April 2019

Documenting Evolution: Comparing and Contrasting Late Mesozoic and Late Cenozoic Molluscan Patterns

Joshua Slattery
University of South Florida, dinohyus@gmail.com

Documenting Evolution: Comparing and Contrasting Late Mesozoic and Late Cenozoic Molluscan Patterns

by

Joshua Slattery

A dissertation submitted in partial fulfillment
of the requirement of the degree of
Doctor of Philosophy
School of Geosciences
College of Arts and Sciences
University of South Florida

Co-Major Professor: Peter Harries, Ph.D.
Co-Major Professor: Paul Wetmore, Ph.D.
Brian Andres, Ph.D.
Neil Landman, Ph.D.
Matthew Olney, Ph.D.

Date of Approval:
May 7, 2019

Keywords: Western Interior Seaway, ammonite biostratigraphy, *plus ça change*, phylogeny, bivalves, *Baculites*

Dedication

I would like to dedicate this dissertation to my mom and Ashley, who have always helped and encouraged me.

ACKNOWLEDGMENTS

I would like thank co-advisers and committee members, who made this dissertation possible. I especially want to show my appreciation to P. Harries for his support and guidance throughout this project. I also want to acknowledge P. Wetmore for his support and invaluable discussions related to the tectonics of western North America. I am also thankful to my committee members B. Andres, N. Landman, and M. Olney for their support, guidance, helpful suggestions, and critical input on all aspects related to this dissertation.

Invaluable discussions and suggestions were also provided by D. Boyd, M. Bingle-Davis, R. Blakey, G. Brown, JP Cavigelli, A. Cardenas, J. Crampton, W. Cobban, D. Dockery, L. Edwards, D. Geary, J. Hartman, J. Hoganson, C. Ifrim, K. Irwin, M. Jarrett, J. Kennedy, B. King, J. Lillegraven, R. Lynds, C. Mehta, M. Meyer, J. Sliko-Meyer, S. Paul, G. Phillips, G. Plint, R. Portell, K. Minor, R. Johnson, D. Sawyer, R. Scott, W. Stinnesbeck, D. Wohr, M. Zaleha, P. Yacobucci, and R. Ostrander.

I also appreciate the various landowners, museums, and collection managers for assisting me with obtaining specimens used in this study. I particularly want to thank the landowners in Wyoming, South Dakota, Nebraska, Colorado, Montana, Mississippi, and Tennessee for giving me permission to carry out field work on their land. I would like to acknowledge R. Martin, JD and L. Williams, R. Pfister, A. and B. Carrol, D. De Boer, R. Moulton, G. Feiner, C. Wilkins, C. and K. Sanders, P. Sanders, J. and D. Lesmeister, Mr. and Mrs. Perino, M. and J. McGraw, K. Schuricht, C. and A. Shaffer, D. and A. Cameron, S. Neugebauer, Mr. and Mrs. Conger, B. Bailey, Mr. and Mrs. Strauch, M. Gibson (University of Tennessee Martin), W. Creel (Pink

Palace Museum), P. Broadbent (Coon Creek Scince Center), and Jennifer Shanahan. I also want to thank R. Portell (Florida Museum of Natural History), G. Phillips (Mississippi Museum of Natural Science), K. McKinney (United States Geological Survey), B. Hussaini (American Museum of Natural History), and S. Butts (Yale Peabody Museum of Natural History), J. Utrup (Yale Peabody Museum), and K. Nelson (Timber Lake and Area Museum) and M. Marshall (Timber Lake and Area Museum) for help accessing and photographing museum specimens.

Credit should also be given to my family, friends, and 'The Truckers' for their help and support. I especially want to recognize A. Sandness for her unwavering support, love, patience, and Adobe Illustrator skills. I also want to express gratitude to my mother, S. Slattery, for her encouragement through the years and with help in the field. I would like to thank L. Bechtholdt for his support with my research. I would also like to thank S. and L. Sandness for there help and support over the year. Acknowledge should be given to J. Mejia and A. Farrell for help with preparing for my defense. This dissertation would have been unlikely to have been undertaken without the influence of my middle school science teacher P. Crips, who inspired me to pursue a PhD in the sciences. I would also like to thank the Z. Salmon and S. Stoddard of the McNair Scholars Program at the University of Wyoming for help during my undergraduate career in achieving my goal of getting accepted into the PhD program at the University of South Florida.

Partial funding for this research has been provided by National Science Foundation through Grant EAR 1053517 to P. Harries. Funding was also provided by the Tampa Bay Fossil Club Louis Villei Memorial Grant and Research Grant, respectively, St. Petersburg Shell Club, Research Grant, University of South Florida School of Geosciences Richard A. Davis Jr. Endowed Fellowship in Geology Research, Paleontological Research Institute's J. Thomas Dutro Jr. Student Award in Systematic Paleontology, Association of Applied Paleontological Services

Rene M. Vandervelde Research Grant, USF School of Geosciences Tharp Award, American Museum of Natural History Collection Study Grant, Geological Society of America Student Research Grant, Florida Paleontological Society Gary S. Morgan Award, Gulf Coast Association of Geological Societies Student Grant Program, Yale Peabody Museum of Natural History Schuchert and Dunbar Grant in Aid Program, American Museum of Natural History, Lerner Gray Fund for Marine Research, and Sigma-Xi Student Research Grant.

TABLE OF CONTENTS

LIST OF TABLES

.

LIST OF FIGURES

ABSTRACT

Despite major advances, evolutionary theory still has numerous shortcomings in terms of fully understanding the controls on speciation and diversification. A major factor limiting our knowledge is how biology and paleobiology view speciation from separate micro- and macro-evolutionary perspectives, respectively. Biologists typically examine microevolutionary changes within species from various biogeographic, behavioral, morphological, and genetic perspectives, which contrasts to the macroevolutionary approach of most paleobiologists, who have examined the same phenomena at larger scales but with the standpoint of time, have also concentrated on aspects of global or regional diversification (e.g., richness, origination rates, and extinction rates) over the long-term. Noticeably absent from speciation research has been a serious reexamination of evolutionary tempo and mode (i.e., the rate and style of transformation) over the long-term framed within an environmental and phylogenetic context. These issues indicate that an assessment of evolutionary patterns set within an environmental and phylogenetic context is needed to improve our understanding of evolutionary drivers and their roles in influencing speciation and cladogenesis. Thus, the goal of this dissertation is to investigate the role that broad-scale climatic regimes (i.e., ice- vs. greenhouse conditions) play in controlling evolutionary patterns and how phylogenetic analysis can be used to reconstruct a hidden evolutionary history of a group.

To examine the role broad-scale climatic variation might exert on evolutionary dynamics, this dissertation examines evolutionary changes among nuculid and lucinid bivalves from the stable climate of the Cretaceous greenhouse to the moderately stable mixed-house climate of the

Neogene to the less stable icehouse climate of the Quaternary. The bivalves used for this study include *Nucula*, *Lucina,* and *Anodontia*, which are well-represented in the fossil record. Morphological change through time was evaluated using both size data and elliptical fourier analysis of outline shape data. *Nucula* show evolutionary change during the Cretaceous and Neogene with no change from the Pliocene to Modern. *Lucina*, which is relatively evolutionarily conservative, show no change in shape from the Miocene to Pleistocene with substantial change in size during the Miocene and limited change in size from the Pliocene to Modern. *Anodontia* show change in shape during the Neogene and then no change during the Quaternary. *Anodontia* also shows substantial change in size and shape during the late Miocene but limited to no change in size and shape during the middle Miocene and Pliocene to Quaternary. In all cases, most evolutionary change coincided with the more stable climate regimes, whereas stasis was primarily concentrated during the less stable climate regimes. These cases provide strong support for Sheldon's (1996) '*Plus ça change*' model, which predicts that relatively more stable environmental settings (such as during a greenhouse or mixed-house climate regime) will display evolutionary change, whereas a more frequently changing environment (such as during an icehouse) will display stasis.

Another critical element in examining evolution in the fossil record is the reconstruction of rigorous phylogenies that allow for understanding of evolutionary relationships and modes, which usually remain hidden using traditional morphometric and biostratigraphic approaches. To reveal the hidden evolutionary history of a clade, the final chapter of this dissertation examines the evolutionary relationships of the biostratigraphically important Late Cretaceous ammonite *Baculites* in the Western Interior Seaway (WIS). This study used both continuous and discrete character data to construct a single most parsimonious tree using the software TNT (Tree search

using New Technology). This tree has excellent biostratigraphic congruence, which is interpreted as independent corroboration of underlying evolutionary relationships among *Baculites* in the seaway. The tree topology reveals that middle Campanian to early Maastrichtian *Baculites* belong to multiple clades, which likely reflects successive extinctions of endemic lineages and replacement by new unrelated species that would evolve into new, short-lived endemic lineages. The causes for repeated clade extinction are unknown, however, they are likely related to the unique environmental conditions of the epicontinental WIS. These results suggest that non-vertebrate groups, which have typically been assumed to have a limited number of available morphological characters, can be analyzed to establish a robust phylogeny with a careful morphological analysis. The resulting phylogenetic patterns can be utilized to reveal the hidden evolutionary history of a chosen group as exemplified here for *Baculites.*

CHAPTER ONE:

INTRODUCTION

The fossil record is known to be an excellent natural archive of the history of life and evolution as documented by numerous studies (e.g., Erwin and Anstey, 1995; Gould, 2002). However, following the publication of *Origin of Species* by Charles Darwin in 1859, many evolutionary biologists typically regarded the fossil record as too incomplete to provide any significant or meaningful information about evolutionary patterns and processes. This resulted in paleontology remaining a sub-discipline of stratigraphy and playing a relatively minor role in the early growth of evolutionary theory. This long-held perspective, however, was challenged with the development of the modern evolutionary synthesis during the mid-20th century, and paleontology's rise to prominence with the publication of *Tempo and Mode in Evolution* by George Gaylord Simpson in 1944. Simpson along with many others who followed his lead (e.g., Newell, 1962; Eldredge and Gould, 1972, Gould and Eldredge, 1977) led what has come to be known as the 'paleobiological revolution', which over several decades elevated paleontology from the 'handmaiden of stratigraphy' to a major player in modern evolutionary theory (Allmon et al., 2008). During this interval, paleobiology, as it has come to be known, has revealed the relative importance of the fossil record to understanding history of life, evolutionary patterns, and evolutionary processes. Despite these major developments within the field of paleobiology, numerous questions about evolution remain.

Thus, the goal of this doctoral dissertation is to examine a range of questions related to evolutionary patterns, the techniques used to examine evolution, and specific hypotheses about the history of life using a variety of different methodologies. Before delving into these topics, Chapters

Two and Three of this dissertation examine the geological and chronological context of the Late Cretaceous Western Interior and Atlantic/Gulf Coastal Plains, respectively, which provides key background and context for the following chapters that relate to the Cretaceous. These sections are then followed with a chapter outlining the methods used in Chapters Five and Six, which are case studies that examine the broad-scale climatic context of different evolutionary patterns using bivalves from the Cretaceous and Neogene–Quaternary of the Gulf Coast. Finally, Chapter Seven examines whether morphological systematics can be used to effectively determine molluscan phylogenies at the species level, even for those clades that are thought to possess relatively few preserved characters.

Early Cretaceous to Paleocene Paleogeographic Evolution of the Western Interior Seaway

Chapter Two provides a broad overview of the Early Cretaceous to Paleocene paleogeographic evolution of the Western Interior Seaway (WIS). This summary delved into its geological setting as well as the various eustatic controls that modulated water depth and the location of the seaway's shorelines. Documentation of western North America's physiography during this interval is necessary to understand how the seaway became established, evolved, and ultimately retreated from the continent. This broad overview of the seaway's paleogeographic evolution will provide insights for a better understanding of the stratigraphic architecture of Lower Cretaceous through Paleocene strata, assist in elucidating the distinctive sedimentation patterns in the Western Interior, and provide a framework against which to compare paleontological trends and patterns.

Campanian–Maastrichtian Ammonite Zonation of the Gulf and Atlantic Coastal Plains

The primary objective of Chapter Three is to compile the existing data on ammonite ranges from the Campanian–Maastrichtian of the Gulf and Atlantic Coastal Plain (GCP and ACP, respectively) to produce biozonations for each region. The impetus behind this chapter lies in the fact that the generally accepted zonal scheme for the GCP is based on the decades old work of Young

(1959, 1963, 1969, 1982, 1985, 1986), and there is currently no existing framework below the upper Maastrichtian in the ACP. Over the past several decades a substantial new focus has been devoted to describing and re-evaluating many of the Campanian–Maastrichtian ammonite assemblages in the ACP and GCP, which has greatly improved our ability to erect a comprehensive biostratigraphy. These studies have enhanced our knowledge of how the ammonite assemblages in the GCP and ACP correlate with more refined biostratigraphic schemes in other parts of the world (e.g., Kennedy et al., 1992; Cobban and Kennedy, 1995; Landman et al., 2004a, b, 2007; Cobban et al., 2008; Ifrim et al. 2015; Larina et al., 2016). However, these studies have not been comprehensive and considerable biostratigraphic information lies scattered throughout numerous publications, which will be reviewed in this chapter. Furthermore, this chapter will also examine the basic geological setting of the ACP and GCP during the Cretaceous.

Broad-Scale Climatic Context of Different Evolutionary Patterns

Chapter Four is specifically focused on methodology and examines the morphometric techniques used in Chapters Five and Six, which compare evolutionary patterns among three bivalve lineages during contrasting climatic regimes (ice- vs. mixed- vs. green-house climates). The origin of these chapters, which are part of a broader National Science Foundation funded project, stems from the fact that most evolutionary tempo and mode studies have focused on testing the legitimacy and frequency of different evolutionary patterns, while ignoring their environmental context and/or controls (e.g., Erwin and Anstey, 1995). Studies that have examined evolutionary controls within an environmental framework have traditionally utilized the taxic ranges to examine long-term drivers on diversity, origination, and extinction patterns (e.g., Foote, 2006; Cardenas and Harries, 2012). Exacerbating this issue has been our inability to obtain a consensus on evolutionary patterns due to most investigations differing in their chosen taxonomic groups, phylogenetic framework, stratigraphic

completeness, temporal range, spatial coverage, and methodologies. These various issues necessitated this reassessment of evolutionary patterns but set within an environmental framework utilizing standardized methodologies at more refined taxonomic and temporal scales than previous studies. This chapter will attempt to improve our understanding of how microevolutionary analyses of tempo and mode integrate with macroevolutionary studies of diversification.

Phylogeny of the Late Cretaceous Ammonite *Baculites* Lamark 1799 in the Western Interior Seaway

Another critical element in examining evolution in the fossil record is the reconstruction of rigorous phylogenies. These allow for detailed understanding of evolutionary relationships and modes, which typically remain concealed using with traditional morphometric and biostratigraphic approaches. In the seventh and final chapter of this dissertation, a phylogenetic approach is utilized to test whether a group that possesses relatively few characters can be used to effectively reconstruct the evolutionary relationships among their constituent species. To do this, the chapter examines the evolutionary relationships among the biostratigraphically important Late Cretaceous ammonite *Baculites* Lamark 1799 in the Western Interior using a cladistic approach. This heteromorphic ammonite is among the most distinctive, abundant, and wide spread Late Cretaceous molluscs. Despite extensive knowledge of their biostratigraphy, biogeography, and paleoecology (e.g., Klinger and Kennedy, 2001; Kruta et al., 2011; Klug, 2012; Westermann, 2013), relatively little is known concerning the phylogenetic relationships among the various described species that comprise this important clade. This poor understanding of their phylogenetic relationships stems at least in part from their simple shell morphologies, which displays a paucity of obvious characters and shares numerous putative convergences among species (Klinger and Kennedy, 2001) thus making phylogenetic work challenging. This study endeavors to identify and define the separate *Baculites* clades that inhabited

the WIS as well as determine the evolutionary role of immigrant/emigrant stocks into the basin during the last 15 million years of the Late Cretaceous. It also compares the phylogenetic hypothesis against earlier, pre-cladistic evolutionary reconstructions developed by Kennedy (1977), Cobban (1993), and Klinger and Kennedy (2001).

References

Allmon, W.D., Kelley, P.H., and Ross, R.M., 2008, Stephen Jay Gould: Reflections on His View of Life: *Oxford University Press*, 416 pp.

Cardenas-Rozo, A.L. and Harries, P.J., 2016, Planktic foraminiferal diversity: logistic growth overprinted by a varying environment: *Acta Biológica Colombiana*, 21, 501–508.

Cobban, W.A., 1993, Upper Cretaceous Ammonite Diversity in the Western Interior Seaway: *in* Caldwell, W.G.E., and Kauffman, E.G., eds., Evolution of the Western Interior Basin: *Geological Association of Canada Special Paper*, 39, 297–318.

Cobban, W.A. and Kennedy, W.J. 1995, Maastrichtian ammonites chiefly from the Prairie Bluff Chalk in Alabama and Mississippi. *The Paleontological Society Memoir*, 44, 40 pp.

Cobban, W.A., Hook, S.C. and McKinney, K.C. 2008, Upper Cretaceous molluscan record along a transect from Virden, New Mexico, to Del Rio, Texas. *New Mexico Geology*, 3, 75–92.

Darwin, C., 1859, The origin of species by means of natural selection: or, the preservation of favored races in the struggle for life: *John Murray Publisher*, 502 pp.

Erwin, D. H., and Anstey, R. L., Editors, 1995, New approaches to speciation in the fossil record: *Columbia University Press*, 288 pp.

Eldredge, N., and Gould, S.J., 1972, Punctuated equilibria: an alternative to phyletic gradualism: *in* Schopf, T.J.M., Eds., *Models in Paleobiology*, 82–115.

Foote, M. 2006, Substrate affinity and diversity dynamics of Paleozoic marine animals: *Paleobiology*, 32, 345–366.

Gould, S.J. and Eldredge, N., 1977, Punctuated equilibria: the tempo and mode of evolution reconsidered: Paleobiology, 3, 115–151.

Gould, S.J., 2002, The Structure of Evolutionary Theory: *Harvard University Press*, 1464 pp.

Ifrim, C., Stinnesbeck, W., and Flores Ventura, J., 2013, An Endemic Cephalopod Assemblage from the Lower Campanian (Late Cretaceous) Parras Shale, Western Coahuila, Mexico: *Journal of Paleontology*, 87, 881–901.

Kennedy W J., 1977, Ammonite Evolution: *in* Hallam, A., ed. *Patterns of Evolution as Illustrated in the Fossil Record*, 251–304.

Kennedy, W.J., Cobban, W.A. and Scott, G.R., 1992, Ammonite correlation of the uppermost Campanian of Western Europe, the US Gulf Coast, Atlantic Seaboard, and the numerical age of the base of the Maastrichtian: *Geological Magazine*, 129, 497–500.

Klinger, H. C. and Kennedy, W.J., 2001, Stratigraphic and geographic distribution, phylogenetic trends, and general comments on the ammonite family Baculitidae Gill, 1871 (with an annotated list of the species referred to the family): *Annals of the South African Museum*, 107, 290 pp.

Klug, C., Riegraf, W., and Lehmann, J., 2012, Soft–part preservation in heteromorph ammonites from the Cenomanian–Turonian Boundary Event (OAE 2) in north–west Germany: *Palaeontology*, 55, 1307–1331.

Kruta, I., Landman, N.H., Rouget, I., Cecca, F., and Tafforeau, P., 2011, The role of ammonites in the Mesozoic marine food web revealed by jaw preservation: *Science*, 331, 70–72.

Lamarck, J. P. B. A. de M. de., 1799, Prodrome d'une nouvelle classification des coquilles: *Memoires de la Societe d'Histoire naturelle de Paris* (for 1799): 63-90.

Landman, N.H.; Johnson, R.O.; and Edwards, L.E. 2004a, Cephalopods from the Cretaceous/Tertiary Boundary Interval on the Atlantic Coastal Plain, with a Description of the Highest Ammonite Zones in North America, Part 1, Maryland and North Carolina. *American Museum Novitates*, 3454, 64 pp.

Landman, N.H.; Johnson, R.O., and Edwards, L.E. 2004b, Cephalopods from the Cretaceous/Tertiary Boundary Interval on the Atlantic Coastal Plain, with a description of the highest ammonite zones in North America, Part 2, Northeastern Monmouth County, New Jersey: *American Museum Bulletin*, 287, 107 pp.

Landman, N.H.; Johnson, R.O.; Garb, M.P.; Edwards, L.E., and Kyte, F.T. 2007, Cephalopods from the Cretaceous/Tertiary boundary interval on the Atlantic Coastal Plain, with a description of the highest ammonite zones in North America. Part 3. Manasquan River Basin, Monmouth County, New Jersey: *American Museum Bulletin*, 303, 112 pp.

Larina, E., Garb, M., Landman, N., Dastas, N., Thibault, N., Edwards, L., Phillips, G., Rovelli, R., Myers, C. and Naujokaityte, J., 2016, Upper Maastrichtian ammonite biostratigraphy of the Gulf Coastal Plain (Mississippi Embayment, southern USA): *Cretaceous Research*, 60, 128–151.

Newell, N. D., 1962, Paleontological gaps and geochronology: *Journal of Paleontology*, 36, 592–610.

Simpson, G. G., 1944, Tempo and mode in evolution: *Columbia University Press*, 237 pp.

Westermann, G.E.G, 2013, Hydrostatics, propulsion and life-habits of the Cretaceous ammonoid *Baculites*: *Revue de Paleobiologie*, 32, 249–265.

Young, K.P. 1959, Techniques of mollusc zonation in Texas Cretaceous: *American Journal of Science*, 257, 752–769.

Young, K.P. 1963, Upper Cretaceous Ammonites from the Gulf Coast of the United States: *University of Texas Publication*, 6304, 373 pp.

Young, K.P. 1969, Ammonite zones of northern Chihuahua. *in* Cordoba, D.A., Wengerd, S.A., and Shomaker, J.W., Eds., *The Border Region (Chihuahua, Mexico, & USA), New Mexico Geological Society Annual Field Conference Guidebook*, 20, 97–101.

Young, K.P. 1982, Cretaceous rocks of central Texas—biostratigraphy and lithostratigraphy: *in* Maddocks, R. F. Ed., *Texas Ostrocoda: guidebook of excursions and related papers for the Eighth Annual International Symposium on Ostracoda*, 8, 111–126.

Young, K.P. 1985, The Austin Division of Central Texas: *in* K. Young, and C.M. Woodruff, Eds. *Austin chalk in its type area--stratigraphy and structure, Austin Geological Society Field Guidebook*. 7, 3–52.

Young, K.P. 1986, Cretaceous, Marine inundations of the San Marcos Platform, Texas: *Cretaceous Research*, 7, 117–140.

CHAPTER TWO:

EARLY CRETACEOUS TO PALEOCENE PALEOGEOGRAPHY OF THE WESTERN INTERIOR SEAWAY: THE INTERACTION OF EUSTASY, TECTONISM, AND SEDIMENTATION

Note to Reader

This work has been previously published in Wyoming Geological Association Field Guide, *Cretaceous Conference: Evolution and Revolution*, 22–60, and has been reproduced with permission by the publisher (see Appendix A).

Introduction

In the west-central portion of North America, Lower Cretaceous through middle Paleocene strata representing sedimentation in the Western Interior Foreland Basin (WIFB) form a thick and complex mosaic of interfingering marine and terrestrial deposits recording successive transgressions and regressions of the Western Interior Seaway (WIS). Throughout most of its history, this epeiric sea (i.e., a sea covering the interior of a continent) connected the Arctic Ocean (or Boreal Ocean) with the Gulf of Mexico (or Tethys Sea) and was joined to the North Atlantic Ocean, possibly episodically, via the Hudson Seaway (Williams and Stelck, 1975; Kauffman and Caldwell, 1993; Roberts and Kirschbaum, 1995; Ziegeler and Rowley, 1996).

Since the publication of Schuchert's (1910) "Paleogeography of North America", numerous studies have dealt with aspects of the WIS's paleogeography, but most of these have only focused on relatively specific time intervals and restricted geographical areas (e.g., Schuchert, 1955; Reeside, 1957; Sloss et al., 1960; Birkelund, 1965; Sohl, 1967; Jeletzky, 1971;

McGookey, 1972; Gill and Cobban, 1973; Williams and Stelck, 1975; Witzke et al., 1983; Cobban and Hook, 1984; Kauffman, 1984; Lillegraven and Ostresh, 1991; Dixon, 1993; Kauffman and Caldwell, 1993; Stott et al., 1993; Cobban et al., 1994; Sageman and Arthur, 1994; Ziegeler and Rowley, 1996; Kennedy et al., 1998; Erickson, 1999; Roberts and Kirschbaum, 1995; White et al., 2000; Stelck et al., 2007; Miall et al., 2008; Nielsen et al., 2008; Boyd and Lillegraven, 2011; Landman et al., 2012; Blakey, 2013; Schröder-Adams, 2014; Berry, 2017). The most detailed studies of the seaway's paleogeography and its transgressive/regressive successions have been primarily concentrated along its western margin in an area spanning from Alberta south to west Texas where strata of this age are thick, well-exposed, and relatively biostratigraphically complete (Reeside, 1957; Sloss et al., 1960; McGookey, 1972; Gill and Cobban, 1973; Williams and Stelck, 1975; Cobban and Hook, 1984; Kauffman, 1984; Lillegraven and Ostresh, 1991; Stott et al., 1993; Cobban, 1994; Sageman and Arthur, 1994; Roberts and Kirschbaum, 1995; Boyd and Lillegraven, 2011; Landman et al., 2012). Relatively fewer studies have attempted detailed reconstructions in its northern and eastern parts because of substantial post-Mesozoic erosion and/or rarity of exposures due to greater cover (e.g., Jeletzky, 1971; Williams and Stelck, 1975; Witzke et al., 1983; Cobban et al., 1994; Roberts and Kirschbaum, 1995; Ziegeler and Rowley, 1996; Erickson, 1999; Stelck et al., 2007; Nielsen et al., 2008; Schröder-Adams, 2014). Similar problems hamper our understanding of the WIS's paleogeography throughout its final regressions and transgressions during the late Maastrichtian to middle Paleocene (e.g., Witzke et al., 1983; Erickson, 1999; Boyd and Lillegraven, 2011). The combination of these factors and paucity of studies synthesizing paleogeographic knowledge have resulted in an incomplete understanding of the spatial evolution of the WIS and the WIFB.

In this paper, we provide a broad overview of the Early Cretaceous to Paleocene paleogeographic evolution of the WIS and the WIFB that it flooded. This summary will also delve into the geological setting, the methodologies used for paleogeographic reconstruction, as well as the various controls that modulated sea level and the location of the seaway's shorelines. A detailed documentation of western North America's physiography during this interval is necessary to understand how the WIS formed, transformed, and eventually ceased to exist. This overall consideration of the seaway's paleogeographic evolution should provide insights for a better understanding of the stratigraphic architecture of Lower Cretaceous through Paleocene strata, assist in elucidating the distinctive sedimentation patterns in the WIFB, and provide a framework against which to compare paleontological trends and patterns.

Physiographic and Geological History of the Western Interior Foreland Basin

The WIS's paleogeography primarily reflects the interplay between sea level and the physiography of North America, which were both influenced to varying degrees by tectonics (Gill and Cobban, 1973; Williams and Stelck, 1975; Jeletzky, 1980; Lillegraven and Ostresh, 1991; Krystinik and DeJarnett, 1995; Kauffman and Caldwell, 1993; Miall et al., 2008). Tectonic forces shaped western North America's physiography during the Late Jurassic to the Eocene through various processes, including volcanism, uplift, subsidence, and fold-thrust-belt migration. These processes, in turn, influenced shoreline patterns and lithofacies distributions.

The most prominent physiographic feature of western North America during this time interval, as well as subsequently, has been and remains the Cordilleran Orogenic Belt, which spans nearly 6,000 km from Alaska to southern Mexico, reaching its maximum width of over 1000 km in the western coterminous United States and southwestern Canada (Fig. 2.1; Monger,

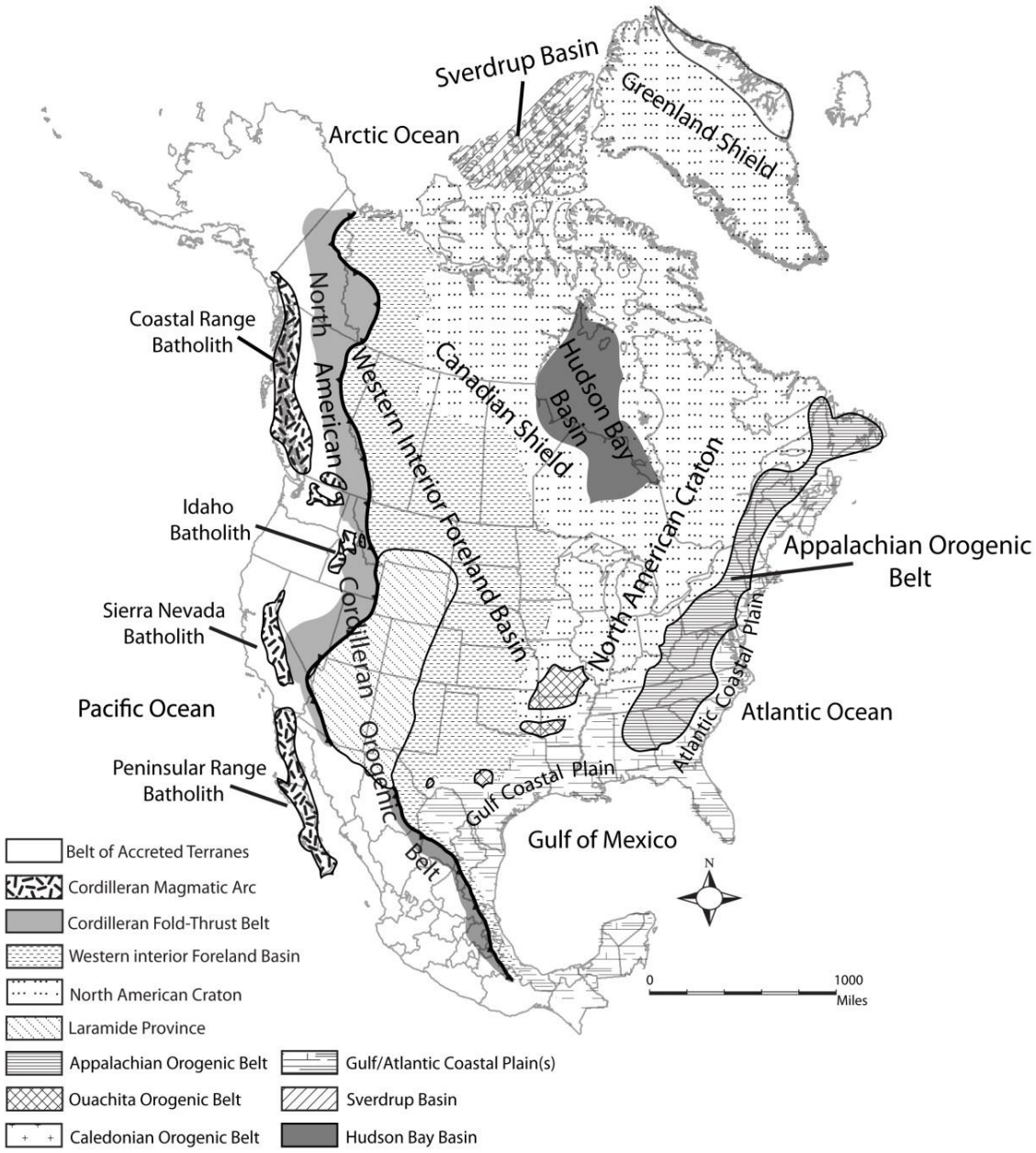

Figure 2.1. Tectonic map of North America showing key geological and physiographic features of the Cordilleran Orogenic Belt, Western Interior Foreland Basin, Hudson Bay Basin, North American Craton, Paleozoic orogenic belts, and Gulf and Atlantic Coastal plains (modified from Bally et al., 1989; DeCelles, 2004).

1993; DeCelles, 2004). This mountain belt and its associated basins (including the WIFB) comprise approximately a seventh of the 40,000 km Circum-Pacific Orogenic Belt (more

colloquially the 'Ring of Fire') that fringes the Pacific Ocean (DeCelles, 2004). Since the Late Jurassic, this geographic feature has acted as a significant oceanographic, climatic, and biogeographic barrier between the Panthalassan or Pacific Ocean and the Western Interior (Williams and Stelck, 1975). Prior to the uplift of the Cordilleran Orogenic Belt, most Mesozoic marine transgressions the flooded the Western Interior came from the Pacific Ocean (Williams and Stelck, 1975).

During the Late Triassic through Middle Jurassic, prior to the development of the Cordilleran Orogenic Belt and the WIFB, western North America was the site of numerous fringing arcs and interarc basins (Harper and Wright, 1984; Wright and Fahan, 1988; Saleeby and Busby-Spera, 1992; Dickinson et al., 1996; DeCelles, 2004). The precursor events that eventually resulted in the Cordilleran Orogenic Belt and WIFB's formation initiated with the westward drift of North America relative to Europe and Africa (Monger, 1993; DeCelles, 2004). This westward drift resulted in the subduction of Panthalassan oceanic crust beneath the North America Plate accompanied by regional shortening and thickening of the continental crust (Monger, 1993; DeCelles, 2004). This movement resulted in a coherent continental margin arc-trench tectonic system that was tectonically similar to the modern continental margin arc-trench tectonic system of western South America (Monger, 1993; DeCelles, 2004).

Like the modern Andes Mountains and Amazon Basin in South America, this region included a forearc system (including a forearc basin), a magmatic arc, and a retroarc (Figs. 2.1; 2.2). The retroarc included both the Cordilleran Fold-Thrust Belt and resulting foreland-basin system (or WIFB; Monger, 1993; DeCelles and Giles, 1996; DeCelles, 2004) with the stable North American craton situated to the east (Figs. 2.1, 2.2; Kauffman and Caldwell, 1993; DeCelles, 2004; Miall et al., 2008). The spatial position and extent of these various tectonic

subdivisions changed through time both perpendicular and parallel to the Cordillera's strike (Monger, 1993; DeCelles, 2004; Miall et al., 2008). These changes played a critical role in the evolution of the WIFB and consequently the geography of the WIS. Broadly, within the Cordilleran Orogenic Belt, different tectonic processes were expressed diachronously from south to north, which were reflected in the physiographic changes that occurred from the Jurassic to Eocene. In Canada, the Cordilleran Orogenic Belt and WIFB arose during the Late Jurassic from the collision of terranes that could not be subducted beneath the North American plate (Coney et al., 1980; Ricketts, 2008). Each new terrane collision, starting in the Jurassic and continuing into the Eocene, increased tectonic loading on the Canadian Shield and initiated a new cycle of fold-thrust belt tectonism, uplift, and the formation of clastic wedges in the WIFB (Stockmal et al., 1992; Miall et al., 2008). The Cordilleran Orogenic Belt and WIFB in the United States were initiated in the Late Jurassic due to the accretion of the fringing arcs associated with the closure of marginal oceanic basins (e.g., the Mezcalera plate) along with the start of Panthalassan oceanic crust subduction (DeCelles and Currie, 1996; DeCelles, 2004; Miall et al., 2008).

The forearc region along the western margin of North America was mainly composed of Mesozoic accretionary terranes and thick deposits of arc- and oceanic-slab-derived sediments deposited into forearc basins (Figs. 2.1, 2.2; Monger, 1993; DeCelles, 2004; Ingersoll, 2008; Ricketts, 2008). A magmatic arc (or the western Cordillera) was positioned eastward of the forearc and was the site of active melting and related arc magmatism above the eastward-dipping subduction zone (Figs. 2.1, 2.2; Monger, 1993; Ducea, 2001; DeCelles, 2004). The volcanoes produced by this arc have long since eroded away, although evidence for their former presence exists in the form of calc-alkaline granitoid intrusions preserved as batholiths in the Peninsular Range of Baja California, the Sierra Nevadas of California, the Idaho Batholith of Idaho and

Montana, and within the Coast Range of British Columbia (Fig. 2.2; Ducea, 2001; DeCelles, 2004). Additional evidence for this volcanism includes the numerous widespread ash beds found throughout the stratigraphic sequences of the WIFB (i.e., Utah, Colorado, Wyoming, Montana, as well as North and South Dakota), which have been used to radiometrically date and correlate Upper Jurassic through Eocene strata in this region (Elder, 1988; Kauffman and Caldwell, 1993; Obradovich, 1993; Kowalis et al., 1995; Cobban et al., 2006).

The retroarc, which included the Cordilleran Fold-Thrust Belt (or eastern Cordillera) and the adjacent WIFB, were situated in southern Nevada, Arizona, Utah, Wyoming, Idaho, Montana, eastern British Colombia, Alberta, Saskatchewan, eastern Yukon Territory, and Northwest Territories (Figs. 2.1, 2.2; Kauffman and Caldwell, 1993; Monger, 1993; DeCelles, 2004). Deformation in the eastern Cordillera was characterized by numerous folds and thrust faults, now obscured by Neogene and Quaternary erosion, igneous events, structural features, and metamorphic processes related to extension as well as migration of the Yellowstone Hot Spot (DeCelles and Mitra, 1995; DeCelles, 2004). Paleobotanical and associated geological evidence suggests that the region between the Cordilleran magmatic arc and Cordilleran Fold-Thrust Belt was the site of a high plateau (i.e., "Nevadaplano") similar to the Altiplano in the central Andes (Fig., 2.2; DeCelles, 2004; Colgan and Henry, 2009; Ernst, 2009; Chamberlain et al., 2012). The retroarc region was the primary location of deformational shortening in western North America during the Late Jurassic to Eocene (Monger, 1993; DeCelles, 2004).

Further east, tectonic loading by the Cordilleran Fold-Thrust Belt depressed the crust (i.e., load-induced flexural subsidence) and resulted in the formation of the WIFB (Figs. 2.1, 2.2) Kauffman and Caldwell, 1993; DeCelles and Giles, 1996; Miall et al., 2008). At its maximum extent, the WIFB was over 1,500 km in width, extending from modern-day central Arizona,

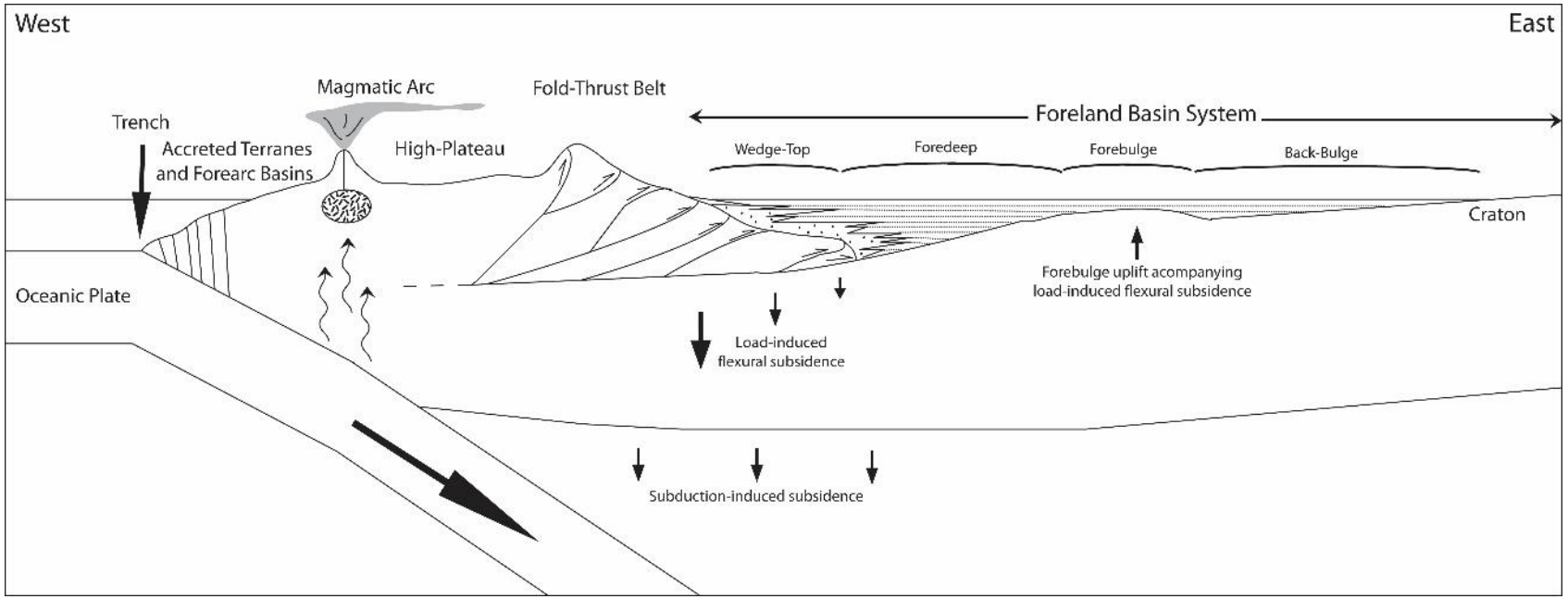

Figure 2.2. Generalized tectonic, structural, and stratigraphic cross-section across the Cordilleran Orogenic Belt and Western Interior Foreland Basin System in North America during the Late Cretaceous (modified from DeCelles and Giles, 1996; Miall et al., 2008).

central Utah, western Wyoming, western Montana, and western Alberta to eastern Kansas, Iowa, western Minnesota, and eastern Manitoba (Cross, 1986; Kauffman and Caldwell, 1993; DeCelles and Giles, 1996; Miall et al., 2008). The basin's overall width is much greater than would be expected based on a typical load-induced flexural-subsidence basin model (e.g., Kauffman, 1977) as WIFB subsidence was likely enhanced by subduction-induced subsidence involving "viscous coupling between the base of the continental plate and downward circulating mantle-wedge that is entrained by the subducting slab" (DeCelles and Giles, 1996, p. 105; Fig. 2.2). This subsidence, along with load-induced flexural subsidence from sediment accumulation and the Cordilleran Fold-thrust Belt, were the primary mechanisms for creating accommodation space in the WIFB (Kauffman and Caldwell, 1993; DeCelles and Giles, 1996; Miall et al., 2008).

The WIFB system consisted of four distinct depositional zones (Fig. 2.2), including from east to west: 1) the wedge-top depozone, filled with sediment that accumulated above the frontal part of the orogenic wedge and thickens toward the foredeep; 2) the foredeep depozone, a cratonward tapering, thick accumulation of sediment located between the tip of the deformation front and the proximal flank of the forebulge; 3) the forebulge depozone, a broad region of potential flexural uplift between the foredeep and backbulge basin; and 4) the backbulge depozone, a mass of sediment collected in a shallow, but expansive zone of possible flexural subsidence cratonward of the forebulge (McMechan and Thompson, 1993; DeCelles and Currie, 1996; DeCelles and Giles, 1996). With the addition of the wedge-top depozone by DeCelles and Currie (1996) and DeCelles and Giles (1996) as part of the WIFB, the basin's geometry becomes a doubly tapered prism instead of the classically asymmetric wedge suggested by earlier studies of the basin (e.g., Kauffman, 1977; Kauffman and Caldwell, 1993).

Latitudinally, the WIFB contains several different, relatively minor pre-existing tectonic elements or basement features that are thought to have exerted substantial influence over the region's physiography, the WIS's paleogeography, and the lithofacies patterns within the basin (Fig. 2.3). These tectonic elements consist of various arches, block-uplifts, and sub-basins that were hypsographically expressed throughout the basin's history or became expressed because of tectonic activity (Weimer, 1978; Stott et al., 1993; Stelck et al., 2007; Miall et al., 2008). Most of these structural features reflect reactivated basement elements that produced various topographic highs and lows that acted as local sediment sources, sediment sinks, and barriers to sea-level rise (Weimer, 1978; Stelck et al., 2007; Miall et al., 2008). In the northern part of the WIFB, transverse structural features or highs, such as the Dave Lord-Eskimo Lake Arch (Canada), Peace River Arch (Canada), and Sweetgrass Arch (US-Canadian border) limited or exerted substantial controls on the initial marine transgression into the WIFB from the Arctic Ocean (Stelck et al., 2007). Further south in the United States, the Transcontinental Arch isolated the northerly-influenced sea from connecting with the Gulf of Mexico during intervals characterized by low sea level (e.g., early Albian-early Cenomanian; Weimer, 1978; Carlson, 1999; Erickson, 1999; Miall et al., 2008).

During the early (Late Jurassic-Early Cretaceous) and late (late Paleocene-Eocene) phases of its history, the WIFB was predominantly a site of terrestrial sedimentation, whereas its middle stage (late Early Cretaceous-middle Paleocene) was dominated by marine sedimentation (i.e., the WIS; Kauffman and Caldwell, 1993; DeCelles, 2004; Miall et al., 2008). Regional tectonics had significant control over the seaway's shoreline position(s) as well as on sedimentation rates and patterns across the basin (Miall et al., 2008). Gill and Cobban's (1973) survey of the Montana Group in the northern Great Plains is among the first studies to recognize

the influence of active tectonic controls on the paleogeography and sedimentary record of the WIS. Their study of Campanian and Maastrichtian biostratigraphy and lithostratigraphy revealed that transgressions in Montana were correlative with regressions in Wyoming, which they interpreted as a tectonically driven regression that was associated with the initiation of Laramide-style uplift (Gill and Cobban, 1973). Hancock and Kauffman's (1979) study of sea-level change in the WIS showed that eustasy dominated sea level during the Cenomanian to Santonian but became increasingly overprinted by tectonic controls during the Campanian through Maastrichtian. Krystinik and Dejarnett's (1995) study of the Campanian and Maastrichtian sequence architecture of the west-central part of North America documented that tectonic controls were more significant in the United States segment of the WIS than in the Canadian part where eustatic controls dominated its stratigraphic record and its western shoreline position.

Throughout the region's history, the deformation front moved further eastward, and ultimately the WIFB was subdivided into a series of smaller basins by block uplift of basement rocks in the United States segment of the Cordillera (Fig. 2.1; Gill and Cobban, 1973; Lillegraven and Ostresh, 1991; DeCelles, 2004; Lawton, 2008; Miall et al. 2008). Despite an alteration in shortening mechanisms in the United States, thrust faulting and folding remained dominant in Canada and Mexico (DeCelles, 2004). This alteration in shortening mechanisms can be attributed to a shallowing of the subduction angle and to differences in the composition of the overlying crust (DeCelles, 2004; Lawton, 2008). This change in deformation styles (i.e., thin-skinned to thick-skinned) marks the onset of the Laramide Orogeny and the cessation of significant compressional deformation in the United States portion of western North America (DeCelles, 2004; Lawton, 2008). This increase in orography combined with a drop in eustatic sea level forced the final retreat of the WIS and initiated the renewal of terrestrial deposition in the

Figure 2.3. Map of structural features that were active during the Late Jurassic to Paleocene in the Western Interior Foreland Basin (modified from Stott et al., 1993; Stelck et al., 2007; Miall et al., 2008). Abbreviations as indicated: BLT, Blow Trough; KT, Keele Trough, PT, Peel Trough; KA, Keele Arch; CMA, Coppermine Arch; PA, Punnichy Arch; CMU Central Montana Uplift; CMT, Central Montana Trough; CCA, Cedar Creek Anticline; BS, Beartooth Shelf; BU, Bighorn Uplift; PRB; Powder River Basin; BHU, Black Hills Uplift; BT, Bighorn Trough; MCA, Miles City Arch; CA; Casper Arch; ChA, Chadron Arch; GRT, Green River Trough; LU; Laramie Uplift; AB, Alliance Basin; UU, Uncompahgre Uplift; US, Utah Shelf; CCT, Central Colorado Trough; FRU, Front Range Uplift; DB, Denver Basin; PB, Paradox Basin; BMB, Bisbee-McCoy Basin; CHT, Chihuahua Trough; MB, Marathon Basin.

WIFB during the Paleogene (Gill and Cobban, 1973; Lillegraven and Ostresh, 1991; Miall et al., 2008; Boyd and Lillegraven, 2011).

Situated east of the WIFB was the stable North American Craton that was characterized by relatively low topographical relief (Figs. 2.1, 2.2). The eastern and southern margins of this region were bounded by the elevated Appalachian and Ouachita (e.g., Ouachita-Ozark Interior Highlands) orogenic belts, which were formed during the Paleozoic (Fig. 2.1; Arbenz, 1989; Rast, 1989). During the Mesozoic and Cenozoic, the Appalachian Mountains acted as barrier that prevented marine inundations into the continental interior of North America from the Atlantic Ocean (Williams and Stelck, 1975). During the Late Cretaceous and Paleogene, uplifted regions, such as the Ouachita-Ozark Interior Highlands, prevented marine flooding into the WIFB from the extension of the Gulf of Mexico known as the Mississippi Embayment. Marine flooding into the continental interior was only possible west of the Ouachita-Ozark Interior Highlands and north of the Appalachians on the Canadian Shield and into the Hudson Bay Basin where there was limited topographical relief (Williams and Stelck, 1975).

Reconstructing Western Interior Seaway Paleogeography: Approaches

The ten paleogeographic maps presented in this paper show key changes in the distribution of land and sea in both the Western Interior and North America during the Early Cretaceous to Paleocene. The paleogeographic reconstructions of the southern portion (southern Alberta to Texas) of the WIS were primarily constructed by W. A. Cobban over his career examining the Cretaceous stratigraphy and paleontology of the west-central United States. Several of these reconstructions have been published in earlier works (e.g., Gill and Cobban, 1973; Cobban and Hook, 1984; Cobban et al., 1994). Albian to Paleocene shoreline configurations of the southern part of the WIS are also compiled from detailed maps presented

by many other studies of its paleogeography (e.g., Reeside, 1957; Sloss et al., 1960; Sohl, 1967; McGookey, 1972; Williams and Stelck, 1975; Kauffman, 1984; Lillegraven and Ostresh, 1991; Kauffman and Caldwell, 1993; Sageman and Arthur, 1994; Erickson, 1999; Roberts and Kirschbaum, 1995; Boyd and Lillegraven, 2011; Landman et al.; 2012). Furthermore paleogeographic reconstructions of the eastern and northern portions of the WIS during the Cretaceous are largely based on maps from various sources (e.g., Birkelund, 1965; Jeletzky, 1971; Williams and Stelck, 1975; Witzke et al., 1983; Kauffman, 1984; Cobban et al., 1994; Sageman and Arthur, 1994; Ziegeler and Rowley, 1996; White et al., 2000; Stelck et al., 2007; Nielsen et al., 2008; Schröder-Adams, 2014), as are those used for the Pacific Coast, Arctic Coast, Gulf and Atlantic Coastal plains, and Mexico (e.g., Jeletzky, 1971; Alencaster, 1982; Scott, 1984; Owens and Gohn, 1989; de Cserna, 1989; Sohl et al., 1991; McFarlan, Jr., and Menes, 1991; Galloway et al., 1991; Landman et al., 2004; Umhoefer and Blakey, 2006; Galloway, 2008; Blakey, 2013; Schroder-Adams, 2014).

These WIS paleogeographic reconstructions through time and controls on relative sea level in the WIFB are based on detailed documentation of both global and regional tectonic reconstructions, biogeography, lithostratigraphy, biostratigraphy, and chronostratigraphy. The most common method employed to reconstruct WIS paleogeography has been through detailed measuring and interpretation of lithostratigraphic sections across the region as well as the collection of biostratigraphic data derived from various organisms, especially ammonites and inoceramids (e.g., Gill and Cobban, 1973; Stelck et al., 2007). These data are used to correlate and constrain different lithofacies, distinguish regional from more local changes that influenced the WIS/WIFB, and facilitate recognition of underlying controls (e.g., eustatic vs. tectonic) on

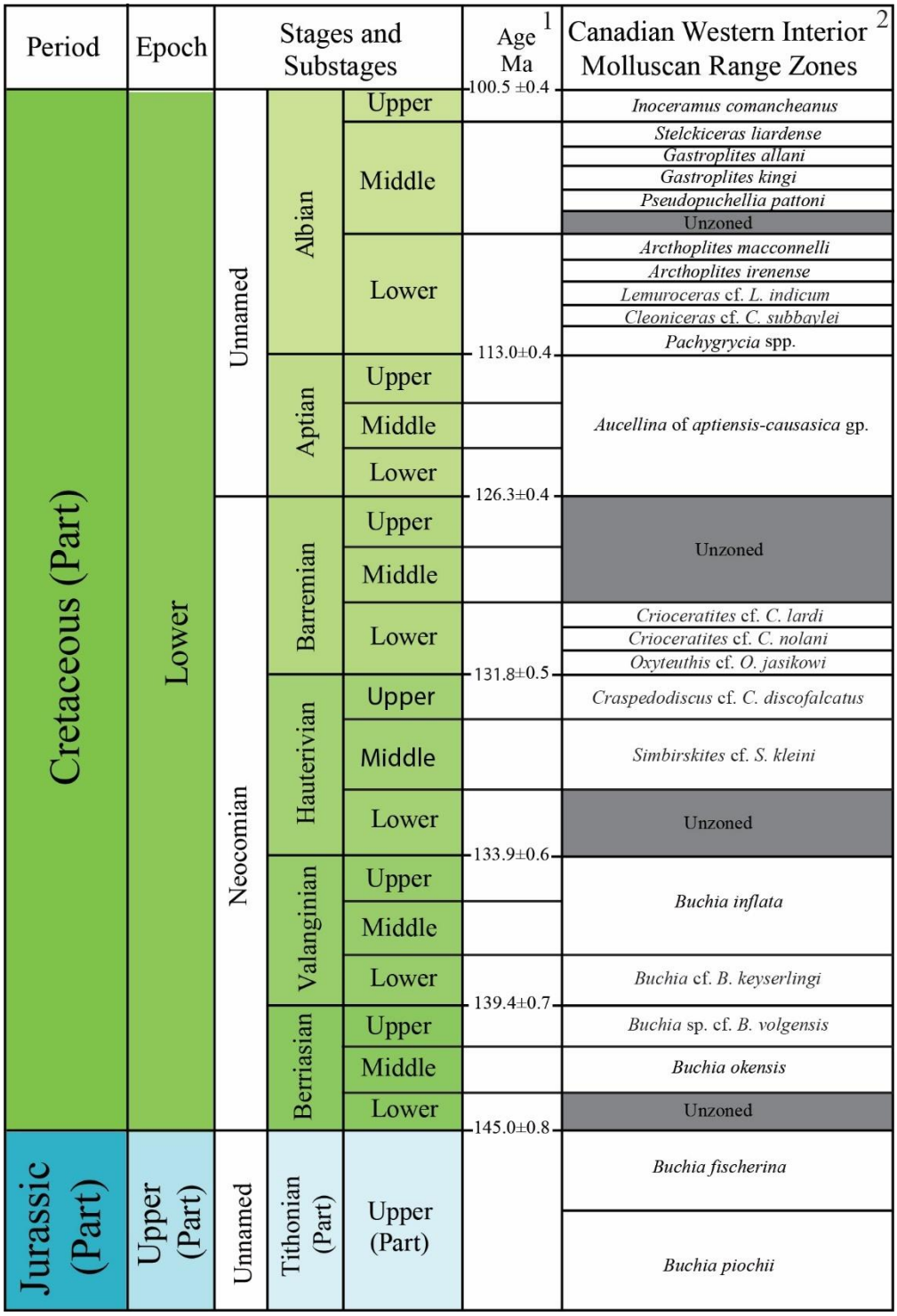

Figure 2.4. Upper Jurassic to Lower Cretaceous biostratigraphic chart for the Canadian Western Interior (1) Gradstein, 2012; 2) Stott et al., 1993).

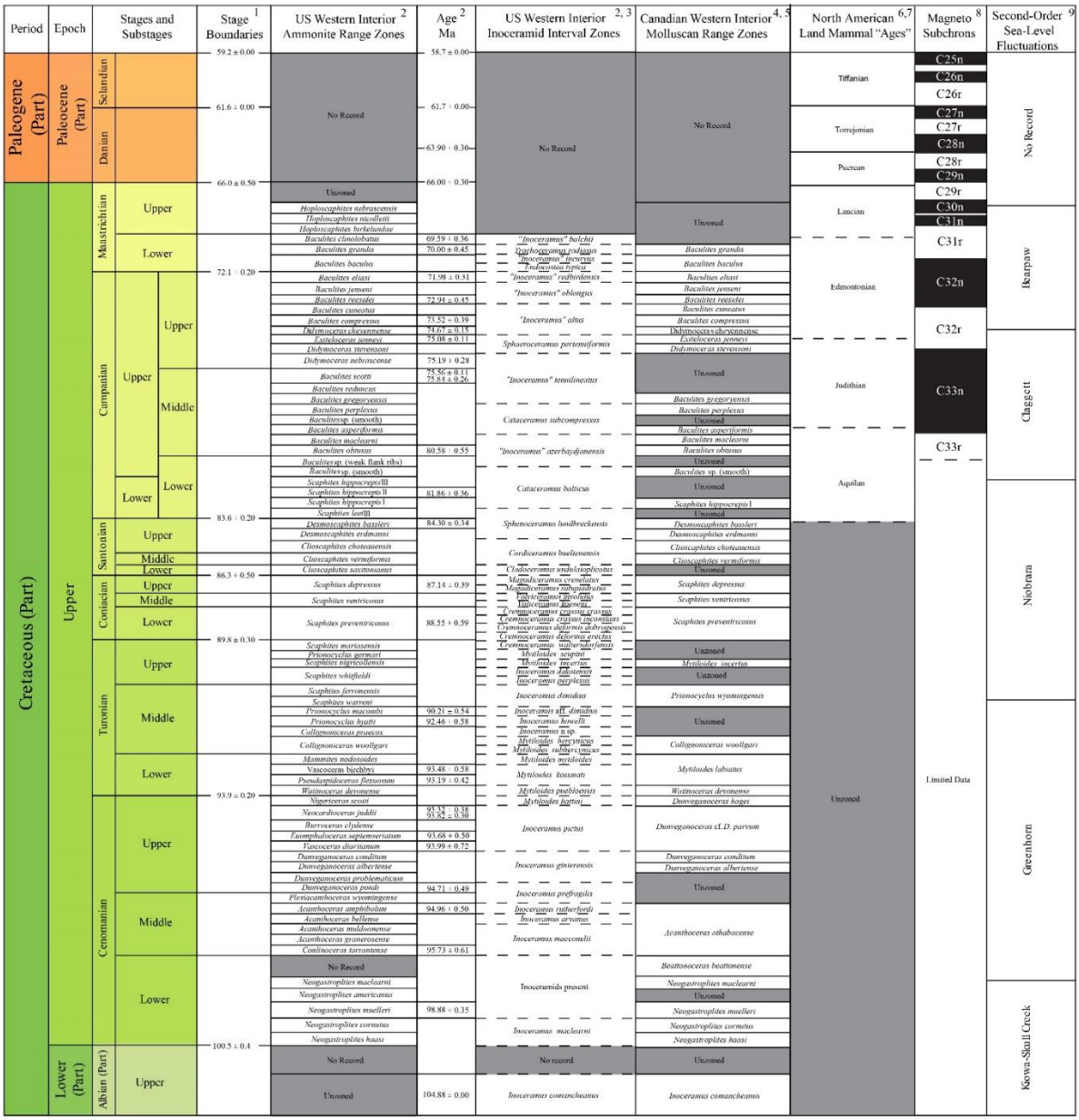

Figure 2.5. Summary chart of Lower Cretaceous to Paleocene chronostratigraphy, biostratigraphy, magnetostratigraphy, and second-order sea-level fluctuations in the US and Canadian Western Interior (1) Gradstein, 2012; 2) Cobban et al., 2006; 3) Scott, 2007 4) Stott et al., 1993 5) Braunberger and Hall, 2001; 6) Lillegraven and Ostresh, 1991; 7) Cifelli et al., 2004; 8) Hicks et al., 1999; 9) Kauffman, 1969).

the sea-level record preserved in the Western Interior. The Lower Cretaceous to Paleocene marine and terrestrial strata of this basin has one of the most continuous and highly resolved 2013; Schröder-Adams, 2014). biostratigraphic frameworks in the world, which is constrained by radiometric dates of ash beds, magneto-, and cyclostratigraphy (Fig. 2.4, 2.5; Fox and Ross, 1942; Fox and Olson, 1969; Lillegraven and Ostresh, 1991; Obradovich, 1993; Kauffman et al., 1993; Kowalis et al., 1995; Hicks et al., 1999; Cifelli et al., 2004; Anderson et al., 2006; Cobban et al., 2006; Scott, 2009; Scott et al., 2009; Wilson et al., 2010). The biostratigraphic frameworks for the northern and southern parts of the WIFB differ slightly due to a paucity of modern biostratigraphic work in the former and because the northern part has a more continuous Lower Cretaceous biostratigraphic record due to its longer interval of marine deposition (Fig. 2.5; Stott et al., 1993).

Another important method used to reconstruct the paleogeography of the WIS is to map the thicknesses of Cretaceous to Paleogene rocks in the Western Interior and use the resulting isopach maps to interpret the changing geometry of the WIFB through time (e.g., Cross, 1986; Roberts and Kirschbaum, 1995; DeCelles, 2004). Isopach maps have been also used to document the migration of different depozones through time and to depict the WIFB breakup into smaller fault-bounded basins during the Laramide Orogeny (e.g., Cross, 1986; Roberts and Kirschbaum, 1995; DeCelles, 2004).

The biogeographic ranges of fossil occurrences within as well as outside of the Western Interior have revealed critical information on how and when the WIS was connected with open-shelf seas (e.g., Arctic Ocean, proto-Gulf of Mexico) along the margins of the North American continent (e.g., Birkelund, 1965; Sohl, 1967; Jeletzky, 1971; Williams and Stelck, 1971; Cobban, 1993; Cvancara and Hoganson, 1993; Boyd and Lillegraven, 2011). This is important for certain

intervals and parts of North America where there is a poor stratigraphic record due to extensive erosion and/or a lack of exposure (i.e., Canadian Shield and eastern North American Craton; Ziegler and Rowley, 1998; White et al., 2000). This type of data can reveal biogeographic connections, which, in the absence of direct stratigraphic data, would remain obscure (e.g., Birkelund, 1965; Sohl, 1967; Jeletzky, 1971; Boyd and Lillegraven, 2011).

Controls on Sea Level in the Western Interior Seaway

As noted above, the paleogeography of the WIS was primarily controlled by the interaction of sea level with physiography (Williams and Stelck, 1971; Gill and Cobban, 1973; Jeletzky, 1980; Lillegraven and Ostresh, 1991; Krystinik and DeJarnett, 1995; Caldwell and Kauffman, 1993; Miall et al., 2008). Sea level in the WIFB was modulated by eustasy, long considered an important driver of sea-level change and, in turn, a control on the paleogeography of the WIS (Kauffman, 1977, 1984; Weimer, 1984; Hallam, 1992), and tectonic controls that altered the basin's physiography through uplift, subsidence, and sedimentation; the interplay of which resulted in localized transgressions and regressions. These different mechanisms interacted both individually and simultaneously, at times in concert and at other times in opposition, on different spatial and temporal scales as primary controls on the seaway's spatial extent, its paleoshorelines, and on its lithofacies (Gill and Cobban, 1973; Jeletzky, 1980; Lillegraven and Ostresh, 1991; Caldwell and Kauffman, 1993; Krystinik and DeJarnett, 1995; DeCelles, 2004; Miall et al., 2008). Several different authors have named and described the various second-order sea-level cycles or transgressive-regressive phases of the WIS that are represented by the history of its shoreline positions and on the stratigraphic record of the WIFB (Fig. 2.5; e.g., Greenhorn Cycle of Kauffman, 1967; Fox Hills Regression of Gill and Cobban,

1973). Each sea-level cycle is characterized by differing degrees of influence from both eustatic and tectonic controls.

In terms of the overall sea-level history, the WIS is characterized by a rise in eustatic sea level during the early Albian to Paleocene accompanied by increased basin subsidence (Fig. 2.6; Kauffman and Caldwell, 1993). The most-accepted explanations for this elevated eustatic record during the Early Cretaceous to Paleocene are: 1) a higher rate of sea-floor spreading that increased the volume of mid-ocean ridges (Pitman, 1978; Pitman and Golovchenko, 1983; Arthur et al., 1985, 1991; Lillegraven and Ostresh, 1991), and 2) the "greenhouse" phenomenon, resulting from higher CO_2 concentrations degassed from elevated volcanic activity and, therefore, the lack of significant ice sheets (e.g., Arthur et al., 1985, 1991; Miller et al., 2003; Hay, 2008). In this hypothesis, these mechanisms could have elevated eustatic sea level to a maximum of approximately 300 m higher than present day and resulted in the expansion of marine environments into continental interiors (Kauffman and Caldwell, 1993).

In contrast, the Miller et al. (2005) analysis of Phanerozoic sea level argued for variation in CO_2 concentration as the primary driver of sea-level change during the Cretaceous and contended that eustatic sea level during the Cretaceous peaked at 100 ± 50 m, which would indicate much slower rates of ocean-crust production than previously estimated. They went on to suggests that short-term variations in sea level were potentially controlled by changes in the volume of Antarctic ice sheets, which in turn would have modulated temperature changes that were associated with tectonically sourced CO_2 input. Several studies have argued that short-term variations in sea level that would have modulated shoreline movement of the WIS during the Cretaceous were controlled by Milankovitch cycles (e.g., Elder et al., 1994; Sageman et al., 1997). Despite recognition of the importance of tectonic controls on sea level in the WIFB, most

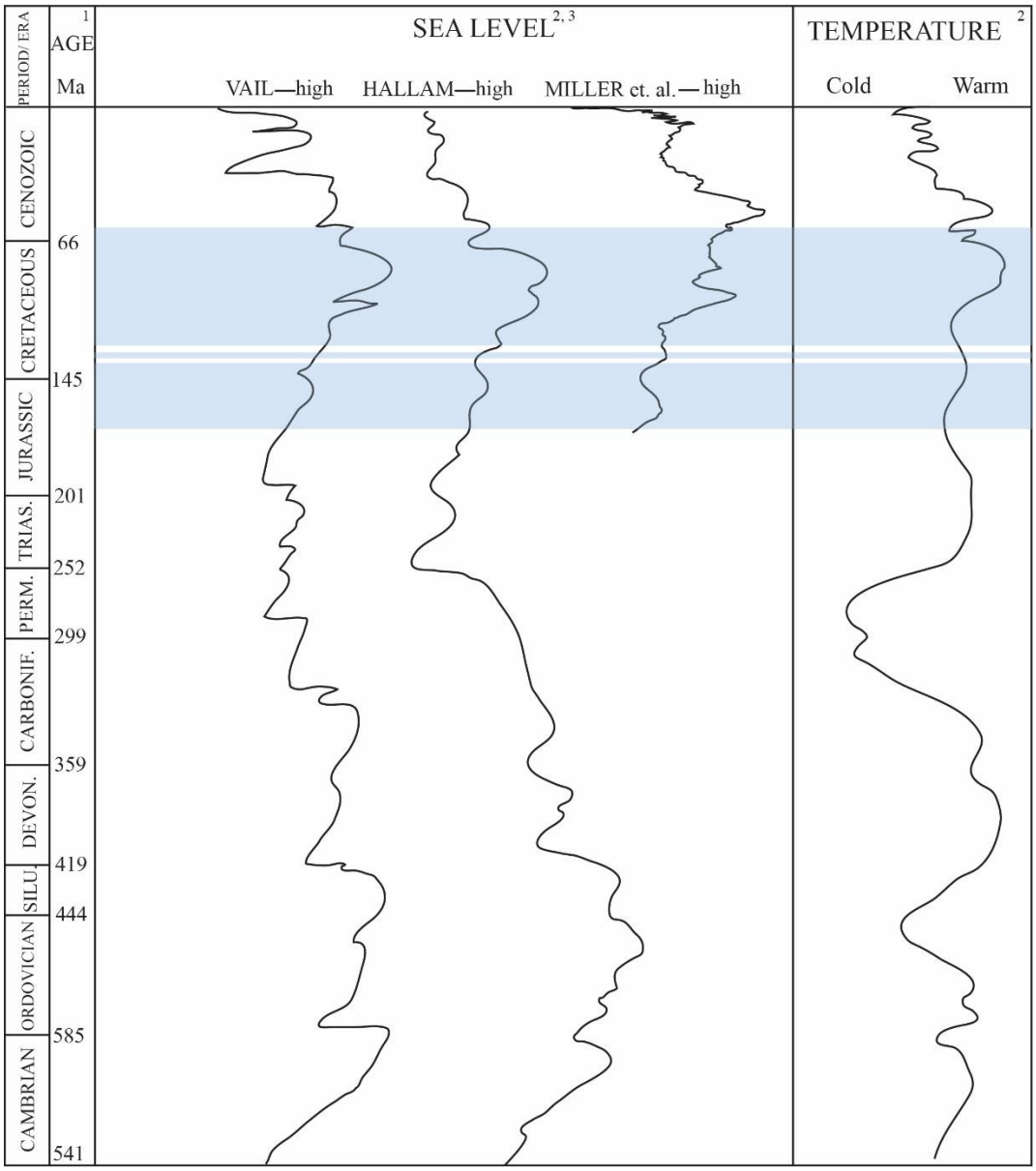

Figure 2.6. Phanerozoic global sea level curves and temperature curve (1) Gradstein, 2012; 2) Frakes et al., 1992; 3) Miller et al., 2005). The shaded area represents the interval characterized by marine flooding in the Western Interior Foreland Basin.

studies have viewed eustasy as the primary driver of cyclic sea-level change and shoreline movement in the WIS (e.g., Weimer, 1984; Kauffman, 1977, 1984). Beginning in the 1970's, this view was criticized, and the importance of tectonics along with eustasy in controlling sea level and shoreline movement became increasingly more recognized (e.g., Gill and Cobban, 1973; Jeletzky, 1979).

Western Interior Seaway Paleogeographic Evolution

Jurassic

During the Early Jurassic, the future location of the WIFB was characterized by predominantly terrestrial passive margin sedimentation (Miall, 2009). Sediments representing this time span were derived from the Appalachian and Ouachita orogenic belts to the east and southeast, respectively (Blakely, 2006). Throughout this interval, western North America was virtually tectonically neutral with transtension governing the plate margin and future retroarc (DeCelles, 2004).

By the Middle Jurassic, a westerly derived sediment source had initiated as a result of the amalgamation of the continental-margin arc-trench tectonic system and the onset of Cordilleran orogenic activity along the western margin of North America (Fuentes et al., 2009; 2011). As this orogenic uplift proceeded and continued to deform the North American craton to the east, it led to the formation the WIFB during the Bajocian (DeCelles and Currie, 1996; DeCelles, 2004; Fuentes et al., 2009; 2011). The basin reflects increased subsidence as a result of the initiation of subduction of the Panthalassan crust beneath western North America (i.e., subduction-induced subsidence) and formation of the Cordilleran Fold-Thrust Belt (i.e., load-induced subsidence; Fuentes et al., 2009, 2011).

Westerly derived sediment sources became dominant during the Middle Jurassic and persisted as such until the latest Eocene (Fuentes et al., 2009, 2011). The Middle Jurassic (i.e., Bajocian) is characterized by the transgression of the shallow, epeiric Sundance Sea into the WIFB (Imlay, 1980; 1984). This sea was an extension of Panthalassa and covered most of modern-day Utah, Idaho, Wyoming, Montana, Alberta, and southern Saskatchewan (Imlay, 1980). During its history the Sundance Sea underwent several different transgressive and regressive phases, which formed numerous, but significant unconformities throughout Middle to Upper Jurassic strata in the Western Interior (McMullens et al., 2014).

During the Late Jurassic (i.e., Kimmeridgian), the shoreline of the Sundance Sea was prograding northward into present-day Alberta in association with a drop in eustatic sea level (Fig. 2.6; Imlay, 1980; 1984). In northern Montana and southern Alberta, this regression is characterized, by marine shales and sandstones of the Upper Jurassic Fernie Formation being overlain by the deltaic and terrestrial coal-rich lithofacies of the Kootenay Formation (Stockmal et al., 1992; Miall et al., 2008). The deltaic deposits of the Kootenay Formation represent the final marine incursion by the Sundance Sea from the Pacific Ocean into the United States portion of the Western Interior during the Jurassic (Imlay, 1980, 1984). In southern Montana, Wyoming, Colorado, Utah, New Mexico, and South Dakota, the post- Sundance stratigraphic record is characterized by riverine and lacustrine deposits of the Morrison Formation (DeCelles and Currie, 1996; Demko et al., 2004; Foster, 2007). As the foredeep depozone was located in central Utah and Idaho during this interval, most of the Morrison Formation was deposited in the WIFB's back-bulge depozone(s) (DeCelles and Currie, 1996; Currie, 1998). Sediments deposited into the wedge-top, foredeep, and backbulge depozone(s) were likely eroded during subsequent Cretaceous thrust-fault uplifts (DeCelles and Currie, 1996; DeCelles, 2004).

Berriasian to Aptian

Terrestrial environments persisted across most of the WIFB (except for the most northern part) throughout the latest Jurassic into the Early Cretaceous (i.e., Kimmeridgian to early Albian; DeCelles, 2004). In British Columbia and northwestern Alberta, Berriasian and Valanginian marine strata deposited in the Peace River Embayment represent the final Mesozoic marine incursion into the Canadian portion of the WIFB from the Pacific (Fig. 2.7; Williams and Stelck, 1975). Post-Valanginian marine inundations into the Western Interior from the Pacific Ocean were most likely prevented by the hypsographic rise of the Cordilleran Orogenic Belt in the western part of Canada (Williams and Stelck, 1975). This rise also shifted the principal drainage of the Western Interior from the Pacific to the Arctic Ocean or Western Interior Sea (i.e., the extension of the Arctic Ocean into the northern part of WIFB that was isolated from the Gulf of Mexico by various topographical highs) until the end of the Early Cretaceous when the WIS formed (Williams and Stelck, 1975).

In the United States, it has been traditionally thought that a widespread unconformity separates the top of the Tithonian or Berriasian–Valanginian (Upper Jurassic to Lower Cretaceous) Morrison Formation from the overlying Aptian–Albian (upper Lower Cretaceous) strata (DeCelles and Burden, 1992; Dyman et al., 1994; Foster, 2007, Zaleha and Wiesemann, 2004; Zaleha, 2006; Elliot et al., 2007). This long-term depositional hiatus primarily reflects inadequate chronostratigraphic sampling from Lower Cretaceous strata and use of outdated biostratigraphic data (Zaleha, 2006; Sames et al., 2010). Recent studies utilizing new biostratigraphic data have revealed that this unconformity represents a much shorter time span than previously thought, varies in duration across the basin, and is represented by multiple

Figure 2.7. Generalized middle Valanginian (*Buchia inflata* time) paleogeographic map of North America showing marine inundation from Pacific Ocean into the Western Interior Foreland Basin (Western Interior shorelines based on Jeletzky, 1971; Williams and Stelck, 1975; shoreline.

unconformities bounding several Lower Cretaceous sequences (Zaleha, 2006; Sames et al., 2010). Zaleha's (2006) use of new chronostratigraphic data identified three Lower Cretaceous

unconformities in the United States that formed prior to the initiation of widespread marine deposition during the Albian. Both Zaleha (2006) and Sames et al. (2010) have shown that strata formerly attributed to Aptian and Albian actually represents Berriasian to Albian deposition within the WIFB.

Fluvial, flood plain, and lacustrine deposition persisted in the southern half of the WIFB up to the start of the early Albian marine transgression that would form the WIS (DeCelles and Currie, 1996; Zaleha, 2006; DeCelles, 2004). Most of the paleochannels found within these strata were deposited as point bars in meandering rivers that show east to north paleoflow direction within the WIFB (Zaleha, 2013). It is even possible that some rivers along the eastern margin of the basin were flowing westward from the vicinity of the Transcontinental Arch (Zaleha, 2013).

Albian to early Cenomanian

Examination of the strata overlying these Berriasian to Aptian beds indicates that load-induced flexural subsidence associated with increased thrusting was active during the Albian (DeCelles, 2004; Miall et al., 2008). This subsidence coincided with the first large-scale marine incursions by the Western Interior Sea or Clearwater Sea, as it is also known, into the WIFB from the Arctic Ocean (Fig. 2.8; Jeletzky, 1971; Williams and Stelck, 1975; Kauffman and Caldwell, 1993; Brenner et al., 2000). This marine transgression is characterized by several punctuated, southward-directed, early to middle Albian flooding events that were primarily restricted to Canada (Williams and Stelck, 1971; Stelck et al., 2007). The limited spatial extent of these transgressions to the Canadian Western Interior and punctuated nature of these transgressions was primarily due to low eustasy and pre-existing, topographically elevated structural features such as the Dave Lord-Eskimo Lakes, Tathlina-Liard River, Peace River, and Sweetgrass arches (Fig. 2.3; Kauffman and Caldwell, 1993; Stelck et al., 2007). As sea level

rose, the advance of the Clearwater Sea was temporally impeded by each of these elevated highs, which would eventually be transgressed with continued sea-level rise (Stelck et al., 2007). Further south, the WIFB was the site of numerous north-flowing fluvial systems that drained into the Clearwater Sea (Stelck et al., 2007; Miall et al. 2008).

During the latest Albian, eustatic-sea-level rise culminated in the first marine connection between the Gulf of Mexico and the Clearwater Sea somewhere in the vicinity of Colorado (i.e., Kiowa-Skull Creek Transgression; Figs. 2.9; Reeside, 1957; Sloss, 1963; Williams and Stelck, 1975; Kauffman and Caldwell, 1993; Brenner et al., 2000; Oboh-Ikuenobe et al., 2009). This transgression formed the Skull Creek Seaway, which divided North America into the isolated landmasses of Appalachia and Laramidia (Fig. 2.9; Archibald, 1996). It was the first transgression to extend past the intracratonic Transcontinental Arch (Fig. 2.3, 2.9; Williams and Stelck, 1975; Kauffman and Caldwell, 1993; Carlson, 1999; Miall et al., 2008; Oboh-Ikuenobe et al., 2009). This unification of northern and southern water masses is indicated by marine sediment deposition on the Transcontinental Arch and by the occurrence of mollusks with strong affinities to the Gulf of Mexico in Canada (Jeletzky, 1971; Williams and Stelck, 1975). Faunal evidence supports a connection with the Arctic Ocean during this interval (Williams and Stelck, 1975). The location of the eastern and western shorelines of the Skull Creek Seaway are well delineated in the southern portion of the Western Interior based on nearshore strata from this interval preserved on both sides of the basin (Fig. 2.9; Witzke et al., 1983; Cobban et al., 1994). Stratigraphic and faunal evidence from Quebec, Ontario, and Labrador suggests that this transgression also resulted in the first marine connection between the Skull Creek Seaway (or WIS) and the Atlantic Ocean via the Hudson Seaway (Fig. 2.9; White et al., 2000).

Figure 2.8. Generalized early Albian (*Lemuroceras* cf. *L. indicum* time) paleogeographic map of North America showing initial marine transgression into the Western Interior Foreland Basin from Arctic Ocean (Clearwater Sea shorelines modified from Stelck et al., 2007; shorelines outside Western interior modified from Alencaster, 1984; Owens and Gohn, 1985; McFarlan and Menes, 1991; Goldhammer, 1999; Blakey, 2013). Shaded areas represent land.

Figure 2.9. Generalized late Albian (*Inoceramus comancheanus* time) paleogeographic map of North America showing first full-marine connection between the Arctic Ocean and Gulf of Mexico in Western Interior Foreland Basin (Skull Creek Seaway shorelines based on unpublished maps of W.A. Cobban; Jeletzky, 1971; shorelines outside Western interior modified from Alencaster, 1984; Owens and Gohn, 1985; McFarlan and Menes, 1991; Goldhammer, 1999; White et al., 2000; Blakey, 2013). Shaded areas represent land.

Figure 2.10. Generalized early Cenomanian, (*Neogastroplites cornutus* time) paleogeographic map of North America showing loss of marine connection between the Arctic Ocean and Gulf of Mexico in the Western Interior Foreland Basin (Mowry Sea shorelines based on unpublished maps of W.A. Cobban; Jeletzky, 1971, Williams and Stelck, 1975; shorelines outside Western interior modified from Alencaster, 1984; Owens and Gohn, 1985; McFarlan and Menes, 1991; Goldhammer, 1999; White et al., 2000; Blakey, 2013). Shaded area represents land.

Eustatic sea level briefly fell during the earliest Cenomanian, and the connection between the Gulf of Mexico and Arctic Ocean was disrupted (i.e., Kiowa-Skull Creek Regression; Figs. 2.10; Miall et al., 2008; Oboh-Ikuenobe et al., 2009; Scott et al., 2009). During this interval, the Mowry Sea (or Western Interior Sea) extended from the Arctic Ocean southward to the Transcontinental Arch (Fig. 2.10; Williams and Stelck, 1975; Cobban et al., 1994; Scott et al., 2009). This structural feature separated the Arctic-Ocean-influenced Mowry Sea from a northern extension of the Gulf of Mexico to the south, which extended northward up to southern Colorado, and Kansas (Williams and Stelck, 1975; Weimer, 1978; Miall et al., 2008; Scott et al., 2009). A connection with the Arctic Ocean is indicated by an endemic fauna with strong affinities to Arctic faunas (Reeside and Cobban, 1960; Williams and Stelck, 1975; Yacobucci, 2004). However, the endemic nature of the fauna suggests that the opening between the Arctic Ocean and Mowry Sea was likely periodically restricted or even closed (Williams and Stelck, 1975; Schröder-Adams, 2014). This biogeographic restriction between the Arctic Ocean and Mowry Sea may have been caused by exceptionally low sea levels or the emplacement of the Mackenzie Salient along the border between the Yukon and Northwest Territories, which resulted in an eastward shift in the western shoreline in this region (Jeletzky, 1971; Williams and Stelck, 1975). The location of the Mowry Sea's western shoreline was situated in western Alberta, western Montana and along the Wyoming-Idaho border, whereas the locations further to the south and along the eastern margin are speculative (Fig. 2.10). The poor stratigraphic record on the Canadian Shield makes it difficult to determine if a marine connection between the Mowry Sea and the Atlantic Ocean was maintained through the Hudson Seaway during this drop in eustatic sea level. The onset of a new transgressive phase and reunification with the Gulf of Mexico is first evident by the appearance of ammonites and foraminifers with affinities to faunas

from the Gulf of Mexico in the *Neogastroplites maclearni* ammonite biozone of Alberta, Montana, and Wyoming (Williams and Stelck, 1975; Yacobucci, 2004).

Middle Cenomanian to Turonian

A eustatic rise resulted in the 'Great Transgression' (or more regionally known as the Greenhorn Transgression) during the middle Cenomanian through the early Turonian, which re-established the interconnection between the Gulf of Mexico and the Arctic Ocean (Fig. 2.11; Hancock and Kauffman, 1979; Kauffman and Caldwell, 1993; Cobban, 1993; Oboh-Ikuenobe et al., 2009; Schröder-Adams, 2014). This continuity persisted at least until the early Maastrichtian and possibly into the Paleocene (Williams and Stelck, 1975; Lillegraven and Ostresh, 1991; Kauffman and Caldwell, 1993; Boyd and Lillegraven, 2011). This connection is represented by a continuous lithostratigraphic record across the basin (including the Transcontinental Arch) and the first occurrence of diverse taxa in the WIS with strong affinities to Gulf of Mexico faunas (Cobban, 1993; Kauffman and Caldwell, 1993). The occurrence of ammonites in Canada with affinities to Alaskan faunas indicates the persistence of a connection with the Arctic Ocean (Jeletzky, 1971). There is strong paleontologic and geologic evidence on the Canadian Shield for the existence of the Hudson Seaway during this time (Williams and Stelck, 1971; Ziegler and Rowley, 1998; White et al., 2000; Schröder-Adams, 2014).

Throughout this interval, the seaway underwent a number of small transgressions and regressions (Jeletzky, 1971; Williams and Stelck, 1975; Cobban and Hook, 1984; Roberts and Kirschbaum, 1995), likely Milankovitch controlled, that strongly influenced the basin's stratigraphic architecture and shoreline positions (Barron et al., 1983; Meyers et al., 2001). The location of the western shoreline during the Cenomanian varied over 600 km in the southwestern part of the United States (i.e., south central Utah to south central New Mexico) and in northern

Figure 2.11. Generalized late Cenomanian (*Neocardioceras juddii* time) paleogeographic map of North America (WIS shorelines based on unpublished maps of W.A. Cobban; Jeletzky, 1971; Roberts and Kirschbaum, 1997; shorelines outside Western Interior modified from Alencaster, 1984; Owens and Gohn, 1985; de Cserna, 1989; McFarlan and Menes, 1991; Goldhammer, 1999; Blakey, 2013). Shaded areas represent land.

Figure 2.12. Generalized late Turonian (*Prionocyclus germari* time) paleogeographic map of North America (WIS shorelines based on unpublished maps of W.A. Cobban; Jeletzky, 1971; Witzke et al., 1990; Roberts and Kirschbaum, 1997; Nielsen et al., 2008; shorelines outside Western interior modified from Alencaster, 1984; Owens and Gohn, 1985; de Cserna, 1989; Sohl et al., 1991; McFarlan and Menes, 1991; Goldhammer, 1999; Blakey, 2013). Shaded areas represent land.

Alberta to less than 100 km in western Wyoming, western Montana, and southwestern Alberta (Roberts and Kirschbaum, 1995). In northern Alberta, the Dunvegan Delta prograded eastward across the basin as a result of increased sediment supply associated with uplift caused by the accretion of the Insular Superterrane (Stockmal et al., 1992; Plint, 2000). During the same interval, the Woodbine Delta prograded westward (in the vicinity of Oklahoma) into the WIFB and southward (in the vicinity of northeast Texas) into the Gulf of Mexico (Roberts and Kirschbaum, 1995). Further north, the positions of the eastern shoreline are poorly constrained, but it most likely varied from western Minnesota and Iowa during peak transgressions to the eastern Dakotas, eastern Nebraska, and eastern Kansas during regressions. This mid-Cretaceous expansion of the WIS was one of the most extensive transgressions in North American history and was characterized by deposition of widespread offshore siliciclastic and carbonate muds across most of the basin and thick successions of nearshore clastic sediments along the coastlines (Reeside, 1957; Jeletzky, 1971; Williams and Stelck, 1975; Kauffman and Caldwell, 1993). During the early Turonian Greenhorn Cycle, the WIS reached its greatest geographic extent (Fig. 2.11; McDonough and Cross, 1991; Kauffman and Caldwell, 1993; Sageman and Arthur, 1994). For the duration of this interval, the sea extended from central Utah to possibly Wisconsin and from Texas to the Arctic Ocean (Fig. 2.11). There is evidence that the sea expanded over the Mackenzie Salient that previously restricted connection between the sea and Arctic Ocean (Jeletzky, 1971). Faunal similarities between the WIS and Pacific coastal fauna led Lang and McGugan (1987) to tentatively suggest that a marine connection formed along the Alberta-Montana border between the Pacific Ocean and WIS during the Turonian peak transgression. Despite some faunal similarities, relatively little additional research has been devoted to testing

this hypothesis and, in light of current geological (e.g., tectonic, stratigraphic) evidence, it seems unlikely.

The Turonian is the youngest interval with direct stratigraphic and paleontological evidence preserved on the Canadian Shield for the existence of the Hudson Seaway (Fig. 2.11; Williams and Stelck, 1975; Ziegler and Rowley, 1998). The areal extent of this sea over the Canadian Shield during this interval is still poorly constrained due to post-Mesozoic erosion. However, it could have been much more extensive than the area depicted on typical paleogeographic maps (e.g., Jeletzky, 1971; William and Stelck, 1975; Ziegler and Rowley, 1998; White et al., 2000). Limestone-marl couplets were deposited across northern Texas to northern North Dakota and from western Colorado to eastern Kansas (Elder et al., 1994; Sageman and Arthur, 1994; Roberts and Kirschbaum, 1995; Sageman et al., 1998; Meyers et al., 2001; Keller et al., 2004). These carbonate deposits can be correlated across the basin to clastic sequences along its margins (Elder et al., 1994).

Carbonate deposition ended during the middle Turonian in association with a drop in sea level that was controlled by tectonics and eustatic changes (Greenhorn Regression; Reeside, 1957; Williams and Stelck, 1975; Roberts and Kirschbaum, 1995; Merewether et al., 2007; Nielsen et al., 2008; Miall et al., 2008). The surface area of the WIS shrunk drastically during this interval, and it is possible that the connection between the WIS and the Atlantic Ocean was lost or restricted (Fig. 2.12; Nielsen et al., 2008). During the middle to late Turonian, the location of the western shoreline varied over 300 km in areas south of the Montana-Wyoming border to less than 150 km north of this border (Roberts and Kirschbaum, 1995). This regression is associated with the deposition of major sand complexes across the basin during the late

Figure 2.13. Generalized middle Coniacian (*Scaphites ventricosus* time) paleogeographic map of North America (WIS shorelines based on unpublished maps of W.A. Cobban; Jeletzky, 1971; Witzke et al., 1990; Roberts and Kirschbaum, 1997; Nielsen et al., 2008; shorelines outside Western interior modified from Alencaster, 1984; Owens and Gohn, 1985; de Cserna, 1989; Sohl et al., 1991; McFarlan and Menes, 1991; Goldhammer, 1999; Blakey, 2013). Shaded areas represent land.

Turonian, such as the upper Frontier Formation in Wyoming and the Cardium Formation in Alberta (Williams and Stelck, 1975; Roberts and Kirschbaum, 1995).

Coniacian to Santonian

Relative sea level rose rapidly during Coniacian and Santonian time (i.e., Niobrara Transgression), resulting in a resurgence of carbonate deposition in the center of the basin, widespread deposition of muds across much of Alberta, Montana, Wyoming, Colorado, and Utah, as well as the development of clastic wedges along the basin margin in central Utah, eastern Idaho, Montana, Alberta, and northeastern British Columbia (Fig. 2.13; Roberts and Kirschbaum, 1995; Merewether et al., 2007; Nielsen et al., 2008). The location of the western shoreline during the Coniacian and Santonian remained fairly static, but probably varied within a 150 km range along most of its length (Roberts and Kirschbaum, 1995). The location of the eastern shoreline during this interval is poorly known but was probably located in central Iowa and Minnesota (Witzke et al., 1983). Isopach maps of this interval also show a significant change in the basin's geometry reflecting the demise of the well-organized flexural-foreland-basin system (Cross, 1986; DeCelles, 2004).

The Coniacian and Santonian represent the greatest marine inundation of the Canadian Western Interior and Arctic Archipelago during the Cretaceous (Fig. 2.13; Jeletzky, 1971). This fact lends support for a possible connection between the WIS and the Atlantic Ocean via the Hudson Seaway during this interval (Fig. 2.13; Williams and Stelck, 1975). The presence of Western Interior ammonite species in western Greenland during the Late Turonian to Santonian supports this hypothesis (Birkelund, 1965; Williams and Stelck, 1975). However, it is possible, as suggested by Birkelund (1965), that these faunas were using an Arctic route since a connection (i.e., the Teichert Strait of Ziegler and Rowley, 1998) was likely made between the

Sverdrup Basin and Baffin Bay during this interval (Jeletzky, 1971; Williams and Stelck, 1975) forming the Labrador Seaway (Fig. 2.13).

Campanian to early Maastrichtian

Tectonic activity, closely associated with the accretion of the Insular Superterrane and uplift of the Purcell Anticlinoform (Stockmal et al., 1992), increased along the Cordilleran Fold-Thrust Belt during the Campanian. Furthermore, Lawton (1994) suggested that this activity was amplified in the United States portion due to an increase in the rate of orthogonal convergence between the Farallon and North American plates. Isopach maps of Campanian–Maastrichtian strata indicate a broad area of thick strata in central Wyoming and Colorado, eastward of the foredeep, indicating a strong influence of subduction-induced subsidence (Cross, 1986). This change in tectonic activity coincided with a permanent shift from carbonate to siliciclastic mud deposition in the basin center (Niobrara Regression; Miall et al., 2008). This interval is stratigraphically represented in the central part of the Western Interior by the transition from the Niobrara Formation to the Pierre Shale (Gill and Cobban, 1973; Roberts and Kirschbaum, 1995). The locations of the western and eastern shorelines in the United States during this time were probably similar to the Coniacian and Santonian (Fig. 2.14; Witzke et al., 1983). However, in Canada the western shoreline began to migrate back and forth within distances spanning 250–650 km (Roberts and Kirschbaum, 1995). The shared occurrence of ammonites in Greenland and the WIS supports a northern connection into the middle Campanian (Fig. 2.14; Birkelund, 1965). However, whether this biogeographic route was through the Arctic Ocean or Hudson Seaway is unclear in the absence of direct evidence (Birkelund, 1965). Schröder-Adams (2014) argued that

Figure 2.14. Generalized middle Campanian (*Baculites obtusus* time) paleogeographic map of North America (WIS shorelines based on unpublished maps of W.A. Cobban; Jeletzky, 1971; Roberts and Kirschbaum, 1997; shorelines outside Western interior modified from Alencaster, 1984; Owens and Gohn, 1985; de Cserna, 1989; Sohl et al., 1991; McFarlan and Menes, 1991; Goldhammer, 1999; Umhoefer and Blakey, 2006; Blakey, 2013). Shaded areas represent land.

biogeographic similarities between the WIS and Labrador Seaway were most likely maintained by the Hudson Seaway.

Beginning in the middle Campanian, a major tectonic reorganization associated with the onset of the Laramide Orogeny resulted in a cratonward shift in marine sedimentation and the expansion of a broad coastal plain that persisted into the Maastrichtian (Clagget and Bearpaw marine cycles; Fig. 2.15; Gill and Cobban, 1973; Roberts and Kirchsbaum, 1995; Miall et al., 2008). The western shoreline shifted eastward to central Montana, central Wyoming, and western Colorado during the peak transgressions of the middle Campanian (Gill and Cobban, 1973; Lillegraven and Ostresh, 1990; Roberts and Kirschbaum, 1995). During regressions it was situated in eastern Montana, eastern Wyoming, central Colorado, and central to eastern New Mexico (Gill and Cobban, 1973; Lillegraven and Ostresh, 1990; Roberts and Kirschbaum, 1995). The location of the eastern shoreline for the Campanian, Maastrichtian, and Danian is completely unknown because of erosion and a lack of available exposures representing nearshore strata along the cratonic side of the basin (Witzke et al., 1983; Erickson, 1999). However, the location of the eastern shoreline for the latest Cretaceous and earliest Paleogene was probably similar to earlier intervals. Williams and Stelck (1975) suggested that the seaway might have been connected to the northern part of the Mississippi Embayment along its eastern side and that the Ouachita-Ozark Interior Highlands might have been multiple islands (or an island) during the Campanian and Maastrichtian. Despite being possible, this hypothesis remains untested and without further study will remain tentative. Lithostratigraphic evidence for a connection to the Arctic Ocean ends at this time due to a substantial regression; however, faunal data provide support for the retention of an Arctic connection throughout this interval (Cobban, 1993; Erickson, 1999). There is currently no paleontologic or stratigraphic evidence for a connection to

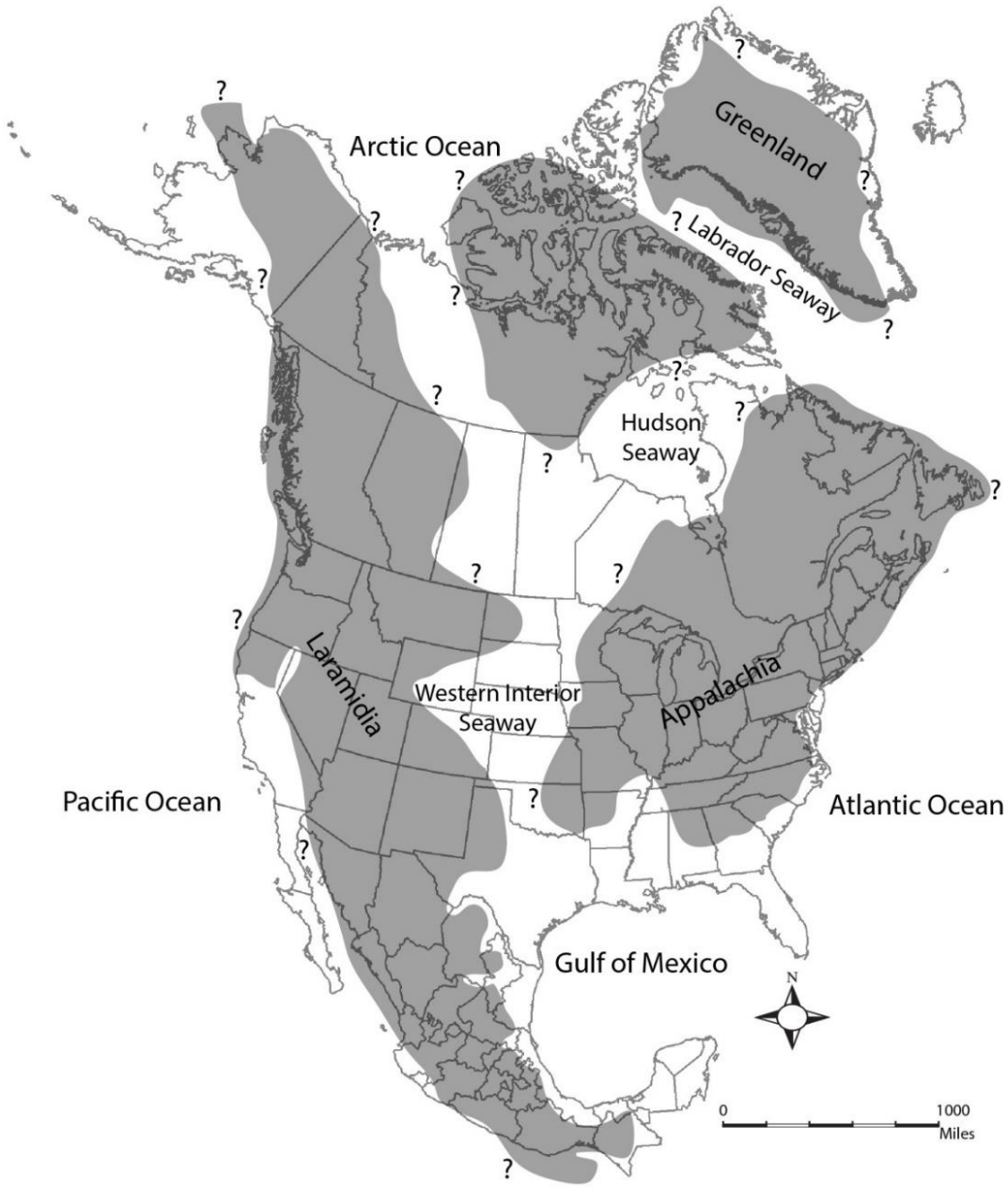

Figure 2.15. Generalized early Maastrichtian (*Baculites clinolobatus* time) paleogeographic map of North America (WIS shorelines based on unpublished maps of W.A. Cobban; Jeletzky, 1971; Roberts and Kirschbaum, 1997; shorelines outside Western interior modified from Alencaster, 1984; Owens and Gohn, 1985; de Cserna, 1989; Sohl et al., 1991; McFarlan and Menes, 1991; Goldhammer, 1999; Landman et al., 2004; Umhoefer and Blakey, 2006; Blakey, 2013). Shaded areas represent land.

Figure 2.16. Generalized Danian paleogeographic map of North America (Cannonball Sea shorelines based on Catuneanu and Sweet, 1999; Catuneanu et al., 2000; Boyd and Lillegraven, 2011; shorelines outside Western interior modified from Owens and Gohn, 1985; de Cserna, 1989; Galloway et al., 1991; Blakey, 2013). Shaded areas represent land.

the northern Atlantic Ocean through the Hudson Seaway in the late Campanian, but it is possible that faunas with affinities to the Arctic Ocean were entering into the WIS via the Hudson Seaway, as the connection that opened up during the Coniacian between the Sverdrup Basin and Baffin Bay was maintained into the Maastrichtian (Ziegler and Rowley, 1998).

Late Maastrichtian to Paleocene

Throughout the Maastrichtian, the western shoreline migrated basinward as eustatic sea level fell and the WIFB started to segregate into marine and non-marine sub-basins with the onset of the Laramide Orogeny (Bearpaw Regression; Waagé, 1968; Gill and Cobban, 1973; Dickinson et al., 1988; Kauffman and Caldwell, 1993; Lillegraven and Ostresh, 1991; Miall et al., 2008). The western shoreline retreated during the early to late Maastrichtian in northeastern Wyoming, Montana, and in the western Dakotas due to the Sheridan Delta's progradation across the basin (Fig. 2.15; Gill and Cobban, 1973; Krystinik and Dejarnett, 1996, Kennedy et al., 1998; Pyles and Slatt, 2007). The western shoreline's location is not clearly resolved for the late Maastrichtian; however, recent studies of the preserved stratigraphic and paleontological marine record have revealed that it extended from southwestern South Dakota to south central North Dakota (Landman et al., 2012). Based on the available evidence, the seaway was most likely located to the east of the current outcrop belt in the vicinity of the Great Plains (Williams and Stelck, 1975). Occurrences of marine taxa in upper Maastrichtian strata with affinities to both the Gulf Coast and Arctic regions also strongly support a through-going connection with both areas during the late Maastrichtian either through the McKenzie Basin or Hudson Seaway (Erickson, 1999; Ziegler and Rowley, 1998).

It has been traditionally postulated that a complete marine withdrawal and continental draining occurred prior to end of the Maastrichtian and that subsequent Paleocene marine

deposition was part of a separate transgression into the Western Interior (e.g., McGookey, 1972; Gill and Cobban, 1973; Williams and Stelck, 1975; Lillegraven and Ostresh, 1990). This interpretation, however, has been questioned by recent studies that suggest the WIS persisted through the latest Maastrichtian and into the earliest Paleocene (Erickson, 1999; Hoganson and Murphy, 2002; Hartman and Kirkland, 2002; Wroblewski, 2004, 2008; Boyd and Lillegraven, 2011). There is evidence for marginal marine condition during the late Maastrichtian occurring as far west as eastern Wyoming and along the Montana-North Dakota border (Schlaikjer, 1935; Boyd and Lillegraven, 2011). These data suggest that what remained of the WIS during the latest Maastrichtian and subsequent Paleocene was probably located in the Great Plains or along the cratonic side of the basin where subsequent Cenozoic erosion has removed any record of its existence or is covered by younger strata and vegetation (Boyd and Lillegraven, 2011). Additional evidence, for the presences of a continuous seaway dividing North America is provided by limited mixing of Laramidian and Appalachian floras and faunas up to the K/Pg Mass Extinction Boundary (Holtz Jr., pers. comm., 2014). If a permeant land connection had been made between Laramidia and Appalachia near the end of the Maastrichtian, then a mixing of terrestrial vertebrate faunas from the two regions should have occurred. Currently, there are only two documented reports of mixing of Appalachian and Laramidian floras and dinosaur faunas during the late Maastrichtian, which suggests that a connection was made, at least ephemerally, during this interval (Berry, 2017; Farke and Phillips, 2017).

Lithostratigraphic as well as biostratigraphic data on foraminifers and mollusks indicate that marine deposition in the WIS persisted into the Danian and Selandian ages of the early and middle Paleocene (66.0–59.2 Ma) as the Cannonball Seaway (Fig. 2.5; Fox et al., 1942; Fox and Ross, 1969; Cvancara, 1976; Garvie, 2013). This age designation is also supported by

mammalian index fossils found in terrestrial strata that directly under- and overly marine tongues in the Cannonball Formation in North Dakota (Anderson et al., 2006; Boyd and Lillegraven, 2011). This relationship indicates that marine incursions occurred during at least the Puercan, Torrejonian, and Tiffanian Land Mammal Ages of the lower to middle Paleocene (Fig. 2.5; Anderson et al., 2006; Boyd and Lillegraven, 2011). Although the paleogeographic extent of the seaway is poorly constrained during the Paleocene, faunal data from the WIFB have been cited to support expansions of both the Gulf of Mexico and the Arctic Ocean into the Great Plains region of the United States and southern Canada (Fig. 2.16; Cvancara, 1976; Boyd and Lillegraven, 2011). There is even strong faunal evidence to suggest full connections between the Gulf of Mexico, Arctic Ocean, and Atlantic, although this was possibly ephemeral (Fig. 2.16; Cvancara and Hoganson, 1993; Boyd and Lillegraven, 2011). The location of the western shoreline(s) of the Cannonball Seaway is poorly known during transgression (Boyd and Lillegraven, 2011). However, stratigraphic and fossil evidence suggests that the sea may have extended at least as an ephemeral water body as far west as Saskatchewan, eastern Montana, and southcentral Wyoming (Belt et al., 1997, 2000; 2004; Catuneanu and Sweet, 1999; Catuneanu et al., 2000; Kroeger and Hartman, 1997; Boyd and Lillegraven, 2011). There is some evidence to suggest that the seaway was split into an arm of the Arctic Ocean and an arm of the Gulf of Mexico by the Sheridan Delta in the location of the Dakotas (Hartman, pers. comm., 2013). As with the Campanian and Maastrichtian, the location of the eastern shoreline is completely unknown.

The final withdrawal of the Cannonball Seaway from the interior of North America most likely occurred no earlier than the middle Paleocene, however, the timing is poorly constrained due to a paucity of preserved strata from this age across most of the Great Plains. Mapping upper

Paleocene strata in the Gulf Coastal Plain indicates that the Late Paleocene shoreline closely mirrors the modern shoreline offset by ~150 km inland (Galloway et al., 1989; Ziegler and Rowley, 1998). This shoreline data shows no deviations extending up into the direction of the Western Interior for upper Paleocene strata, which does not hold for lower to middle Paleocene strata (Galloway et al., 1989; Ziegler and Rowley, 1998). This shoreline data lends strong support for the complete retreat of the sea from the interior during the latest Paleocene.

Conclusion

- The WIS is one of the largest post-Paleozoic epeiric seas and covered most of west-central North America for ~46 Mya.
- The seaway's location within this actively subsiding foreland basin and its proximity to a continually uplifting sediment source resulted in a thick, but complicated mosaic of interfingering marine and terrestrial deposits that record sea-level fluctuations within the seaway.
- This thick stratigraphic record on the tectonically actively subsiding portion of the WIFB has made it possible through the detailed analysis of lithofacies and fossils to paleogeographically reconstruct the successive changes in the position of the sea's western shoreline at a fine scale of temporal resolution.
- The evolution of the northern and eastern shorelines remains poorly resolved due to condensed sections, higher erosion rates, and limited exposures along the cratonic side of the basin.
- The seaway's well-documented paleogeography along with its detailed lithostratigraphic, biostratigraphic, and chronostratigraphic frameworks make it a perfect laboratory to examine a range of questions related to paleobiology, sequence stratigraphy, sea level

change, paleoceanography, and paleoclimatology within a highly refined temporal and spatial framework.

- Detailed paleogeographic reconstructions will aid in developing and testing new hypotheses concerning evolution, faunal dynamics, and biogeography during greenhouse climatic intervals.
- It should also be noted that future research utilizing paleogeographic reconstructions of the WIS must consider the inherent biases that are found in the preserved or available stratigraphic record of the WIFB.

References

Alencaster, G., 1982, Late Jurassic- Cretaceous molluscan paleogeography of the southern half of Mexico: *in* Westermann, G.E.G., eds., Jurassic-Cretaceous biochronology and paleogeography of North America: *Geological Association of Canada Special Paper*, 27, 77–98.

Anderson, L.C., Hartman, J.H., and Wesselingh, F., 2006, Close evolutionary affinities between freshwater corbulid bivalves from the Neogene of western Amazonia and Paleogene of the northern Great Plains, USA: *Journal of South American Earth Sciences*, 21, 28–48.

Arbenz, J.K., 1989, The Ouachita System: *in* Bally, A.W. eds., The Geology of North America–An overview: The Geological Society of America, *The Geology of North America*, A, 371–396.

Archibald, J.D., 1996, Dinosaur Extinction and the End of an Era: What the Fossils Say, New York, NY: *Columbia University Press*, 240 pp.

Armstrong, R.L., and Ward, P. L., 1993, Late Triassic to earliest Eocene magmatism in the North American Cordillera: implications for the Western Interior Basin: *in* Caldwell, W.G.E., and Kauffman, E.G., eds., Evolution of the Western Interior Basin: *Geological Association of Canada Special Paper*, 39, 49–72.

Arthur, M.A., and Dean, W.E., Schlanger, S.O., 1985, Variations in the Global Carbon Cycle during the Cretaceous related to Climate, Volcanism, and Changes in the Atmospheric CO_2: *in* Sundquist, E.T., and Broeker, W.S., eds., *The carbon cycle and atmospheric CO_2: Natural variation Archean to Present: American Geophysical Union Monograph*, 32, 504–529.

Arthur, M.A., Kump, L.R., Dean, W.E., and Larson, R. L., 1991, Superplume, Supergreenhouse?: *EOS, Transactions of the American Geophysical Union Abstract with Programs*, 72, 301.

Bally, A.W., Scotese, C.R., and Ross, M.I., 1989, North America; Plate tectonic setting and tectonic elements: *in* Bally, A.W., eds., *The Geology of North America–An overview: The Geological Society of America, The Geology of North America*, A, 1–15.

Barron, E. J., 1983, A warm, equable Cretaceous: *The nature of the problem: Earth Science Reviews*, 19, 305–338.

Beaumont, C., Quinlan, G.M., and Stockmal, G.S., 1993, The evolution of the Western Interior Basin; causes, consequences and unsolved problems: *in* Caldwell, W.G.E., and Kauffman, E.G., eds., *Evolution of the Western Interior Basin: Geological Association of Canada Special Paper*, 39, 97–119.

Belt, E.S., Diemer, J.A., and Beutner, E.C., 1997, Marine ichnogenera within Torrejonian facies (Paleocene) of the Fort Union Formation, southeastern Montana: Contributions to Geology, University of Wyoming, v. 32, p. 3–18.

Belt, E.S., Hartman, J.H., Diemer, J.A., Kroeger,T.J., Tibert, N.E., and Curran, H.A., 2004, Unconformities and age relationships, Tongue River and older members of the Fort Union Formation (Paleocene), western Williston Basin, U.S.A.: *Rocky Mountain Geology*, 39, 113–140.

Belt, E.S., Tibert, N.E., Curran, H.A., Diemer, J.A., Hartman, J.H., Kroeger, T.J., Harwood, D.M., 2005, Evidence for marine influence on a low-gradient coastal plain: Ichnology and invertebrate paleontology of the lower Tongue River Member (Fort Union Formation, middle Paleocene), western Williston Basin, U.S.A.: *Rocky Mountain Geology*, 40, 1–24.

Berry, K. 2017, New paleontological constraints on the paleogeography of the Western Interior Seaway near the end of the Cretaceous (late Campanian–Maastrichtian) with a special emphasis on the paleogeography of southern Colorado, U.S.A., *Rocky Mountain Geology*, 52, 1–16.

Birkelund, T., 1965, Ammonites from the Upper Cretaceous of West Greenland: *Gronlands Geologiske Undersogelse*, 179, 192 pp.

Blakey, R., 2013, Regional paleogeographic views of earth history: Colorado Plateau Geosystmems, inc.: web page: http://cpgeosystems.com/globaltext2.html (accessed October 2013).

Boyd, D.W., and Lillegraven, J.A., 2011, Persistence of the Western Interior Seaway Historical background and significance of ichnogenus Rhizocorallium in Paleocene strata, south-central Wyoming: *Rocky Mountain Geology*, 46, 43–69.

Braunberger, W.F., and Hall, R.L., 2001, Ammonoid faunas from the Cardium Formation (Turonian–Coniacian, Upper Cretaceous) and contiguous units, Alberta, Canada: 1. Scaphitidae: Canadian Journal of Earth Sciences, 38, 333–346.

Brenner, R.L., Ludvigson, G.A., Witzke, B.J., Zawistoski, A.N., Kvale, E.P., Ravn, R.L., and Joeckel, R.M., 2000, Late Albian Kiowa-Skull Creek Marine Transgression, Lower Dakota Formation, Eastern Margin of Western Interior Seaway, USA: Journal of Sedimentary Research, 70, 868–878.

Caldwell, W.G.E., Diner, R., Eicher, D.L., Fowler, S.P., North, B.R., Stelck, C.R., and von Holdt Wilhelm, L., 1993, Foraminiferal biostratigraphy of Cretaceous marine cyclothems, *in* Caldwell, W.G.E., and Kauffman, E.G., eds., Evolution of the Western Interior Basin: Geological Association of Canada Special Paper, 39, 477–520.

Carlson, M.P., 1999, Transcontinental Arch—A pattern formed by rejuvenation of local features across central North America: Tectonophysics, 305, 225–233.

Catuneanu, O., and Sweet, A.R., 1999, Maastrichtian-Paleocene foreland-basin stratigraphies, western Canada: a reciprocal sequence architecture: Canadian Journal of Earth Sciences, 36, 685–703.

Catuneanu, O., Sweet, A.R., and Miall, A.D., 2000, Reciprocal stratigraphy of the Campanian–Paleocene Western Interior of North America: *Sedimentary Geology*, 134, 235–255.

Chamberlain, C.P., Mix, H.T., Mulch, A., Hren, M.T., Kent-Corson, M.L., Davis, S.J., and Graham, S.A., 2012, The Cenozoic climatic and topographic evolution of the western North American Cordillera: *American Journal of Science*, 312, 213–262.

Cifelli, R.L., Eberle, J.J., Lofgren, D. L., Lillegraven, J.A., and Clemens, W.A., 2004, Mammalian biochronology of the latest Cretaceous: *in* Woodburne, M.O., ed., *Late Cretaceous and Cenozoic mammals of North America: Columbia University Press*, New York, 21–42.

Cobban, W.A., and Hook, S.C., 1984, Mid-Cretaceous molluscan biostratigraphy and paleogeography of southwestern part of Western Interior, United States *in* Westermann, G.E.G., eds., *Jurassic-Cretaceous Biochronology and Paleogeography of North America: Geological Association of Canada Special Paper*, 27, p. 257–271.

Cobban, W.A., 1993, Upper Cretaceous Ammonite Diversity in the Western Interior Seaway, *in* Caldwell, W.G.E., and Kauffman, E.G., eds., *Evolution of the Western Interior Basin: Geological Association of Canada Special Paper*, 39, 297–318.

Cobban, W.A., Merewether, E.A., Fouch, T.D., and Obradovich, J.D., 1994, Some Cretaceous shorelines in the western interior of the United States: *in* Caputo, M.V., Peterson, J.A.,

and Franczyk, K.J., eds., *Mesozoic Systems of the Rocky Mountain Region USA: Rocky Mountain Section (SEPM)*, 393–414.

Cobban, W.A., Walaszczyk, I., Obradovich, J.D., and McKinney, K.C., 2006, A USGS zonal table for the Upper Cretaceous middle Cenomanian-Maastrichtian of the Western Interior of the United States based on ammonites, inoceramids, and radiometric ages: *United States Geological Survey Open-File Report*, 1240, 50 pp.

Colgan, J.P., and Henry, C.D., 2009, Rapid middle Miocene collapse of the Mesozoic orogenic plateau in north-central Nevada: *International Geology Review*, 5, 920–961.

Coney, P.J., Jones, D.L., and Monger, J.W.H., 1980; Cordilleran suspect terranes: *Nature*, 288, 329–333.

Cross, T.A., 1986, Tectonic controls of foreland basin subsidence and Laramide style deformation, western United States: *in* Allen, P.A., and Homewood, P., eds., *Foreland basins, International Association of Sedimentologists Special Publications*, 8, 15–39.

Currie, B.S., 1998, Upper Jurassic-Lower Cretaceous Morrison and Cedar Mountain formations, NE Utah-NW Colorado; relationships between nonmarine deposition and early Cordilleran foreland-basin development: *Journal of Sedimentary Research*, 68, 632–652.

Cvancara, A.M., 1976, Geology of the Fox Hills Formation (late Cretaceous) in the Williston Basin of North Dakota, with reference to uranium potential: *North Dakota Geological Survey, Report of investigation*, 55, 16 pp.

Cvancara, A.M.,1976, Geology of the Cannonball Formation (Paleocene) in the Williston Basin, with Reference to Uranium Potential: *North Dakota Geological Survey, Report of investigation*, 57, 22 pp.

Cvancara, A.M., and Hoganson, J.W., 1993; Vertebrates of the Cannonball Formation (Paleocene) in North and South Dakota: *Journal of Vertebrate Paleontology*, 13, 23 pp.

Dahlstrom, D.C.A., 1969, Balanced cross sections: *Canadian Journal of Earth Sciences*, 6, 743–757.

Dahlstrom, D.C.A., 1970, Structural geology in the eastern margin of the Canadian Rocky Mountains: *Bulletin Canadian Petroleum Geologists*, 18, 332–406.

DeCelles, P.G., 1994, Late Cretaceous-Paleocene synorogenic sedimentation and kinematic history of the Sevier thrust belt, northeast Utah and southwest Wyoming: *Geological Society of America Bulletin*, 106, 32–56.

DeCelles, P.G., and Gautam, M., 1995, History of the Sevier orogenic wedge in terms of critical taper models, northeast Utah and southwest Wyoming: *Geological Society of America Bulletin*, 107, 454–462.

DeCelles, P.G., Lawton, T.F., and Gautam, M., 1995, Thrust timing, growth of structural culminations, and synorogenic sedimentation in the type Sevier orogenic belt, western United States: *Geology*, 23, 699–702.

DeCelles, P.G., and Mitra, G., 1995, History of the Sevier orogenic wedge in terms of critical taper models, northeast Utah and southwest Wyoming: *Geological Society of America Bulletin*, 107, 454–462.

DeCelles, P.G., and Currie, B.S., 1996, Long-term sediment accumulation in the Middle Jurassic–early Eocene Cordilleran retroarc foreland-basin system: *Geology*, 24, 591–594.

DeCelles, P.G., and Giles, K.A., 1996, Foreland basin systems: *Basin Research*, 8, 105–123.

DeCelles, P.G., and Horton, B.K., 2003, Early to middle tertiary foreland basin development and the history of Andean crustal shortening in Bolivia: *Geological Society of America Bulleting*, 115, 58–77.

DeCelles, P.G., 2004, Late Jurassic to Eocene evolution of the Cordilleran Thrust Belt and Foreland Basin System, Western United States of America, American Journal of Science, 304, 105–168.

de Cserna, Z., 1989, An outline of the geology of Mexico: *in* Bally, A. W. eds., The Geology of North America–An overview: *The Geological Society of America, The Geology of North America*, A, 233–264.

Demko, T.M., Currie, B.S., and Nicoll, K.A., 2004, Regional paleoclimatic and stratigraphic implications of paleosols and fluvial/overbank architecture in the Morrison Formation (Upper Jurassic), Western Interior, USA: *Sedimentary Geology*, 167, 115–135.

Dickinson, W.R., Klute, M.A., Hayes, M.J., Janecke, S.U., Lundin, E.R., McKittrick, M.A., and Olivares, M.D.,1988, Paleogeographic and paleotectonic setting of Laramide sedimentary basins in the central Rocky Mountain region: *Geological Society of America Bulletin*, 100, 1023–1039.

Dickinson, W.R., Hopson, C. A., Saleeby, J.B., Schweickert, R.A., Ingersoll, R.V., Pessagno Jr, E.A., and Blome, C.D.,1996, Alternate origins of the Coast Range ophiolite (California): Introduction and implications: *Geological Society of America Today*, 6, 1–10.

Dixon, G.R., 1993, Cretaceous tectonics and sedimentation in northwest Canada: *in* Caldwell, W.G.E., and Kauffman, E.G., eds., Evolution of the Western Interior Basin: *Geological Association of Canada Special Paper*, 39, 119–129.

Ducea, M., 2001, The California arc: Thick granitic batholiths, eclogitic residues, lithospheric-scale thrusting, and magmatic flare-ups: *GSA today*, 11, 4–10.

Dyman, T.S., Merewether, E.A., Molenaar, C.M., Cobban, W.A., Obradovich, J.D., Weimer, R. J., and Bryant, W. A., 1994, Stratigraphic transects for Cretaceous rocks, Rocky Mountains and Great Plains regions: in Caputo, M.V., Peterson, J.A. and Franczyk, K.J., eds., *Mesozoic systems of the Rocky Mountain Region, USA: Rocky Mountain Section Society for Economic Geology*, 365–391.

Eicher, D.L., 1960, Stratigraphy and micropaleontology of the Thermopolis Shale: *Peabody Museum of Natural History Bulletin*, 15, 126 pp.

Elder, W.P., Gustason, E.R., and Sageman, B.B., 1994, Correlation of basinal carbonate cycles to nearshore parasequences in the Late Cretaceous Greenhorn seaway, Western Interior USA: *Geological Society of America Bulletin*, 106, 892–902.

Erickson, J.M., 1999, The Dakota Isthmus—closing the Late Cretaceous Western Interior Seaway: *Proceedings of the North Dakota Academy of Science*, 53, 124–129.

Ernst, W.G., 2009, Rise and fall of the Nevadaplano: *International Geology Review*, 51, 583–588.

Fan, M., Quade, J., Dettman, D., and DeCelles, P.G., 2011, Widespread basement erosion during the late Paleocene–early Eocene in the Laramide Rocky Mountains inferred from 87Sr/86Sr ratios of freshwater bivalve fossils: *Geological Society of America Bulletin*, 123, 2069–2082.

Fielding, C.R., 2011, Foreland basin structural growth recorded in the Turonian Ferron Sandstone of the Western Interior Seaway Basin, USA: *Geology*, 39, 1107–1110.

Foster, J., 2007, Jurassic West: the dinosaurs of the Morrison Formation and their world: *Indiana University Press*, 416 pp.

Fox Jr, S.K., and Ross Jr, R.J., 1942, Foraminiferal evidence for the Midway (Paleocene) age of the Cannonball Formation in North Dakota: *Journal of Paleontology*, 16, 660–673.

Fox, S.K. and Olsson, R.K., 1969, Danian planktonic foraminifera from the Cannonball Formation in North Dakota: *Journal of Paleontology*, 43, 1397–1404.

Frakes, L.A., Francis, J.E, and Syktus, J.I., 1992, Climate modes of the Phanerozoic: *Cambridge University Press*, 280 pp.

Fuentes, F., DeCelles, P.G., Constenius, K.N., and Gehrels, G.E., 2011, Evolution of the Cordilleran foreland basin system in northwestern Montana, USA: *Geological Society of America Bulletin*, 123, 507–533.

Galloway, W.E., 2008, Depositional Evolution of the Gulf of Mexico Sedimentary Basin: *in* Miall, A.D., ed., *Sedimentary basins of the world*, 5, 506–549.

Galloway, W.E., Bebout, D.G., Fisher, W.L., Dunlap, Jr., J.B., Cabrera-Castro, R., Lugo-Rivera, J.E., and Scott, T.M., 1991, Cenozoic: *in* Salvador, A., eds., *The Gulf of Mexico, The Geological Society of America, The Geology of North America Series*, J, 181–204.

Garvie, C.L., 2013, Studies on the molluscan paleomacrofauna of the Texas Paleogene: *Bulletins of American Paleontology*, 384, 216 pp.

Gill, J.R., and Cobban, W. A., 1973, Stratigraphy and Geological History of the Montana Group and Equivalent rocks, Montana, Wyoming, and North and South Dakota: *United States Geological Survey Professional Paper*, 776, 1–37.

Goldhammer, R.K. and Johnson, C.A., 1999, Mesozoic sequence stratigraphy and paleogeographic evolution of northeast Mexico: *Geological Society of America Special Papers*, 340, 1–58.

Gradstein, F.M., 2012, Introduction: in Gradstein, F.M., Ogg, J.G., Schmitz, M.D., and Ogg, G.M., eds., *The Geological Time Scale 2012, Elsevier*, 1–29.

Gregory-Wodzicki, K.M., 2000, Uplift history of the Central and Northern Andes: A review: *Geological Society of America, Bulletin*, v. 112, p. 1091–1105.

Hallam, A., 1992, Phanerozoic sea-level changes: *Columbia University Press*, 266 pp.

Hancock, J.M., and Kauffman, E.G., 1979, The great transgressions of the Late Cretaceous: *Journal of the Geological Society*, 136, 175–186.

Harper, G.D., and Wright, J.E., 1984, Middle to Late Jurassic tectonic evolution of the Klamath Mountains, California- Oregon: *Tectonics*, 3, 759–772.

Hartman, J.H., 1999, The paleontologic and geologic record of North Dakota—Important sites and current interpretations, a symposium overview and geologic framework: *Proceedings of the North Dakota Academy of Science*, 53, 116–118.

Hartman, J.H., and Kirkland, J.I., 2002, Brackish and Marine Mollusks of the Hell Creek Formation of North Dakota: Evidence for a persisting Cretaceous Seaway: *in* Hartman, J.H., Johnson, K.R., and Nichols, D.J., eds. *The Hell Creek Formation and the Cretaceous-Tertiary Boundary in the Northern Great Plains: An integrated Continental Record of the End of the Cretaceous: Geological Society of America Special Papers*, 361, 271–296.

Hay, W.W., 2008, Evolving ideas about the Cretaceous climate and ocean circulation: *Cretaceous Research*, 29, 725–753.

Heller, P.L., and Paola, C., 1989, The paradox of Lower Cretaceous gravels and the initiation of thrusting in the Sevier orogenic belt, United States Western Interior: *Geological Society of America Bulletin*, 101, 864–875.

Hicks, J.F., Obradovich, J.D., and Tauxe, L., 1999, Magnetostratigraphy, isotopic age calibration, and intercontinental correlation of the Red Bird section of the Pierre Shale, Niobrara County, Wyoming, USA: *Cretaceous Research*, 20, 1–27

Hicks, J.F., Johnson, K.R., Obradovich, J.D., Tauxe, L., Clark, D. 2002, Magnetostratigraphy and geochronology of the Hell Creek and Basal Fort Union Formations of southwestern North Dakota and a recalibration of the age of the Cretaceous-Tertiary boundary: *in* Hartman, J.H., Johnson, K.R., and Nichols, D.J., eds. The Hell Creek Formation and the Cretaceous-Tertiary Boundary in the Northern Great Plains: An integrated Continental Record of the End of the Cretaceous: *Geological Society of America Special Papers*, 361, 35–55.

Hoganson, J.W., and Murphy, E.C., 2002, Marine Breien Member (Maastrichtian) of the Hell Creek Formation in North Dakota: Stratigraphy, vertebrate fossil record, and age: *in* Hartman, J.H., Johnson, K.R., and Nichols, D.J., eds. The Hell Creek Formation and the Cretaceous-Tertiary Boundary in the Northern Great Plains: An integrated Continental Record of the End of the Cretaceous: *Geological Society of America Special Papers*, 361, 247–270.

Horton, B.K., Hampton, B.A., and Waanders, G., 2001, Paleogene synorogenic sedimentation in the Altoplano plateau and implications for initial mountain building in the central Andes: *Geological Society of America Bulletin*, 113, 1387–1400.

Imlay, R.W., 1980, Jurassic paleobiogeography of the conterminous United States in its continental setting: *United States Geological Survey Professional Paper*, 1062, 134 pp.

Imlay, R.W., 1984, Jurassic ammonite successions in North America and biogeographic implications: *in* Westermann, G.E.G., eds., Jurassic-Cretaceous biochronology and paleogeography of North America: *Geological Association of Canada Special Paper*, 27, 1–12.

Ingersoll, R.V., 2008, Subduction-related sedimentary basins of the USA Cordillera: *in* Miall, A.D., eds., *Sedimentary basins of the world*, 5, 395–428.

Jeletzky, J.A., 1971, Marine Cretaceous biotic provinces and paleogeography of western and Arctic Canada: illustrated by a detailed study of ammonites: Geological Survey of Canada, Paper, 70, 92 pp.

Jeletzky, J.A., 1978, Causes of Cretaceous oscillations of sea level in Western and Arctic Canada and some general geotectonic implications: *Geological Survey of Canada Bulletin*, 77, 44 pp.

Jowett, D.M.S., Schröder-Adams, C.J., and Leckie, D., 2007, Sequences in the Sikanni Formation in the frontier Liard Basin of northwestern Canada—evidence for high frequency late Albian relative sea-level changes: *Cretaceous Research*, 28, 665–695.

Kauffman, E.G., 1969, Cretaceous marine cycles of the Western Interior: *The Mountain Geologist*, 6, 227–245.

Kauffman, E.G., 1977, Geological and biological overview: Western Interior Cretaceous basin: *The Mountain Geologist*, 14, 75–99.

Kauffman, E.G., 1984, Paleobiogeography and evolutionary response dynamic in the Cretaceous Western Interior Seaway of North America: *in* Westermann, G.E.G., eds., Jurassic-Cretaceous Biochronology and Paleogeography of North America: *Geological Association of Canada, Special Paper*, 27, 273–306.

Kauffman, E.G. and Caldwell, W.G.E., 1993, Evolution of the Western Interior Basin, *in* Caldwell, W.G.E., and Kauffman, E.G., eds., *Evolution of the Western Interior Basin: Geological Association of Canada Special Paper*, 39, 1–46.

Kauffman, E.G., Sageman, B.B., Kirkland, J.I., Elder, W.P., Harries, P.J., and Villamil, T., 1993, Molluscan biostratigraphy of the Cretaceous Western Interior Basin, North America, *in* Caldwell, W.G.E., and Kauffman, E.G., eds., *Evolution of the Western Interior Basin: Geological Association of Canada, Special Paper,* 39, 397–434.

Keller, G., Berner, Z., Adatte, T., and Stueben, D., 2004, Cenomainian-Turonian $\delta^{13}C$, and $\delta^{18}O$, sea level and salinity variation at Pueblo Colorado: *Palaeogeography, Palaeoclimatology, Palaeoecology*, 211, 19–43.

Kennedy, W.J., Landman, N.H., Christensen, W.K., Cobban, W.A. and Hancock, J.M., 1998, Marine connections in North America during the late Maastrichtian: Palaeogeographic and palaeobiogeographic significance of Jeletzkytes nebrascensis Zone cephalopod fauna from the Elk Butte Member of the Pierre Shale, SE South Dakota and NE Nebraska, *Cretaceous Research*, 19, 745–775.

Kowallis, J., Christiansen, E.H., Deino, A.L., Kunk, M.J., Heaman, L.M., 1995, Age of the Cenomanian–Turonian boundary in the Western Interior of the United States: *Cretaceous Research*, 16, 109–129.

Krystinik, L.F., and DeJarnett, B.B., 1995, Lateral variability of sequence stratigraphic framework in the Campanian and Lower Maastrichtian of the Western Interior Seaway: *in* Van Wagoner, J.C. and Bertram, G.T., eds., Sequence Stratigraphy of Foreland Basin Deposits: *American Association of Petrolum Geologists Memoirs*, 64, 11–26.

Kroeger, T.J., and Hartman, J.H., 1997, Paleoenvironmental distribution of Paleocene palynomorph assemblages from brackish water deposits in the Ludlow, Slope, and Cannonball Formations, southwestern North Dakota: *Contributions to Geology*, 32, 115–129.

Landman, N.H., Johnson, R.O., and Edwards, L.E., 2004, Cephalopods from the Cretaceous/Tertiary boundary interval on the Atlantic Coastal Plain, with a description of the highest ammonite zones in North America, Part 2, Northeastern Monmouth County, New Jersey: *Bulletin of the American Museum of Natural History*, 287, 107 pp.

Landman, N.H., Remin, Z., Garb, M.P., and Chamberlain Jr, J.A., 2013, Cephalopods from the Badlands National Park area, South Dakota: Reassessment of the position of the Cretaceous/Paleogene boundary: *Cretaceous Research*, 42. 1–27.

Lang, H.R., and McGugan, A., 1987, Cretaceous (Albian–Turonian) foraminiferal biostratigraphy and paleogeography of northern Montana and southern Alberta: *Canadian Journal of Earth Sciences*, 25, 316–342.

Lawton, T.F., 1994, Tectonic setting of Mesozoic sedimentary basins, Rocky Mountain region, United States, *in* Caputo, M.V., Peterson, J.A., and Franczyk, K.J., eds., *Mesozoic systems of the Rocky Mountain region, USA: Denver, Colorado, Rocky Mountain Section SEPM*, 1–26.

Lawton, T.F., 2008, Laramide sedimentary basins: *in* Miall, A.D., ed. *Sedimentary basins of the world*, 5, 429–450.

Leckie, D.A., and Reinson, G.E., 1988, Effects of middle to late Albian sea level fluctuations in the Cretaceous Interior Seaway, western Canada: *in* Caldwell, W.G.E., and Kauffman, E.G., eds., Evolution of the Western Interior Basin: Geological Association of Canada, Special Paper, 39, 151–176.

Leithold, E.L., 1994, Stratigraphical architecture at the muddy margin of the Cretaceous Western Interior Seaway, southern Utah: *Sedimentology*, 41, 521–542.

Lillegraven, J.A., and Ostresh, L.M., 1990, Late Cretaceous (earliest Campanian/ Maastrichtian) evolution of western shorelines of the North American Western Interior Seaway in relation to known mammalian faunas: *Geological Society of America Special Papers*, 243, 1–30.

Liu, S., and Nummedal, D., 2004, Late Cretaceous subsidence in Wyoming: Quantifying the dynamic component: *Geology*, 32, 397–400

Liu, S., and Nummedal, D., and Liu, L., 2011, Migration of dynamic subsidence across the Late Cretaceous United States Western Interior Basin in response to Farallon plate subduction: *Geology*, 39, 555–558.

Livaccari, R.F., 1991, Role of crustal thickening and extensional collapse in the tectonic evolution of the Sevier-Laramide orogeny, western United States: *Geology*, 19, 1104–1107.

Martinson, V.S., Heller, P. L., and Frerichs, W.E., 1998, Distinguishing middle Late Cretaceous tectonic events from regional sea-level change using foraminiferal data from the US Western Interior: *Geological Society of America Bulletin*, 110, 259–268.

McGookey, D.P., Haun, J.D., Hale, L.A., Goodell, H.G., McCubbin, D.G., Weimer, R., and Wulf, G.R.,1972, Cretaceous system: in Mallory, W.W., eds., *Geologic Atlas of the Rocky Mountain Region: Rocky Mountain Association of Geologists*, 190–228.

McFarlan, Jr., E., and Menes, L.S., 1991, Lower Cretaceous: *in* Salvador, A., eds., The Gulf of Mexico, *The Geological Society of America, The Geology of North America Series*, J, 181–204.

McMechan, M.E., and Thompson, R.I., 1993, The Canadian Cordilleran fold and thrust belt south of 66º N and its influenceon the Western Interior Basin, in Caldwell, W.G.E., and Kauffman, E.G., eds., Evolution of the Western Interior Basin: *Geological Association of Canada Special Paper*, 39, 73– 90.

Merewether, E.A., Cobban, W.A., and Obradovich, J.D., 2007, Regional disconformities in Turonian and Coniacian (Upper Cretaceous) strata in Colorado, Wyoming, and adjoining states—biochronological evidence: *Rocky Mountain Geology*, 42, 95–122.

Merewether, E.A., Cobban, W.A., and Obradovich, J.D., Biostratigraphic data from Upper Cretaceous Formations: eastern Wyoming, central Colorado, and northeastern New Mexico: *United States Geological Survey Scientific Investigation Map*, 3175, 11 pp.

Meyers, S.R., Sageman, B.B., and Hinnov, L.A. ,2001, Integrated quantitative stratigraphy of the Cenomanian-Turonian Bridge Creek Limestone Member using evolutive harmonic analysis and stratigraphic modeling: *Journal of Sedimentary Research*, 71, 628–644.

Miall, A.D., Catuneanu, O., Vakarelov, B.K., and Post, R., 2008, The Western interior basin: *in* Miall, A.D., ed. *Sedimentary basins of the world*, 5, 329–362.

Miller, K.G., Sugarman, P.J., Browning, J.V., Kominz, M.A., Hernández, J.C., Olsson, R.K., and Van Sickel, W.,2003, Late Cretaceous chronology of large, rapid sea-level changes: Glacioeustasy during the greenhouse world: *Geology*, 31, 585–588.

Miller, K.G., Kominz, M.A., Browning, J.V., Wright, J.D., Gregory S. Mountain, Katz, M.E., Sugarman, P.J., Cramer, B.S., Christie-Blick, N., Pekar, S.F., 2005, The Phanerozoic Record of Global Sea-Level Change: *Science*, 310, 1293–1298.

Monger, J.W.H., 1993, Cretaceous tectonics of the North American Cordillera., *in* Caldwell, W.G.E., and Kauffman, E.G., eds., *Evolution of the Western Interior Basin: Geological Association of Canada Special Paper*, 39, 31–47.

Nielsen, K.S., Schröder-Adams, C.J., Leckie, D.A., Haggart, J.W., and Elberdak, K., 2008, Turonian to Santonian paleoenvironmental changes in the Cretaceous Western Interior Sea: The Carlile and Niobrara formations in southern Alberta and southwestern Saskatchewan, Canada: *Palaeogeography, Palaeoclimatology, Palaeoecology*, 270, 64–91.

Oboh-Ikuenobe, F.E., Holbrook, J.M., Scott, R.W., Akins, A.L., Evetts, M.J., Benson D.G. and, Pratt, L.M., 2009, Anotomy of epicontinental flooding: Late Albian-Early Cenomanian of the southern U.S., Western Interior Basin: *in* Pratt, B.R. and Holmden, C., *Dynamics of Epeiric seas: Geological Association of Canada Special Paper*, 48, 201–208.

Obradovich, J.D., 1993, A Cretaceous time scale, *in* Caldwell, W.G. E. and Kauffman, E.G., eds., *Evolution of the Western Interior Basin: Geological Association of Canada, Special Paper*, 39, 379–396.

Owens, J.P., and Gohn, G.S., 1985, Depositional history of the Cretaceous series in the US Atlantic Coastal Plain: Stratigraphy, paleoenvironments, and tectonic controls of sedimentation. Geologic Evolution of the United States Atlantic Margin: *Van Nostrand Reinhold*, 25–86.

Pang, M., and Nummedal, D., 1995, Flexural subsidence and basement tectonics of the Cretaceous Western Interior basin, United States: *Geology*, 23, 173–176.

Parra, M., Mora, A., Jaramillo C., Strecker M.R., Sobel E.R., Quiroz, L. Rueda, M., and Torres, V., 2009, Orogenic wedge advance in the northern Andes: Evidence from the Oligocene-Miocene sedimentary record of the Medina Basin, Eastern Cordillera, Colombia, *Geological Society of America*, 121, 780–800.

Price, R.A., and Mountjoy, E.W., 1970, Geological structure of the Canadian Rocky Mountains between Bow and Athabascarivers—Progress report: *in* Wheeler, J. O., eds.: *Geological Association of Canada Special Paper*, 6, 7–25.

Pitman, W.C., III, 1978, Relationship between eustacy and stratigraphic sequences of passive margins: *Geological Society of America Bulletin*, 89, 1389–1403.

Pitman, W.C., III, and Golovchenko, X., 1983, The effect of sea-level change on the shelf edge and slope of passive margins: *Society of Economic Paleontologists and Mineralogists Special Publication*, 33, 41–58.

Plint, A.G., 2000, Sequence stratigraphy and paleogeography of a Cenomanian deltaic complex: the Dunvegan and lower Kaskapau formations in subsurface and outcrop, Alberta and British Columbia, Canada: *Bulletin of Canadian Petroleum Geology*, 48, 43–79.

Poulton, T.P., Braun, W.K., Brooke, M.M., and Davis, E.H., 1993, Jurassic: *in* Stott, D.F., and Aitken, J.D., eds., Sedimentary Cover of the Craton in Canada: *The Geological Society of America, The Geology of North America Series*, D-1, 321–357.

Pyles, D. R., and Slatt, R.M., Applications to understanding shelf edge to base-of-slope changes in stratigraphic architecture of prograding basin margins: Stratigraphy of the Lewis Shale, Wyoming, USA, *in* T.H. Nilsen, R.D. Shew, G.S. Steffens, and J.R.J. Studlick, eds., *Atlas of deep-water outcrops: AAPG Studies in Geology*, 56, 1–19.

Ramos, V.A., 1999, Plate tectonic setting of the Andean Cordillera: *Episodes*, 22, 183–190.

Rast, N., 1989, The evolution of the Appalachian Chain: *in* Bally, A. W. eds., The Geology of North America–An overview: *The Geological Society of America, The Geology of North America* Series, A, 323–348.

Reeside, J. B., 1957, Paleoecology of the Cretaceous seas of the Western Interior of the United States: *Geological Society of America Memoirs*, 67, 505–542.

Reeside, J.B., and Cobban, W. A., 1960, Studies of the Mowry Shale (Cretaceous) and Contemporary Formations in the United States and Canada: *United States Geological Survey Professional Paper*, 355, 126 pp.

Ricketts, B.D., 2008, Cordilleran Sedimentary Basins of Western Canada Record 180 Million Years of Terrane Accretion: *in* Miall, A.D., eds. *Sedimentary basins of the world*, 5, 364–394.

Roberts, L.N.R., and Kirschbaum, M.A., 1995, Paleogeography of the Late Cretaceous of the Western Interior of middle North America-coal distribution and sediment accumulation: *United States Geological Survey Professional Paper*, 1561, 115 pp.

Royse, F. Jr., Warner, M.A., and Reese, D.L.,1975, Thrust belt structural geometry and related stratigraphic problems, Wyoming-Idaho-northern Utah, in Bolyard, D. W., ed., *Deep drilling frontiers of the central Rocky Mountains Sysmposium: Rocky Mountain Association of Geologist*, 41–54.

Sageman, B.B., and Arthur, M.A., 1994, Early Turonian paleogeographic/paleobathymetric map, western interior, US: *Mesozoic Systems of the Rocky Mountain Region, SEPM*, 457–469.

Sageman, B.B., Rich, J., Arthur, M.A., Birchfield, G.E. and Dean, W.E., 1997, Evidence for Milankovitch periodicities in Cenomanian–Turonian lithologic and geochemical cycles, Western Interior, U.S.A. *Journal of Sedimentary Research*, 67, 286–302.

Saleeby, J.B., and Busby-Spera, C.J., 1992, Early Mesozoic tectonic evolution of the western U.S. Cordillera, in Buchfiel, B.C., et al., *The Cordilleran Orogen: Coterminous U.S.: Geology of North America, Geological Society of America*, G-3, 107–168

Sames, B., Cifelli, R.L., and Schudack, M.E., 2010, The nonmarine Lower Cretaceous of the North American Western Interior foreland basin: New biostratigraphic results from ostracod correlations and early mammals, and their implications for paleontology and geology of the basin—An overview: *Earth-Science Reviews*, 101, 207–224.

Schlaikjer, E.M., 1935, Contributions to the stratigraphy and palaeontology of the Goshen Hole area, Wyoming. II. The Torrington Member of the Lance Formation and a study of a new *Triceratops*: *Harvard College, Museum of Comparative Zoology, Bulletin*, 76, 31–68.

Schlanger, S.O. and Jenkyns, H.C., 1976, Cretaceous Oceanic Anoxic Events-Causes and Consequences: *Geologie en Mijnbouw*, 55, 179–184.

Schröder-Adams, C., Herrle, J.O., and Tu, Q., 2012, Albian to Santonian carbon isotope excursions and faunal extinctions in the Canadian Western Interior Sea: Recognition of eustatic sea-level controls on a forebulge setting: *Sedimentary Geology*, 281, 50–58.

Schröder-Adams, C., 2014, The Cretaceous Polar and Western Interior Seas: Paleonenvironmental History and Paleoeceanographic linkages: *Sedimentary Geology*, 301, 26–40.

Schuchert, C., 1910, Paleogeography of North America: *Geological Society of America Bulletin*, 20, 427–606.

Schuchert, C., 1955, Atlas of paleogeographic maps of North America: *John Wiley and Sons*, 177 pp.

Scott, R.W., 1984, Mesozoic biota and depositional systems of the Gulf of Mexico-Caribbean region: *in* Westermann, G.E.G., ed., Jurassic-Cretaceous biochronology and paleogeography of North America: *Geological Association of Canada Special Paper*, 27, 49–64.

Scott, R.W., 2007, Calibration of the Albian/Cenomanian boundary by ammonite biostratigraphy: US Western Interior: *Acta Geologica Sinica - English Edition*, 81, 940–948.

Scott, R.W., 2009, Uppermost Albian biostratigraphy and chronostratigraphy: *Carnets de Géologie, Notebooks on Geology*, 3, 1–16.

Scott, R.W., Oboh-Ikuenobe, F.E., Benson, Jr., D.G., and Holbrook, J.M., 2009, Numerical age calibration of the Albian/Cenomanian boundary: *Stratigraphy*, 6, 17–32.

Sloss, L.L., Dapples, E.C., and Krumbein, W.C., 1960, Lithofacies maps: an atlas of the United States and southern Canada: *John Wiley and Sons*, 108 pp.

Sohl, N.F., Martinez, R., Salmeron-Urena, P., and Soto-Jaramillo, F., 1991, Upper Cretaceous: *in* Salvador, A., eds., *The Gulf of Mexico, The Geological Society of America, The Geology of North America Series*, J, 206–245.

Sohl, N.F., 1967, Upper Cretaceous gastropod assemblages of the Western Interior of the United States: *in* Kauffman, E.G., and Kent, H.C., *Paleoenvironments of the Cretaceous seaway in the Western Interior*, 1–37.

Stelck, C.R., Trollope, F. H., Norris, A.W., and Pemberton, S.G., 2007, McMurray Formation foraminifera within the lower Albian (Lower Cretaceous) Loon River shales of northern Alberta: *Canadian Journal of Earth Sciences*, 44, 1627–1651.

Stockmal, G.S., Cant, D.J., and Bell, J.S., 1992, Relationship of the stratigraphy of the Western Canada foreland basin to Cordilleran tectonics: insights from geodynamic models: *in* Macqueen, R.W., and Leckie, D.A., eds., Foreland Basins and Fold Belts: *American Association of Petroleum Geologists Memoir*, 55, 107–124.

Stott, D.F., 1993, Evolution of Cretaceous foredeeps: a comparative analysis along the length of the Canadian Rocky Mountains. Evolution of the Western Interior Basin: *in* Caldwell, W.G.E., and Kauffman, E.G., eds., Evolution of the Western Interior Basin: *Geological Association of Canada, Special Paper*, 39, 131–150.

Stott, D.F., Caldwell, W.G.E., Cant, D.J., Christopher, J.E., Dixon, J. Koster, E.H., McNeil, D.H., and Simpson, F., 1993; Cretaceous: *in* Stott, D.F., and Aitken, J.D., eds., *Sedimentary Cover of the Craton in Canada, The Geological Society of America, The Geology of North America Series*, D-1, 358–438.

Umhoefer, P.J. and Blakey, R.C., 2006, Moderate (1600 km) northward translation of Baja British Columbia from southern California: An attempt at reconciliation of paleomagnetism and geology: *in* Haggart, J.W., Enkin, R.J. and Monger, J.W.H., eds., Paleogeography of the North American Cordillera: *Evidence For and Against Large-Scale Displacements: Geological Association of Canada, Special Paper*, 46, 305–327.

Waagé, K.M., 1968, The type Fox Hills Formation, Cretaceous (Maestrichtian, South Dakota; Part 1, Stratigraphy and Paleoenvironments: *Peabody Museum of Natural History Bulletin*, 27, 175 pp.

Weimer, R.J., 1984, Relation of unconformities, tectonics, and sea-level changes, Cretaceous of Western Interior, USA: *AAPG Special Volumes*, M36, 7–35.

Weimer, R.J., 1978, Influence of Transcontinental Arch on Cretaceous marine sedimentation, a preliminary report, in Pruit, J.D., and Coffin, P.E., eds., *Energy resources of the Denver basin: Rocky Mountain Association of Geologist Symposium*, 211–22.

Weimer, R.J., 1984, Relation of unconformities, tectonics, and sea-level changes, Cretaceous of Western Interior, USA: *AAPG Memoir*, 7–35.

White, T.S., Witzke, B.J., and Ludvigson, G.A., 2000, Evidence for an Albian Hudson arm connection between the Cretaceous Western Interior Seaway of North America and the Labrador Sea: *Geological Society of America Bulletin*, 112, 1342–1355.

Williams, G.D., and Stelck, C.R., 1975, Speculations on the Cretaceous paleogeography of North America, The Cretaceous System in the Western Interior of North America: *Geological Association of Canada Special Paper*, 13, 1–20.

Wilson, G.P., Dechesne, M., and Anderson, I.R., 2010, New latest Cretaceous mammals from northeastern Colorado with biochronologic and biogeographic implications: *Journal of Vertebrate Paleontology*, 30, 499–520.

Witzke, B.J., Ludvigson, G.A., Poppe, J.R., and Ravn, R.L. ,1983, Cretaceous Paleogeography along the Eastern Margin of the Western Interior Seaway, Iowa Southern Minnesota, Eastern Nebraska and South Dakota: *Rocky Mountain Section (SEPM)*, 2, 225–252.

Wright, J.E., and Fahan, M.R., 1988, An expanded view of Jurassic orogenesis in the western U.S. Cordillera: Middle Jurassic (pre-Nevadan) regional metamorphism and thrust faulting within an active arc environment, Klamath Mountains, California, *Geological Society of America Bulletin*, 100, 859–876.

Wroblewski, A.F-J., 2008, Paleoenvironmental Significance of Cretaceous and Paleocene *Psilonichnus* in southern Wyoming: *Palaios*, 23, 370–379.

Wroblewski, A.F-J., 2004, New Selachian paleofaunas from ‘‘fluvial’’ deposits of the Ferris and lower Hanna formations (Maastrichtian–Selandian: 66–58 Ma): Southern Wyoming: *Palaios*, 19, 249–258.

Yacobucci, M.M., 2004, *Neogastroplites* meets *Metengonoceras*: morphological response of an endemic hoplitid ammonite to a new invader in the mid-Cretaceous Mowry Sea of North America: *Cretaceous Research*, 25, 927–944.

Zaleha, M.J., and Wiesemann, S.A., 2005, Hyperconcentrated flows and gastroliths: sedimentology of diamictites and wackes of the upper Cloverly Formation, Lower Cretaceous, Wyoming, USA: *Journal of Sedimentary Research*, 75, 43–54.

Zaleha, M.J., 2006, Sevier orogenesis and nonmarine basin filling: Implications of new stratigraphic correlations of Lower Cretaceous strata throughout Wyoming, USA: *Geological Society of America Bulletin*, 118, 886–896.

Zaleha, M.J., 2013, Paleochannel hydraulics, geometries, and associated alluvial architecture of Early Cretaceous rivers, Sevier Foreland Basin, Wyoming, USA: *Cretaceous Research*, 45, 321–341

Ziegler, A.M., and Rowley, D.B., 1998, The vanishing record of epeiric seas, with emphasis on the late Cretaceous Hudson Seaway: *Oxford Monographs on Geology and Geophysics*, 39, 147–168.

CHAPTER THREE:

BIOSTRATIGRAPHIC COMPILATION OF THE CAMPANIAN AND MAASTRICHTIAN AMMONITES BIOZONES IN THE GULF AND ATLANTIC COASTAL PLAINS

Introduction

Ammonites are among the most useful macrofossils for Mesozoic biostratigraphy. This utility stems from their rapid evolutionary rates, facies independence, high preservation potential, and ready species recognition (e.g., Kennedy and Cobban, 1976; Lehmann, 2015). These features make them ideal index fossils and explains why this era's chronological framework is so integrally linked to ammonite zones (e.g., Cobban et al., 2006; Ogg and Hinnov, 2012; Lehmann, 2015). Due to their habitat preference for open-shelf and epeiric seas, ammonites also facilitate high-resolution correlation of strata deposited in shallow-marine continental settings (Lehmann, 2015). However, due to provincialism among ammonite species, different regional biozonations have been erected across the globe, which is clearly apparent for the North American and European zonations (e.g., Küchler, 1998; Cobban et al., 2006; Ward et al., 2012; Ogg and Hinnov, 2012). The general utility of ammonites as outlined above is clearly manifest in the Campanian–Maastrichtian, although some regions still require further refinement.

Whereas extensive focus has been given to the ammonite zonation of the North American Western Interior (WI) and Pacific Coast, the generally accepted zonal scheme for the Gulf Coastal Plain (GCP) is primarily based on the decades old work of Young (1959, 1963, 1969, 1982, 1985, 1986), and there is presently no existing framework below the upper Maastrichtian

in the Atlantic Coastal Plain (ACP). Over the past few decades a significant new focus has been devoted to describing and re-evaluating many of the Campanian–Maastrichtian ammonite assemblages in the ACP and GCP, which has greatly improved our ability to erect a comprehensive biostratigraphy. These studies have enhanced our knowledge of how the ammonite assemblages in the GCP and ACP correlate with more refined biostratigraphic schemes in other parts of the world (e.g., Kennedy et al., 1992, Kennedy and Cobban, 1997; Cobban and Kennedy, 1995; Landman et al., 2004a, b, 2007; Cobban et al., 2008; Ifrim et al. 2015; Larina et al., 2016). However, these recent studies have not been comprehensive and considerable biostratigraphic information lies distributed throughout numerous publications.

The primary objective of this paper is to compile and synthesize the existing data on ammonite ranges from the ACP and GCP Campanian–Maastrichtian and use those data to produce biozonations for each region. In addition, the aim is to correlate them to the ammonite zonations in the Western Interior as well as the current biochronologic framework for the Late Cretaceous established by Ogg and Hinnov (2012).

Geographic and Geologic Setting of the Atlantic and Gulf Coastal Plains.

The ACP and GCP comprise an extensive passive margin that formed in response to the opening of basins related to Pangaea's breakup during the Triassic through Jurassic (Galloway, 2008; Miall et al., 2008). The ACP spans from Nova Scotia to Florida and is bounded to the east by the Atlantic Oceanic Basin and to the west by Appalachian Orogenic Belt (Fig. 3.1). The GCP is part of the Gulf of Mexico Basin that stretches from Florida to the Yucatan Peninsula and is bounded to the north by the Appalachian-Ouachita Orogenic belts and to the west by the Cordilleran Orogenic Belt (Fig. 3.1). During the Cretaceous, high global sea level resulted in various transgressions across the ACP and GCP (Owens and Gohn, 1985; McFarlan and Menes,

Figure 3.1. Map of structural features that influenced sedimentation patterns and paleogeography along the Gulf and Atlantic coastal plains during the Campanian–Maastrichtian (modified from Owens and Gohn, 1985; Salvador, 1991; Sohl et al., 1991; Slattery et al., 2015).: LIP, Long Island Platform; RE, Raritan Embayment; SNJH, South New Jersey High; NH, Norfolk or Ft. Monroe High, , AE, Albemarle Embayment; CFA, Cape Fear Arch; SEGE, Southeast Georgia Embayment; SGH, South Georgia High; SS, Suwannee Straits; APE, Apalachicola or Southwest Georgia Embayment; ME, Mississippi Embayment; MSB, Mississippi Salt Basin; JD, Jackson Dome; MU, Monroe Uplift; SU, Sabine Uplift; ETB, East Texas Basin; SMA, San Marcos Arch; EP, Edwards Plateau; WIFB, Foreland Basin, RGE, Rio Grande Embayment; BB, Burgos Basin; SB, Sabinas Basin; VSPP, Valles San Luis Potosi Platform; TMB, Tampico Misantia Basin; VB, Veracruz Basin; ISB, Isthmus Saline Basin; MB, Macuspana Basin; YP, Yucatan Platform.

Figure 3.2. Map of Upper Cretaceous rocks exposed along the Gulf and Atlantic coastal plains (modified from Reed et al., 2005).

1991; Sohl et al., 1991; Miller et al., 2005). These transgressions forced shorelines to the margins of the bounding uplifts (or highlands) that defined these regionsboundaries (see Fig. 3.1) and formed a marine connection between the Gulf of Mexico to the south and the WI Seaway to the north. During the Santonian to early Campanian, the shoreline of the Gulf of Mexico transgressed past the Appalachian-Ouachita Orogenic Belt northward into the Mississippi Embayment.

The ACP and GCP Campanian–Maastrichtian deposits form a discontinuous outcrop belt that extends from New Jersey to southern Texas (Fig. 3.2). In northern Mexico, these strata are exposed in and along the Sierra Madre Oriental and Occidental, both of which are parts of the North American Cordilleran Orogenic Belt (Figs. 3.1 and 3.2). Campanian–Maastrichtian strata are represented by various formations (e.g., Fig. 3.3 and 3.4) that were deposited in a wide range of depositional environments ranging from terrestrial to marine shelf settings (Stephenson et al., 1942; Sohl et al., 1991). Most of the ammonite records discussed here derive from the northern GCP and the central ACP, which is primarily due to greater exposure of Campanian–Maastrichtian strata, preservational influences, and collecting biases towards these regions. The southern GCP is also characterized by rudist-dominated biofacies, which rarely preserve ammonites (Sohl et al., 1991).

As is typical for passive-margin settings, ACP and GCP Cretaceous strata formed wedge-shaped packages that thicken in a down dip or offshore direction (Galloway, 2008; Miall et al., 2008). During the Campanian–Maastrichtian, siliciclastic sedimentation dominated the ACP, whereas both siliciclastic and carbonate deposition occurred along the GCP (Sohl et al., 1991; Galloway, 2008; Miall et al., 2008). However, due to limited sediment supply in conjunction with low subsidence rates in these passive-margin settings, sediments were frequently reworked

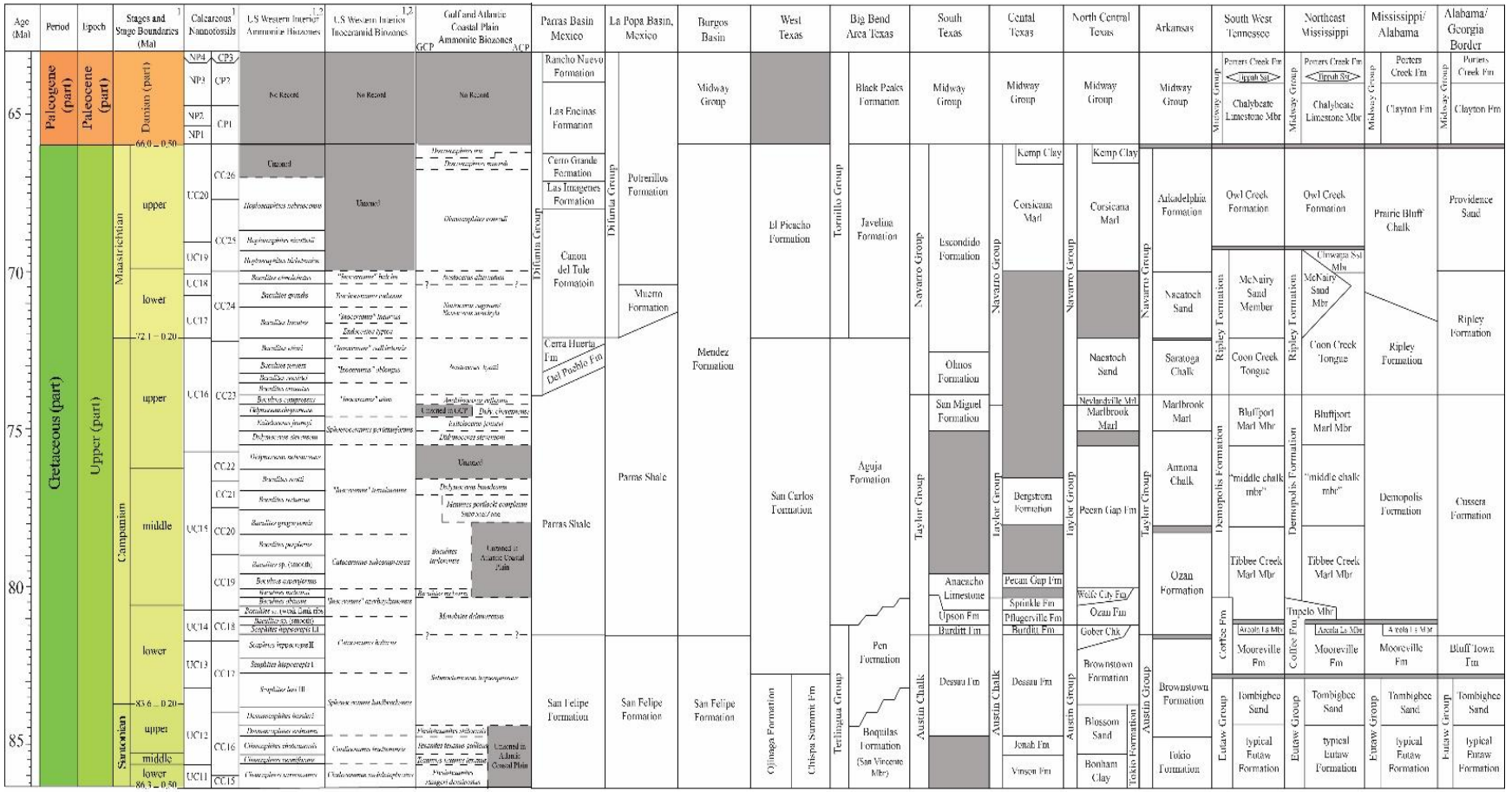

Figure. 3 Correlation chart of Campanian–Maastrichtian formations exposed along the Gulf Coastal plain (Chrono- and biostratigraphy based on 1) Ogg and Hinnov, 2012; 2) Cobban et al., 2006; Lithostratigraphy predominately based on data contained in Stephenson, 1941, Stephenson et al., 1942; Sohl, 1960; 1964; Maxwell et al., 1967; Pessagno, 1969; McBride et al., 1974; Sohl and Koch, 1986; Young, 1985; 1986; Sohl et al., 1991; Dockery, 1990, 1996; Mancini et al., 1996; Kennedy and Cobban, 1993a, b, d, e; 1999; 2001; Cobban and Kennedy, 1991b, c; 1992a, b; 1993a; 1994a, b; 1995; Kennedy et al., 1997a, b, c; 2001; Goldhammer, 1999; Ifrim et al., 2005; Cobban et al., 2008; Ifrim and Stinnesbeck, 2010; Larina et al., 2016; Dockery and Thompson, 2016). Dashed lines indicate approximate placement of biozonal boundaries. Boundaries or biozones with question marks indicate questionable placement of boundaries or biozones in region, respectively.

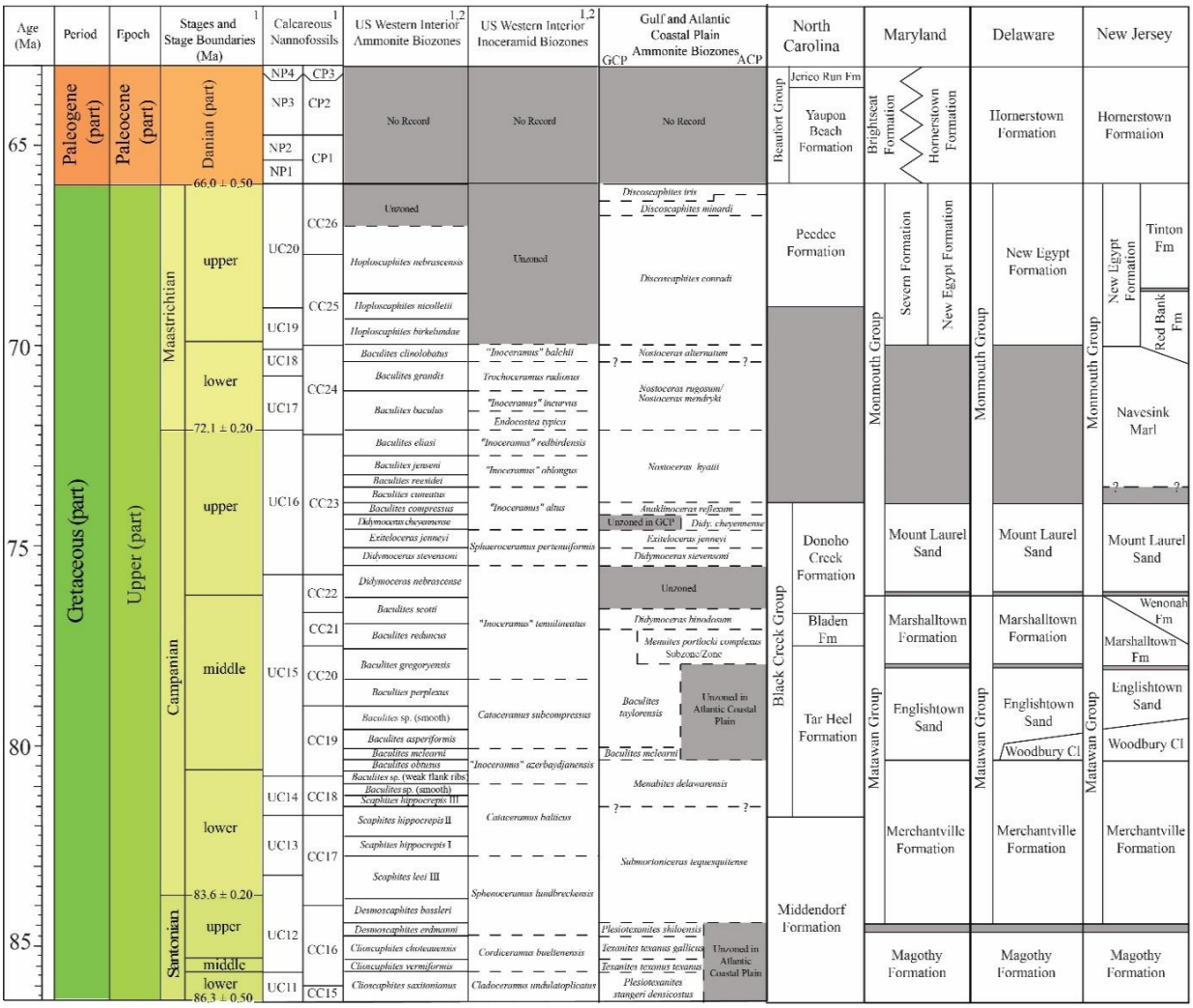

Figure 3.4. Correlation chart of Campanian–Maastrichtian formations exposed along the Atlantic Coastal plain (Chrono- and biostratigraphy based on 1) Ogg and Hinnov, 2012; 2) Cobban et al., 2006; Lithostratigraphy predominately based on data contained in Stephenson et al., 1942; Minard, 1980; McLaurin and Harris, 2001; Sohl et al., 1991; Kennedy and Cobban, 1991, 1993c, 1994a, b, 1996; 1997; Kennedy et al., 1997a, b, c; 2000c; Pierson, 2003; Landman et al., 2004a, b; 2007;). Dashed lines indicate approximate placement of biozonal boundaries. Boundaries or biozones with question marks indicate questionable placement of boundaries or biozones in region, respectively.

resulting in numerous condensed beds (Becker et al., 1996; 1998). Siliciclastic sedimentation and subsidence rates were highest in the western parts (e.g., Rio Grande Embayment) of the GCP due to their proximity to the active Cordilleran Orogenic Belt, which resulted in more expanded sedimentary sequences in southern Texas and northeast Mexico (Sohl et al., 1991; Galloway,

2008). Carbonate deposition was most prevalent in tropical to subtropical areas, such as in the Florida and Yucatan peninsulas (Sohl et al., 1991).

The entire area is underlain by various structural features that resulted in a series of basins or embayments separated by structural highs or arches (Fig. 3.1). Most of these structural elements are the result of pre-existing basement features, volcanism, and extensional mechanisms related to the opening of oceanic basins (Owens and Gohn, 1985; Sohl et al., 1991; Cox and Van Arsdale, 1997, 2002; Galloway, 2008; Miall et al., 2008; Dockery and Thompson, 2016). The structural geology of the GCP has also been influenced by the formation of diapirs, which are driven by upward mobilization of Jurassic salts (Owens and Gohn, 1985; Galloway, 2008; Miall et al., 2008). These structural elements controlled sediment supply, accommodation space, and accumulation patterns (Sheridan, 1974; Galloway, 2008). Campanian–Maastrichtian strata may be absent over structural highs but can range up to 1300 m in thickness in basins or embayments (Sohl et al., 1991).

Biostratigraphic Zonal Concepts

Different biostratigraphic zonal concepts have been applied to the ACP and GCP over the past century, including total range, interval, assemblage, and abundance or Oppel biozones (Fig. 3.5A-E). Early workers rarely defined the biozonal concepts used in their zonal schemes. However, most appear to be total range biozones (Fig. 3.5A), which are favored when index species are common to abundant both spatially and stratigraphically. Consequently, many ACP and GCP biozones erected in the early 20th century selected the most abundant taxa in a stratigraphic interval, which typically only had local use for correlation due to uneven preservation and limited facies distribution. Relatively abundant fossils and widespread depofacies is why most ammonite- and bivalve-based biozones in the Cretaceous WI are defined

as total range biozones. However, in contrast to the WI, ammonites in the ACP and GCP are generally rare to uncommon in most stratigraphic sections, which is likely due to various taphonomic and preservational artefacts (see discussion below). As a result, most modern workers, until recently, have used assemblage biozones to define the ACP and GCP ammonite biostratigraphy (i.e., Young, 1963; Cobban and Kennedy, 1995; Kennedy *et al*., 1997c). Assemblage biozones, which are a body of strata characterized by three or more fossil taxa, are generally useful in regions with uneven distribution of fossils since the identification of a biozone relies on multiple taxa (Fig. 3.5B and C). For these types of biozones to be meaningful, it is necessary to define their boundaries (e.g., lowest and upper boundaries defined by the first and last appearances of multiple taxa). However, most proposed ACP and GCP assemblage biozones do not follow the formal definition for this type of biostratigraphic unit as defined in the North American and International stratigraphic codes. Instead these zonations are typically defined by the total range of the eponymous taxa and correlated across the broader regions based on their associated molluscan assemblages (e.g., Young, 1963). More recently, workers have begun to use abundance and interval biozones to define the biostratigraphic schemes for the upper Maastrichtian. Abundance biozones (Fig. 3.5D), which are a body of strata characterized by the maximum abundance of index species, have been used in the ACP (i.e., Landman et al., 2004a) and likely only have local significance due to changes in facies and population dynamics. The use of interval biozones (i.e., Larina et al., 2016), which are defined by a body of strata constrained by two specified datums (usually the first or last occurrence of two separate species), is typically favored by most modern biostratigraphers and used here to define the ACP and GCP biozones (Fig. 3.5E).

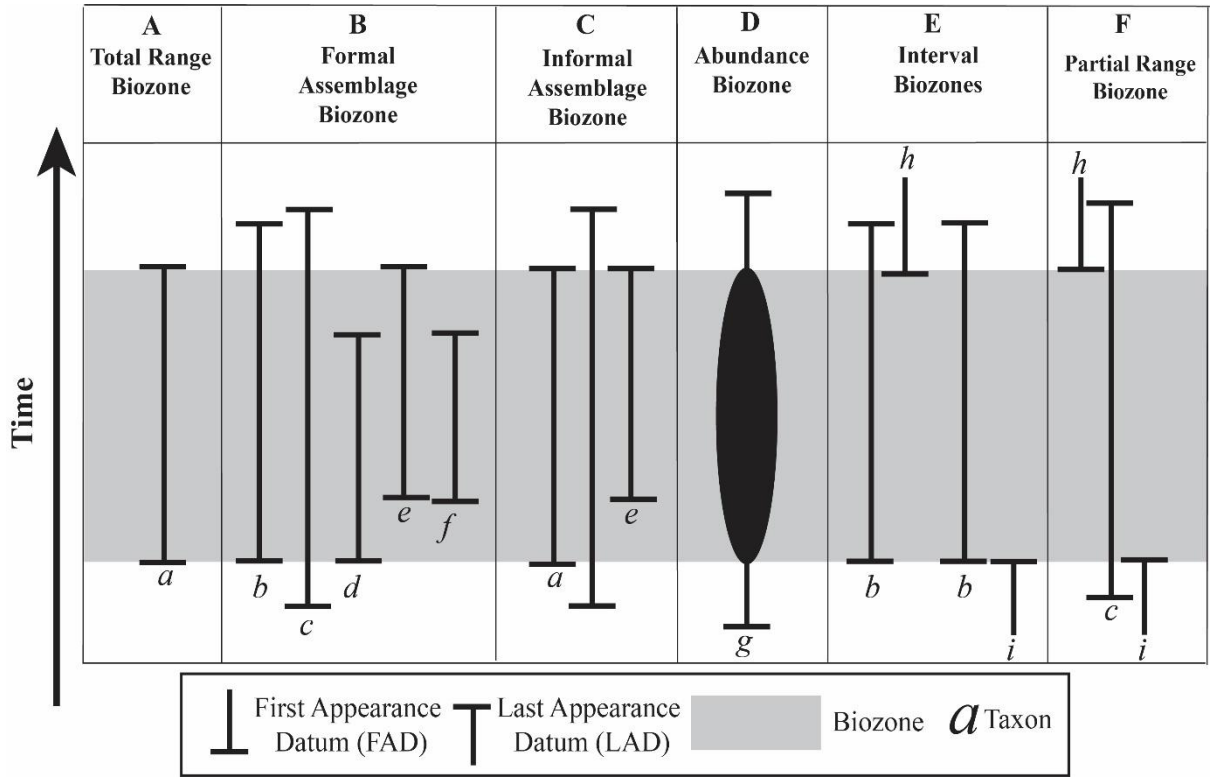

Figure 3.5. Examples of different biozone concepts used in the Gulf and Atlantic Coastal Plains.

Ammonite and Inoceramid Zonation of the Western Interior

Both the ACP and GCP share numerous ammonite and inoceramid bivalve species with the WI; the latter has one of most refined macrofossil biostratigraphic frameworks globally that has been calibrated using $^{40}Ar/^{39}Ar$ and $^{206}Pb/^{238}U$ dating of numerous ash beds (Obradovich, 1993; Kowalis *et al*., 1995; Cobban *et al*., 2006; Meyers *et al*., 2012; Ogg and Hinnov, 2012; Eldrett et al., 2015). These shared species allow for high-resolution correlations, which are used in this compilation to constrain (or bracket) the age and duration of GCP and ACP ammonite zones. Here, we provide a brief overview of the currently accepted biozonation used for the Campanian–Maastrichtian in the WI used in this analysis.

The Campanian–Maastrichtian ammonite and inoceramid biostratigraphic frameworks in the WI consist of 29 and 13 range zones, respectively (Fig. 3.6; also see Cobban *et al*., 2006).

The WI ammonite zones range from 0.4 to 0.9 Ma in duration, whereas the inoceramid zones range from 0.4 to 2.7 Ma. The ammonite and inoceramid record in the WI ends well-below the K/Pg boundary due to regression and the deposition of mainly terrestrial lithofacies across the region (e.g., Slattery *et al*., 2015). The highest ammonite zone (i.e., *Hoploscaphites nebrascensis* Biozone) in the WI occurs in the Breien Member of the Hell Creek Formation of North Dakota (see Hoganson and Murphy, 2002), which was deposited between 66.5 to 67 Ma (see Johnson *et al*., 2002). The highest inoceramid record (i.e., *Endocostea*) in the WI occurs in the *H. nicolletti* Biozone of the Fox Hills Formation, which ranges from 69.30 to 68.69 Ma (Ward *et al*., 1991; Ogg and Hinnov, 2012). The lack of ammonites and inoceramids above this interval makes it impossible to use the WI record to constrain the ages of the highest Cretaceous ammonite zones present in the ACP and GCP. Thus, it is necessary to use other taxonomic groups, such as dinoflagellates, to determine their age (e.g., Larina *et al*., 2016).

Correlation between the WI and other parts of the globe (e.g., Europe; North Africa) relies on bio-, magneto-, and chemostratigraphic frameworks. Traditionally, biostratigraphic coorelation has been a challenge due to the lack of cosmopolitan ammonites and a paucity of microfossils typically used for global correlation (Cobban *et al*., 2006; Walaszczyk et al., 2008; Ogg and Hinnov, 2012). Most index ammonites used for the WI and/or North American biozonation are endemic; however, a few species, such as *Didymoceras stevensoni, D. nebrascense,* and *D. cheyennense*, are also found in Europe and the Middle East (Larson *et al*.,

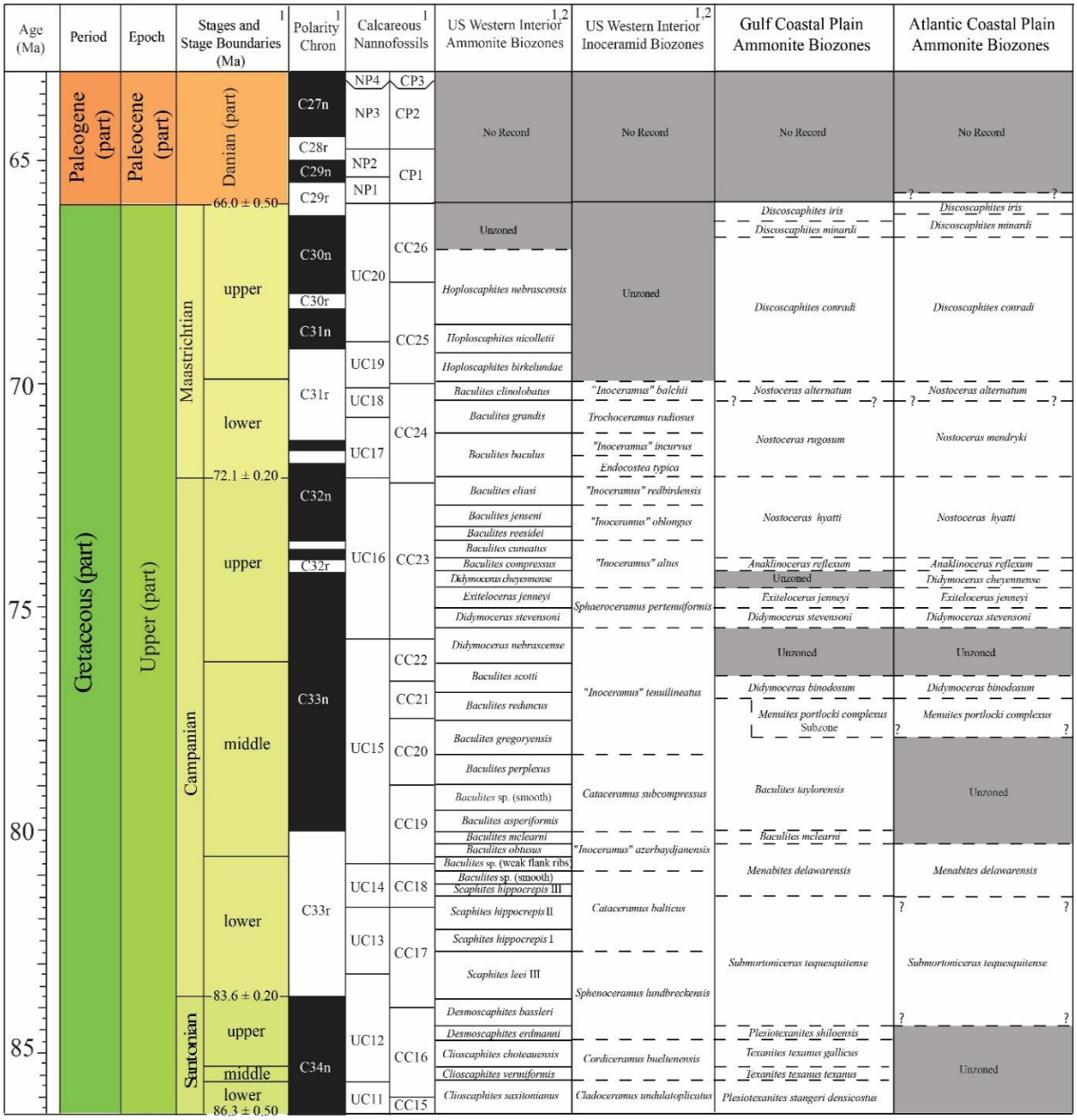

Figure 3.6. Biozonal table for the Campanian and Maastrichtian of the Western Interior, Atlantic Coastal Plain, and Gulf Coastal Plain calibrated to the currently accepted geochronological time scale (Chrono-, magneto-, and biostratigraphy based on 1) Ogg and Hinnov, 2012; 2) Cobban et al., 2006). Dashed lines indicate approximate placement of biozonal boundaries. Boundaries or biozones with question marks indicate questionable placement of boundaries or biozones in region, respectively.

1997; Cobban *et al*., 2006). Also, due to the widespread biogeographic distribution of inoceramids during the Campanian–Maastrichtian, numerous species found in the WI and their associated biozones are shared with the European Cretaceous (Cobban *et al*., 2006). This similarity in inoceramid zonation and faunas has enabled biostratigraphic correlation between most European macrofossil zones and global microfossil zones (e.g., planktic foraminifera, calcareous nannofossils) to that of North American. Campanian–Maastrichtian correlation has also been facilitated via magneto- and Sr-isotope stratigraphy (Hicks *et al*., 1999, 2002; Cobban *et al*.; 2006; McArthur *et al*., 2016), which are independent correlation methods.

Stage and Substage Divisions

To date, the definitions of the stage and substage boundaries of the Campanian and Maastrichtian, with the exception of the boundary between these two stages, remain provisional (Fig. 3.6). Therefore, most authors typically use the recommendations of the 1995 Brussels' Symposium on Cretaceous Stage Boundaries for the biozonation of the Campanian–Maastrichtian (Rawson *et al*., 1996; Ogg and Hinnov, 2012) as briefly outlined below in combination with more-recent revisions.

The Santonian-Campanian boundary is provisionally defined by the extinction of the cosmopolitan crinoid *Marsupites testudinarius* (Hancock and Gale, 1996; Gale *et al*., 2008). However, this species is likely facies restricted and is not a useful index fossil for this boundary in all settings (Ogg and Hinnov, 2012). Thus, the Campanian Working Group has suggested using the base of Chron C33r as the primary boundary marker due to its position close to the extinction of *M. testudinarius* (see Ogg and Hinnov, 2012). In the WI, the base of the Campanian is typically correlated with the base of the *Scaphites leei* III Biozone (Fig. 3.6; Cobban *et al*.,

2006), which has been constrained by $^{40}Ar/^{39}Ar$ dates from ash beds to 84.2 ± 0.4 Ma (Sageman *et al*., 2014).

The classic European Campanian has traditionally been subdivided into lower and upper parts; however, Rawson et al. (1996) recommended a tripartite subdivision, similar to that used in the WI. Since there are no formal definitions for these substages, we follow those established for the WI. Cobban *et al*. (2006) defined the bases of the middle and upper Campanian on the first appearance of the *Baculites obtusus* and *Didymoceras nebrascense*, respectively. However, owing to endemism of these taxa or rarity in other parts of the world, correlation outside the WI requires the use of Euroamerican inoceramid bivalves '*Inoceramus*' *vorhelmensis*, and '*I.*' *tenuilineatus*, which are geographically more widespread (Walaszczyk et al. 2001, 2002a, b; Odin and Walaszczyk, 2003; Walaszczyk, 2004).

The position of the Campanian–Maastrichtian stage boundary was ratified by the International Commission on Stratigraphy based on the average stratigraphic position of 12 bioevents recognized at the Tercis les Bains (SW France) stratotype section that have potential for correlation with other regions (Odin, 1996, 2001; Odin and Lamaurelle, 2001). In terms of inoceramids, this boundary correlates with the upper part of the '*I.*' *redbirdensis* Biozone and the first appearance of *Endocostea typica* (Walaszczyk et al., 2002a; Odin and Walaszczyk, 2003; Ogg and Hinnov, 2012). The classification of this boundary correlates with the basal Maastrichtian *B. baculus* Biozone in the WI, which has an age date based on spline fitting of ash beds of 72.1 ± 0.2 Ma (Cobban et al., 2006; Ogg and Hinnov, 2012).

The Maastrichtian is currently subdivided into lower and upper parts (Odin, 1996; Ogg and Hinnov, 2012). In northern Europe, the lowest upper Maastrichtian is defined by the base of the *Belemnitella junior* Biozone, which closely correlates with the first appearance of the

ammonite *Menuites fresvillensis* (Schulz *et al.* 1984; Odin, 1996; Walaszczyk et al., 2010). This boundary is equivalent to the upper part, or potentially the top of the biozone defined by the inoceramid *Trochoceramus radiosus* (see Walaszczyk et al., 2009, 2010; Walaszczyk and Kennedy, 2011). In the WI, the lowest upper Maastrichtian is informally placed as the first appearance of the index ammonite *Hoploscaphites birkelundae* (Landman and Waage, 1993; Cobban, 1993; Cobban et al., 2006).

The base of the Danian, which is delineated by the Cretaceous-Paleogene (K-Pg) boundary, was ratified by the International Commission on Stratigraphy based on a section near El Kef, Tunisia (Molina *et al*., 2006; Vandenberghe *et al*., 2012). It is defined as the base of a rusty colored, 50–cm-thick boundary clay, which contains an iridium anomaly, microtektites, Ni-rich spinel crystals and shocked quartz formed during a bolide impact. Similar features can be traced across the globe, including North America (Molina *et al*., 2006; Vandenberghe *et al*., 2012; Landman *et al*., 2007; 2012). The K/Pg boundary in the GCP is characterized by a hiatus and, in certain localities such as Moscow Landing, evidence of deformation and downcutting (Hart *et al*., 2013; Larina *et al*., 2016). The exact amount of time missing at the boundary in the GCP is debated, but recent biostratigraphic work suggest it is less than 350 ka (Hart *et al*., 2013; Larina *et al*., 2016). The iridium anomaly is known from the ACP; however, it is debated if this record is continuous (like El Kef, Tunisia) or represents a deposit that was eroded and then reworked into slightly older beds through bioturbation or chemical diffusion (Landman *et al*., 2007; 2012). For the ACP and GCP, we define the base of the Danian as the distinct K-Pg boundary beds and/or the lowest appearance of *in situ* Danian fauna, including the bivalve *Pycnodonte pulaskensis* and dinoflagellate *Carpatella cornuta*.

Nature of the Record

The ACP and GCP Campanian–Maastrichtian ammonite biostratigraphic record, as with any paleontological record, has been influenced by various sampling, geologic, and taphonomic biases. These biases have led to an incomplete/fragmentary record of ammonite ranges at the local scale, which in turn have resulted in a much more poorly resolved understanding of ammonite biostratigraphic and temporal distributions from these areas as compared to other regions, such as the Western Interior. Each of these biases were expressed at different temporal and spatial scales along the ACP and GCP due to changes in local structural features, accommodation space, sedimentation patterns, and water depths through time across the ACP and GCP. These factors have contributed to dissimilar paleontologic records due to the differential preservation across these regions, leading to large variability in ammonite occurrences between sections.

The amount of available exposed sedimentary rock area is one of the most important factors that influence the ACP and GCP ammonite records. This variable exerts a significant control on reconstructed species diversity and also determines the age coverage of strata exposed in a given area (e.g., Raup, 1976). Even where units are potentially exposed at the surface, there are three constraints that limit their accessibility: soil development, overgrowth by vegetation, and urbanization. Thick soil horizons and vegetation throughout the ACP and GCP limit exposures to areas where natural river cuts or manmade features, such as borrow pits, construction sites, mines/quarries, and road/railroad cuts, expose the underlying geology. Even where exposures are available, many outcrops have been lost from the expansion of invasive plant species, such as kudzu, which has overgrown many localities in the southern ACP and eastern GCP (G. Phillips and N. Landman, pers. comm.). Given these limitations, they usually

only reveal relatively limited portions of much more extensive strata, which has, on a number of occasions, resulted in limited understanding of ammonite ranges and confusion over the exact stratigraphic placement of some biozones (e.g., see discussion on the *Discoscaphites iris* and *D. conradi* biozones below). Only in the arid western part of the GCP (i.e., Big Bend area, Texas and northern Mexico) are more widespread natural exposures relatively common due to a limited vegetation cover, which has, at least to a degree, contributed to the more extensively documented Cretaceous biostratigraphic record as compared to the eastern portion of the GCP or the ACP (e.g., Cobban et al., 2008). However, even in the western GCP, most Campanian–Maastrichtian rocks, besides being predominantly non-marine, are only exposed in association with tectonic uplifts and in areas where Cenozoic strata have been stripped by erosion. A more contemporary factor impacting the amount of available outcrop area for sampling of ammonites and strata of different ages is the growing loss of fossil localities due to manmade developments, encompassing stabilization of road cuts or canals, building over fossil sites, and increasingly limited access to exposures on private and/or public lands. This has resulted in the loss of numerous classic localities along the GCP and almost 50% of the localities along the ACP in the last 40 years (Johnson, pers. obser.).

While the extent of biostratigraphic sampling is undoubtedly impacted by ground cover and human activities, the ultimate limiting factors influencing preservation and biostratigraphic ranges of fossils are the total volume and thickness of available strata in the rock record, which is directly controlled by the tectonic setting, sedimentation, and eustasy. For example, the huge sediment influx and tectonically driven basin subsidence produced as a result of the Cordilleran Orogeny, generated widespread and relatively thicker packages of strata in westernmost part of the GCP and Western Interior Foreland Basin (WIFB) during the Campanian–Maastrichtian

(Sohl et al., 1991; Robinson Roberts and Kirschbaum, 1995; Slattery et al., 2015). This active tectonic setting created accommodation space for hundreds to thousands of meters of section, widespread exposures, numerous volcanic ash beds useful for radiomentric dating, and an extensive fossil record for high resolution bio- and chronostratigraphic analysis (Kauffman, 1977; Kauffman et al., 1993). Such a high-resolution bio- and chronostratigraphic analysis is not possible for the passive margin settings of the eastern GCP and ACP, where the equivalent rock record is condensed into tens to hundreds of meters of strata with numerous unconformities, few dateable volcanic sediments, and fossils concentrated within relatively short stratigraphic intervals (e.g., Becker et al., 1996; 1998; Larina et al., 2016). In these Late Cretaceous passive-margin settings, sediment deposition was primarily controlled by eustatic changes, long-term (>1 Ma) sediment starvation, and low subsidence rates (Sohl et al., 1991; Galloway, 2008). Even where greater tectonic control was influential due to the proximity of the Cordilleran Orogen, sedimentation rates were still much lower than in the WIFB thus producing relatively thinner sections (Sohl et al., 1991; Galloway, 2008).

As in many shallow-water settings, ACP and GCP ammonites are usually not evenly distributed throughout stratigraphic sections but are commonly concentrated into discrete fossiliferous beds or stratigraphic horizons reflecting different degrees of time averaging as well as favorable taphonomic/diagenetic histories and which are separated by non- to poorly fossiliferous strata (Becker et al., 1996, 1998; Kidwell, 1998). This distributional pattern makes it unlikely that sampled specimens will represent an ammonite's entire stratigraphic/age range, even if large exposures are available. This poses challenges, especially if attempts are made to use the local appearance or disappearance of ammonites in the stratigraphic record as benchmarks for chronostratigraphic correlation/determination. These fossil concentrations

typically reflect sequence or parasequence boundaries formed through sediment starvation, sediment reworking resulting in the mixing of different aged fossils, or through differential preservation and dissolution of aragonite (Becker et al., 1996, 1998; Kidwell, 1998).

In the ACP and eastern GCP, ammonites are frequently concentrated with other fossils at sequence boundaries into thin fossiliferous beds termed condensed zones or 'biostratigraphically condensed zones' (*sensu* Heim, 1934; Kidwell, 1998) that are separated by meters or in some cases hundreds of meters of poorly fossiliferous or non-fossiliferous strata. These biostratigraphically condensed zones form in areas of low sedimentation as a result of erosion of the sea bottom, which results in the accumulation of fossils with different ranges/ages being hydrodynamically transported/sorted and eventually deposited into a lag on the erosional surface. These beds are eventually preserved through burial during the next transgressive pulse (Becker et al., 1996; 1998). A classic example of this is a 30 cm layer of reworked fossils, matrix, and nodules at the base of the Navesink Formation called the 'basal lag deposit' (*sensu* Becker, et al., 1996). During this time, sediment-starved conditions had a sufficiently long duration to allow fossils of late Campanian age to accumulate and mix with fossils of early Maastrichtian age (Kennedy et al., 2000c).

Third-order (<1 Ma) sea-level changes also contributed to the concentration of ammonite and other fossils into discrete beds and/or concretionary horizons. These types of shell beds usually reflect flooding surfaces or parasequence boundaries formed through sediment starvation during sea-level rise (e.g., see Elder et al., 1994; McMullen et al., 2014). During these events, shells and organic debris accumulate on the sea floor, which can potentially lead to shell bed lithification or concretion formation during early diagenesis (Gautier, 1982, Maeda, 1987, Carpenter et al., 1988; Landman and Klofak, 2012; Feldman et al., 2012; Landman et al., 2015;

Slattery et al., 2018). Beds deposited under these conditions usually reflect much shorter durations of time averaging and generally preserve ammonites with similar known ranges representing a single ammonite biozone (e.g., the concretionary horizon documented in the Bergstrom Formation by Kennedy and Cobban, 1999).

Diagenesis of fossiliferous beds has also played a significant factor in limiting the abundances of ammonites and other molluscs in many beds in the ACP and GCP. For example, aragonitic fossils in the basal lag deposit of the Navesink Formation were dissolved prior to or after lithification, which left only coarse-grained, glauconitic internal molds whose juvenile/inner whorls are typically not preserved due to the coarseness of the sediments. This preservational issue has led to the misinterpretation that ammonites, as well as other molluscs, are underrepresented in this biostratigraphically condensed deposit (Johnson, pers. obser.). The dissolution of aragonitic taxa prior to or during the lithification of carbonates and marls have obliterated numerous ammonite records in many stratigraphic sections and restricted the biostratigraphic ranges of countless ammonite species to singles beds or 'taphonomic windows' in the GCP. The degree of loss of aragonitic taxa through diagenesis can be difficult to determine but is usually indicated by the relative abundance of calcitic taxa with a rarity of aragonitic forms typically preserved through bioimmuration or as xenomorphic features on the shells of calcitic forms. So-called 'taphonomic windows' typically preserve aragonitic taxa, such as ammonites, as molds or cast within beds, whereas the overlying and underlying strata are usually devoid of any evidence of aragonitic fossils. The dissolution of aragonitic ammonites has resulted in restricted stratigraphic ranges for many species across the GCP even when there are relatively expanded sections (e.g., see Gale et al., 1995).

These natural influences have partially resulted in disjunct biostratigraphic and biogeographic ranges of certain ammonite biozones and species across the ACP and GCP, which have also been confounded by research-related biases. For example, the lack of detailed biostratigraphic analysis of many areas and stratigraphic intervals with known ammonite occurrences has contributed greatly to the limited knowledge of Campanian–Maastrichtian ammonites in the southern ACP (e.g., North Carolina) and in Mexico In addition, some workers in the ACP and GCP have traditionally favored using museum collections over doing field work and have generally failed to document ammonite ranges within detailed measured sections. In these collection-based investigations, specimens are typically from exposures that no longer exist. While important from a taxonomic standpoint, specimens in older collections may often lack stratigraphic and even location data.

The rarity and concentration of ammonites at many sections in the ACP and GCP have led many workers to define most Campanian–Maastrichtian ammonite biozones in these regions as assemblage biozones instead of range or interval biozones as is done in the Western Interior or in Europe (e.g., Young, 1963). However, the use of assemblage biozones over other types of biozones in areas where ammonites are rare provides a means to correlate and determine the age of strata without having to locate a specific index species (Young, 1963).

Many of the biases and issues discussed here are beginning to be overcome through the re-examination and, in some cases, the redescription of many well-known ammonites faunas (e.g., Cobban and Kennedy 1995; Kennedy et al., 2000c) as well as detailed biostratigraphic studies over broad regions, as exemplified by Larina et al.'s (2016) recent analysis of the upper Maastrichtian ammonite biostratigraphy of the Mississippi Embayment in the GCP. Future work, utilizing modern quantitative stratigraphic and biochronolological techniques, such as graphic

correlation or constrained optimization, will likelyimprove correlation between sections and overcome many of the biases influencing the ACP and GCP biostratigraphic record.

Previous studies

Numerous authors have published biostratigraphic schemes for the Campanian–Maastrichtian of the ACP and GCP based on molluscs (Figs. 3.7–3.9). Many early works varied greatly in their biostratigraphic definitions for stages and substages, which resulted in differing opinions on boundary placement (Fig. 3.10). Most early biostratigraphic schemes were also only applicable to the local regions where they were erected and typically reflect the relative stratigraphic successions of index species within different formations without defining their precise stratigraphic/temporal ranges. This limited knowledge of stratigraphic/age ranges for specific biozones is indicated by the lack of zonal boundaries seen in Figure 3.7.

Stephenson (1914) was the first worker to propose a biostratigraphic scheme for the GCP and ACP using the bivalve *Exogyra* (Fig. 3.7). He proposed a lower *Exogyra ponderosa* Biozone with a *Mortoniceras* Subzone and an upper *E. costata* Biozone with a *Liopistha protexta* Subzone for the eastern GCP and ACP. Later, Stephenson (1923; 1928, 1933) and Stephenson et al. (1942) used the range of *E. ponderosa* to define the Campanian and *E. costata* as well as *E. cancellata* to delineate two distinct overlapping biozones for the Maastrichtian, which have retained their utility for correlation and age determination (Sohl et al., 1991). Until the early 1990s, this biozone transition was used to define the Campanian–Maastrichtian boundary in the ACP and GCP (e.g., Sohl et al., 1991). However, the current definition of this stage boundary (see Odin and Lamaurelle, 2001; Walaszczyk et al., 2001, 2002a,b; Ogg and Hinnov, 2012) places the top of Stephenson's Campanian–Maastrichtian boundary within the currently defined middle upper Campanian, and, as such, well below the base of the Maastrichtian (Fig. 3.10).

Böse and Cavins (1928) and Böse (1928) subdivided the Campanian–Maastrichtian of Texas and Mexico into two bivalve- and five ammonite-based biozones, respectively (Fig. 3.7). Adkins' (1928; 1933) review of the Texas Cretaceous subdivided the Campanian–Maastrichtian into 12 biozones, laying the groundwork for future biozonations of the Campanian in the GCP (Fig. 3.4). Stephenson (1936a) used ostreid and inoceramid bivalves for the zonal subdivision of the Coniacian to lower Campanian Austin Chalk of Texas; however, as noted by Young (1963), most of this work only allowed for local correlation among stratigraphic sections.

The mid-20th century saw the refinement of many of these earlier molluscan-based biostratigraphic frameworks and the development of the modern ammonite-based scheme used across the GCP (Fig. 3.7 and 3.8). Young and Marks (1952) refined the biozonation for the Austin Chalk developed by Stephenson (1936a) and correlated this local biozonation into Müller and Schenck's (1943) broader Cretaceous biostratigraphic framework. Richards (1958) used Stephenson's *Exogyra* framework for the Campanian–Maastrichtian to correlate the central ACP formations to those of the southern ACP and GCP. Sohl (1960; also see Sohl, 1977; Sohl and Koch, 1986) further subdivided Stephenson's *Exogyra* biozonation by proposing several new molluscan-based range and assemblage zones, which are useful for correlation across the ACP and GCP. Young (1963) proposed a fully ammonite-based biozonal scheme for the lower and middle Campanian of the GCP that integrated earlier biozonations from other authors with his studies on the ammonites of Texas. He subdivided the lower and middle Campanian of Texas into three assemblage biozones and one assemblage biozone, respectively. Similarly, Cooper (1970; 1971) built upon Böse and Cavin (1928) and Böse (1928) by refining and updating their earlier sphenodiscid-based biostratigraphic scheme for the Maastrichtian in South Texas and Mexico.

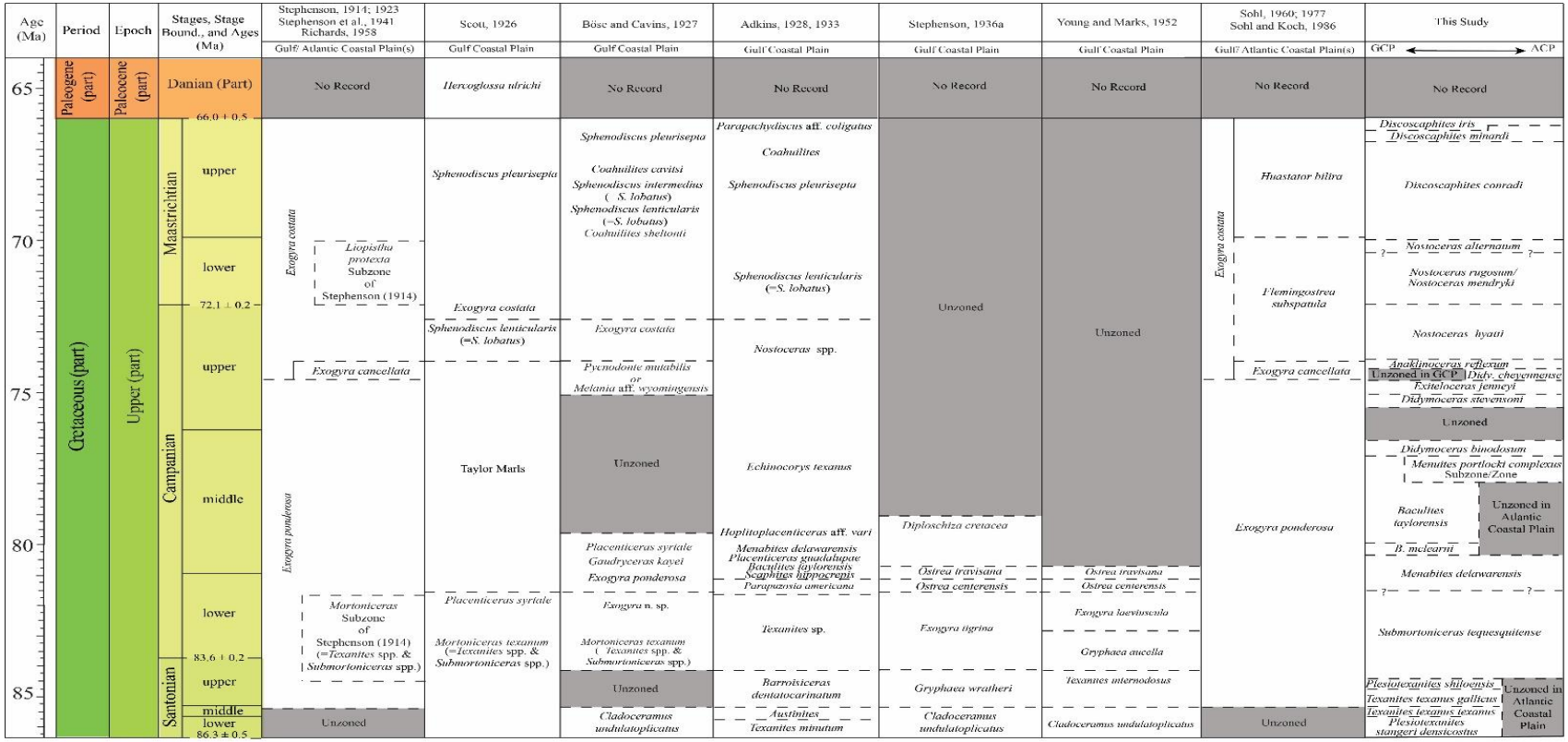

Figure 3.7. Comparison of Campanian–Maastrichtian biostratigraphic schemes for the Gulf and Atlantic Coastal Plains by different early to mid-20th century authors calibrated to the geochronological time scale of Ogg and Hinnov (2012) and the biostratigraphic framework proposed here. Dashed lines indicate approximate placement of biozonal boundaries. Boundaries or biozones with question marks indicate questionable placement of these elements.

In the late 20th century, ammonite workers continued building on the work of Young (1963) by expanding his biozonation into the upper Campanian and Maastrichtian as well as across the GCP (Fig. 3.8). Some workers also began linking these biozones to the Cretaceous chronostratigraphy based on radiometric dates as well as through correlation with well-dated biozones in the WI and Europe (e.g., Kauffman, 1979). This improved correlation with other regions resulted in greater consistency in stage and substage boundary placement (Fig. 3.5). Young (1969; 1982; 1985; 1986) expanded on his earlier ammonite zonation for Texas by informally proposing various different biostratigraphic schemes for the entire Campanian–Maastrichtian. He repeatedly redefined and adjusted the placement of several of his biozones through each successive study, but it is clear that he was uncertain about the full biostratigraphic and temporal ranges of his biozones. Kauffman (1979) expanded on Stephenson's (1914, 1923, 1928; 1933, 1936a) and Young's (1963) biozonation for the GCP by proposing several new biozones as well as correlating them with biozones in the WI and Europe. However, many of these proposed biozones were correlated to biozones in other regions without any explicit data supporting their assignments, which resulted in temporally misplaced biozones. A similar correlation problem is also apparent from Metz's (2000) Texas biozonation for the Campanian (Fig. 3.4).

Starting in the 1970s, Cobban, and later in collaboration with Kennedy and Landman, began a systematic description of the ACP and GCP Campanian–Maastrichtian ammonite faunas, which resulted in a better-defined biostratigraphic scheme for the GCP and the first ammonite zones defined for the ACP (Fig. 3.9). In addition, these authors proposed several new ammonite zones and redefined others (see below). These workers also clearly showed how these ammonite faunas and biozones correlated with more established biostratigraphic schemes in the

WI and Europe (e.g., Kennedy *et al*., 1992; Cobban and Kennedy, 1995). In the central ACP, such efforts

were, in no small part, made possible by extensive sampling by local collectors and societies, which contributed significant numbers of new ammonite specimens to this region's paleontological record. In spite of this extensive work, these workers never defined a biostratigraphic scheme for the middle to lower upper Campanian in the GCP or for the interval below the uppermost Campanian in the ACP (Fig. 3.4).

Further biostratigraphic definition and refinement continued into the early 21st century, although greater emphasis was placed on constraining the exact stratigraphic placement of different ammonite species and defining formal biozones. Landman *et al*.'s (2004a,b, 2007) and Larina *et al*.'s (2016) biostratigraphic studies in the ACP and GCP redefined the biozonal framework for the upper Maastrichtian proposed by Cobban and Kennedy (1995) and split this interval into three separate biozones. These authors also demonstrated that the K/Pg boundary is relatively biostratigraphically conformable throughout the ACP and GCP, which previously was thought to be marked by a long-term, widespread hiatus based on lithological evidence of an unconformity and the absence of upper Maastrichtian planktic foraminifera (e.g., Cepek and Hay, 1969; Mancini *et al*., 1996). In contrast, they showed this boundary to be much more stratigraphically complete with most unconformities having limited temporal and spatial extent

Cobban et al. (2008) redescribed the lower to middle Campanian biozones of west Texas and northeast Mexico, which, because of faunal similarities with the WI, improved correlation between these regions. During this same period, Ifrim and Stinnesbeck (2010, 2013) and Ifrim *et al*. (2004, 2010, 2013, 2015) began a systematic description of Mexican Campanian–Maastrichtian ammonite faunas, which resulted in biozonal extensions from the WI into the GCP

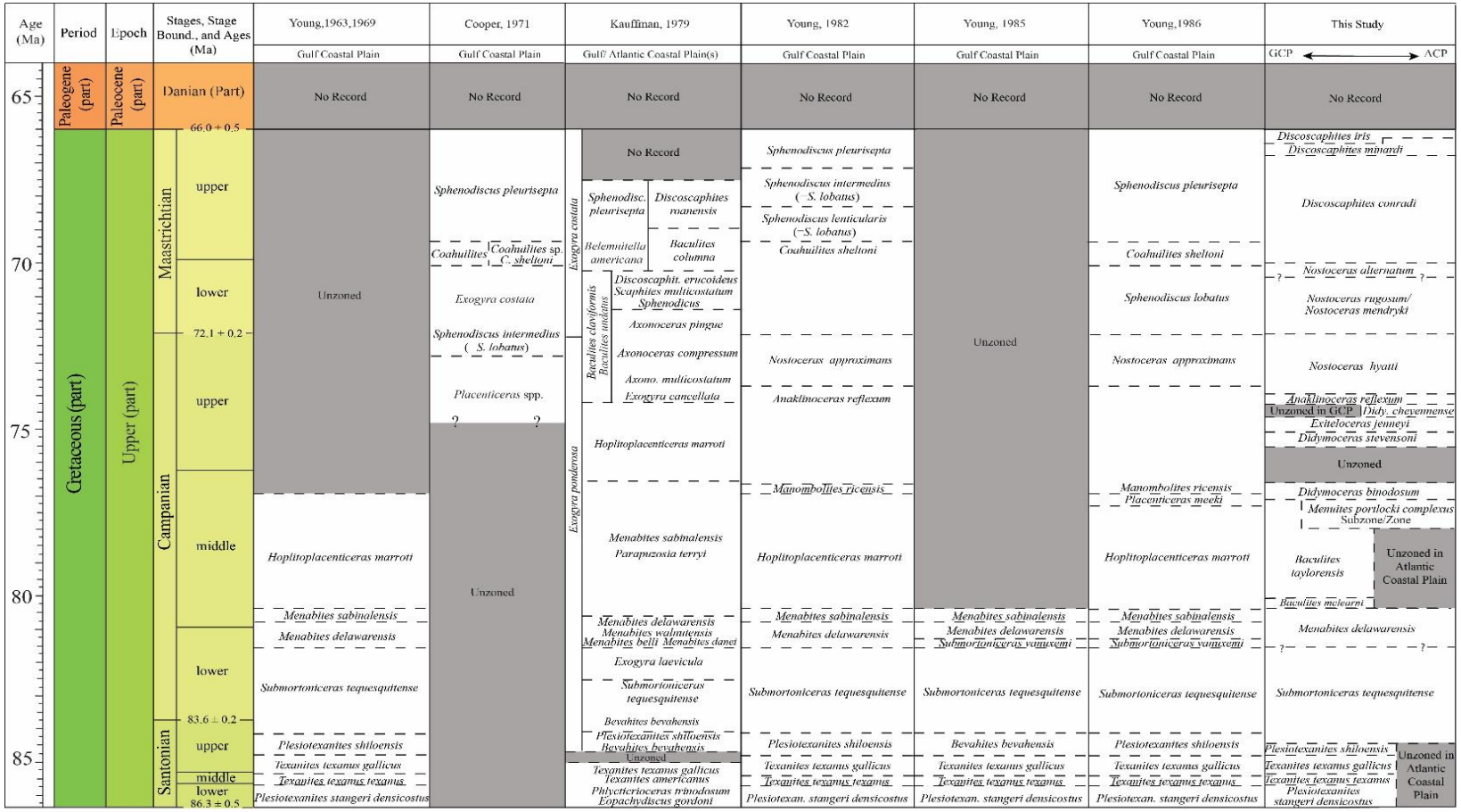

Figure 3.8. Comparison of Campanian–Maastrichtian biostratigraphic schemes for the Gulf and Atlantic Coastal Plains by different mid- to late-20th century authors calibrated to the geochronological time scale of Ogg and Hinnov (2012) and the biostratigraphic framework proposed here. Dashed lines indicate approximate placement of biozonal boundaries. Boundaries or biozones with question marks indicate questionable placement of these elements.

as well as improved correlation with the European scheme. Ifrim *et al*. (2005) also re-examined the sphenodiscid taxonomy and biostratigraphy established by Böse and Cavin (1928), Böse (1928), and later revised by Cooper (1970; 1971) for south Texas and northeast Mexico. This work revealed that this framework only had local significance for correlation and that it had a relatively poor biostratigraphic resolution due to the use of long-ranging taxa. Most recently, Larson (2016) proposed an ammonite zonation for the eastern GCP. However, many of his proposed ammonite zones were miscorrelated to the biozonation in the WI, which resulted in temporally misplaced biozones.

Methods

The age range of both ammonites and ammonite zones described below are based on the numerous published studies compiled in the reference list. All upper Maastrichtian ammonite biozones in the ACP and GCP are based on high-resolution stratigraphic sampling at various sections, which have provided an excellent record of the ranges of the species found within this interval (Landman et al., 2007; Larina et al., 2016). The exact range of ammonites found below the upper Maastrichtian are less well constrained due limited high-resolution biostratigraphic sampling of this interval, limited exposure of fossiliferous strata, and the occurrence of numerous condensed beds, which often correlate with two or more ammonite zones in the Western Interior. In these cases, age ranges were constrained by the association among ACP and GCP ammonites with taxa (i.e., ammonites, inoceramids) that are well-known biostratigraphically in the Western Interior. This method did not provide the true age range of a species; however, it did constrain the minimum and maximum ages of a biozone and species.

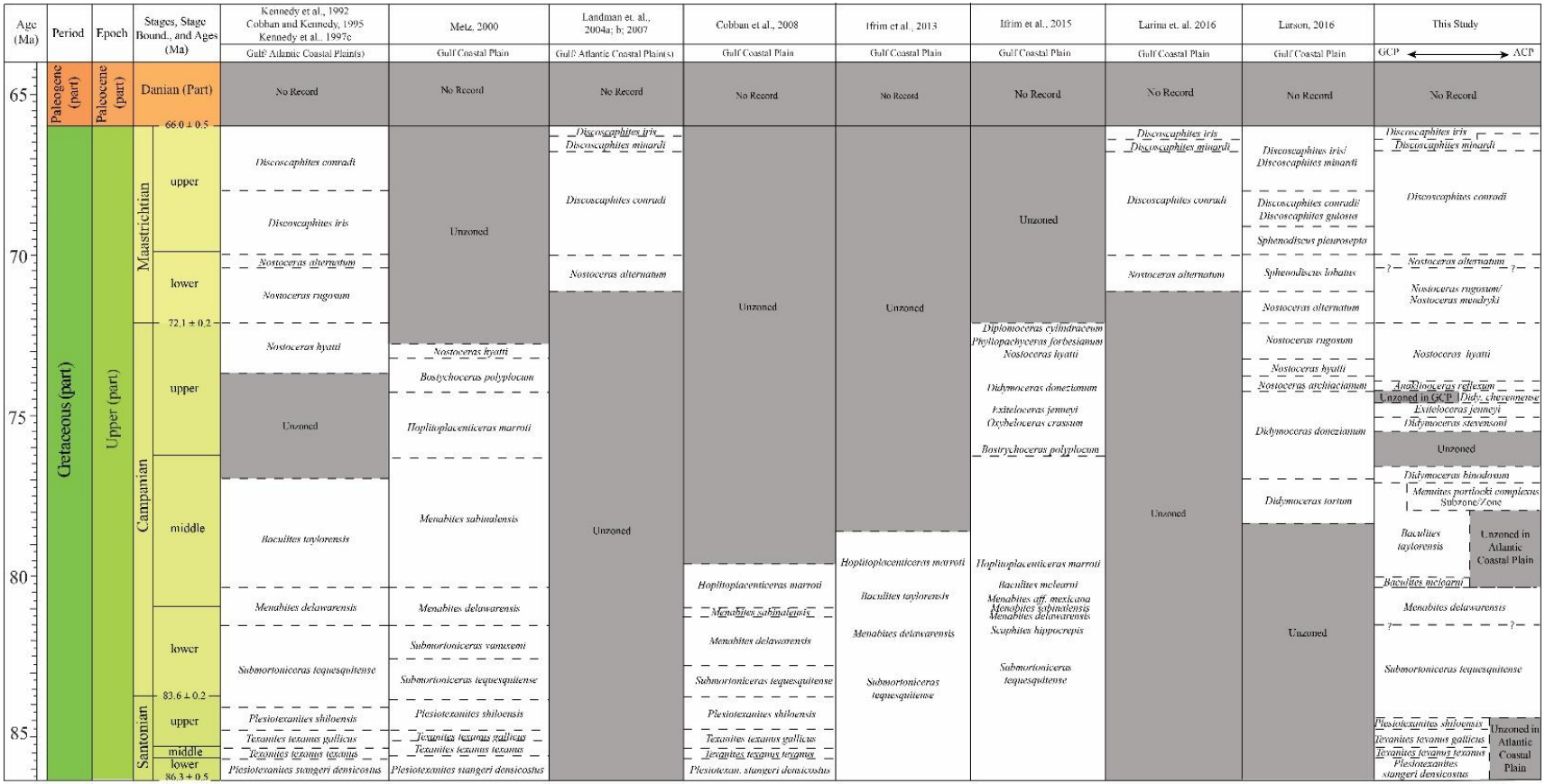

Figure 3.4. Comparison of Campanian–Maastrichtian biostratigraphic schemes for the Gulf and Atlantic Coastal Plains by different late-20th century authors calibrated to the geochronological time scale of Ogg and Hinnov (2012) and the biostratigraphic framework proposed here. Dashed lines indicate approximate placement of biozonal boundaries. Boundaries or biozones with question marks indicate questionable placement of these elements.

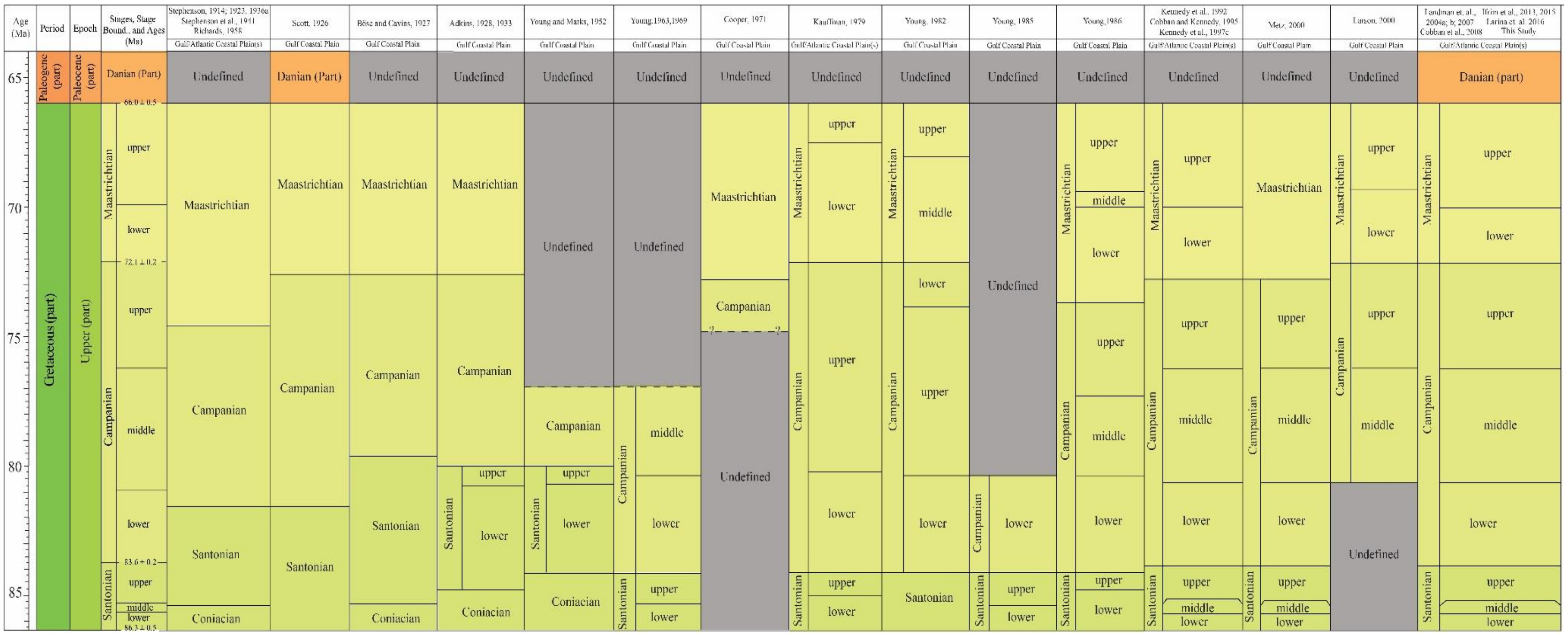

Figure 3.10. History of Campanian and Maastrichtian stage boundary placement from different authors molluscan-based biostratigraphic schemes shown in Figs. 3.3, 3.7, 3.8, and 3.9 for the Gulf and Atlantic Coastal Plains. Dashed lines indicate approximate placement of biozonal boundaries. Boundaries or biozones with question marks indicate questionable placement of these elements.

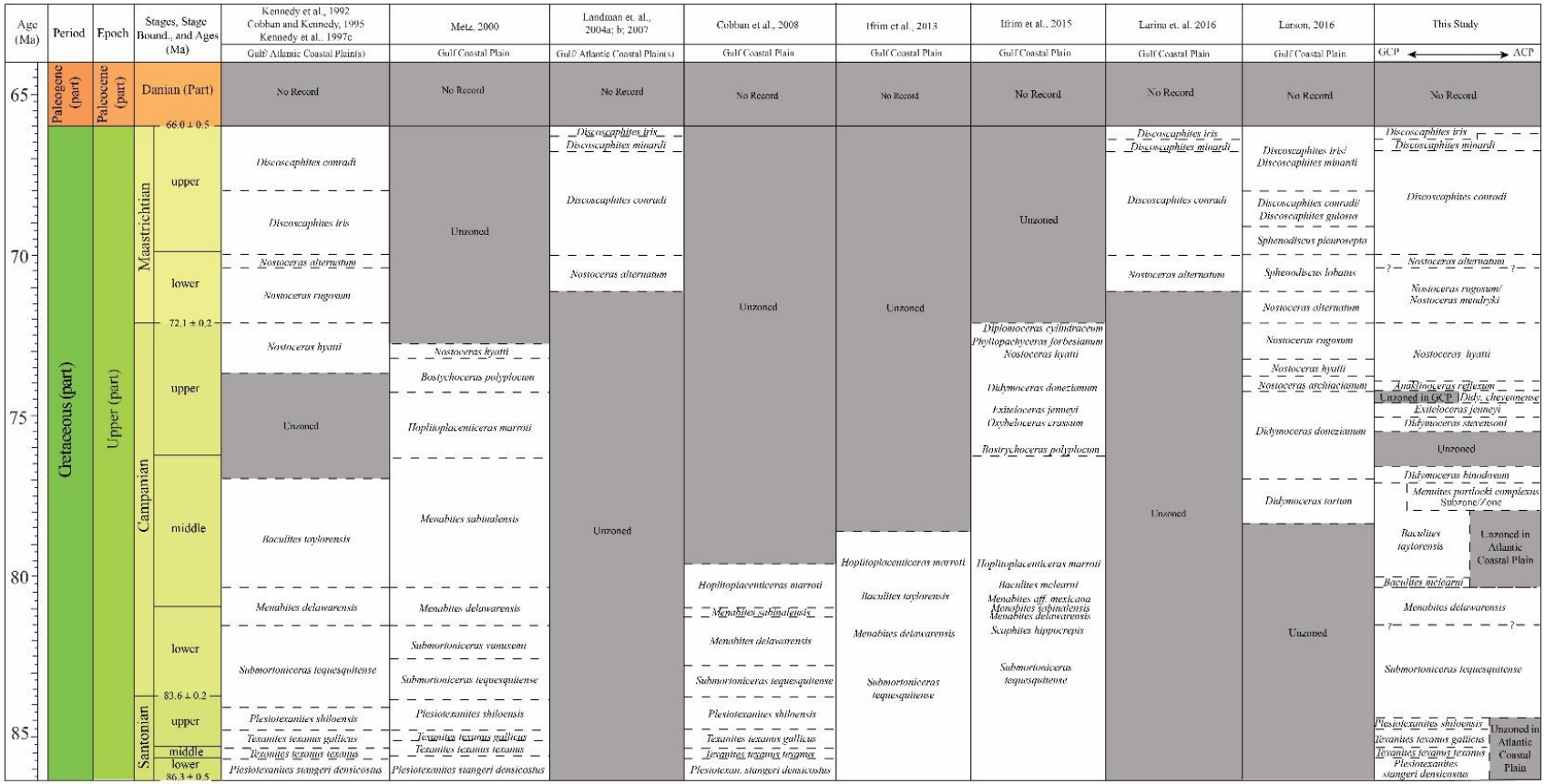

Figure 3.5. Comparison of Campanian–Maastrichtian biostratigraphic schemes for the Gulf and Atlantic Coastal Plains by different late-20th century authors calibrated to the geochronological time scale of Ogg and Hinnov (2012) and the biostratigraphic framework proposed here. Dashed lines indicate approximate placement of biozonal boundaries. Boundaries or biozones with question marks indicate questionable placement of these elements.

Definition of Ammonite Zones

Campanian Biostratigraphic Zones

We subdivide the Campanian (83.6–72.1 Ma) of the ACP and GCP into ten and eight ammonite zones, respectively (Fig. 3.6). In ascending order, the Campanian biozones include: *Submortoniceras tequesquitense*, *Menabites delawarensis*, *Baculites mclearni* (GCP only), *B. taylorensis* (GCP only), *Menuites portlocki complexus* (biozone in ACP and subzone of *B. taylorensis* in GCP), *Didymoceras binodosum*, *D. stevensoni*, *Exiteloceras jenneyi*, *D. cheyennense* (ACP only), *Anaklinoceras reflexum*, and *Nostoceras hyatti* biozones. Both regions are left unzoned for an interval roughly equivalent to the upper part of the WI *Baculites scotti* and *Didymoceras nebrascense* biozones (Fig. 3.6). Similarly, the GCP is left unzoned at a level corresponding to the WI's upper Campanian *Didymoceras cheyennense* Biozone, whereas the ACP is unzoned at an interval approximately equivalent to the GCP's middle Campanian *B. mclearni* and *B. taylorensis* biozones (Fig. 3.6). Six of these biozones, *B. mclearni*, *M. portlocki complexus*, *D. binodosum*, *D. stevensoni*, *E. jenneyi*, and *D. cheyennense*, are newly established for these regions and either replace biozones proposed by earlier authors or populate unzoned intervals for the middle to upper Campanian identified in Figure 3.4 as well as noted by Kennedy and Cobban (1993b). The Campanian ammonite zones range from ~0.3 to ~3.3 Ma induration (see Table 1). The ACP and GCP represent extensive areas with complex paleontological and geological records, and these biozones have not been identified throughout these regions (Fig. 3.7); therefore, the biostratigraphic schemes discussed below and shown in Fig. 3.6 are considered a composite regional biozonation.

Table 3.1. Campanian–Maastrichtian Gulf and Atlantic Coastal Plains ammonite zone ranges.

Biozone	Basal Age (Ma)	Top Age (Ma)	Duration
Discoscaphites iris	66.4	66.0	0.4
Discoscaphites minardi	66.8	66.4	0.4
Discoscaphites conradi	69.9	66.8	3.1
Nostoceras alternatum	70.4	69.9	0.5
Nostoceras mendryki	72.1	70.4	1.7
Nostoceras rugosum	72.1	70.4	1.7
Nostoceras hyatti	73.9	72.1	1.8
Anaklinoceras reflexum	74.2	73.9	0.3
Didymoceras cheyennense	74.6	74.2	0.4
Exiteloceras jenneyi	75.1	74.6	0.5
Didymoceras stevensoni	75.6	75.1	0.5
Didymoceras binodosum	76.8	76.2	0.6
Menuites portlocki complexus	77.9	76.8	1.1
Baculites taylorensis	80.2	76.9	3.3
Baculites mclearni	80.7	80.2	0.5
Menabites delawarensis	81.5	80.7	0.8
Submortoniceras tequesquitense	84	81.5	2.5

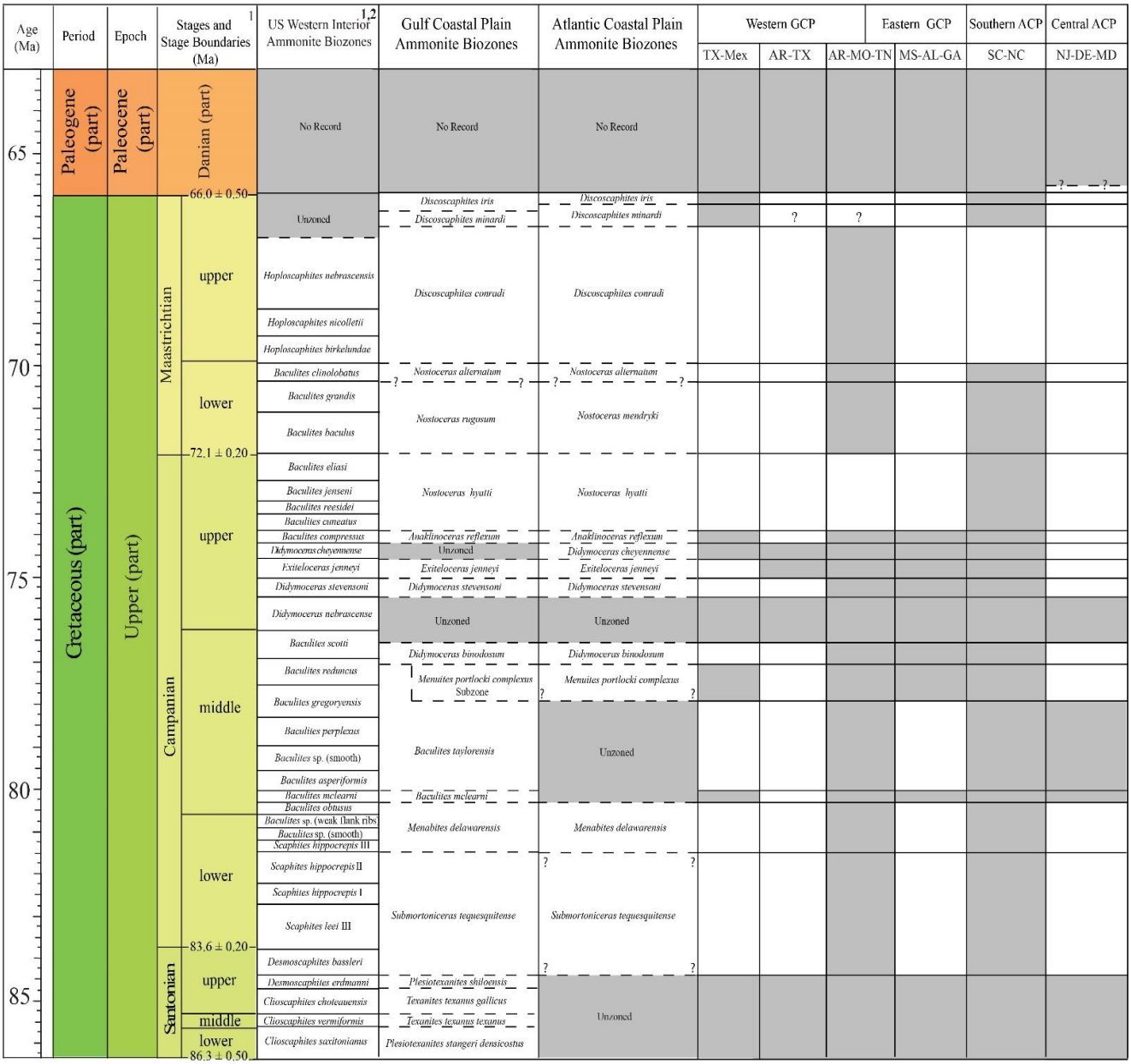

Figure 3.6. Table showing distribution of Campanian–Maastrichtian biozones across the Gulf and Atlantic Coastal Plains for the Santonian-Maastrichtian (Chrono-, magneto-, and biostratigraphy based on 1) Ogg and Hinnov, 2012; 2) Cobban et al., 2012). Dashed lines indicate approximate placement of biozonal boundaries. Boundaries or biozones with question marks indicate questionable placement of boundaries or biozones in region, respectively.

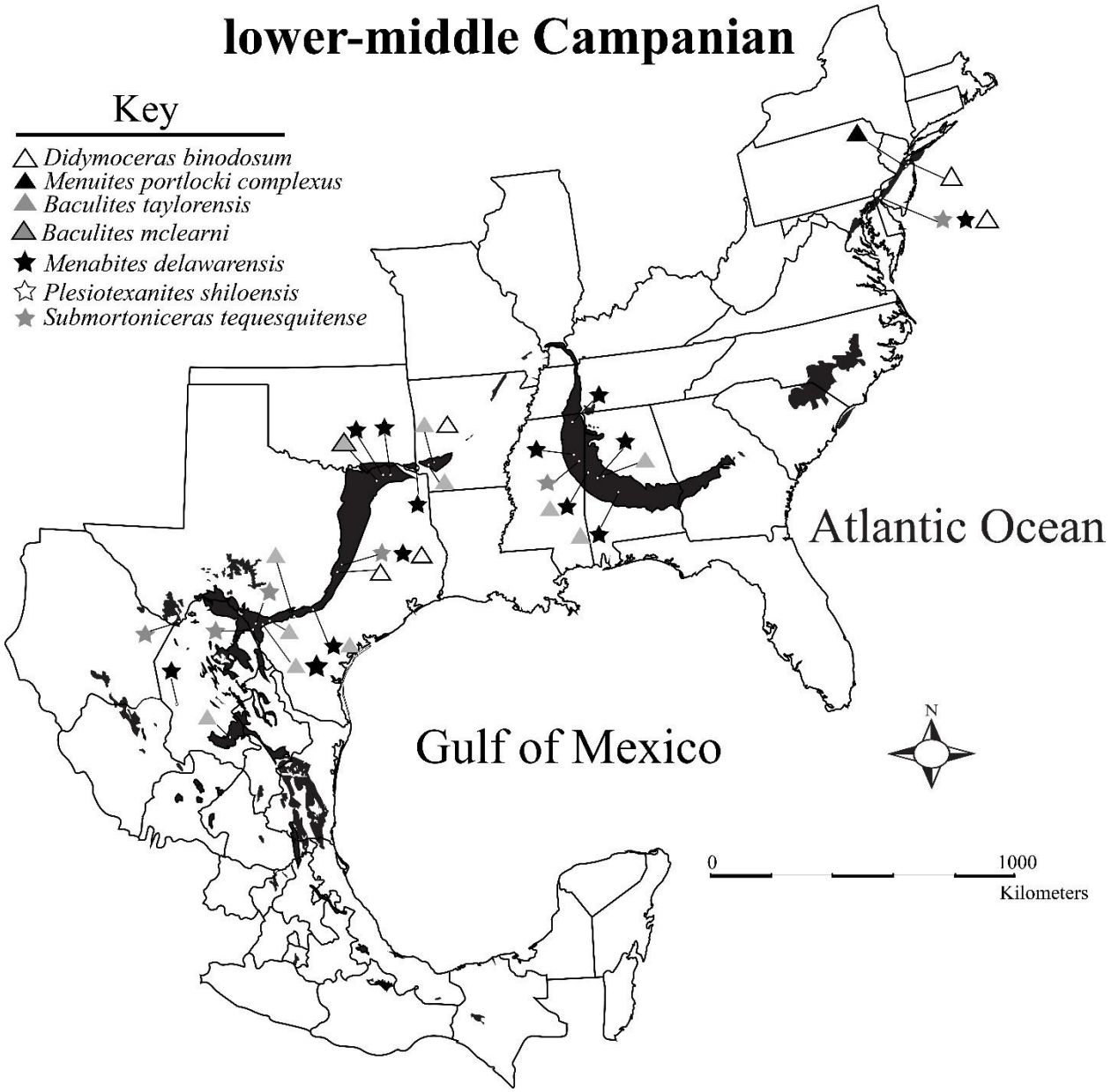

Figure 3.7. Map depicting the distribution of published localities (discussed and cited in text) with lower to middle Campanian biozones along the Gulf and Atlantic Coastal Plains.

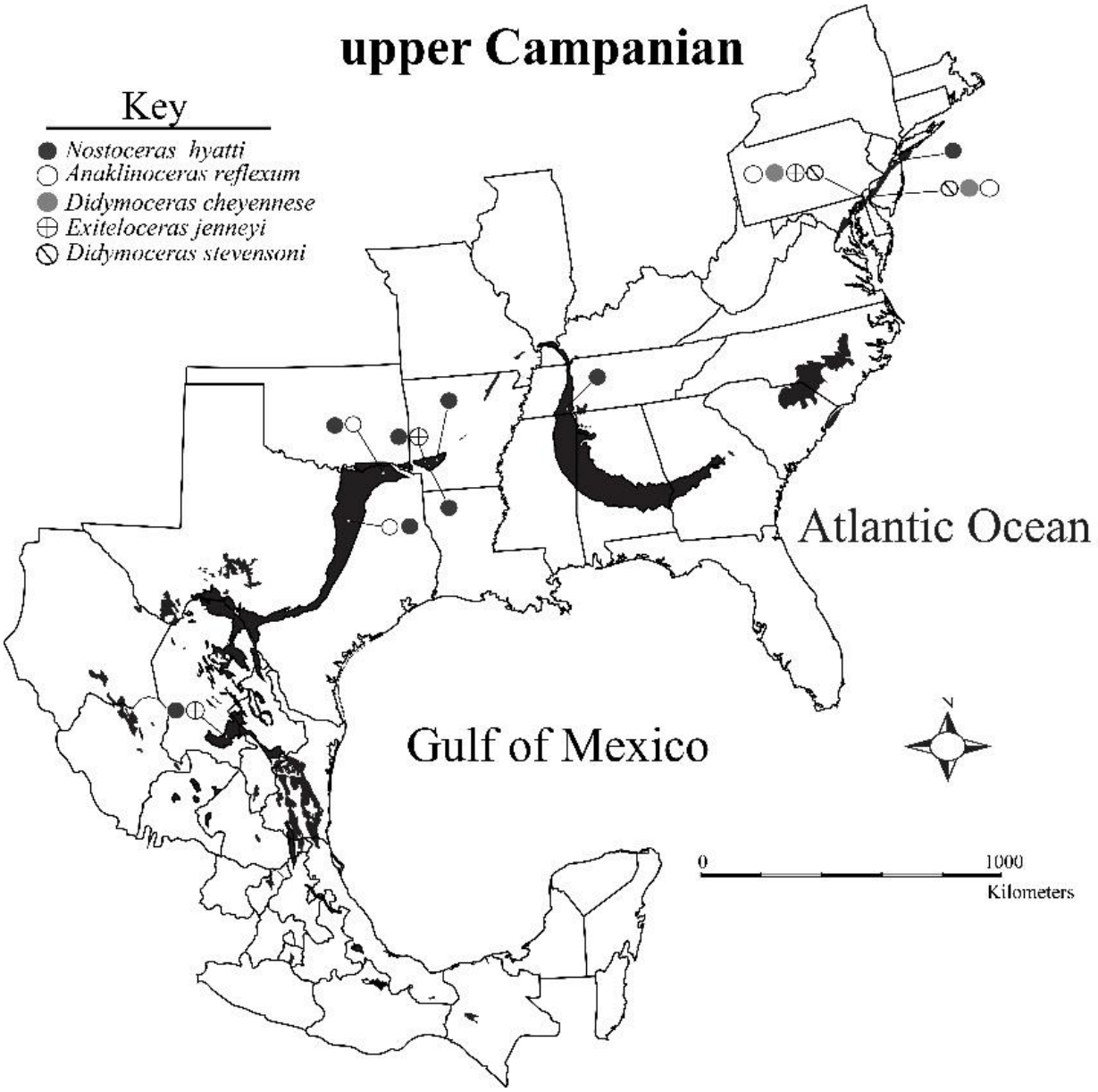

Figure 3.8. Map depicting the distribution of published localities (discussed and cited in text) with upper Campanian biozones along the Gulf and Atlantic Coastal Plains.

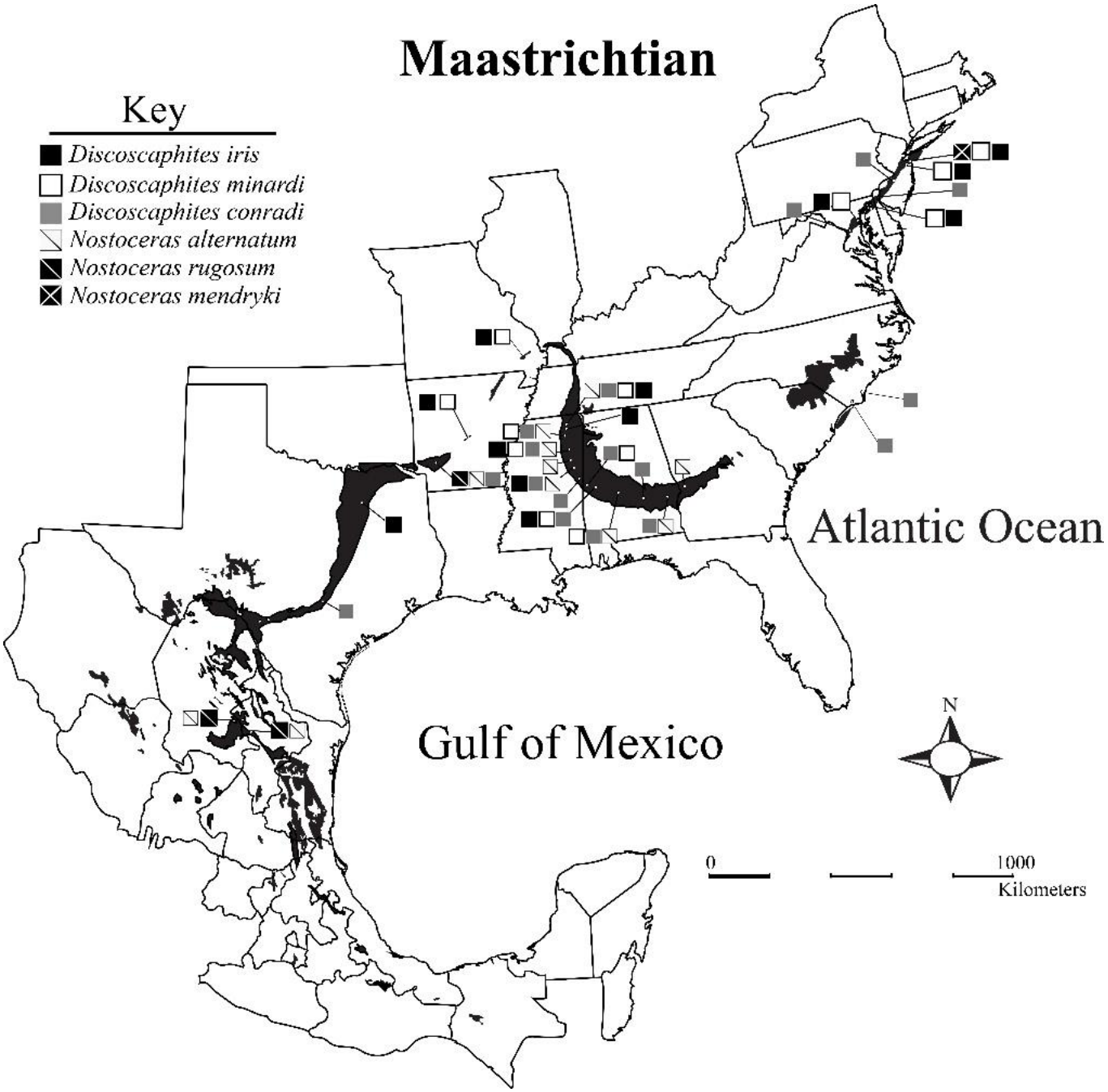

Figure 3.9. Map depicting the distribution of published localities (discussed and cited in text) with Maastrichtian biozones along the Gulf and Atlantic Coastal Plains.

Submortoniceras tequesquitense Biozone

Definition: This biozone is defined as an interval zone for the GCP and possibly ACP. The base of this biozone is defined by the first appearance of *S. tequesquitense*, while the top of this biozone is defined by the first occurrence of *Menabites delawarensis.* Young (1963) originally proposed the *S. tequesquitense* Biozone to define the base of the lower Campanian.

Occurrence: This biozone has been documented in the GCP but has not yet been directly recorded from the ACP (Figs. 3.11 and 3.12). However, the presence of elements of the *S. tequesquitense* biozone ammonite assemblage including *S. uddeni* and *Pseudoschloenbachia chispaensis*, which were found in float possibly derived from the Merchantville Formation (Fig. 3.3, also see Kennedy and Cobban, 1993c), suggest that this biozone exists in the ACP. In the GCP, this biozone has been documented in the Eutaw Formation (top of the Tombigbee Sand Member), Mooreville Formation (main body), Austin Group: middle and upper Dessau Chalk, Terlingua Group: Boquillas Limestone (Upper San Vicente Member), Chispa Summit Formation, Ojinaga Formation, and San Carlos Formation (Figs. 3.3 and 3.4; also see Young, 1963; Wollenben, 1967; Kennedy and Cobban, 1991; Cobban et al., 2008; Gale et al., 2008; Kennedy et al., 1997b). *Submortoniceras tequesquitense* has also been documented at the top of the Mancos Shale of New Mexico in the WI (Cobban and Kennedy, 1991a).

Stratigraphic and Age Range: The *S. tequesquitense* Biozone ranges from the uppermost Santonian to lowermost Campanian (Fig. 3.6). The top of this biozone is poorly constrained, but it is thought to range to the base of the overlying *M. delawarensis* Biozone, which correlates to the WI *Scaphites hippocrepis* III Biozone. This suggests, however, that the upper limit most likely correlates with the WI *Sc. hippocrepis* II Biozone. *Submortoniceras tequesquitense* has also been documented in association with *Sc. hippocrepis* I (82.7 to 82.0 Ma) below the upper

contact of the Mancos Shale in New Mexico (Cobban and Kennedy, 1991a). The bottom of this biozone is underlain by the upper Santonian *Plesiotexanites shiloensis* Biozone, which, based on its association with the WI species *Sc. leei* I, is correlative with the upper Santonian WI *Desmoscaphites erdmanni* Biozone (84.5 to 84.0 Ma; Kennedy et al., 1997b). This biostratigraphic position is supported by the last appearance of the Santonian-Campanian stage boundary marker index fossil *Marsupites testudinarius* within the *S. tequesquitense* Biozone in both Mississippi and Texas (Gale *et al*., 1995; 2008; Kennedy *et al*., 1997b). Based on these biostratigraphic data, we can confidently correlate the *S. tequesquitense* Biozone with the WI biozones of *De. bassleri* to *Sc. hippocrepis* II ranging between 84.0 to 81.5 Ma (Fig. 3.6; Table 3.1).

***Menabites delawarensis* Biozone**

Definition: This biozone is defined as an interval zone for both the ACP and GCP (Table 3.1). The base of this biozone is defined by the first appearance of *M. delawarensis*, while the top of this biozone is defined by the first occurrence of *B. taylorensis.* It was initially erected by Young (1963) as a middle lower Campanian ammonite biozone stratigraphically below and above his *M. sabinalensis* and *S. tequesquitense* biozones, respectively. Cobban and Kennedy (1992a) later reported the occurrence of *M. delawarensis* in association with *Trachyscaphites spiniger spiniger* in the Ozan Formation near Ladonia, Texas, which is younger than the *M. delawarensis* Biozone fauna from the underlying Roxton Member of the Gober Chalk (see Cobban and Kennedy, 1992b). This establishes an upper age limit for this index species that is younger than previously thought. Kennedy, et al. (1997b, p. 3) consequently revised Young's original biozonation by merging his *M. sabinalensis* and *M. delawarensis* biozones, thus extending the range of the latter to the base of Young's *Hoplitoplacenticeras marroti* Biozone

(now *B. mclearni* and *B. taylorensis* Biozone, see discussion below). These revisions greatly strengthened the GCP biozonation scheme by adjusting the boundaries to better coincide with the actual ranges of the index species.

Occurrence: The *M. delawarensis* Biozone is well represented within the ACP and GCP (Figs. 3.8 and 3.11). Occurrences include the Matawan Group: Merchantville and Woodbury formations in the central ACP (Fig. 3.4; also see Kennedy and Cobban, 1993c; Kennedy et al., 1997b). Documented occurrences in the GCP include the Mooreville Formation (Arcola Limestone Member), Coffee Sand: Tupelo Tongue (Chapelville Fossiliferous Horizon), Austin Group: Burditt Marl, Pflugerville Formation, Gober Chalk (Roxton Limestone Member), Taylor Group: Ozan Formation and lower Anacacho Formation, and Terlingua Group: upper Pen Formation (Fig. 3.3; also see Dockery, 1990; Cobban and Kennedy, 1992b; Kennedy et al., 1997b; Dockery and Thompson, 2016; Swezey and Sullivan, 2004). The index species has also been documented in France, South Africa, and possibly Madagascar (Cobban and Kennedy, 1992b; Kennedy et al., 1997b).

Stratigraphic and Age Range: The range of *M. delawarensis* is now known to extend well above the WI *Scaphites hippocrepis* III Biozone (~80.9 to 80.6 Ma). Dockery (1990), based on a personal communication with W.A. Cobban, indicated that the upper part of the *M. delawarensis* Biozone was concurrent with the *Baculites* sp. (smooth), *B.* sp. (weak flank ribs), and *B. obtusus* (81.2 to 80.9 Ma) biozones of the WI. Its upper limit is suggested by the occurrence of *M. danei*, a *M. delawarensis* Biozone ammonite, in the WI *B. obtusus* Biozone (~80.9 to 80.6 Ma) in Colorado (Cobban and Kennedy, 1991a). Since there is no record of *M. delawarensis* Biozone faunal components in the succeeding WI biozones, the lowermost middle Campanian *B. obtusus* Biozone is taken to be the upper limit for its range (Cobban and Kennedy,

1993a; Kennedy et al., 1997b). The association between *M. delawarensis* and the WI species *Sc. hippocrepis* III indicates an extension of this biozone down into the lower Campanian. Based on this data, we suggest that the *M. delawarensis* Biozone spans the late early Campanian to early middle Campanian and corresponds to the *Sc. hippocrepis* III to *B. obtusus* biozones in the WI, which places its age between 81.5 to 80.7 Ma (Fig. 3.6; Table 3.1).

***Baculites mclearni* Biozone**

Definition: This is a proposed geographic extension of the WI *B. mclearni* Biozone into the GCP. It is classified as an interval biozone defined at its base by the first occurrences of *B. mclearni* and at its top by the first occurrence of *B. taylorensis* (Table 3.1). Cobban and Kennedy (1993a) were the first to document this index species in the GCP from the Wolfe City Sand.

Occurrence: In North America, this biozone is known from numerous sites in the WI and from one locality in the Wolfe City Sand of the western GCP (Figs. 3.3, 3.11, and 3.12; also see Cobban, 1962; Cobban and Kennedy, 1993a; Cobban et al., 2006). There are currently no known occurrences of this index species or its associated ammonite fauna in the eastern GCP or ACP.

Stratigraphic and Age Range: This biozone is contained within the lower middle Campanian in the WI (Fig.3.6; also see Cobban, 1962; Cobban and Kennedy, 1993a). This placement is supported by its stratigraphic position in the Wolfe City Sand, which is stratigraphically above the lower Ozan Formation that contains the *M. delawarensis* biozone and is stratigraphically below the Pecan Gap Chalk that contains the middle Campanian index ammonite *Baculites taylorensis* (Cobban and Kennedy, 1993b, 1994b). Ogg and Hinnov (2012) place the chronostratigraphic range for the middle Campanian *B. mclearni* Biozone between 80.7 to 80.2 Ma, which gives it the duration of ~0.5 Ma (Fig. 3.6; Table 3.1).

Baculites taylorensis Biozone

Definition: This biozone is defined as an interval zone for the GCP (see section on age and Table 3.1), and was initially proposed by Kennedy et al. (1997c) to replace Young's (1963) *Hoplitoplacenticeras marroti* Biozone based on the abundance and widespread distribution of *B. taylorensis* across the GCP. The base of this biozone is defined by the first appearance of *B. taylorensis*, while the top of this biozone is defined by the first occurrence of *Didymoceras binodosum.*

Occurrence: Baculites taylorensis has only been documented in the GCP; however, faunal components of the highest parts of this biozone are known from the ACP (Figs. 3.11 and 3.12). The *B. taylorensis* Biozone has been documented from the Demopolis Formation, Taylor Group: Annona Chalk, Pecan Gap Chalk, and upper Anacacho Limestone, Mooreville Formation (Arcola Limestone Member), and also from the Parras Shale within the Mexican GCP (Fig. 3.3; also see Elder, 1994; Kennedy and Cobban, 1993b,d; 2001, Kennedy et al., 1997c; Swezey and Sullivan, 2004; Ifrim et al., 2015). Species belonging to this biozone have been documented in the basal Aguja Formation in West Texas (see Fig. 3.3; also see Cobban et al., 2008).

Stratigraphic and Age Range: Kennedy et al. (1997c) indicated that the *B. taylorensis* Biozone overlies the *M. delawarensis* Biozone, based on this species' occurrence in the basal Demopolis Chalk, which is stratigraphically above the Arcola Limestone Member of the Mooreville Formation that contains specimens of *M. delawarensis.* Given the correlation between the *M. delawarensis* and the WI *Baculites obtusus* biozones (80.9 to 80.7 Ma), this stratigraphic position suggests that the base of the *B. taylorensis* Biozone is younger than the *B. obtusus* Biozone, which would make it equivalent to either the WI *B. mclearni* or *B. asperiformis* biozones. *Trachyscaphites spiniger porchi,* a characteristic component of the lower *B.*

taylorensis assemblage, is known to co-occur in the WI with *B. mclearni* and *B. asperiformis*, suggesting correlation with the biozones these species define (Cobban and Kennedy, 1993a; Kennedy et al., 1997c; Larson et al., 1997). The first appearance of *B. taylorensis* in the Pecan Gap Chalk, stratigraphically above the *B. mclearni* Biozone in the Wolfe City Sand, indicates that the base of this biozone correlates with the *B. asperiformis* biozone (80.2 to 79.6 Ma) (Cobban and Kennedy, 1993b; 1994b). The upper limit of this biozone is well below the top of the middle Campanian, which is based on the absence of *B. taylorensis* within the overlying *D. binodosum* Biozone (see below), a biostratigraphic level equivalent to the top and lower portion of the WI *B. reduncus* and *B. scotti* biozones, respectively. The upper portion of the *B. taylorensis* Biozone (defined by the *M. portlocki complexus* Subzone) appears to be equivalent to the WI *B. gregoryensis* and *B. reduncus* biozones (78.3 to 76.9 Ma), based on the co-occurrence in the GCP of *B. taylorensis* with the WI index fossils *B. reduncus, T. redbirdensis, Menuites* cf. *portlocki,* and *Didymoceras cochleatum* (Kennedy and Cobban, 1993b). This biozone potentially ranges into the uppermost middle Campanian or lower upper Campanian; however, this is unlikely as the documented association between *Baculites taylorensis* with younger ammonite species (e.g., *D. binodosum*, *Nostoceras monotuberculatum*, *B. crickmayi*) are from a condensed zone in the basal Annona Formation with phosphatic fossils (Kennedy and Cobban 1993d). Based on its stratigraphic position and its correlation to the WI *B. asperiformis* to *B. reduncus* biozones, the *B. taylorensis* Biozone is estimated to span the early middle Campanian with a range from about 80.2 to 76.9 Ma (see Fig. 3.6). This biozone has a duration of ~3.3 Ma, which makes it the longest ammonite zone in the Campanian (see Table 1).

Menuites portlocki complexus Biozone/Subzone

Definition: This zone is defined as an interval biozone for the ACP and as a subzone in the GCP representing the top of the *Baculites taylorensis* Biozone (Figs. 3.6). The base of this biozone/subzone is defined by the first appearance of *M. portlocki complexus*, while the top of this biozone is defined by the first occurrence of *D. binodosum*. Kennedy and Cobban (1993b,d) first defined the *M. portlocki complexus* including the associated ammonite fauna in the GCP, and suggested its biostratigraphic utility due to its restricted stratigraphic range. Kennedy and Cobban (1994a, 1997) later documented this index species in the ACP from biostratigraphically condensed beds that also preserve slightly younger faunal elements associated with the overlying *D. binodosum* Biozone.

Occurrence: In the ACP, the *M. portocki complexus* Biozone is known from the Matawan Group: Marshalltown and Wenonah formations (Figs. 3.4, 3.7, and 3.8; also see Kennedy and Cobban, 1994a; 1997). In the GCP, the subzone has been documented from the basal phosphatic zone of the Annona Formation (Figs. 3.3, 3.11, and 3.12; also see Kennedy and Cobban, 1993d). *Menuites portlocki complexus* along with many of the other species that define this biozone have also been documented across the WI (Cobban and Kennedy, 1993b; Larson et al., 1997).

Stratigraphic and Age Range: Menuites portlocki complexus and its associated ammonite assemblage are known to range from the upper part of the *Baculites gregoryensis* to the base of the *B. scotti* biozones (77.6–76.8 Ma) in the WI (Cobban and Kennedy, 1993b). This range overlaps with the range of *B. taylorensis* in the GCP; thus, it is erected as a subzone representing the top of that biozone. The range of *Menuites portlocki complexus* also overlaps with the base of the overlying *D. binodosum* Biozone, which can make it difficult to distinguish these two

biozones if other faunal components of the *M. portlocki complexus* ammonite assemblage are absent (Table 2). However, we favor using the first occurrence of *D. binodosum* as the top of this biozone. Based on this biostratigraphic correlation, the *M. portlocki complexus* Biozone in the ACP and GCP is late middle Campanian with an age range between 77.9 to 76.8 Ma (Fig. 3.6; Table 3.1).

***Didymoceras binodosum* Biozone**

Definition: The *D. binodosum* Biozone is an interval biozone for the GCP and possibly ACP (Table 3.2). The stratigraphic extent of this biozone is unclear due limited exposures and preservational biases, but its base is defined by the first appearance of *D. binodosum.* This biozone, as defined here, replaces Young's (1986) *Manambolites ricensis* and *Placenticeras meeki* biozones, which he defined for the upper and lower Bergstrom Formation, respectively (Figs. 3.3 and 3.8). They were proposed without specific details on their stratigraphic or age relationships. However, *M. ricensis* is found in association with *D. binodosum* in the Kimbro Nodule Bed in the upper part of the Bergstrom Formation (see Fig. 3.3). Kennedy and Cobban (1999) correlated the fauna from the Kimbro Nodule Bed to the upper middle Campanian, which is stratigraphically below the known upper Campanian range of *P. meeki* and not above, as indicated by Young (1986). Based on this stratigraphic information and on its greater geographic distribution, we prefer *D. binodosum* as the index fossil to either *M. ricensis* or *P. meeki*, (e.g., Kennedy and Cobban, 1994a; 1997; 1999).

Occurrence: The *D. binodosum* Biozone is known from the Taylor Group: Bergstrom Formation (Kimbro nodule bed) and Annona Chalk (basal phosphatic zone) in the GCP, and from the Matawan Group: upper Marshalltown and Wenonah formations in the ACP (Figs. 3.3; 3.4; 3.11, and 3.12; also see Kennedy and Cobban, 1993d, 1994a, 1997, 1999). *Didymoceras*

binodosum and many of the ammonites found with this index species are also common in the upper middle Campanian *Baculites scotti* Biozone in the WI (Kennedy et al., 2000b).

Stratigraphic and Age Range: The biostratigraphic placement of the *D. binodosum* Biozone is based on its stratigraphic position above the older *B. taylorensis* in the GCP, as well as its placement below the upper Campanian Mount Laurel Sand that contains the younger index species *D. stevensoni* and *Exiteloceras jenneyi* in the ACP (Kennedy and Cobban, 1994a, 1997, 1999). *Didymoceras binodosum* and the co-occurring ammonites *B. texanus*, *Spiroxybeloceras kimbroense*, and *Trachyscaphites pulcherrimus* directly correlate this biozone with the WI *Baculites scotti* Biozone, which ranges from 76.9 to 76.3, specifically the *D. binodosum* Subzone (Kennedy and Cobban, 1999; Kennedy et al., 2000b; Ogg and Hinnov, 2012). The senior author has discovered relatively complete specimens of *D. binodosum* below the *B. scotti* Biozone near the top of the *B. reduncus* Biozone (77.6–77.9 Ma) in Wyoming, which indicates a slightly earlier first appearance. Based on these data we suggest that this biozone correlates with the top of the *B. reduncus* and lower portion of the *B. scotti* biozones, which places it in the upper middle Campanian with a range of 77.2 to 76.6 Ma (Fig. 3.6; Table 3.1).

***Didymoceras stevensoni* Biozone**

Definition: This is a proposed geographic extension of this WI biozone into both the ACP and GCP (Fig. 3.6). It is classified as an interval biozone defined by the first occurrence of the eponymous index species (Table 3.2). Cobban (1970) was the first to document this index species alongside the younger index species *E. jenneyi* in the ACP. As these specimens were found in float but were apparently from different stratigraphic horizons based on lithological and preservational differences, Cobban (1970) initially suggested that *D. stevensoni* and *E. jenneyi* came from the Marshalltown Formation and Mount Laurel Sand, respectively. However, in a

subsequent study, Kennedy and Cobban (1997) documented *in situ D. stevensoni* from a condensed zone near the base of the Mount Laurel Formation closely associated with float specimens of *E. jenneyi*. Despite being closely associated, these authors maintained that the two different index species were likely derived from distinct stratigraphic levels in the basal Mount Laurel Sand. Ifrim et al. (2015) suggested the presence of this biozone in the GCP in their biostratigraphic correlations; however, their study did not document an actual occurrence of *D. stevensoni*.

Occurrence: Didymoceras stevensoni and faunal elements assigned to this biozone have been documented in the Monmouth Group: basal Mount Laurel Sand of the ACP (Figs. 3.4, 3.11, and 3.13). A few faunal elements (i.e., *B. crickmayi*, *Solenoceras elegans*, *Oxybeloceras crassum Nostoceras monotuberculatumn*) assigned to this biozone in the WI have also been documented in the Annona Chalk in southwestern Arkansas and from the Parras Shale of the Mexican GCP (Figs. 3.3, 3.11, and 3.13; also see Kennedy and Cobban, 1997; Ifrim et al., 2015). The components assigned to this biozone are well known from numerous localities in the WI ranging from New Mexico to Montana (Kennedy et al., 2000d). Outside of North America, *D. stevensoni* has been documented in France and possibly Egypt (Kennedy and Bilotte, 1995; Luger and Gröschke, 1989).

Stratigraphic and Age Range: The *D. stevensoni* Biozone occurs during the lower upper Campanian in the WI (Fig. 3.6; also see Kennedy et al., 2000d). This placement is supported by its stratigraphic position in the basal Mount Laurel Sand, which is stratigraphically above the upper middle Campanian Wenonah and Marshalltown formations that contain *D. binodosum* (Kennedy and Cobban, 1994a, 1997). This age is also supported by specimens of *N. monotuberculatum* co-occurring with *D. stevensoni* in the ACP and GCP, which in the WI ranges

from the *D. nebrascense* to the *D. stevensoni* biozones (Kennedy and Cobban, 1997; Kennedy et al., 2000d). However, in the ACP and GCP, *D. stevensoni* fauna occurs stratigraphically below and above beds that contain the younger index species *D. cheyennense* and older index species *D. binodosum*, respectively. Ogg and Hinnov (2012) indicate that the *D. stevensoni* Biozone spans the early late Campanian and ranges from 75.6 to 75.1 Ma (Fig. 3.6; Table 3.1).

***Exiteloceras jenneyi* Biozone**

Definition: This is a biozonal extension of a WI index species into the ACP and GCP. This biozone is classified as an interval biozone defined by the first occurrence of the *E. jenneyi* (Table 2). Cobban (1970) was the first to document this index species in the ACP, and, more recently, Ifrim et al. (2015) proposed the *E. jenneyi* Biozone as a distinct biostratigraphic unit in the GCP based on the occurrence of *E. jenneyi* and species typically associated with this index fossil, such as *Solenoceras elegans*, in the Parras Shale of Mexico.

Occurrence: Exiteloceras jenneyi and its associated ammonite fauna have been documented in the basal Mount Laurel Sand (Delaware) of the ACP, and from the Parras Shale (Mexico) in GCP (Fig. 3.3, 3.4, 3.11, and 3.13; also see Kennedy and Cobban, 1997; Ifrim et al., 2015). *E. jenneyi* is also known from numerous WI localities (Kennedy et al., 2000).

Stratigraphic and Age Range: The *E. jenneyi* Biozone encompasses the lower upper Campanian in the WI (Fig. 3.6; also see Kennedy et al., 2000d). Ogg and Hinnov (2012) places the *E. jenneyi* Biozone in the early late Campanian with a range between 75.1 to 74.6 Ma (see Fig. 3.6; Table 3.1).

***Didymoceras cheyennense* Biozone**

Definition: This is a proposed geographic extension of the WI *D. cheyennense* Biozone into the ACP. This ammonite zone is classified as an interval biozone defined by the first

occurrence of *D. cheyennense* (Table 2.1). Kennedy and Cobban (1994b) were the first to document this index species in the ACP from a condensed, phosphatic zone in the Mount Laurel Sand.

Occurrence: In North America, this biozone is known from numerous sites in the WI and from one locality in the Mount Laurel Sand of the ACP (Figs. 3.4, 3.11, and 3.13; also see Kennedy et al., 2000d; Kennedy and Cobban, 1994b). There are currently no known localities for this index species or its associated ammonite fauna in the GCP.

Stratigraphic and Age Range: This biozone is contained within the middle upper Campanian in the WI (Fig. 3.6; also see Kennedy et al., 2000d). This placement is supported by its stratigraphic position in the Mount Laurel Sand, which contains the lower upper Campanian ammonites *D. stevensoni* and *E. jenneyi* at its base and is stratigraphically below the Navesink Formation that contains the upper upper Campanian index ammonite *Nostoceras hyatti* (Kennedy and Cobban, 1994b). These correlations place it stratigraphically below the *Anaklinoceras reflexum* Biozone in the ACP and GCP. Ogg and Hinnov (2012) place the chronostratigraphic range for late Campanian *D. cheyennense* Biozone between 74.6 to 74.2 Ma, which gives it the shortest duration of any biozone in the Campanian of ~0.4 Myr (Fig. 3.6; Table 3.1).

***Anaklinoceras reflexum* Biozone**

Definition: This biozone is defined as an interval zone for both the ACP and GCP (Table 2), and it is defined by the first occurrence of the eponymous index species (Table 2). Stephenson (1941) was the first to document *A. reflexum* in the GCP and suggested it might be useful for biostratigraphic purposes because of its restricted stratigraphic range. Young (1982) used *A. reflexum* to define a biozone above and below his *M. ricensis* and *Nostoceras stantoni*

(=*N. approximans*) biozones, respectively. Young (1982) correlated this biozone with the Neylandville Marl and noted that this biozone might eventually be included in his *M. ricensis* Biozone due to limited bio- and lithostratigraphic range data. Kennedy and Cobban (1994b) were the first to document this index species in the ACP from the same biostratigraphically condensed beds, which also contain *D. cheyennense*.

Occurrence: In North America, the *A. reflexum* Biozone is known from the Navarro Group, Neylandville Marl in GCP, and from a condensed, phosphatic zone in the Monmouth Group, Mount Laurel Sand of the ACP (Figs. 3.3, 3.11, and 3.13). *Anaklinoceras reflexum* and the other species that define this assemblage biozone have also been documented in Colorado in the WI (Cobban et al., 1993). Outside of North America, it has been documented in Israel (Lewy, 1986).

Stratigraphic and Age Range: In both the ACP and GCP, *A. reflexum* is found in units below strata containing *Nostoceras hyatti*, which defines the overlying upper Campanian biozone. *Anaklinoceras reflexum* and many of the species that occur in this biozone are found in the WI *Baculites compressus* Biozone, indicating correlation with this biostratgraphic unit, which in this region overlies the *D. cheyennense* Biozone (Cobban et al., 1993). Based on this correlation, the *A. reflexum* Biozone is late late Campanian, with a temporal range between 74.2 to 73.9 Ma (Fig. 3.6), which gives this biozone the shortest duration in the Campanian of 0.3 Ma (Table 1).

***Nostoceras hyatti* Biozone**

Definition: In the ACP and GCP, this biozone is defined as an interval zone (Table 2). The base of this biozone is defined by the first appearance of *N. hyatti*, while the top of this biozone is defined by the first appearance of *N. rugosum.* It was first defined by Kennedy et al.

(1992) based on its shared ranges with uppermost Campanian faunas in the WI and Europe as well as its relative superposition below known lower Maastrichtian faunas.

Occurrence: This biozone has been documented within the basal lag of the Navesink Formation in the ACP, as well as in the Ripley Formation (Coon Creek Tongue), Saratoga Chalk, Nacatoch Sand, Cerro del Pueblo (of Mexico), and Parras Shale (of Mexico) in the GCP (Figs. 3.3, 3.11, and 3.13; also see Stephenson, 1941; Cobban, 1974; Cobban and Kennedy, 1994a; Kennedy and Cobban, 1993a; Larson, 2012, 2016; Ifrim et al., 2015). The index taxon has also been recorded from Colorado (Kennedy et al., 1992) as well as in Poland, Austria, France, Spain, Iraq, Israel, Angola, and Colombia (Howarth, 1965; Lewy, 1967; Kennedy et al., 1992; Etayo-Serna, 1989; Kennedy and Lunn, 2000; Ward and Orr, 1997; Küchler, 2000; Eberth et al., 2004; Summesberger et al., 2007; Machalski, 2012).

Stratigraphic and Age Range: The *N. hyatti* Biozone in ACP and GCP represents the highest ammonite-based biostratigraphic unit in the upper Campanian. This is based on its stratigraphic position in the GCP below the *Endocostea typica* inoceramid biozone (72.1–71.8 Ma), which correlates with the base of the Maastrichtian in both Europe and the WI (Walaszczyk et al., 2001, 2002a,b; Walaszczyk, 2004). This range/age is also reinforced by correlation with the Euroamerican inoceramids zonation (i.e., '*Inoceramus*' *altus* to '*I.' redbirdensis* biozones) that span the *N. hyatti* Biozone in Europe, which correlates this biozone to the *D. cheyennense* to *B. eliasi* biozones in the WI (Walaszczyk et al., 2002a,b; Walaszczyk, 2004). This range is supported by the ammonites associated with *N. hyatti* in the ACP and GCP, which correlate with the upper Campanian WI biozonation (Kennedy et al., 1992; Cobban and Kennedy, 1994a; Larson, 2012, 2016). Most notably, a portion of a *N. hyatti* specimen was found by the senior author in the *B. eliasi* Biozone (72.7–72.1 Ma) approximately 10 m below the first occurrence of

basal Maastrichtian index fossil *E. typica* at the Red Bird section in Wyoming. *N. hyatti* is also known to occur in the upper Campanian *B. jenseni* Biozone (73.3–72.7 Ma) in the Pierre Shale of Colorado (Kennedy at al., 1992). Many of the co-occurring ammonite species with *N. hyatti* in the Nacatoch Sand, Saratoga Chalk, the Coon Creek Tongue of the Ripley Formation, and Navesink Formation are known from the *B. compressus* to *B. jenseni* biozones (74.2–72.7 Ma) of the WI (Kennedy et al., 1992; Kennedy and Cobban, 1993a; Larson, 2012, 2016). A significant portion of the *N. hyatti* fauna in the APC and GCP includes species typical of the *B. cuneatus*-*B. reesidei* biozones of Colorado (Kennedy et al., 1992; Kennedy and Cobban, 1993a; Larson, 2012; 2016). Landman et al. (2010) indicate that most of the *Hoploscaphites* documented in the *N. hyatti* Biozone in the ACP and GCP represent species found in the *B. reesidei* to *B. jenseni* biozones (73.6–72.7 Ma) of the WI. The use of these various biostratigraphic criteria indicates that the *N. hyatti* Biozone corresponds to the *B. cuneatus* through the *B. eliasi* biozones of the WI. Based on this correlation with the WI ammonite biochronology (see Ogg and Hinnov, 2012), the *N. hyatti* Biozone ranges from ~73.9 to 72.1 Ma (Fig. 3.6; Table 3.1).

Maastrichtian

The Maastrichtian (72.1–66.0 Ma) is subdivided into five ammonite zones (Fig. 3.6). They range in duration from ~0.4 to ~3.1 Ma (also see Table 1). In ascending order, the lower Maastrichtian biozones are: *Nostoceras mendryki* in the ACP and the equivalent *N. rugosum* in the GCP, and *N. alternatum* biozones for both regions (Cobban, 1974; Cobban and Kennedy, 1995; Kennedy *et al*., 2000c). The upper Maastrichtian biozonation consists of the *Discoscaphites conradi*, *D. minardi*, and *D. iris* biozones (Cobban and Kennedy, 1995; Landman *et al*., 2004a,b, 2007; Larina *et al*., 2016). The *N. mendryki* Biozone is a new biostratigraphic unit for the ACP and is positioned between the *N. hyatti* and *N. alternatum* biozones (see Fig.

3.6). These ammonite biozones occur across the ACP and GCP with significant gaps in the record in the Southern ACP as well as along the border between the western and eastern GCP (Figs. 3.6, 3.11, and 3.14).

***Nostoceras rugosum* Biozone**

Definition: The *N. rugosum* Biozone is defined as an interval zone for the GCP (Table 2). This biozone is defined by the first appearance of *N. rugosum*, whereas the upper limit is defined by the first occurrence of *N. alternatum.* This biozone remains relatively poorly studied since it was first defined by Cobban and Kennedy (1991b).

Occurrence: The *N. rugosum* Biozone has been documented from the Nacatoch Sand and Mendez Formation (Mexico) in the GCP (Figs. 3.3, 3.11, and 3.14 also see Cobban and Kennedy, 1991b; Ifrim *et al*., 2004).

Stratigraphic and Age Range: This biozone is the lowest ammonite zone in the Maastrichtian ammonite sequence in the GCP based on its relative stratigraphic position 46 m above the uppermost Campanian *Nostoceras hyatti* Biozone and its occurrence below the upper lower Maastrichtian *N. alternatum* Biozone in Hempstead County, Arkansas (Cobban and Kennedy, 1991b; 1995). This placement is supported by the co-occurrence at this locality of *N. rugosum* with the inoceramid index species *E. typica*, which correlates to the base of the Maastrichtian in the WI and Europe (Cobban, 1974; Cobban and Kennedy 1991b; Walaszczyk *et al*., 2001, 2002a,b; Walaszczyk, 2004; Cobban *et al*., 2006). According to Ogg and Hinnov (2012), this would place the basal age of this biozone at ~72.1 Ma (also see Fig. 3.6; Table 3.1). The top of this biozone is unknown and could range as high as the base of the WI *B. clinolobatus* Biozone that was correlated with the *N. alternatum* Biozone in the ACP and GCP. Thus, we

place its top at ~70.4 Ma, which is equivalent to the first half of the early Maastrichtian (Fig. 3.6; Table 1).

***Nostoceras mendryki* Biozone**

Definition: The *N. mendryki* Biozone is an interval zone defined for the ACP, and which is approximately age equivalent to the GCP's *N. rugosum* Biozone based on its stratigraphic position and its associated fauna (discussed below; also see Table 2). This biozone is defined by the first appearance of *N. mendryki*, while the top is delimited by the first occurrence of *N. alternatum.* Cobban (1974) was the first to describe *N. mendryki* from the basal Navesink Formation along the ACP. Machalski (2012) suggested that *N. mendryki* might be conspecific with the European ammonite *N. schloenbachi;* however, due to the rarity of material on both continents, this awaits confirmation.

Occurrence: This biozone has been documented from the basal Navesink Formation in the ACP and the Prairie Bluff Formation in the GCP (Figs. 3.3, 3.4, 3.11, and 3.14; also see Cobban, 1974; Cobban and Kennedy, 1995; Kennedy *et al*., 2000c). If *N. mendryki* is conspecific with *N. schloenbachi*, then this species also occurs in Poland, Ukraine, and Bulgaria (Machalski, 2012).

Stratigraphic and Age Range: This biozone is the lowest ammonite zone in the ACP's Maastrichtian ammonite sequence based on its relative stratigraphic position 0.2 m above the Upper Campanian *N. hyatti* Biozone at the Atlantic Highlands locality in New Jersey (Kennedy *et al*., 2000c). Cobban (1974) documented *N. mendryki* in the upper of two ammonite-bearing beds that occurred within the basal lag deposit of the Navesink Formation and recognized that it was slightly older than *N. alternatum*. Kennedy, *et al*. (2000c) also documented the cephalopod fauna from the two ammonite-bearing beds within the basal lag deposit of the Navesink

Formation, and considered *N. mendryki* to be Maastrichtian in age, citing its occurrence in the Prairie Bluff Formation in Alabama. A specimen of *Hoploscaphites plenus* may be derived from the same beds, which suggest that this biozone is equivalent to the uppermost Campanian *B. eliasi* or lower Maastrichtian *Baculites baculus* biozones of the WI (Kennedy *et al*., 2000c). This range would also be supported if *N. mendyki* is conspecific with *N. schloenbachi*, which in Europe ranges from the uppermost Campanian to the lowermost Maastricthian (Machalski, 2012). The lack of *N. hyatti* specimens co-occurring with *N. mendryki* suggest that it occurs above the top of the Campanian. The top of this biozone is unknown and could range as high as the base of the WI *B. clinolobatus* Biozone that is correlated with the overlying *N. alternatum* Biozone. This would place its top, as is the case with the *N. rugosum* Biozone, at ~70.4 Ma. Based on this correlation and utilizing the recent biochronology of Ogg and Hinnov (2012), this correlates the *N. mendryki* Biozone to the basal Maastrichtian with a range from ~72.1 to 70.4 Ma (Fig. 3.6; Text 3.1).

***Nostoceras alternatum* Biozone**

Definition: The *N. alternatum* Biozone is considered an interval zone for both the ACP and GCP (Table 1; also see Cobban, 1974; Cobban and Kennedy, 1991c, 1995). This biozone extends from the first appearance of *N. alternatum* to the first occurrence of *D. conradi.* This biozone was first defined as a biostratigraphic unit by Cobban (1974) for occurrences in the eastern GCP. Subsequently, Cobban and Kennedy (1991c) determined the stratigraphic position of this biozone in the GCP using superposition relative to the underlying *N. rugosum* and overlying *Discoscaphites*-dominated biozones.

Occurrence: In the GCP, this biozone has been recorded from the Ripley Formation (undifferentiated and Coon Creek Tongue), Prairie Bluff Chalk, and Nacatoch Sand, (Cobban,

1974; Cobban and Kennedy, 1991c, 1995; Ifrim *et al*., 2004). Ifrim *et al*. (2004) also recorded the occurrence of the *N. alternatum* Biozone in the Mendez Formation from Mexico. In the ACP, *N. alternatum* has only been recorded in float from the Navesink Formation (Kennedy *et al*., 2000c).

Stratigraphic and Age Range: This biozone is considered lower Maastrichtian based on its relative stratigraphic position below the various upper Maastrichtian biozones defined on *Discoscaphites* and its location above the lower Maastrichtian *N. rugosum* Biozone (Cobban and Kennedy, 1991c; 1995). Cobban and Kennedy (1991c) argued that this biozone is stratigraphically equivalent to the lower Maastrichtian *Baculites clinolobatus* Biozone of the WI based on the co-occurring inoceramids and scaphitids. This correlation with the *B. clinolobatus* Biozone gives it an age between ~70.4 to 69.9 Ma (Fig. 3.6; Table 3.1; Ogg and Hinnov, 2012).

***Discoscaphites conradi* Biozone**

Definition: The *D. conradi* Biozone is currently recognized as an interval biozone and the lowest ammonite zone of the upper Maastrichtian sequence in the ACP and GCP (Landman *et al*., 2004a, b; 2007; Larina *et al*., 2016). Following Larina *et al*. (2016), the base of this interval biozone is defined by the first appearance of *D. conradi*, whereas its upper limit is defined by the first occurrence of *D. minardi*. Cobban and Kennedy (1995) were the first to erect the *D. conradi* Biozone; however, in contrast to its current designation, it was defined as an assemblage biozone and was placed as the highest biozone in the upper Maastrichtian based on the absence of long-ranging *Baculites claviformis* (discussed below) as well as limited information on this biozones relative to its stratigraphic position. Landman *et al*. (2004a, b) redefined the stratigraphic position of this biozone and placed it as the lowest biozone in the upper Maastrichtian ammonite sequence of the ACP based on its stratigraphic superposition relative to *D. minardi* Biozone and

associated dinoflagellates. This placement was corroborated by Larina *et al's* (2016) study of GCP ammonites.

Occurrence: This biozone has been documented in the Navesink, New Egypt, Peedee, and Severn formations in the ACP (Figs. 3.4, 3.11; 3,14; also see Kennedy *et al*., 1997a; Landman *et al*., 2004a, b). In the GCP, it has been documented in the Prairie Bluff Chalk of Alabama and Mississippi, the Arkadelphia Marl in Arkansas, and the Corsicana Formation in Texas (Figs. 3.3, 3.11; 3.14; also see Cobban and Kennedy, 1995; Woehr, 2013; Larina *et al*., 2016). *D. conradi* and associated ammonites have also been documented in the *Hoploscaphites nebrascensis* Biozone of the Fox Hills Formation of North and South Dakota as well as the Pierre Shale of South Dakota and Nebraska. However, *D. conradi* is not employed as an index fossil for the WI.

Stratigraphic and Age Range: In the ACP, the *D. conradi* Biozone correlates to the CC25b/UC20a nannofossil subzone, which has been assigned to the earliest part of the upper Maastrichtian (Landman *et al*., 2004a; Larina *et al*., 2016). Larina *et al*. (2016) indicated that the base of this biozone is currently poorly known due to limited exposure of appropriate aged strata and extensive reworking of the lower upper Maastrichtian. However, based on the association between *D. conradi* and *Coahuilites sheltoni* in the Prairie Bluff Chalk of Mississippi, the base of this biozone most likely corresponds to the informally defined lower upper Maastrichtian, which correlates to the WI *Hoploscaphites birklundae* Biozone (Cobban and Kennedy, 1995). A similar interpretation for the range of this biozone was also given by Larina *et al*. (2016; see their Fig. 3.12), which placed the base of this biozone above the upper lower Maastrichtian *N. alternatum* Biozone. Larina *et al*. (2016) also stated that the top of this biozone is poorly constrained, but likely correlates with either the CC26a/UC20c or CC25c/UC20b^{TP} nannofossil

subzones. The co-occurrence of *D. conradi* and *H. nebrascensis* in the Severn Formation of ACP and in the Fox Hills Formation of the WI indicates that these two biozones named for these species are at least partially equivalent (Kennedy *et al*., 1997a). However, it is unclear if *H. nebrascensis* ranges throughout the *D. conradi* Biozone or just at the top of its range. Kennedy *et al*. (1998) also suggested correlation between the *D. conradi* and the WI *H. nicolletti* or *H. nebrascensis* biozones (~69.3–67.2 Ma), based on their similar ammonite faunas (e.g., *D. gulosus, Trachybaculites columna, S. lobatus, S. pleurisepta*). Based on these various biostratigraphic data, the *D. conradi* Biozone spans from the base of the informally defined late Maastrichtian substage boundary to the younger *D. minardi* biozone or from ~69.9 to 66.8 Ma making it the longest biozone in the Maastrichtian with a duration of ~3.1 million years (also see Fig. 3.6; Table 3.1).

***Discoscaphites minardi* Biozone**

Definition: Following Larina *et al*. (2016), the base and top of this interval biozone are defined by the first appearance of *D. minardi,* and the first appearance of *D. iris*, respectively. This contrasts with Landman *et al*. (2004a), who were the first to define this biozone, and used the lowest occurrence of abundant *D. iris* specimens as the top of this biozone. The reason for the definition change from an abundance zone to an interval zone was not given by Larina *et al*. (2016) but it does follow modern biostratigraphic convention.

Occurrence: In the ACP, Landman *et al*. (2004a, b) identified the *D. minardi* Biozone in the Severn and the New Egypt formations (Figs. 3.4, 3.11; 3.14). In the GCP, Larina *et al*. (2016) recorded this biozone in the middle of the Prairie Bluff Chalk (Figs. 3.3, 3.11; 3.14). It has also been suggested, although unconfirmed, that this biozone occurs in the Arkadelphia and Owl Creek formations based on the occurrence of *D. minardi* near the base of the *D. iris* Biozone

(Kennedy *et al*., 2001; Landman *et al*. 2004a; Larina *et al*., 2016). Landman et al. (2004a) suggested this biozone might also occur in the Corsicana Formation based on the similarity of specimens described by Kennedy and Cobban (1993) to *D. minardi*.

Stratigraphic and Age Range: Using dinoflagellates, Landman *et al*. (2004a) correlated the *D. minardi* Biozone in the ACP with the base of the CC26b/UC20d and the highest part of CC26a/UC20c nannofossil subzones indicating an age equivalent with the middle of the upper Maastrichtian (Landman *et al*., 2004a). More recently, Larina *et al*. (2016) argued that the this biozone is restricted to the CC26a/UC20c nannofossil subzones based on the presence and absence of the dinoflagellates *Deflandrea galeata* and *Isabelidinium* aff. *I. cooksoniae*, respectively, which would place it between ~66.4–66.8 Ma. This age range makes it the shortest ammonite zone in the Maastrichtian in the ACP and GCP (Fig. 3.6; Table 3.1).

***Discoscaphites iris* Biozone**

Definition: This biozone is currently recognized as an interval zone and the youngest ammonite zone in the ACP and GCP upper Maastrichtian sequences, which has an upper limit of the K/Pg boundary (Landman *et al*., 2004a, b; 2007; Larina *et al*., 2016). In the GCP, Larina *et al*. (2016) defined this biozone's base as the first appearance of *D. iris* and the top by the lowest appearance of *in situ* Danian fauna (e.g., *Pycnodonte pulaskensis* and/or *Carpatella cornuta*). In the central ACP, Landman et al. (2012) found evidence of non-reworked ammonites (i.e., *Eubaculites latecarinatus*, *Discoscaphites* sp.) in strata directly above the K/Pg boundary, which suggests that this biozone may extend into the lowest Danian in this region.

The biozone was first tentatively erected by Cobban and Kennedy (1995) as an assemblage zone, however, in contrast to its current placement as the highest ammonite zone in the upper Maastrichtian, these authors tentatively placed it below their *D. conradi* Assemblage

Biozone (now an interval biozone). These authors based its placement on *Baculites claviformis*, a temporally long-ranging taxon spanning the upper Campanian *Nostoceras hyatti* to the *N. alternatum* biozones, which is absent in the overlying upper Maastrichtian *D. conradi* Biozone, and then reappears in the *D. iris* Biozone. These authors logically assumed, in the absence of continuous sequences and given the lack of detailed faunal data from measured sections, that the absence of *B. claviformis* in the *D. conradi* Biozone and its presence in the *D. iris* Biozone indicated that the latter was stratigraphically equivalent to the *N. alternatum* Biozone that also contains *B. claviformis*. Reflecting on this perceived absence, Cobban and Kennedy (1995) also mistakenly established this biozone at the base of the upper Maastrichtian. In contrast, Landman *et al*. (2004a,b; 2007) placed the biozone in the uppermost Maastrichtian in the ACP based on the co-occurrence with diagnostic dinoflagellates and stratigraphic position within the uppermost Maastrichtian Prairie Bluff Chalk, which directly underlies the Danian Clayton Formation. Most recently, Larina *et al*. (2016) also designated it as the highest biozone in the GCP and altered the definition of this biozone from an assemblage to an interval biozone.

Occurrence: The *D. iris* Biozone has been documented in the Corsicana, Arkadelphia, and Owl Creek formations, as well as in the Prairie Bluff Chalk of the GCP (Figs. 3.3, 3.11; 3.14; also see Cobban and Kennedy, 1995; Kennedy and Cobban, 2000; Kennedy *et al*., 2001; Larina *et al*., 2016). In the ACP, this biozone has been recorded in the Severn, New Egypt, and Tinton formations; it also present as reworked material in the Danian Hornerstown Formation (Figs. 3.4, 3.11; 3.14; also see Kennedy and Cobban, 1996; Landman *et al*., 2004a, b, 2007). *D. iris* is also known from Libya (Machalski *et al*., 2009).

Stratigraphic and Age Range: The dinoflagellates in the ACP co-occurring with *D. iris* indicate a correlation with the CC26b/UC20d nannofossil subzone, which is positioned near the

top of the Maastrichtian directly below the appearance of Danian fauna (Landman *et al*., 2004a). In the GCP, Larina *et al*. (2016) used the presence and absence of several different dinoflagellate species and nannofossils, stratigraphic superposition and other fossil molluscs in the *D. iris* Biozone to show age equivalence between the GCP and ACP (Larina *et al*., 2016). Based on these data and correlations, it represents the highest (youngest) ammonite zone in the ACP and GCP with an approximate range between ~66.0–66.4 Ma (Fig. 3.6; Text 3.1). However, if certain ammonite species survived for a short time following the K/Pg mass extinction as suggested by Landman et al. (2012), then this ammonite zone might extend up into the lowest Danian or up to ~59.9 Ma.

Discussion

Regional Significance of New Biostratigraphic Framework

The ACP and GCP biostratigraphic schemes presented here are compilations based on systematic and biostratigraphic studies of the ammonites in these regions by various authors over the past half century (e.g., Young, 1963; Kennedy *et al*., 2000c; Landman *et al*., 2004a,b; 2007; Cobban *et al*., 2008; Larina *et al*., 2016). The influence from these studies is clearly seen when our biostratigraphic framework is compared against earlier schemes for the ACP and GCP (Figs. 3.8; 3.9; 3.10). However, in contrast to the previous studies, we have compiled significantly more ammonite data from the ACP and GCP, which allows refinement of the ammonite biozonations for these regions as well as constraining previously unidentifiable unzoned intervals. We are also able to produce a single unified scheme for each respective region with well-defined biozones that are temporally scaled within the modern biochronological framework for the Late Cretaceous established by Ogg and Hinnov (2012). This provides a means to improve correlation among regions as well as to evaluate the approximate chronostratigraphic

age of specific strata in the ACP and GCP, which due to their geological setting are lacking in geochronologically datable units, such as ash beds.

The biostratigraphic resolution of the ACP and GCP ammonite zones for the Campanian–Maastrichtian are comparable and are represented by 14 biozones each. These numbers are less than half of the 30 ammonite zones defined for the same interval in the WI (see Fig. 3.6 and Kauffman, 1977; Kauffman and Caldwell, 1993; Kauffman *et al*., 1993; Cobban *et al*., 2006; Ogg and Hinnov, 2012). The ACP and GCP ammonite zones have average durations of ~1.2 ± 1.0 Ma, which is considerably longer than the ~0.5 ± 0.2 Ma average biozonal durations for the WI (Ogg and Hinnov, 2012). ACP and GCP biozones range from ~0.3 to ~3.7 Ma in duration, which is much more variable than the ~0.4 to ~0.9 Ma biozone durations documented for the WI (see Table 1; also see Ogg and Hinnov, 2012).

Remaining Gaps in the ACP and GCP Biostratigraphic Records

Despite the addition of new biozones to previously unzoned intervals in the ACP and GCP, there are still significant gaps in our ammonite-based biostratigraphic record. In our scheme, the ACP has more unzoned levels with longer durations than that of the GCP, which can be seen in Fig. 3.6. Biostratigraphic gaps are also seen locally across both these regions (see Fig. 3.11); however, the GCP has an overall better record than the ACP due to its more complete stratigraphic coverage likely reflecting the greater number of exposures. Many of these local gaps in both regions are related to the nature of the record (as discussed above) and also prevailing paleoenvironmental conditions during the Late Cretaceous that controlled the distribution of ammonites locally. The poor record of ammonite biozones in the southern ACP and the border between the eastern and western GCP is most likely related to the limited number taxonomic studies on ammonites and other mollusks in these regions. For example, the only

taxonomic descriptions of ammonites known to the authors in the southern ACP are Stephenson (1923) and Landman et al. (2004a). Similarly, the only descriptions of ammonites along the border between the eastern and western GCP have primarily focused on either the Coon Creek Beds in McNairy, Tennessee or on the uppermost Maastrichtian faunas in southeastern Missouri or northeastern Arkansas (e.g., Wade, 1926; Stephenson, 1955; Cobban and Kennedy, 1994a; Larson, 2012, 2016; Larina et al., 2016).

The only intervals in both ACP and GCP left unzoned at the same level is roughly equivalent to the WI *Didymoceras nebrascense* Biozone to upper part of the *Baculites scotti* Biozone (Fig. 3.6). Kennedy and Cobban (1994b) did note the occurrence *D. nebrascence* in the Mount Laurel Sand in the ACP, but the specimen was not shown in any of the plates, and we were not able to find any other reports of this species. The lack of localities and specimens corresponding to these biozones in the GCP is likely due to limited exposures, preservational potential of these aragonitic taxa, and study. The Annona Chalk and Demopolis Formation are of the right age, but fossils, especially aragonitic taxa, are typically rare in these formations (K. Irwin and G. Phillips, pers. comm.). However, future research may uncover new data that will allow biozonation of this cross-regional gap in the ammonite record.

Regional-scale biozonal gaps include levels equivalent to *D. cheyennense* Biozone in the GCP as well as with intervals correlative with the Santonian and lower middle Campanian in the ACP (Fig. 3.6). The absence of ammonites equivalent to the *D. cheyennense* Biozone in the GCP is probably due to similar issues causing a lack of ammonites corresponding to the WI's upper *Baculites scotti* to *Didymoceras nebrascense* biozones in the GCP. The Marlbrook Marl, Blufftown Marl, and Demopolis Formation are the right age for *D. cheyennense* (see Figs. 3.3 and 4), but these formations are typically poorly- to unfossiliferous (K. Irwin and G. Phillips,

pers. comm.). The extreme rarity or even complete absence of ammonites in the unzoned levels of the upper Santonian and middle Campanian of the ACP can be attributed to relatively low sea levels during these time periods (see Miller, et al., 2004; Kulpecz, et al., 2008). In outcrop, the Santonian and lower middle Campanian strata (equivalent to the *Baculites taylorensis* Biozone) are mostly nonmarine to marginal marine in origin, such as the Magothy and Englishtown formations, where ammonites are scarce or completely absent. However, these formations are replaced by marine formations downdip, and the corresponding biozones are likely represented in subsurface. The gap along the middle-upper Campanian boundary appears to coincide with one of the several transgressive-regressive cycles identified along the ACP (Owens and Gohn, 1985). However, along the ACP, formations are thin, exposures are very small, and fossils are scare, so it is possible that this unzoned level is represented despite lacking fossils corresponding to these intervals.

Conclusions

- In this chapter, we revise the Campanian–Maastrichtian biozonation of the ACP and GCP. The biostratigraphic schemes proposed here are based on various systematic and biostratigraphic studies undertaken over the past 50 years on the ammonites of these two regions.
- The ACP and GCP schemes are represented by 14 ammonite zones each. The average durations differ considerably from the high-resolution biostratigraphic framework of the Western Interior.
- In this biozonation, eight new biozones are erected that occupy previously unzoned intervals. However, even with these additions, significant biozonal/temporal gaps in the record in the ACP and GCP record remain. These gaps in the ammonite-based

biostratigraphic record most likely reflect preservational gaps in the record, deposition of non-marine sediments due to low sea levels, and preferential collecting of specific intervals and regions.

References

Adkins, W.S., 1928, Handbook of Texas Cretaceous fossils: *University of Texas Bulletin*, 2838, 385 pp.

Adkins, W.S., 1933, Mesozoic Systems in Texas: *in* E.H. Sellards, W.S. Adkins, and F.B. Plummer Eds., *The Geology of Texas, vol. 1, Stratigraphy, University of Texas Bulletin*, 3232, 240–518.

Becker, M.A., Slattery, W., and Chamberlain, J.A., 1996, Reworked Campanian and Maastrictian macrofossils in a sequence bounding, transgressive lag deposit, Monmouth County, New Jersey: *Northeastern Geology and Environmental Sciences*, 18, 322–322.

Becker, M.A., Slattery, W., and Chamberlain, J.A., 1998, Mixing of Santonian and Campanian chondrichthyan and ammonite macrofossils along a transgressive lag deposit, Greene County, western Alabama: *Southeastern Geology*, 37, 205–216.

Böse, E., 1928, Cretaceous ammonites from Texas and Northern Mexico: *University of Texas Bulletin*, 2748, 143–357.

Böse, E., and Cavins, O.A., 1928, The Cretaceous and Tertiary of Southern Texas and Northern Mexico: *University of Texas Bulletin*, 2748, 142 pp.

Carpenter, S.J., Erickson, J.M., Lohmann, K.C., and Owen, M.R. 1988, Diagenesis of fossiliferous concretions from the Upper Cretaceous Fox Hills Formation, North Dakota: *Journal of Sedimentary Petrology*, 58, 706–723.

Cepek, P., and Hay, W.W., 1969, Calcareous nannoplankton and biostratigraphic subdivision of the Upper Cretaceous: *Gulf Coast Association of Geological Societies*, 19, 323–336.

Cobban, W.A., 1962, Baculites from the lower part of the Pierre Shale and equivalent rocks in the Western Interior: *Journal of Paleontology*, 36, 704–718.

Cobban, W.A., 1970, Occurrence of the Late Cretaceous ammonites *Didymoceras stevensoni* (Whitfield) and *Exiteloceras jenneyi* (Whitfield) in Delaware. *United States Geological Survey Professional Paper*, 700, 71–76.

Cobban, W.A. 1974, Ammonites from the Navesink Formation at Atlantic Highlands, New Jersey: *United States Geological Survey Professional Paper*, 845, 11 pp.

Cobban, W.A. and Kennedy, W.J. 1991a, New records of the Ammonite subfamily Texanitinae in Campanian (Upper Cretaceous) rocks in the Western Interior of the United States. *United States Geological Survey Bulletin,* 1985–B, 1–4.

Cobban, W.A. and Kennedy, W.J. 1991b, Some Upper Cretaceous ammonites from the Nacatoch Sand of Hempstead County, Arkansas: *United States Geological Survey Bulletin*, 1985–C, 1–5

Cobban, W.A. and Kennedy, W.J. 1991c, Upper Cretaceous (Maastrichtian) ammonites from the *Nostoceras alternatum* zone in southwestern Arkansas*: Unites States Geological Survey Bulletin*, 1985–E, 1–6.

Cobban, W.A. and Kennedy, W.J. 1992a, Campanian *Trachyscaphites spiniger* ammonite fauna in North-East Texas: *Palaeontology*, 35, 63–93.

Cobban, W.A. and Kennedy, W.J. 1992b, Campanian ammonites from the Upper Cretaceous Gober Chalk of Lamar County, Texas: *Journal of Paleontology*, 66, 440–454.

Cobban, W.A. and Kennedy, W.J. 1993a, Middle Campanian ammonites and inoceramids from the Wolfe City Sand in northeastern Texas: *Journal of Paleontology*, 67, 71–82.

Cobban, W.A. and Kennedy, W.J., 1993b, The Upper Cretaceous dimorphic pachydiscid ammonite Menuites in the Western Interior of the United States. *United States Geological Survey*, 1533, 14 pp.

Cobban, W. A., and Kennedy, W. J., 1994a, Upper Cretaceous ammonites from the Coon Creek Tongue of the Ripley Formation at its type locality in McNairy County, Tennessee: *United States Geological Survey Bulletin*, 2073–B, 12 pp.

Cobban, W.A., and Kennedy, W.J., 1994b, Middle Campanian (Upper Cretaceous) Ammonites from the Pecan Gap Chalk of Central and Northeastern Texas: *United States Geological Survey Bulletin*, 2073–D, 1–9.

Cobban, W.A. and Kennedy, W.J. 1995, Maastrichtian ammonites chiefly from the Prairie Bluff Chalk in Alabama and Mississippi: *The Paleontological Society Memoir*, 44, 40 pp.

Cobban, W.A., Kennedy, W.J., and Scott, G.R, 1993, Upper Cretaceous heteromorph ammonites from the *Baculites compressus* zone of the Pierre Shale in north central Colorado: *United States Geological Survery Bulletin*, 2024, 1–11.

Cobban, W.A., Mckinney, K., Obradovich, J.D. and Walaszczyk, I. 2006, USGS zonal table for the Upper Cretaceous Middle Cenomanian-Maastrichtian of the Western Interior of the United States Based on ammonites, inoceramids, and radiometric ages: *United States Geological Survey Open-File Report*, 1240, 50 pp.

Cobban, W.A., Hook, S.C. and McKinney, K.C., 2008, Upper Cretaceous molluscan record along a transect from Virden, New Mexico to Del Rio, Texas: *New Mexico Geology*, 3, 75–92.

Cooper, J.D. 1970, Stratigraphy and paleontology of Escondido Formation (Upper Cretaceous), Maverick County, Texas, and Northern Mexico: *Unpublished PhD Dissertation, University of Texas at Austin*, 288 pp.

Cooper, J.D. 1971, Maestrichtian (Upper Cretaceous) biostratigraphy, Maverick County, Texas, and northern Coahuila, Mexico: *Transactions of the Gulf Coast Association of Geological Societies*, 21, 57–65.

Cox, R.T.; and Van Arsdale, R.B. 1997, Hotspot origin of the Mississippi Embayment and its possible impact of contemporary seismicity: *Engineering Geology*, 46, 201–216.

Cox, R.T. and Van Arsdale, R.B., 2002, The Mississippi Embayment, North America: a first order continental structure generated by the Cretaceous super plume mantle event*: Journal of Geodynamics*, 34, 163–176.

Dockery III, D.T., 1990, The Chapelville fossiliferous Horizon of the Coffee Sand: A Window into the Campanian Molluscan Faunas of the northern Gulf: *in* Zullo, V.A., Burleigh Harris, W., and Price, V., *Savannah River region: transition between the Gulf and Atlantic coastal plains: proceedings of the Second Bald Head Island Conference on Coastal Plains Geology, Hilton Head Island, University of North Carolina at Wilmington*, 83–90.

Dockery III, D.T., 1996, Toward a revision of the generalized stratigraphic column of Mississippi: *Mississippi Geology*, 17, 8 pp.

Dockery III, D.T. and Thompson, D.E. 2016, The geology of Mississippi: *The University Press of Mississippi*, 175 pp.

Eberth, D.A., Delgado-de Jesús, C.R., Lerbekmo, J.F., Brinkman, D.B., Rodríquez-de la Rosa, R.A., Sampson, S.D., 2004, Cerro del Pueblo Fm (Difunta Group, Upper Cretaceous), Parras Basin, southern Coahuila, Mexico: reference sections, age, and correlation, *Revista Mexicana de Ciencias Geológicas*, 21, 335–352.

Elder, W.P., 1994, Some macrofossils from the Cretaceous (Campanian) Anacacho Limestone of Texas: *United States Geological Survey Open-File Report*, 94–551, 23.

Eldrett, J.S.; Ma, C.; Bergman, S.C.; Lutz, B.; Gregory, F.J.; Dodsworth, P.; Phipps, M.; Hardas, P.; Minisini, D.; Ozkan, A.; Ramezani, J., 2015, An astronomically calibrated stratigraphy of the Cenomanian, Turonian and earliest Coniacian from the Cretaceous Western Interior Seaway, USA: Implications for global chronostratigraphy. *Cretaceous Research*, 56, 316–344.

Etayo-Serna, F., 1989, Campanian to Maastrichtian fossils in the northeastern Western Cordillera, Colombia: *Geología Norandina*, 11, 23–32.

Feldman, R. M., Franţescu, A., Frantescu, O. D., Klompmaker, A. A., Logan, G., Robins, C. M., and Waugh, D. A., 2012, Formation of lobster-bearing concretions in the Late Cretaceous Bearpaw Shale, Montana, United States, in a complex geochemical environment: *Palaios*, 27, 842–856.

Gale, A.S., Hancock, J.M., Kennedy, W.J., Petrizzo, M.R., Lees, J.A., Walaszczyk, I. and Wray, D.S. 2008. An integrated study (geochemistry, stable oxygen and carbon isotopes, nannofossils, planktonic foraminifera, inoceramid bivalves, ammonites and crinoids) of the Waxahachie Dam Spillway section, north Texas: a possible boundary stratotype for the base of the Campanian Stage: *Cretaceous Research*, 1, 131–167.

Gale, A.S.; Montgomery, P.; Kennedy, W.J.; Hancock, J.M.; Burnett, J.A, and McArthur, J.M. 1995, Definition and global correlation of the Santonian-Campanian boundary: *Terra Nova*, 7, 611–622.

Galloway, W.E. 2008. Depositional Evolution of the Gulf of Mexico Sedimentary Basin. *in* A.D., Miall Ed., *Sedimentary basins of the world*, 5, 505–549.

Gautier, D.L., 1982. Siderite Concretions: Indicators of Early Diagenesis in the Gammon Shale (Cretaceous): *Journal of Sedimentary Petrology*. 52, 859–871.

Goldhammer, R.K. and Johnson, C.A. 1999, Mesozoic sequence stratigraphy and paleogeographic evolution of northeast Mexico: *Geological Society of America Special Papers*, 340, 58 pp.

Hancock, J.M. and Gale, A.S., 1996, The Campanian Stage: Bulletin de I'lnstitut royal des Sciences naturelles de Belgique, Sciences de la Terre, 66, 103–109.

Hart, M.B., Harries, P.J. and Cárdenas, A.L., 2013, The Cretaceous/Paleogene boundary events in the Gulf Coast: comparisons between Alabama and Texas: *Gulf Coast Association of Geological Societies Transactions*, 235–256.

Heim, N. 1934, Stratigraphische Kondensation: *Eclogae Geologica Helvetica*, 27, 372–383.

Hicks, J.F., Obradovich, J.D., and Tauxe, L., 1999, Magnetostratigraphy, isotopic age calibration, and intercontinental correlation of the Red Bird section of the Pierre Shale, Niobrara County, Wyoming, USA: *Cretaceous Research*, 20, 1–27

Hicks, J.F., Johnson, K.R., Obradovich, J.D., Tauxe, L., Clark, D. 2002, Magnetostratigraphy and geochronology of the Hell Creek and Basal Fort Union Formations of southwestern North Dakota and a recalibration of the age of the Cretaceous-Tertiary boundary: *in* Hartman, J.H., Johnson, K.R., and Nichols, D.J., eds. The Hell Creek Formation and the Cretaceous-Tertiary Boundary in the Northern Great Plains: An integrated Continental

Record of the End of the Cretaceous: *Geological Society of America Special Papers*, 361, 35–55.

Hoganson, J.W., and Murphy, E.C., 2002, Marine Breien Member (Maastrichtian) of the Hell Creek Formation in North Dakota: Stratigraphy, vertebrate fossil record, and age: *in* Hartman, J.H., Johnson, K.R., and Nichols, D.J., eds. The Hell Creek Formation and the Cretaceous-Tertiary Boundary in the Northern Great Plains: An integrated Continental Record of the End of the Cretaceous: *Geological Society of America Special Papers*, 361, 247–270.

Howarth, M.K. 1965, Cretaceous Ammonites and Nautiloids from Angola: *Bulletin of the British Museum*, 10, 335–412.

Ifrim, C. and Stinnesbeck, W. 2010, Migration pathways of the late Campanian and Maastrichtian shallow facies ammonite *Sphenodiscus* in North America: *Palaeogeography, Palaeoclimatology, Palaeoecology*, 292, 96–102.

Ifrim, C. and Stinnesbeck, W. 2013, Ammonoides del Maastrichtiano (Cretácico Tardío) en El Zancudo, Nuevo Laredo, Tamaulipas. México: *Boletín de la Sociedad Geológica Mexicana*, 65, 189–200.

Ifrim, C. Stinnesbeck, W. and López- Oliva, J.G. 2004, Maastrichtian cephalopods from Cerralvo, north- eastern Mexico: *Palaeontology*, 6, 1575–1627.

Ifrim, C. Stinnesbeck, W., and Schafhauser, A. 2005, Maastrichtian shallow-water ammonites of northeastern Mexico: *Revista Mexicana de Ciencias Geológicas*, 22, 48–64.

Ifrim, C., Stinnesbeck, W., Garza, R.R. and Ventura, J.F. 2010, Hemipelagic cephalopods from the Maastrichtian (Late Cretaceous) Parras Basin at La Parra, Coahuila, Mexico, and their implications for the correlation of the lower Difunta Group: *Journal of South American Earth Sciences*, 29, 597–618.

Ifrim, C.; Stinnesbeck, W.; and Flores Ventura, J. 2013, An Endemic Cephalopod Assemblage from the Lower Campanian (Late Cretaceous) Parras Shale, Western Coahuila, Mexico*: Journal of Paleontology*, 87, 881–901.

Ifrim, C., Stinnesbeck, W., Espinosa, B. and Ventura, J.F., 2015, Upper Campanian (Upper Cretaceous) cephalopods from the Parras Shale near Saucedas, Coahuila, Mexico. *Journal of South American Earth Sciences*, 64, 229–257.

Johnson, K.R., Nichols, D.J. and Hartman, J.H., 2002, Hell Creek Formation: A 2001 synthesis: *Geological Society of America Special Papers*, 361, 503–510.

Kauffman, E. G., 1977, Geological and biological overview: Cretaceous basin, *in* Kauffman, E.G. Ed, *Cretaceous Facies, Faunas, and Paleoenvironments Across the Western Interior*

Basin: Field Guide: North American Paleontological Convention II. Mountain Geologist, 14, 75–99.

Kauffman, E.G., 1979, Cretaceous: *Treatise on invertebrate paleontology,* A, 418–487.

Kauffman, E.G., 1977, Evolutionary rates and biostratigraphy, *in* Kauffman, E.G., Hazel, J.E. and Heffernan, B.D. eds., Concepts and methods of biostratigraphy: *Dowden, Hutchinson & Ross,* 109–141.

Kauffman, E.G. and Caldwell, W.G.E. 1993, Evolution of the Western Interior Basin, In: W.G.E. Caldwell and E.G. Kauffman (Eds.), Evolution of the Western Interior Basin. *Geological Association of Canada Special Paper*, 39, 1–46.

Kauffman, E.G., Sageman, B.B., Kirkland, J.I., Elder, W.P.; Harries, P.J., and Villamil, T., 1993, Molluscan Biostratigraphy of the Western Interior Basin, North America. *in* Caldwell, W.G.E., and Kauffman E.G., Ed., *Evolution of the Basin: Geological Association of Canada Special Paper*, 39, 397–434.

Kennedy, W.J., and Bilotte, M., 1995, A new ammonite fauna from the Sub-Pyrenean Campanian (Upper Cretaceous): *Geobios*, 28, 359–370.

Kennedy, W.J., and Cobban, W.A., 1976, Aspects of ammonite biology, biogeography, and biostratigraphy: *The Paleontological Association Special Papers in Palaeontology*, 17, 98 pp.

Kennedy, W.J.; and Cobban, W.A. 1991, Upper Cretaceous (upper Santonian) *Boehmoceras* fauna from the Gulf Coast region of the United States: *Geological Magazine*, 128, 167–189.

Kennedy, W.J. and Cobban, W.A. 1993a, Ammonites from the Saratoga Chalk (Upper Cretaceous), Arkansas: *Journal of Paleontology*, 67, 404–434.

Kennedy, W.J. and Cobban, W.A. 1993b, Lower Campanian (Upper Cretaceous) ammonites from the Merchantville formation of New Jersey, Maryland, and Delaware*: Journal of Paleontology*, 67, 828–849.

Kennedy, W.J. and Cobban, W.A. 1993c, Maastrichtian ammonites from the Corsicana Formation in northeast Texas: *Geological Magazine*, 130, 57–67.

Kennedy, W.J. and Cobban, W.A. 1993d, Upper Campanian ammonites from the Ozan-Annona Formation boundary in southwestern Arkansas: *Bulletin of the Geological Society of Denmark*, 40, 115–148.

Kennedy, W.J. and Cobban, W.A. 1994a, Ammonite fauna from the Wenonah Formation (Upper Cretaceous) of New Jersey*: Journal of Paleontology*, 68, 95–110.

Kennedy, W.J. and Cobban, W.A. 1994b, Upper Campanian ammonites from the Mount Laurel Sand at Biggs Farm, Delaware: *Journal of Paleontology*, 68, 1285–1305.

Kennedy, W.J. and Cobban, W.A. 1996, Maastrichtian ammonites from the Hornerstown Formation in New Jersey: *Journal of Paleontology*, 70, 798–804.

Kennedy, W.J.; and Cobban, W.A. 1997, Upper Campanian (Upper Cretaceous) Ammonites from the Marshalltown Formation-Mount Laurel Boundary Beds in Delaware: *Journal of Paleontology*, 71, 62–73.

Kennedy, W. and Cobban, W. 1999, Campanian (late Cretaceous) ammonites from the Bergstrom Formation in central Texas: *Acta geologica polonica*, 49, 67–80.

Kennedy, W. and Cobban, W. 2000, Maastrichtian (Late Cretaceous) ammonites from the Owl Creek Formation in northeastern Mississippi, USA*: Acta Geologica Polonica*, 50, 175–190.

Kennedy, W. and Cobban, W. 2001, Campanian (Late Cretaceous) ammonites from the upper part of the Anacacho Limestone in south-central Texas: *Acta geologica polonica*, 51, 15–30.

Kennedy, W.J. and Lunn, G., 2000, Upper Campanian (Cretaceous) ammonites from the Shinarish formation, Djebel Sinjar, Northwest Iraq: *Journal of Paleontology*,74, 464–473.

Kennedy, W.J., Cobban, W.A. and Scott, G.R., 1992, Ammonite correlation of the uppermost Campanian of Western Europe, the US Gulf Coast, Atlantic Seaboard and, and the numerical age of the base of the Maastrichtian: *Geological Magazine*, 129, 497–500.

Kennedy, W.J., Cobban, W.A., and Landman, N.H. 1997a, Maastrichtian ammonites from the Severn Formation of Maryland: *American Museum Novitates*, 3210, 30 pp.

Kennedy, W.J., Cobban, W.A., Landman, N.H. and Johnson, R.O. 1997b, New ammonoid records from the Merchantville Formation (Upper Cretaceous) of Maryland and New Jersey: *American Museum Novitates*, 3193, 17 pp.

Kennedy, W.J., Cobban, W.A., and Landman, N.H., 1997c, Campanian ammonites from the Tombigbee Sand Member of the Eutaw Formation, the Mooreville Formation, and the basal part of the Demopolis Formation in Mississippi and Alabama*: American Novitates*; 3201, 44 pp.

Kennedy, W., Cobban, W. and Scott, G., 2000b, Heteromorph ammonites from the middle Campanian *Baculites scotti* Zone in the US: *Acta Geologica Polonica*, 50, 223–241.

Kennedy, W.J., Landman, N.H., Cobban, W.A. and Johnson, R.O. 2000c. Additions to the ammonite fauna of the Upper Cretaceous Navesink Formation of New Jersey: *American Museum Novitates*, 3306, 30 pp.

Kennedy, W.J., Landman, N.H., Cobban, W.A. and Scott, G.R., 2000d, Late Campanian (Cretaceous) heteromorph ammonites from the Western Interior of the United States: *American Museum Bulletin*, 251, 86 pp.

Kennedy, W.J., Gale, A.S., and Hansen, T.A. 2001, The last Maastrichtian ammonites from the Brazos River sections in Falls County, Texas: *Cretaceous Research*, 22, 163–171.

Kidwell, S.M., 1998, Time averaging in the marine fossil record: overview of strategies and uncertainties: *Geobios*, 30, 977–995.

Klinger, H. C. and Kennedy, W.J., 2001, Stratigraphic and geographic distribution, phylogenetic trends, and general comments on the ammonite family Baculitidae Gill, 1871 (with an annotated list of the species referred to the family): *Annals of the South African Museum*, 107, 290.

Kowallis, B.J., Christiansen, E.H., Deino, A.L., Kunk, M.J., Heaman, L.M., 1995, Age of the Cenomanian-Turonian boundary in the Western Interior of the United States. *Cretaceous Research*, 16, 109–129.

Küchler, T., 2000, Upper Cretaceous of the Barranca (Navarra, northern Spain); integrated litho-, bio-and event stratigraphy. Part 2, Campanian and Maastrichtian: *Acta Geologica Polonica*, 50, 441–499.

Küchler, T. 1998, Upper Cretaceous of the Barranca (Navarra, northern Spain); integrated litho-, bio-and even stratigraphy 1, Cenomanian through Santonian: *Acta Geologica Polonica*, 48, 157–236.

Kulpecz, A.A., Miller, K.G., Sugarman, P.J. and Browning, J.V., 2008, Response of Late Cretaceous migrating deltaic facies systems to sea level, tectonics, and sediment supply changes, New Jersey Coastal Plain, USA: *Journal of Sedimentary Research*, 78, 112–129.

Landman, N. H., and Klofak, S. M., 2012, Anatomy of a concretion: Life, death, and burial in the Western Interior Seaway: *Palaios*, 27, 671–692.

Landman, N.H., Johnson, R.O., and Edwards, L.E., 2004a, Cephalopods from the Cretaceous/Tertiary Boundary Interval on the Atlantic Coastal Plain, with a Description of the Highest Ammonite Zones in North America, Part 1, Maryland and North Carolina: *American Museum Novitates*, 3454, 64 pp.

Landman, N.H., Johnson, R.O., and Edwards, L.E., 2004b, Cephalopods from the Cretaceous/Tertiary Boundary Interval on the Atlantic Coastal Plain, with a description of

the highest ammonite zones in North America, Part 2, Northeastern Monmouth County, New Jersey: *American Museum Bulletin*, 287, 107 pp.

Landman, N.H.; Johnson, R.O.; Garb, M.P.; Edwards, L.E., and Kyte, F.T., 2007, Cephalopods from the Cretaceous/Tertiary boundary interval on the Atlantic Coastal Plain, with a description of the highest ammonite zones in North America. Part 3. Manasquan River Basin, Monmouth County, New Jersey: *American Museum Bulletin*, 303, 112 pp.

Landman, N.H., Garb, M.P., Rovelli, R., Ebel, D.S., and Edwards, L.E., 2012, Short-term survival of ammonites in New Jersey after the end-Cretaceous bolide impact: *Acta Palaeontologica Polonica*, 57, 703–716.

Landman, N. H. Grier, J.C., Grier, J. W., Cochran, J.K., and Klofak, S.M., 2015, 3–D orientation and distribution of ammonites in a concretion from the Upper Cretaceous Pierre Shale of Montana: *Swiss Journal of Paleontology*, 1–23.

Larina, E., Garb, M., Landman, N., Dastas, N., Thibault, N., Edwards, L., Phillips, G., Rovelli, R., Myers, C. and Naujokaityte, J., 2016, Upper Maastrichtian ammonite biostratigraphy of the Gulf Coastal Plain (Mississippi Embayment, southern USA): *Cretaceous Research*, 60, 128–151.

Larson, N.L. 2012, The late Campanian (Upper Cretaceous) cephalopod fauna of the Coon Creek Formation at the type locality: *Journal of Paleontological Sciences*, 1, 68 pp.

Larson, N.L., 2016, The Late Cretaceous (upper Campanian) cephalopod fauna from the Coon Creek Science Center, McNairy County, Tennessee: *Bulletin of the Alabama Museum of Natural History*, 21–58.

Larson, N.L.; Jorgensen, S.D.; Farrar, R.A.; and Larson, P.L., 1997, Ammonites and the Other Cephalopods of the Pierre Seaway Identification Guide, *Geoscience Press*, 148 pp.

Lewy, Z., 1967, Some late Campanian nostoceratid ammonites from southern Israel: *Israel Journal of Earth-Science*, 16, 165–173.

Lewy, Z., 1986, *Anaklinoceras reflexum* Stephenson in Israel and its stratigraphic significance: *Newsletters on Stratigraphy*, 16, 1–8.

Luger, P., and Gröschke, M., 1989, Late Cretaceous ammonites from the Wadi Qena area in the Egyptian Eastern Desert: *Palaeontology*, 32, 355–407.

Machalski, M., Jagt, J.W.M., Landman, N.H.; and Janusz, U., 2009, First record of the North American scaphitid ammonite *Discoscaphites iris* from the upper Maastrichtian of Libya: *Neues Jahrbuch für Geologie und Paläontologie*, 254, 373–378.

Machalski, M., 2012, Stratigraphically important ammonites from the Campanian–Maastrichtianboundary interval of the Middle Vistula River section, central Poland: *Acta Geologica Polonica*, 62, 91–116.

Maeda, H., 1987. Taphonomy of Ammonites from the Cretaceous Yezo Group in Tappu Area, Northewestern Hokkaido, Japan: *Transactions and Proceedings of the Paleontological Society of Japan*, 148, 285–305.

Mancini, E.A., Puckett, T.M., and Tew, B.H., 1996, Integrated biostratigraphic sequence stratigraphic framework for Upper Cretaceous strata of the eastern Gulf Coastal Plain, USA: *Cretaceous Research*, 17, 645–669.

Maxwell, R. A., Lonsdale, J. T., Hazzard, R. T., and Wilson, J. A., 1967, Geology of Big Bend National-Park, Brewster County, Texas: *University of Texas, Bureau of Economic Geology, Publication*, 6711, 320 pp.

McArthur, J.M., Steuber, T., Page, K.N. and Landman, N.H., 2016, Sr-isotope stratigraphy: Assigning time in the Campanian, Pliensbachian, Toarcian, and Valanginian: *The Journal of Geology*, 124, 569–586.

McBride, E.F., Weidie, A.E., Wolleben, J.A. and Laudon, R.C., 1974, Stratigraphy and structure of the Parras and La Popa basins, northeastern Mexico: *Geological Society of America Bulletin*, 85, 1603–1622.

McFarlan, E., Jr., and Menes, L. S., 1991, Lower Cretaceous, In: A. Salvador (Ed.), The Gulf of Mexico Basin: *Geological Society of America, The Geology of North America Series*, J, 181–204.

McLaurin, B.T. and Harris, W.B., 2001, Paleocene faulting within the Beaufort Group, Atlantic Coastal Plain, North Carolina: *Geological Society of America Bulletin*, 113, 591–603.

McMullen, S.K., Holland, S.M., and O'Keefe, F.R., 2014, The occurrence of vertebrate and invertebrate fossils in a sequence stratigraphic context: The Jurassic Sundance Formation, Bighorn Basin, Wyoming, USA: *Palaios*, 29, 277–294.

Meyers, S.R.; Siewert, S.E.; Singer, B.S.; Sageman, B.B.; Condon, D.J.; Obradovich, J.D.; Jicha, B.R.; Sawyer, D.A. 2012, Intercalibration of radioisotopic and astrochronologic time scales for the Cenomanian-Turonian boundary interval, Western Interior Basin, USA: *Geology*, 40, 7–10.

Miall, A.D., Catuneanu, O., Vakarelov, B.K., and Post, R., 2008, The Western Interior basin. *In* Miall, A.D., Ed., *Sedimentary basins of the world*, 5, 329–362.

Miller, K.G., Sugarman, P.J., Browning, J.V., Kominz, M.A., Olsson, R.K., Feigenson, M.D., and Hernandez, J.C., 2004, Upper Cretaceous sequences and sea-level history, New Jersey Coastal Plain: *Geological Society of America Bulletin*, 116, 368–393.

Miller, K.G., Kominz, M.A., Browning, J.V., Wright, J.D., Gregory S. Mountain, Katz, M.E., Sugarman, P.J., Cramer, B.S., Christie-Blick, N., and Pekar, S.F., 2005, The Phanerozoic record of global sea-level change: *Science*, 310, 1293–1298.

Minard, J.P. 1980, Geology of the Round Bay quadrangle, Anne Arundel County, Maryland: *United States Geological Survey Professional Paper*, 1109, 30 pp.

Molina, E., Alegret, L., Arenillas, I., Arz, J.A., Gallala, N., Hardenbol, J., von Salis, K., Steurbaut, E., Vandenberghe, N., Zaghbib-Turki, D., 2006, The Global Boundary Stratotype Section and Point for the base of the Danian Stage (Paleocene, Paleogene, "Tertiary", Cenozoic) at El Kef, Tunesia-Original definition and revision: *Episodes*, 29, 263–273.

Müller, S.W. and Schenck, H.G. 1943, Standard of Cretaceous System: *American Association of Petroleum Geologists Bulletin*, 27, 262–278.

Pierson, J.A., 2003, Late cretaceous (Campanian and Maastrichtian) sequence stratigraphy, southeastern North Carolina, USA*: Unpublished* Masters *Thesis, University of North Carolina at Wilmington,* 75 pp.

Obradovich, J.D. 1993, A Cretaceous time scale: *in* Caldwell, W.G.E.; Kauffman, E.G., eds., *Evolution of the Western Interior Basin. Geological Association of Canada, Special Paper*, 39, 379–396.

Odin, G.S., 1996, Le site de Tercis (Landes): Observations stratigraphiques sur le Maastrichtien. Arguments pour la localisation et la corre´lation du Point Stratotype Global de la limite Campanien-Maastrichtien: *Bulletin de la Socie´te´ ge´ologique de France*, 167, 637–643.

Odin, G.S. (Ed.), 2001, The Campanian–Maastrichtian Boundary: Characterisationat Tercis les Bains (France) and correlation with Europe and other Continents. *Developments in Palaeontology and Stratigraphy*, 19, 910 pp.

Odin, G.S. and Lamaurelle, M.A., 2001, The global Campanian–Maastrichtian stage boundary: *Episodes*, 24, 229–238.

Odin, G.S. and Walaszczyk, I., 2003, Sur les inocérames de Tercis (Landes, France): le meilleur outil corrélatif entre Europe et Amérique du Nord autour de la limite Campanien-Maastrichtian: *Comptes Rendus Geoscience*, 335, 239–246.

Ogg, J. G., L. A. Hinnov, and Huang, C. 2012, "Cretaceous.": in Gradstein, F.M., Ogg, J.G., Schmitz, M.D., and Ogg, G.M., *The Geologic Time Scale*, 793–853.

Owens, J.P.; and Gohn, J.S., 1985, Depositional history of the Cretaceous Series in the U.S. Atlantic Coastal Plain: stratigraphy, paleoenvironments, and tectonic controls of sedimentation: *in* Poag, C.W., Ed., *Geological Evolution of the United States Atlantic Margin*, 25–86.

Pessagno, E.A., 1969, Upper Cretaceous stratigraphyof the Western Gulf Coast area of Mexico, Texas, and Arkansas: *Geological Society of America Memoir*, 111, 139 pp.

Raup, D.M., 1976, Species Diversity in the Phanerozoic: An Interpretation: *Paleobiology*, 2, 289–297.

Rawson, P.F., Dhondt, A.V., Hancock, J.M., Kennedy, W.J. (Eds.), 1996. Proceedings of the Second International Symposium on Cretaceous Stage Boundaries, Brussels, 8–16 September 1995: *Bulletin de l'Institut Royal des Sciences Naturelles de Belgique, Sciences de la Terre*, 66, 117 pp.

Reed Jr., J.C., Wheeler, J.O. and Tucholke, B.E., 2005, Geological map of North America with explanatory notes: *Geological Society of North America Continent Scale Map*, 001, 36 pp

Richards, H.G., 1958, The Cretaceous Fossils of New Jersey, Part 1: *New Jersey Geological Survey*, 266 pp.

Robinson Roberts, L.N. and Kirschbaum, M.A. 1995, Paleogeography of the Late Cretaceous of the Western Interior of Middle North America-Coal Distribution and Sediment Accumulation. *United States Geological Survey Professional Paper*, 1561, 115 pp.

Sageman, B.B., Singer, B.S., Meyers, S.R., Siewert, S.E., Walaszczyk, I., Condon, D.J., Jicha, B.R., Obradovich, J.D. and Sawyer, D.A., 2014, Integrating 40Ar/39Ar, U-Pb, and astronomical clocks in the Cretaceous Niobrara Formation, Western Interior Basin, USA. Bulletin, 126, 956–973.

Salvador, A., 1991, Origin and development of the Gulf of Mexico basin: *in* Salvador A. (Ed.), *The Gulf of Mexico Basin, The Geology of North America Series*, J, 389–444.

Schulz, M. G., Ernst, G., Ernst, H., and Schmid, F., 1984, Coniacian to Maastrichtian stage boundaries in the standard sections for the Upper Cretaceous white chalk of N.W. Germany (Lagerdorf–Kronsmoor–Hemmoor): *Definitions and proposals. Bulletin of the Geological Society of Denmark,* 33, 203–215.

Sheridan, R.E., 1974, Conceptual model for the block-fault origin of the North American Atlantic continental margin geosyncline. *Geology*, 2, 465–468.

Slattery, J.S., Cobban, W.A., McKinney, K.C., Harries, P.J., and Sandness, A.L., 2015, Early Cretaceous to Paleocene Paleogeography of the Western Interior Seaway of North America and its relation to tectonics and eustasy, *in* Bingle-Davis, M., Ed., *Cretaceous Conference. Evolution and Revolution, WGA Field Guide*, 22–60.

Slattery, J.S., Harries, P.J. and Sandness, A.L., 2018, Do marine faunas track lithofacies? Faunal dynamics in the Upper Cretaceous Pierre Shale, Western Interior, USA: *Palaeogeography, Palaeoclimatology, Palaeoecology*, 496, 205–224.

Sohl, N.F., 1960, Archeogastropoda, mesogastropoda, and stratigraphy of the Ripley, Owl Creek, and Prairie Bluff Formations: *United States Geological Survey Profession Paper*, 331–A, 151 pp.

Sohl, N.F., 1964, Gastropods from the Coffee Sand (Upper Cretaceous) of Mississippi, *United States Geological Survey Profession Paper*, 331–C, 345–394.

Sohl, N. F., 1977, Utility of gastropods in biostratigraphy: *in* Kauffman, K.G. and J. E. Hazel, J. E. Ed., *Concepts and Methods of Biostratigraphy. Dowden, Hutchinson and Ross*, 510–539.

Sohl, N.F., and Koch, C.F., 1986, Molluscan biostratigraphy and biofacies of the Haustator bilira Assemblage zone (Maastrichtian) of the east Gulf Coastal Plain: *in* Reinhardt, J. Ed., Stratigraphy and sedimentology of continental nearshore and marine Cretaceous sediments of the Eastern Gulf Coastal Plain: *Society of Economic Paleontologists and Mineralogists Annual Meeting Field Trip*, 3, 45–56.

Sohl, N. F., Martinez R. E., Salmeron-Urena, P., and Soto-Jaramillo, F., 1991, Upper Cretaceous. *in* A. Salvador A. Ed., *The Gulf of Mexico Basin, The Geology of North America Series*, J, 205–244.

Stephenson, L.W., 1914, Cretaceous deposits of the eastern Gulf region and species of *Exogyra* from the eastern Gulf region and the Carolinas: *United States Geological Society Professional Paper*, 81, 55 pp.

Stephenson, L.W., 1923, Invertebrate Fossils of the Upper Cretaceous Formations: *in* The Cretaceous Formations of North Carolina: *North Carolina Geological and Economic Survey*, 5, 389 pp.

Stephenson, L.W., 1928, Correlation of the Upper Cretaceous or Gulf series of the Gulf Coastal Plain: *American Journal of Science*, 96, 485–496.

Stephenson, L.W., 1933, The zone of *Exogyra cancellata* traced twenty-five hundred miles: *American Association of Petroleum Geologists Bulletin*, 17, 1351–1361.

Stephenson, L.W., 1936a, Stratigraphic relations of the Austin, Taylor, and equivalent formations in Texas: *United States Geological Survey Professional Paper*, 186–G, 133–146.

Stephenson, L.W., 1941, The Larger Invertebrate Fossils of the Navarro Group of Texas (Exclusive of Corals and Crustaceans and Exclusive of the Fauna of the Escondido Formation): *The University of Texas Publication*, 4101, 641 pp.

Stephenson, L.W., King, P.B., Monroe, W.H. and Imlay, R.W., 1942, Correlation of the outcropping Cretaceous formations of the Atlantic and Gulf Coastal Plain and trans-Pecos Texas: *Geological Society of America Bulletin*, 53, 435–448.

Stephenson, L.W., 1955, Owl Creek (Upper Cretaceous) fossils from Crowleys Ridge, southeastern Missouri: *United States Geological Survery Professional Paper*, 274–E, 140 pp.

Summesberger, H.; Machalski, M.; Wagreich, M., 2007, First record of the late Campanian heteromorphy ammonite *Nostoceras hyatti* from the Alpine Cretaceous (Grünbach, Gosau Group, Lower Austria): *Acta Geologica Polonica*, 57, 443–451.

Swezey, C.S. and Sullivan, E.C., 2004, Stratigraphy and sedimentology of the Upper Cretaceous (Campanian) Anacacho Limestone, Texas, USA: *Cretaceous Research*, 25, 473–497.

Vandenberghe, N., Hilgen, F.J., Speijer, R.P., Ogg, J.G., Gradstein, F.M., Hammer, O., Hollis, C.J., and Hooker, J.J., 2012, The Paleogene Period: *in* Gradstein, F.M., Ogg, J.G., Schmitz, M., and Ogg, G. eds., *The Geologic Time Scale 2012*, *Elsevier*, 855– 921.

Walaszczyk, I., Cobban, W.A., and Harries, P. J., 2001, Inoceramids and inoceramid biostratigraphy of the Campanian and Maastrichtian of the United States Basin: *Revue Paleobiology*, 20, 117–234.

Walaszczyk, I., Odin, G., and Dhondt, A., 2002a, Inoceramids from the Upper Campanian and Lower Maastrichtian of the Tercis section (SW France), the Global Stratotype Section and Point for the Campanian–Maastrichtian boundary; taxonomy, biostratigraphy and correlation potential: *Acta Geologica Polonica*, 52, 269–305.

Walaszczyk, I., Cobban, W.A., and Odin, G.S., 2002b, The inoceramid succession across the Campanian–Maastrichtianboundary: *Bulletin of the Geological Society of Denmark*, 49, 53–60.

Walaszczyk, I., 2004, Inoceramids and inoceramid biostratigraphy of the Upper Campanian to basal Maastrichtian of the Middle Vistula River section, central Poland: *Acta Geologica Polonica*, 54, 95–168.

Walaszczyk, I., Cobban, W.A., Wood, C.J. and Kin, A., 2008, The "Inoceramus" azerbaydajensis fauna (Bivalvia) and its value for chronostratigraphic calibration of the European Campanian (Upper Cretaceous): *Bulletin de l'Institut Royal des Sciences Naturelles de Belgique*, 78, 229–238.

Walaszczyk, I., Kennedy, W.J., and Klinger, H.C., 2009, Cretaceous faunas from Zululand and Natal, South AfricaSystematic palaeontology and stratigraphical potential of the upper Campanian–Maastrichtian Inoceramidae (Bivalvia), *African Natural History*, 5, 49–132.

Walaszczyk, I., Jagt, J.W.M., and Keutgen, N., 2010, The youngest Maastrichtian 'true'inoceramids from the Vijlen Member (Gulpen Formation) in northeast Belgium and the Aachen area (Germany): *Netherlands Journal of Geosciences*, 89, 147–167.

Wade, B., 1926, The fauna of the Ripley formation on Coon Creek, Tennessee: *United States Geological Survey Professional Paper*, 137, 137 pp.

Ward, P.D., Kennedy, W.J., MacLeod, K.G. and Mount, J.F., 1991, Ammonite and inoceramid bivalve extinction patterns in Cretaceous/Tertiary boundary sections of the Biscay region (southwestern France, northern Spain): *Geology*, 19, 1181–1184.

Ward, P. and Orr, W., 1997, Campanian–Maastrichtian ammonite and planktonic foraminiferal biostratigraphy from Tercis, France: implications for defining the stage boundary: *Journal of Paleontology*, 71, 407–418.

Ward, P.D., Haggart, J.W., Mitchell, R., Kirschvink, J.L. and Tobin, T., 2012, Integration of macrofossil biostratigraphy and magnetostratigraphy for the Pacific Coast Upper Cretaceous (Campanian–Maastrichtian) of North America and implications for correlation with the Western Interior and Tethys: *Geological Society of America Bulletin*, 124, 957–974.

Woehr, D.A. 2013, Die Fauna der Corsicana-Formation (Maastrichtian) von Süd-Texas (USA): *Der Steinkern*, 14, 67 pp.

Wolleben, J.A., 1967, Senonian (Cretaceous) mollusca from Trans-Pecos Texas and northeastern Chihuahua, Mexico. *Journal of Paleontology*, 41, 1150–1165.

Young, K.P., 1959, Techniques of mollusc zonation in Texas Cretaceous: *American Journal of Science*, 257, 752–769.

Young, K., 1963, Upper Cretaceous Ammonites from the Gulf Coast of the United States: *University of Texas Publication*, 6304, 373 pp,

Young, K., 1969, Ammonite zones of northern Chihuahua: *in* Cordoba, D.A., Wengerd, S.A., and Shomaker, J.W., Eds., *The Border Region (Chihuahua, Mexico, & USA), New Mexico Geological Society Annual Field Conference Guidebook*, 20, 97–101.

Young, K., 1982, Cretaceous rocks of central Texas—biostratigraphy and lithostratigraphy. In: Maddocks, R. F., Ed., *Texas Ostrocoda: guidebook of excursions and related papers for the Eighth Annual International Symposium on Ostracoda*, 8, 111–126.

Young, K., 1985, The Austin Division of Central Texas: *in* K. Young, K., and Woodruff, C.M., Eds., *Austin chalk in its type area--stratigraphy and structure*, *Austin Geological Society Field Guidebook*, 7, 3–52.

Young, K., 1986, Cretaceous, Marine inundations of the San Marcos Platform, Texas: *Cretaceous Research*, 7, 117–140.

CHAPTER FOUR:

MORPHOMETRIC METHODS USED FOR DOCUMENTING EVOLUTIONARY PATTERNS

Introduction

There is a broad array of techniques to document and examine evolution in the fossil record, including, but not limited to, analyses of origination and extinction, phylogenetic relationships, and morphological form. Studies of origination and extinction can reveal broad-scale macroevolutionary patterns of diversification, whereas analysis of phylogenetic relationships can typically reveal important information on evolutionary processes (e.g., allopatric vs. sympatric speciation). Of all these techniques, examination of morphological form is the most commonly used method to test for stasis, punctuated equilibrium, and phyletic gradualism within species and lineages due to its ability to identify virtually imperceptible evolutionary modifications or similarities in form. Morphological change between both taxa and lineages is typically evaluated using morphometric analyses, which usually involve the quantitative analysis of form (i.e., shape and size) and/or landmarks.

Chapters Five and Six document and compare the evolutionary patterns among the bivalves *Nucula* Lamarck 1799, *Lucina* Bruguière 1797, and *Anodontia* Link 1807 during contrasting climatic regimes using two morphometric elements: size measurements and outline shapes. Here, they are utilized to test for stasis by measuring morphologic change within various lineages. The methodology follows Jarrett's (2016) procedures in terms of measuring and analyzing both size and shape data in large numbers of specimens.

Photography

To obtain the bivalve measurements and outline shapes, specimens were initially, photographed using a high-resolution Olympus Tough camera (12–megapixel resolution) set to macro and mounted onto an adjustable stand with good-lighting. This provides higher quality images and reduces potential motion blur caused by vibrations in low-light conditions, which could impact the quality of an extracted outline. The adjustable camera stand provided a means to standardize the working distance between the specimens and the lens, which, if varied between photographs, could potentially impact the scale of the image for collection of measurement data. All specimens were photographed against a clean, low-reflectivity, black cloth surface, which made image processing (e.g., altering the image contrast) easier and less time consuming. Each bivalve specimen was placed concave surface down with its umbo oriented towards the bottom of the image. All specimens were centered in each image frame with the specimen information card and a scale bar placed at their sides (Fig. 4.1).

Image Editing

Once specimen image files were uploaded onto a computer, they were sorted and relabeled with a coding scheme based on their taxonomy, valve (i.e., right or left), and field data to make them easier to identify and verify. For example, an image of a left valve of *Nucula proxima* from the Tamiami Formation of south Florida, was renamed NPTL1, with the first two letters signifying the genus and species, the third letter indicating the formation, fourth letter identifying either right (R) or left (L) valves, and a number to signify the specimen. For the most part, taxonomic and age assignment were based on the sample labels associated with the specimens. For specimens collected by the author, taxonomic identifications were based on the

literature, whereas geological information was based on the regional geological map information, biostratigraphic age determination, and detailed stratigraphic description of fossil localities.

Images used for collection of shape data were uploaded into the GNU Image Manipulation Program (GIMP) (Solomon, 2009). In GIMP, images were converted to grayscale, and their contrast or threshold was adjusted to make a black and white silhouette to promote the ready extraction of shape data. Images were then cleaned up to remove small specks (e.g., loose sediment particles) surrounding the valves, which could potentially result in inaccurate outlines (Fig. 4.2A and 4.2B).

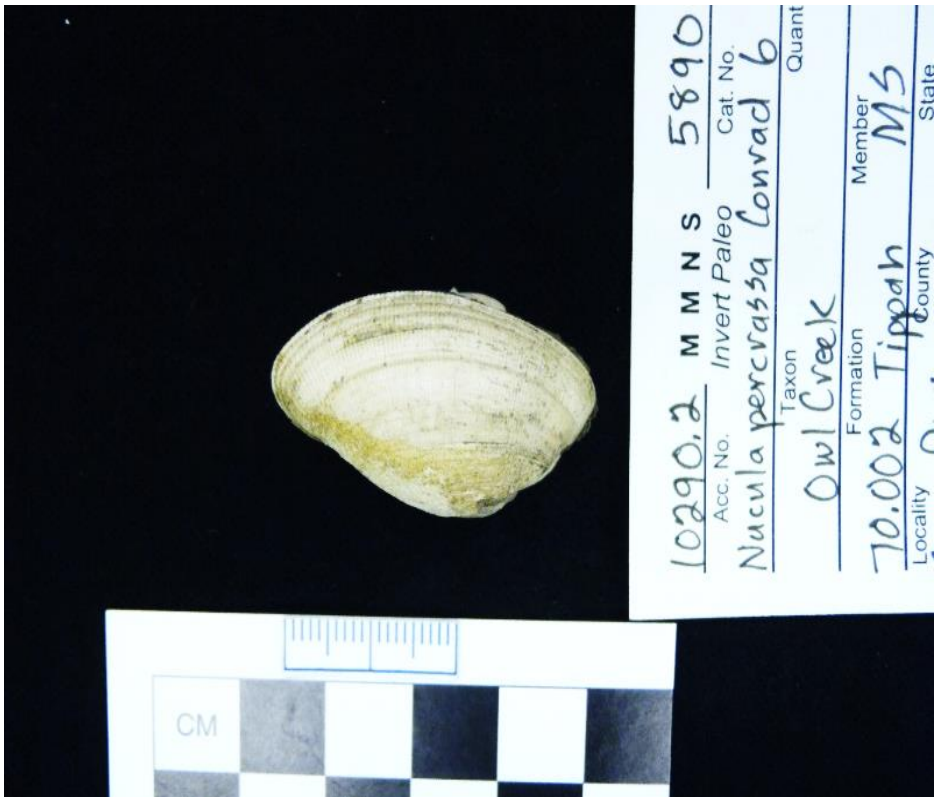

Figure 4.1. Example of how bivalve images were taken with specimen centered in each image frame with the specimen information card and a scale set to their sides.

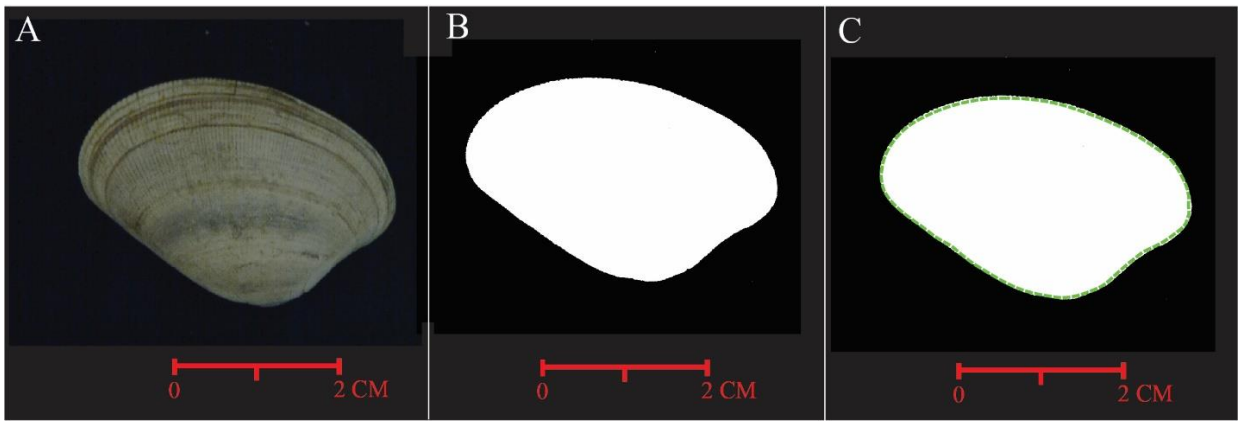

Figure 4.2. The steps followed for creating outline data from a bivalve specimen. (A) a raw unedited specimen photograph (B) image adjusted to create black and white silhouette of specimen (C) generation of shape outline as defined by the green dashed line.

Outline Shape and Size Data Extraction

The National Institutes of Health shareware program FIJI (a modified version of ImageJ; Schindelin et al., 2012) was used to automatically collect outline-shape data. Edited bivalve images were imported into FIJI, where the shells were selected using the Wand Tracing Tool to replicate the outline (Fig. 4.2C). Once the shell outline was demarcated, the xy-coordinates were extracted by selecting: Process Menu → Find Edge Command. These xy-coordinates were exported out of FIJI as text files by selecting: Select File → Save as → XY coordinates. These text files were labeled and organized into folders based on their taxonomy, field information, and valve (i.e., right or left).

FIJI was also used to obtain height and width data from the imported bivalve images (Fig. 4.3). To determine the image's scale, the Line Tool was utilized to measure a 10–mm segment taken from the scale included in the image during photographing. Then, the image scale was set by selecting: Analyze Menu → Set Scale. After this was established, the wand tool was used to obtain the outline of the shell and measurements were taken by selecting: Analyze Menu → Set

Measurements → Measure. The height and width data were then exported as an Excel file for easy analysis.

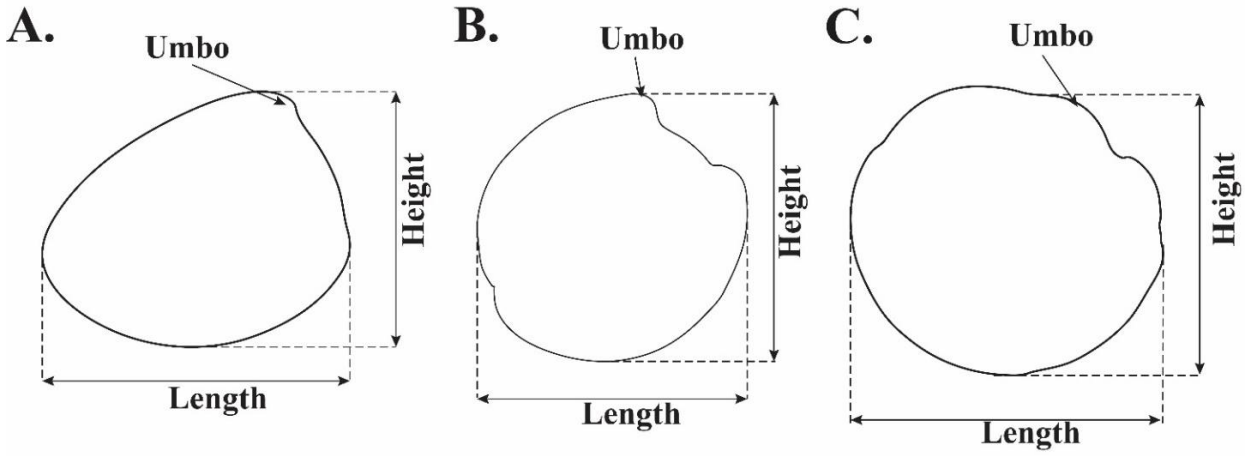

Figure 4.3. Height and width measurements for *Nucula* (A), *Lucina* (B), and *Anodontia* (C) bivalve shells analyzed in chapters Five and Six.

Preparation of Outline Data for Elliptical Fourier Analysis

Before calculating Fourier harmonics used to define a specimen's shape, outline data were smoothed as well as aligned to remove potential data artifacts caused by variation in raw xy-coordinate position, size, translation, rotation, and starting position. The xy-coordinates defining the outline shapes of the bivalves were processed in the R packages 'MOMOCS' (morphometrics using R) and 'geomorph' (Bonhome *et al*., 2014; R Development Core Team, 2018), as well as using the coo_rotate and coo_setstart programs developed by Jarrett (2016). Initially, outline data were smoothed over 100 iterations to make the xy-coordinates evenly spaced as well as to eliminate variation in xy-coordinate position (Fig. 4.4). Without smoothing, raw outlines, which are composed of small pixels, have a sawtooth pattern and are usually undulatory. This uneven and undulatory appearance, called digitization noise, if not removed by the smoothing routine, can partially obscure the true outline shape of a specimen. Because raw outlines typically vary in their size, translation, and rotation due to the imaging and outline

extraction processes, post-processing methods were employed to remove these variations not related to shape. First, all outlines were scaled to a unit centroid size that was identical for every specimen (i.e., all centroid sizes = 1; Fig. 4.5A). Second, because the orientation of specimens can be influenced by their initial position during photography, the 'coo_rotate' method was also used to rotate each outline into a standard position based on the rotation of the first ellipse (Fig. 4.5B). Finally, a standardized starting position for the outline trace was calculated using the program, 'coo_setstart', which converts each raw outline to a new outline comprised of 360 equally spaced coordinates with an identical starting position (Fig. 4.5C). This is important because the analytical method (i.e., Elliptical Fourier Analysis, see discussion below) used here to evaluate outline shape is highly sensitive to the starting position, and could, without correction, reflect variation in starting position rather than shape (Haines and Crampton, 2000).

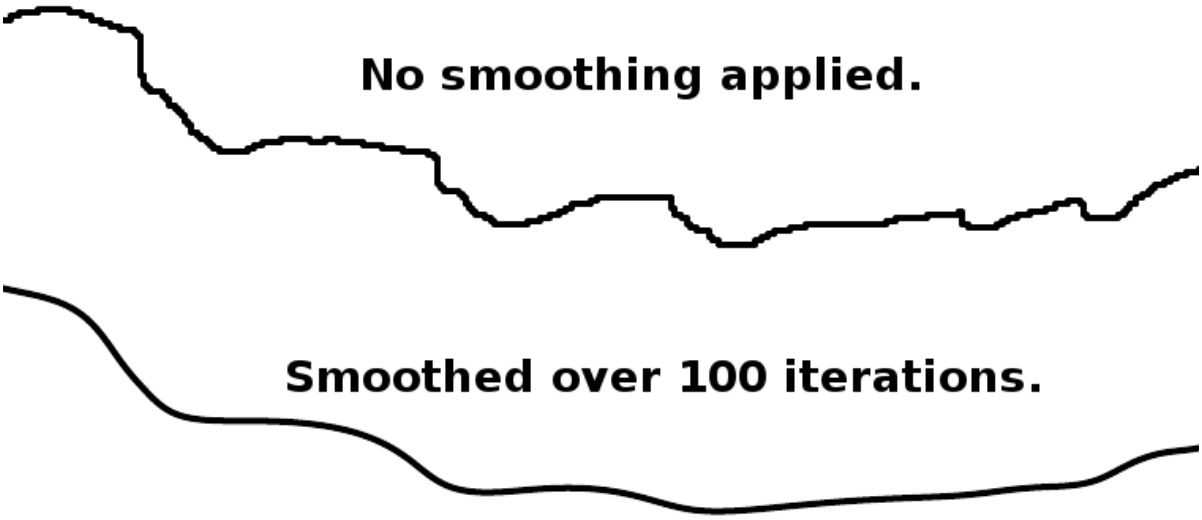

Figure 4.4. Example of how digitized shell outlines were smoothed to over 100 iterations to make the xy-coordinates evenly spaced as well as to eliminate variation in xy-coordinate position (courtesy of M. Jarrett).

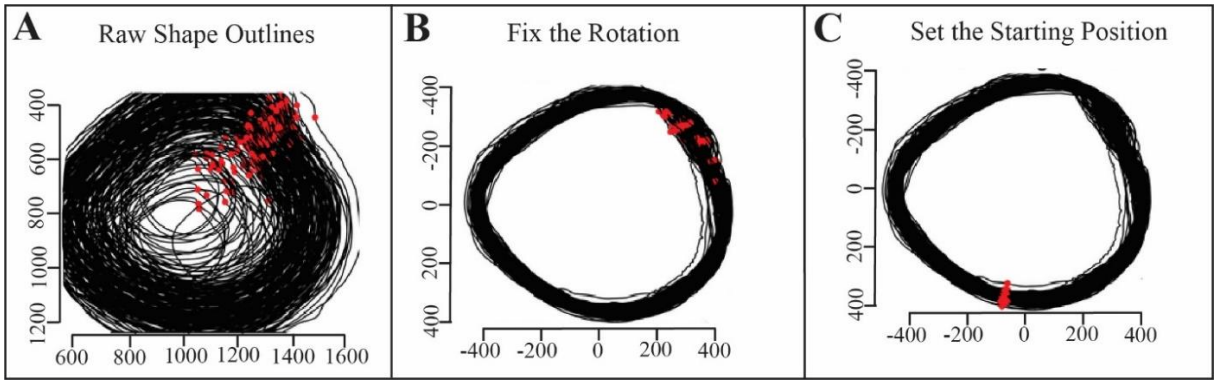

Figure 4.5. Examples of the steps involved in the preparation of bivalve shape outlines, including A) raw shape outline, B) Jarrett's (2016) 'coo_rotate' method used to rotate each outline into a standard position, and C) Jarrett's (2016), 'coo_setstart' program, which changes raw outlines to new outlines comprised of 360 equally spaced coordinates with matching starting positions. Figure modified from Jarrett (2016).

Elliptical Fourier Analysis of Outlines

Elliptical Fourier Analysis (EFA) was utilized to calculate Fourier coefficients from the corrected xy-coordinates using the 'MOMOCS' package in R developed by Bonhome *et al*. (2014). EFA works best on specimens or characters with comparatively simple shapes (e.g., outlines shapes that are roughly ovals), like the outline of many bivalves and brachiopods (Haines and Crampton, 2000).

Allometry

To examine how variability in the outline shape relates to specimen size, the relative warp scores (i.e., a measure of the bending energy required to warp one shape to a 'mean shape' representative of the outline population; see also Claude, 2008; Zelditch et al., 2012) were compared to centroid size, which is a measure of size used in geometric morphometrics (Bookstein, 1989; 1997; Rohlf and Bookstein, 2003; Freissias, 2003; Jonke *et al*., 2003; Hammer and Harper, 2008). The warp scores were derived from the fitted outlines and the centroid sizes were calculated by summing the squared distances between all landmarks on specimens

(Webster and Sheets, 2010). Therefore, if shape variation is reflected by the relative warp scores as a relationship of centroid size, the primary element being compared in the analysis is dependent upon size and is, therefore, an inaccurate measure of morphology if used without corrective procedures, commonly a simple log transform of the data (Zelditch et al., 2012).

Analysis of Fourier Coefficients and Size Data

To determine evolutionary patterns, the variance in Fourier coefficients for the different species from various time intervals were analyzed using the ordination techniques Principle Component Analysis (PCA) and Canonical Variate Analysis (CVA) in the statistical package R. PCA is used to examine the variance among specimens, whereas CVA was employed to maximize differences among groups (Mitteroecker and Bookstein, 2011; Zelditch et al., 2012). PCA is an eigenvalue-eigenvector technique that sorts variation in multivariate datasets along two or more independent (uncorrelated) axes, which are ranked in order of decreasing importance (Zelditch et al., 2012). Axis 1 explains the most amount of variation in PCA, followed successively by axis 2, axis 3, and so on. The amount variation explained by each axis (i.e., loadings) is given as a percent, which can be used to interpret the data. Here we only examine the first three axes on the PCA plots because they explain a preponderance of the morphologic variation. Similarly, CVA, which is an extension discriminant analysis, plots multivariate data along two or more dimensions so differences among three or more groups are maximized (Mitteroecker and Bookstein, 2011; Zelditch et al., 2012). The mean PCA and CVA scores were plotted along each axis and 80% confidence ellipsoids were calculated to show the amount of variation each species from the different formations reflected. An 80% confidence interval was chosen because it encompasses the variance in sample sizes, especially samples with few specimens, better than 95% confidence intervals. The groupings observed in both PCA and

CVA plots were then statistically tested by analyzing PCA and CVA scores using Hotelling's T^2 test, which is a modified Student's t-test intended for multivariate datasets (Hotelling, 1931). An alpha value of 0.05 was used as a metric of significance for these statistical tests as well as all other tests.

Length (L) and height (H) data of each specimen was converted to the geometric mean $\left(gm = \sqrt{(LxH)}\right)$ as this proxy for body size correlates with more complex measures of specimen shape (i.e., centroid size; see Koznik *et al*., 2008) to analyze size through time. Size data was analyzed by time interval using: 1) box and whisker plots, and 2) tables displaying summary statistics for each size distribution. Size data was also compared among time intervals using the Mann–Whitney *U* test statistic (Mann and Whitney, 1947). This test is a non-parametric equivalent to a two-sample t-test and is best utilized for small sample sizes (n<10), which are common in the data sets analyzed here.

References

Bookstein, F.L., 1989, Principal warps: Thin-plate splines and the decomposition of deformations: *IEEE Transactions on pattern analysis and machine intelligence*, 11, 567–585.

Bookstein, F.L., 1997, Morphometric tools for landmark data: geometry and biology: *Cambridge University Press*, 456 pp.

Bonhomme, V., Picq, S., Gaucherel, C., and Claude, J., 2014, Momocs: outline analysis using R: *Journal of Statistical Software*, 56, 24 pp.

Claude, J., 2008, Morphometrics with R: *Springer Science & Business Media*, 317 pp.

Friessias, M., 2003, An Application of the Relative Warps Analysis to Problems in Human Paleontology – With Notes on Raw Data Quality: *Image Analysis and Stereology*, 22, 63–72.

Haines A.J. and Crampton, J.S., 2000, Improvements to the method of fourier shape analysis as applied in morphometric studies: *Palaeontology*, 43, 765–783.

Hammer, O. and Harper, D.A.T., 2006, Paleontological Data Analysis: *Blackwell*, 356 pp.

Hotelling, H., 1931, The generalization of Student's ratio: *Annals of Mathematical Statistics*, 2, 360–378.

Jarrett, M., 2016, Lilliput Effect Dynamics across the Cretaceous-Paleogene Mass Extinction: Approaches, Prevalence, and Mechanisms: *Unpublished doctoral dissertation, University of South Florida*, 188 pp.

Jonke E., Schaefer, K. Freudenthaler, J.W., Prossinger H., and Bookstein, F.L., 2003, A Cephalometric Comparison of Skulls from Different Time Periods – The Bronze Age, the 19th Century and the Present: *Collective Anthropology*, 27, 789–801.

Kosnik, M. A., Jablonski, D., Lockwood, R., and Novack-Gottshall, P. M., 2006, Quantifying molluscan body size in evolutionary and ecological analyses: maximizing the return on data-collection efforts: *Palaios*, 21, 588–597.

Mann, H. B., and Whitney, D. R., 1947, On a test of whether one of 2 random variables is stochastically larger than the other: *Annals of Mathematical Statistics*, 18, 50–60.

Mitteroecker, P. and Bookstein, F., 2011, Linear discrimination, ordination, and the visualization of selection gradients in modern morphometrics: *Evolutionary Biology, 38*, 100–114.

R Core Team 2015, R: A Language and Environment for Statistical Computing. R Foundation for Statistical Computing, URL http://www.R-project.org/.

Rohlf, F.J. and Bookstein, F.L., 2003, Computing the uniform component of shape variation: *Systematic Biology*, *52*, 66–69.

Schindelin, J., Arganda-Carreras, I., Frise, E., Kaynig, V., Longair, M., Pietzsch, T., Preibisch, S., Rueden, C., Saalfeld, S., Schmid, B. and Tinevez, J.Y., 2012, Fiji: an open-source platform for biological-image analysis: *Nature methods*, 9, 676.

Solomon, R.W., 2009, Free and open source software for the manipulation of digital images: *American Journal of Roentgenology*, 192, 330–334.

Webster, M. and Sheet, H.D., 2010, A Practical Introduction to Landmark-based Geometric Morphometrics. *in* Alroy, J. and Hunt, G., eds., *Quantitative Methods in Paleobiology, Paleontological Society Short Course*, 16, 163–188.

Zelditch, M.L., Swiderski, D.L. and Sheets, H.D., 2012, Geometric morphometrics for biologists: a primer: *Academic Press*, 488 pp.

CHAPTER FIVE:

PUTTING EVOLUTIONARY PATTERNS IN CONTEXT: A COMPARISON OF NUCULID BIVALVE EVOLUTION FROM CONTRASTING BROAD-SCALE CLIMATIC REGIMES

Introduction

Eldredge and Gould (1972) placed patterns of speciation, especially the differences between punctuated equilibrium and phyletic gradualism (Fig. 5.1), as a primary focus of evolutionary paleobiology (e.g., Erwin and Anstey, 1995; Gould, 2002; Hunt, 2006, 2007). Despite the substantial knowledge gleaned on this topic, many questions related to the processes that drive these different patterns remain unresolved (e.g., Lieberman *et al*., 1995; Lieberman and Dudgeon, 1996; Eldredge *et al*., 2005). This reflects most evolutionary studies focusing on documenting the legitimacy and frequency of different evolutionary patterns, while ignoring their underling controls (see Erwin and Anstey, 1995). Studies that have examined the relationship between physical environmental change and evolution have typically utilized the Paleobiology Database (www.paleodb.org) to look at broad-scale controls on macroevolutionary patterns of diversification (i.e., origination, extinction) over broad spans of geologic time (e.g., Alroy *et al*., 2000; Cardenas and Harries, 2010; 2016). This lack of focus on the environmental context or controls on microevolutionary processes is likely due to the assumption that evolutionary responses to environmental change almost always results in adaptive evolutionary change or extinction and that it has little influence on traits (especially morphological traits) remaining unchanged for long intervals of time (i.e., evolutionary stasis; McKinney, 1993). In

contrast, evolutionary stasis has been traditionally considered to be controlled by more intrinsic mechanisms, such as developmental and genetic homeostasis, habitat tracking, stabilizing selection, or metapopulation dynamics (Hecht *et al*., 1974; Lieberman and Dudgeon, 1996; Gould, 2002; Eldredge *et al*., 2005).

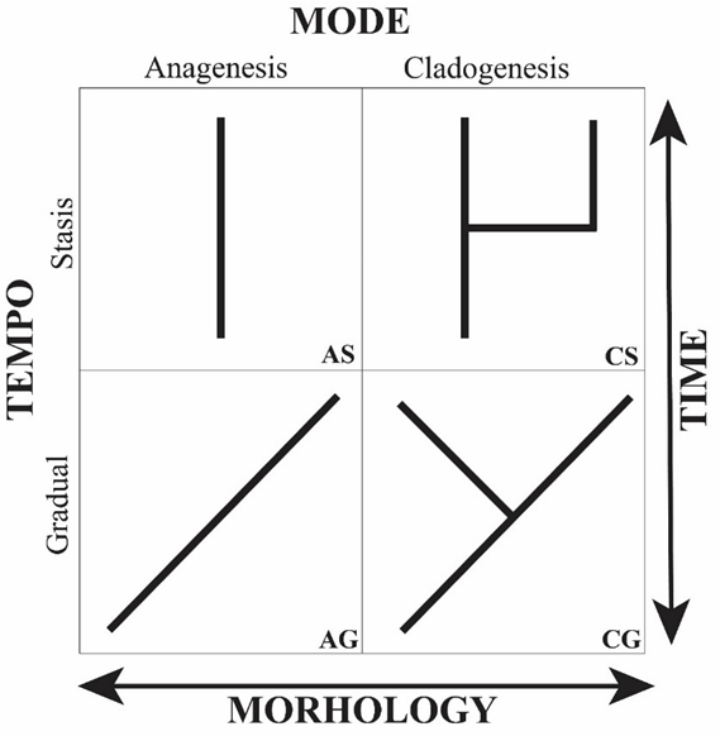

Figure 5.1. Diagram depicting different expressions of evolutionary patterns of speciation (modified from Jablonski, 2007; Harries and Allmon, 1997).

This assumption, however, has been placed into question by Sheldon's (1996) 'Plus ça Change' model, which translates as 'the more things change, the more the stay the same.' From an evolutionary perspective, this model hypothesizes that rapid and pronounced environmental variability will result in morphologic stasis until a threshold is met and speciation occurs, whereas reduced environmental variability, particularly when it approximates the rate of adaptation in a given clade, will drive more gradual morphologic changes (Fig. 5.2). In this

model, short and frequent physical environmental changes limit the amount of time phenotypic change can accumulate in response to a given set of environmental variables before those conditions vary, thus stabilizing selection dominates and morphological stasis is maintained. When environmental conditions change more slowly and consistently, new phenotypes have more time to evolve due to the longer intervals between significant environmental changes, resulting in the gradual morphologic variation. Furthermore, this model predicts that species inhabiting more unstable environmental settings, such as shallow shelves and temperate or high-latitude regions, are more likely to display stasis, whereas settings with more stable environments, such as that characteristic of the deep sea and the tropics, should be more likely to display gradualism.

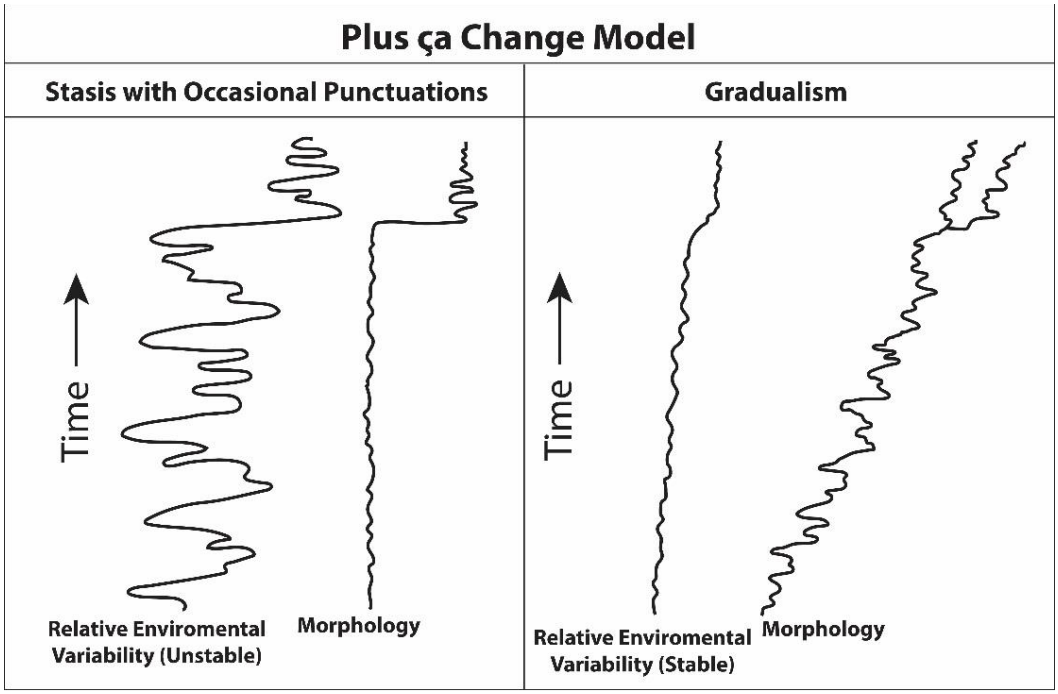

Figure 5.2. Sheldon's (1996; 1997) 'Plus ça change' model of environmental control on evolutionary patterns.

These predictions for the environmental context of different evolutionary patterns in the 'Plus ça Change' model should also be influenced by the Earth's broad-scale climatic patterns

through the Phanerozoic (Fig. 5.3). These climate patterns are known to have broadly oscillated between ice-, mixed-, and greenhouse climatic regimes, which are controlled by plate tectonics and orbital-forcing over the long-term (Frakes *et al*., 1992; Zachos *et al*., 2001; De Vleeschouwer *et al*., 2017). Icehouse conditions show the greatest amount of short-term environmental fluctuations largely within the Milankovitch frequencies, whereas greenhouse conditions display dampened variation and mixed-house being intermediate, although difficult to precisely define. Despite being important for understanding both micro- and macroevolutionary drivers, relatively little attention has been given to examining evolutionary tempo and mode within a broad-scale climatic context. Harries and Allmon (2007) re-analysis of the various studies contained within Erwin and Anstey (1995) revealed that all examples of gradual change, with or without stasis, are limited to greenhouse climate regimes. That preliminary analysis indicates that a reassessment of evolutionary patterns set within an environmental framework is necessitated.

The goal of this chapter is to examine and compare the morphological variability among different species of the marine bivalve *Nucula* Lamark 1799 from contrasting climatic regimes to test the predictions of Sheldon's (1996) 'Plus ça Change' model and to understand the broad-scale climate context of different evolutionary patterns. Furthermore, this chapter aims to expand our understanding of how changing rates of morphological evolution integrate with microevolutionary analyses of speciation and macroevolutionary studies of diversification.

Background

Broad-Scale Climatic Setting

To test the 'Plus ça Change' model's prediction that reduced environmental variability drives evolutionary change, this study traces the evolution of the bivalve *Nucula* through the

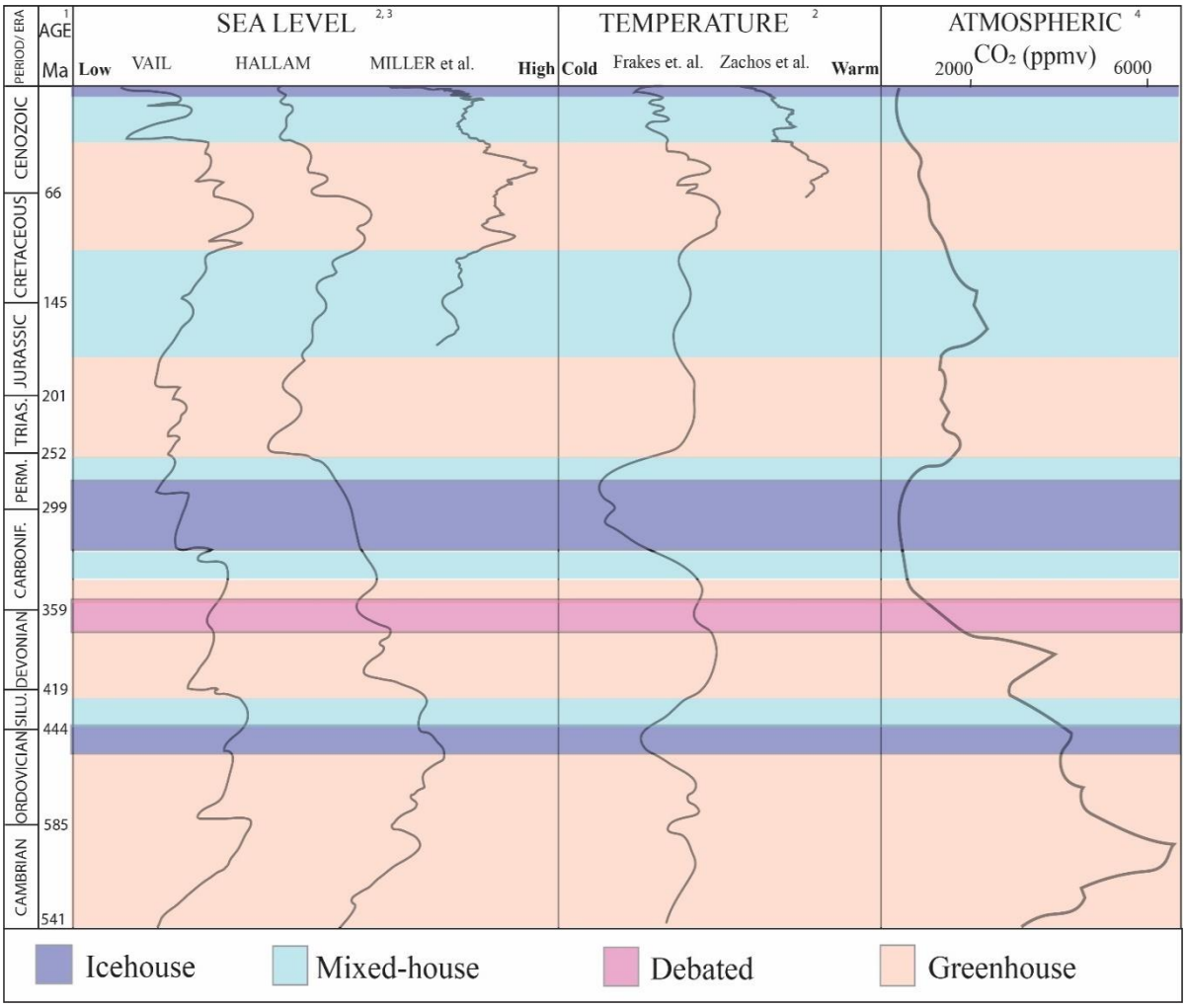

Figure 5.3. Phanerozoic climate history depicting global sea-level and temperature curves as well as different climate regimes as defined by the amount of glaciation. The purple band around the Devonian-Carboniferous boundary represents an interval where there is still considerable debate as to the extent of glaciation (modified from Frakes et al., 1992; Zachos et al., 2001; Miller et al., 2005; Gradstein et al., 2012; McKenzie et al., 2016.

stable climate regime of the Late Cretaceous as well as the variable climates associated with the Neogene and Quaternary (Fig. 5.3). The Late Cretaceous was an equitable, ice-free world characterized by elevated global temperatures and sea levels typical of a greenhouse climate regime (Frakes *et al*., 1992; Miller *et al*., 2005). These conditions were primarily driven by elevated atmospheric pCO_2 levels caused by increased magmatism, especially at mid-ocean ridges but also associated with subduction-derived volcanism (Arthur *et al*., 1985, 1991; McKenzie et al., 2016). Due to these greenhouse conditions, the effects of higher-order (10^4 to 10^5 years) Milankovitch-controlled climate and sea-level changes were substantially dampened as compared to cooler climatic intervals, which resulted in relatively stable environmental conditions (i.e., little change in marine shelf areas or temperature) over long-intervals. The most prominent environmental changes during the Late Cretaceous were primarily expressed as lower-order (10^5 to 10^7 years) tectonically driven changes in temperature and sea level.

In contrast, the Neogene was dominated by two 6.0 to 8.0 Ma long mixed-housed climates regimes that were interrupted by shorter (~0.4 to 2.7 Ma) ice- as well as warm-house intervals (Fig. 5.3). Neogene temperatures and sea levels were substantially higher than those in the Quaternary, but were slowly declining (Zachos *et al*., 2001; Miller *et al*., 2005; De Vleeschouwer *et al*., 2016). These declines were primarily due to an overall decrease in pCO_2 levels as well as modifications to the Earth's oceanic-atmospheric circulation patterns related to changes in continental geography and hypsography (Zachos *et al*., 2001; Miller *et al*., 2005; De Vleeschouwer *et al*., 2016). Temperature and sea-level fluctuations were still relatively moderated during the Neogene and were, for the most part, expressed on the 41ka obliquity band (Zachos *et al*., 2001: Miller *et al*., 2005). These fluctuations in the climatic spectrum were primarily controlled by glaciation in the Southern hemisphere, which was largely ephemeral until

the Eastern and Western Antarctic ice sheets became permanently established during the mid-late to late late Miocene, respectively (Zachos *et al*., 2001). Glaciation in the Northern Hemisphere would remain ephemeral through the Miocene and Pliocene (Zachos *et al*., 2001; De Vleeschouwer *et al*., 2016).

These declines in temperature and sea level accelerated in the Quaternary in association with permanent northern hemisphere glaciation (Zachos *et al*., 2001). This resulted in a greater expression of Milankovitch-scale variations in temperatures, sea-level, and continental ice-coverage that defined the various glacials and interglacials that characterize this interval (Zachos *et al*., 2001; Miller *et al*., 2005). By the middle Pleistocene (~950 ka), there was a major shift in the amplitude and frequency of the glacial-interglacial cycles from the 41 ka obliquity band with low amplitude variations to the 100 ka eccentricity cycle with high amplitude changes (Zachos *et al*., 2001). This middle Pleistocene shift resulted in a change from more temporally symmetrical glacial-interglacial cycles to more asymmetrical cycles with very long, cold glacial periods punctuated by short, warmer interglacials (Mudelsee and Schulz., 1997; Zachos *et al*., 2001; Tziperman and Gildore, 2003). Overall, the Pleistocene is characterized by an increase in variance in the climatic spectrum (Frakes *et al*., 1992).

Geological Setting

This study analyzed *Nucula* specimens from the Gulf and Atlantic Coastal Plains (GCP and ACP, respectively). These regions represent passive-margin settings that formed during the breakup of Pangaea during the Triassic through Jurassic (Galloway, 2008; Miall *et al*., 2008). During the Late Cretaceous, elevated sea levels associated with the greenhouse conditions caused the Gulf of Mexico and Atlantic Ocean to transgress across the coastal plains up to and, in cases such as of the Mississippi Embayment, past the Appalachian-Ouachita Orogenic Belt

(Chapter Three). This transgression resulted in the deposition of marine siliciclastic (i.e., nearshore to proximal facies) and carbonate (distal facies) strata across the area. Upper Cretaceous localities sampled in this study are characterized as sandy clay-rich units with well-preserved aragonitic shells, which were originally deposited in shallow, proximal-offshore shelf-settings.

In contrast to the Cretaceous record, the Neogene–Quaternary sea-level records are substantially lower and more varied due to the relatively higher amplitude, shorter term eustatic changes. Most Neogene–Quaternary strata in the GCP and ACP were deposited during highstands and are separated by lowstand unconformities. Neogene–Quaternary *Nucula* localities sampled in this study are represented by sandy shell-rich units with well-preserved aragonitic shells, which were originally deposited in shallow, nearshore settings.

Systematic Overview

This study examined one Cretaceous and two Neogene–Quaternary species of *Nucula*, respectively. Species within this genus were selected for study because of their generally excellent preservation, abundance, and long stratigraphic records in both the Cretaceous and Neogene–Quaternary strata of the GCP and ACP. These characteristics made *Nucula* an excellent organism to obtain a statistically robust sample to test the 'Plus ça Change' model.

The Cretaceous portion of this study is focused on the nuculid bivalve *Nucula percrassa* Conrad 1858 (Fig. 5.4A), which ranges across the GCP, ACP, and into the Western Interior (Speden, 1970; Wingard and Sohl, 1990). *Nucula percrassa* is one of the largest members, both extant and extinct, of the family Nuculidae with some specimens obtaining lengths of up to 45 mm (Wingard and Sohl, 1990). Cretaceous *N. percrassa* specimens are most common in micaceous, clayey, fine sands deposited in shallow-marine, inner-shelf settings with normal

salinity (Wingard and Sohl, 1990). They are typically rare in lagoonal and deeper-water settings characterized by marls (Wingard and Sohl, 1990). In the ACP, steinkerns of *N. percrassa* are found in the lower middle Campanian Woodbury Clay and upper middle Campanian Merchantville Formation (R. Johnson, pers. comm., 2018). *Nucula* then disappear from the ACP record until the lower upper Maastrichtian *Discoscaphites conradi* Biozone (R. Johnson, pers. comm., 2018). In the GCP, this species appears in the lower Campanian *Submortoniceras tequesquitense* Biozone and ranges up to the K–Pg boundary (Wingard and Sohl, 1990).

The Neogene–Quaternary component of this analysis include two taxa: *N. chipolana* Dall 1898 and *N. proxima* Say 1821 (Fig. 5.4B and C). The former is known only from the middle Miocene of the Florida Panhandle and ranges from the Burdigalian to Serravallian (Fig. 5.7; Dall, 1898; Gardner, 1926; Portell *et al*., 2006), whereas the latter is known from the middle Miocene to Holocene of the ACP and easternmost GCP (Fig. 5.7; Richard and Harbison, 1942; Gardner, 1943; Edwards *et al*., 2005). The first record of *N. proxima* occurs in the Serravallian Shoal River Formation of Florida (see Fig. 5.10), where it co-occurs with *N. chipolana* and *N. chipolana waltonia* Gardner 1926 (Portell *et al*., 2006). Living *N. proxima* inhabit shallow marine shelf settings with soft sand or soft sandy mud bottoms with normal salinities (Hampson, 1971).

Evolutionary Relationships among *Nucula* Analyzed in this Study

The evolutionary relationship between the different *Nucula* species analyzed in this study are poorly known. This primarily stems from a lack of comprehensive phylogenetic analyses of this group in both the fossil record and among living species. This is further exacerbated by the numerous homeoplasies observed in this group and, given the relative simplicity of their shells,

the relative paucity of usable morphological characters that could be used to reconstruct a robust phylogeny. Also, despite having a relatively similar biogeographic range, the Cretaceous

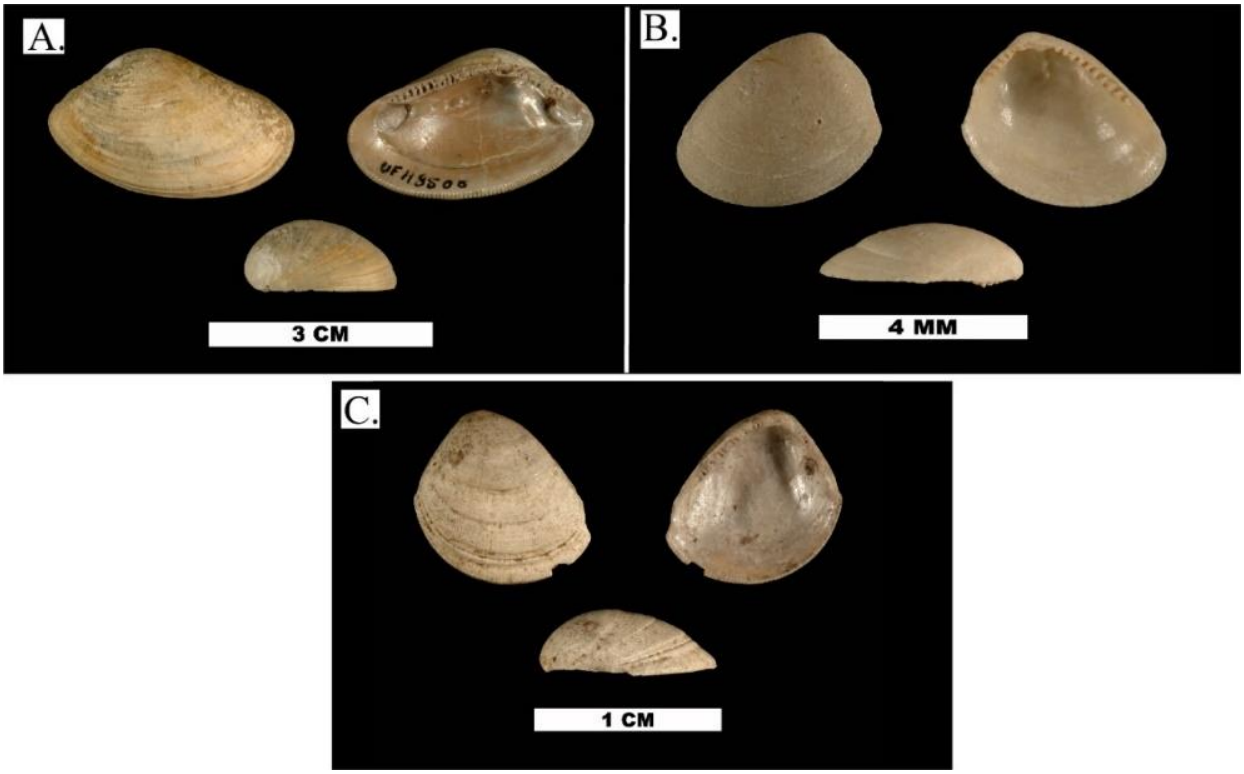

Figure 5.4. Examples of *Nucula* species examined in this study, including: A) Cretaceous *N. percrassa* (UF118500, B) Miocene *N. chipolana* (UF133012), and C) Pliocene to Holocene *N. proxima* (UF267837) (photos courtesy of R. Portell, FLMNH).

species are separated in time from the Neogene–Quaternary species by ~40 Ma. Based on these issues, it is unclear at this point whether the latter are descendants of the former or whether the latter represent an unrelated lineage with characteristically smaller sizes.

In contrast, the two Neogene–Quaternary species are much more likely part of the same evolutionary lineage and could possibly be the same species. This is based on numerous morphological similarities, including similar shape outline, inflation, hinge line, and relatively thin shell thicknesses. The most substantial difference between the two species is their size with *N. chipolana* typically having a mean length of 3–4 mm, whereas *N. proxima* typically have a

mean length of 10 mm. Also, both *N. chipolana* and *N. proxima* overlap in their biogeographic range and the last appearance of the former species overlaps with the first appearance of the latter species during the early Serravallian (see Fig. 5.6, also see discussion above).

Nucula Life Habits and Habitats

Nuculids are shallow-infaunal bivalves that prefer well-oxygenated soft, muddy to coarse sandy substrates, which they actively move through using their planar foot. They are generally deposit feeders and use an extensile palp probocides to feed on detritus below the sediment surface. They are also known to filter feed, particularly as juveniles, but this can continue as a feeding mode into adulthood. Today, they are common in many marine environments, but are especially diverse in the deep sea (Mikkelsen and Bieler, 2008).

Methods

Sample Localities

Cretaceous *Nucula* specimens analyzed in this study came from four GCP and ACP localities (Figs. 5.5 and 5.6). *Nucula percrassa* specimens are from three classic localities in the GCP: the Upper Campanian Coon Creek locality in Tennessee, lower Maastrichtian Blue Springs locality in Mississippi, and the upper Maastrichtian Owl Creek locality in Mississippi. The age of these localities are constrained by ammonite and inoceramid biostratigraphy; however, due to their condensed biostratigraphic records and the extended age ranges of ACP–GCP ammonite biozones, many of these localities span relatively long intervals of time (i.e., >1–2 Ma; see Chapter Two). The Coon Creek locality samples correlate with the GCP *Nostoceras hyatti* Biozone, which places it between 73.8 to 72.1 Ma (see Chapter Two). The Blue Springs locality correlates with the GCP *N. rugosum* biozones, which range from 72.1.8 to 70.5 Ma (see Chapter Two). The Owl Creek locality correlates with the GCP *Discoscaphites minardi* and *D. iris*

biozones, which places it between 76.8 to 66 Ma. ACP specimens came from one lower upper Maastrichtian locality in Maryland, which correlates to the ACP *Discoscaphites conradi* Biozone and Western Interior *Hoploscaphites nebrescensis* Biozone (see Chapter Two). This range places the age of these specimens between 68.9 to 69.8 Ma. This indicates that the samples studied here span an~7.8 Ma interval during the late Campanian to late Maastrichtian.

Neogene and Quaternary *Nucula* specimens analyzed in this study come from numerous formation and localities across the GCP and ACP (Figs. 5.5 and 5.7). These formations span ~17 Ma; however, this record is not continuous since all these formations are bounded by hiatuses or unconformities, which span from 10's of Ma to 100's of ka. *Nucula chipolana* specimens come from the middle Miocene Chipola Formation at a single locality in the Florida Panhandle. The Chipola Formation has an age range from 17 to 16.3 Ma (Huddlestun, 1984). There is then a long gap in our *Nucula* record, which spans from the middle Miocene Chipola Formation to the Pliocene Yorktown and Tamiami Formations (Fig. 5.7). This gap ranges from 16.3 to 5.0 Ma or a time span of 11.3 Ma. It primarily reflects a lack of available material due to numerous and relatively long unconformities that span >1 Ma as well as relatively poor preservation of mollusc fossils (i.e., steinkerns). Our Pliocene to Pleistocene *Nucula* record spans ~5 Ma and is relatively more complete due to greater better representation of specimen from different intervals in museum collections. This relatively better representation is due to shorter unconformities as well as better preservation of specimens from the Pliocene to Pleistocene. The Pliocene *N. proxima* specimens come from localities in Florida (n = 3), Georgia (n = 1), South Carolina (n = 1), and Virginia (n = 1). These specimens span the Zanclean to Piacenzian, which gives them an age range from 5.0 to 2.6 Ma. Some of the Tamiami Formation specimens from Florida might also be earliest Pleistocene in age, which would give these specimens an age range from 4.0 to 2.2

Ma. Quaternary *N. proxima* specimens come from both Florida (n = 6) and North Carolina (n = 1). The specimens from Florida formations span the entire Pleistocene and range in age from 2.2 to 0.04 Ma. The Quaternary specimens from North Carolina are from the James City Formation, which spans the middle Pleistocene and ranges in age from 2.0 to 1.0 Ma.

Morphometric and Quantitative Analysis

The morphometric and statistical methodologies used on *Nucula* are identical to those found in Chapter Three.

Samples

A total of 961 Cretaceous and Neogene–Quaternary *Nucula* specimens were analyzed from various collections for this study (Table 5.1). Cretaceous *Nucula* specimens were found to be highly underrepresented in most museum collections in comparison to Neogene–Quaternary *Nucula*. This underrepresentation in museum collections is likely due to combination of lower abundances in most sampled Cretaceous lithofacies and a preference by collectors to ignore bivalves, while focusing on sampling rarer and/or more notable Cretaceous taxa (e.g., ammonites, crabs, echinoids). A total of 147 right and left valves of Cretaceous *N. percrassa* specimens were analyzed from the Coon Creek Tongue of the Ripley Formation of Tennessee, Ripley Formation of Mississippi, Severn Formation of Maryland, and Owl Creek Formation of Mississippi (Table 5.1). A total of 107 of these specimens are reposited in the collections at the Mississippi Museum of Natural Sciences (MMNS), Florida Museum of Natural History (FLMNH), Yale Peabody Museum of Natural History (YPM), and Monmouth Amateur Paleontologist's Society (MAPS). The 30 remaining specimens, which were collected from the Coon Creek Tongue, Ripley Formation, and Owl Creek Formation, were taken from the author's private research collection. A total of 814 right and left valves of Neogene–Quaternary *Nucula*

specimens were analyzed from the ACP and GCP (Table 5.1). These specimens are all reposited in the FLMNH collection.

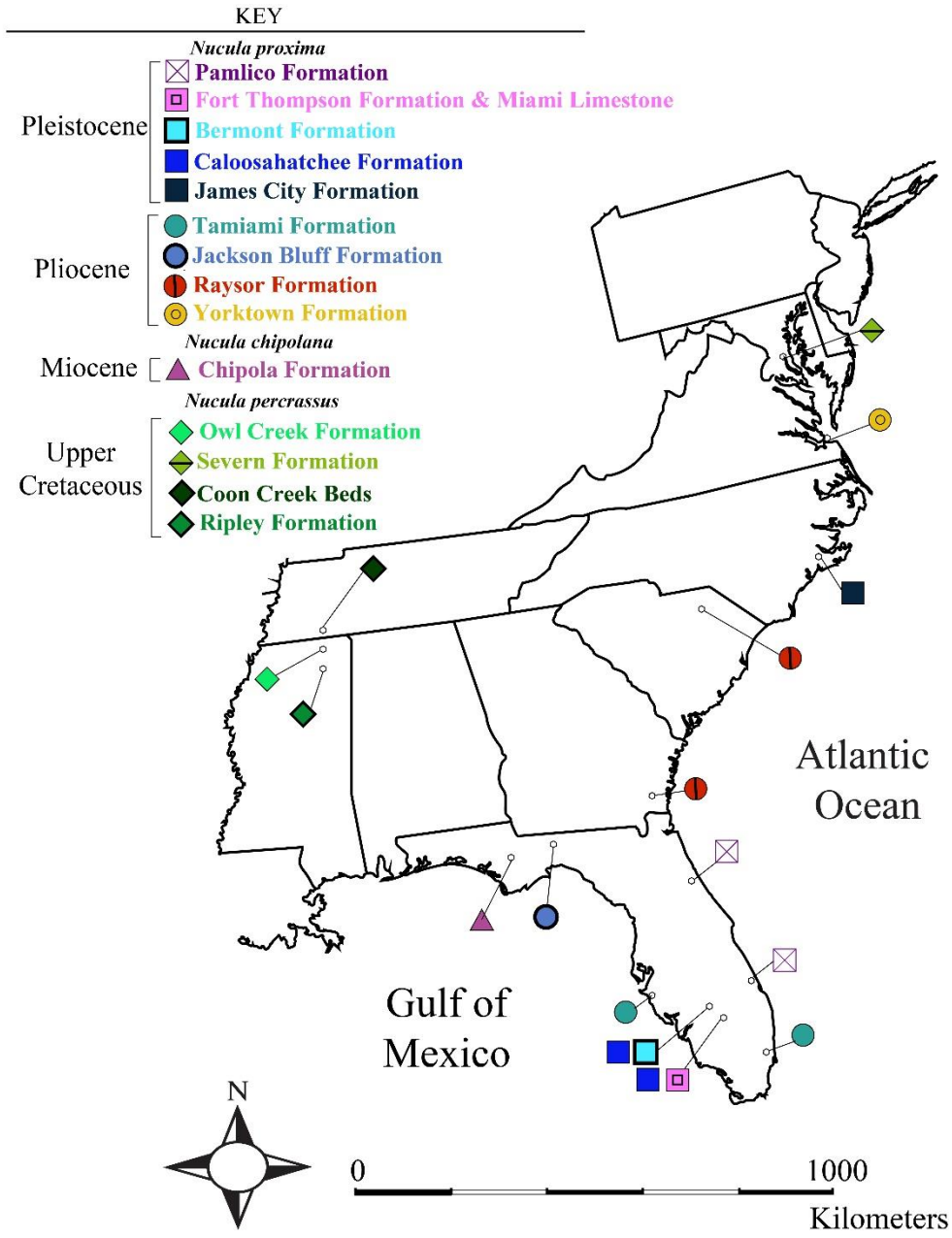

Figure 5.5. Localities for Cretaceous and Neogene–Quaternary *Nucula* specimens used this study.

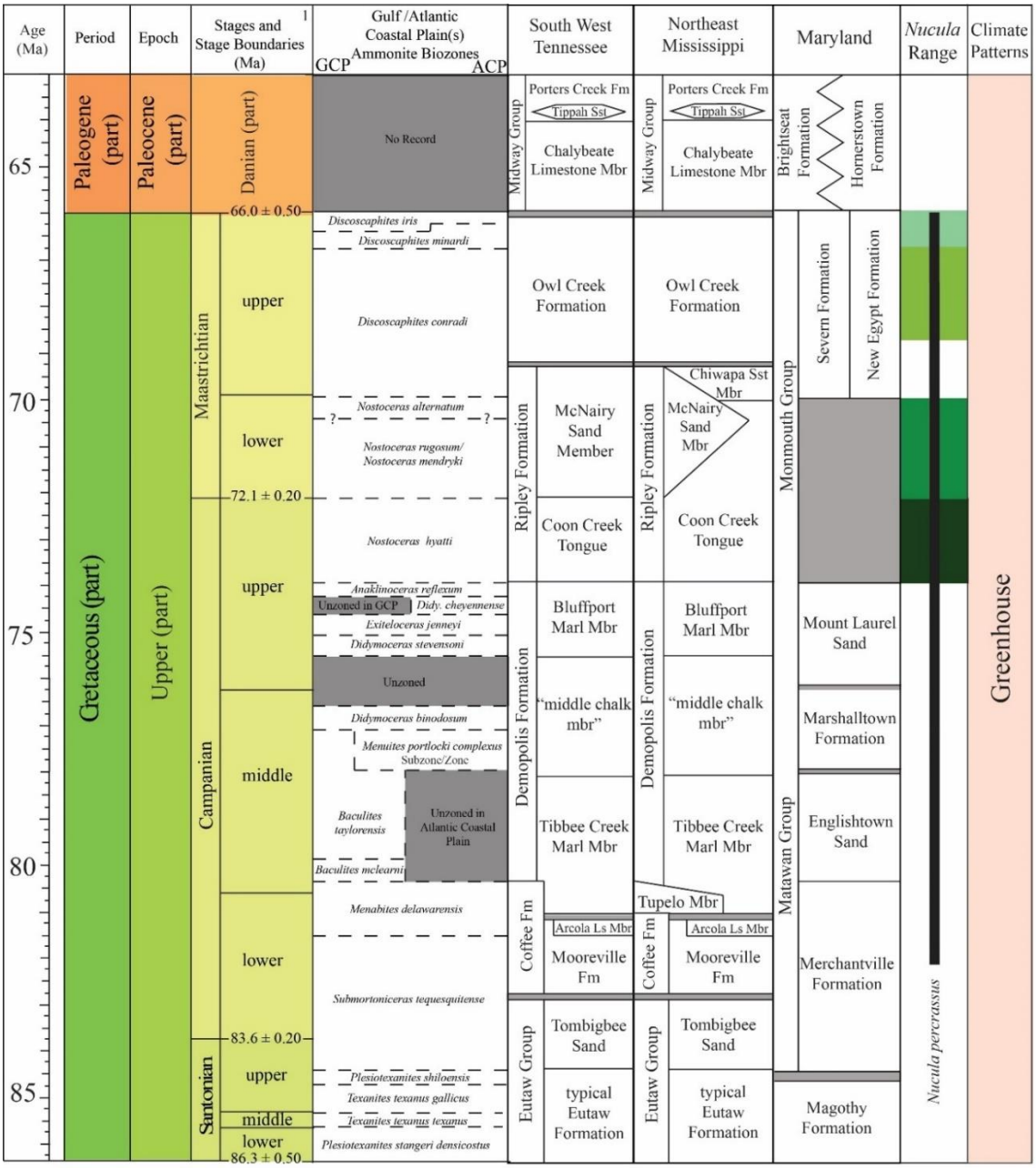

Figure 5.6. Stratigraphic position of Cretaceous *Nucula percrassa* samples in ACP and GCP used in study (see Fig. 5.5 for geographic distribution), range of Cretaceous *N. percrassa*, and broad-scale climate patterns (see Fig. 5.3 for key) (figure modified from Slattery et al. in revision). Colored formations and intervals on range chart correspond to time intervals sampled for this study.

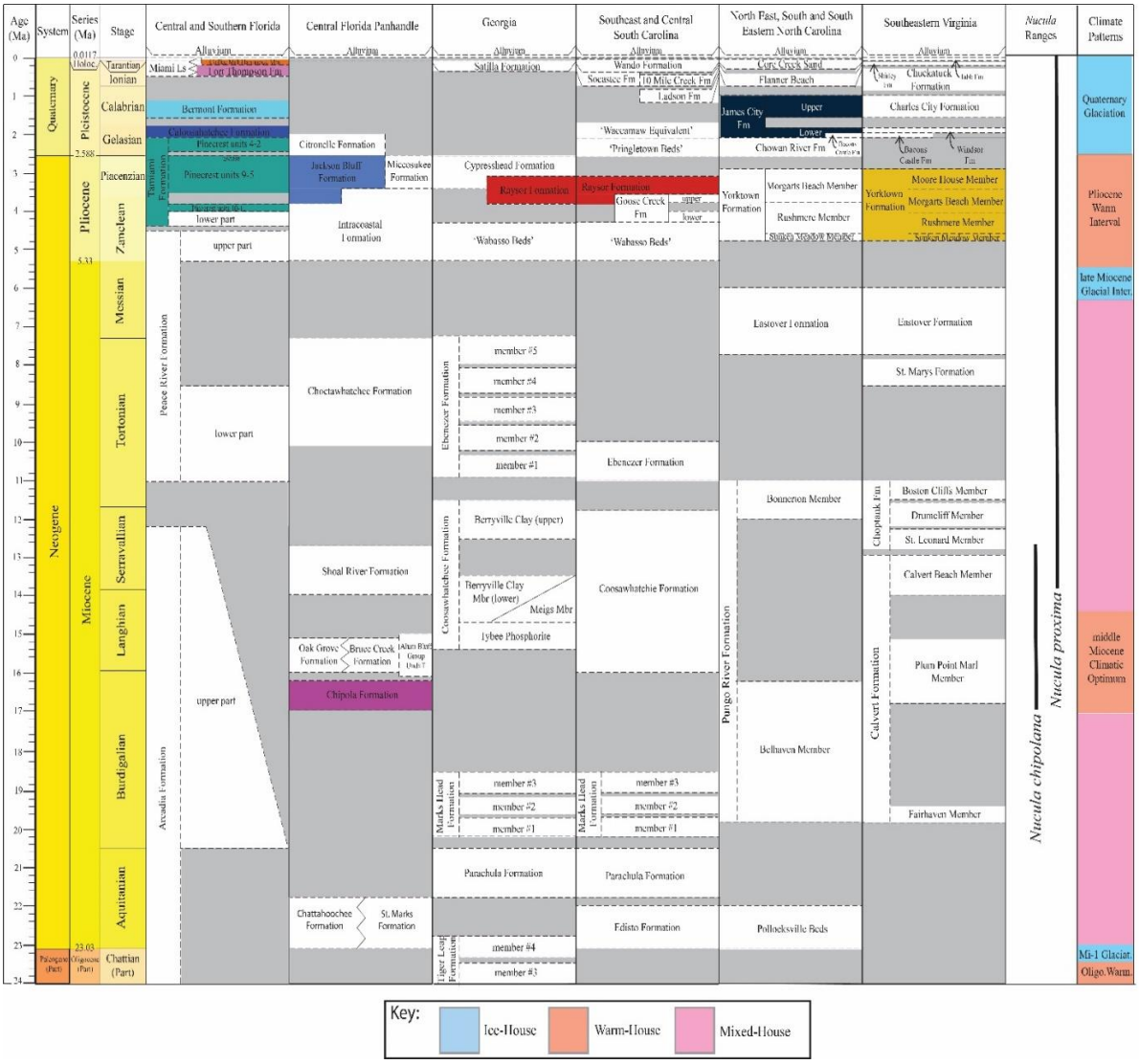

Figure 5.7. Stratigraphic position of Neogene–Quaternary *Nucula* samples in ACP and GCP used in study (see Fig. 5 for geographic distribution), range of *Nucula* species, and broad-scale climate patterns (modified from Huddlestun, 1984; Weems and Edwards, 2001; Zachos et al., 2001; Weems and Lewis, 2002; Edwards et al., 2005; Weems and George, 2013; Weems et al., 2004; Saupe et al., 2014; Hastings and Dooley, 2017).

Results

Allometry

The relationship between size and shape (i.e., allometry) for the Cretaceous and Neogene–Quaternary *Nucula* shows no correlation. For example, the trend between the relative warp scores (i.e., a measure of shape) and centroid sizes (i.e., a measure of size) of Cretaceous *N. percrassa* as well as the Late Cenozoic *N. chipolana* and *N. proxima* left and right valves had very small R^2 values (see Figs. 5.8 and 5.9).

Size Change

Cretaceous *N. percrassa* show an overall decrease in size over 7.8 Ma, but taken *in toto* are significantly larger than Neogene–Quaternary specimens (Fig. 5.10; Table 5.2; also see Appendix B, Table B1). For example, *N. percrassa* displays a 23.1% decrease in left valves size (i.e., from 26.8 ± 4.1 to 20.6 ± 0.9 mm for left) and a 21.6% decrease in right valves size (i.e., from 24.8 ± 3.6 to 20.4 ± 0.9 mm for right valves) during the Campanian to Maastrichtian. The only exception to this pattern is the difference in size between Severn Formation and Ripley Formation specimens, which are similar for left valves, but the Severn Formation right valves are larger.

Neogene *Nucula* display an increase in size between species and then little to no change from the late Neogene to Quaternary. (Fig. 5.10; Table 5.2). This increase in size is greater among ACP specimens than for GCP specimens, since the former are typically larger. For example, ACP *N. proxima* left and right valves are 106.1% and 120.6% larger, respectively as

Table 5.1. Number of *Nucula* specimens used in study along with their repositories.

Species	Formation	Source	Age	Total Left Valves	Total Right Valves
Nucula proxima Say 1820	Pamlico Fm	FLMNH	Pleistocene	41	38
Nucula proxima Say 1820	Fort Thompson Fm	FLMNH	Pleistocene	102	95
Nucula proxima Say 1820	Caloosahatchee Fm/ Bermont Fm	FLMNH	Pleistocene	118	73
Nucula proxima Say 1820	James City Fm	FLMNH	Pleistocene	3	5
Nucula proxima Say 1820	Tamiami Fm	FLMNH	Pliocene	9	3
Nucula proxima Say 1820	Jackson Bluff Fm	FLMNH	Pliocene	90	54
Nucula proxima Say 1820	Raysor Fm	FLMNH	Pliocene	62	52
Nucula proxima Say 1820	Yorktown Fm	FLMNH	Pliocene	3	5
Nucula chipolana Dall 1898	Chipola Fm	FLMNH	Miocene	34	27
Nucula percrassa Conrad 1856	Owl Creek Fm	MMNS	Cretaceous	18	29
Nucula percrassa Conrad 1856	Severn Fm	MAPS	Cretaceous	2	5
Nucula percrassa Conrad 1856	Ripley Fm	MMNS	Cretaceous	33	32
Nucula percrassa Conrad 1856	Coon Creek Tongue	FLMNH and YPM	Cretaceous	16	12
			Total:	531	430

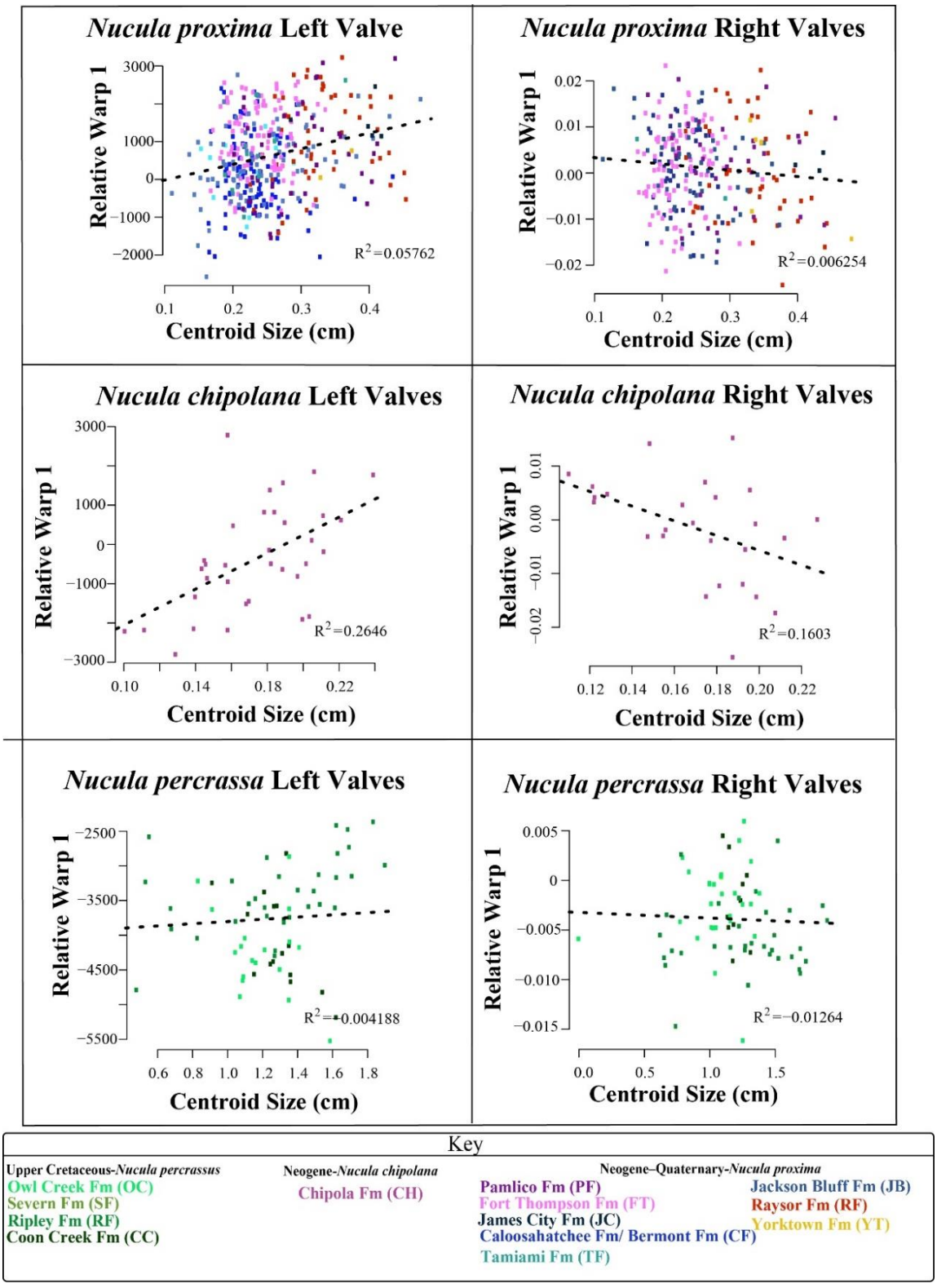

Figure 5.8. Allometric test for right valves of *Nucula* from the Cretaceous and Neogene–Quaternary.

compared to *N. chipolana* specimens. In contrast, GCP *N. proxima* left and right valves are 63.6% and 55.9% larger, respectively, as compared to *N. chipolana* specimens. Following this increase, *N. proxima* displays little change from the Pliocene to the Pleistocene with the geographic differences. Most GCP specimens range between 4.5 to 6 mm in size, whereas ACP specimens vary between 6.5 to 9 mm.

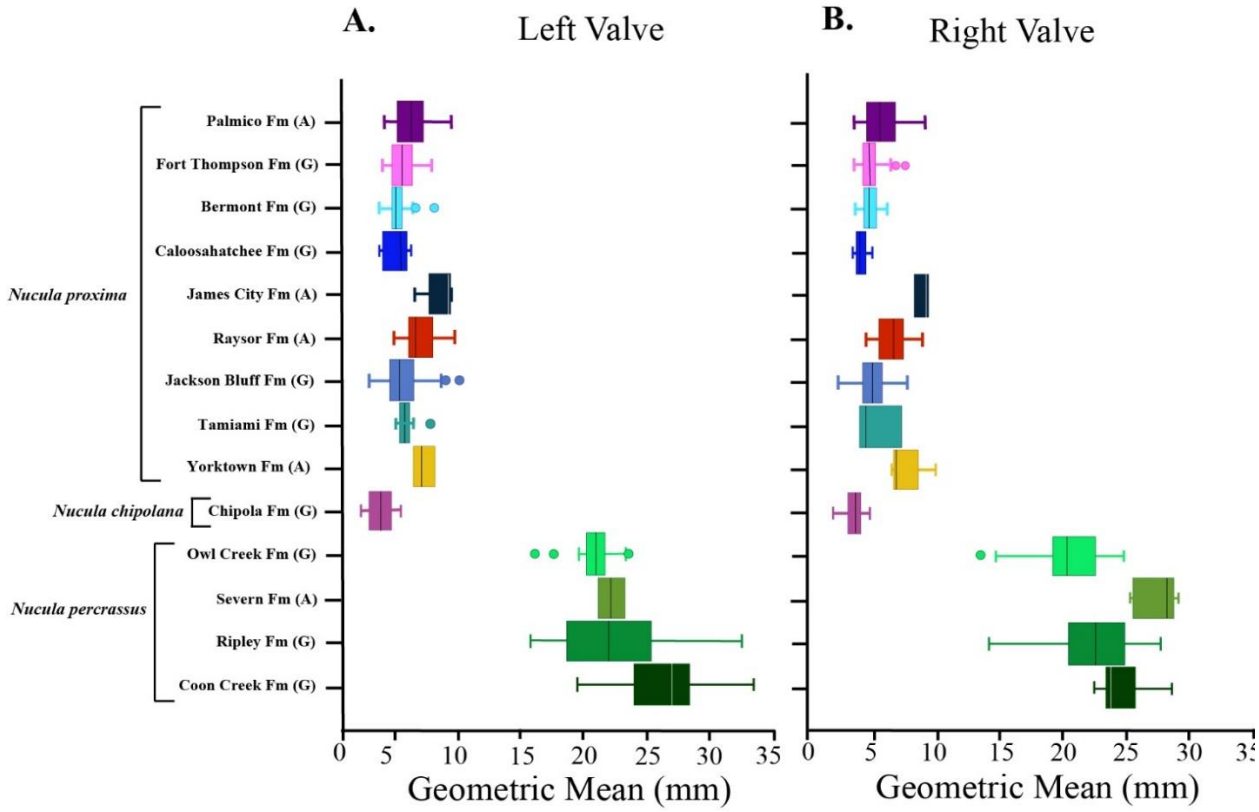

Figure 5.9. Size of Cretaceous and Neogene–Quaternary *Nucula* for right (A) and left (B) valves. Letter in parentheses next to formation indicates if samples from the respective formations are from the Gulf (G) and Atlantic (A) Coastal Plains.

Table 5.2. Summary parameters for geometric means of right and left *Nucula* valves shown in Figure 5.10.

Right Valves										
Formation	Species	Min	Quartile 1	Median	Mean	Quartile 3	Max	Variance	Standard Deviation	Total # of Valves
Palmico Formation	Nucula proxima	3.524805952	4.503370071	5.573877465	5.76716878	6.736251925	9.245320546	2.383865385	0.484154596	38
Fort Thompson Formation	Nucula proxima	3.529753108	4.315928097	4.787465405	4.896485805	5.266504024	7.574233229	0.568729842	0.60487411	95
Caloosahatchee/Bermont	Nucula proxima	3.520318167	4.469072597	4.830054064	4.739294194	5.21447218	6.168554612	0.365872689	1.072171193	73
Callosahatchee	Nucula proxima	3.520318167	3.865003304	4.106351889	4.150018279	4.310840421	4.985068004	0.234405673	0.754141791	-
James City Formation	Nucula proxima	8.478193911	8.891112648	9.304031384	9.07889852	9.379250825	9.454470265	0.276292485	1.156597222	5
Raysor	Nucula proxima	4.589093048	5.739120142	6.646287686	6.57457893	7.325355964	8.918121551	1.149551068	0.525635315	52
Jackson Bluff Formation	Nucula proxima	2.367252838	4.359535755	5.043682385	5.070532372	5.695903833	7.749455594	1.337717133	1.543977132	54
Taimiami Formation	Nucula proxima	4.042471398	4.30510577	4.567740141	5.290721757	5.914846937	7.261953732	2.983293437	1.727221305	3
Yorktown Formation	Nucula proxima	6.590231787	6.909436446	6.943082889	7.515546897	7.118463458	10.0165199	1.990958554	1.411013308	5
Chipoloa	Nucula chipolana	1.901927443	3.176293818	3.712294169	3.481851692	4.087523399	4.739938396	0.723635787	1.677696615	27
Owl Creek Formation	Nucula percrassus	13.6300391	19.42408572	20.49413106	20.43379281	22.48983174	24.96717495	8.366479175	0.850667848	29
Severn Formation	Nucula percrassus	25.58762345	26.12800674	28.49963851	27.63572958	28.52280975	29.44056946	2.814665931	1.78259509	5
Ripley Formation	Nucula percrassus	14.37269181	20.95675387	22.72984647	22.2984172	24.9575364	27.92636043	12.70214007	2.892486677	32
Coon Creek Formation	Nucula precrassus	22.61551109	23.76245165	23.99117298	24.8422947	25.85848323	28.8788916	3.177645253	3.564006183	12

Left Valves										
Formation	Species	Min	Quartile 1	Median	Mean	Quartile 3	Max	Standard Deviation	Variance	Total Left Valves
Palmico Formation	Nucula proxima	3.582430879	4.75965545	5.808043388	5.968972088	6.771992838	9.024019947	1.029580764	1.968747695	41
Fort Thompson Formation	Nucula proxima	3.45392733	4.356923915	5.121765614	5.110790073	5.737460065	7.425136228	0.678741703	0.718472888	102
Caloosahatchee/Bermont	Nucula proxima	3.219159052	4.27074076	4.624639554	4.680207828	4.989670659	7.622972976	1.292407038	0.4606903	118
Callosahatchee	Nucula proxima	3.204060549	3.464903959	4.972880922	4.510402319	5.382129307	5.854156216	0.8476278	1.060036549	-
James City Formation	Nucula proxima	6.114190707	8.599766741	8.792214909	8.283065984	8.834315197	9.074842368	1.403168839	1.498584375	3
Raysor	Nucula proxima	4.470419891	5.67461241	6.26221159	6.64701408	7.236698142	9.405344013	1.224166809	1.670315953	62
Jackson Bluff Formation	Nucula proxima	2.344822595	4.210460392	4.81994759	5.070237424	5.887321395	9.71699259	1.403120699	1.96888279	90
Taimiami Formation	Nucula proxima	4.540025	4.868130339	5.300881719	5.399350765	5.427748705	7.325378352	0.827513812	0.684779109	9
Yorktown Formation	Nucula proxima	6.047526767	6.363697477	6.679868187	6.801917422	7.179112749	7.678357311	0.822237239	0.676074078	3
Chipoloa	Nucula chipolana	1.637506336	2.375760244	3.388348665	3.326290416	4.063311019	5.022962273	1.374892765	0.875069376	34
Owl Creek Formation	Nucula percrassus	15.88991781	20.22888032	20.7788454	20.60466294	21.2929342	23.43842136	0.935451429	3.186112496	18
Severn Formation	Nucula percrassus	21.15508601	21.64118401	22.12728201	22.12728201	22.61338	23.099478	3.314969594	1.890330115	2
Ripley Formation	Nucula percrassus	15.44724461	18.70796704	21.98297613	22.22120299	25.12179337	32.6562285	1.784968486	17.26132633	33
Coon Creek Formation	Nucula precrassus	19.38983174	24.48246289	27.10588622	26.78234721	28.32768528	33.62648071	4.154675238	10.98902341	16

The Mann-Whitney test of the geometric mean of size for both left and right valves of *Nucula* from Cretaceous and Neogene–Quaternary formations are drawn from populations with different median values (Table 5.2), which supports the differences in specimen size for populations observed in Figure 5.10. For example, the geometric means of size values for Cretaceous left and right valves are statistically different. The only exception to this pattern is the association among the Severn Formation *N. percrassa* with that of specimens from the Ripley and Owl Creek formations. The geometric means of size values for Neogene–Quaternary left and right valves are also statistically different. However, the statistical associations among all Tamiami as well as half of the Jackson Bluff (e.g., Pamlico vs. Jackson Bluff) and Yorktown (e.g., James City vs. Yorktown) *Nucula* associations lack statistically significant differences. A lack of statistically significant differences, indicative of no size change, are also identified for valves of *N. proxima* from the Caloosahatchee compared to Caloosahatchee–Bermont and Fort Thompson.

Shape Change: Principal Component Analysis

PCA Axes 1 to 3 scores for both left and right valves of *Nucula* reveal pronounced shape morphospace similarities among Neogene–Quaternary specimens, but substantial morphospace differences for the Cretaceous specimens (Fig. 5.11). This is despite the Neogene–Quaternary specimens spanning a greater amount of time as compared to the Cretaceous specimens. PCA axis 1 for both left and right valves of Cretaceous and Neogene–Quaternary *Nucula* explains 75.2% and 73.2% of the observed shape variation, respectively, whereas, PCA axis 2 for both left and right valves explains 13.4% and 15.0% of the observed shape variation, respectively. PCA axis 3 for left and right valves explains 5.0% and 4.1% of the observed shape variation, respectively. The variation along axis 1 primarily reflects changes in shell width, whereas

Table 5.3. Summary statistics for size measurements of left (top) and right (bottom) *Nucula* valves. Yellow boxes indicate statistically significant differences when compared with opposite samples, whereas gray boxes indicate a lack of statistically significant differences.

Right Valves													
Species	*Nucula proxima*								*Nucula chipolana*	*Nucula percrassus*			
Formation	Fort Thompson	Caloosa/Bermont	Caloosahatchee	James City	Raysor	Jackson Bluff	Tamiami	Yorktown	Chipola	Severn	Owl Creek	Ripley	Coon Creek
Pamlico	2.49E-03	3.56E-03	2.74E-04	6.50E-03	5.33E-03	5.39E-02	6.81E-01	1.98E-02	1.33E-08	3.52E-04	1.17E-11	2.09E-13	2.21E-08
Fort Thompson		8.85E-01	6.24E-04	3.41E-03	4.52E-14	2.98E-01	9.34E-01	2.59E-04	2.61E-11	1.78E-04	2.65E-15	1.21E-18	5.59E-10
Caloosa/Bermont			2.96E-04	3.87E-03	1.94E-13	3.19E-01	8.34E-01	2.33E-04	4.08E-11	2.33E-04	1.11E-13	3.09E-16	2.62E-09
Caloosahatchee				4.40E-03	2.77E-07	2.01E-03	1.80E-01	1.87E-03	2.34E-02	3.23E-04	8.91E-07	2.88E-07	1.26E-05
James City					5.63E-03	4.11E-03	1.00E-01	2.50E-01	5.68E-03	3.57E-02	5.69E-03	4.80E-03	9.15E-03
Raysor						1.61E-08	1.36E-01	1.85E-01	1.96E-12	2.92E-04	1.66E-12	1.43E-14	8.76E-09
Jackson Bluff							9.40E-01	1.43E-03	2.17E-08	2.63E-04	4.97E-13	2.63E-15	5.07E-09
Tamiami								3.93E-01	3.81E-02	3.57E-02	5.69E-03	4.80E-03	2.45E-03
Yorktown									5.06E-04	7.94E-03	5.07E-04	3.63E-04	1.29E-04
Chipola										5.06E-04	3.03E-10	1.55E-11	1.14E-07
Severn											5.07E-04	1.17E-03	1.46E-02
Owl Creek												1.08E-02	8.10E-06
Ripley													2.49E-02
Left Valves													
Species	*Nucula proxima*								*Nucula chipolana*	*Nucula percrassus*			
Formation	Fort Thompson	Caloosa/Bermont	Caloosahatchee	James City	Raysor	Jackson Bluff	Tamiami	Yorktown	Chipola	Severn	Owl Creek	Ripley	Coon Creek
Pamlico	6.77E-04	1.13E-07	4.55E-03	4.26E-03	1.89E-02	7.08E-04	3.37E-01	2.26E-01	8.65E-12	1.95E-02	1.31E-09	1.24E-13	1.31E-09
Fort Thompson		2.91E-04	7.90E-02	4.13E-04	3.99E-13	3.73E-01	4.13E-01	9.26E-03	1.28E-13	1.63E-02	1.61E-11	3.29E-18	1.61E-11
Caloosa/Bermont			9.96E-01	2.11E-04	7.45E-21	1.07E-01	4.25E-03	4.45E-03	1.13E-11	1.62E-02	1.30E-11	1.88E-18	1.30E-11
Caloosahatchee				3.23E-04	5.07E-06	2.86E-01	2.47E-01	4.40E-03	4.89E-03	2.20E-02	5.34E-06	3.57E-07	5.34E-06
James City					3.50E-02	9.23E-04	5.11E-03	1.43E-01	3.85E-04	9.52E-02	9.10E-04	3.86E-04	5.94E-05
Raysor						2.53E-10	2.14E-03	6.57E-01	1.17E-15	1.77E-02	1.45E-10	8.50E-16	1.45E-10
Jackson Bluff							2.66E-01	3.02E-02	1.53E-09	1.66E-02	2.74E-11	1.35E-17	2.74E-11
Tamiami								3.64E-02	1.06E-05	3.64E-02	3.47E-05	5.30E-06	3.47E-05
Yorktown									4.95E-03	2.00E-01	1.50E-03	4.96E-03	1.50E-03
Chipola										2.07E-02	4.19E-09	1.41E-12	4.19E-09
Severn											3.16E-01	9.17E-01	4.21E-02
Owl Creek												4.16E-06	4.16E-06
Ripley													3.34E-04

variation along axis 2 reflects differences in shell height. For example, Miocene *N. chipolana* and all Pliocene to Pleistocene *N. proxima* specimen 80% confidence intervals around mean scores overlap along both PCA axes 1 and 2. In contrast, *N. percrassa* specimen 80% confidence intervals mean scores from different Cretaceous formations show distinctly reduced overlap. The ACP Severn Formation *N. percrassa* 80% ellipse and mean are the most distinct for the Cretaceous suggesting that there was either pronounced ecophenotypic variation or physical, oceanographic, and/or climatic barriers with populations from the GCP; however, they are morphologically closest to Ripley Formation specimens, which are the most similar in age. The only Neogene–Quaternary 80% ellipse that deviate substantially from the other Cenozoic 80% ellipses around the means are the right valves of Caloosahatchee Formation specimens along PCA axis 2.

Statistical analysis of the PCA axes 1 and 2 associations indicate statistically significant differences among Cretaceous specimens but limited statistically significant differences for Neogene–Quaternary specimens (Table 5.3). Nearly all Cretaceous *N. percrassa* right and left valve PCA scores are statistically different with the exception of the relationship between the Severn and Ripley and Coon Creek and Owl Creek right valves. Neogene–Quaternary specimens show a much greater number of PCA mean scores with no statistical differences, which supports the PCA associations. However, less than half of the associations lack statistically differentiation, which suggests that the PCA associations are not as similar as they appear on the PCA plot (see Fig. 11). Notable exceptions to these results include statistically significant differences among associations between most Chipola and Jackson Bluff left valves and all other samples. Also, less than half of Chipola and Jackson Bluff right valves show statistically significant differences among associations.

Shape Change: Canonical Variance Analysis

The CVA axis 1 to 3 scores for both right and left valves of the *Nucula* species investigated here show a similar pattern to the PCA plots with obvious shape similarities among Neogene–Quaternary specimens, but major differences for the Cretaceous specimens (Fig. 5.12). The 80% confidence intervals for the CVA mean scores for most left and right valves of *N. chipolana* and *N. proxima* overlap along both axes 1 and 2, however, right valve 80% confidence intervals mean scores for specimens from the Yorktown and Caloosahatchee have slightly lower CVA axis 1 scores. In contrast, *N. percrassa* specimen scores from different Cretaceous formations show much greater variance and less overlap along CVA axes 1 and 2 in comparison to Neogene–Quaternary specimens.

The statistical results for the CVA axis 1 to 3 associations are almost identical to the results of the PCA statistical analysis with statistically significant differences among Cretaceous specimens but limited statistically significant differences for Neogene–Quaternary specimens (Table 5.4). For example, all Cretaceous *Nucula* right and left valve CVA scores are statistically different. In contrast, Neogene–Quaternary specimens show a much greater number of CVA scores with no statistical differences. As with the PCA statistical results, there are statistically significant differences among associations between most Chipola and Jackson Bluff left valves and all other samples. The associations among Chipola as compared to Jackson Bluff, Raysor, and Fort Thompson right valves are significantly different. The associations among Jackson Bluff as compared to Yorktown, Raysor, and Caloosahatchee–Bermont right valves are also statistically significantly different among associations.

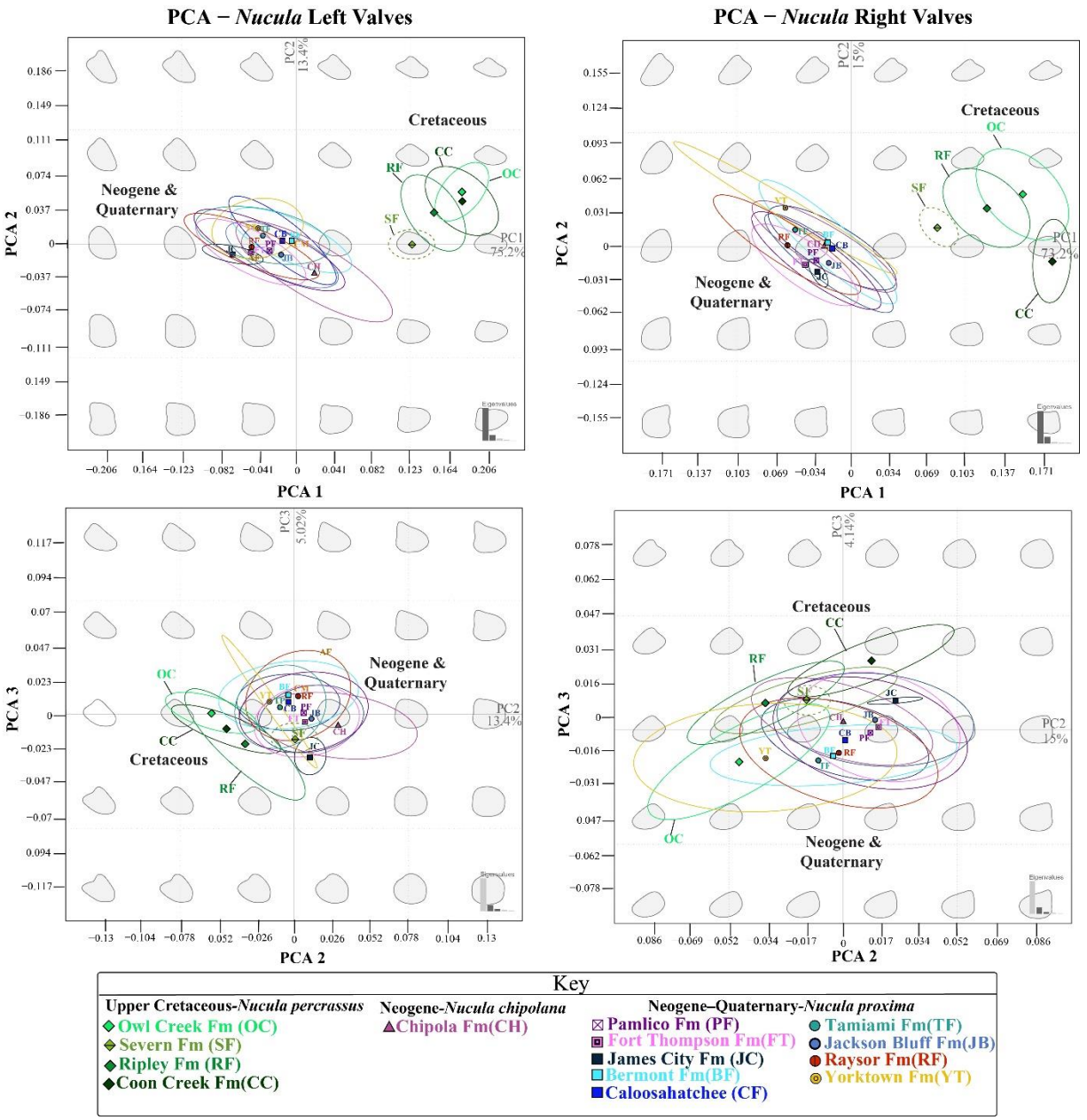

Figure 5.10. PCA axis 1 to 3 scores for Cretaceous and Neogene–Quaternary *Nucula* right (A) and left (B) valves. Backtransform shapes (gray) in background show Nucula outline shape variation in morphospace. Ellipses represent 80% confidence intervals around mean PCA scores.

Table 5.4. Summary statistics for PCA axes 1 to 3 scores of left (top) and right (bottom) *Nucula* valves. Yellow boxes indicate statistically significant differences when compared with opposite samples, whereas gray boxes indicate a lack of statistically significant differences.

PCA RIGHT VALVES												
Species	*Nucula proxima*							*Nucula chipolana*	*Nucula percrassus*			
Formation	Fort Thompson	Caloosahatchee/Bermont	James City	Raysor	Jackson Bluff	Tamiami	Yorktown	Chipola	Severn	Owl Creek	Ripley	Coon Creek
Pamlico	3.04E-02	5.66E-03	2.38E-01	7.78E-02	3.83E-01	2.44E-01	6.91E-03	6.63E-02	3.33E-11	1.34E-35	2.85E-34	1.33E-22
Fort Thompson		8.96E-09	6.66E-01	8.78E-04	2.97E-04	8.66E-02	4.52E-04	1.65E-05	6.58E-16	1.75E-66	1.55E-62	8.64E-42
Caloosahatchee/Bermont			2.90E-01	5.36E-07	5.19E-02	5.42E-01	3.67E-01	7.81E-02	1.49E-06	5.41E-36	3.54E-33	4.83E-22
James City				1.27E-01	2.55E-01	1.03E-03	1.82E-03	4.58E-02	5.56E-07	1.95E-12	3.50E-12	3.42E-08
Raysor					3.96E-04	2.72E-01	9.00E-03	5.64E-03	3.14E-10	6.62E-41	5.68E-39	6.23E-24
Jackson Bluff						2.19E-01	6.65E-03	2.52E-02	1.70E-12	1.72E-45	1.11E-42	2.31E-28
Tamiami							8.41E-01	4.75E-01	1.72E-03	1.54E-09	5.84E-09	1.92E-06
Yorktown								1.28E-01	2.14E-03	1.68E-12	8.91E-12	3.48E-07
Chipola									4.34E-06	5.50E-27	2.40E-25	1.29E-15
Severn										3.84E-07	7.03E-04	2.09E-05
Owl Creek											5.04E-07	9.06E-08
Ripley												5.01E-09
PCA LEFT VALVES												
Species	*Nucula proxima*							*Nucula chipolana*	*Nucula percrassus*			
Formation	Fort Thompson	Caloosahatchee/Bermont	James City	Raysor	Jackson Bluff	Tamiami	Yorktown	Chipola	Severn	Owl Creek	Ripley	Coon Creek
Pamlico	4.26E-03	1.17E-07	9.34E-03	1.37E-01	3.68E-01	2.23E-01	3.87E-01	4.71E-03	1.01E-05	1.21E-29	5.60E-34	1.84E-30
Fort Thompson		6.19E-29	6.10E-02	4.37E-01	4.16E-08	3.24E-03	6.34E-02	2.18E-10	2.55E-11	1.96E-62	3.37E-69	3.71E-62
Caloosahatchee/Bermont			6.14E-08	9.27E-17	2.59E-10	1.61E-01	4.59E-01	1.18E-07	7.12E-06	9.57E-56	4.31E-58	1.05E-54
James City				2.58E-02	6.95E-04	2.17E-02	1.06E-01	8.11E-04	4.49E-03	3.67E-14	5.05E-19	7.32E-14
Raysor					4.18E-04	2.23E-02	1.19E-01	4.70E-06	6.16E-08	7.19E-40	9.38E-45	8.87E-41
Jackson Bluff						8.65E-02	2.45E-01	3.05E-03	1.45E-07	2.91E-50	7.11E-55	5.34E-50
Tamiami							9.30E-01	3.18E-02	2.19E-02	1.25E-12	5.64E-17	9.72E-13
Yorktown								1.99E-01	1.20E-01	1.96E-10	1.18E-12	2.99E-09
Chipola									7.60E-05	2.83E-26	8.90E-30	4.09E-27
Severn										8.24E-03	1.07E-01	5.45E-04
Owl Creek											1.91E-05	8.54E-01
Ripley												4.26E-05

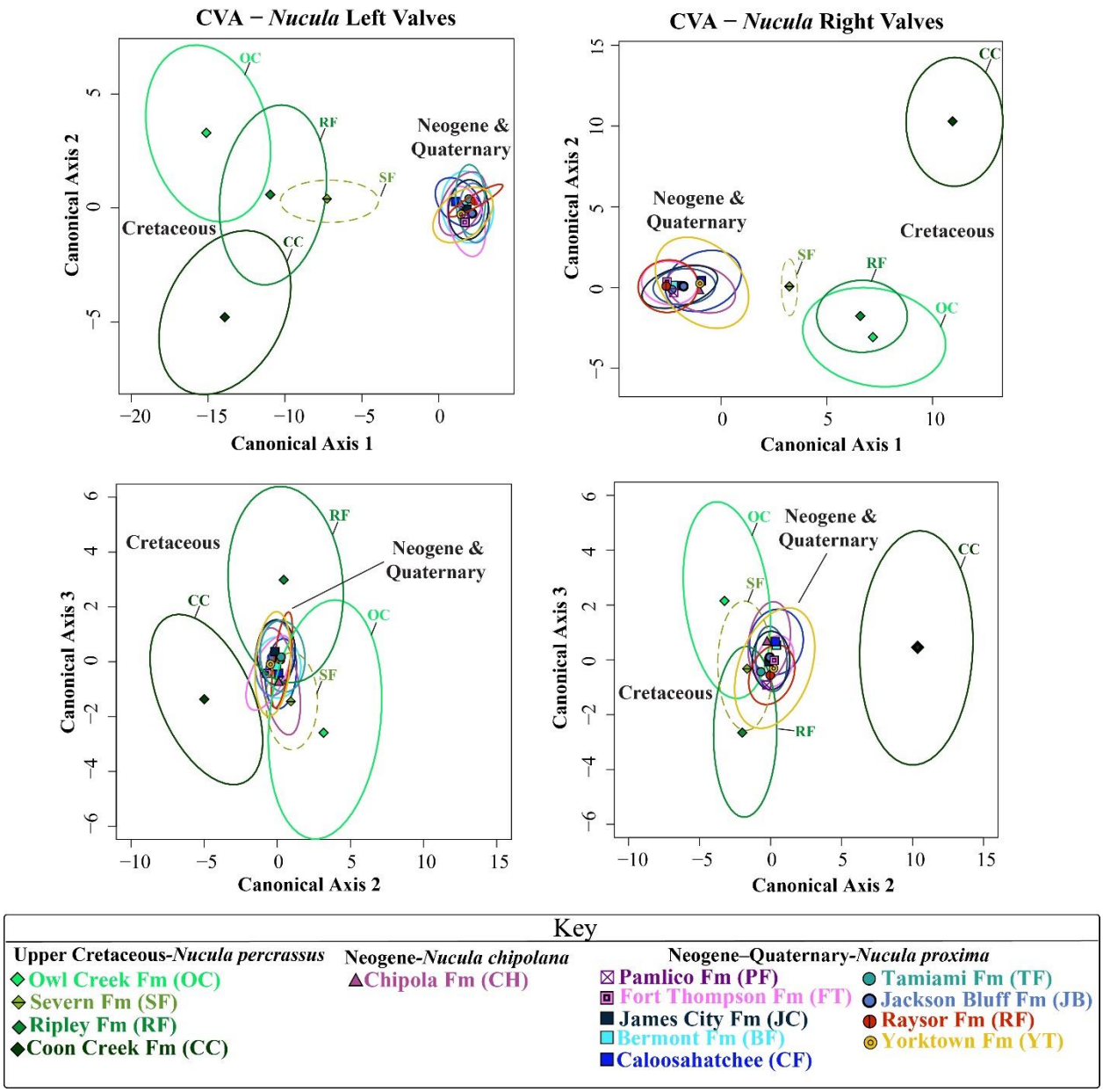

Figure 5.11. CVA axis 1 to 3 scores for of Upper Cretaceous and Neogene–Quaternary *Nucula* right (A) and left (B) valves. Ellipses represent 80% confidence intervals around mean CVA scores.

Table 5.5. Summary statistics for PCA axes 1 to 3 scores of left (top) and right (bottom) *Nucula* valves. Yellow boxes indicate statistically significant differences when compared with opposite samples, whereas gray boxes indicate a lack of statistically significant differences.

CVA RIGHT VALVES												
Species	*Nucula proxima*							*Nucula chipolana*	*Nucula percrassus*			
Formation	Fort Thompson	Caloosahatchee/Bermont	James City	Raysor	Jackson Bluff	Tamiami	Yorktown	Chipola	Severn	Owl Creek	Ripley	Coon Creek
Pamlico	3.04E-02	5.66E-03	2.38E-01	7.78E-02	3.83E-01	2.44E-01	6.91E-03	6.63E-02	3.33E-11	1.34E-35	2.85E-34	1.33E-22
Fort Thompson		8.96E-09	6.66E-01	8.78E-04	2.97E-04	8.66E-02	4.52E-04	1.65E-05	6.58E-16	1.75E-66	1.55E-62	8.64E-42
Caloosahatchee/Bermont			2.90E-01	5.36E-07	5.19E-02	5.42E-01	3.67E-01	7.81E-02	1.49E-06	5.41E-36	3.54E-33	4.83E-22
James City				1.27E-01	2.55E-01	1.03E-03	1.82E-03	4.58E-02	5.56E-07	1.95E-12	3.50E-12	3.42E-08
Raysor					3.96E-04	2.72E-01	9.00E-03	5.64E-03	3.14E-10	6.62E-41	5.68E-39	6.23E-24
Jackson Bluff						2.19E-01	6.65E-03	2.52E-02	1.70E-12	1.72E-45	1.11E-42	2.31E-28
Tamiami							8.41E-01	4.75E-01	1.72E-03	1.54E-09	5.84E-09	1.92E-06
Yorktown								1.28E-01	2.14E-03	1.68E-12	8.91E-12	3.48E-07
Chipola									4.34E-06	1.68E-12	2.40E-25	1.29E-15
Severn										3.84E-07	7.03E-04	2.09E-05
Owl Creek											5.04E-07	9.06E-08
Ripley												5.01E-09
CVA LEFT VALVES												
Species	*Nucula proxima*							*Nucula chipolana*	*Nucula percrassus*			
Formation	Fort Thompson	Caloosahatchee/Bermont	James City	Raysor	Jackson Bluff	Tamiami	Yorktown	Chipola	Severn	Owl Creek	Ripley	Coon Creek
Pamlico	2.55E-03	2.66E-03	4.08E-01	7.08E-02	6.90E-01	4.03E-01	6.00E-01	4.44E-03	5.17E-11	1.30E-41	8.44E-47	2.34E-38
Fort Thompson		5.46E-19	1.37E-01	3.60E-06	2.33E-04	5.82E-04	2.89E-02	5.80E-08	2.57E-31	2.10E-96	3.52E-100	2.16E-90
Caloosahatchee/Bermont			2.30E-02	3.14E-08	2.20E-07	1.83E-01	8.22E-01	1.91E-08	5.30E-21	9.42E-96	1.81E-98	8.57E-93
James City				6.45E-04	1.38E-01	2.05E-01	3.83E-01	1.63E-02	8.85E-03	8.80E-13	2.10E-16	4.10E-11
Raysor					6.45E-04	1.18E-02	3.16E-01	2.61E-07	4.51E-20	2.31E-58	5.28E-63	2.88E-54
Jackson Bluff						2.10E-01	3.00E-01	5.08E-04	2.05E-21	3.77E-80	2.89E-84	6.65E-75
Tamiami							4.08E-01	3.07E-01	7.35E-04	2.30E-16	1.56E-20	1.90E-14
Yorktown								2.12E-01	2.50E-02	9.61E-10	4.79E-12	2.15E-08
Chipola									1.19E-12	4.64E-39	3.74E-44	8.39E-36
Severn										8.95E-05	8.95E-11	4.63E-04
Owl Creek											1.43E-03	4.74E-12
Ripley												4.61E-11

Discussion

Allometric Effects on Shape

Allometric effects must be considered prior to shape analysis as the potential exists for morphologic differences from both an individual sample as well as from different ones to reflect variation in size due to ontogeny rather than evolutionary change. The weak correlation between size and shape for the Cretaceous and Neogene–Quaternary *Nucula* indicates that size is playing at most a limited role in impacting specimen shape. This correlation indicates that the different *Nucula* species were undergoing isometric growth through ontogeny such that all shell dimensions were growing at approximately the same rate and that shell proportions of large individuals are not significantly different from those of the small individuals. Potential allometric effects (i.e., changes in the shape proportions with growth) are important to consider as size is well-known to influence shape through ontogeny in many species (Bonner, 2006).

In groups that display allometric growth, body size increases through ontogeny can change the shape of an organism to compensate for structural and functional requirements associated with increased size (Bonner, 2006). These modifications are usually related to an organism changing its life habit and habitat through ontogeny (Bonner, 2006). However, these types of changes are not required for *Nucula*, since this group of bivalves maintains roughly the same life habits and habitat preferences throughout their life.

Size Trends

Cretaceous and Neogene–Quaternary *Nucula* differ substantially in their shell size variance through time with the former examples being much more variable than the latter, however, interpreting this variance in size can be challenging. This primarily stems from size

variance being influenced by various factors, including ontogeny of specimens, ecophenotypic effects, taphonomy, sample sizes, and collecting biases towards larger bivalve specimens.

Examining the data for each interval individually, both the box plots and statistical analysis of geometric means of size for Cretaceous *Nucula* indicates a clear pattern of evolutionary change for this time interval, which is similar for both right and left valves. This is indicated by the 22–23% evolutionary decrease in size for both right and left valves of *N. percrassa* over a 7.8 Ma interval spanning the late Campanian to the end-Maastrichtian. This size decrease is likely related to either progressively shorter life spans through the end-Cretaceous and/or heterochronic changes in development (e.g., see McKinney and McNamara, 2013). The former explanation would require a descrease in longevity through time, whereas the latter explanation could be the result of progressively more recent forms reaching maturity at a smaller size. Both factors would have likely been driven by changes in extrinsic environmental factors through the end-Cretaceous. Although beyond the scope of this study, a combination stratigraphic and sclerochronological approach would be needed to better understand if this decrease in size was driven by either the ecologic or evolutionary controls.

The Cretaceous *N. percrassa* are substantially larger and thicker shelled as compared to the Neogene–Quaternary *N. chipolana–proxima* lineage as can be seen in Figures 5.4 and 5.10. The exact cause of this size difference is unclear but could be due to either phylogeny or an evolutionary change in growth patterns from the Late Cretaceous to Neogene–Quaternary. As noted above, the exact evolutionary relationship between these Late Cretaceous and Neogene–Quaternary *Nucula* are unknown, so it is unclear whether the latter are descendants of the former or whether the latter represents an unrelated lineage with characteristically smaller individuals. If *N. percrassa* is ancestral to the *N. chipolana–proxima* lineage then the substantial decrease in

size could be due heterochronic changes in development, which resulted in Neogene–Quaternary lineages reaching maturity at a smaller size. Furthermore, Jones (1988) documented a similar heterochronic changes in growth rates for the bivalve *Arctica* Schumacher 1817 in the Late Cretaceous and Recent, with the former populations growing much more rapidly than Modern forms, although the adult sizes were not significantly different.

The *N. chipolana–proxima* lineage displays a substantial increase in mean size during the Neogene, indicating evolutionary change. This increase in size among middle Miocene and younger species is common in Western Atlantic bivalves and has been documented in numerous other clades (e.g., see Chapter Six; Gardner, 1926; Thompson, 2001). It likely reflects 'Cope's Rule,' which is characterized as an evolutionary trend for a lineage to increase in size over geological time (e.g., Cope, 1887; 1896; Newell, 1949; Stanley, 1973; Jablonski, 1997; Alroy, 1998). This interpretation is strengthened by the fact that *N. chipolana–proxima* represent a lineage.

If considered geographically, Neogene–Quaternary *Nucula* in the GCP show a 63.6% and 55.9% increase in mean size for left and right valves, respectively, for the transition from *N. chipolana* to *N. proxima*. In contrast, the ACP populations display approximately a 106.1% and 120.6% increase in mean size for left and right valves, respectively, for this same transition. The cause of this greater mean size for ACP *N. proxima* populations is unclear but could be due to either differences in sampling procedures by collectors (i.e., screening for smaller shells versus picking larger exposed shells on outcrop), population genotypes, or ecophenotypic variation (e.g., larger shells in the ACP versus smaller shells in the GCP due to environmental conditions). The substantially greater mean shell size percent increase in the ACP *Nucula* compared to GCP populations, although intriguing, could potentially be due to the use of GCP Miocene *Nucula* as

the original base line value for the percent increase calculation. As we did not analyze Miocene ACP *Nucula* samples, it is not clear if they were already larger than the Miocene GCP population as is documented in the younger *N. proxima* samples from the two regions. The presence of ACP Miocene *Nucula* data would potentially allow us to determine if the size change was truly greater in the ACP or relatively more comparable to the increase documented in the GCP. Furthermore, the contrast in size increases for the left and right valves of *Nucula* during the Neogene is notable and is likely due to slight morphological variation in the valves.

The box plots show that GCP populations of *N. proxima* maintain a relatively similar mean size of ~6 mm from the Pliocene into the late Pleistocene, whereas the mean size of ACP populations vary around ~8 mm during the same interval. This contrast among ACP and GCP *N. proxima* samples indicate that this species shows greater interspecific differences in size geographically among populations of equivalent age (e.g., Tamiami in GCP vs. Yorktown in ACP; Caloosahatchee/Bermont in GCP vs. James City in ACP) than they do temporally among populations from a smaller geographic area (e.g., Florida samples from the Pliocene to late Pleistocene). This high geographic and temporal interspecific variance among populations likely explains why large numbers of samples from different formations display overlap in size in the box plots (Fig. 5.10) but have statistically different median values among populations (Table 5.2). Stanley and Yang (1987) suggested that if geographic interspecific difference in morphology were greater than temporal differences, as in this study, then the evolutionary trend was likely trivial as seen here. This implies that *N. proxima* were in stasis during the late Pliocene to late Pleistocene. Some of the differences between the box plots and statistical results are also likely due to the sensitivity of the statistical test and the low samples size for certain populations (e.g., Tamiami and Yorktown). This limited size change suggests that *N. proxima*

was under stasis for a minimum of 3.6 Ma during the mid-Pliocene to late Pleistocene. Stasis in size could be longer, but the lack of Miocene *N. proxima* samples in the data set prohibit the ability to identify earlier evolutionary transitions.

Shape Trends

As with size, comparison among changes in outline shape for Cretaceous *N. percrassa* indicates clear evolutionary change. This is demonstrated by a considerable lack of overlap in PCA and CVA 80% confidence intervals. The shift from high to low CVA scores is suggestive of a gradual change in shape from the late Campanian to the end-Maastrichtian, however, as with size, the sampling resolution is too limited to confirm this pattern. The slight difference in the plotting positions of PCA and CVA scores for left and right valves suggests that the *Nucula* shells are somewhat inequivalved (i.e., valves not possessing same size and/or shape), although imperceptibly to the naked eye.

In contrast, Neogene–Quaternary *Nucula* PCA and CVA scores all overlap, which indicates that they share the same outline shape through time. Some of the differences between the PCA and CVA plots and the statistical results are, as with the size data, likely due to the sensitivity of the statistical test and the small sample sizes for certain populations (e.g., data for the Tamiami and Yorktown). This lack of change in outline shape suggests that this trait was in stasis in the *N. chipolana–proxima* lineage from the mid-Miocene to late Pleistocene. It also supports the possibility discussed above that *N. chipolana* and *N. proxima* are the same species; however, a greater range of characters would have to be analyzed before this interpretation can be more rigorously evaluated.

Cretaceous *Nucula* shape PCA and CVA scores show larger 80% ellipses as compared to Neogene–Quaternary species, which indicates greater variability among the former. This high

interspecific variability in shape is important because variation provides the raw material for natural selection to act upon (e.g., see West-Eberhard, 1989, 2003; Lloyd and Gould, 1993; Sheldon, 1993; Day and McPhail, 1996, Yacobucci, 2004). For example, reduced variability likely limits the amount of shape diversity natural selection can draw upon to drive evolutionary change. The exact cause of for high and low variability are still debated; however, it is thought to related to either the degree of ecological interactions with other organisms and/or the environment that the species inhabits (Simpson, 1944; Parsons, 1987; Ayala *et al*., 1975; Sheldon, 1993; Yacobucci, 2004). A few authors, such as Parsons (1987), have suggested that high-phenotypic variability is characteristic of high-stress environments since greater variability would be advantages to adapting to these settings. Other authors, such as Ayala *et al*. (1975) and Sheldon (1993), have suggested that high variability might be more likely to occur in stable environmental settings with limited environmental constraints due to reduced selection pressures and greater opportunity for greater phenotypic experimentation. The greater variability documented here for Cretaceous *Nucula* suggests that the reduced environmental stresses associated with this time interval relaxed selection pressures and created greater opportunity for greater shape variation. In contrast, the reduced variability documented here for Neogene–Quaternary *Nucula* outline shapes suggests that the greater and more frequent environmental changes associated with this time interval increased selection pressures and reduced the opportunity for greater shape variation.

Evolutionary Integration of Size and Shape Traits

The size and outline shape traits in the different *Nucula* species and lineages share congruent evolutionary patterns during their respective time intervals. Given the similarities in evolutionary pattern, this likely reflects ‘evolutionary integration’ among these traits (Hunt,

2007; Hopkins and Lidgard, 2012). This pattern suggests that size and outline shape were responding to selection pressures in a similar fashion during the Late Cretaceous and Neogene–Quaternary.

The only exception to this pattern is associated with the evolutionary transition from *N. chipolana* to *N. proxima*, which shows an increase in mean shell size, while outline shape remained in stasis. This variance in evolutionary patterns among traits in *Nucula* during the Neogene is not unusual and has been documented in numerous taxa and lineages (Hunt, 2007; Hopkins and Lidgard, 2012). Hunt (2007) has shown that evolutionary patterns typically vary among traits in a broad range of taxa, and, as in my study, size was significantly less likely than shape characters to display stasis.

Difficulties with Determining Evolutionary Patterns

Comparison among changes in size and outline shape patterns for Cretaceous and Neogene–Quaternary *Nucula* indicates contrasting evolutionary patterns of evolution and stasis for these respective time intervals. However, despite being able to identify these different evolutionary trajectories, it is difficult to differentiate between the modes of gradualism versus punctuated equilibrium. This inability to identify these evolutionary patterns is due to the resolution of our sampling regime, because we only examined a limited number of intervals that are separated by substantial temporal gaps caused by the lack of completeness in the depositional record, preservational issues (i.e., a change from aragonitic to steinkern preservation), and changes in facies (i.e., oxygen-rich, soft-substrate, *Nucula*-rich facies to oxygen-poor, firmer substrate *Nucula*-poor facies). If a higher-resolution sampling regime was possible, then potentially the evolutionary pattern could be more effectively identified using Hunt's (2006)

technique to statistically test whether data describe patterns of gradualism, stasis, or random walk.

Implications for the 'Plus ça Change' model

The size and shape patterns documented here for Cretaceous *Nucula* support Sheldon's (1996) 'Plus ça Change' prediction that reduced environmental variability will drive evolutionary responses. The change in size and shape documented for *N. percrassa* occurred against the backdrop of the Late Cretaceous greenhouse, which, as noted above, was characterized by relative environmental stability (Frakes *et al*., 1992; Miller *et al*., 2005; De Vleeschouwer *et al*., 2017). This suggests that the more slowly changing environment of the Late Cretaceous reduced environmental selection pressures, which allowed for *Nucula* to evolve new phenotypes due to the longer intervals of reduced environmental changes helping to promote continuing morphologic transformations.

The change in size displayed for the transition from the *N. chipolana* to *N. proxima* during the Neogene also supports the 'Plus ça Change' prediction that reduced environmental variability will drive an evolutionary change. Although the precise timing of this evolutionary transition is poorly constrained due to preservational issues (i.e., stratigraphic gaps, poor shell preservation) that limit the use of analytical methods used to identify such transitions (e.g., Hunt, 2007), it likely occurred either during the latter part of the middle Miocene Climatic Optimum or during the middle Miocene Climatic transition. These intervals are characterized by a relatively stable climate regime with high-global temperatures and sea level, which, like the Late Cretaceous, had reduced environmental stresses compared to the remainder of the Neogene or Quaternary. These diminished environmental stresses would have reduced selection pressures on *Nucula* and would likely have played a role in this evolutionary transition. Gardner (1926) noted

that each successive formation of middle Miocene age in the Florida Panhandle was associated with the appearance of a new *Nucula* species, which were defined by differences in their shell size, thickness, degree of inflation, hinge morphology, and escutcheon morphology. The appearance of each of these new species suggests that origination rates were relatively high within this group during the middle Miocene. This high-origination rate among *Nucula* in the ACP and GCP during the middle Miocene is unique as the remainder of the Neogene–Quaternary in these regions is inhabited by the much longer-ranging *N. proxima.* However, it should be considered that some of these middle Miocene species in the GCP might be oversplit, because, as noted by Mikklesen and Bieler (2008) as well as Wingard and Sohl (1990), *Nucula* are known to vary greatly in their size, shape, and color depending on environmental conditions. Nonetheless, the great variance seen among these middle Miocene species supports reduced selection pressures for this interval characterized by relative environmental stability.

The lack of size and shape change documented here for the Pliocene to Pleistocene *N. proxima* support the 'Plus ça Change' prediction that increased environmental variability, such as associated with the late Cenozoic, will result in stasis. This evolutionary stasis in size and shape for *N. proxima* spans ~3.6 Ma during the Pliocene warmhouse through Quaternary icehouse. The first 1.0 Ma of this interval was characterized by warmhouse conditions with elevated temperatures and sea levels as well as dampened climatic variation, similar to those in the Miocene (Fig. 5.7). The remaining 2.6 Ma was characterized by greater frequency of high-amplitude variations in temperatures and sea-level fluctuations that defined the various glacial and interglacial periods (Mudelsee and Schulz., 1997; Zachos *et al*., 2001; Tziperman and Gildore, 2003, Miller *et al*., 2005; De Vleeschouwer *et al*., 2017). This suggests that the rapidity

of the cyclically changing environmental conditions did not provide sufficient time for *Nucula* to adapt and hence led to morphological stasis.

Paleobiological Implications

The empirical data presented in this study both supports and refutes elements of Sheldon's (1996) 'Plus ça Change' model, which hypothesizes that evolutionary patterns vary with environmental stability over the long-term. More specifically, the results presented here support the prediction that the degree of environmental stability during different climatic regimes can influence evolutionary patterns. However, the discovery of gradual evolutionary change in Cretaceous *Nucula* from shallow-marine settings conflicts with Sheldon's (1996) original formulation, which considered these types of environments (i.e., shelf settings between 0 to 200 m depth) to be unlikely settings for evolutionary gradualism. Instead, he considered these environments as probable settings for evolutionary stasis and deep-oceanic environments as likely marine settings for gradual evolutionary change. He suggested that shallow-marine settings were too dynamic to produce gradualistic evolutionary patterns as they are influenced by various environmental factors (e.g., oxygen, salinity, temperature, depth) that vary relatively rapidly on very short time scales (i.e., daily to seasonally). However, this sort of variability is predictable to organisms that have at least annual life spans and must be adapted to if an organism and its species are going to survive in those settings.

Alternatively, the results presented here indicate that the degree of environmental stability during different climatic regimes can influence evolutionary patterns in shallow-marine settings. This suggests that ocean-climate interactions likely play a larger role in influencing shallow-marine environmental stability, and in turn selection pressures, than just marine dynamics alone. For example, during icehouse regimes, the Earth is relatively colder, with a less

active hydrologic cycle, and typically with the high latitude land masses and high elevations covered in ice, which markedly reduces sea levels and the geographic coverage of shallow marine habitats (Frakes *et al*., 1992; Zachos *et al*., 2001). When combined with the effects of Milankovitch-scale cyclicity, which controls global ice volumes over geologically relatively short timescales, marine habitats can be substantially impacted over relatively short temporal intervals due to rapid environmental changes (e.g., sea level, temperature, salinity). These abiotic fluctuations can be so rapid that they can considerably influence the stability and persistence of marine habitats and communities, which causes biotic selection pressures on marine species to vary throughout an icehouse (Roy et al., 1996). These fluxes also drive species to track their shifting habitats, which results in populations constantly fragmenting and then reforming over time (Potts, 1983; Pease et al., 1989). As a result, populations are prohibited from isolating and differentiating genetically. Over the long-term, this instability reduces the ability of species to evolutionarily respond before the dynamic environmental system changes once again (Roy et al., 1996). Under these conditions, organisms do not vary much morphologically over geological time scales and accommodate most of these changes ecologically.

In contrast, greenhouse intervals are warmer, wetter, and typically ice-free, which maintains high-sea levels and geographic coverage of shallow-marine habitats (Frakes *et al*., 1992). These conditions substantially reduce the amplitude of Milankovitch-scale variations in sea level, which decreases and slows the changes in the geographic coverage of shallow-marine environmental settings during each cycle. The amplitude of change in various environmental parameters (e.g., sea level, temperature) are sufficiently reduced that they do not substantially alter marine habitats over the long-term, which creates greater stability and persistence for

marine communities. This gives marine faunas greater time to evolutionarily respond to broad-scale environmental changes.

Despite this support for Sheldon's (1996) 'Plus ça Change' model, this case study is only one example of extrinsic controls influencing evolutionary patterns. Over the two decades since Sheldon (1996) used various examples from literature to show that evolutionary patterns vary with environmental stability, and, more importantly to this paper, different climatic regimes, relatively few published studies have tested this hypothesis or other extrinsic controls. The two empirical studies that have tested Sheldon's (1996) 'Plus ça Change' model have, based on their findings, argued against it.

Kim *et al*. (2009) documented a 3–Ma pattern of stasis in the trilobite *Triarthus beckii* Green 1832, which they used to argue against the 'Plus ça Change' model based on this species' occurrence within a relatively environmentally stable, low-oxygen, offshore setting of the Appalachian Foreland Basin. They framed their argument based on the model's prediction that gradualism should be more common at substantial depths due to greater environmental stability. However, it is more likely that the pattern they documented actually supports the 'Plus ça Change' model because the interval they studied coincides with a well-documented, although brief icehouse interval (Sheehan, 1973; Brenchley *et al*., 1994; Sutcliffe *et al*., 2000; Finnegan *et al*., 2011), compounded by the fact that the paleoenvironmental study they relied on to estimate depth (Cisne *et al*., 1982) was based upon an outdated approach to estimate the depth range of low-oxygen settings in epicontinental seas. Therefore, the depth is also likely vastly overestimated as most current evidence suggests that foreland basins were likely never deeper than 200 m (e.g., see Slattery *et al*., 2018).

Another study to have argued against the 'Plus ça Change' model is Ostrander (2013), who documented a clear pattern of evolutionary change as well as greater morphological variance in bivalves from the Neogene–Quaternary icehouse and stasis with limited variance in bivalve from the Cretaceous greenhouse. Ostrander (2013) suggested that the greater evolutionary change observed in the icehouse species relative to greenhouse representatives most likely reflects the requirement of the species to adapt to a broad range of changing environmental conditions, given the rapid fluctuations in climatic change during an icehouse. Despite these findings, Ostrander (2013) had substantial methodological problems, which could have skewed his results including comparing data from both steinkerns and well-preserved shells, not considering problems with shell ornamentation, not considering allometric differences among species, and not accounting for data artifacts caused by variation in raw xy-coordinate position, size, translation, rotation, and starting position.

These few examples indicate that a greater number of studies are needed to test the 'Plus ça Change' model, especially within a climatic context, to better constrain how the frequency of different evolutionary patterns varied with broad-scale climatic regimes. As Gould, Eldredge, and others frequently stressed, the debate over contrasting evolutionary patterns was not over which tempos and modes occur (see Fig. 5.1), but instead over their relative frequencies through geological time. A greater number of case studies, especially with standardized methodologies and examining multiple traits, would also help to facilitate future metanalyses of evolutionary patterns.

Conclusions

- Comparison among changes in size and outline shape patterns for Late Cretaceous and Neogene–Quaternary *Nucula* indicates that stasis and evolutionary change dominated these respective time intervals, respectively.
- The size and outline shape traits in the different *Nucula* species and lineages share congruent evolutionary patterns during their separate time intervals, which reflects evolutionary integration among these traits and that they were responding to respective prevailing selection pressures in a similar manner.
- The size and shape patterns documented here for Late Cretaceous and Neogene–Quaternary *Nucula* support Sheldon's (1996) 'Plus ça Change' model, which hypothesizes that increased environmental variability will result in stasis, whereas reduced environmental variability will drive progressive, potentially gradualistic morphologic responses.
- The paucity of studies examining the 'Plus ça Change' model, especially within a climatic context, indicate that a greater number of evolutionary tempo and mode studies set within a broad-scale climatic framework are required to understand the frequency of different patterns.

References

Alroy, J., 1998, Cope's rule and the dynamics of body mass evolution in North American fossil mammals: *Science*, 280, 731–734.

Alroy, J., Koch, P.L. and Zachos, J.C., 2000, Global climate change and North American mammalian evolution: *Paleobiology*, 26, 259–288.

Arthur, M.A., Dean, W.E. and Schlanger, S.O., 1985, Variations in the global carbon cycle during the Cretaceous related to climate, volcanism, and changes in atmospheric CO2: *The carbon cycle and atmospheric CO2: Natural variations Archean to present*, 32, 504–529.

Arthur, M.A., Kump, L.R., Dean, W.E., and Larson, R. L., 1991, Superplume, Super greenhouse?: *EOS, Transactions of the American Geophysical Union Abstract with Programs*, 72, 301 pp.

Ayala, F.J., Valentine, J.W., Delaca, T.E., Zumwalt, G.S., 1975, Genetic variability of the Antarctic brachiopod Liothyrella notorcadensis and its bearing on mass extinction hypotheses: *Journal of Paleontology*, 49, 1–9.

Bonner J.T., 2006, Why size matters: from bacteria to blue whales: *Princeton University Press*, 176 pp.

Brenchley, P.J., Marshall, J.D., Carden, G.A.F., Robertson, D.B.R., Long, D.G.F., Meidla, T., Hints, L., and Anderson, T.F., 1994, Bathymetric and isotopic evidence for a short-lived Late Ordovician glaciation in a greenhouse period: *Geology*, 22, 295–298.

Cárdenas, A.L. and Harries, P.J., 2010, Effect of nutrient availability on marine origination rates throughout the Phanerozoic Eon: *Nature Geoscience*, 3, 430–434.

Cardenas-Rozo, A.L. and Harries, P.J., 2016, Planktic foraminiferal diversity: logistic growth overprinted by a varying environment: *Acta Biológica Colombiana*, 21, 501–508.

Cisne, J.L., Karig, D.E., Rabe, B.D. and Hay, B.J., 1982, Topography and tectonics of the Taconic outer trench slope as revealed through gradient analysis of fossil assemblages: *Lethaia*, 15, 229–246.

Cope, E.D., 1887, The origin of the fittest: essays on evolution: *D. Appleton Press*, 1–466.

Cope, E.D., 1896, The primary factors of organic evolution: *Open Court Publishing, Company*, 547 pp.

Dall, W.H., 1898, Contributions to the Tertiary Fauna of Florida: With Especial Reference to the Miocene Silex-beds of Tampa and the Pliocene Beds of the Caloosahatchie River: *Wagner free institute of science*, 3, 511–947.

Day, T., McPhail, J.D., 1996, The effect of behavioural and morphological plasticity on foraging efficiency in the threespine stickleback (Gasterosteus sp.): *Oecologia*, 108, 380–388.

De Vleeschouwer, D., Vahlenkamp, M., Crucifix, M. and Pälike, H., 2017, Alternating Southern and Northern Hemisphere climate response to astronomical forcing during the past 35 my: *Geology*, 45, 375–378.

Edwards, L.E., Barron, J.A., Bukry, D., Bybell, L.M., Cronin, T.M., Poag, C.W., Weems, R.E. and Wingard, G.L., 2005, Paleontology of the upper Eocene to Quaternary postimpact section in the USGS-NASA Langley core, Hampton, Virginia: *United States Geological Survey professional paper*, 1688-H, 47 pp.

Erwin, D. H., and Anstey, R. L., Editors, 1995, New approaches to speciation in the fossil record: *Columbia University Press*, 288 pp.

Eldredge, N., Thompson, J. N., Brakefield, P. M., Gavrilets, S., Jablonski, D., Jackson, J. B., Lenski, R.E., Lieberman, B.S., McPeek A.M., and Miller III, W., 2005, *The dynamics of evolutionary stasis: Paleobiology*, 31, 133–145.

Eldredge, N., and Gould, S.J., 1972, Punctuated equilibria: an alternative to phyletic gradualism: *in* Schopf, T.J.M., Eds.: *Models in Paleobiology*, 82–115.

Finnegan, S., Bergmann, K., Eiler, J.M., Jones, D.S., Fike, D.A., Eisenman, I., Hughes, N.C., Tripati, A.K. and Fischer, W.W., 2011, The magnitude and duration of Late Ordovician–Early Silurian glaciation: *Science*, 331, 903–906.

Frakes, L.A., Francis, J.E., and Syktus, J.I., 1992, Climate modes of the Phanerozoic, *Cambridge University Press*, 288 pp.

Galloway, W.E., 2008, Depositional Evolution of the Gulf of Mexico Sedimentary Basin: *in* Miall, A.D., ed. *Sedimentary Basins of the World*, 5, 506–549.

Gardner, J.A. and Mansfield, W.C., 1943, Mollusca from the Miocene and lower Pliocene of Virginia and North Carolina:, *United States Geological Survey, Professional Paper*, 199–A, 177 pp.

Gardner, J., 1926, The molluscan fauna of the Alum Bluff Group of Florida, Part I, Prionodesmacea and Anomalodesmacea: *United States Geological Survey, Professional Paper*, 142–A, 79 pp.

Gould, S.J., 2002, The Structure of Evolutionary Theory: *Harvard University Press*, 1464 p.

Gradstein, F.M., 2012, Introduction: in Gradstein, F.M., Ogg, J.G., Schmitz, M.D., and Ogg, G.M., eds., *The Geological Time Scale 2012, Elsevier*, 1–29.

Hampson, G.R., 1971, A species pair of the genus *Nucula* (Bivalvia) from the eastern coast of the United States: *Journal of Molluscan Studies*, 39, 333–342.

Hastings, A.K. and Dooley, A.C., 2017, Fossil-collecting from the middle Miocene Carmel Church Quarry marine ecosystem in Caroline County, Virginia: *Geological Society of America Field Guides*, 47, 77–88.

Harries, P. J., and Allmon, W. D., 2007, Is there a relationship between sea level and evolutionary pattern among macroinvertebrates?: *Geological Society of America Abstracts with Programs*, 39, 587.

Hopkins, M.J. and Lidgard, S., 2012, Evolutionary mode routinely varies among morphological traits within fossil species lineages: *Proceedings of the National Academy of Sciences*, 109, 20520–20525.

Huddlestun, P.F., 1984, The Neogene stratigraphy of the Central Florida Panhandle: Unpublished *PhD dissertation, Florida State University*, 210 pp.

Hunt, G., 2007, The relative importance of directional change, random walks, and stasis in the evolution of fossil lineages: *Proceedings of the National Academy of Sciences*, 104, 18404–18408.

Hunt, G., 2006, Fitting and comparing models of phyletic evolution: random walks and beyond: *Paleobiology*, 32, 578–601.

Hecht, M.K., Eldredge, N. and Gould, S.J., 1974, Morphological transformation, the fossil record, and the mechanisms of evolution: a debate: *in* Evolutionary biology, Springer, 295–308.

Jablonski, D., 1997, Body-size evolution in Cretaceous molluscs and the status of Cope's rule: *Nature*, 385, 250 pp.

Jablonski, D., 2007. Scale and hierarchy in macroevolution: *Palaeontology*, 50, 87–109.

Jones, D.S., 1988, Sclerochronology and the size versus age problem: *in* Heterochrony in evolution, Springer, 93–108.

Kim, K., Sheets, H.D. and Mitchell, C.E., 2009, Geographic and stratigraphic change in the morphology of Triarthrus beckii (Green)(Trilobita): a test of the Plus ça change model of evolution: *Lethaia*, 42, 108–125.

Lamarck, J. P. B. A. de M. de., 1799, Prodrome d'une nouvelle classification des coquilles: *Memoires de la Societe d'Histoire naturelle de Paris* (for 1799): 63-90.

Lieberman, B. S., and Dudgeon, S., 1996, An evaluation of stabilizing selection as a mechanism for stasis: *Palaeogeography, Palaeoclimatology, Palaeoecology*, 127, 229–238.

Lieberman, B. S., Brett, C. E., and Eldredge, N., 1995, A study of stasis and change in two species lineages from the Middle Devonian of New York State: *Paleobiology*, 21, 15–27.

Lloyd, E.A. and Gould, S.J., 1993, Species selection on variability: *Proceedings of the National Academy of Sciences*, 90, 595–599.

McKenzie, N.R., Horton, B.K., Loomis, S.E., Stockli, D.F., Planavsky, N.J. and Lee, C.T.A., 2016, Continental arc volcanism as the principal driver of icehouse-greenhouse variability, *Science*, 352, 444–447.

McKinney, M.L., 1993, Evolution of Life: Processes, Patterns, and Prospects: *Prentice Hall*, 415 pp.

McKinney, Michael L., and Kenneth J. McNamara, 2013, Heterochrony: the evolution of ontogeny: *Springer*, 327–347.

Miall, A.D., Balkwill, H.R. and McCracken, J., 2008, The Atlantic margin basins of North America: *Sedimentary Basins of the World*, 5, 473–504.

Mikkelsen, P. M., and Bieler, R., 2007, Seashells of Southern Florida: Living Marine Mollusks of the Florida Keys and Adjacent Regions; Bivalves: *Princeton University Press, Princeton*, 446 pp.

Miller, K.G., Kominz, M.A., Browning, J.V., Wright, J.D., Mountain, G.S., Katz, M.E., Sugarman, P.J., Cramer, B.S., Christie-Blick, N. and Pekar, S.F., 2005, The Phanerozoic record of global sea-level change: *Science*, 310, 1293–1298.

Mudelsee, M. and Schulz, M., 1997, The Mid-Pleistocene climate transition: onset of 100 ka cycle lags ice volume build-up by 280 ka: *Earth and Planetary Science Letters*, 151, 117–123.

Newell, N.D., 1949, Phyletic size increase, an important trend illustrated by fossil invertebrates, *Evolution*, 103–124.

Ostrander, R.J., 2013, Effects of Climate Variability on Evolutionary Tempo and Mode in Cretaceous and Neogene Marine Molluscs: *Unpublished Masters Thesis, University of Wisconsin-Madison*, 119 pp.

Parsons, P.A., 1987, Evolutionary rates under environmental stress: *Evolutionary Biology*, 21, 311–347.

Pease, C.M., Lande, R. and Bull, J.J., 1989, A model of population growth, dispemal and evolution in a changing environment: *Ecology*, 70, 1657–1664

Potts, D.C., 1983, Evolutionary disequilibrhun among Indo-Pacific corals, *Bull. Mar. Sci*., 33, 619–632

Portell, R. W, Polites, G. L, and Schmelz, G. W., 2006, Mollusca, Shoal River Formation (Middle Miocene,): Florida Paleontological Society, Florida Fossil Invertebrates, 9.

Roy, K., Valentine, J.W., Jablonski, D. and Kidwell, S.M., 1996, Scales of climatic variability and time averaging in Pleistocene biotas: implications for ecology and evolution: *Trends in Ecology & Evolution*, 11, 458–463.

Richards, H.G. and Harbison, A., 1942, Miocene invertebrate fauna of New Jersey: *Proceedings of the Academy of Natural Sciences of Philadelphia*, 167–250.

Saupe, E.E., Hendricks, J.R., Portell, R.W., Dowsett, H.J., Haywood, A., Hunter, S.J., and Lieberman, B.S., 2014, Macroevolutionary consequences of profound climate change on niche evolution in marine molluscs over the past three million years: *Proceedings of the Royal Society B*, 281, 1–9.

Sheehan, P.M., 1973, The relation of Late Ordovician glaciation to the Ordovician- Silurian changeover in North American brachiopod faunas: *Lethaia*, 6, 147–154.

Sheldon, P. R., 1996, Plus ça change—a model for stasis and evolution in different environments: *Palaeogeography, Palaeoclimatology, Palaeoecology*, 127, 209–227.

Sheldon, P.R., 1997, The Plus ça change model: Explaining stasis and evolution in response to abiotic stress over geological timescales: *in* Bijlsma, R. Loeschcke, V. Eds., *Environmental Stress, Adaptation, and Evolution*: Basel, *Birkhäuser Verlag*, 307–326.

Sheldon, P.R., 1993, Making sense of microevolutionary patterns: *in* Lees, D.R., Edwards, D. Eds., *Evolutionary Patterns and Processes, Linnean Society, Symposium, Academic Press*, 14, 19–31.

Simpson, G. G., 1944, Tempo and mode in evolution: *Columbia University Press*, 237 pp.

Slattery, J.S., Harries, P.J. and Sandness, A.L., 2018, Do marine faunas track lithofacies? Faunal dynamics in the Upper Cretaceous Pierre Shale, Western Interior, USA: *Palaeogeography, Palaeoclimatology, Palaeoecology*, 496, 205–224.

Speden, I.G., 1970, The type Fox Hills Formation, Cretaceous (Maestrichtian), South Dakota. Systematics of the Bivalvia: *Bulletin of the Peabody Museum, Yale University*, 33, 222 pp.

Stanley, S.M., 1973, An explanation for Cope's rule: *Evolution*, 27, 1–26.

Stanley, S.M. and Yang, X., 1987, Approximate evolutionary stasis for bivalve morphology over millions of years: a multivariate, multilineage study: *Paleobiology*, 13, 113–139.

Sutcliffe, O.E., Dowdeswell, J.A., Whittington, R.J., Theron, J.N. and Craig, J., 2000, Calibrating the Late Ordovician glaciation and mass extinction by the eccentricity cycles of Earth's orbit: *Geology*, 28, 967–970.

Thompson, M.D., 2001, Gigantism and Dolomite Replacement in the Dean's Trucking Pit Mollusks (early to Middle Miocene), Sarasota County, Florida: *Unpublished Doctoral dissertation, University of South Florida*, 369 pp.

Tziperman, E. and Gildor, H., 2003, On the mid- Pleistocene transition to 100- kyr glacial cycles and the asymmetry between glaciation and deglaciation times: *Paleoceanography*, 18, 1–4.

Weems, R.E. and Edwards, L.E., 2001, Geology of Oligocene, Miocene, and younger deposits in the coastal area of Georgia: *Georgia Geologic Survey Bulletin*, 124 pp.

Weems, R.E., Self-Trail, J.M. and Edwards, L.E., 2004, Supergroup stratigraphy of the Atlantic and Gulf coastal plains (Middle? Jurassic through Holocene, eastern North America): *Southeastern Geology*, 42, 191–216.

Weems, R.E. and George, R.A., 2013, Amphibians and nonmarine turtles from the Miocene Calvert Formation of Delaware, Maryland, and Virginia (USA): *Journal of Paleontology*, 87, 570–588.

Weems, R.E. and Lewis, W.C., 2002, Structural and tectonic setting of the Charleston, South Carolina, region: Evidence from the Tertiary stratigraphic record: *Geological Society of America Bulletin*, 114, 24–42.

West-Eberhard, M.J., 1989, Phenotypic plasticity and the origins of diversity: *Annual review of Ecology and Systematics*, 20, 249–278.

West-Eberhard, M.J., 2003, Developmental plasticity and evolution: *Oxford University Press*, 794 pp.

Wingard, G.L. and Sohl, N.F., 1990, Revision of the *Nucula percrassa* Conrad, 1858 group in the Upper Cretaceous of the Gulf and Mid-Atlantic Coastal Plains: An example of bias in the nomenclature: *United States Geological Survey of Bulletin*, 1881-D, 25 pp.

Yacobucci, M.M., 2004, Neogastroplites meets Metengonoceras: morphological response of an endemic hoplitid ammonite to a new invader in the mid-Cretaceous Mowry Sea of North America: *Cretaceous Research*, 25, 927–944.

Zachos, J., Pagani, M., Sloan, L., Thomas, E. and Billups, K., 2001, Trends, rhythms, and aberrations in global climate 65 Ma to present: *Science*, 292, 686–693.

CHAPTER SIX:

THE EVOLUTIONARY TEMPO OF LUCINIDS IN FLORIDA DURING THE CONTRASTING CLIMATIC REGIMES OF THE NEOGENE AND QUATERNARY

Introduction

Understanding the tempo (i.e., stasis, gradualism) of morphological change is a critical component of evolutionary theory (Fig. 6.1). Since the publication of Eldredge and Gould (1972) substantial focus has been given to understanding the frequency of different evolutionary patterns. Based on countless studies, punctuated equilibrium is now thought to be the dominant evolutionary pattern for metazoans through the Phanerozoic (e.g., Barnosky, 1987; Gould and Eldredge, 1993; Jackson and Cheetham, 1999; Benton and Pearson, 2001; Gould, 2002;). However, Erwin and Anstey's (1995) compilation concluded that no single pattern predominates the evolutionary record and that many lineages show both punctuated equilibrium and gradualism through their history. The exact reason many lineages show contrasting evolutionary patterns through time remains poorly understood due to a limited investigation of the environmental context and controls of evolutionary patterns.

One possible explanation for different evolutionary patterns is Sheldon's (1996) 'Plus ça Change' model, which hypothesizes that frequent and pronounced environmental fluctuations will result in evolutionary stasis, whereas more static or slowly changing environmental conditions will drive gradual evolutionary change (Fig. 6.2). His hypothesis suggests that frequent and pronounced environmental changes limit the amount of time a new phenotype has to evolve, whereas environments with longer intervals of stability provide opportunity for new

phenotypes to gradually evolve. This model predicts that more stable environmental settings (e.g., deep seas) should promote gradualism, whereas more variable settings (e.g., shallow shelf) should result in stasis until an environmental threshold is met and relatively rapid evolution occurs.

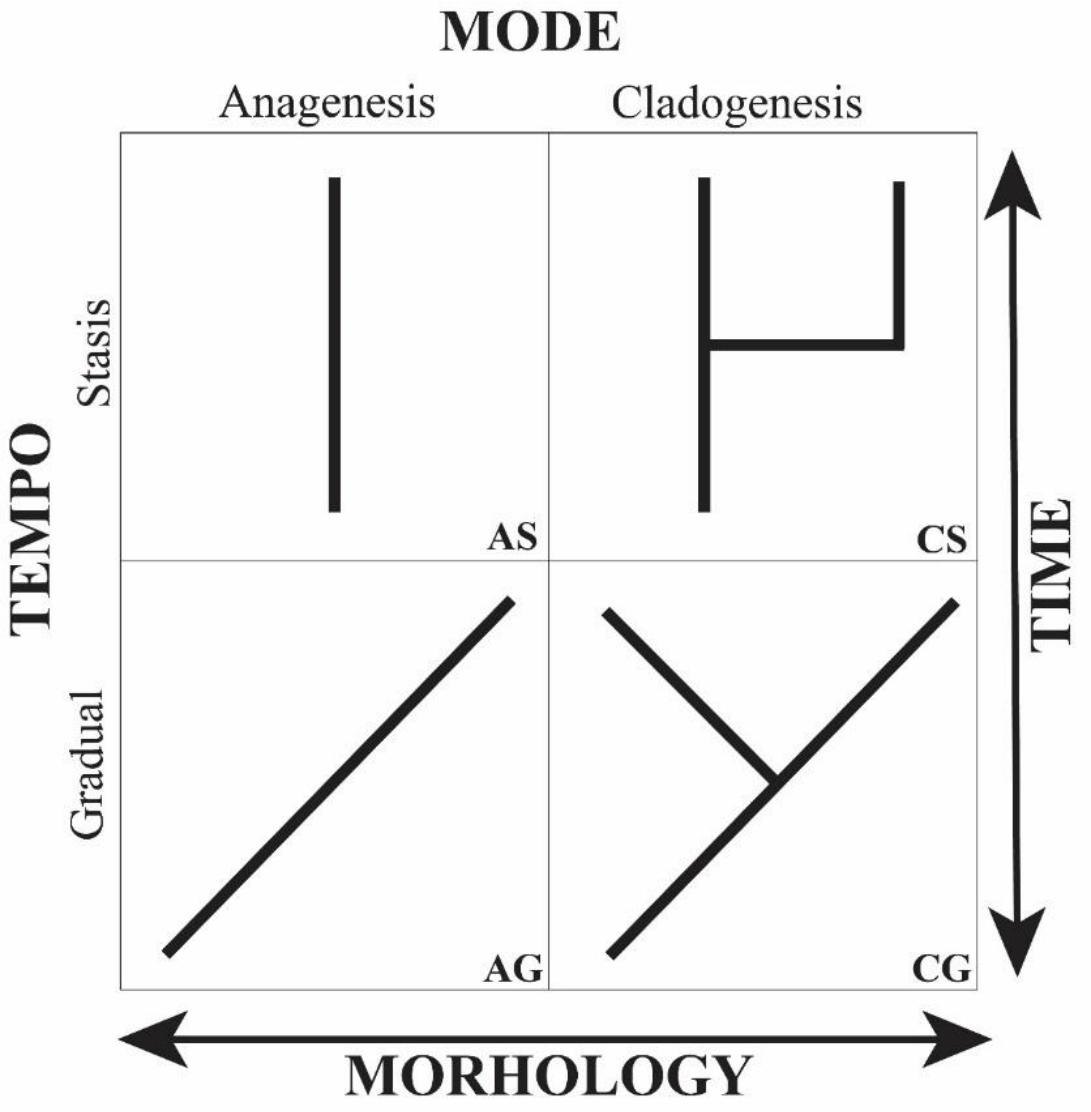

Figure 6.1. Diagram depicting different expressions of evolutionary patterns of speciation (modified from Jablonski, 2007; Harries and Allmon, 2007).

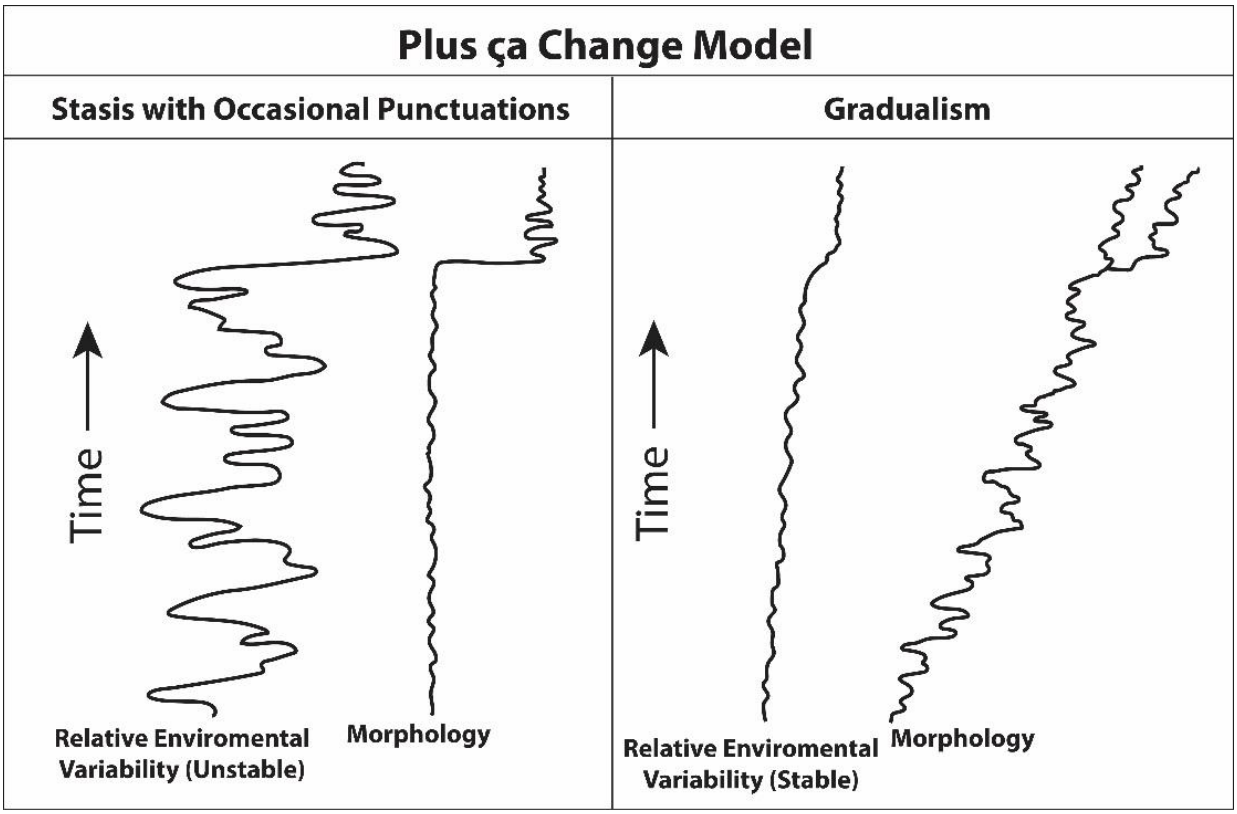

Figure 6.2. Sheldon's (1996, 1997) 'Plus ça change' model of environmental control on evolutionary patterns.

These evolutionary patterns should also be associated with broad-scale climatic regimes documented over the Phanerozoic (Fig. 6.3). These regimes fluctuated between ice-, mixed-, and greenhouse climatic conditions with each respective interval characterized by greater to lesser amounts of environmental variability (Frakes et al., 1992). However, it is currently poorly understood if different evolutionary patterns are associated with these long-term climatic patterns. Harries and Allmon's (2007) re-examination of the data compiled within Erwin and Anstey (1995) concluded that all the examples of gradualism are associated with greenhouse intervals. This indicates that a reassessment of evolutionary patterns examined from a broad-scale climatic context may provide important insights into the evolutionary process(es).

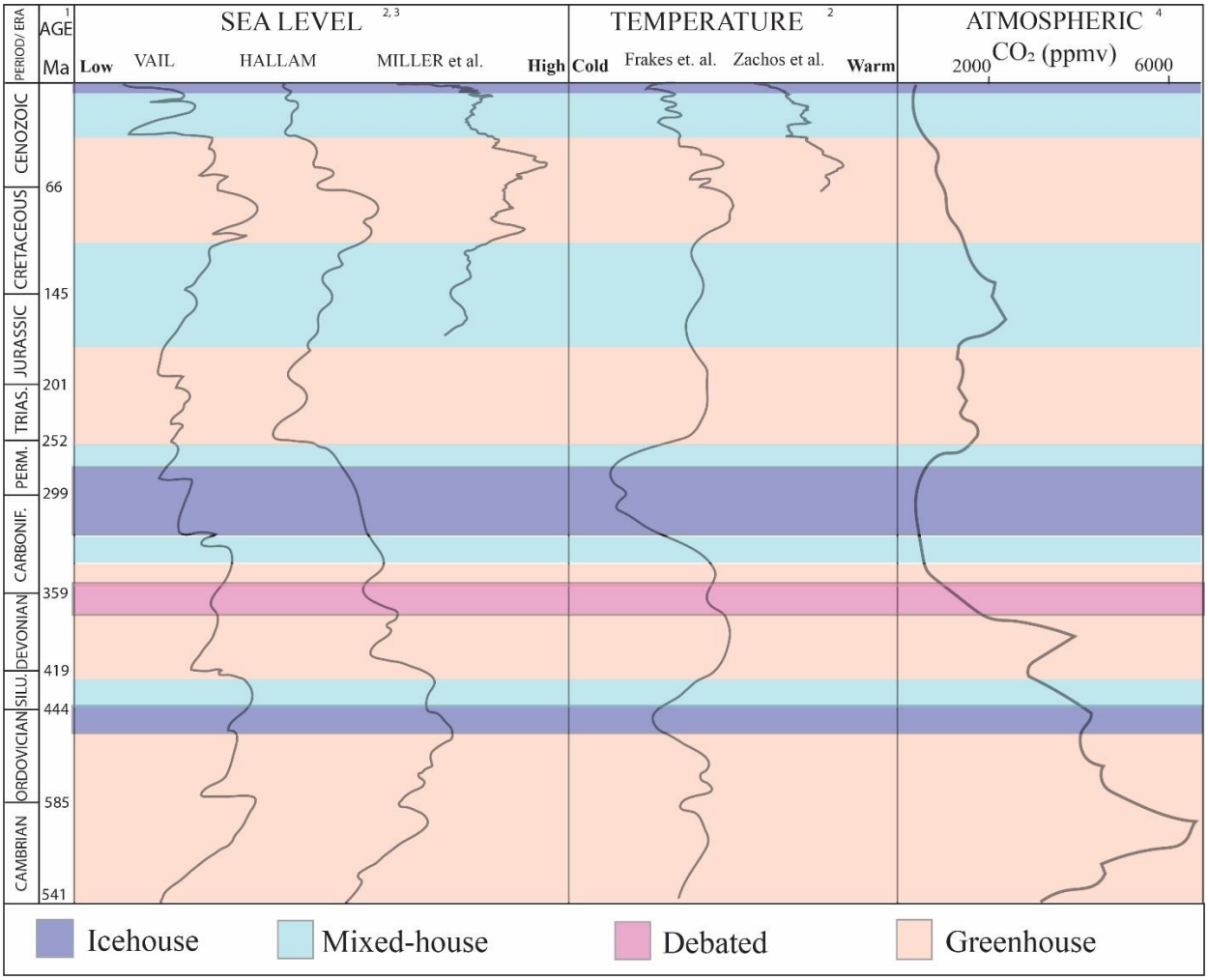

Figure 6.3. Phanerozoic climate history depicting global sea level curves, temperature curves, as well as different climate regimes as defined by the amount of glaciation. The purple band around the Devonian–Carboniferous boundary represents an interval where there is still considerable debate as to the extent of glaciation (modified from Frakes et al., 1992; Zachos et al., 2001; McKenzie et al., 2016).

The goal of this chapter is to examine the changes in evolutionary patterns among two different genera of lucinid bivalves through the relatively more stable mixed-house climate regime of Neogene to the less stable icehouse climatic regime of the Quaternary in a shallow shelf setting. This study will test Sheldon's (1996) 'Plus ça Change' model and will expand our understanding of broad-scale climatic controls on evolutionary patterns. Furthermore, this study

will test for the morphological distinctiveness or similarity, of taxa currently placed into the separate genera and/or species based on factors besides morphology (i.e., time, molecular data).

Background

Broad-Scale Climatic Setting

The Neogene and Quaternary display substantial differences in their broad-scale climatic patterns (Fig. 6.4), which make them a well-suited study interval for understanding how evolutionary tempos in lucinids potentially varied under differing climatic regimes. This interval is represented by an overall decrease in global temperature and sea level in association with an increase in continental glaciation (Fig. 6.4; Frakes et al., 1992; De Vleeschouwer et al., 2017; Zachos et al., 2001; Miller et al., 2005). This trend was primarily driven by a shift from high to low pCO2 levels in the atmosphere in combination with changes in the Earth's ocean-atmospheric circulation patterns because of geographic and topographic changes to the continents (Zachos et al., 2001; Royer et al., 2004; Beerling and Royer, 2011; McKenzie et al., 2016). These differences resulted in greater expression of Milankovitch-scale changes, which made the Earth increasingly more environmentally variable.

The Miocene to Pliocene Epochs were characterized by higher temperature and sea level than the Quaternary (Fig. 6.4), which for the most part varied relatively moderately in response to the 41 ka obliquity frequency (De Vleeschouwer et al., 2017; Zachos et al., 2001; Miller et al., 2005). The Miocene began with a short, but significant Southern Hemisphere glaciation event, which lasted ~0.4 Ma (Zachos et al., 1997, 2001; Pälike et al., 2006). This was then followed by a 6.0 Ma long mixed-house climate regime that was characterized by an overall warming trend punctuated by several ephemeral glaciation events in the southern hemisphere (De Vleeschouwer et al., 2016). This overall warming trend culminated in the mid-Miocene Climatic Optimum by

17 Ma, which was an interval characterized by 2.7 Ma of limited Southern-Hemisphere continental ice-sheet coverage as well as elevated global temperatures and sea level (Fielding et al., 2011; Griener et al., 2015; De Vleeschouwer et al., 2016; Zachos et al., 2001; Miller et al., 2005). Temperatures and sea level declined rapidly from ~14 to 12.5 Ma during the mid-Miocene climatic transition, which resulted in the establishment of a permanent East Antarctic Ice Sheet (Zachos et al., 2001). The drop in temperature and sea level continued into the late Miocene but at a substantially reduced rate, which resulted in the establishment of ephemeral ice-sheets in the northern-hemisphere by ~7.5 Ma and the permanent formation of the West Antarctic Ice Sheet during late Miocene glacial interval. This overall trend continued until the late Pliocene warm period (~3.6–2.6 Ma) when global temperature increased and continental ice coverage decreased resulting in higher sea levels (Zachos et al., 2001; Wara et al., 2005; Dowsett et al., 2007; Miller et al., 2012).

The late Pliocene warm period was followed by a substantial drop in global temperatures and sea level at the beginning of the Pleistocene, which marks the beginning of the so-called Quaternary Glaciation (Fig. 6.4; Frakes et al., 1992; Zachos et al., 2001; Miller et al., 2005). This interval is noted for a substantial increase in both climatic fluctuations, seasonality, and continental ice coverage (Zachos *et al*., 2001; Miller *et al*., 2005; Hennison et al., 2015). Initially, these fluctuations that defined the glacial-interglacial cycles of the Quaternary, varied at the 41 ka obliquity band; however, by the mid-Pleistocene (~950 ka), these cycles had shifted to 100 ka eccentricity frequency (Mudelsee and Shulz., 1997; Zachos et al., 2001; Tziperman and Gildore, 2003). This shift during the mid-Pleistocene along with the continued drop in pCO_2 levels resulted in high-amplitude changes in climate with longer and colder glacial periods and comparatively shorter and warmer interglacials periods. Prior to the mid-Pleistocene climatic

shift, most glacial-interglacial cycles were relatively more temporally symmetrical with similar length glacial and interglacial intervals (Mudelsee and Shulz., 1997; Tziperman and Gildore, 2003; Zachos et al., 2001).

Lucinid Systematics

This study examines six species of Neogene–Quaternary lucinids belonging to two separate clades. Lucinids were chosen because of their abundance, excellent preservation, and extensive stratigraphic record in the Neogene and Quaternary. These features made lucinids an excellent organism to quantitatively test the 'Plus ça Change' model.

One of the Neogene–Quaternary lucinid clades examined includes *Lucina* (Fig. 6.5A-C and 6.6)**.** The oldest species in this study is *L. glenni* (Fig. 6.5A), which is known from the middle Miocene of Florida and Brazil (Gardner, 1947; Couto, 1967; Toledo, 1989; Tavora et al., 2010). There is then a gap in the *Lucina* record until the Pliocene, which is due to a lack of middle Miocene *Lucina* specimens in museum collections and a dearth of available shell beds from this age in Florida. The Pliocene to Holocene focus of this analysis is on *L. pensylvanica* (Fig. 6.5B). This species is known from the Atlantic Coast (Maryland to Florida), the Gulf of Mexico (including Gulf Coastal Plain [GCP]), Bermuda, the Bahamas, West Indies, Caribbean Central America, and South America (Mikkelsen and Bieler, 2008 Taylor and Glover, 2016). This study also examined *L. roquesana* (Fig. 6.5C), which is morphologically similar *L. pensylvanica*, but is substantially smaller. This species has been documented from Bermuda, the Bahamas, Cayman Islands, Jamaica, Cuba, Haiti, Dominica, Virgin Islands, St Vincent, Guadeloupe, Martinique, Barbuda, Barbados, Central America, and northern South America (Taylor and Glover, 2016).

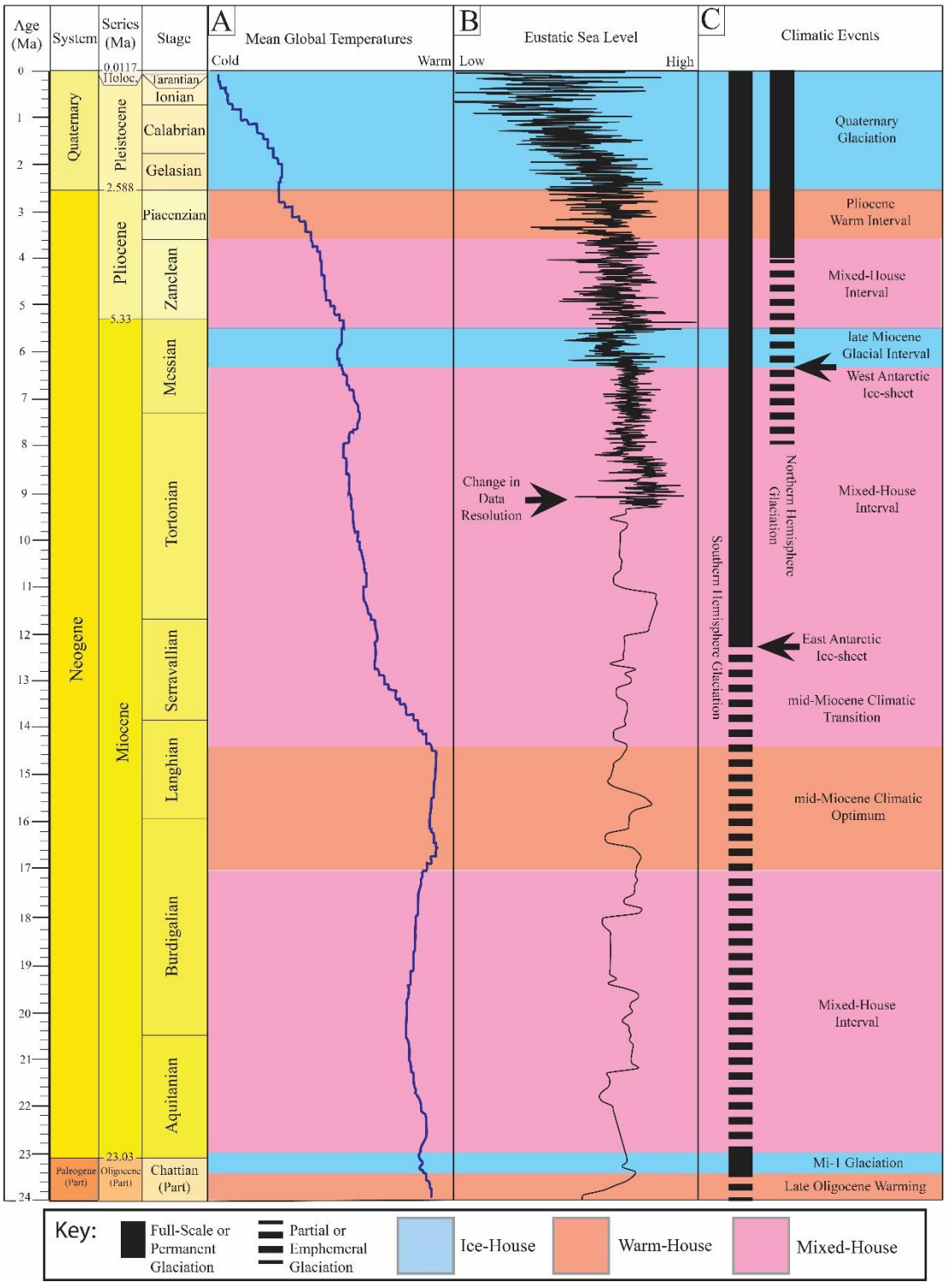

Figure 6.4. Neogene and Quaternary climate history depicting global temperature curves, sea level curves, as well as different climate regimes as defined by the amount of glaciation. The dashed and black lines show the appearance of ephemeral and permanent glaciation in the southern and northern hemispheres (modified from Frakes et al., 1992; Zachos et al., 2001).

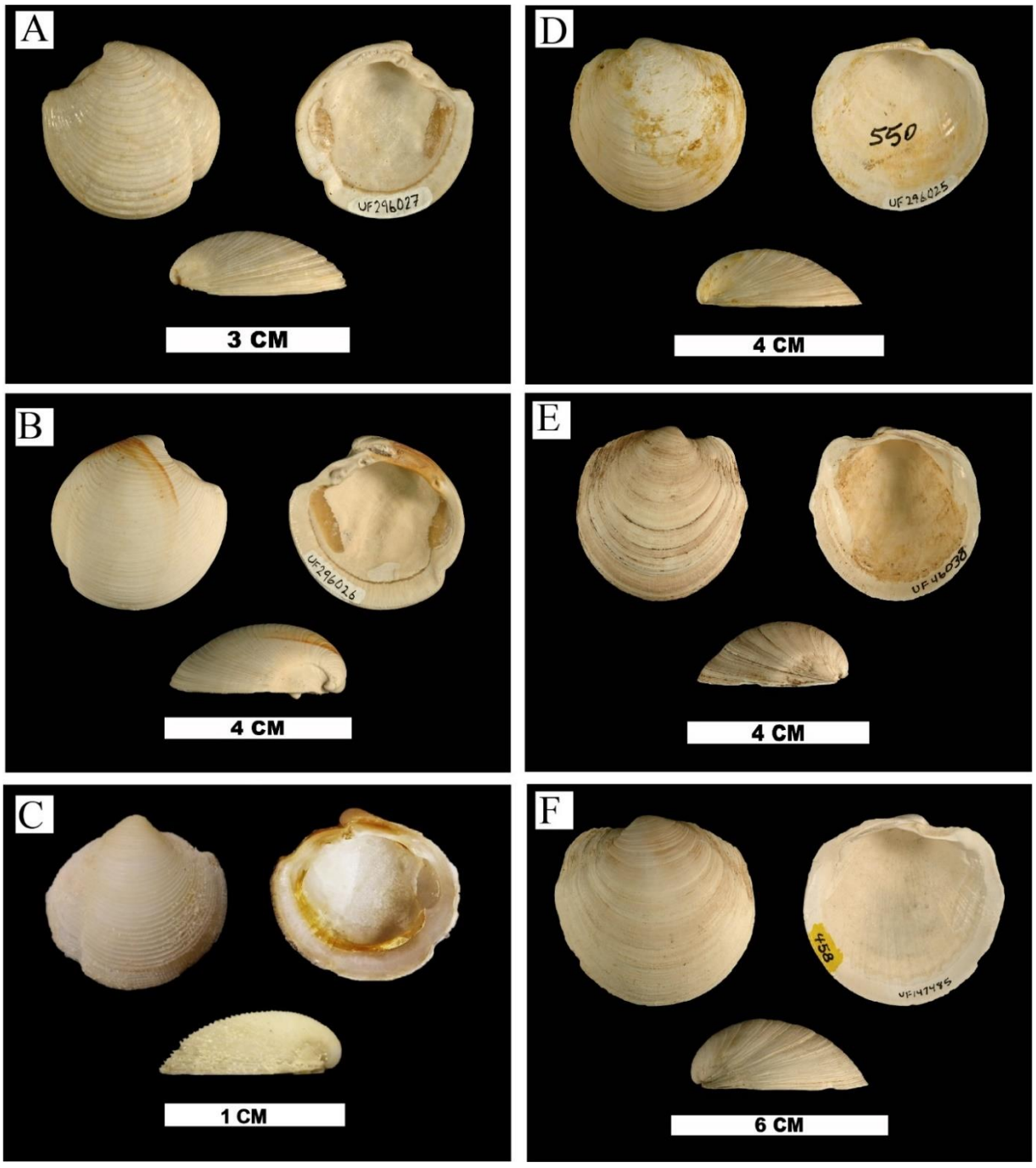

Figure 6.5. Examples of *Lucina* and *Anodontia* species examined in study with outside, inside, and side profiles. A) *Lucina glenni* (Left valve; UF296027), B) *Lucina pensylvanica* (Right valve; UF296026), C) *Lucina roquesana* (Left valve; author's personal collection), D) *Anodontia janus* (Left valve; UF296025), E) *Anodontia santarosana* (Right valve; (UF46038), and F) *Anodontia alba* (Left valve; UF147485).

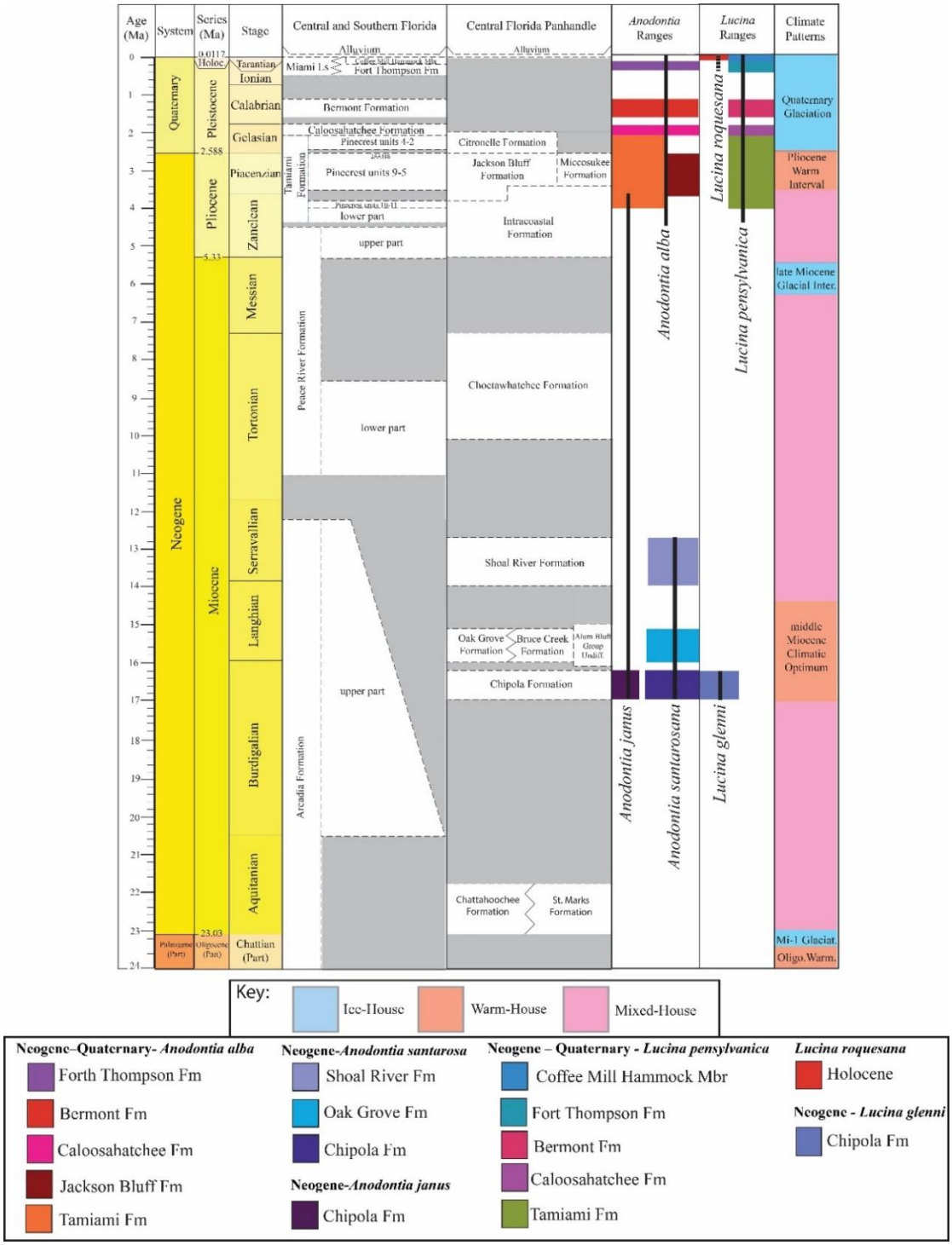

Figure 6.6. Stratigraphic position of Neogene to Quaternary *Lucina* and *Anodontia* samples from Florida used in study (see fig. 6.9 and 6.10 for geographic distribution) and broad scale climatic regimes (modified from Huddlestun, 1984; Zachos et al., 2001; Saupe et al., 2014). Solid black lines reflect total known range of species, whereas colored boxes reflect sampled ranges.

This study also examined the evolution of the Neogene–Quaternary lucinid genus *Anodontia* (Figs. 6.7 and 6.8)**.** The Miocene species analyzed in this study include *A. janus* and *A. santarosana* (Fig. 6.7A and B). *Anodontia janus* is known from the Miocene of Florida and Panama as well as the Pliocene of Dominican Republic (Smith, 1941; Gardner, 1947; Woodring, 1957; Hendy et al., 2008), whereas *A. santarosana* is only known from the Miocene of Florida (Gardner, 1947). The Pliocene to Holocene focus of this analysis is on *A. alba* (Fig. 6.7C and D), which ranges from North Carolina to Florida as well as into the Gulf of Mexico (including the GCP), Bermuda, the Bahamas, West Indies, Caribbean Central America, and South America (to Venezuela; Mikkelsen and Bieler, 2008; Taylor and Glover, 2016).

Evolutionary Relationships among Lucinids Analyzed in this Study

The evolutionary relationship among the taxa analyzed in this study, until recently, have been poorly constrained. As with most bivalves, this poor understanding stems from their various homeomorphies and their comparatively simple shell morphologies with few identifiable characters that can be used to effectively differentiate taxa based on morphology or to establish a phylogeny. These shortcomings, however, have been challenged by recent phylogenetic analysis of extant species by Taylor et al. (2016) using molecular data, which has revealed five major clades with many species and two minor clades with only a few species of extant western Atlantic lucinids. Taylor et al. (2016) has shown that *Lucina* and *Anodontia* belong to the lucinid clades Lucininae and Leucosphaerinae, respectively. Leucosphaerinae is moderately speciose and is relatively distantly related to the highly speciose Lucininae (see Taylor et al., 2016).

The evolutionary relationship among *L. glenni*, *L. pensylvanica*, and *L. roquesana* are all considered phylogenetically very close. Taylor and Glover (2016) suggested that Miocene *L. glenni* was the antecedent of the Pliocene to Holocene *L. pensylvanica*. This evolutionary

relationship is established based upon their striking shell resemblances and their biogeographic overlap in the Western Atlantic. Taylor et al.'s (2016) phylogenetic analysis of lucinid molecular data revealed that *L. pensylvanica* and *L. roquesana* are sister taxa.

The evolutionary relationship among *A. alba*, *A. janus*, and *A. santarosana* is poorly understood. However, based on their numerous shared shell traits (i.e., similar shape outlines, inflation patterns, muscle scars, and hinge features) and similar biogeographic ranges it is likely that *A. janus* and *A. santarosana* are either sister taxa or variants of the same species. Based on their similar shell morphology, overlap in biogeographic range, and the close relationship between the extinction of *A. janus* and the origination of *A. alba* during the Zanclean, it is likely younger species (depending upon their evolutionary relationship and if they are separate species) is ancestral to the older species. The most noteworthy contrast between *A. alba* and the two Miocene species is their size with *A. janus* and *A. santarosana* typically displaying a mean length of 40 ± 10 mm, whereas *A. alba* has a mean length of 60 ± 12 mm.

Lucinid Life Habits and Habitats

Lucinids are deep-infaunal bivalves that prefer soft, fine- to coarse-grained substrates with high sulfide contents (e.g., mangrove and seagrass habitats, anoxic substrates). They are generally chemosymbiotic suspension feeders, which incorporate sulfide-oxidizing endosymbiotic bacteria into their gills. The high-sulfide content of the sediments lucinids inhabit support the sulfide-oxidizing bacteria, which in turn are employed by the bivalves for food (Mikklesen and Bieler, 2008; Stanley, 2014). Lucinids are most abundant in oxygen-deficient substrates where other bivalves are uncommon. Lucinids are globally distributed and range in depth from the intertidal zone to the deep sea (Mikkelsen and Bieler, 2008). Numerous lucinid species prefer cold seeps, but they are most diverse and abundant in shallow-shelf settings, such

as seagrass beds, unvegetated sands near reefs, and mangrove habitats (Mikklesen and Bieler, 2008; Stanley, 2014).

The Holocene representatives of the genera analyzed in this study typically prefer shallow-water habits with either vegetated or unvegetated substrates. Both *Lucina pensylvanica* and *L. roquesana* typically prefer very shallow (<3 m depth), nearshore habitats with unvegetated substrates (Mikklesen and Bieler, 2008); but the latter is also known from dead specimens down to 60 m depth (Mikklesen and Bieler, 2008; Taylor and Glover, 2016). *Anodontia alba* has a similar preference for very shallow (<3 m depth), nearshore habitats, but is typically most abundant in seagrass beds (Mikklesen and Bieler, 2008; Taylor and Glover, 2016). *Lucina* and *Anodontia* both typically live less 30 cm beneath the sediment-water interface (Giere, 1985; Redfern, 2013; Taylor and Glover, 2016).

Geological Setting and Sample Localities

This study analyzed lucinid specimens from the Neogene and Quaternary records of Florida. This passive margin tectonic setting lies at the junction between the Gulf- and Atlantic coastal plains, which initiated during the break-up of the supercontinent Pangea during the mid-Mesozoic (Galloway, 2008; Miall *et al*., 2008). During the Cretaceous to Paleogene, Florida was characterized as a distinct carbonate platform, which was isolated from the North American mainland by a deep-water channel referred to as the Suwannee or Georgia Straits. Beginning at the start of the Neogene, siliciclastic sediments shed from the rejuvenated Appalachian Uplift (Gallen et al, 2013), negatively impacted carbonate production across most of the Florida Platform. These Neogene–Quaternary siliciclastic-dominated strata were deposited in various shallow, nearshore-shelf environments during sea-level highstands. As a result of sediment starvation across the Florida Platform, these siliciclastics were repeatedly reworked resulting in a

condensed stratigraphic succession. Due to dense vegetation and reduced topographic relief, these strata are only exposed in river cuts and in manmade excavations, such as construction sites or in mines.

The fossil lucinids examined in this study were collected from various sandy shell-rich localities across Florida, which usually are characterized by well-preserved aragonitic shells (Figs. 6.6 and 6.9). These shell rich units range from the mid-Miocene to Pleistocene, a temporal span of ~17 Ma. This record is quite discontinuous due to numerous inter- and intra-formational hiatuses or unconformities as well as gaps in sampling.

The oldest *Lucina* analyzed in this study are *L. glenni*, which comes from two mid-Miocene Chipola Formation (17–16.3 Ma) localities in the Florida Panhandle (Figs. 6.6 and 6.9; Huddlestun, 1983; Brown et al., in review). There is then a 11.3 Ma (16.3 to 5 Ma) break in our *Lucina* record, which stretches from the mid-Miocene Chipola Formation to the Pliocene Tamiami Formation (Fig. 6.7). This gap is primarily due to a lack samples from this interval in museum collections and poor preservation of specimens (i.e., mainly steinkerns) in the formations that span this interval in Florida (e.g., upper part of Arcadia Formation, Peace River Formation, Choctawhatchee Formation).

The Pliocene to Pleistocene record examined in this study is represented by the lucinid species *L. pensylvanica*, which has a relatively complete record for the past ~5 Ma (Figs. 6.6 and 6.9). This substantially more complete record for *L. pensylvanica* is primarily due to improved preservation of specimens and better representation in museum collections. The Pliocene to lower Pleistocene *L. pensylvanica* specimens come from one locality in the Florida Panhandle and three localities in southern Florida. Tamiami Formation specimens range from 5 to 2.2 Ma, which correlates to the Zanclean to middle Gelasian. Quaternary *L. pensylvanica* specimens were

collected from six localities in Florida that span the entire Pleistocene and range in age from 2.2 to present. Quaternary specimens came from the Caloosahatchee, Bermont, and Fort Thompson formations, which span the middle Pleistocene and range in age from 2.2 to 0.18 Ma.

Holocene *Lucina* specimens come from Florida's Gulf Coast and San Salvador, Bahamas, which is part of the Bahamian Archipelago. Holocene Florida *L. pensylvanica* examined for this study were collected from the shell-rich, sandy beaches at Honey Moon Island State Park on the Gulf Coast (Fig. 6.9). These shells were typically collected from shell-lags concentrated by the surf during low-tide or from shell concentrations concentrated higher up on the beach that formed during storms. *Lucina rosquesana* specimens were collected from Graham's Harbor on the island of San Salvador (Fig. 6.10). Specimens were found at 5 m depth in seagrass meadows formed in a carbonate skeletal sand and typically dug up from less than 10 cm below the sediment surface (Brown, pers. comm., 2017).

Neogene and Quaternary *Anodontia* specimens analyzed in this study are derived from several different formations and localities in Florida (Figs. 6.5 and 6.7). Many of the specimens co-occur in the same formations as *L. glenni and L. pensylvanica*. *Anodontia janus* specimens come only from the early middle Miocene Chipola Formation (17–16.3 Ma), whereas *Anodontia santarosana* specimens were collected from the middle Miocene Chipola, Oak Grove (16.8–15 Ma) and Shoal River formations (13.8–12.6 Ma) (Huddlestun, 1984; Brown et al., in review). This gives *A. janus* and *A. santarosana* specimens an age range of 0.7 and 4.4 Ma, respectively. The Miocene *Anodontia* specimens were derived from three localities in the Florida Panhandle (Fig. 6.11). As with *Lucina*, there is an extensive gap in the record of *Anodontia* that spans the middle Miocene to Pliocene, which is due to the issues discussed above. The record of *A. alba* in this study initiates in the Tamiami Formation (4–2.6 Ma) and spans the Pliocene to upper

Pleistocene or a time interval ranging for ~5 Ma. Most *A. alba* specimens were collected from one Pliocene Jackson Bluff Formation locality in the Florida Panhandle and 15 sites in Peninsular Florida (Fig. 6.11). Holocene *Anodontia* specimens were collected from the same shell-rich, sandy beach concentrations where the *L. pensylvanica* specimens were found in Florida (see above; Fig. 6.9).

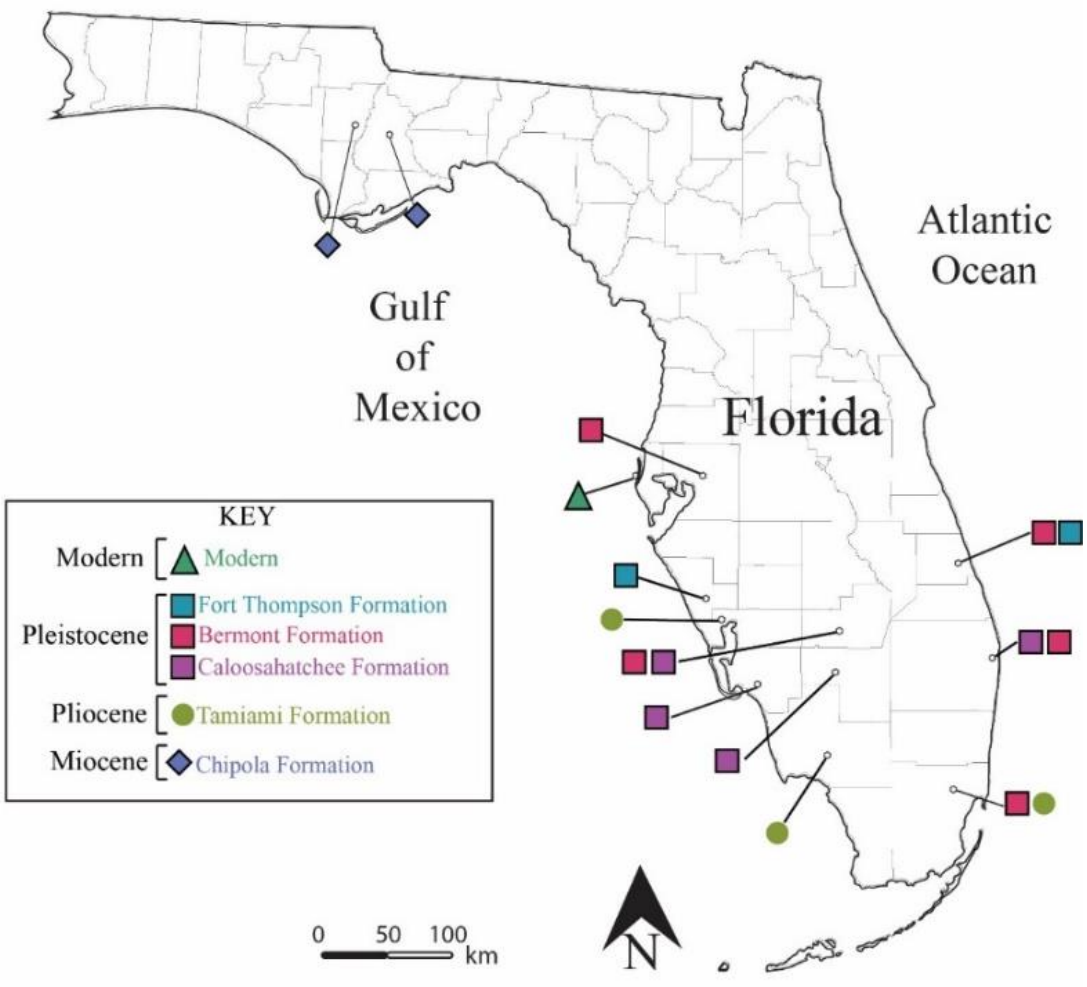

Figure 6.7. Localities for Florida Neogene and Quaternary *Lucina* specimens used in this study.

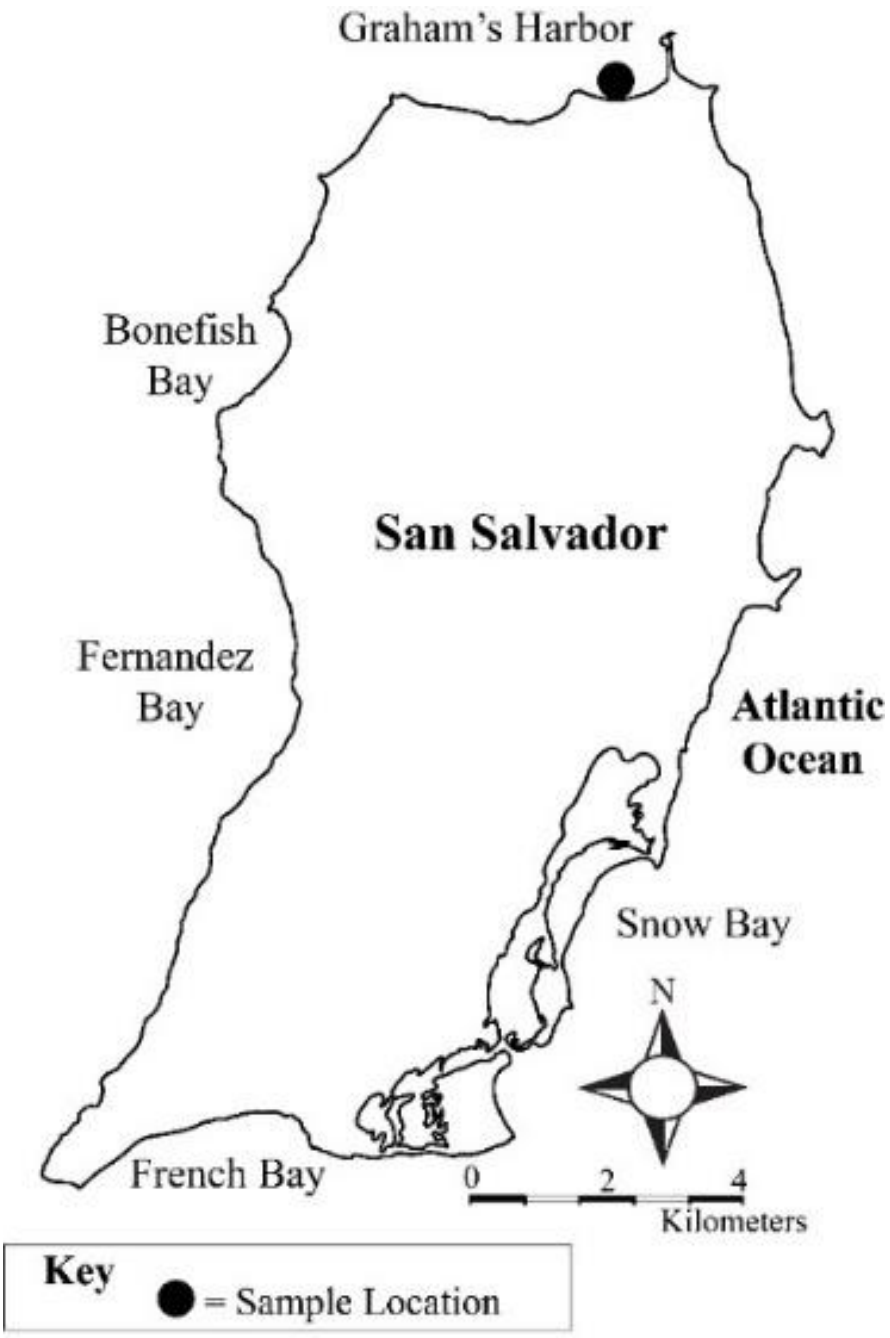

Figure 6.8. Locality for Holocene *Lucina roquesana* specimens used in this study from San Salvador, Bahamas.

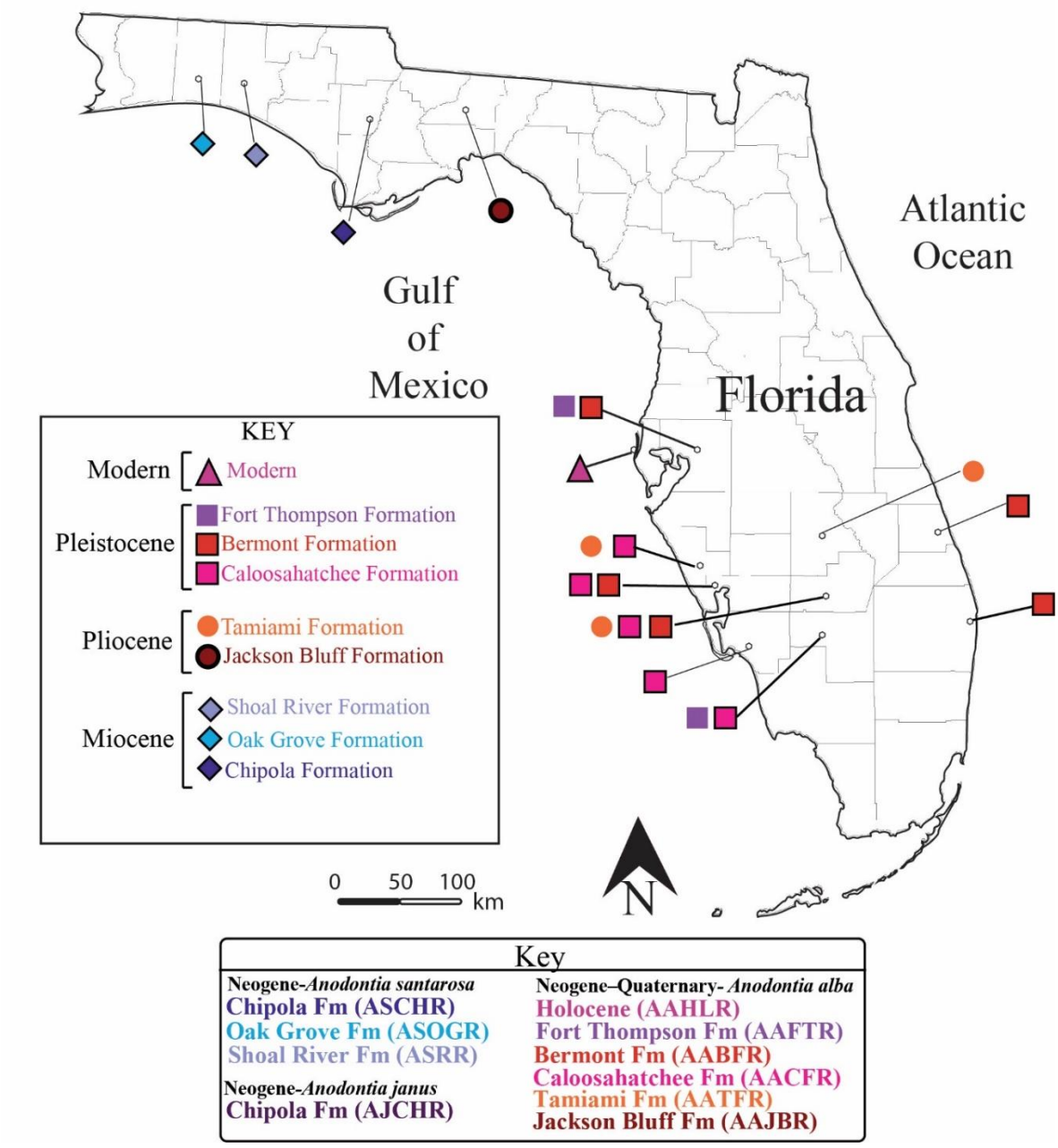

Figure 6.9. Localities for Florida Neogene and Quaternary *Anodontia* specimens used in this study.

Methods

Samples

A total of 1,430 Neogene–Quaternary specimens of *Lucina* and *Anodontia* were analyzed for this study (Table 6.1–6.3). All fossil specimens are reposited in the collections at Florida Museum of Natural History (FLMNH), whereas Holocene examples are in the author's personal research collection. Both *Lucina* and *Anodontia* were found to be well represented in the museum collection. A total of 657 left and right valves are represented by *Lucina* specimens with 140 of these being comprised of *L. glenni* valves from the Miocene and the remaining 507 specimens representing *L. pensylvanica* from the Pliocene to Holocene (Table 6.1). A total of 720 left and right valves of Neogene–Quaternary *Anodontia* specimens were analyzed for this study (Table 6.2). In terms of individual anodontid species, there are 146 *A. santarosana* valves, 131 *A. janus* valves, and 443 valves of *A. alba*.

Table 6.1. Number of *Lucina* specimens used in study along with their repositories

Species	Authority	Formation	Source	Age	Total Left Valves	Total Right Valves
Lucina roquesana	Gibbson-Smith (1982)	Holocene Beach Deposits	Personal Coll.	Holocene	35	29
Lucina pensylvinica	Linnaeus (1758)	Holocene Beach Deposits	Personal Coll.	Holocene	39	40
Lucina pensylvinica	Linnaeus (1758)	Fort Thompson Fm	FLMNH	Pleistocene	6	5
Lucina pensylvinica	Linnaeus (1758)	Bermont Fm	FLMNH	Pleistocene	43	51
Lucina pensylvinica	Linnaeus (1758)	Caloosahatchee Fm	FLMNH	Pleistocene	55	64
Lucina pensylvinica	Linnaeus (1758)	Tamiami Fm	FLMNH	Pliocene	81	69
Lucina glenni	Dall (1903)	Chipola Fm	FLMNH	Miocene	69	71
				Total:	328	329

Table 6.2. Number of *Anodontia* specimens used in study along with their repositories.

Species	Authority	Formation	Source	Age	Total Left Valves	Total Right Valves
Anodontia alba	Link (1807)	Modern	Personal Coll.	Holocene	69	71
Anodontia alba	Link (1807)	Fort Thompson	FLMNH	Pleistocene	17	15
Anodontia alba	Link (1807)	Bermont	FLMNH	Pleistocene	49	45
Anodontia alba	Link (1807)	Caloosahatchee	FLMNH	Pleistocene	107	100
Anodontia alba	Link (1807)	Jackson Bluff	FLMNH	Pliocene	15	13
Anodontia alba	Link (1807)	Bermont	FLMNH	Pliocene	10	18
Anodontia janus	Dall (1903)	Tamiami.	FLMNH	Miocene	73	58
Anodontia santarosana	Dall (1903)	Chipola	FLMNH	Miocene	50	41
Anodontia santarosana	Dall (1903)	Shole River	FLMNH	Miocene	12	5
Anodontia santarosana	Dall (1903)	Oak Grove	FLMNH	Miocene	17	21
				Total:	333	387

Morphometric and Quantitative Analysis

See Chapter Four for a description of the morphometric and statistical methodologies used.

Results

Allometric Relationships: *Lucina* and *Anodontia*

There is no correlation between size and shape (i.e., allometry) for the Neogene and Quaternary *Lucina* and *Anodontia*. For example, the trend between the relative warp scores (i.e., a measure of shape) and centroid sizes (i.e., a measure of size) for left and right valves of *L. glenni*, *L. pensylvanica*, and *L. roquesana* all have low R^2 values (see Figs. 6.12 and 6.13). The trend between the relative warp scores and centroid sizes for the different species of *Anodontia* for both left and right valves also have low R^2 values (see Figs. 6.14 and 6.15).

Size Change: *Lucina*

Both the right and left valves of the *L. glenni–L. pensylvanica* lineage show a 59% increase in size (see Chapter Four for methods) from the middle Miocene to middle Pleistocene and then an 11% decrease into the Holocene (Fig. 6.16; Table 6.4; also see Appendix C, Table C1). In comparison to this lineage, Holocene *L. roquesana* from the Bahamas are substantially smaller and are less variable in size. The geometric mean of size for Miocene Chipola *L. glenni* is 25.4 mm ± 3.6 and 25.1 mm ± 3.9 for left and right valves, respectively, whereas Pliocene Tamiami *L. pensylvanica* specimens have means of 32.7 mm ± 5.6 and 34.5 mm ± 6.2 for left and right valves, respectively and middle Pleistocene Bermont specimens are 40.2 mm ± 5.9 and 39.7 mm ± 3.5 for left and right valves, respectively. There is a decrease in the geometric mean of size to 33.5 mm ± 4.7 and 29.6 mm ± 6.4 for left and right valves, respectively, in the upper Pleistocene Fort Thompson specimens followed by a slight increase in Holocene specimens to 35.3 mm ± 3.7 and 35.4 mm ± 9.3 for left and right valves, respectively. Both Fort Thompson and Holocene *L. pensylvanica* valves have similar sizes to the Pliocene Tamiami specimens. Variation in the geometric mean of size is relatively stable throughout the Miocene to Holocene, however, the right valves of Fort Thompson *L. pensylvanica* are slightly more variable as compared to the left valves. The geometric mean of size for *L. roquesana* is 7.7 mm ± 3.1 and 7.2 mm ± 4.9 for left and right valves, respectively.

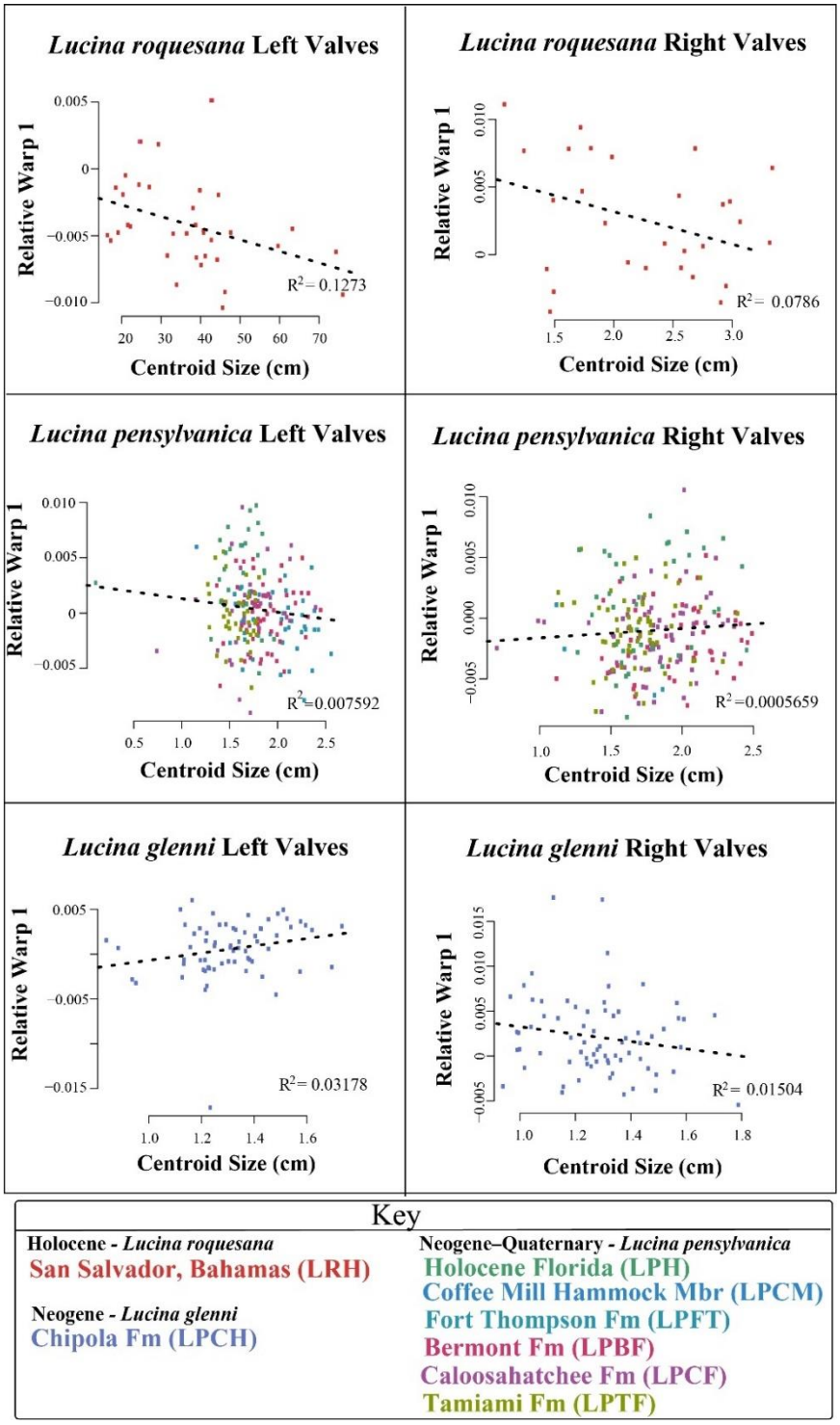

Figure 6.10. Allometric test for left and right valves of the different *Lucina* species from the Neogene–Quaternary.

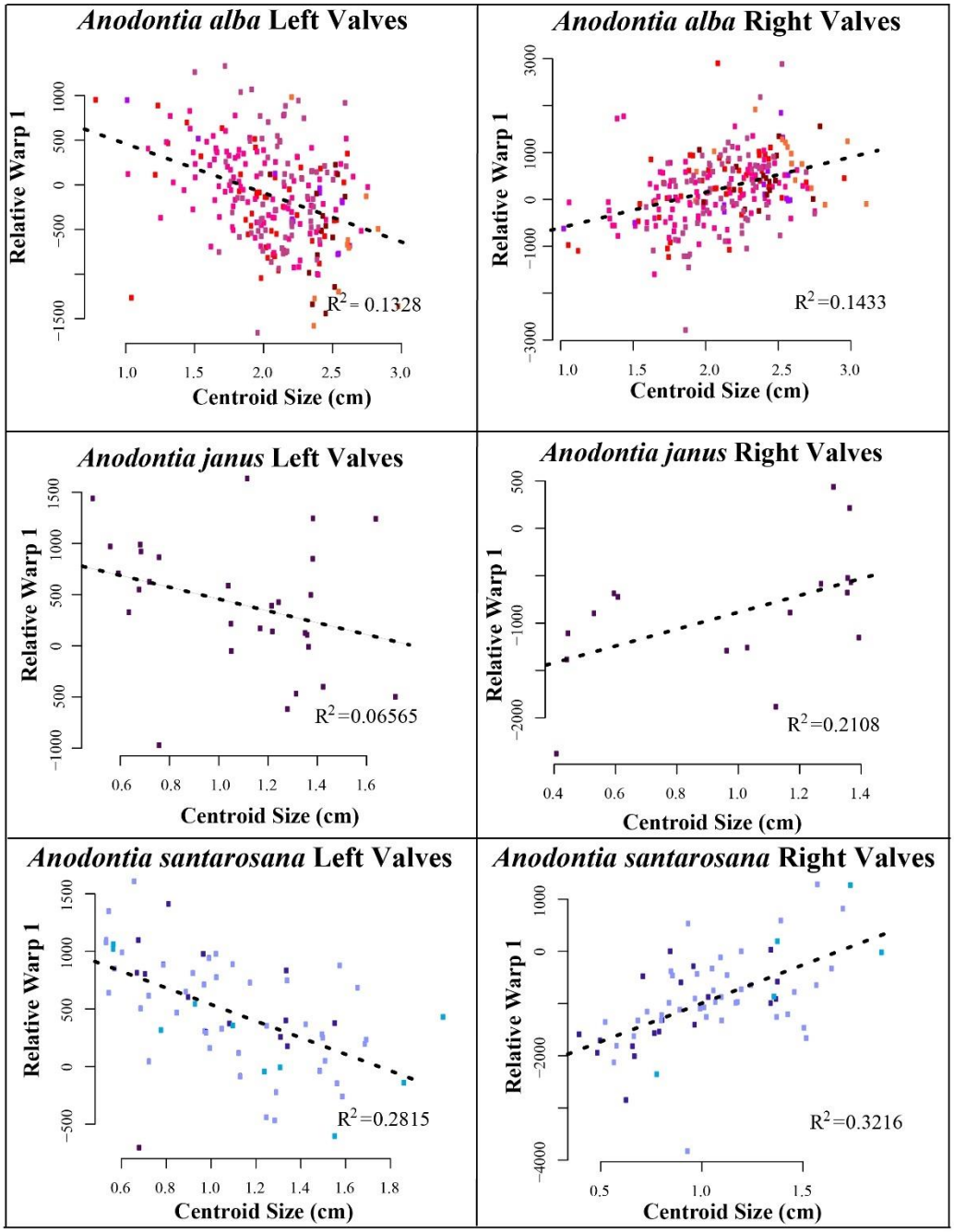

Key			
Neogene-*Anodontia santarosana*	Neogene-*Anodontia janus*	Neogene–Quaternary- *Anodontia alba*	
Shoal River Fm (ASR)	Chipola Fm (AJCH)	Caloosahatchee Fm (AACF)	Holocene (AAHL)
Oak Grove Fm (ASOG)		Tamiami Fm (AATF)	Fort Thompson Fm (AAFT)
Chipola Fm (ASCH)		Jackson Bluff Fm (AAJB)	Bermont Fm (AABF)

Figure 6.11. Allometric test for left and right valves of the the different *Anodontia* species from the Neogene–Quaternary.

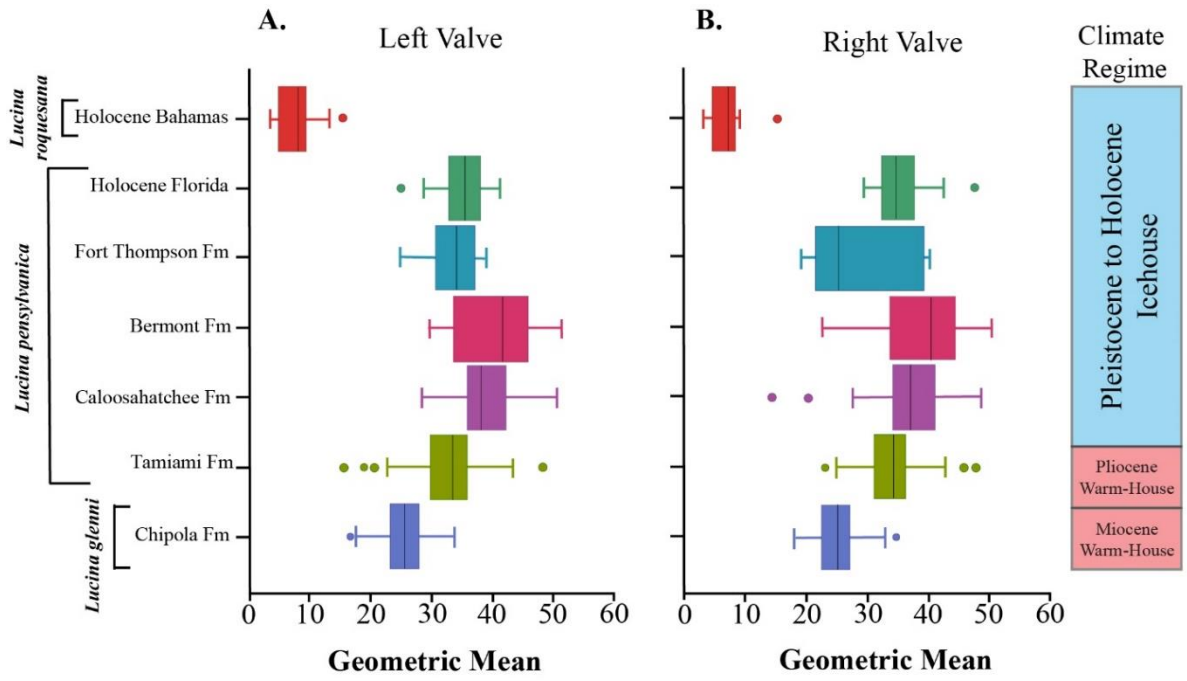

Figure 6.12. Size of the Neogene–Quaternary *Lucina* left (A) and right (B) valves from Florida and the Bahamas.

The Mann-Whitney U test of the geometric means of size for both left and right valves of Lucina from the Neogene–Quaternary supports an overall increase in size from the middle Miocene to middle Pleistocene and then a decrease into the Holocene (Table 6.5). The data also support a statistically significant size difference for *L. roquesana* and the *L. glenni–L. pensylvanica* lineages. For example, a statistical comparison among the geometric means of size values for the right and left valves of the middle Miocene to middle Pleistocene *L. glenni* and *L. pensylvanica* populations display a statistically significant difference in size. In contrast, the geometric means of size for the Fort Thompson and Holocene left and right valve as well as Bermont and Caloosahatchee left valves are not statistically different in size. Furthermore, *L. roquesana* and the *L. glenni–pensylvanica* samples are also statistically different in size.

Table 6.3. Summary parameters for geometric means of right and left *Lucina* valves shown in Figure 6.12.

Right Valves									
Formation	**Species**	**Min**	**Quartile 1**	**Median**	**Mean**	**Quartile 3**	**Max**	**Standard Deviation**	**Total # of Valves**
Holocene	*Lucina roquesana*	3.37621978	5.081506273	7.497031346	7.20929819	8.54749332	15.47671254	4.87341532	29
Holocene	*Lucina pensylvanica*	29.47895414	32.47274057	34.70410676	35.448199	37.6567222	47.70797166	9.315623691	40
Fort Thompson	*Lucina pensylvinica*	19.28094982	24.27855498	25.43747776	29.5770602	38.674776	40.21354254	6.373350958	5
Bermont	*Lucina pensylvanica*	22.92380222	34.0685023	40.39134867	39.6972053	44.1585864	50.25926183	3.53390622	51
Caloosahatchee	*Lucina pensylvanica*	14.64386015	34.45064012	37.16304794	37.2369438	41.20268	48.55460728	2.906270192	64
Tamiami	*Lucina pensylvanica*	23.05293842	31.72120631	34.38553585	34.4871251	36.2332429	47.84366861	6.182243714	69
Chipola	*Lucina glenni*	18.31509279	22.75065128	25.25542007	25.1114178	26.9918512	34.78677181	3.904018919	71

Left Valves									
Formation	**Species**	**Min**	**Quartile 1**	**Median**	**Mean**	**Quartile 3**	**Max**	**Standard Deviation**	**Total # of Valves**
Holocene	*Lucina roquesana*	3.434591096	5.103689915	8.031691976	7.71137925	9.00551999	15.50338963	3.072017798	35
Holocene	*Lucina pensylvanica*	24.94359122	33.16212597	35.57239189	35.3037579	37.7986692	41.11850189	3.722901323	39
Fort Thompson	*Lucina pensylvanica*	24.87476203	32.90677952	34.09471907	33.4646665	35.7905429	38.85718132	4.739646687	6
Bermont	*Lucina pensylvanica*	29.71099924	33.77147882	41.48583614	40.2015	45.2560947	51.14861769	5.939693159	43
Caloosahatchee	*Lucina pensylvanica*	28.20683091	35.91596969	38.0190022	38.909066	41.6373624	50.40267283	4.975638882	55
Tamiami	*Lucina pensylvanica*	15.54963871	29.94986175	33.44648831	32.7283367	35.4374146	48.05438508	5.555990118	81
Chipola	*Lucina glenni*	16.52373671	23.53136906	25.41418126	25.377006	27.6218619	33.57601875	3.586374145	69

Table 6.4. Summary statistics for size measurements of right (top) and left (bottom) *Lucina pensylvanica* and *L. roquesana*. valves. Yellow boxes indicate statistically significant differences when compared with opposite samples, whereas gray boxes indicate a lack of statistically significant differences.

Size Right Valves (P-Values)							
Species	**Species**	*Lucina pensylvanica*		*Lucina glenni*	*Lucina pensylvanica*		
	Formation	Bermont	Caloosahatchee	Chipola	Fort Thompson	Modern	Tamiami
Lucina roquesana	Holocene	1.40E-13	1.65E-14	5.43E-15	4.63E-04	4.36E-12	7.08E-15
Lucina pensylvanica	Bermont		4.42E-02	5.23E-19	1.71E-02	7.44E-04	9.54E-06
	Caloosahatchee			2.75E-19	1.08E-01	1.80E-02	2.81E-04
Lucina glenni	Chipola				5.43E-01	2.49E-16	1.39E-19
Lucina pensylvanica	Fort Thompson					2.60E-01	2.91E-01
Lucina pensylvanica	Holocene						3.20E-01

Size Left Valves (P-Values)							
Species	**Species**	*Lucina pensylvanica*		*Lucina glenni*	*Lucina pensylvanica*		
	Formation	Bermont	Caloosahatchee	Chipola	Fort Thompson	Modern	Tamiami
Lucina roquesana	Modern	1.01E-16	1.69E-15	1.01E-16	1.16E-04	1.54E-13	1.56E-17
Lucina pensylvanica	Bermont		3.03E-01	1.98E-18	3.15E-02	3.76E-04	5.05E-08
	Caloosahatchee			8.36E-21	1.82E-02	6.20E-04	3.72E-10
Lucina glenni	Chipola				1.07E-03	7.68E-16	4.43E-16
Lucina pensylvanica	Fort Thompson					3.41E-01	5.86E-01
Lucina pensylvanica	Modern						3.32E-03

Shape Change: *Lucina*

Eighty percent ellipses surrounding the mean PCA scores for both left and right valves of *Lucina* (Fig. 6.13) reveal clear shape similarities in variance among Neogene and Quaternary specimens. PCA axis 1 for both left and right valves of Neogene and Quaternary *Lucina* explains 46.1% and 28.4% of the observed shape variation, respectively, whereas, PCA axis 2 for both left and right valves explains 17.7% and 22.7% of the observed shape variation, respectively. PCA axis 3 for both left and right valves explain 12.5% and 17.7% of the observed shape variation, respectively. For example, Miocene *L. glenni* and all Pliocene to Pleistocene *L. pensylvanica* 80% ellipses overlap along both PCA Axes 1 to 3. The left valves of Holocene *L. pensylvanica* form a distinct group on PCA axis 2 and 3 and are longer as well as shorter than other specimens. In contrast, the right valves of Holocene *L. pensylvanica* overlap completely with Miocene specimens and partially with Pliocene to Pleistocene examples along PCA axis 2 and 3. Also, based on the size of the ellipses, both the right and left valves of Pleistocene Coffee Mill Hammock specimens show greater variance as compared to the other Neogene and Quaternary specimens along PCA axis 1 and 2. The only exception to the general pattern are the right and left valves of Holocene *L. roquesana,* which form distinct shape fields along PCA axis 1 to 3 from all *L. pensylvanica*.

Statistical analysis of the PCA axes 1 to 3 scores suggest some variance in the degree of outline shape similarities for Miocene to Pleistocene *Lucina* specimens and support for all Holocene examples forming distinct shape groupings (Table 6.6). Miocene to Pleistocene *Lucina* left valve specimens lack statistically significant differences with the exception of the association between Bermont as compared to Coffee Mill Hammock, Caloosahatchee, Tamiami, and Chipola specimens. Similarly, Miocene to Pleistocene Lucina right valves lack statistically significant

differences with exception of the association between Chipola as compared to Bermont, Caloosahatchee, and Tamiami. Holocene L. *pensylvanica* and *L. roquesana* specimens are also statistically different from all other samples. The only exceptions to this pattern are the lack of statistically significant differences between the right valves of Holocene *L. pensylvanica* with that of Coffee Mill Hammock and Fort Thompson specimens as well as with *L. glenni* specimens from the Chipola.

Eighty percent ellipses around mean CVA scores for both right and left valves of *Lucina* (Fig. 6.14) show substantial overlap along axes 1 to 3, which indicates similarities in outline shape among different Pliocene–Pleistocene populations, with Miocene and Holocene specimens plotting as distinct fields. For example, the left valves of Miocene *L. glenni* and all Pliocene to Pleistocene *L. pensylvanica* specimen 80% ellipses overlap along both CVA axes 1 to 3. Right valves along axes 1 to 3 show a virtually identical pattern; however, *L. glenni* specimens have lower CVA axes 2 and 3 scores compared to the others. The left and right valves of Holocene *L. pensylvanica* form distinct fields along CVA axes 1 to 3 values compared to other *L. pensylvanica*. Also, the right valves of Holocene *L. pensylvanica* overlap with the right valves of Miocene *L. glenni* along CVA 2. As with the PCA, both right and left valves of Pleistocene Fort Thompson Formation and Coffee Mill Hammock Member specimens show greater variance in the 80% ellipses along CVA axis 2 as compared to the other Neogene–Quaternary specimens. Both right and left valves of *L. roquesana* specimens form a distinct field from the *L. glenni–L. pensylvanica* specimens along CVA axis 1 and 2.

Statistical analysis of the CVA axes 1 to 3 scores for Neogene–Quaternary *Lucina* specimens suggest that these populations significantly differ in outline shape (Table 6.7). For

example, most Miocene to Holocene CVA scores are statistically different from populations from other formations. The only exception to this pattern is the association among Coffee Mill

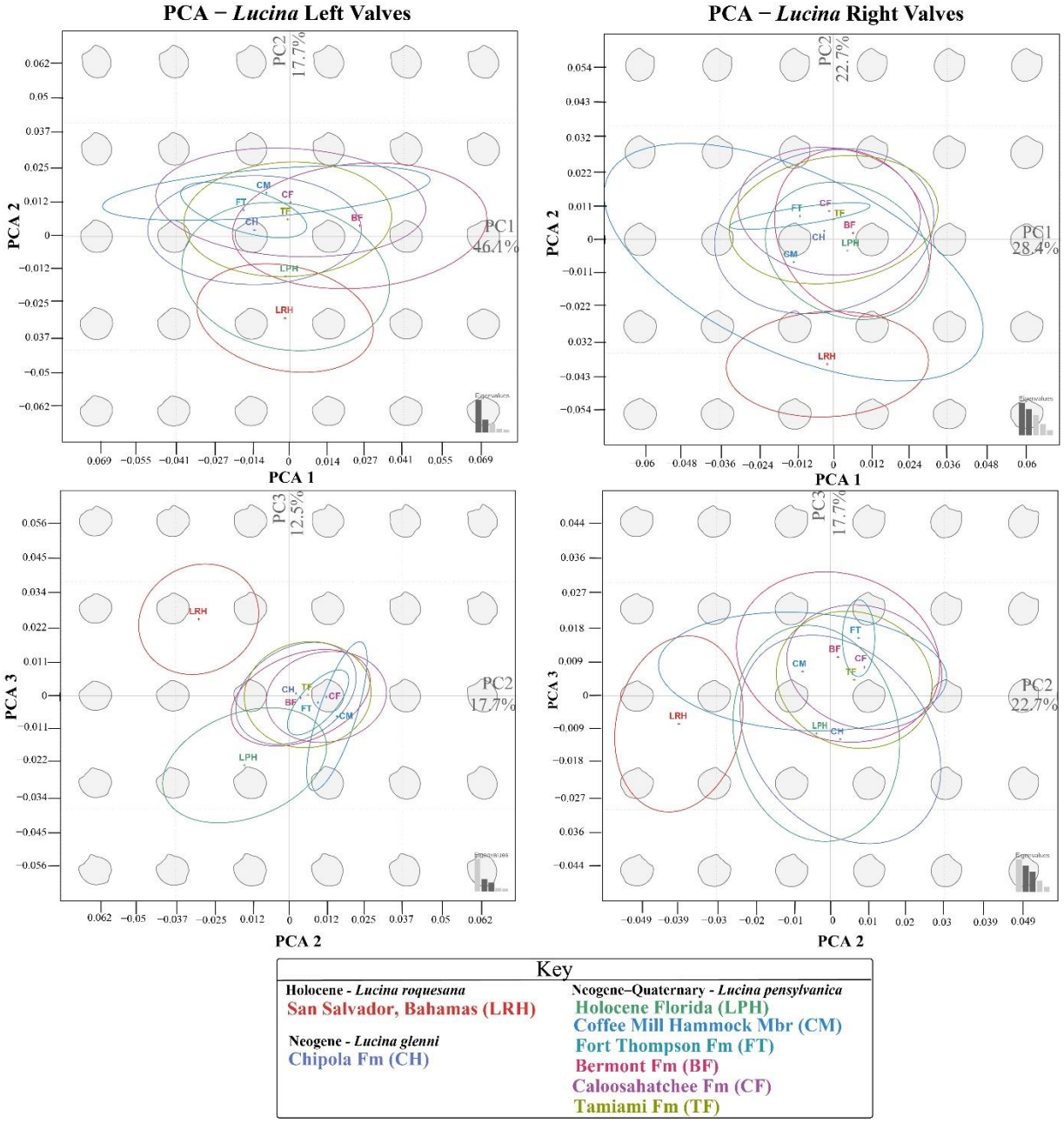

Figure 6.13. PCA axis 1 to 3 scores for Neogene–Quaternary *Lucina* right (A) and left (B) valves. Backtransform shapes (gray) in background show *Lucina* outline shape variation in morphospace. Ellipses represent 80% confidence intervals around mean PCA scores.

Table 6.5. Summary statistics for PCA axes 1 to 3 scores of left (top) and right (bottom) *Lucina* valves. Yellow boxes indicate statistically significant differences when compared with opposite samples, whereas gray boxes indicate a lack of statistically significant differences.

PCA RightValve								
Species		*Lucina pensylvanica*						*Lucina glenni*
	Formation	Holocene	Coffee Mill	Fort Thompson	Bermont	Caloosahatchee	Tamiami	Chipola
Lucina roquesana	Bahama Holocene	6.48E-12	1.06E-03	1.91E-06	6.77E-15	5.31E-24	2.34E-22	4.41E-15
Lucina pensylvanica	Holocene		1.27E-01	6.18E-02	4.55E-05	3.55E-08	1.08E-05	1.65E-01
	Coffee Mill			3.94E-01	8.92E-02	5.55E-02	1.70E-01	1.87E-01
	Fort Thompson				3.68E-01	4.46E-01	2.36E-01	6.79E-02
	Bermont					8.51E-02	1.11E-01	7.48E-09
	Caloosahatchee						2.79E-01	1.82E-09
	Tamiami							4.12E-06
PCA Left Valve								
Species		*Lucina pensylvanica*						*Lucina glenni*
	Formation	Holocene	Coffee Mill	Fort Thompson	Bermont	Caloosahatchee	Tamiami	Chipola
Lucina roquesana	Bahama Holocene	7.32E-23	1.53E-08	3.81E-06	2.87E-21	3.69E-26	4.02E-25	5.89E-25
Lucina pensylvanica	Holocene		1.79E-02	2.57E-02	7.36E-11	7.07E-14	3.44E-14	9.95E-13
	Coffee Mill				3.34E-02	6.41E-01	3.47E-01	7.53E-02
	Fort Thompson				9.86E-02	7.91E-01	6.87E-01	6.87E-01
	Bermont					1.10E-03	4.07E-04	9.60E-07
	Caloosahatchee						1.83E-01	4.69E-04
	Tamiami							5.45E-02

Hammock and Fort Thompson specimens with each other and with populations from the Tamiami, Caloosahatchee, and Bermont formations. There is also a lack of statistically significant differences among Caloosahatchee and Bermont L. pensylvanica right valves.

Size Change: *Anodontia*

Both the right and left valves of the Miocene *Anodontia* are relatively smaller than the Pliocene to Holocene *A. alba* specimens (Fig. 6.15; Table 6.8; also see Appendix C, Table C2). For example, the geometric mean of size for both Miocene *Anodontia* species is ~22.0 mm, which changes little among samples from different formations. Chipola Formation *Anodontia janus* specimens have a mean size of 20.9 mm ± 6.4 and 20.1 mm ± 6.4 for left and right valves, respectively. In contrast, *A. santarosana* specimens in the Chipola Formation have a mean size of 20.9 mm ± 7.1 and 19.0 mm ± 7.1 for left and right valves, respectively, which then increases to 23.4 mm ± 8.7 and 28.3 mm ± 8.4 for left and right valves, respectively, in the Oak Grove and then declines in the Shoal River to 21.4 mm ± 6.6 and 21.3 mm ± 6.0 for left and right valves, respectively. In contrast, Pliocene to Holocene *A. alba* right and left valves have a mean size ~41.0 mm. Specimens from the Fort Thompson are the only exception to this pattern with a mean size 48.0 mm ± 11.7 and 50.4 mm ± 9.8 for left and right valves, respectively. The Mann-Whitney U test of the geometric means of size for both left and right valves of *Anodontia* supports a lack of size change in Miocene specimens and a somewhat greater variance in size for Pliocene to Holocene specimens (Table 6.9). The geometric means of size values for right and left valves of Miocene *Anodontia* indicate that these samples are not statistically different in size. When Miocene *Anodontia* specimens are compared against Pliocene to Holocene *A. alba*, these associations are statistically different in size. Statistical results suggest that Pliocene to Holocene *A. alba* samples vary in mean size values through this interval. However, Pliocene Tamiami and

Jackson Bluff *A. alba* lack statistically significant differences with specimens from each other and with populations from the Caloosahatchee, Bermont, and Holocene, which indicates similar sizes.

Shape Change: *Anodontia*

The 80% ellipses around PCA mean scores for both the right and left valves of *Anodontia* (Fig. 6.16) show substantial overlap with Neogene samples displaying greater variance in plotting position of mean scores than Quaternary examples, which plot more closely. PCA axis 1 scores for both left and right valves of Neogene–Quaternary *Anodontia* explains 40.4% and 53.5% of the observed shape variation, respectively, whereas, PCA axis 2 for both left and right valves explains 17.0% and 12.8% of the observed shape variation, respectively. PCA axis 3 for both left and right valves explain 10.2 and 7.8% of the observed shape variation, respectively. The left valves of *Anodontia* along PCA axis 1 all overlap but show a loose temporal progression (i.e., Miocene to Holocene samples) from high to low scores along PCA axis 2. The right valves for *Anodontia* also form a weak temporal progression along PCA axis 1 with Miocene samples having higher scores, Pliocene samples having lower scores, and Quaternary samples plotting compactly between the Miocene and Pliocene samples. Along PCA axis 2 there is also a loose temporal progression with Miocene samples having lower scores and all Pliocene to Holocene samples displaying higher scores. Along PCA axes 2 and 3 left and right valves have similar patterns with 80% ellipses for *Anodontia* splitting into both a Miocene cluster and a Pliocene to Holocene cluster. Right valve 80% ellipses are more tightly clustered compared to the left valves which show a greater variance. The outline shapes for Miocene species show the greatest variability and have shorter lengths as well as reduced heights relative to *A. alba.* All Pliocene to Holocene *A. alba* have similar shapes with mid-range PCA axis 1 to 3 score.

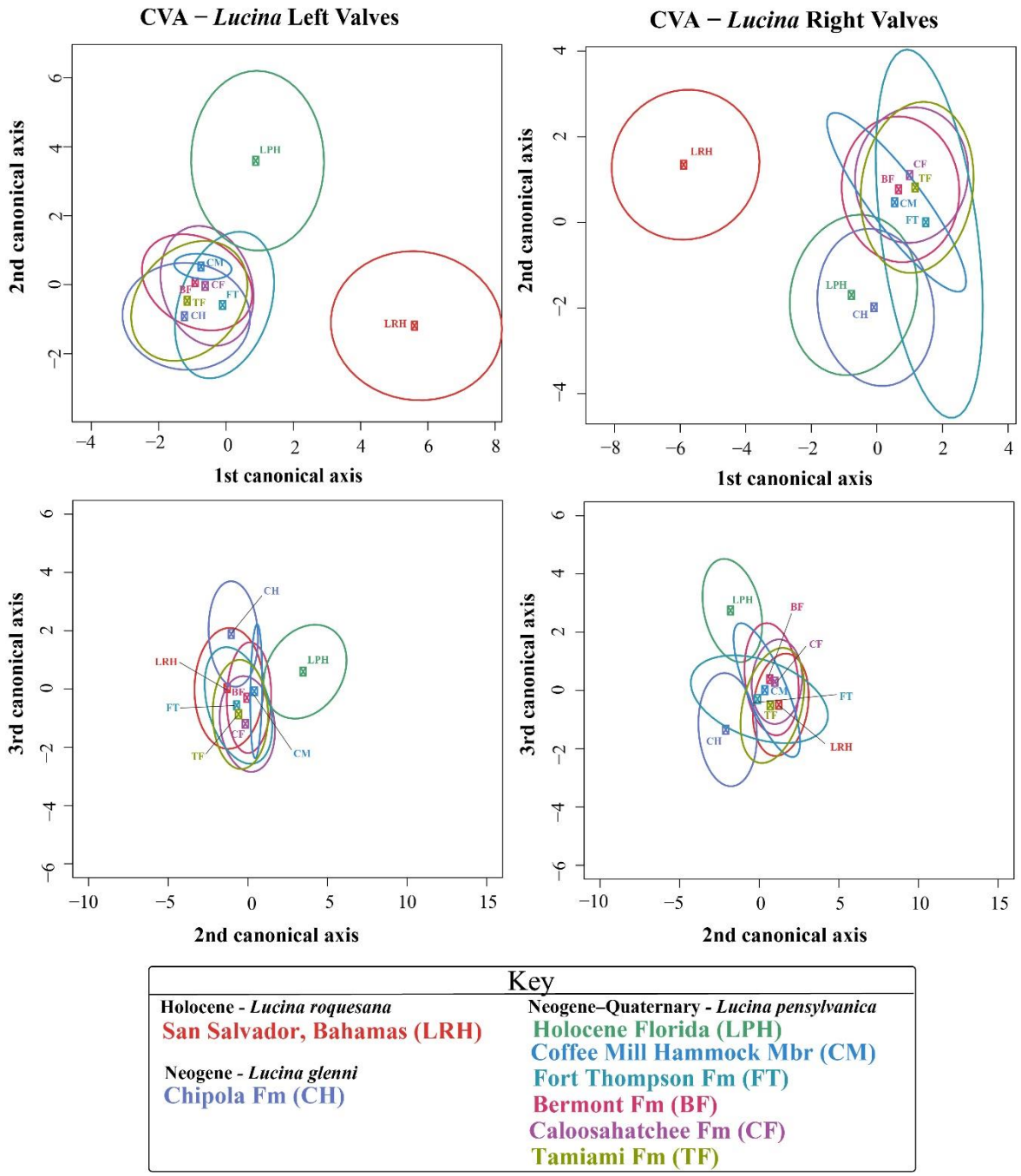

Figure 6.14. CVA axis 1 to 3 scores for Neogene–Quaternary *Lucina* left and right valves from Florida and the Bahamas. Ellipses represent 80% confidence intervals around mean CVA scores.

Table 6.6. Summary statistics for CVA axes 1 to 3 scores of left (top) and right (bottom) *Lucina* valves. Yellow boxes indicate statistically significant differences when compared with opposite samples, whereas gray boxes indicate a lack of statistically significant differences.

CVA Left Valve								
Species		*Lucina pensylvanica*						*Lucina glenni*
	Formation	Holocene	Coffee Mill	Fort Thompson	Bermont	Caloosahatchee	Tamiami	Chipola
Lucina roquesana	Bahama Holocene	4.25451E-31	6.64599E-11	2.45948E-08	9.92123E-37	3.34126E-43	4.29424E-53	4.18571E-46
Lucina pensylvanica	Holocene		2.61755E-05	1.40555E-05	3.9111E-26	1.55824E-30	8.75864E-37	1.07186E-40
	Coffee Mill			0.1059686	0.500355042	0.03366232	0.052913577	2.36903E-05
	Fort Thompson				0.209607388	0.25509871	0.162006641	0.000138174
	Bermont					8.77214E-05	0.000558725	1.56126E-20
	Caloosahatchee						0.000219585	4.34567E-33
	Tamiami							7.93775E-32

CVA Right Valve								
Species		*Lucina pensylvanica*						*Lucina glenni*
	Formation	Holocene	Coffee Mill	Fort Thompson	Bermont	Caloosahatchee	Tamiami	Chipola
Lucina roquesana	Bahama Holocene	9.62E-33	3.57E-12	7.14E-11	8.26E-37	8.33E-46	6.79E-47	1.21E-45
Lucina pensylvanica	Holocene		7.93E-09	1.23E-07	2.01E-24	1.35E-35	1.72E-37	2.70E-36
	Coffee Mill			2.74E-01	5.90E-01	1.52E-01	1.66E-01	1.61E-09
	Fort Thompson				1.03E-01	5.93E-02	3.60E-01	1.04E-05
	Bermont					7.71E-02	3.31E-05	1.02E-35
	Caloosahatchee						6.71E-05	5.64E-45
	Tamiami							1.37E-33

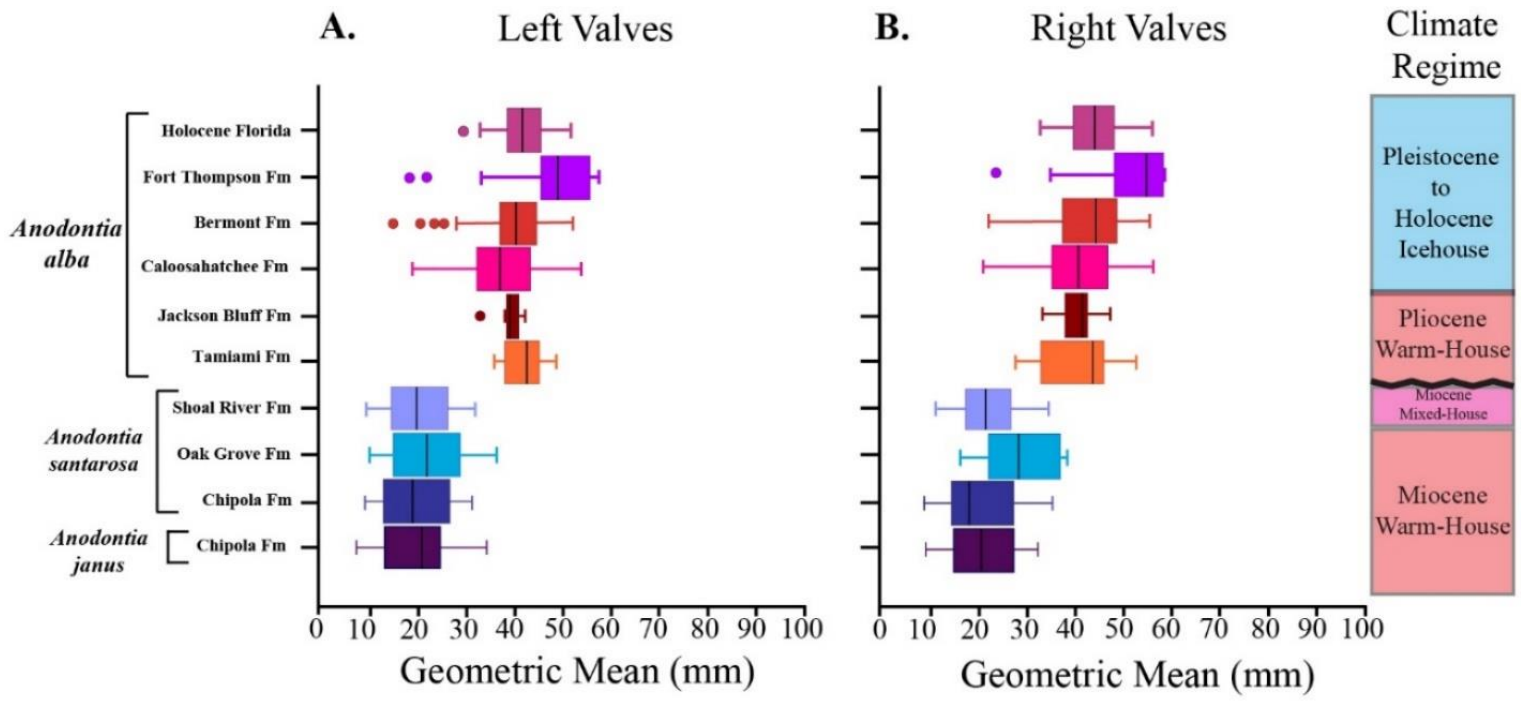

Figure 6.15. Size of the Neogene–Quaternary *Anodontia* for left (A) and right (B) valves.

Table 6.7. Summary parameters for geometric means of right and left *Anodontia* valves shown in Figure 6.15.

Right Valves									
Formation	**Species**	**Min**	**Quartile 1**	**Median**	**Mean**	**Quartile 3**	**Max**	**Standard Deviation**	**Total # of Valves**
Holocene	*Anodontia alba*	31.785166	38.533622	42.96368	42.758041	46.59214	54.80813	5.247506768	71
Fort Thompson	*Anodontia alba*	22.782579	48.842988	53.576207	50.449022	56.54501	57.376889	9.775602829	15
Bermont	*Anodontia alba*	21.479553	37.0717	43.166398	41.589442	47.210422	54.270032	7.099737389	45
Caloosahatchee	*Anodontia alba*	20.072211	34.494336	39.39615	39.510751	45.684131	54.72042	7.531755173	100
Jackson Bluff	*Anodontia alba*	32.503389	37.625481	40.439523	39.705934	41.138004	46.299494	3.343182608	13
Tamiami	*Anodontia alba*	26.74598	32.66406	42.638782	39.689196	44.211523	51.568632	7.828707752	18
Shoal River	*Anodontia santarosa*	10.610352	16.831641	20.785086	21.284077	24.329401	33.510031	6.012872746	41
Oak Grove	*Anodontia santarosa*	15.595137	26.970482	27.384673	28.340457	34.426072	37.325924	8.411403677	5
Chipola	*Anodontia santarosa*	8.244655	13.752816	17.455087	19.006047	25.419906	34.302826	7.076214504	21
Chipola	*Anodontia janus*	8.4796521	14.387993	19.806025	20.076484	25.885937	31.402582	6.434773891	58

Left Valves									
Formation	**Species**	**Min**	**Quartile 1**	**Median**	**Mean**	**Quartile 3**	**Max**	**Standard Deviation**	**Total # of Valves**
Holocene	*Anodontia alba*	30.308632	39.813039	42.707899	42.677002	45.840585	52.594079	4.571213437	69
Fort Thompson	*Anodontia alba*	19.516895	46.89692	50.037524	48.008917	56.309855	58.443741	11.71228625	17
Bermont	*Anodontia alba*	16.017213	38.395972	41.502508	40.527983	45.414673	53.009986	7.922287271	49
Caloosahatchee	*Anodontia alba*	20.028012	33.666512	38.0838	38.346571	44.198912	54.783659	7.596350426	107
Jackson Bluff	*Anodontia alba*	34.256241	39.536584	40.611076	40.484269	41.822954	43.250361	2.153182857	15
Tamiami	*Anodontia alba*	37.079885	40.143132	43.454547	43.094993	45.00041	49.688531	3.817379189	10
Shoal River	*Anodontia santarosa*	10.530645	16.182336	21.091273	21.441975	26.223949	33.050201	6.641654594	50
Oak Grove	*Anodontia santarosa*	11.180677	17.719705	23.069399	23.365295	27.755187	37.340394	8.705115913	12
Chipola	*Anodontia santarosa*	10.01126	14.378164	19.91296	20.864505	27.282237	32.25338	7.080940808	17
Chipola	*Anodontia janus*	8.3032524	14.878989	22.070427	20.882432	25.625644	35.302596	6.432582901	73

Table 6.8. Summary statistics for size measurements of right (top) and left (bottom) *Anodontia* valves. Yellow boxes indicate statistically significant differences when compared with opposite samples, whereas gray boxes indicate a lack of statistically significant differences.

Size Right Valves (P-Values)										
Species	**Species**	*Anodontia alba*					*Anodontia janus*	*Anodontia santarosa*		
	Formation	Caloosahatchee	Fort Thompson	Holocene	Jackson Bluff	Tamiami	Chipola	Chipola	Oak Grove	Shoal River
Anodontia alba	Bermont	8.54E-02	1.14E-04	6.46E-01	5.84E-02	3.90E-01	6.96E-17	3.44E-10	3.61E-03	1.98E-14
	Caloosahatchee		1.18E-05	4.76E-03	8.94E-01	9.25E-01	2.60E-23	1.27E-11	1.08E-02	3.43E-18
	Fort Thompson			6.80E-05	1.32E-04	4.85E-04	1.78E-08	1.49E-06	3.74E-03	6.57E-08
	Modern				1.35E-02	2.26E-01	1.91E-22	5.10E-12	5.90E-04	1.99E-18
	Jackson Bluff					3.93E-01	2.93E-12	1.96E-08	2.71E-03	5.30E-11
	Tamiami						3.74E-09	1.18E-06	3.03E-02	3.03E-08
Anodontia janus	Chipola							4.74E-01	4.07E-02	4.20E-01
Anodontia santarosa	Chipola								5.74E-02	1.26E-01
	Oak Grove									9.03E-02
	Shoal River									

Size Left Valves (P-Values)										
Species	**Species**	*Anodontia alba*					*Anodontia janus*	*Anodontia santarosa*		
	Formation	Caloosahatchee	Fort Thompson	Holoncene	Jackson Bluff	Tamiami	Chipola	Chipola	Oak Grove	Shoal River
Anodontia alba	Bermont	3.28E-02	4.33E-04	2.40E-01	4.37E-01	3.58E-01	1.78E-17	3.83E-08	3.89E-06	8.64E-15
	Caloosahatchee		5.53E-05	3.72E-05	1.82E-01	3.57E-02	7.19E-26	1.57E-09	8.50E-06	3.60E-09
	Fort Thompson			3.05E-04	1.96E-03	1.71E-02	2.76E-08	1.04E-05	1.53E-04	7.38E-08
	Modern				3.98E-02	8.54E-01	1.10E-24	2.41E-10	1.36E-07	2.20E-20
	Jackson Bluff					7.14E-02	1.37E-09	1.62E-06	1.96E-05	5.51E-09
	Tamiami						3.41E-07	2.21E-05	1.15E-04	7.46E-07
Anodontia janus	Chipola							9.67E-01	4.42E-01	7.59E-01
Anodontia santarosa	Chipola								5.50E-01	6.92E-01
	Oak Grove									5.04E-01
	Shoal River									

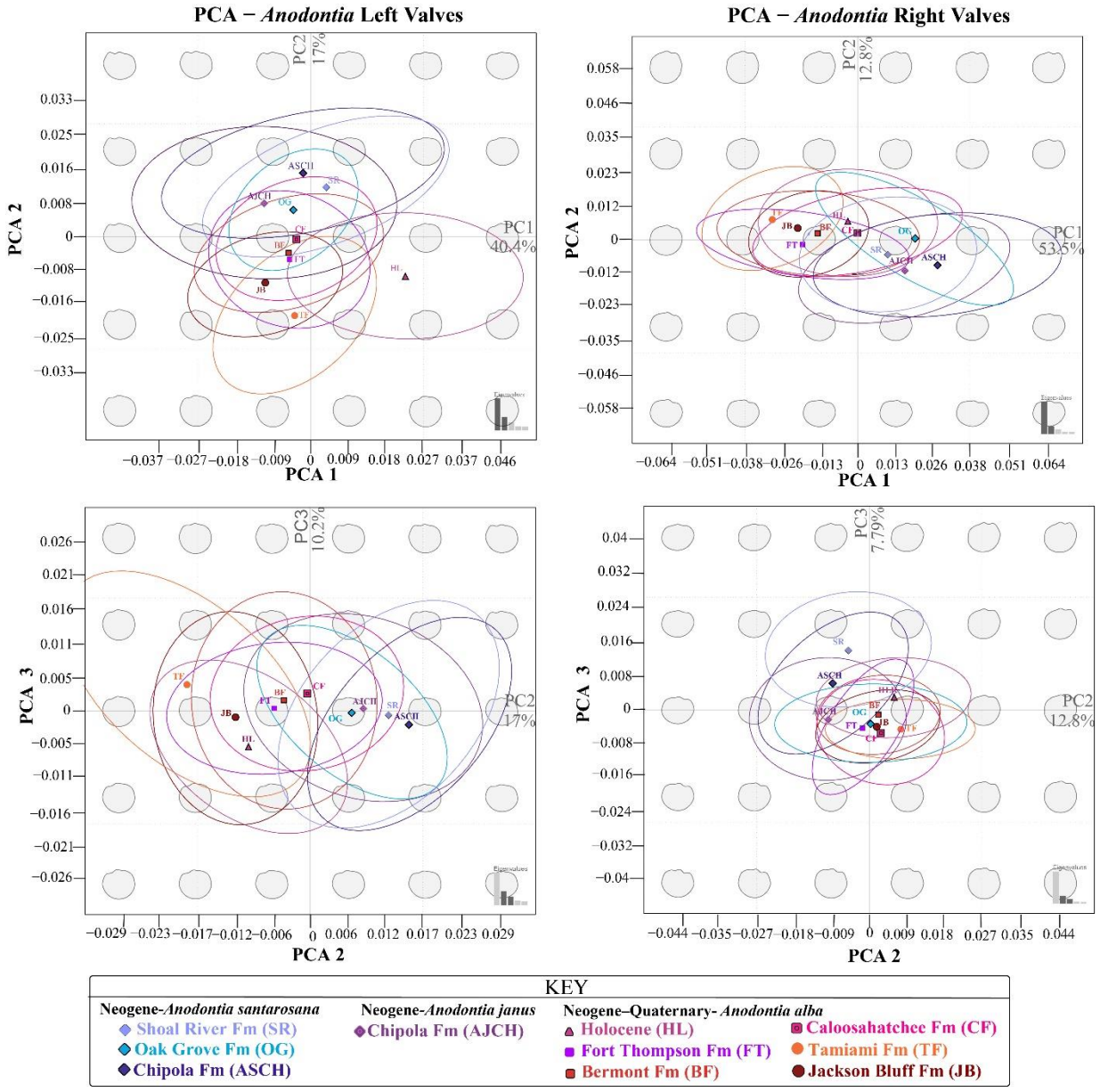

Figure 6.16. PCA axis 1 to 3 scores for the Neogene–Quaternary *Anodontia* left and right valves.

Statistical analysis of PCA mean scores both support and refute the associations on PCA axes 1 to 3 (Table 6.9). Analyses of both left and right valves of Miocene species indicate a lack of statistically significant differences among the two Miocene species and among samples from different intervals in the Miocene. The only exceptions to this pattern include the association between Chipola *A. janus* and Shoal River *A. santarosana* right and left valves as well as the right valves of Shoal River *A. santarosana* with that of specimens from the Chipola and Oak Grove formations. The two Miocene species' PCA scores are generally statistically significantly different when compared with *A. alba* scores. The only exception to this pattern is the association between specimens from the Oak Grove with that of specimens from Fort Thompson (left valves only), Bermont, and Caloosahatchee formations. The PCA scores for right and lefts valves of *A. alba* from the Pliocene to Pleistocene are statistically significantly different when compared among specimens from different time intervals. For left valves, the exception to this pattern is the association among specimens from Tamiami with that of the Caloosahatchee and Bermont as well as the association between the Caloosahatchee and Jackson Bluff. The same exceptions are true for right valves, however, Bermont and Caloosahatchee specimens are statistically significantly different rather than Caloosahatchee and Jackson Bluff specimens. Finally, all right and left valves of Holocene *A. alba* are statistically significantly different from all others.

The CVA axes 1 to 3 scores for both left and right left valves of *Anodontia* (Fig. 6.17) overlap in outline shape but show greater variance in both plotting position of mean sample scores and ellipse size compared to the PCA. For example, axes 1 and 2 show substantial scatter in ellipses and mean scores. In contrast, axes 2 and 3 show substantial overlap, especially among ellipses. The 80% ellipses for the left valves of Miocene *Anodontia* all overlap except for Shoal

River *A. santarosana* specimens. *Anodontia alba* left valve ellipses also substantially overlap with only the Holocene and Jackson Bluff samples displaying less overlap. All *Anodontia* right valve ellipses overlap except for *A. janus* from the Miocene Chipola Formation and *A. alba* from the Pliocene Tamiami and Jackson Bluff formations. The only samples displaying less overlap along axis 2 and 3 include the left valves of *A. santarosana* from the Shoal River and right valves of *A. janus* from the Chipola.

Statistical analysis of the CVA axes 1 to 3 scores for right and left valves suggests that most samples are statistically significantly different with just a few exceptions (Table 6.11). Statistics for the CVA scores for both left and right valves of Miocene species indicate statistically significant differences between the two species and among the different samples from the different time intervals. Exceptions to this include the relationship between *A. janus* from the Chipola with *A. santarosana* right and left valves from the Oak Grove and Chipola formations, respectively. There is also a lack of statistically significant differences among the right valves of *A. santarosana* with Caloosahatchee and Fort Thompson *A. alba* specimens. There is a lack of statistically significant differences between the left valves of *A. alba* specimens from the Caloosahatchee vs. Holocene, Fort Thompson, and Jackson Bluff formations and Fort Thompson *A. alba* right valve specimens. CVA scores for *A. alba* are generally statistically significantly different when compared among the same species from different time intervals. However, right valves lack a statistically significant difference between Caloosahatchee and Fort Thompson specimens. There is also a lack of statistically significant differences between the left valves of *A. alba* from the Caloosahatchee as compared to specimens from the Holocene, Fort Thompson, and Jackson Bluff formations as well as between the Fort Thompson and Holocene, as well as between the Tamiami and Jackson Bluff.

Table 6.9. Summary statistics for PCA axes 1 to 3 scores of left (top) and right (bottom) *Anodontia* valves. Yellow boxes indicate statistically significant differences when compared with opposite samples, whereas gray boxes indicate a lack of statistically significant differences.

PCA Left Valve										
Species	**Species**	*Anodontia alba*					*Anodontia janus*	*Anodontia santarosana*		
	Formation	FortThompson	Bermont	Caloosahatchee	Jackson Bluff	Tamiami	Chipola	Chipola	Oak Grove	Shoal River
Anodontia alba	Holocene	1.10E-03	5.11E-13	2.42E-23	7.34E-06	7.77E-04	1.93E-21	3.46E-10	2.57E-06	2.44E-17
	FortThompson		9.58E-01	5.34E-01	5.10E-01	2.36E-01	3.17E-02	3.52E-03	2.45E-01	1.51E-03
	Bermont			3.49E-01	1.29E-01	3.13E-03	1.92E-05	1.49E-05	7.01E-02	1.39E-07
	Caloosahatchee				4.15E-03	1.15E-04	8.93E-06	2.74E-05	2.35E-01	7.19E-08
	Jackson Bluff					1.98E-01	4.06E-05	2.07E-05	4.63E-03	8.58E-07
	Tamiami						9.01E-06	8.99E-05	1.29E-04	1.39E-07
Anodontia janus	Chipola							2.21E-01	8.12E-01	1.34E-02
Anodontia santarosana	Chipola								3.81E-01	4.71E-01
	Oak Grove									5.86E-01

PCA RightValve										
Species	**Species**	*Anodontia alba*					*Anodontia janus*	*Anodontia santarosana*		
	Formation	FortThompson	Bermont	Caloosahatchee	Jackson Bluff	Tamiami	Chipola	Chipola	Oak Grove	Shoal River
Anodontia alba	Holocene	4.75E-03	8.83E-03	1.68E-07	1.55E-03	9.59E-05	2.65E-12	6.82E-07	2.30E-02	1.83E-11
	FortThompson		4.06E-01	1.26E-01	6.77E-01	8.04E-02	1.25E-06	5.27E-05	2.08E-02	6.26E-09
	Bermont			8.67E-03	4.07E-01	2.97E-02	1.97E-10	3.97E-07	9.87E-02	1.08E-13
	Caloosahatchee				1.16E-01	3.30E-05	5.52E-14	4.94E-11	2.85E-01	1.78E-21
	Jackson Bluff					4.85E-02	9.92E-10	6.35E-07	1.74E-02	9.17E-12
	Tamiami						6.83E-13	1.16E-07	2.70E-03	1.16E-12
Anodontia janus	Chipola							1.65E-01	5.65E-01	2.96E-09
Anodontia santarosana	Chipola								1.70E-01	5.50E-03
	Oak Grove									8.14E-03

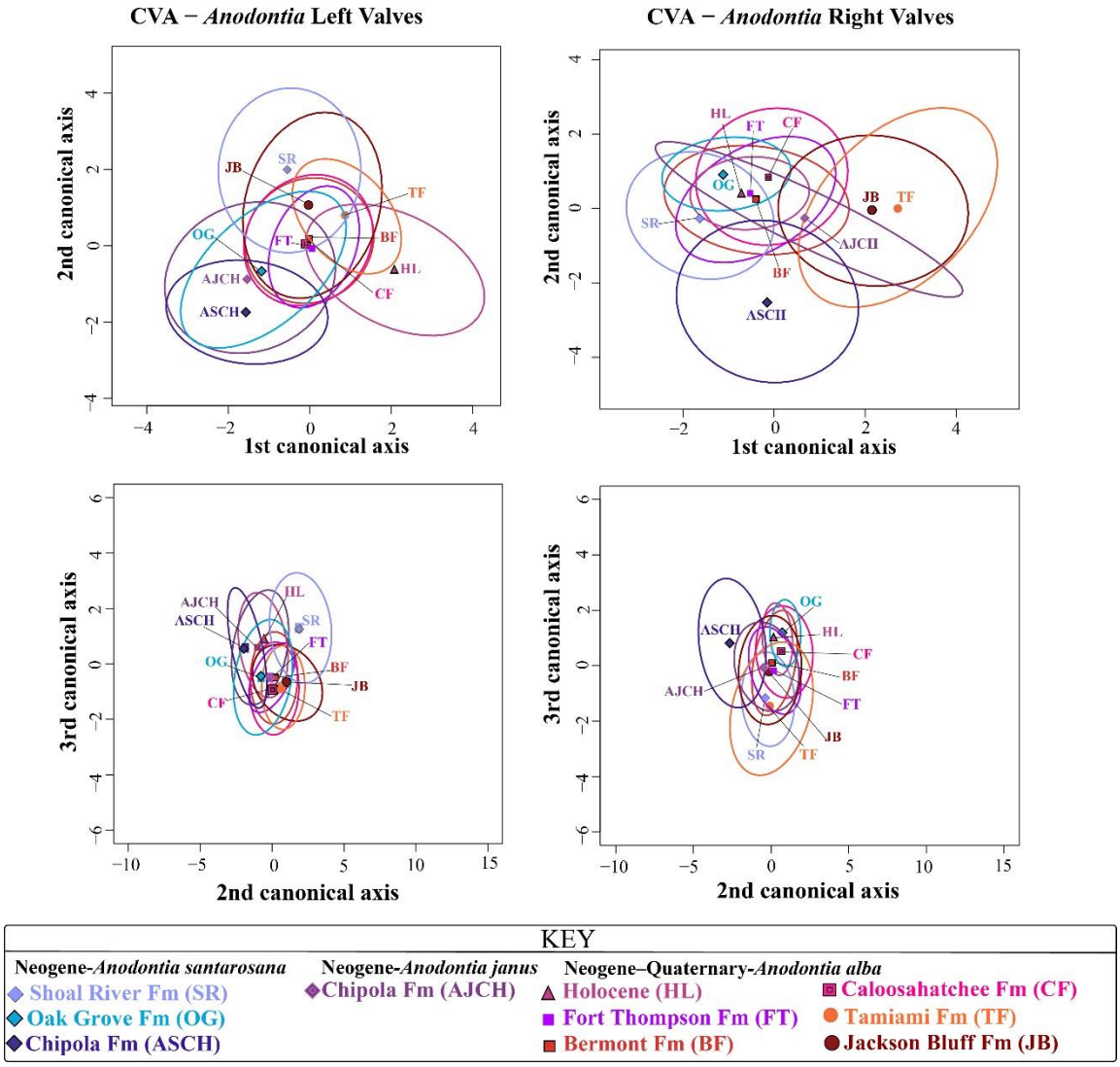

Figure 6.17. CVA axis 1 to 3 scores for Neogene–Quaternary *Anodontia* left and right valves from Florida

Table 6.10. Summary statistics for CVA axes 1 to 3 scores of left (top) and right (bottom) *Anodontia* valves. Yellow boxes indicate statistically significant differences when compared with opposite samples, whereas gray boxes indicate a lack of statistically significant differences.

CVA Right Valve										
Species	**Species**	*Anodontia alba*					*Anodontia janus*	*Anodontia santarosana*		
	Formation	Caloosahatchee	FortThompson	Holocene	Jackson Bluff	Tamiami	Chipola	Chipola	Oak Grove	Shoal River
Anodontia alba	Bermont	6.50E-07	3.73E-14	7.24E-37	6.81E-17	2.97E-16	1.06E-40	7.14E-28	3.22E-06	9.42E-27
	Caloosahatchee		8.40E-01	5.23E-03	8.52E-04	1.24E-05	2.75E-09	1.02E-08	2.41E-01	7.25E-09
	FortThompson			2.48E-04	9.70E-03	1.55E-04	1.26E-17	1.93E-14	1.77E-01	1.93E-19
	Holocene				7.62E-03	4.79E-05	8.24E-29	4.34E-25	1.02E-02	1.49E-32
	Jackson Bluff					5.44E-03	1.47E-15	5.73E-13	1.55E-03	8.47E-14
	Tamiami						2.77E-16	1.41E-12	3.49E-04	2.68E-14
Anodontia janus	Chipola							1.61E-04	8.33E-02	1.45E-24
Anodontia santarosana	Chipola								2.26E-02	1.53E-15
	Oak Grove									6.81E-04

CVA Left Valve										
Species	**Species**	*Anodontia alba*					*Anodontia janus*	*Anodontia santarosana*		
	Formation	Caloosahatchee	FortThompson	Holocene	Jackson Bluff	Tamiami	Chipola	Chipola	Oak Grove	Shoal River
Anodontia alba	Bermont	3.38E-06	1.13E-18	7.33E-35	5.98E-10	6.48E-06	2.94E-35	1.44E-19	5.22E-11	3.24E-29
	Caloosahatchee		9.14E-01	4.57E-01	1.22E-01	1.64E-02	3.16E-06	1.45E-05	3.61E-02	2.81E-08
	FortThompson			1.39E-01	2.74E-02	4.48E-03	5.81E-17	3.81E-11	2.89E-03	4.49E-19
	Holocene				1.10E-02	4.66E-03	1.66E-29	3.91E-15	5.62E-04	7.26E-32
	Jackson Bluff					1.28E-01	1.50E-11	9.79E-07	8.74E-03	4.72E-08
	Tamiami						2.75E-11	1.80E-08	6.71E-04	9.61E-08
Anodontia janus	Chipola							4.86E-02	2.58E-02	2.56E-22
Anodontia santarosana	Chipola								2.68E-02	5.07E-15
	Oak Grove									1.85E-09

Discussion

Allometry: *Lucina* and *Anodontia*

The different species of *Lucina* and *Anodontia* all show a weak correlation between size and shape, which indicates that changes in size are not influencing the shell outline shape of these lucinids. This weak correlation suggests that the different *Lucina* and *Anodontia* species were undergoing isometric growth through ontogeny, which means that all shell features were growing at approximately the same rate. Thus, small, more juvenile specimens for each species have the same shape as larger, more mature specimens.

If these traits were correlated, then it would indicate an allometric growth pattern for both *Lucina* and *Anodontia*. Such a correlation would signify that different shell components were growing at different rates and that outline shape was changing through growth (e.g., Bonner, 2006). Changes in shape with growth would likely only occur to accommodate for functional and structural requirements for a greater size or for changes in life habit and/or environment through ontogeny (Bonner, 2006). However, for bivalves, such as *Lucina* and *Anodontia*, which only reach a few centimeters at maximum size and maintain the same life habits as well as habitats, there is little necessity to make substantial changes to their shell shape with growth since there is little change in their habitat, physiology, functioning, and structural requirements with ontogeny.

Size Trends: *Lucina* and *Anodontia*

The box plots and statistical tests of geometric means of size for both the left and right valves of the *L. glenni–L. pensylvanica* lineage show an evolutionary increase in size during the Neogene to middle Pleistocene and then a decrease into the Holocene. Holocene *L. roquesana* from the Bahamas are also differentiated from the larger *L. glenni–L. pensylvanica* lineage by their smaller sizes. Florida *Lucina* show the greatest amount of size increase (i.e., ~36%

increase) during the Neogene, which is associated with the transition from *L. glenni* to *L. pensylvanica*. *Lucina pensylvanica* continued to increase in size by ~18% up to the middle Pleistocene but then decrease by ~11% in size over the past ~1 Ma.

This increase in size is a common evolutionary pattern among many different Neogene–Quaternary bivalve genera in the Western Atlantic, which has been recognized by several authors (e.g., see Chapter Five; Gardner, 1926; Thompson, 2001). This long-term increase likely reflects Cope's Rule, which is defined as an evolutionary tendency for animals to increase in size over time within a lineage (e.g., Cope, 1887; 1896; Newell, 1949; Stanley, 1973; Jablonski, 1997; Alroy, 1998). This is supported by the interpretation that *L. glenni–L. pensylvanica* represent a distinct lineage, something that was not always established in previous investigations of Cope's Rule, but a critical element of evaluating its manifestation in the fossil record.

In contrast, the size decrease in *Lucina* over the past ~1 Ma could be due to either increasingly shorter life spans among *Lucina* and/or heterochronic changes in development where progressively more recent forms attain maturity at a smaller size. (e.g., see McKinney,1986, 1988, 2012; McKinney and McNamara, 1991; McKinney et al., 2013). This shift from an increase to a decrease in size closely corresponds to the mid-Pleistocene climatic transition and was likely regulated by the long-term environmental changes that corresponded with this event. However, to disentangle the ecological and evolutionary underpinnings of this shift would require high-resolution stratigraphic and sclerochronological approaches.

The box plots and statistical analysis of geometric means of size for both the left and right valves of *Anodontia* suggest that stasis predominated during most of this group's evolutionary record over the past ~17 Ma. For example, middle Miocene *Anodontia* show no difference in size between species and little to no change in size among an interval of at least 4.4

Ma. Similarly, *A. alba* maintains an average geometric mean of size of ~41.0 mm over 4.0 Ma from the Pliocene to Holocene. The only substantial evolutionary change is associated with an ~86% increase in shell size, which is associated with the transition from *A. janus* to *A. alba*. This size increase is similar to patterns documented for *Lucina* and many other bivalves in the Western Atlantic (e.g., see Chapter Five; Gardner, 1926; Thompson, 2001). As with *Lucina*, the exact tempo of this evolutionary transition is unknown due to limited knowledge of the upper Miocene and early Pliocene molluscan fossil record in the Florida and other parts of the Western Atlantic. However, as *A. janus* and *A. alba* likely represent a lineage, the mode of this transition was likely anagenetic.

Lucina and *Anodontia* show substantially different variances in their geometric size means through the Neogene and Quaternary, yet, understanding this change in variance in shell size can be problematic. This difficulty originates from shell size variance being controlled by numerous influences, including ecophenotypic variation, ontogenetic stage, preservational controls, sample size, and preferential collecting of specific size classes. Ecophenotypic variance can be somewhat difficult to determine, but the narrow range of variance revealed by the PCA plots and limited difference shown by the CVA plots suggests that there was some ecophenotypic variation among populations but that it was relatively limited. This study attempted to account for ontogenetic stage, sample size, and preferential collecting biases towards specific size classes by utilizing large numbers of specimens with roughly similar sized shells, however, certain time intervals were not as well represented in museum collections as others (e.g., Fort Thompson *L. pensylvanica* or Tamiami *A. alba*). Due to this and other issues mentioned above, size variance cannot be effectively examined in greater detail.

Shape Trends: *Lucina* and *Anodontia*

Lucina show limited to no change in outline shape among the Miocene to Holocene species indicating evolutionary stasis. Stasis is indicated by the PCA and CVA 80% confidence ellipses for the right and left valves of Miocene to Holocene species that display substantial overlap and *Lucina* sharing a relatively narrow range of outline shapes (e.g., see Fig. 6.13). The most distinct outline shape for *L. pensylvanica* is seen for the Holocene. The cause of this difference is unclear but could be due to ecophenotypic variance or recent evolution of outline shape traits. The minor variance in plotting positions of PCA and CVA mean values and statistical results for both median PCA and CVA scores likely indicates that *Lucina* populations display ecophenotypic variation. However, this variation was likely limited based on how proximity among mean PCA and CVA scores. The distinctiveness of the *L. glenni* right valves from the other *Lucina* on the CVA plot (i.e., Fig. 6.14) supports that these are separate species. It is also likely that these *Lucina* are subtly inequivalved since the left valves do not show this same pattern on the CVA. In addition, the clear separation between *L. pensylvanica* from Florida and *L. roquesana* from the Bahamas supports that these are distinct species.

Neogene to Quaternary *Anodontia* left and right valves possess a narrow range of outline shapes, which show a limited temporal pattern of evolutionary change from the Miocene to Pliocene and then stasis during the Quaternary. The distinctiveness of the Neogene species is shown by Miocene and Pliocene *Anodontia* forming distinct fields at the 80% confidence intervals as compared to Quaternary *A. alba*. The substantial overlap in shape between Chipola Formation *A. janus* and *A. santarosana* suggest that these two Miocene taxa could potentially be the same species. However, shell outlines only represent a two-dimensional character and since these are complex three-dimensional shells it is likely that these are different species. Gardner

(1926) noted that the shells of *A. santarosana* closely resembled *A. janus*, but with the former species had several distinct characters. Four of these characters are captured by the shell outline, including: a slightly more anterior beak, a distinct posterior dorsal area, and a more emphatic anterior. However, four characters noted by Gardner (1926) are not captured with the shell outline, including stronger concentric striation, shorter and wider lunule, and a surface that retains traces of four or five lighter and darker color bands. The similarities in size and outline shape, but differences in other character states indicate that these are separate species, which are likely closely related.

The statistical tests of the PCA and CVA median values both support and refute the evolutionary interpretations based on the PCA and CVA plots for *Lucina* and *Anodontia*. This discrepancy between the PCA and CVA plots and the statistical results likely relates to the question of what are biologically compared to statistically meaningful. The overlap in 80% confidence intervals, scatter in mean values, and varying statistical results (including differences between right and left valves) are likely reflecting variance in outline shape among different populations of *Lucina* and *Anodontia* through time and not statistically meaningful differences in evolution through time. This is indicated by the relatively narrow range of PCA and CVA scores as well as how *Lucina* and *Anodontia* plot in a relatively limited zone in morphospace (e.g., see Fig. 6.14; 6.16). Since the statistical tests used here are highly sensitive to subtle differences in median values it is likely that the tests are distinguishing among only minor differences among outline shape PCA and CVA scores.

Evolutionary integration of size and shape traits

The degree of evolutionary integration (i.e., how closely two or more traits follow the same evolutionary pattern) between size and outline shape patterns for *Lucina* are relatively

consistent through the Neogene and Quaternary. For example, *Lucina* show evolutionary size change in association with stasis in outline shape from the Miocene to Holocene suggesting limited integration in these elements (Fig. 6.18). The change in *Lucina*'s size, while shape remained in stasis is a common evolutionary pattern, is frequently associated with a switch in the developmental timing of the species (e.g., Gould, 1982). This suggests that *L. glenni* and *L. pensylvanica* are synonymous, with the principle difference between them reflected in their sizes. However, this possibility must remain equivocal until a greater number of characters are analyzed. Evolutionary divergence in size and shape traits has been documented in a diverse range of species and lineages (Hunt, 2007; Hopkins and Lingard, 2012). Hunt (2007) showed that size is readily more evolvable than shape traits, which more frequently remain in stasis for long periods.

In contrast, *Anodontia* show change in shape with no change in size during the middle Miocene and no constant size and shape during the Pliocene to Holocene (Fig. 6.18). There is major change in both size and outline shape in *Anodontia* associated with the transition from *A. janus* to *A. alba*, which occurred during the late Miocene or early Pliocene. These patterns in *Anodontia* suggest that size and shape were not well integrated in the Miocene but were during the Pliocene to Holocene. This indicates that selection pressures switched from factors that drove solely shape change in the middle Miocene to factors that could drive both shape and size change during the late Miocene to early Pliocene.

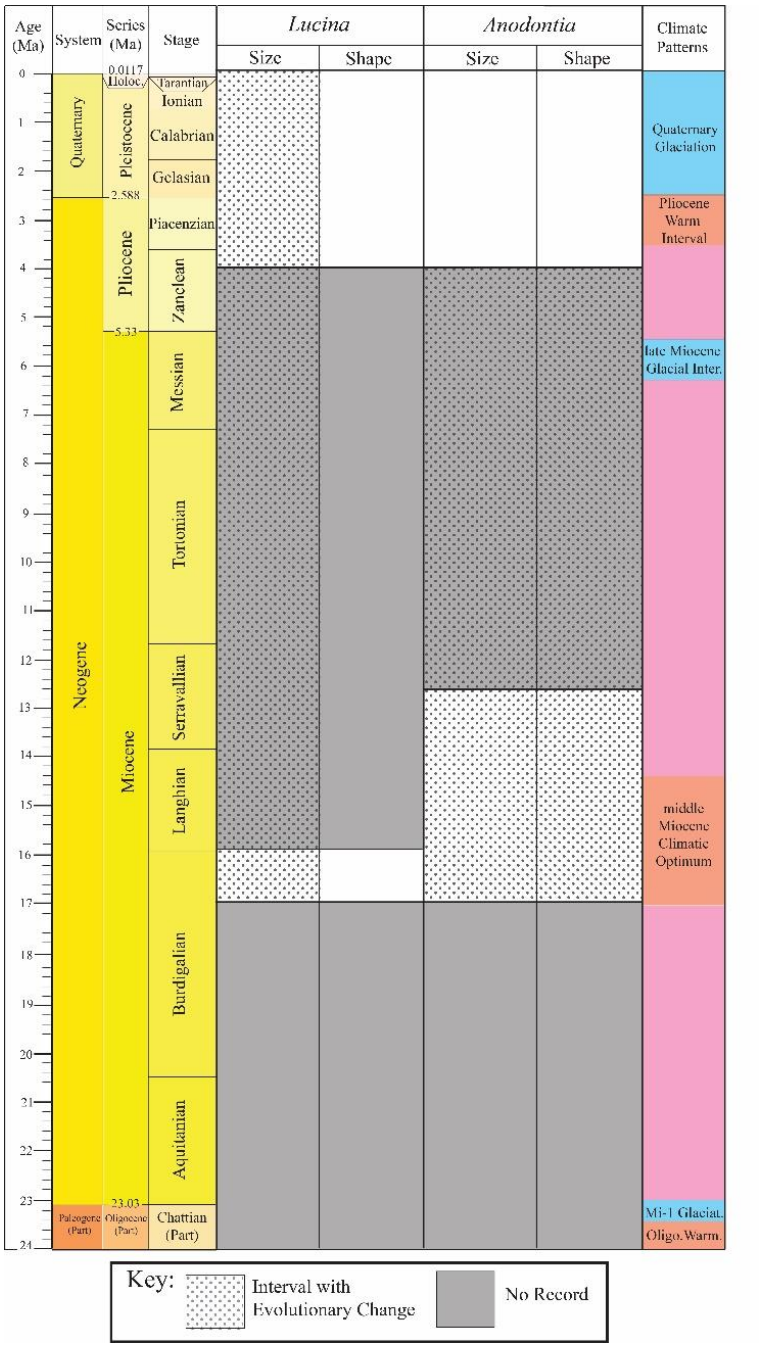

Figure 6.18. Summary of evolutionary size and shape changes in *Lucina* and *Anodontia* during Neogene to Quaternary with broad-scale climatic regimes shown on the right (modified from Huddlestun, 1984; Zachos et al., 2001; Saupe et al., 2014). See Figure 6.4 for key to broad-scale climate regimes.

Variability Trends: *Lucina* and *Anodontia*

The 80% ellipses around mean scores on the *Anodontia* PCA plots shows substantial variability in the Miocene but little variability in the Pliocene to Holocene. The precise reason for this pattern is unclear but could be driven by either the species environmental setting and/or the scale of ecological interactions with other species (Simpson, 1944; Ayala et al., 1975; Parsons, 1987; Sheldon, 1993; Yacobucci, 2004). This is crucial to consider because variability controls the range of morphospace organisms can evolve into overtime (e.g., see West-Eberhard, 1989, 2003; Lloyd and Gould, 1993; Sheldon, 1993; Yacobucci, 2004). Parsons (1987) suggested that increased morphological variability is frequently associated with high-stress settings because of its adaptational benefits. In contrast, Ayala et al. (1975) and Sheldon (1993) proposed that elevated variability might be more common in relatively stable settings with restricted environmental limits because of a depression of selection pressures and more opportunity for morphological experimentation. The relatively greater variability documented in Miocene *Anodontia* supports the latter hypothesis since the reduced and less frequent environmental changes associated with this interval likely decreased evolutionary pressures, thus increasing the opportunity for greater outline shape variation. Similarly, the limited variability documented for Pliocene to Holocene *Anodontia* suggests that the elevated and more frequent environmental changes associated with icehouse conditions amplified evolutionary pressures and decreased the opportunity for greater outline shape variation.

The 80% ellipses around mean scores on the PCA plots shows little variability in Miocene to Holocene *Lucina*. As the trends in this group do not mirror those characterizing *Anodontia* it likely that this pattern is reflecting the relatively evolutionarily conservative nature of *Lucina*. Some *Lucina* groups do not follow these patterns and show greater variability on the

PCA and CVA plots (e.g., Bermont; Coffee Mill Hammock Member of the Fort Thompson). The cause of greater variability seen in certain groups is difficult to determine but could be due to various factors including greater time averaging, ecophenotypic variance, or genetic variance among separate geographic populations. Since many of these groups reflect individuals from different localities in Florida, it is most likely this pattern is reflecting the latter two explanations.

Difficulties with Determining Evolutionary Patterns among *Lucina* and *Anodontia*

Lucina and *Anodontia* display clear patterns of change in both size and shape, however, the resolution of the data is too limited to determine the exact evolutionary tempo. This would require a greater number of samples from more horizons/time intervals than analyzed here (Fig. 6.6). If a greater number of sample horizons with well-preserved fossils were present in the Florida record, then it could be possible to utilize Hunt's (2007) methodology to analytically determine if the patterns represent stasis, gradualism, or random walk.

Future studies could potentially analyze a greater number of time intervals, but this would require sampling a broader geographic range to locate specimens from the missing time intervals. Such a study would have to account for the huge, possibly insurmountable challenges with temporal correlation among stratigraphic units in the western Atlantic. Correlation among western Atlantic stratigraphic units can be challenging due to a paucity of index fossils and age-defining geological constraints, such as ash beds or event horizons. Stratigraphic units and lithofacies are also not uniformly distributed across this region due to shifting facies and differential preservation related to local tectonic and stratigraphic architectures. Thus, certain regions have substantially more gaps between stratigraphic units than other areas. Besides geological and preservational issues, a study utilizing a broader sampling would have to account

for geographic variation in populations and how these differences changed through time at both the local and regional scales.

Implications for the 'Plus ça Change' model

The changes in shell size documented for *Lucina* both support and refute the predictions of Sheldon's (1996) 'Plus ça Change' model. For example, the transition from *L. glenni* to *L. pensylvanica*, which was characterized by the greatest amount of size change in this lineage, transpired during the relatively equitable climatic regime of the middle to late Miocene (Fig. 6.4; Frakes et al., 1992; De Vleeschouwer et al., 2017; Zachos et al., 2001; Miller et al., 2005). Its co-occurrence with an interval known for diminished climatic fluctuations, suggests that these conditions likely played a role in reducing selection pressures on growth patterns, which would have influenced the change in size and possibly the evolution of *L. pensylvanica*. The continued change in size during the Pleistocene icehouse (see Fig. 6.18), argues against this model's expectation that stasis should be associated with greater climate variability. Instead it suggests that increased climate variability was either playing no part in this lineages size change or that it was possibly driving these changes. The latter idea that climate was influencing these changes is suggested by a switch from an increasing size trends to a decreasing size trend at around the same time as the mid-Pleistocene climatic transition.

The lack of change in shell outline shape for *Lucina* also provides confirmation and refutation of the 'Plus ça Change' model. For example, the lack of change in outline shape during the Miocene to Pliocene counters the model's prediction that diminished environmental variability will result in evolution (Fig. 6.18). Alternatively, it suggests that selection pressures were elevated during the Miocene to Pliocene, which kept *Lucina* in stasis. In contrast, the evolutionary stasis among *Lucina* during the Pleistocene supports the idea that elevated

environmental variability will result in reduced evolutionary change. However, this lack of change in shape might also be due to reduced evolvability of shape characters, which makes it more difficult to change without substantial alterations to selection pressures (Hunt, 2007). Lucinids are well-known to be an evolutionarily conservative group, which show little variance in shape among different closely related species and clades (e.g., Taylor and Glover, 2016). There is evidence that some lucinids have remained unchanged in morphology for millions of years. For example, the seep-adapted lucinids *Nymphalucina occidentalis* from the Upper Cretaceous Western Interior (Fig. 6.19A) and *Lucina aquequizonata* from the Holocene of the Pacific Shelf of North and South America (Fig. 6.19B), although attributed to different genera, are morphologically similar, which suggests that they have remained relatively unchanged in shape since the Late Cretaceous (Landman, pers. comm., 2018). This suggests that rather than confirming or supporting the 'Plus ça Change' model that the evolutionary patterns documented here for *Lucina* instead reflect the evolutionary conservatism of this group.

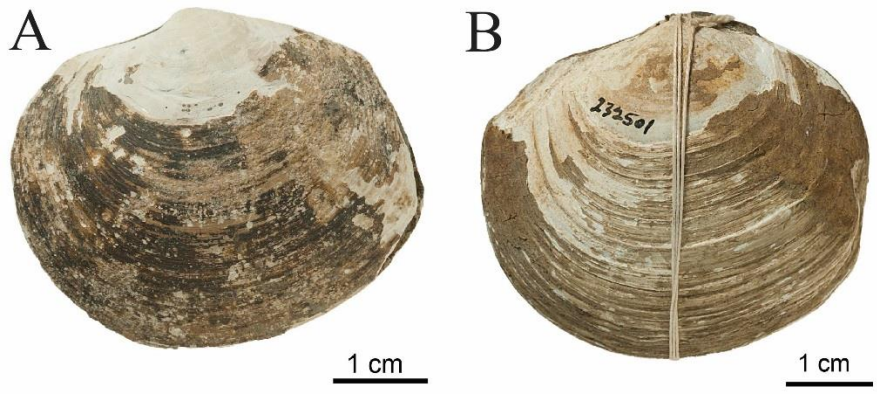

Figure 6.19. Examples of morphological similarities between the Upper Cretaceous seep lucinid (A) *Nymphalucina occidentalis* (AMNH 66246) from the Western Interior and the Holocene seep lucinid (B) *Lucina aquequizonata* (AMNH 232501) from the Pacific shelf of California (photos courtesy of Neil H. Landman).

In contrast to *Lucina*, the evolutionary patterns of *Anodontia* provides strong evidence for the predictions of the 'Plus ça Change' model. The changes in *Anodontia* shape throughout the stable mixed-house climate regime of the Neogene and the increase in its size during the late Miocene or early Pliocene supports the 'Plus ça Change' model's prediction that evolution should be associated with an interval characterized by relatively limited environmental variability (Fig. 6.18). Furthermore, the lack of changes in *Anodontia* shape and size throughout the icehouse climate regime of the Quaternary supports the 'Plus ça Change' model's prediction that stasis should be associated with an interval characterized by relatively limited environmental variability. The lack of size change in *Anodontia* during the middle Miocene climatic optimum is the only interval that does not support the prediction of the 'Plus ça Change' model. This discrepancy suggests, alternatively, that selection pressures on size were elevated during the middle Miocene, which kept *Anodontia* in stasis.

Paleobiological Implications

This analysis of *Lucina* and *Anodontia* offers robust empirical evidence both for and against Sheldon's (1996) 'Plus ça Change' model. Although the evidence is derived from closely related groups with quite comparable ecologies, the results are somewhat contradictory despite the general expectation that they should respond similarly to evolutionary drivers. However, these differences likely reflect a combination of the degree of evolutionary 'potential' that a species or trait possesses to respond to the natural selection pressures that control different evolutionary patterns. The phenomena of evolutionary 'potential' or 'evolvability' has been documented in numerous case studies and is known to vary among groups and traits (e.g., size vs. shape; Ebner et al., 2001; Hunt, 2007; Hansen and Houle, 2008; Hopkins and Lingard, 2012;). Here, the long-term evolutionary stasis in shell outline shape documented in *Lucina*

likely reflects low 'evolvability', whereas the long-term change in size reflects greater evolvability for traits that control growth rates and in turn size patterns. In contrast, the long-term evolutionary patterns in size and shape in *Anodontia* suggest that this group's traits are relatively more responsive to evolutionary drivers as compared to *Lucina*. This suggests that the degree of evolutionary conservatism or 'evolvability' likely plays a substantial role in how evolutionary patterns are expressed during different climatic regimes and what taxa or traits will respond evolutionarily to these changes. Thus, a taxon, such as *Lucina*, with low evolutionary 'potential' might not be as good a candidate as *Anodontia* to examine long-term evolutionary patterns within a broad-scale climatic context.

Of two lineages analyzed in this study, *Anodontia* offers the strongest empirical support for the 'Plus ça Change' model, which hypothesizes that evolutionary tempo and mode vary with environmental stability. Evidence from *Anodontia* indicate that the environmental stability associated with different broad-scale climatic regimes can affect evolutionary tempos. However, as with the bivalve *Nucula* analyzed in Chapter Six, this interpretation differs from Sheldon's (1996) initial proposal, which hypothesized that shallow-marine environments were unlikely to display gradualisms because these settings changed too often over the long-term to drive evolutionary change since they are influenced by various environmental factors (e.g., depth, oxygen, temperature, turbidity, salinity) that alter relatively frequently over short time intervals (i.e., daily to seasonally). Alternatively, Sheldon (1996) proposed that deep-oceanic and shallow-marine environments would be more likely to display evolutionary gradualism and stasis, respectively.

The data presented here for *Anodontia* supports the hypothesis presented in Chapter Six that broad-scale ocean-climate changes (i.e., icehouse vs. mixed-house vs. greenhouse) can more

strongly influence shallow-marine environmental stability, and in turn selection pressures, then just oceanic dynamics by themselves. For instance, warm-house climate regimes are characteristically wetter, warmer, and have limited continental ice-coverage, which sustains higher sea levels and persistence of shallow-shelf habitats (Frakes et al., 1992; Miller et al., 2005). These ocean-climate states are associated with diminished amplitudes of Milankovitch-frequency sea-level variations, which reduces the changes in the distributions of shallow-marine environments on continents throughout each respective cycle. The amplitude and frequency of climate and sea-level fluctuations during these warm-house intervals are sufficiently reduced that they do not result in pronounced variations in numerous factors (e.g., temperature, water depth, geographic change to the area of certain biomes) that influence marine habitats, which results in pronounced stability and persistence for shallow marine communities over the long-term. This offers marine organisms substantially more time to evolutionarily respond to marine environmental dynamics.

During icehouses, the planet is dryer, colder, and has more extensive ice coverage at high elevations and latitudes as compared to greenhouse conditions. This results in a fall in eustatic sea level and the geographic area of shallow-shelf habitats (Frakes et al., 1992; Zachos et al., 2001; Miller et al., 2005). When conjoined with the influences of Milankovitch-frequency cycles, which control global ice distributions, environmental conditions in shallow-shelf habitats vary significantly over relatively short intervals due to rapid and pronounced changes in various factors (e.g., sea level, temperature, salinity). These environmental oscillations vary so frequently that they reduce the long-term stability and persistence of marine habitats and their faunal associations (Roy et al., 1996). This results in rapidly varying abiotic and biotic selection pressures on species throughout an icehouse climate regime. It is also likely that as these

fluctuations occur species track their shifting preferred habitats, which cause populations to repeatedly break up and reform, thus inhibiting genetic isolation and differentiation over the long-term (Potts, 1983; Pease et al., 1989). These various factors in turn decrease the ability for organisms to evolutionarily respond before the environmental settings, habitats, and communities' change once again.

Even with the support for the 'Plus ça Change' model suggested by the *Anodontia* data, this analysis is only one of a handful of cases that have examined how broad-scale environmental drivers shape evolutionary tempos. Since the publication of Sheldon (1996), only two studies have tested this model and, based on their results, have disputed it predictions. For instance, Kim et al. (2009) identified a 3–Ma pattern of evolutionary stasis in the Late Ordovician trilobite *Triarthus beckii*, which was used to argue against the 'Plus ça Change' model. In their study, they based their contention on the model's prediction that evolutionary change should occur more frequently at great water depths due to elevated stability and the fact that *T. beckii* occurs within a relatively stable, low-oxygen, deep-water (~500 m) facies of the Appalachian Foreland Basin. Despite their contention, it is more reasonable to suggest that the evolutionary pattern that they recognized actually corroborates the 'Plus ça Change' model as the study they relied on to infer the environmental settings (Cisne et al., 1982) was contingent upon an antiquated hypothesis for the depth range of low-oxygen environments in epeiric seas and the fact that foreland basin systems are generally shallower than 200 m (e.g., see Slattery et al., 2018). Ostrander (2013) is another study to have tested and argued against the 'Plus ça Change' model. In this study, Ostrander (2013) examined changes in morphological variability within the bivalve family Cardiidae in Florida, the Gulf Coast, and the Western Interior. His findings identified pronounced variability during Neogene to Quaternary and reduced variability during the Late

Cretaceous. Regardless of these results, this study had several methodological problems, which potentially altered the findings. These include not considering allometric disparities among species, not considering methodological issues related to using shells with prominent shell ornamentation, comparing shape data from shells with different preservational modes (i.e., steinkerns vs. well-preserved shells), and not considering data discrepancies produced by difference in raw outline position and size.

These two examples suggest that a larger number of case studies are needed to test the 'Plus ça Change' model. In contrast to previous investigations, these studies must be undertaken within a climatic and environmental framework, to better understand how the incidences of different evolutionary tempos and modes varied within a broad-scale climatic context in different environmental settings. As has been emphasized by numerous authors (e.g., Gould and Eldredge, 1977; Erwin and Antsey, 1995), the discussion over different evolutionary tempo and modes was not over which patterns occur (see Fig. 6.1), but rather over their relative frequencies over long spans of time. A larger quantity of studies examining multiple traits within lineages, utilizing a set standard of methodologies, and placed within an environmental context are needed to advance future analyses of evolutionary patterns. This would provide a better understanding of the interactions between evolutionary patterns and environmental changes as well as how they influence broad-scale patterns of macroevolutionary diversification.

Conclusions

- Data for Neogene and Quaternary *Lucina* indicates evolutionary change dominated this group's size patterns, but that its shape traits remained in stasis, likely due to evolutionary conservatism within this group.

- Both size and shape traits in *Anodontia* show evolutionary change and stasis during the Neogene and Quaternary, respectively.
- The size and outline shape traits in the *Lucina* share incongruent evolutionary patterns during their respective time intervals, which reflects a lack of evolutionary integration among these traits, which suggests they responded to selection pressures in different ways.
- The size and outline shape traits in the different *Anodontia*, with the exclusion of the middle Miocene examples, share congruent evolutionary patterns during their respective time intervals, which reflects evolutionary integration among traits and that these traits were responding to selection pressures in an identical manner.
- Analysis of *Lucina* and *Anodontia* offers robust empirical evidence for and against Sheldon's (1996) 'Plus ça Change' model, which seems contradictory, but is likely reflecting a combination of the degree of species or trait evolvability and the selection pressures that controlled the different evolutionary patterns.
- Of the two lineages analyzed in this study, *Anodontia* offers the strongest empirical support for the 'Plus ça Change' model, which hypothesizes that increased environmental variability will result in stasis, whereas reduced environmental variability will drive progressive, potentially gradualistic morphologic responses.
- The rarity of studies testing the 'Plus ça Change' model, specifically set within a climatic and environmental context, suggests that a larger number of case studies are required to understand the controls on the frequency of different patterns.

References

Alroy, J., 1998, Cope's rule and the dynamics of body mass evolution in North American fossil mammals: *Science*, 280, 731–734.

Ayala, F.J., Valentine, J.W., Delaca, T.E., Zumwalt, G.S., 1975, Genetic variability of the Antarctic brachiopod Liothyrella notorcadensis and its bearing on mass extinction hypotheses: *Journal of Paleontology*, 49, 1–9.

Barnosky, A.D., 1987, Punctuated equilibrium and phyletic gradualism: *in Current mammalogy*, 109–147.

Benton, M.J. and Pearson, P.N., 2001, Speciation in the fossil record: *Trends in Ecology & Evolution*, 16, 405–411.

Beerling, D.J. and Royer, D.L., 2011, Convergent cenozoic CO 2 history: *Nature Geoscience*,4, 1–418.

Bonner J.T., 2006, Why size matters: from bacteria to blue whales: *Princeton University Press*, 1–176.

Cisne, J.L., Karig, D.E., Rabe, B.D. and Hay, B.J., 1982, Topography and tectonics of the Taconic outer trench slope as revealed through gradient analysis of fossil assemblages: *Lethaia*, 15, 229–246.

Cope, E.D., 1887, The origin of the fittest: essays on evolution: *D. Appleton Press*, 1–466.

Cope, E.D., 1896, The primary factors of organic evolution: *Open Court Publishing, Company*, 1–547.

Couto, P. C., 1967, Contribuicao a paleontologia do Estado do Para. Um Sirenio na Formacao Pirabas: *Atas so Simposio Sobre a Biota Amazonica*,1, 345–357

De Vleeschouwer, D., Vahlenkamp, M., Crucifix, M. and Pälike, H., 2017, Alternating Southern and Northern Hemisphere climate response to astronomical forcing during the past 35 my: *Geology*, 45, 375–378.

Dowsett, H.J., Robinson, M.M., and Foley, K.M., 2009, Pliocene three-dimensional global ocean temperature reconstruction: *Climate of the Past*, 5, 769–783.

Ebner, M., Shackleton, M., and Shipman, R., 2001, How neutral networks influence evolvability: *Complexity*,7, 19–33.

Erwin, D. H., and Anstey, R. L., Editors, 1995, New approaches to speciation in the fossil record: *Columbia University Press*, 288 pp.

Eldredge, N., Thompson, J. N., Brakefield, P. M., Gavrilets, S., Jablonski, D., Jackson, J. B., Lenski, R.E., Lieberman, B.S., McPeek A.M., and Miller III, W., 2005, The dynamics of evolutionary stasis: *Paleobiology*, 31, 133–145.

Eldredge, N., and Gould, S.J., 1972, Punctuated equilibria: an alternative to phyletic gradualism: *in* Schopf, T.J.M., Ed. *Models in Paleobiology*, 82–115.

Fielding, C.R., Browne, G.H., Field, B., Florindo, F., Harwood, D.M., Krissek, L.A., Levy, R.H., Panter, K.S., Passchier, S., and Pekar, S.F., 2011, Sequence stratigraphy of the ANDRILL AND-2A drillcore, Antarctica: A long-term, ice-proximal record of Early to Mid-Miocene climate, sea-level and glacial dynamism: *Palaeogeography, Palaeoclimatology, Palaeoecology*, 305, 337–351

Frakes, L.A., Francis, J.E. and Syktus, J.I., 1992, Climate modes of the Phanerozoic: *Cambridge University Press.*

Galloway, W.E., 2008, Depositional Evolution of the Gulf of Mexico Sedimentary Basin: *in* Miall, A.D., ed.: *Sedimentary Basins of the World*, 5, 506–549.

Gallen, S.F., Wegmann, K.W. and Bohnenstiehl, D.R., 2013, Miocene rejuvenation of topographic relief in the southern Appalachians: *GSA Today*, 23, 4–10.

Gardner, J.A. and Mansfield, W.C., 1943, Mollusca from the Miocene and lower Pliocene of Virginia and North Carolina (Vol. 199), *United States Geological Survey, Professional Paper*, 199–A, 177 pp.

Gardner J., 1947, Molluscan Fauna of Alum Bluff Group of Florida, *United States Geological Survey Professional Paper* 142–H, 493–656

Gardner, J., 1926, The molluscan fauna of the Alum Bluff Group of Florida, Part I, Prionodesmacea and Anomalodesmacea: *United States Geological Survey Professional Paper*, 142–A, 79 pp.

Giere, O., 1985, Structure and position of bacterial endosymbionts in the gill filaments of Lucinidae from Bermuda (Mollusca, Bivalvia): *Zoomorphology*, 105, 296–301

Gould, S.J. and Eldredge, N., 1977, Punctuated equilibria: the tempo and mode of evolution reconsidered: *Paleobiology*, 3, 115–151.

Gould, S.J., 1982, Change in developmental timing as a mechanism of macroevolution. *in Evolution and development*, Springer, 333–346.

Gould, S.J. and Eldredge, N., 1993, Punctuated equilibrium comes of age: *Nature*, 366, 223.

Gould, S.J., 2002, The Structure of Evolutionary Theory: *Harvard University Press*, 1464 pp.

Griener, K.W., Warny, S., Askin, R., and Acton, G., 2015, Early to middle Miocene vegetation history of Antarctica supports eccentricity-paced warming intervals during the Antarctic icehouse phase: *Global and Planetary Change*, 127, 67–78.

Hansen, T.F. and Houle, D., 2008, Measuring and comparing evolvability and constraint in multivariate characters: *Journal of evolutionary biology*, 21,1201–1219.

Harries, P. J., and Allmon, W. D., 2007, Is there a relationship between sea level and evolutionary pattern among macroinvertebrates?: *Geological Society of America Abstracts with Programs,* Vol. 39, 587.

Hendy, A. J. W., Buick, D. P., Bulinski, K. V., Ferguson, C. A., and Miller A. I.. 2008, Unpublished census data from Atlantic coastal plain and circum-Caribbean Neogene assemblages and taxonomic opinions: *Paleobiology Database* (http://www.paleobiodb.org/classic/displayRef erence?reference_no=19909).

Hennissen, J.A., Head, M.J., De Schepper, S. and Groeneveld, J., 2015, Increased seasonality during the intensification of Northern Hemisphere glaciation at the Pliocene–Pleistocene boundary~ 2.6 Ma: *Quaternary Science Reviews*,129, 321–332.

Hopkins, M.J. and Lidgard, S., 2012, Evolutionary mode routinely varies among morphological traits within fossil species lineages: *Proceedings of the National Academy of Sciences*, 109, 20520–20525.

Huddlestun, P.F., 1984, The Neogene stratigraphy of the Central Florida Panhandle: Florida State University *unpublished PhD dissertation,* 210 pp.

Hunt, G., 2007, The relative importance of directional change, random walks, and stasis in the evolution of fossil lineages: *Proceedings of the National Academy of Sciences*, 104, 18404–18408.

Jablonski, D., 1997, Body-size evolution in Cretaceous molluscs and the status of Cope's rule: *Nature*, 385, 250–252.

Jablonski, D., 2007, Scale and hierarchy in macroevolution: *Palaeontology*, *50*, 87–109.

Jackson, J.B. and Cheetham, A.H., 1999, Tempo and mode of speciation in the sea: *Trends in Ecology & Evolution*,14, 72–77.

Jones, D.S., 1988, Sclerochronology and the size versus age problem, *in Heterochrony in Evolution,* 93–108.

Kim, K., Sheets, H.D. and Mitchell, C.E., 2009, Geographic and stratigraphic change in the morphology of Triarthrus beckii (Green)(Trilobita): a test of the Plus ça change model of evolution, *Lethaia*, 42, 108–125.

Lieberman, B. S., and Dudgeon, S., 1996, An evaluation of stabilizing selection as a mechanism for stasis: Palaeogeography: *Palaeoclimatology, Palaeoecology*, 127, 229–238.

Lieberman, B. S., Brett, C. E., and Eldredge, N., 1995, A study of stasis and change in two species lineages from the Middle Devonian of New York State: *Paleobiology*, 21, 15–27.

Lloyd, E.A. and Gould, S.J., 1993, Species selection on variability: *Proceedings of the National Academy of Sciences*, 90, 595–599.

McKenzie, N.R., Horton, B.K., Loomis, S.E., Stockli, D.F., Planavsky, N.J. and Lee, C.T.A., 2016, Continental arc volcanism as the principal driver of icehouse-greenhouse variability, *Science*, 352, 444–447.

McKinney, M.L., 1988. Classifying Heterochrony. In *Heterochrony in evolution*, 17–34). Springer, Boston, MA.

McKinney, M.L., 1988. Heterochrony in evolution. In *Heterochrony in Evolution*, 327–340. Springer, Boston, MA.

McKinney, M.L. and McNamara, K.J., 1991, Heterochrony. In *Heterochrony*, Springer Publishing, 1-12.

McKinney, Michael L., and Kenneth J. McNamara, 2013, Heterochrony: the evolution of ontogeny: *Springer*, 327–347.

Miall, A.D., Balkwill, H.R. and McCracken, J., 2008, The Atlantic margin basins of North America: *Sedimentary Basins of the World*, 5, 473–504.

Mikkelsen, P. M., and Bieler, R., 2008, Seashells of Southern Florida: Living Marine Mollusks of the Florida Keys and Adjacent Regions; Bivalves: *Princeton University Press, Princeton*, 446 pp.

Miller, K.G., Wright, J.D., Browning, J.V., Kulpecz, A., Kominz, M., Naish, T.R., Cramer, B.S., Rosenthal, Y., Peltier, W.R., and Sosdian, S., 2012, High tide of the warm Pliocene: Implications of global sea level for Antarctic deglaciation: *Geology*, 40, 407–410

Miller, K.G., Kominz, M.A., Browning, J.V., Wright, J.D., Mountain, G.S., Katz, M.E., Sugarman, P.J., Cramer, B.S., Christie-Blick, N. and Pekar, S.F., 2005, The Phanerozoic record of global sea-level change: *Science*, 310, 1293–1298.

Mudelsee, M. and Schulz, M., 1997, The Mid-Pleistocene climate transition: onset of 100 ka cycle lags ice volume build-up by 280 ka: *Earth and Planetary Science Letters*, 151, 117–123.

Newell, N.D., 1949, Phyletic size increase, an important trend illustrated by fossil invertebrates, *Evolution*, 3, 103–124.

Ostrander, R.J., 2013, Effects of Climate Variability on Evolutionary Tempo and Mode in Cretaceous and Neogene Marine Molluscs: *Unpublished Masters Thesis, University of Wisconsin-Madison*, 119 pp.

Pälike, H., Norris, R.D., Herrle, J.O., Wilson, P.A., Coxall, H.K., Lear, C.H., Shackleton, N.J., Tripati, A.K., and Wade, B.S., 2006, The heartbeat of the Oligocene climate system: S*cience*, 314,1894–1898.

Parsons, P.A., 1987, Evolutionary rates under environmental stress: *Evolutionary Biology*, 21, 311–347.

Pease, C.M., Lande, R. and Bull, J.J., 1989, A model of population growth, dispemal and evolution in a changing environment: *Ecology*, 70,1657–1664

Potts, D.C., 1983, Evolutionary disequilibrhun among Indo-Pacific corals, *Bull. Mar. Sci*., 33, 619–632

Redfern, C., 2001. Bahamian Seashells: 1161 Species from Abaco, Bahamas: *Bahamian Seashells, Inc., Florida*, 501 pp.

Roy, K., Valentine, J.W., Jablonski, D. and Kidwell, S.M., 1996, Scales of climatic variability and time averaging in Pleistocene biotas: implications for ecology and evolution: *Trends in Ecology & Evolution*, 11, 458–463.

Royer, D.L., Berner, R.A., Montañez, I.P., Tabor, N.J. and Beerling, D.J., 2004, Co~ 2 as a primary driver of phanerozoic climate: *GSA today*,14,4–10.

Saupe, E.E., Hendricks, J.R., Portell, R.W., Dowsett, H.J., Haywood, A., Hunter, S.J., and Lieberman, B.S., 2014, Macroevolutionary consequences of profound climate change on niche evolution in marine molluscs over the past three million years: *Proceedings of the Royal Society* B, 281, 20160654, http://dx.doi.org/10.1098/rspb.2016.0654.

Sheldon, P. R., 1996, Plus ça change—a model for stasis and evolution in different environments: *Palaeogeography, Palaeoclimatology, Palaeoecology*, 127, 209–227.

Sheldon, P.R., 1997, The Plus ça change model: Explaining stasis and evolution in response to abiotic stress over geological timescales, *in* Bijlsma, R. Loeschcke, V. Eds., *Environmental Stress, Adaptation, and Evolution*: *Basel, Birkhäuser Verlag*, 307–326.

Sheldon, P.R., 1993, Making sense of microevolutionary patterns. In: Lees, D.R., and Edwards, D. Eds., *Evolutionary Patterns and Processes: Linnean Society, Symposium, Volume 14: Academic Press*, 19–31.

Simpson, G. G., 1944, Tempo and mode in evolution: *Columbia University Press*, 237 pp.

Slattery, J.S., Harries, P.J. and Sandness, A.L., 2018, Do marine faunas track lithofacies? Faunal dynamics in the Upper Cretaceous Pierre Shale, Western Interior, USA: *Palaeogeography, Palaeoclimatology, Palaeoecology*, 496, 205–224.

Speden, I.G., 1970, The type Fox Hills Formation, Cretaceous (Maestrichtian), South Dakota. Systematics of the Bivalvia: *Bulletin of the Peabody Museum, Yale University*, 33, 222 pp.

Stanley, S.M., 1973, An explanation for Cope's rule: *Evolution*, 27, 1–26.

Stanley, S.M., 2014, Evolutionary radiation of shallow-water Lucinidae (Bivalvia with endosymbionts) as a result of the rise of seagrasses and mangroves: *Geology*, 42, 803–806.

Taylor, J.D. and Glover, E.A., 2016, Lucinid bivalves of Guadeloupe: diversity and systematics in the context of the tropical Western Atlantic (Mollusca: Bivalvia: Lucinidae): *Zootaxa*,4196, 301–380.

Taylor, J.D., Glover, E.A., Smith, L., Ikebe, C. and Williams, S.T., 2016, New molecular phylogeny of Lucinidae: increased taxon base with focus on tropical Western Atlantic species (Mollusca: Bivalvia): *Zootaxa*, 4196, 381–398.

Tavora, V.A., dos Santos, A.A.R., and Araujo, R.N., 2010, Localidades fossiliferas da Formacao Pirabas (Mioceno Inferior): *Boletim do Museu Paraense Emílio Goeldi Ciências Naturais, Belém* 5**,** 207–224

Thompson, M.D., 2001, Gigantism and Dolomite Replacement in the Dean's Trucking Pit Mollusks (early to Middle Miocene), Sarasota County, Florida: *unpublished Doctoral dissertation, University of South Florida*, 369 pp.

Toledo, P.M. 1989, Sobre novos achados de sirenios (*Sirenotherium pirabense* Paula Couto, 1976) na Formacao Pirabas (Para, Brasil): *Boletim do Museu Paraense Emilio Goeldi Serie Ciencias da Terra*, 1**,**5 -10

Tziperman, E. and Gildor, H., 2003, On the mid- Pleistocene transition to 100- kyr glacial cycles and the asymmetry between glaciation and deglaciation times: *Paleoceanography*, 18, 1–8.

Wara, M.W., Ravelo, A.C., and Delaney, M.L., 2005, Permanent El Niño-like conditions during the Pliocene warm period: *Science*, 309, 758–761.

West-Eberhard, M.J., 1989, Phenotypic plasticity and the origins of diversity: *Annual review of Ecology and Systematics*, 20, 249–278.

West-Eberhard, M.J., 2003, Developmental plasticity and evolution: *Oxford University Press*.

Yacobucci, M.M., 2004, Neogastroplites meets *Metengonoceras*: morphological response of an endemic hoplitid ammonite to a new invader in the mid-Cretaceous Mowry Sea of North America: *Cretaceous Research*, 25, 927–944.

Zachos, J., Pagani, M., Sloan, L., Thomas, E. and Billups, K., 2001, Trends, rhythms, and aberrations in global climate 65 Ma to present: *Science*, 292, 686–693.

Zachos, J.C., Flower, B.P. and Paul, H., 1997, Orbitally paced climate oscillations across the Oligocene/Miocene boundary: *Nature*,388, 567–570.

CHAPTER SEVEN:

THE PHYLOGENY OF THE MIDDLE CAMPANIAN TO LATE MAASTRICHTIAN AMMONITE *BACULITES* LAMARK 1799 IN THE WESTERN INTERIOR OF NORTH AMERICA

Introduction

The heteromorphic ammonite *Baculites* Lamark 1799 and other members of the Baculitidae are among the most distinct, yet common Late Cretaceous molluscs. They were especially prominent during the Campanian and Maastrichtian globally. Morphologically, this ammonite clade is characterized by gradually expanding, straight to slightly curved, orthoconic conchs that terminate in an aperture with prominent dorsal and ventral lappets (Fig. 7.1A; Larson et al., 1997; Klinger and Kennedy, 2001). Baculitidae also vary greatly in adult size from a few centimeters in a small number of species to over one meter in length among most species (Larson et al., 1997; Jagt et al., 2003; Machalski and Heinberg, 2005, Landman et al., 2007). They are revered for their biostratigraphic utility, which results from a combination of their short temporal ranges (i.e., 500–900 ka) as well as their abundance in a wide variety of marine facies (Klinger and Kennedy, 2001).

Despite extensive knowledge of their biostratigraphy, biogeography, ecology, and biology (e.g., Klinger and Kennedy, 2001; Kruta et al., 2011; Klug, 2012; Westermann, 2013), relatively little is known concerning the evolutionary relationships among the various described species that comprise this important clade. To date, only Klinger and Kennedy (2001) have proposed a hypothesis for the evolutionary relationships among baculitid genera, whereas three

reviews have briefly discussed the phylogeny of various *Baculites* species in the Western Interior and Gulf Coastal Plain of North America (i.e., Kennedy,1977; Cobban, 1993; Klinger and Kennedy, 2001). Knowledge of a clade's phylogenetic relationships is critical for many reasons including: understanding a group's evolutionary tempo and mode, distinguishing endemic evolutionary lineages from more geographically widespread ones, as well as identifying migrant/emigrant species in various regions.

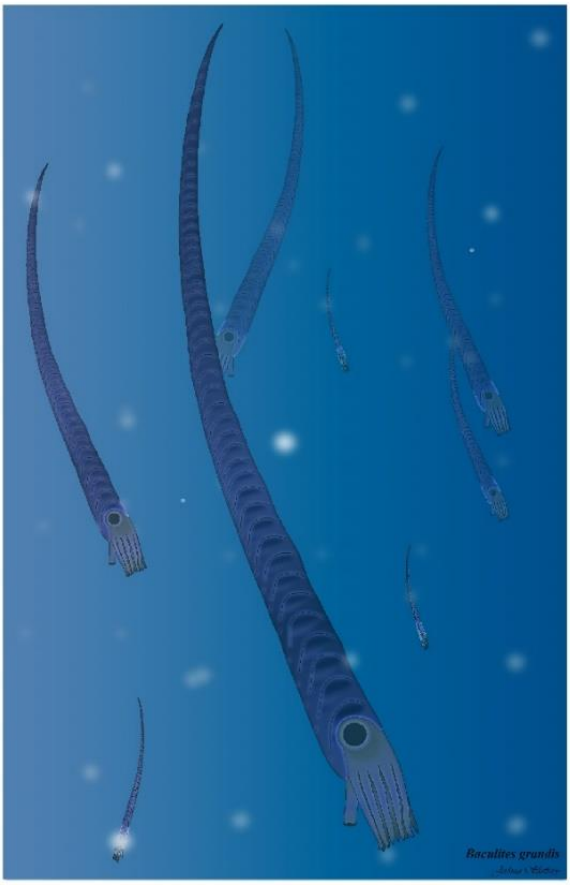

Figure 7.1. Reconstruction of living *Baculites grandis* Hall and Meek1854 in the Western Interior Seaway during the early Maastrichtian (~70.6 Ma). Baculitid arm length and shape are speculative, whereas large eyes and number of arms are based on Klug et al. (2012) and Klug et al. (2015), respectively.

One reason there has been no attempt to phylogenetically analyze the various *Baculites* species is likely related to their simple shell morphology that limits the number of obvious characters and is further compounded by numerous instances of morphologic homoplasy between species in terms of basic shape (Klinger and Kennedy, 2001; Yacobucci, 2012; Bardin et al., 2014). These features that complicate determining evolutionary relationships are common among many molluscan groups and other phyla, which results in their being poorly constrained phylogenetically because of their limited character suite. This has resulted in numerous studies (e.g., Newell and Boyd, 1975; Mikesh, 1988; Wingard, 1993) devoted to reconstructing fossil molluscan phylogenies using a combination of biostratigraphic distributions and personal opinions on species relations to infer evolutionary relationships, while not applying more modern and less subjective cladistic approaches. Most studies that have analyzed molluscan phylogenies cladistically have usually only defined clades at taxonomically higher levels (e.g., Ponder and Lindberg, 1997; Moyne and Neige, 2004; Stoger et al., 2013), whereas only a handful have been undertaken at the species level (e.g., Landman et al., 1989; Bardin et al., 2017).

Thus, the goal of this study will be to test whether a group, such as *Baculites*, that possesses relatively few apparent characters can be used to effectively reconstruct the evolutionary relationships among its constituent species. Therefore, this study focuses on determining evolutionary the relationships among the Campanian and Maastrichtian *Baculites* from the Western Interior Seaway using a cladistic approach. This region's *Baculites* fauna was chosen because they are the primary index fossils used for this interval and are among the best-known ammonites from both traditional taxonomic and biostratigraphic perspectives (e.g., Cobban et al., 2006). This study will also compare its phylogenetic results with the earlier, pre-cladistic reconstructions of *Baculites* evolutionary relationships developed by Kennedy (1977),

Cobban (1993), and Klinger and Kennedy (2001) (Fig. 7.3). Specifically, this chapter will test if there were endemic Western Interior *Baculites* lineage(s) as well as to identify the evolutionary role of migrant/emigrant stocks into the Western Interior Seaway during the last 15 Ma of the Late Cretaceous.

Background on Baculitidae

Baculitids are among the most widely distributed and abundant heteromorphic ammonites in the Cretaceous (Gill and Cobban, 1966, 1973; Larson et al., 1997). They range from the lower Albian to the top of the Maastrichtian and possibly into the lowest Danian directly above the Cretaceous–Paleogene (K–Pg) boundary (Larson et al., 1997; Klinger and Kennedy, 2001; Jagt et al., 2003; Machalski and Heinberg, 2005, Landman et al., 2007). *Baculites*, a cosmopolitan genus (Klinger and Kennedy, 2001), ranges from the base of the Turonian to the top of Maastrichtian and consists of the most common species of the family. However, most of its constituent species are regionally endemic, which limits their biostratigraphic utility for global correlation. However, they are used on a regional basis in many instances, including for the North American Pacific Coast, Western Interior, and Gulf/Atlantic Coastal Plains, as biostratigraphic index fossils for the Campanian and Maastrichtian (e.g., Cobban et al., 2006; Ward et al., 2012; Chapter Two).

At first glance baculitids appear to have comparatively simple shells with few defining characters; however, closer examination reveals substantial variation in morphology. Most variation is reflected in differences among curvature, taper, taper angle, ornamentation, aperture shape, cross-sectional shape, and sutures (Fig. 7.2A–C; Gill and Cobban, 1966; 1973; Larson et al., 1997). Despite this great morphological variation, most baculitid species have been traditionally defined by only a small combination of characters (i.e., typically two to five

characters), with their evolutionary relationships being mostly based on their biostratigraphic ranges and one or two characters as chosen by individual investigators. In contrast to previous work on baculitids, this study used as many characters and character states as possible to produce a robust phylogeny that was independent of biostratigraphic ranges. To do this, baculitids and their traits were examined in detail, which resulted in the identification of a greater number of characters than used in any previous study of this group.

Baculites were likely nektic planktivores that inhabited the middle to upper portions of the water column in open-shelf and epeiric seas (Fig. 7.1; Westermann, 1996; Tsujita and Westermann, 1998; Kruta et al., 2011). This life habit is suggested by light stable isotope evidence from well-preserved Western Interior and Gulf Coastal Plains specimens, which show values that differ from benthic molluscs (Tourtelot and Rye, 1969; Wright, 1987; Tsujita and Westermann, 1998; He et al., 2005; Sessa et al., 2015). It is also based on their shell morphology, inferred poor motility and shell orientation during life, evidence of predation by nektic marine vertebrates (e.g., fish, reptiles), and broad facies distribution (Westermann, 1996; Tsujita and Westermann, 1998; Slattery, 2011; Slattery et al., 2018). This life-habit is also supported by their jaw and radula structures as well as probable remains of their prey, which indicate a preference for feeding on small plankton (e.g., planktic gastropods and crustaceans) rather than larger benthic prey (Kruta et al., 2011). Slattery et al. (2018) showed that juvenile *Baculites* typically preferred shallow-water habits, whereas larger mature individuals preferred more offshore settings with relatively deeper-water conditions.

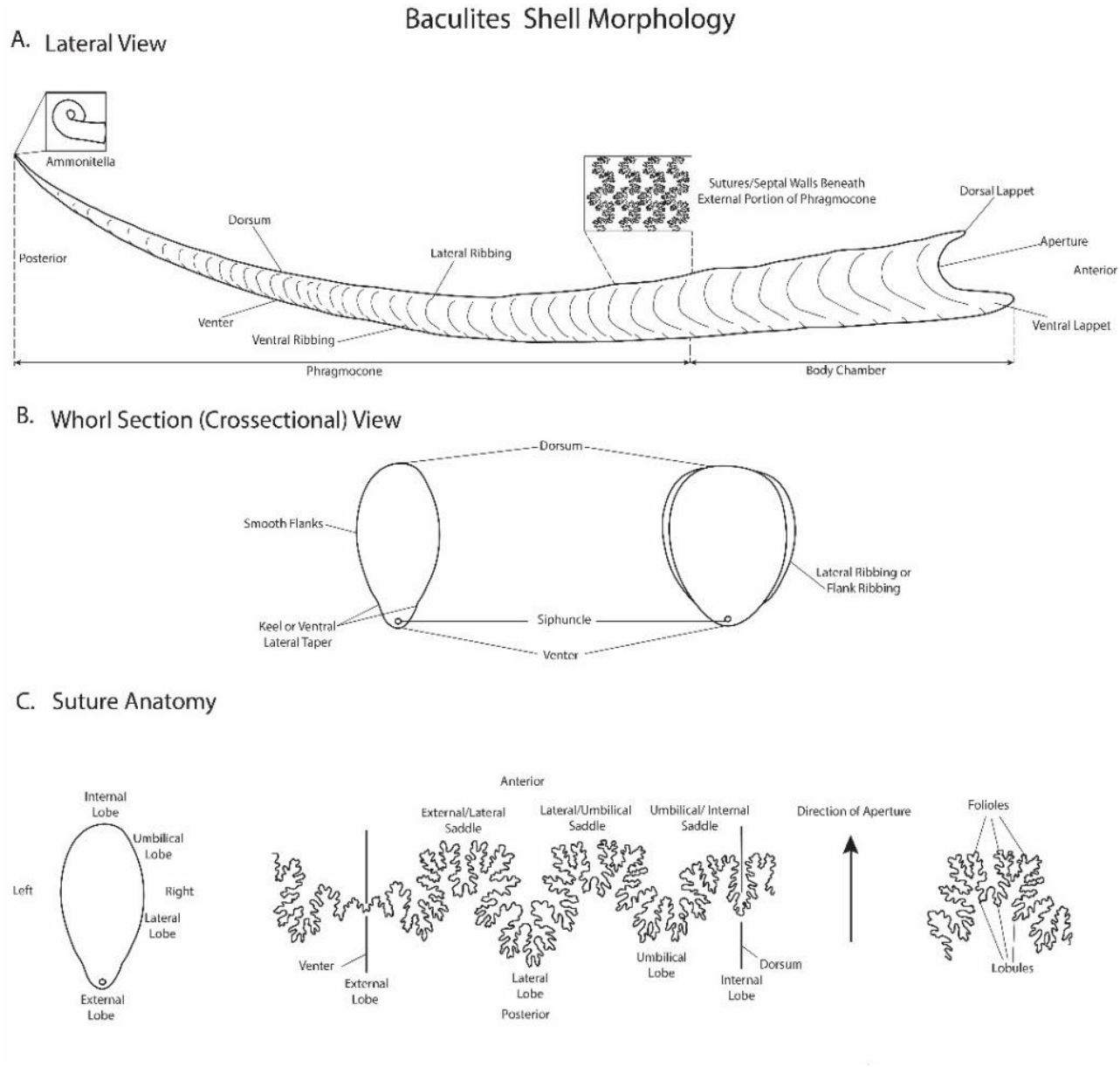

Figure 7.2. The shell and suture element terminology for *Baculites.*

Geological and Paleogeographic Setting

The specimens used in this study were primarily collected from the Cretaceous of the Western Interior. These strata are represented by thick monotonous successions of shale, siltstone, and sandstone that contain numerous concretionary horizons (Slattery et al, 2018). Many of these concretions are fossiliferous and are the primary source of well-preserved

Baculites (e.g., Landman and Klofak, 2012; Landman et al., 2015; Slattery et al., 2018). These concretionary horizons are thought to reflect weakly defined flooding surfaces (i.e., parasequence boundaries) due to fourth- or fifth-order sea-level rises (Elder et al., 1994; McMullen et al., 2014; Slattery et al., 2018). At many localities, *Baculites* are found loose in the shale, where they are either lithified and well-preserved or unlithified and crushed (e.g., Slattery et al., 2018).

This Upper Cretaceous succession was deposited in the Western Interior Foreland Basin (WIFB), a north-south oriented depression that covered the central part of North America from the middle Jurassic to the earliest Paleocene (Kennedy, 1977; Kauffman and Caldwell, 1993; DeCelles, 2004; Fuentes et al., 2009; 2011; Slattery et al., 2015). This basin was bounded to the west by an actively rising cordilleran fold-thrust belt and to the east by the stable cratonic part of eastern North America. During the late Early Cretaceous, the WIFB became flooded in association with elevated global sea levels and temperatures forming the Western Interior Seaway (WIS; Fig. 7.3, Kaufman and Caldwell, 1993; Slattery et al., 2015). This shallow (<100 m depth) epeiric sea stretched from the Arctic Ocean to the Gulf of Mexico and persisted for ~42 Ma (Slattery et al., 2018). Beginning in the Campanian and continuing into the Paleogene, the WIFB began to break into smaller basins that were delimited by structural uplifts related to the Laramide Orogeny (DeCelles, 2004). This switch in the tectonic regime along with a drop eustasy resulted in the final transgression of the WIS, which finally drained from the interior of the continent by the early Paleocene (Slattery et al., 2018).

Figure 7.3. Middle Campanian (*Baculites obtusus* age) paleogeographic reconstruction of North America showing the distribution of land and sea (modified from Slattery et al., 2015). Shaded areas represent land.

Background on Western Interior *Baculites*

In the Western Interior, Campanian and Maastrichtian baculitids are represented by 37 identified species belonging to four genera (Fig. 7.4). Approximately 33 of these species are assigned to *Baculites* (Fig. 7.4A), whereas the four remaining species are placed in *Pseudobaculites* Cobban 1952, *Trachybaculites* Cobban and Kennedy 1995, and *Criobaculites* Klinger and Kennedy 1997 (Fig. 7.4B; Kennedy et al., 1998; Klinger and Kennedy, 2001). Most of these species are endemic; however, a small number of these species co-occur in the Gulf and Atlantic Coastal Plains in low abundances (e.g., Cobban, 1993; Kennedy and Cobban, 1994). A total of 17 *Baculites* species are used to define discrete biozones for the Campanian and Maastrichtian of the Western Interior, which span most of this interval (Klinger and Kennedy, 2001). The average duration of these biozones is ~700 ± 200 ka, which is relatively short compared to 2.0 ± 0.5 Ma ranges of *Baculites* biozones for the Pacific Coast and Gulf/Atlantic Coastal Plains.

Despite its exceptional fossil record, relatively little work has been done on the evolutionary relationships of *Baculites*. Most phylogenetic hypotheses about this genus are based on stratigraphic occurrences, biogeography, and various authors' personal opinions. Traditionally, middle Campanian and Maastrichtian *Baculites* species in the Western Interior have been separated into a long-lived endemic anagenetic lineage (Fig. 7.5A; i.e., *B. compressus* Say 1821, *B. eliasi* Cobban 1958), a lineage of migrant species from the Atlantic and Gulf of Mexico (e.g., *B. texanus* Kennedy and Cobban, 1999, *B. undatus* Stephenson 1941) that eventually established a distinct early Maastrichtian endemic lineage (Fig. 7.5B; e.g., *B. baculus* Meek and Hayden 1861–*grandis* Hall and Meek 1854–*clinolobatus* Elias 1933), and a late Maastrichtian fauna with uncertain affinities (Fig. 7.5C; e.g., *B. larsoni* Cobban and Kennedy

1992). The endemic lineage of Western Interior *Baculites* is thought to have initiated when individuals migrated into the seaway during the Turonian (i.e., *B. yokoyamai* Tokunaga and Shimizu 1926) where they evolved into different species up to the end of the Campanian when they became extinct (Kennedy and Cobban, 1976; Kennedy, 1977; Cobban, 1993). These endemic species are occasionally associated with species that belong to stocks that had their primary range in the Atlantic and Gulf Coastal Plains. These species, including *B. texanus, B. undatus*, and an early form of *B. baculus*, are thought to have migrated into the seaway from the Atlantic and Gulf of Mexico shelves. *Pseudobaculites* also appeared in the Western Interior during *B. jenseni* Cobban 1962b to *B. eliasi* time and is considered to have been the only baculitid to migrate into the WIS from the north (Cobban, 1993; Cobban and Kennedy, 1994). These migrant species, which are typically rare to uncommon, never fully established a major population in the Western Interior during the Campanian (Cobban, 1993). This, however, changed with the extinctions of the long-lived endemic lineage at the end of the Campanian and the appearance of abundant *B. baculus* during the early Maastrichtian. *Baculites baculus* is thought to have established a new lineage in the Western Interior, which persisted until the end of the early Maastrichtian (Cobban, 1993).

This *Baculites* lineage was then thought to be replaced by *Trachybaculites*, *Criobaculites*, and two new *Baculites* species during the late Maastrichtian (Fig.7.4; Cobban and Kennedy, 1992; Kennedy et al., 1998; Landman and Cobban, 2003; Larson pers. comm., 2012). These taxa are relatively small (i.e., whorl diameters < 2.5 cm) compared to earlier species. However, the undescribed smooth species found in the *Hoploscaphites nebrescensis* Biozone in South Dakota is known to have relatively large whorl diameters (Kennedy et al., 1999). These late Maastrichtian baculitids are not well known from both biostratigraphic and evolutionary

perspectives due to their rarity in the Western Interior fossil record. This is especially true for the diminutive *B. larsoni*, which is only known from a small number of specimens from South Dakota (Fig. 7.5C).

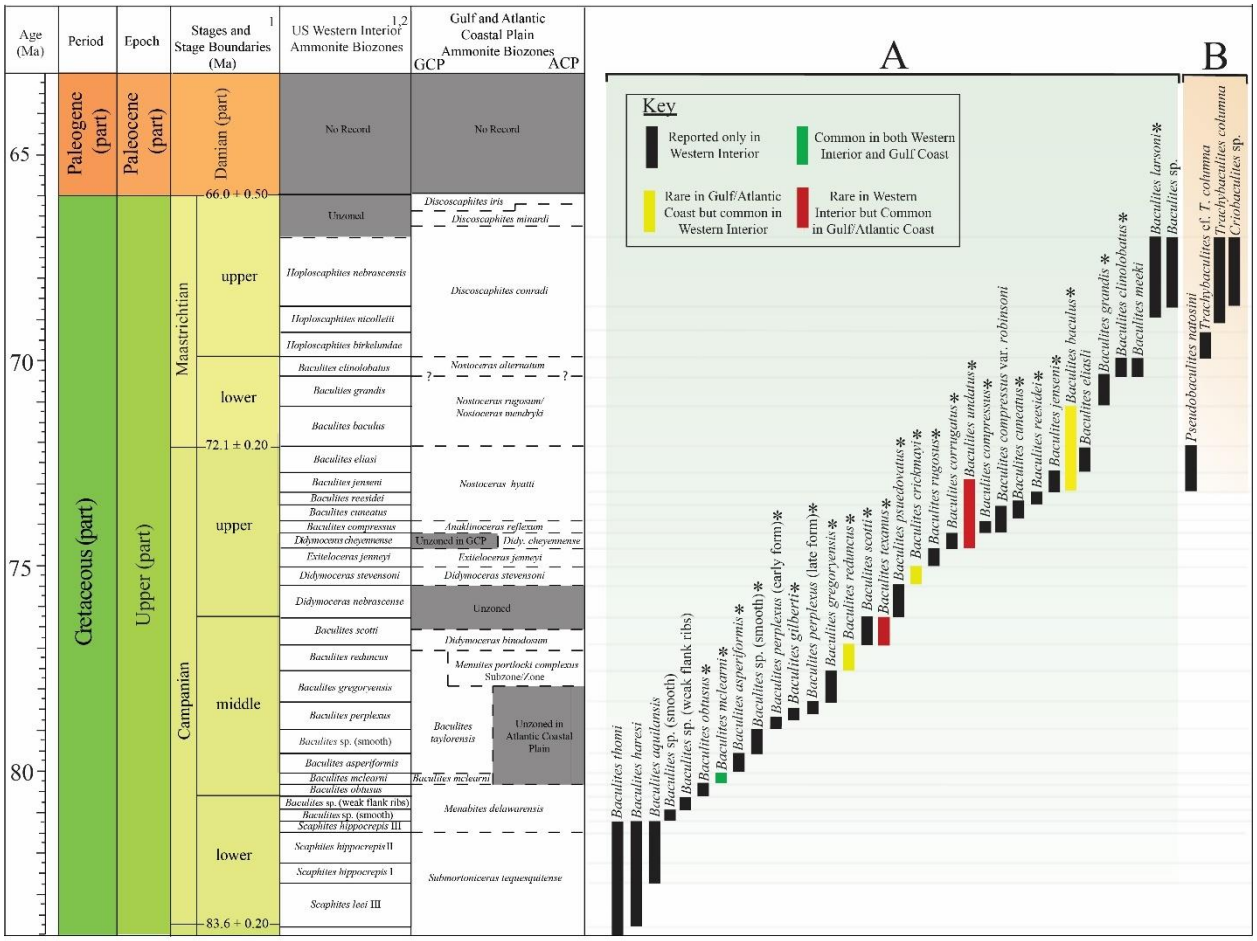

Figure 7.4. Documented ranges for Campanian and Maastrichtian *Baculites* (A) and closely related baculitid genera (B) (baculitid ranges based on Elias, 1933; Gill and Cobban, 1966; 1973; Cobban and Kennedy, 1992; Larson et al., 1997; Kennedy et al., 1998; Klinger and Kennedy, 2001). Species with * next to them represent species analyzed in this study.

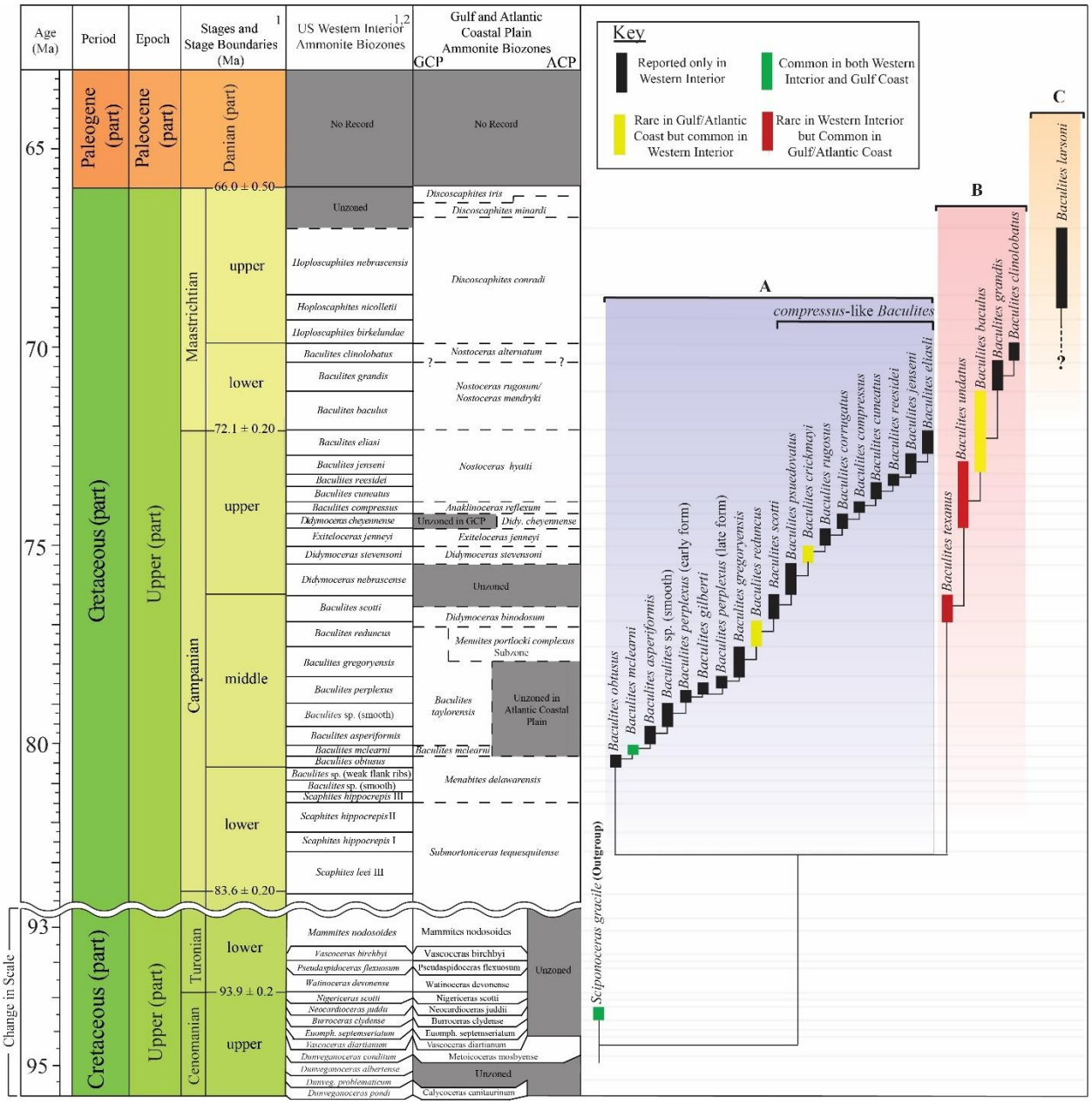

Figure 7.5. Pre-cladistic hypothesis for the evolutionary relationships of the Baculites species analyzed in this study (evolutionary relationships based on Cobban, 1993; Klinger and Kennedy, 2001; Baculites ranges based on Elias, 1933; Gill and Cobban, 1966; 1973; Cobban and Kennedy, 1992; Larson et al., 1997; Kennedy et al., 1998; Klinger and Kennedy, 2001).

Data

Ingroup Selection

This study focused on 25 *Baculites* species from the middle Campanian to upper Maastrichtian of the Western Interior. These species were chosen because they are abundant, well-preserved, and well-defined in literature (e.g., Cobban, 1962a,b; Larson et al., 1997). Pre-middle Campanian species as well as members belonging to *Pseudobaculites, Criobaculites*, and *Trachybaculites* (see Cobban and Kennedy, 1992, 1994; Larson et al., 1997; Landman and Cobban, 2003) were excluded from this analysis due to a paucity of specimen for study. *Baculites compressus* var. *robinsoni* Cobban 1962b and *B. meeki* Elias 1933 were also excluded from this analysis due to a lack of available samples for study. Finally, a relatively large, undescribed upper Maastrichtian *Baculites* species known from the Pierre Shale in South Dakota and Nebraska was omitted due to the paucity of well-reserved specimens and the inability to effectively determine this taxon's character states (Kennedy et al., 1998).

The morphology of most of these species were described and coded from examination of specimens, including type specimens, in museum/repository collections and from published studies. Most of the specimens in the former span the middle Campanian to lower Maastrichtian and were collected from outcrops exposed in the Black Hills, Front Range of Colorado, Middle Park Basin, Laramie Basin, and central Montana. Museums/repositories visited for this study include: the National Museum of Natural History, the United States Geological Survey Denver Mesozoic Collection, the American Museum of Natural History, Yale Peabody Museum of Natural History, Mississippi Museum of Natural Science, and Florida Museum of Natural History. Published literature (i.e., Hall and Meek, 1855; Williams, 1930; Elias, 1933; Landes, 1940; Stephenson, 1941; Cobban, 1951; 1958; 1962a; b; 1973; 1977; 1990; Gill and Cobban,

1966; 1973; Cobban and Kennedy, 1992; Cobban et al., 1993; Larson et al., 1997; Kennedy and Cobban, 1999a; Klinger and Kennedy, 2001) was used to primarily collect data related to suture traces, taper angles, and cross sections.

Outgroup Selection

Because *Baculites* is a sister group of *Sciponoceras* Hyatt 1894 (Klinger and Kennedy, 2001), one upper Cenomanian member of the latter family was selected as the outgroup: *Sciponoceras gracile* Shumard 1860. This taxon was chosen because it is well-known from morphologic, biostratigraphic, and biogeographic perspectives (Klinger and Kennedy, 2001).

Character Argumentation

Sereno's (2007) format for character argumentation (i.e., the structure for composing written characters) was followed here for describing characters and character states. Each character statement is written as: primary locator, secondary locator, variable, and variable qualifier character states. The 'primary' and 'secondary locators' are terms that are utilized to specify a character's general and specific location or configuration on a shell, respectively. The 'variable' defines the part of a character that changes, whereas the 'variable qualifier' is a phrase that qualifies the 'variable' and is typically optional. Variables are not written out for presence-absence characters because they describe morphological structures that either exist or not.

Characters

A total of 55 characters were utilized for the data matrix, which included 31 continuous (see Table7.1) and 24 discrete characters (see Table 7.2). These 55 characters consist of 20 sutural, 13 shell ornamentation, five shell cross-sectional-shape, 12 shell shape, and five shell aperture-shape elements (Table 7.1; Fig. 7.2A-C). Several of these characters are defined ontogenetically, such that they are subdivided into juvenile (~20–30 mm adoral whorl heights)

and mature forms (i.e., 40–50 mm adoral whorl heights). For the diminutive *B. larsoni*, which only reaches a maximum size of 10 mm at maturity, the minimum height for juveniles was set as 6 mm. This cutoff was chosen because it corresponds to the size where septal crowding (i.e., a proxy for maturity in ammonites; Seilacher, 1988) was noted in available specimens. Most of the characters included in this study were derived from fragments, often relatively large portions, of *Baculites* because nearly complete specimens are extremely rare in the fossil record. The data for continuous characters was primarily collected using calipers as well as the National Institute of Health shareware program FIJI (i.e., an enhanced version of ImageJ) to measure characters on physical specimens and photographs of specimens with scale bars, respectively.

Table 7. 1 Continuous characters for Western Interior baculitids. Measurement for certain continuous characters shown in Figures 7.6, 7.7, 7.9, and 7.10A

Sutures Line Characters:

0. External lobe, length (B–B') relative to anterior-most width (A–A'): Continuous (B–B/A– A')

1. External/lateral lobule, length D–D'') relative to anterior-most width (C–C'): Continuous (D–D"/C- C')

2. External/lateral folio, length (D–D') relative to total exterior lateral lobe length (D–D"): Continuous (D–D'/D–D")

3. External/lateral saddle central lobule, length (F–F'') relative to anterior-most width (E–E'): Continuous (F–F"/E–E')

4. Lateral lobe folio, length (G–G') relative to total lateral lobe length (G–G""): Continuous (G–G'/G–G"")

5. Lateral lobe, length (G–G"") relative to anterior-most width (H–H'): Continuous (G–G'/H–H')

6. Lateral lobe, medial constriction length (G–G"') relative to medial constriction width (I–I'): Continuous (G–G'/I–I')

7. Lateral lobe, posterior constriction length (G–G"), relative to posterior constriction width (J–J'): Continuous (G–G'/J–J')

8. Lateral/umbilical saddle central lobule, length (L– L"), relative to anterior-most width (K–K'): Continuous (L–L"/K–K')

9. Umbilical lobe, length (N–N") relative to anterior-most width (M–M'): Continuous (N–N"/M–M')

Table 7.1 Continued Continuous characters for Western Interior baculitids. Measurement for certain continuous characters shown in Figures 7.6, 7.7, 7.9, and 7.10A

10. Lateral lobe folio, length (N–N') relative to total lateral lobe length (N–N"): Continuous (N–N'/N–N")

11. Ornam Umbilical lobe, medial constriction length (N–N") relative to medial constriction width (O–O'): Continuous (N–N"/O–O')

12. Umbilical/internal saddle lobule, length (P–P'), relative to anterior-most width (Q–Q'): Continuous (P–P'/ Q–Q')

13. Internal lobe, length (R–R') relative to anterior-most width (S–S'): Continuous (R–R'/S–S')

Ornamentation Characters:

14. Flank ribbing, mature form: number per whorl diameter: Continuous

15. Flank ribbing, juvenile form: number per whorl diameter: Continuous

16. Ventral ribbing, mature: number per whorl diameter: Continuous

17. Lateral ribbing, prominence: Continuous (W2–W1)/2

18. Ventral ribbing, prominence: Continuous (H1–H2)

19. Lateral ribbing, height relative to total height: Continuous (L1/L3)

Shell Cross-section Shape Characters:

20. Shell, whorl-section: height (H1) relative to width at widest point (W1): Continuous

Shell Shape:

21. Shell, anteroposterior taper (mature): Continuous

22. Shell, taper angle (mature): Continuous

23. Shell, anteroposterior Taper: (juvenile): Continuous

24. Shell, taper angle (juvenile): Continuous

25. Shell, curvature along length arc angle (mature): Continuous

26. Shell, curvature along length arc angle (juvenile): Continuous

27. Shell, maximum size: (whorl height in mm): Continuous

Shell Aperture and Body Chamber:

28. Dorsal lappet, length versus height: Continuous (B–B'/A–A')

29. Ventral lappet, length versus height: Continuous (C–C'/A–A')

30. Body chamber, length (C–C') relative to adoral height (A–A'): Continuous (C–C'/A–A')

Table 7.2. Discrete characters for Western Interior baculitids. Examples for certain discrete characters shown in Figures 7.2, 7.8, and 7.10B.

Sutures Line:

31. Suture, degree of incision: Smooth (0), Convoluted (1) Suture Lines
32. Shell lobe shape: Quadrate (0), Triangular (1), Subquadrate (2)
33. Umbilical lobe, medial folio position relative to posterior constriction: Same height (0), Above (1), Below (2)
34. Umbilical lobe posterior constriction: Unconstricted (0), Partial constriction (1), Constricted (2)
35. Lateral lobe, posterior saddle constriction: Absent (0), Present (1)
36. Lateral lobe, medial saddle constriction: Absent (0), Present (1)

Ornamentation:

37. Flank ornamentation shape mature: Inclined (0), Node-like arcuate (1), Arcuate (2)
38. Flank ornamentation shape juvenile: Inclined (0), Arcuate nodes (1), Node-like arcuate (2)
39. Ventral ornamentation shape: Circum peripheral (0), Weak corrugated (1), Corrugated (2), Undulations (3)
40. Ventral ornamentation shape: Circum peripheral (0), Weak corrugated (1), Corrugated (2), Undulations (3)
41. Flank ribbing, mature: Present (0), Absent (1)
42. Flank ribbing, juvenile: Present (0), Absent (1)
43. Ventral ribbing, mature: Present (0), Absent (1)
44. Ventral ribbing, juvenile: Present (0), Absent (1)

Shell Cross-section Shape:

45. Shell, cross-section shape mature: Circular (0), Stout ovate (1), Sub-elliptical (2), Compressed Ovate (3), Compressed (4), Trigonal (5)
46. Shell, cross-section shape juvenile: Circular (0), Moderately Ovate (1), Ovate (2), Compressed ovate (3), Elliptical (4)
47. Shell, cross-section, venter shape: Rounded (0), Flattened (1)
48. Shell, cross-section, dorsum shape: Rounded (0), Flattened (1)
49. Shell, dorsal-lateral taper: Present (0), Absent (1)
50. Shell, ventrolateral taper: Present (0), Absent (1)
51. Shell, keel: Present (0), Absent (1)

Shell Shape:

52. Shell, curvature along length, mature: Present (0), Absent (1)
53. Shell, curvature along length, juvenile: Present (0), Absent (1)

Table 7.2 Continued. Discrete characters for Western Interior baculitids. Examples for certain discrete characters shown in Figures 7.2, 7.8, and 7.10B.

Shell Aperture:
54. Dorsal lappet, shape: Flared (0), Straight (1)
55. Ventral lappet, shape: Broad (0), Attenuated (1)

Out of the 20 sutural characters, there were 14 continuous and six discrete characters (Table 7.1 and 7.2). The continuous characters are represented by aspect ratios (i.e., height-to-width ratios) of various saddles, lobes, lobules, and folioles on the sutures (Fig. 7.6). The discrete characters are represented by high vs. low incision (i.e., smooth suture line vs. convoluted suture line), lobe and saddle shapes, as well as lobules and folioles constriction characters. Sutural character data was primarily collected from suture tracings in the published species descriptions (e.g., Cobban, 1962a,b; 1977). All but one of the *Baculites* species analyzed have at least one suture tracing. However, when multiple tracings were available, measurements were made on each one and averaged to account for variation. Although the sample size of most suture tracings are represented by only one to three examples, they are usually relatively similar, which suggests that one of a small number of tracings are adequate at characterizing the species. *Baculites gilberti* Cobban, 1962 was the only one to have an incomplete trace, which was due to the preservation of the original type material.

Shell ornamentation characters are represented by 14 continuous and six discrete characters (Table 7.1 and 7.2). The data were primarily collected directly from specimens or from photographs. Discrete shell ornamentation characters include the presence-absence of ventral and lateral ribbing (see Fig. 7.2A) in both juvenile and mature stages as well as the shape of lateral and ventral ribs. Continuous ornamentation characters are represented by the number of ventral ribs per adoral whorl height, number of lateral ribs per adoral whorl height, lateral

ribbing prominence, ventral ribbing prominence (i.e., the width of a single rib), and lateral ribbing height relative to adoral whorl height (Fig. 7.7).

Shell cross-section characters include one continuous character and four discrete characters (Table7.1 and 7. 2). The data were collected using published cross-section traces, in the various species description (e.g., Cobban, 1962a;b; Larson et al., 1997), photographs, and actual specimens. Continuous cross-section characters are only represented by the shell cross adoral whorl width:adoral whorl height ratios (Fig. 7.7). Discrete cross-section characters include the shape, cross-venter shape, cross-dorsum shape, presence-absence of shell dorsal-lateral taper, presence-absence of ventral-lateral taper, and presence-absence of a keel (Figs. 7.2B and 7.8).

The 12 shell shape characters are comprised of seven continuous and five discrete characters, and the data were primarily collected using photographs and published information on ontogenetic changes in shell curvature as well as taper angles. The continuous characters are represented by juvenile and mature anteroposterior taper angles, juvenile and mature anteroposterior tapers, juvenile and mature shell curvature angles, and shell size (Fig. 7.9). Discrete shell ornamentation characters are represented by the presence-absence of a keel, shell dorsal-ventral taper, as well as juvenile and mature shell curvatures (Fig. 7.2).

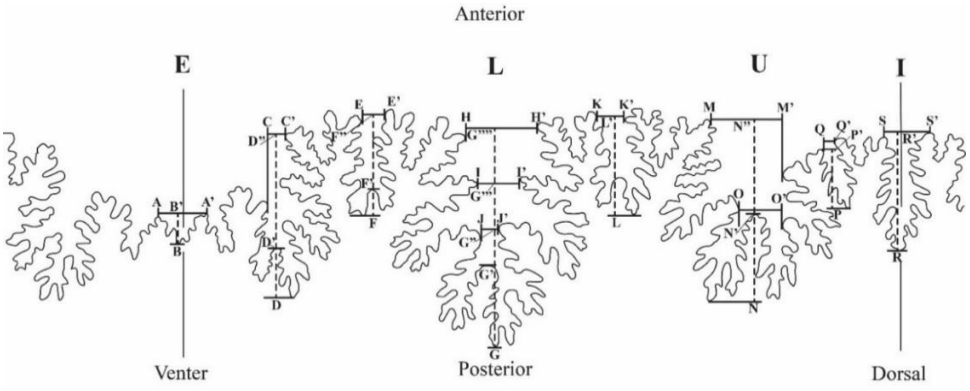

Figure 7.6. Guide for measurements taken on *Baculites* suture tracings for continuous characters 0–13. See Table 1 for character argumentation.

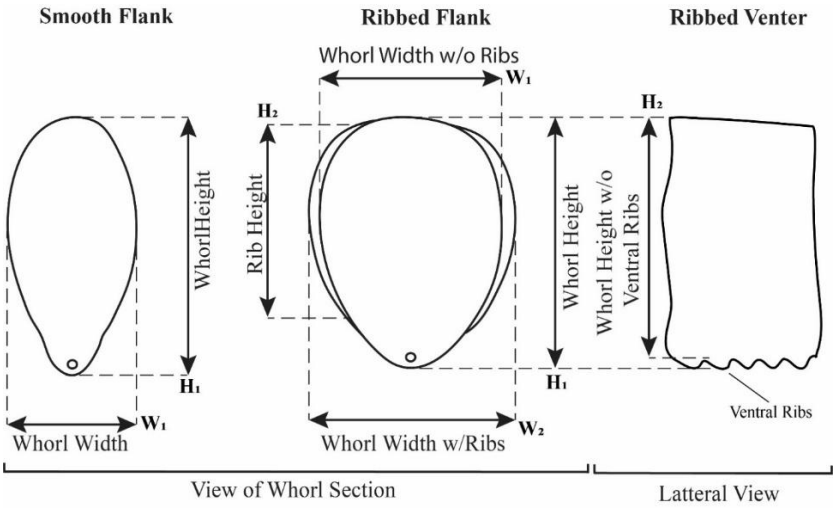

Figure 7.7. Measurements for baculitid shell whorl section and ornamentation continuous character for smooth and ribbed varieties. See Table 7.1 for character argumentation.

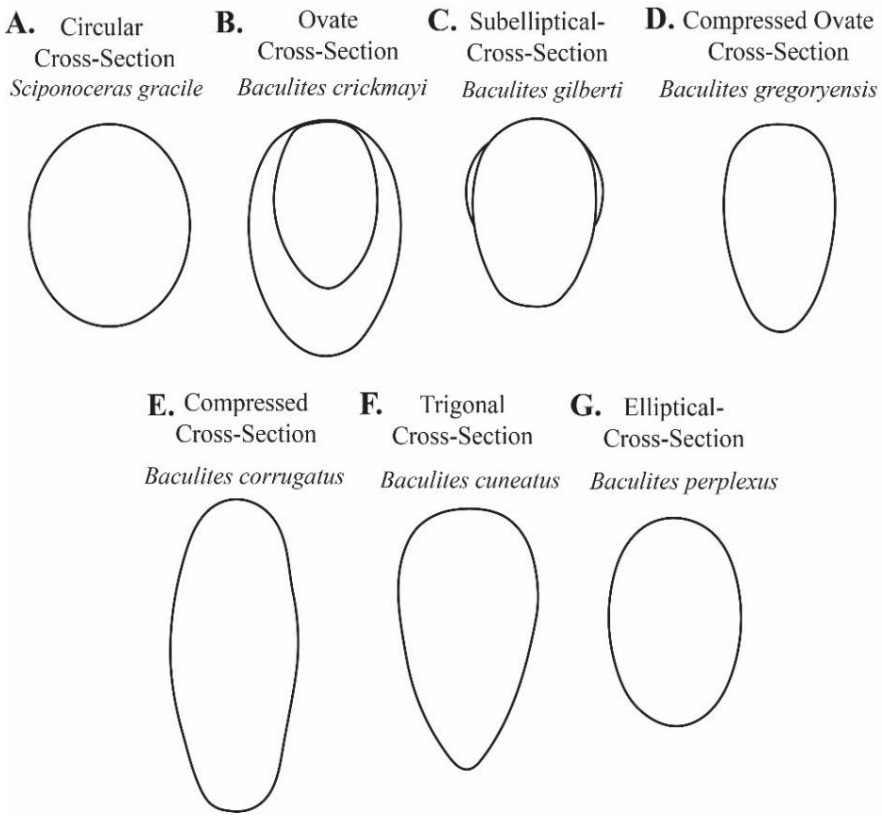

Figure 7.8. Baculitid shell cross section character states. See Table 7.2 for character argumentation.

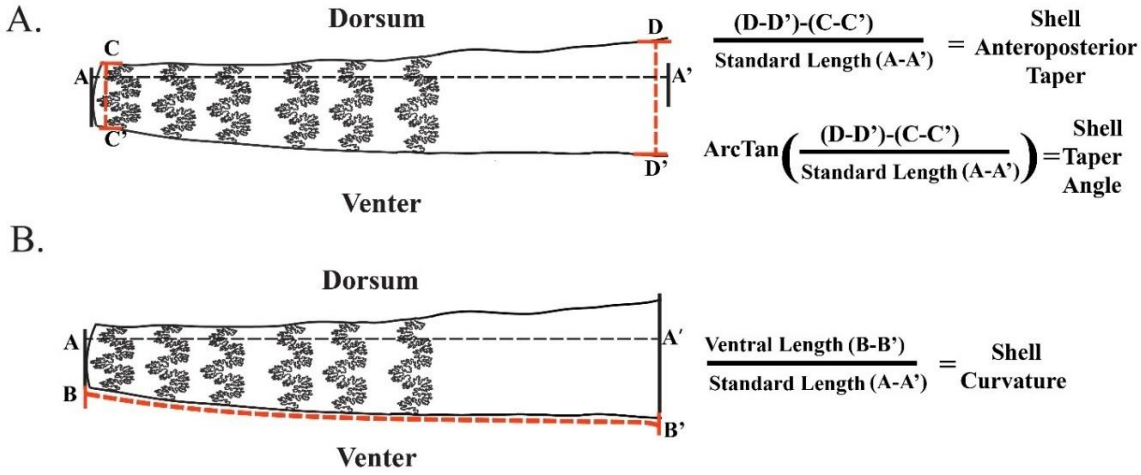

Figure 7.9. Measurements and equations for continuous characters for shell shape, including shell taper (A), taper angle (A), and shell curvature (B). See Table 7.1 for character argumentation.

Shell aperture and body chamber characters include three continuous characters and two discrete. The former includes dorsal lappet length/height and ventral lappet length/height, and body chamber length/adoral height ratios (Fig. 7.10A), whereas the latter are represented by dorsal and ventral lappet shapes (Fig. 7.10B). Complete apertures and body chambers in *Baculites* are rare; as a result, these were the most challenging characters to gather data for and only 25% of the species analyzed in this study have data for these.

Phylogenetic Analysis of Character Matrix

A character matrix was erected for the species (Table 7.1 and7.2; also see Appendix D) in the software program Excel and the software program TNT v1.5 (Tree Analysis using New Technology; Maddison and Maddison, 2008; Goloboff et al., 2008; Goloboff and Catalono, 2016) was used to undertake the parsimony analysis. Character data were all equally-weighted. Continuous character data were scaled to unity (i.e., all were normalized to a scale ranging from 0 to 1). Intraspecific variation was accounted for by utilizing

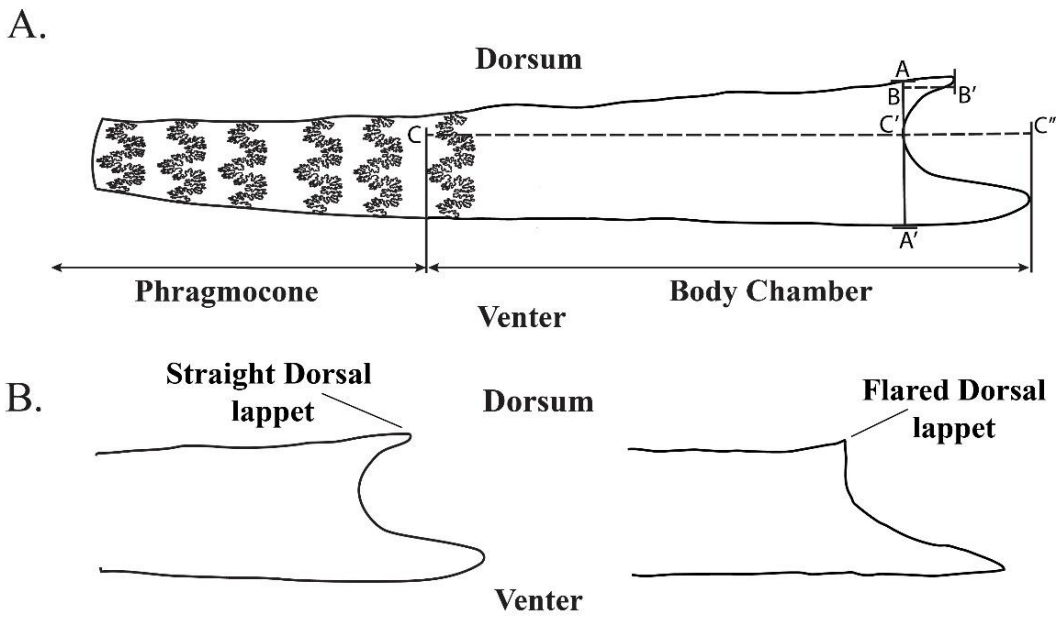

Figure 7.10. Baculitid shell aperture and body chamber continuous (A) and discrete characters (B). See Tables 7.1 and 7.2 for character argumentation.

polymorphic coding, which places two or more-character states within brackets (e.g., [01] for character state 0 and 1 when both are present in a species). Inapplicable character states (i.e., missing or weakly expressed characters) were coded by denoting them with a question mark (?) in the continuous partition and a dash (-) in the discrete partition (i.e., reductive coding). The parsimony analysis was executed in TNT using the following commands:

Nstates stand; HOLD 50000; COLLAPSE auto; MULT= replic 2000 keepall; BEST.

These commands performed a basic tree-search analysis with 2,000 Random Addition Sequence replicates followed by a branch swapping phases using both Tree Bisection and Rerooting as well as Subtree Pruning and Regrafting. The ‘Nstate stand’ command automatically scaled the continuous character data, whereas Hold 50000 set the number of equally parsimonious trees to be retained the during search. Parsimony settings for the tree search did not utilize ambiguous branch support and zero-length branches were automatically collapsed. The resulting phylogenetic trees were then filtered for the best scores.

Descriptive measures were also calculated in TNT for the phylogenetic tree of middle Campanian to upper Maastrichtian *Baculites*. These 'support' measures included the consistency index (CI) and retention index (RI) (Kluge and Farris, 1969; Farris, 1989). The CI measures how well character data fits the tree, whereas RI measures how groupings of characters fit the formation of a tree. These indices were calculated using the Stats.run script available at the PhyloWiki website (http://phylo.wikidot.com/tntwiki#toc2).

Results

The phylogenetic analysis of the middle Campanian to late Maastrichtian *Baculites* in the Western Interior produced a single most parsimonious tree (Fig. 7.11). The tree has 190.25 steps with a CI of 0.36 and RI of 0.54. The taxa distribution within the tree has excellent biostratigraphic congruence, and there are only two apparent inconsistencies between the tree and the documented species' ranges. The first incongruence is associated with *B. reduncus* Cobban, 1977, which plots on the tree prior to the older *B. gregoryensis* Cobban 1951. This second incongruence is associated with the late Maastrichtian *B. larsoni*, which plots closer on the tree closer to outgroup (i.e., *Sciponoceras*) from the late Cenomanian.

The basal-most taxon is the late Maastrichtian *B. larsoni*. The next branch of the tree is represented by middle Campanian to early Maastrichtian species (Fig. 7.11, clade A), which are characterized by two clades (AI and 11AII) united by various sutural characters, their cross-sectional shapes, and sizes (Table 7.3). Clade AI is characterized by early middle Campanian species, whereas the other, AII, is represented by late middle Campanian to early Maastrichtian species. Most of the species comprising these clades are endemic to the WI. However, six species (i.e., *B. mclearni*, *B. reduncus*, *B. crickmayi*, *B. texanus*, *B. undatus*, and *B. baculus*) are known to occur in the WI as well as in the Gulf and Atlantic coastal plains.

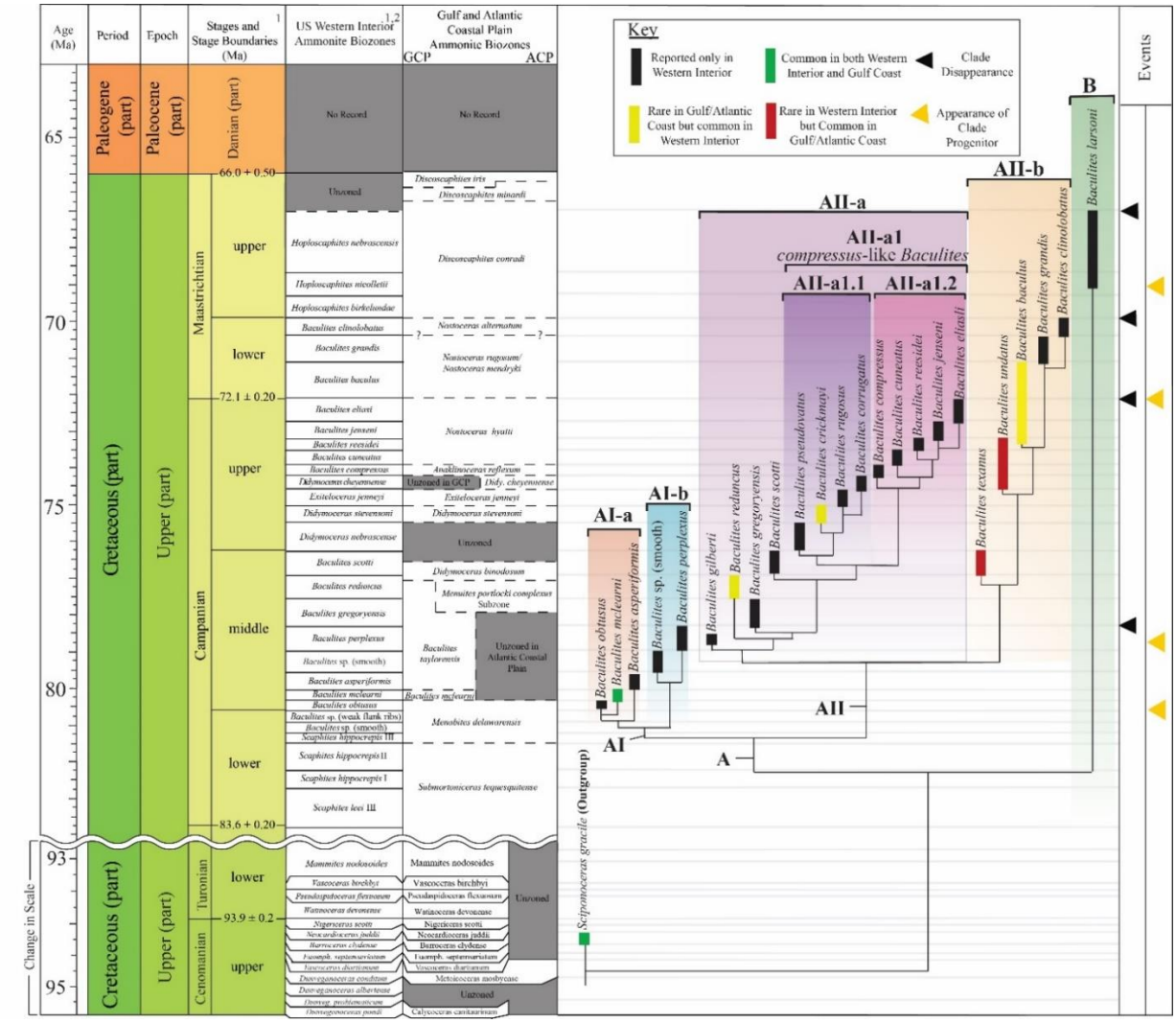

Figure 7.11. The single most parsimonious tree from the phylogenetic analysis of middle Campanian to late Maastrichtian *Baculites* of the Western Interior (*Baculites* ranges based on Elias, 1933; Gill and Cobban, 1966; 1973; Cobban and Kennedy, 1992; Larson et al., 1997; Kennedy et al., 1998; Klinger and Kennedy, 2001).

Table 7.3. List of characters supporting each baculitid clade described in text and shown in Figure 7.11. Character argumentation for each character shown in Tables 7.1 and7. 2.

Node Number	Characters
A	3, 5, 8, 11, 12, 13, 20, 27, 31, 34
AI	19, 21, 22, 45, 54
AI-a	17, 37, 38, 47
AI-b	0, 3, 7, 8, 12, 20, 46
AII	4, 10, 23
AII-a	3, 16, 20, 33
AII-a1	4, 7, 27, 28, 35
AII-a1.1	0, 44
AII-a1.2	0, 7, 9, 20, 27, 28, 45
AII-b	9, 18, 29, 37, 39
B	0, 1, 3, 4, 7,8 ,9, 10, 11, 12, 13, 21, 22, 27, 33, 41, 42, 43

The basal-most branch of the tree is represented by *B. larsoni* from the upper Maastrichtian Fox Hills Formation in South Dakota (B). This branch retains many sutural characters found in the outgroup and in juveniles (see Table 7.3 for defining characters).

The second basal-most clade (AI) is split into two subclades defined by lower middle Campanian species (AI-a and AI-b). The species in this clade typically are moderate in size for *Baculites*, have quadrate sutures, and, except for *Baculites* sp. (smooth), have prominent flank and ventral ornamentation (see Table 7.3 for diagnostic characters). The older subclade consists of (from oldest to youngest) *B. obtusus*, *B. mclearni*, and *B. aperiformis*, whose most distinguishing character are their prominent, node-like flank ribbing that is present through most of their ontogeny. The second and slightly younger subclade consists of *Baculites* sp. (smooth) and *B. perplexus*.

The AII clade is also divided into two subclades (AII-a and AII-b), which are represented by late middle Campanian to early Maastrichtian *Baculites*. The species in the AII-a subclade typically have triangular sutures, substantial variation in ornamentation, and are moderate to

large (see Table 7.3 for defining characters). The late middle Campanian species in this subclade are successive sister groups of the late Campanian species (AII-a1 or the *compressus*-like *Baculites*), which is divided into early late and late late Campanian *Baculites* (AII-a1.1 and AII-a1.2). These two late Campanian subgroups correspond to Cobban's (1962) *compressus*-like *Baculites*, which he united based on the basal constriction of the first lateral lobe's terminal branches. The AII-b clade consists of Campanian migrant species from the Gulf of Mexico and early Maastrichtian species endemic to the Western Interior, with the exclusion of *B. baculus*. The species in this subclade typically have quadrate to subquadrate sutures, prominent flank ornamentation, weak ventral ornamentation, and have moderate-to-large sizes for Baculites (see Table 7.3 for defining characters). This subclade includes (from oldest to youngest) *B. texanus*, *B. undatus*, *B. baculus*, *B. grandis*, and *B. clinolobatus*.

Discussion

Interpretation of Stratigraphic Congruence

The evolutionary history of *Baculites* is derived from both their temporal distributions and their character-based phylogenetic relationships (Wills et al., 2008). Both are independent sources, which provide information about evolutionary rates and evolutionary relationships among *Baculites*, respectively. However, due to phylogenetic assumptions about rooting and evolutionary models as well as temporal margins of error with species ranges, each requires interpretation (Benton and Hitchin, 1997; Wills, 2002; Wills et al., 2008). As such, it is practical to compare the order of taxa on a tree topology with their biostratigraphic ranges (Norell and Novacek, 1992; Benton and Hitchin, 1997; Wills, 1998; Clyde and Fisher, 1997; Angielczyk and Fox, 2006; Pol and Norell, 2006; Wills et al., 2008). Doing so can offer mutual corroboration, which can be assumed to reflect the accurate, underlying evolutionary pattern of the group.

However, where the topology conflicts with the temporal order, additional evidence is required to determine which reconstruction most closely reflects evolutionary reality (Wills, 2007).

The excellent concordance between the tree topology and temporal ranges of *Baculites* suggests strong mutual corroboration for both sources. Therefore, there is strong evidence that the resultant phylogenetic tree reflects the true, underlying evolutionary history of *Baculites* in the WIS during the middle Campanian to late Maastrichtian. This exceptional concordance is likely related to the relatively robust fossil record of *Baculites* in this basin, which is due to the exceptional exposures and sampling of Cretaceous marine faunas in this region for the purpose of biostratigraphy. For example, the United States Geological Survey Denver Collection, which was largely developed by William A. Cobban and his various collaborators, contains ammonites from more than ~3000 Campanian and Maastrichtian localities in the Western Interior (i.e., from New Mexico to Montana). This excellent stratigraphic and geographic sampling has resulted in a relatively robust fossil record, especially compared to other regions globally.

The only species that do not show congruence between their branching pattern on the phylogenetic tree and their ranges are *B. reduncus* and *B. larsoni*. For *B. reduncus*, it is not clear whether this conflict reflects its true evolutionary relationship or whether it is caused by its currently documented stratigraphic range. If this minor incongruence is a result of its true evolutionary relationship, then it could be caused by either a homoplasy or descent from a cryptic taxon that has not yet been discovered. However, *B. reduncus* is only known from a small number of nearshore localities in Wyoming and Colorado, which has resulted in a poor understanding of its true biostratigraphic and biogeographic range (Cobban, pers. Comm., 2002). This has led to the suggestion that *B. reduncus* could also potentially overlap in age or be isochronous with *B. gregoryensis* (Cobban, pers. Comm.).

The placement of the late Maastrichtian *B. larsoni* as the basal-most branch on the phylogenetic tree is peculiar but is likely the result of its distinct character suite. This taxon is the most diminutive Western Interior *Baculites* species included in this analysis and has a suture pattern with limited incision (i.e., least convoluted pattern). These characteristics are found in the earliest baculitid species as well as in early growth stages of larger *Baculites* (i.e., small sizes, sutures with low incision). This suite of characteristics suggests three possibilities: 1) *B. larsoni* is a juvenile; 2) it belongs to a lineage that retains ancestral characteristics; or 3) it is a progenetic species. Evidence that *B. larsoni* is not a juvenile is indicated by septal crowding (Landman, 2018, pers. comm.). This feature has been identified as signifying maturity in various ammonoids (Hölder, 1952; Seilacher, 1988), and it suggests that this taxon reached maturity at very small sizes. The second explanation would require a ghost lineage to explain this pattern, which seems unlikely as Campanian and Maastrichtian *Baculites* with similar primitive character suites in the Western Interior and across the globe are unknown. The more likely explanation is that this pattern reflects progenesis, which is type of paedomorphosis (i.e., the retention of ancestral juvenile traits in the mature descendant) where individuals in the species reach maturity at an earlier growth stage (Gould, 1977; Fink, 1982). Progenesis has been documented in numerous ammonite species and clades in both space and time (e.g., Kennedy, 1977; Landman, 1988; Landman et al., 1991; Yacobucci, 2016). Diminutive forms of baculitids, such as *B. lomaensis*, *Trachybaculites columna*, and *Eubaculites latecarinatus*, are especially common in North America during the late Maastrichtian as compared to earlier time intervals (e.g., Kennedy and Cobban, 1993; 2000; Landman et al., 2004; 2007). This suggests that evolutionary pressures during this interval in North America were selecting for progenetic forms that reached maturity at earlier growth stages.

Paedomorphic species can complicate a phylogenetic analysis due to the retention of juvenile and ancestral characters, which makes it difficult to reconstruct their true evolutionary relationship with other species. Complicating this issue is the fact that juvenile characters are usually weakly developed compared to characters on mature forms, which makes them difficult to evaluate or measure. Several juvenile characters were included in this analysis (e.g., presence-absence of lateral or ventral ribbing); however, most characters were defined for mature forms of *Baculites*. Examination of strictly juvenile characters would likely produce a more accurate representation of the 'true' evolutionary relationship between *B. larsoni* and all other *Baculites* included in this analysis. For example, it could potentially reveal that *B. larsoni* belongs to one of the Campanian or early Maastrichtian clades analyzed in this study rather than its own separate evolutionary branch. However, since *B. larsoni* is so small (i.e., <10 mm whorl diameter), a better comparison would require the smallest growth stages of most *Baculites*, which was not available in the collection analyzed in this study.

Interpretation of Tree Topology and Comparison with Pre-Cladistic View

The tree topology of the middle Campanian to late Maastrichtian *Baculites* in the WI both supports and rejects various elements of the pre-cladistic perspective on their evolutionary relationships (compare Figs. 7.5 and 7.11). As noted above, these species were traditionally divided into a long-lived (i.e., Turonian to Campanian) endemic lineage and a separate lineage composed of migrants from the Gulf of Mexico, which were hypothesized to eventually established a new early Maastrichtian endemic lineage following the extinction of the older endemic lineages at the end-Campanian (e.g., Gill and Cobban, 1966; Kennedy, 1977; Cobban, 1993). This traditional view also suggests that when the early Maastrichtian endemic lineage

went extinct at the beginning of the late Maastrichtian, they were replaced by several new baculitids, including *B. larsoni*.

Here, the tree topology shows that the middle Campanian to early Maastrichtian *Baculites* all belong to the same major clade. This tree topology suggests, in contrast to the pre-cladistic view, that species traditionally placed into the long-lived endemic lineage instead belong to two different but closely related clades (i.e., AI and AII-a). The excellent stratigraphic congruence within each clade and subclade indicates that these potentially represent separate evolutionary lineages.

The tree topology also supports the view that migrant species during the Campanian (i.e., *B. texanus, B. undatus*) and early Maastrichtian (*B. baculus, B. grandis, B. clinolobatus*) belong to a single clade (i.e., AII-b). It supports the hypothesis that the migrant species established a new endemic lineage after the latest Campanian endemic stock (i.e., AII-a) went extinct at end of *B. eliasi* time. However, in contrast to the pre-cladistic view, this subclade (i.e., AII-b) likely represents a sister group to the late middle to late Campanian endemic WI subclade (i.e., AII-a).

Evolutionary Interpretation of Phylogenetic Pattern for *Baculites*

The phylogenetic pattern of multiple lineages of *Baculites* in the Western Interior appears to reflect successive extinctions of endemic clades and replacement by new non-endemic stocks. The extinction of the incumbent endemic clade likely opened a niche in the seaway's ecosystem, which was rapidly filled by a new species that was derived from a separate stock of *Baculites.* These progenitor species appeared abruptly in the Western Interior after the extinction of the incumbent stock, which suggests that they migrated into the WIS from an adjacent sea. There is evidence that some progenitor species (e.g., *B. baculus*) and the earlier evolutionary members of their stock persisted alongside the endemic clades as suggested by migrant species (e.g., *B.*

undatus, *B. texanus*). However, these species were never able to establish large reproducing populations in WIS due to competitive exclusion until the incumbent species was eliminated. The close evolutionary relationships and excellent stratigraphic congruency for each species within the different clades suggests that once a progenitor species (e.g., *B. gilberti*, *B. baculus*) was established in the seaway, the evolution of a new endemic *Baculites* lineage proceeded until the next extinction. A similar repeated pattern of invasion, speciation, and extinction was proposed for the evolution of the various subspecies of the trilobite *Eldredgeops rana* from the Devonian epicontinental sea of eastern North America (Eldredge, 1971; Eldredge and Gould, 1972). This pattern is also strikingly similar to Palmer's (1965, 1984) biomere concept, where several biozones that are defined by a successive lineage of species are bounded by an extinction event and a subsequent invasion of taxonomically different, but morphologically similar separate stock that leads to a new lineage of species. This pattern has been documented across the Cambrian of North America.

The process of repeated extinction and replacement of *Baculites* clades provides a parsimonious explanation for why there are rapid and substantial changes in baculitid morphology during the Campanian and Maastrichtian in the Western Interior, which are not as easily explained by a traditional anagenetic model. This rapid change could be explained by punctuated equilibrium, but it is unlikely that several different characters and character states would rapidly evolve to account for the pronounced morphological change noted among certain species at specific times. This is exemplified by the replacement of the large-sized *B. baculus-grandis-clinolobatus* lineage, by the diminuitive late Maastrichtian *Baculites* like *B. larsoni*. In the traditional anagenetic model, the earlier species are required to change several different character states (i.e., decrease size, change cross section shape, adjust various sutural characters)

to evolve into the smooth forms. In the new clade extinction and replacement model, the early Maastrichtian *Baculites* went extinct in the WI and were then replaced by late Maastrichtian forms. This process explains why different morphotypes, like the smooth form, appear and disappear in the Western Interior over several different intervals throughout the early and middle Campanian.

Causes of *Baculites* Clade Extinction

The causes for repeated *Baculites* clade extinction in the WIS remain unknown, although they are likely related to the unique environmental conditions that characterize this epicontinental sea. The WIS, like most epicontinental seas, was relatively shallow over vast areas (i.e., <200 m depth) and geographically restricted due to its location between the western and eastern landmasses of Laramidia and Appalachia, respectively (Kauffman and Caldwell, 1993; Slattery et al., 2015). Based on its setting in a shallow sea that was geographically isolated, the repeated clade extinctions could be due to or associated with a loss of habitat from regression or even temperature change. This is important since epicontinental sea faunas are considered to have been "perched" in that changes in sea-level or temperature would have resulted in the disappearance of habitats, leading to possible extinctions (Johnson, 1974; Stanley, 2010). However, throughout the study interval there are no substantial lithological or associated faunal changes beyond the origination of a new *Baculites* species until the Maastrichtian (e.g., Gill and Cobban, 1966; Slattery et al., 2018). This suggests that during the Campanian and most of the Maastrichtian, there are no apparent major regressions that resulted in even a partial draining of the basin. It also suggests that the elevated temperatures and stable climate regime of the Cretaceous greenhouse would not have been associated with a substantial change in temperatures, which would have extirpated the seaway's fauna. However, it should be noted that

our current knowledge of the Campanian and Maastrichtian in the WI might be too coarse to detect relatively short-term changes in sea level and temperature. Thus, there is the possibility, that rapid changes in sea level and temperature in the Western Interior could have occurred, which remain unrecognized.

The only apparent exceptions to these patterns occur in the Maastrichtian. For example, at the lower and upper Maastrichtian boundary, there is a shift from offshore to nearshore lithofacies, which is correlated with extinction of endemic *Baculites* (i.e., *B. clinolobatus*) and the rapid decline in abundance or extinction of inoceramid bivalves in the Western Interior. The decline of inoceramids has been well-documented and is traditionally explained by a loss of habitat and/or the evolution of new predators (Ward et al., 1991; Ozanne and Harries, 2002; Berry and Lucas, 2017), although, its correlation with the extinction of *Baculites* has remained unstudied. The uppermost Maastrichtian in the Western Interior is also associated with the extinction of *Baculites* and the regions entire marine fauna, however, this is known to be associated with the last major Cretaceous regression of the WIS (Waage, 1968; Gill and Cobban, 1973). In terms of temperature, there is a relatively short-termed cooling event during the earliest Maastrichtian associated with the extinction of the late Campanian *Baculites*, however, for the most part temperatures varied relatively moderately during the greenhouse conditions of the Campanian and Maastrichtian (Barrera, 1994; Miller et al., 1999).

Other factors besides sea level, such as the seaway's geography and oceanography, could have also likely contributed to the repeated clade extinction of *Baculites* during the Campanian and Maastrichtian. For example, the WIS likely had a sluggish circulation regime as well as a susceptibility to substantial inputs of freshwater, sediment, and nutrients from the adjacent landmasses (Hay et al., 1993; Kauffman and Caldwell, 1993; Fischer et al., 1994; Slingerland et

al., 1996; Pagani and Arthur, 1998; Stanley, 2010). In turn, these environmental conditions could have influenced the seaway's stratification, salinity levels, oxygen concentrations, and turbidity levels (Kauffman, 1977; Kauffman and Caldwell, 1993). It is also possible that sea-level rise could have been associated with changes in temperature, which could have gone beyond the habitable tolerance of the endemic species. This hypothesis has been used to explain the causes for biomere boundaries in the Cambrian and could be a potential cause for the extinction of the *Baculites* in the WIS. These various environmental parameters could have played roles in periodically eliminating the endemic *Baculites* inhabiting the water column allowing for their replacements by new stocks from populations that were not influenced by these perturbations.

Biogeographic Origin of Progenitor Species

The origin of progenitor species are likely from adjacent open-shelf seas (i.e., Gulf of Mexico, Arctic Ocean, Atlantic Ocean) and epicontinental seas (i.e., Hudson Seaway) outside the WIS. Additionally, some of these progenitor species were also possibly derived through parapatric evolution along the peripheral margins of the endemic species' geographic range in the seaway as indicated by evidence of morphological variants. There is extensive evidence for marine faunal exchange between the WI and Gulf, Atlantic, Arctic, and Pacific shelves (e.g., Cobban, 1993; Kennedy and Cobban, 1999b). However, in contrast to the U.S. WI, the taxonomy and biostratigraphy of *Baculites* in other regions in North America, with the exclusion of the Pacific Coast (e.g., Ward, 1978; Ward, et al., 2012), are still relatively poorly known due to lack of study and poor preservation/exposure of appropriate age strata in certain areas, which makes the determination of possible ancestral stocks to the WI species difficult.

The best evidence for this model of *Baculites* evolution in the Western Interior comes from *B. texanus* and *B. undatus*, which are Atlantic and Gulf Coast species that belong to the

same clade as the early Maastrichtian WI endemic species *B. baculus*, *B. grandis*, and *B. clinolobatus*. The close evolutionary relationship among these species, biogeographic overlap, and their successive stratigraphic ranges with minimal age gaps suggest that these represent a single lineage. During the middle to late Campanian *B. texanus*, *B. undatus*, and an early form of *B. baculus* periodically migrated into the WIS where they co-existed at low abundances with the incumbent population of endemic *Baculites* (Cobban, 1993). During the end-Campanian with the extinction of *B. eliasi* and its endemic lineage, the early form of *B. baculus* established a permanent population in the WIS (Cobban, 1993). Similarly, Ward, et al. (2015) suggested that the repeated appearance of smooth and weak flank-ribbed *Baculites* in the WI as well as in other parts of the world might represent repeated invasion events by the same long-lived species of *Baculites* that inhabited a broader region outside the interior. Although the early Campanian smooth-forms of WI *Baculites* were not included in this analysis, the clustering of the late form of *Baculites* sp. (smooth) into its own clade supports Wards et al. (2015) interpretation. However, to fully understand their evolutionary relationships a greater number of smooth forms of *Baculites* will have to be included in future phylogenetic analyses of this enigmatic group.

Evolutionary Patterns of *Baculites* Clades in the Western Interior Seaway

The exact pattern (i.e., punctuated vs. gradual) of evolution within each clade of *Baculites* in the seaway is unclear due limitations in the stratigraphic resolution; however, most evidence points to punctuated equilibrium. Most WI *Baculites* species persisted with relatively little morphologic change on time scales ranging from 0.5 to 0.9 Ma (Kennedy and Cobban, 1976). In stratigraphic terms, this usually reflects 10's of meters of section containing several different concretionary horizons (i.e., flooding surfaces or weakly expressed parasequence boundaries) with no apparent change in form (e.g., Gill and Cobban, 1966). The transition

between species appears to have been relatively rapid with most occurring in a few meters from one concretionary horizon to the next overlying concretionary horizon. Due to this rapid stratigraphic transition in *Baculites* species, Gill and Cobban (1966) typically used the mid-point between two concretionary beds to define the top and bottom of one of their ammonite range zones.

There is some evidence for gradualism in *Baculites* in the Western Interior, but it is relatively poorly documented. For example, Gill and Cobban (1966) noted that the concretionary beds near the tops of many *Baculites* range zones contained transitional forms with the overlying species. It is also possible that some of these species were parapatrically evolving along an environmental gradient in the seaway. The best evidence for this is derived from *B. compressus*, which is split into a regular form in the southern Western Interior (i.e., Colorado, South Dakota) and variety (or subspecies) in the northern part (i.e., northern Montana, Alberta, Saskatchewan) of the WI identified as *B. compressus* var. *robinsoni*. This northern variety, although not included here due to a lack of available specimens for study, has a combination of features that it shares with both *B. compressus* and *B. cuneatus* (Cobban, 1962b; Larson et al., 1997). Specifically, this variety has flank ribbing on early growth stages and a trigonal cross section, which are found in *B. cuneatus* but not in *B. compressus* (Cobban, 1962b). This pattern suggests that morphological features that define *B. cuneatus* originated in the *B. compressus* population that inhabited the northern part of the WIS.

The case of morphologically similar *Baculites* in other parts of the globe

Several authors have noted that morphologically similar species of *Baculites* to those found in the WI appear relatively contemporaneously in other parts of North America and across the globe during the Campanian. These species have been typically assigned to different species

based on their geography, biostratigraphic position, and occasionally by one or a small number of defining characters. For example, morphologically similar smooth species are known to occur in the WI, Pacific, Gulf Coast, Japan, South Africa, and Chile during the early and early middle Campanian (Bookstein and Ward, 2013; Ward et al., 2015). In certain regions, such as the WI, these smooth species are known to repeatedly appear and disappear throughout this interval (e.g., Gill and Cobban, 1973). Another example is the appearance of *B. reduncus* in the Western Interior and *B. rex* in the Pacific Coast during the late middle Campanian. Cobban (1977) noted that these two species share comparable sizes, curvatures, tapers, and suture patterns with only minor differences in their ornamentation. One last example is the occurrence of *B. compressus* and *B. cuneatus* in the WI relatively contemporaneously with the morphologically similar *B. occidentalis* in the Pacific Coast.

These various examples of morphologically similar species occurring in different parts of the world relatively contemporaneously can be explained by three competing hypotheses, including: 1) homoplasy between unrelated species, 2) globally distributed species, and/or 3) that they are closely related species that possibly belong to the same clade. In the pre-cladistic model, which views endemic species as belonging to separate anagenetic lineages, these morphological similarities among different *Baculites* that lived relatively contemporaneously in the different parts of the world relies upon convergence among unrelated stocks to explain these similarities. This model, however, seems unlikely because of the limited possibility that two or more unrelated species in different parts of the globe would evolve a similar morphology during a relatively narrow window of time. Alternatively, as originally proposed by Ward et al., (2015), these taxa could be synonymous and belong to the same widespread species with most of the morphological differences reflecting variance due to their broad geographic distributions. Their

scenario, however, relies on a very broad definition of the species concept, which would lump several species together based on only a small number of characters (e.g., cross-section, lateral lobe complexity). As noted above, many of these species look quite similar, but without analyzing a broader array of characters it is difficult to argue that these are truly the same species. In addition, many of the species that they suggest are potentially synonymous, based on a small number of characters, also display apparent morphological, temporal (although moderate), and geographic differences, which would traditionally be utilized to define separate species rather than to unite them. These differences suggest that these *Baculites*, instead of reflecting widely geographically distributed synonymous taxa, actually reflect separate species that belong to closely related clades.

Broader Paleobiological Implications

The intriguing results of this study suggest that the use of stratigraphic ranges to determine evolutionary records cannot solely provide an accurate understanding of a taxa's evolutionary history. This is an especially important consideration for many paleobiological studies, which only use taxic ranges to examine long-term evolutionary patterns. As exemplified here, much of a groups accurate evolutionary history can only be revealed through detailed phylogenetic analysis. For example, without phylogenetics it would still be assumed that the long succession of middle Campanian to late Maastrichtian *Baculites* in the WI reflect one or two long-lived anagenic lineage rather than four clades, which were shaped by multiple extinction and replacement events. This is especially important for ammonites and other fossil invertebrates, which have been relatively phylogenetically neglected due to their limited number of apparent characters and homoplasy (Neige et al., 2007; Yacobucci, 2012; Bardin et al., 2014). Without a phylogenetic context, many evolutionarily critical patterns might be going

unrecognized, whereas meaningless patterns in the species range data might be over emphasized in current literature.

As exemplified here, the use of continuous character data can result in a much more robust characters matrix for fossil molluscs, which can be used to understand their hidden evolutionary history. This type of study needs to be applied to a broader range of non-vertebrate groups in the Western Interior to determine if the clade extinction and replacement proposed here for *Baculites* was also occurring in other groups and at similar times. Finally, future analysis needs to include a broader range of *Baculites* species from different regions to better define their evolutionary relationships and patterns.

Conclusion

- The phylogenetic analysis of the middle Campanian to late Maastrichtian *Baculites* in the WI produced a single most parsimonious tree. This tree shows excellent stratigraphic congruence, which strongly supports it reflecting the accurate, underlying evolutionary relationships among *Baculites* in the region.
- The tree topology of the middle Campanian to late Maastrichtian *Baculites* in the WI both broadly supports and rejects some components of the pre-cladistic view on their evolutionary relationships.
- The tree shows two branches of *Baculites,* with one spanning the middle Campanian to early Maastrichtian and the other occurring only in the late Maastrichtian. The first branch is composed of single major clade that is characterized by two clades with multiple subclades each. The second major branch is represented by the diminutive *B. larsoni* from the upper Maastrichtian nearshore deposits of the Fox Hills Formation in South Dakota.

- This phylogenetic pattern and biostratigraphic ranges reflects three successive extinctions of endemic lineages and replacement by three unrelated species. These new species or progenitor species evolved into new, short-lived endemic lineages. The causes for repeated clade extinction are unknown, however, they are likely related to the unique environmental conditions of an epicontinental sea.
- The origin of progenitor *Baculites* species are likely from the adjacent open-shelf (e.g., Gulf Shelf) and epicontinental seas (e.g., Hudson Seaway).
- This evolutionary pattern documented here for *Baculites* resembles Palmer's (1965; 1984) biomere concept that has been documented in different groups in the Paleozoic.
- The intriguing results of this study suggest that a greater number of invertebrate groups, which have typically been assumed to have too limited character suite, can be analyzed to establish a robust phylogeny with a careful analysis of various features. The resulting phylogenetic patterns can be utilized to reveal the hidden evolutionary history of a chosen group as exemplified here for *Baculites*.

References

Angielczyk, K. D., and D. L. Fox. 2006, Exploring new uses for measures of fit of phylogenetic hypotheses to the fossil record: *Paleobiology*, 32,147–165.

Bardin, J., Rouget, I. and Cecca, F., 2014, Cladistics in ammonoids: back to the future: *Neues Jahrbuch für Geologie und Paläontologie-Abhandlungen*, 274, 239–253.

Bardin, J., Rouget, I., and Cecca, F., 2017, The phylogeny of Hildoceratidae (Cephalopoda, Ammonitida) resolved by an integrated coding scheme of the conch: *Cladistics*, 33, 21–40.

Benton, M. J., and R. Hitchin. 1997, Congruence between phylogenetic and stratigraphic data on the history of life: *Proceeding of the Royal. Societies London B Biolology.* 264, 885–890.

Barrera, E., 1994, Global environmental changes preceding the Cretaceous-Tertiary boundary: Early-late Maastrichtian transition: *Geology*, 22, 877–880.

Berry, K. and Lucas, S.G., 2018, An astropectinid sea star from the early Maastrichtian Pierre Shale in southern Colorado: *USA, and the extinction of the inoceramid bivalves: Neues Jarbruch für Geologie und Paläontologie–Abhandlungen*, 286, 1–10.

Bookstein, F.L., and Ward, P.D., 2013, A modified Procrustes analysis for bilaterally symmetrical outlines, with an application to microevolution in *Baculites*: *Paleobiology*, 39, 214–234.

Clyde, W. C., and Fisher, D. C., 1997, Comparing the fit of stratigraphic and morphologic data in phylogenetic analysis: *Paleobiology*, 23, 1–19.

Cobban, W. A., 1951, New species of *Baculites* from the Upper Cretaceous of Montana and South Dakota: *Journal of Paleontology* 25, 817–821.

Cobban, W. A., 1958, Two new species of *Baculites* from the Western Interior region: *Journal of Paleontology*, 32, 660–665.

Cobban, W.A., 1962a, *Baculites* from the lower part of the Pierre Shale and equivalent rocks in the Western Interior: *Journal of Paleontology*, 36, 704–718.

Cobban, W.A., 1962b, New *Baculites* from the Bearpaw Shale and equivalent rocks of the Western Interior: *Journal of Paleontology*, 36, 126–135.

Cobban, W.A., 1973, The Late Cretaceous cephalopod *Baculites undatus* Stephenson in Colorado and New Mexico: *United States Geological Survery Journal of Research*, 1, 459–465.

Cobban, W.A., 1977, A new curved baculite from the Upper Cretaceous of Wyoming: *Journal of Research of the United States Geological Survey*, 5, 457–462.

Cobban, W.A., 1990, Ammonites and some characteristic bivalves from the Upper Cretaceous Frontier Formation, Natrona County, Wyoming: *Bulletin of the UnitedStates Geological Survey 1917–B*, 1–13.

Cobban, W.A., 1993, Upper Cretaceous ammonite diversity in the Western Interior Seaway, *in* Caldwell, W.G.E., and Kauffman, E.G., eds., *Evolution of the Western Interior Basin: Geological Association of Canada Special Paper*, 39, 297–318.

Cobban, W.A., and Kennedy, W.J., 1992, The last Western Interior *Baculites* from the Fox Hills Formation of South Dakota: *Journal of Paleontology*, 66, 682–684.

Cobban W.A., and Kennedy, W.J., 1994, A new giant baculite from the Upper Campanian and lower Maastrichtian of the Western Interior: *United States Geological Survey Bulletin*, 2073–C, 1–3.

Cobban, W.A., Kennedy, W.J., and Scott, G.R, 1993, Upper Cretaceous heteromorph ammonites from the *Baculites compressus* zone of the Pierre Shale in north central Colorado: *United States Geological Survey Bulletin*, 2024, 1–11.

Cobban, W.A., Walaszczyk, I., Obradovich, J.D., and McKinney, K.C., 2006, A USGS Zonal Table for the Upper Cretaceous Middle Cenomanian-Maastrichtian of the Western Interior of the United States: *Based on Ammonites, Inoceramids, and Radiometric Ages: United States Geological Survey Open-File Report*, 1240, 50 pp.

DeCelles, P.G., 2004, Late Jurassic to Eocene evolution of the Cordilleran thrust belt and foreland basin system, Western United States of America: *American Journal of Science*. 304, 105–168.

Farris, J.S., 1989, The retention index and the rescaled consistency index: *Cladistics*, 5, 417–419.

Fink, W.L., 1982, The conceptual relationship between ontogeny and phylogeny: *Paleobiology*, 8, 254–264.

Fisher, C.G., Hay, W.W., and Eicher, D. L., 1994, Oceanic Front in the Greenhorn Sea {late middle through late Cenomanian): *Paleoceanography*, 9, 879–892.

Fuentes, F., DeCelles, P.G., Gehrels, G.E., 2009, Jurassic onset of foreland basin deposition in northwestern Montana, USA: implications for along-strike synchroneity of Cordilleran orogenic activity. *Geol. Soc. Am. Bull.* 123, 507–533.

Fuentes, F., DeCelles, P.G., Constenius, K.N., and Gehrels, G.E., 2011, Evolution of the Cordilleran foreland basin system in northwestern Montana, USA: *Geological Society of America Bulletin*, 123, 507–533.

Elder, W.P., Gustason, E.R., Sageman, B.B., 1994, Correlation of basinal carbonate cycle to nearshore parasequences in the Late Cretaceous Greenhorn seaway: Western Interior, USA: *Geolological Society of America Bull*etin, 106, 892–902.

Eldredge, N., 1971, The allopatric model and phylogeny in Paleozoic invertebrates: *Evolution*, 25,156–167.

Elias, M.K., 1933, Cephalopods of the Pierre Formation of Wallace County, Kansas and adjacent area, 289–363.

Gill, J.R., and Cobban, W.A., 1973, Stratigraphy and geological history of the Montana Group and equivalent rocks, Montana, Wyoming, and North and South Dakota: *United States Geological Survey Professional Paper*, 776, 37 pp.

Gill, J.R., and Cobban, W.A., 1966, The Red Bird Section of the Upper Cretaceous Pierre Shale in Wyoming: *United States Geological Survey Professional Paper*, 776, 71 pp.

Goloboff, P. A., Farris, J. S., and Nixon, K. C., 2008, TNT, a free program for phylogenetic analysis: *Cladistics*, 24, 774–786.

Goloboff, P.A. and Catalano, S.A., 2016, TNT version 1.5, including a full implementation of phylogenetic morphometrics: *Cladistics*, 32, 221–238.

Gould, N.E.S.J. and Eldredge, N., 1972, Punctuated equilibria: an alternative to phyletic gradualism, 82-115.

Gould, S.J., 1977, Ontogeny and phylogeny: *Harvard University Press.*, 501 pp.

Hall, J. and Meek, F.B., 1855, Descriptions of New Species of Fossils, from the Cretaceous Formations of Nebraska, with Observations upon Baculites ovatus and B. compressus, and the Progressive Development of the Septa in Baculites, Ammonites, and Scaphites. *Memoirs of the American Academy of Arts and Sciences*, 5, 379–411.

Hay, W.W., Eicher, D.L., and Diner, R, 1993, Physical oceanography and water masses in the CretaceousWestern Interior Seaway, in Caldwell, W.G.E., and Kauffman, E.G., eds., Evolution of the Western Interior Basin: *Geological Association of Canada Special Paper*, 39, 297–318.

He, S., Kyser, T.K. and Caldwell, W.G.E., 2005, Paleoenvironment of the Western Interior Seaway inferred from δ18O and δ13C values of molluscs from the Cretaceous Bearpaw marine cyclothem: *Palaeogeography, Palaeoclimatology, Palaeoecology*, 217, 67–85.

Hölder, H, 1952, Über den Gehäusebau, insbesondere den Hohlkiel jurassischer Ammoniten: *Palaeontol A*, 102, 18–48

Hyatt, A., 1894, Phylogeny of an acquired characteristic: *Proceedings of the American Philosophical Society*, 32: 349-647.

Jagt, J.W.M., Smith, J. and Schulp A. S., 2003, Early Paleocene ammonites and other molluscan taxa from the Angerpoort-Curfs quarry (Geulhem, southern Limburg, the Netherlands): *in* Lamolda, M.A., eds., *Bioevents: their stratigraphical records, patterns, and causes*: *Caravaca*, 113 pp.

Johnson, J.G., 1974, Extinction of perched faunas: *Geology*, 2, 479–482.

Kauffman, E.G., 1977, Geological and biological overview: Western Interior Cretaceous basin: *The Mountain Geologist.*

Kauffman, E.G. and Caldwell, W.G.E., 1993, The Western Interior Basin in space and time, *in* Caldwell, W.G.E., and Kauffman, E.G., eds., Evolution of the Western Interior Basin: *Geological Association of Canada Special Paper*, 39, 1–30.

Klinger, H. C. and Kennedy, W.J., 2001, Stratigraphic and geographic distribution, phylogenetic trends, and general comments on the ammonite family Baculitidae Gill, 1871 (with an annotated list of the species referred to the family): *Annals of the South African Museum*, 107, 290 pp.

Kennedy, W.J., and Cobban, W.A., 1976, Aspects of ammonite biology, biogeography, and biostratigraphy: *The Paleontological Association Special Papers in Palaeontology*, 17, 98 pp.

Kennedy, W.J., 1977, Ammonite evolution. Patterns of evolution as illustrated in the fossil record: *Elsevier*, 251–304.

Kennedy, W.J., and Cobban, W. A., 1999a, Campanian (Late Cretaceous) ammonites from the Bergstrom Formation in central Texas: *Acta Geologica Polonica*, 49, 67–80.

Kennedy, W.J., and Cobban, W.A., 1999b, Pachydiscus (Pachydiscus) hornbyense Jones, 1963, and P.(P.) catarinae (Anderson and Hanna, 1935)(Cretaceous, Campanian: Ammonoidea), Pacific Realm marker fossils in the Western Interior Seaway of North America: *Bulletin de l'Institut Royal des Sciences Naturelles de Belqique, Sciences de la Terre*, 69, 119–127.

Kennedy, W.J. and Cobban, W.A., 1993, Maastrichtian ammonites from the Corsicana Formation in northeast Texas: *Geological Magazine*, 130, 57–67.

Kennedy, W.J. and Cobban, W.A., 2000, Maastrichtian (Late Cretaceous) ammonites from the Owl Creek Formation in northeastern Mississippi, USA: *Acta Geologica Polonica*, 50, 175–190.

Kennedy, W.J. Landman, N.H., Christensen, W.K., Cobban, W.A., and Hancock, J.M. 1999**,** Marine connections in North America during the late Maastrichtian: palaeogeographic and palaeobiogeographic significance of *Jeletzkytes nebrascensis* Zone cephalopod fauna from the Elk Butte Member of the Pierre Shale, SE South Dakota and NE Nebraska: *Cretaceous Research*, 19, 745–775.

Kennedy, W.J., Landman, N.H., Christensen, W.K., Cobban, W.A. and Hancock, J.M., 1998, Marine connections in North America during the late Maastrichtian: Palaeogeographic and palaeobiogeographic significance of Jeletzkytes nebrascensis Zone cephalopod fauna from the Elk Butte Member of the Pierre Shale, SE South Dakota and NE Nebraska, *Cretaceous Research*, 19, 745–775.

Kennedy, W.J. and Cobban, W.A., 1994, Ammonite fauna from the Wenonah Formation (Upper Cretaceous) of New Jersey: *Journal of Paleontology*, 68, 95–110.

Klug, C., Riegraf, W. and Lehmann, J., 2012, Soft–part preservation in heteromorph ammonites from the Cenomanian–Turonian Boundary Event (OAE 2) in northwest Germany: *Palaeontology*, 55, 1307–1331.

Klug, C. and Lehmann, J., 2015, Soft part anatomy of ammonoids: reconstructing the animal based on exceptionally preserved specimens and actualistic comparisons: *in Ammonoid Paleobiology: from anatomy to ecology*, Springer, 507–529.

Kluge, A.G. and Farris, J.S., 1969, Quantitative phyletics and the evolution of anurans: *Systematic Biology*, 18, 1–3.

Kruta, I., Landman, N.H., Rouget, I., Cecca, F., and Tafforeau, P., 2011, The Role of Ammonites in the Mesozoic marine food web revealed by jaw preservation: *Science*, 331, 70–72.

Lamarck, J. P. B. A. de M. de., 1799, Prodrome d'une nouvelle classification des coquilles: *Memoires de la Societe d'Histoire naturelle de Paris* (for 1799): 63-90.

Landes, R. W. 1940, Part 2. Palaeontology of the marine formations of the Montana Group: *Memoirs ofthe Geological Survey of Canada*, 221, 129–223.

Landman, N. H. 1988, Heterochrony in ammonitesin McKinney, M. L. (ed.). Heterochrony *in Evolution. New York, Plenum Press,* 159–182.

Landman, N.H., 1989, Iterative progenesis in Upper Cretaceous ammonites*: Paleobiology*, 15, 95–117.

Landman, N. H., Dommergues, J-L., and Marchand, D. 1991, The complex nature of progenetic species: Examples from Mesozoic ammonites: *Lethaia* 24, 409– 421.

Landman, N.H., Johnson, R.O. and Edwards, L.E., 2004, Cephalopods from the Cretaceous/Tertiary boundary interval on the Atlantic Coastal Plain, with a description of the highest ammonite zones in North America. Part 2. Northeastern Monmouth County, New Jersey: *Bulletin of the American Museum of Natural History*, 107 pp.

Landman, N.H., Johnson, R.O., Garb, M.P., Edwards, L.E., and Kyte, F.T., 2007, Cephalopods from the Cretaceous/Tertiary boundary in New Jersey and Maryland, with a description of the highest ammonite zones in North America. Part 3. Manasquan River Basin, Monmouth County, New Jersey: *Bulletin of the American Museum of Natural History*, 303, 122 p.

Landman, N.H., and Cobban, W.A., 2003, Ammonites from the Upper Part of the Pierre Shale and Fox Hills Formation of Colorado: *AMNH Novitates*, 3388, 24 pp.

Landman, N.H. and Klofak, S.M., 2012, Anatomy of a concretion: life, death, and burial in the Western Interior Seaway: *Palaios*, 27, 671–692.

Larson, N.L., Jorgensen, S.D., Farrar, R.A., and Larson, P.L., 1997, Ammonites and other Cephalopods of the Pierre Seaway: *Geoscience Press*, 97 pp.

Landman, N.H., Grier, J.C., Grier, J.W., Cochran, J.K., Klofak, S.M., 2015, 3–D orientation and distribution of ammonites in a concretion from the Upper Cretaceous Pierre Shale of Montana: *Swiss Journal Paleontol*, 1–23.

Machalski, M., and Heinberg, K., 2005, Evidence for ammonites survival into the Danian (Paleogene) from the Cerithium Limestone at Stevens Klint, Denmark: *Bulletin of the Geological Society of Denmark*, 52, 97–111.

Maddison and Maddison, 2008, Mesquite: a modular system for evolutionary analysis, 2.01.

McMullen, S.K., Holland, S.M., O'Keefe, F.R., 2014, The occurrence of vertebrate and invertebrate fossils in a sequence stratigraphic context: the Jurassic Sundance Formation, Bighorn Basin, Wyoming, USA: *Palaios*, 29, 277–294.

Miller, K., Barrera, E., Olsson, R., Sugarman, P., and Savin, S., 1999, Does ice drive early Maastrichtian eustasy?: Geology, 27, 783–786.

Mikesh, D.L., Glenister, B.F. and Furnish, W.M., 1988, Stenolobulites n. gen., Early Permian ancestor of predominantly Late Permian paragastrioceratid subfamily Pseudogastrioceratinae.

Moyne, S. and Neige, P., 2004, Cladistic analysis of the Middle Jurassic ammonite radiation: *Geological Magazine*, 141, 115–123.

Newell, N.D. and Boyd, D.W., 1975, Parallel evolution in early trigoniacean bivalves: *AMNH Bulletin*, 154, 162 pp.

Neige, P., Rouget, I. and Moyne, S., 2007, Phylogenetic practices among scholars of fossil cephalopods, with special reference to cladistics. *in Cephalopods present and past: new insights and fresh perspectives, Springer*, 3–14.

Norell, M.A. and Novacek, M.J., 1992, Congruence between superpositional and phylogenetic patterns: comparing cladistic patterns with fossil records: *Cladistics*, 8, 319–337.

Ozanne, C.R. and Harries, P.J., 2002, Role of predation and parasitism in the extinction of the inoceramid bivalves: an evaluation: *Lethaia*, 35, 1–19.

Pagani, M., and Arthur, M.A., 1998, Stable isotopic studies of Cenomanian-Turonian proximal marine fauna the U.S. Western Interior Seaway, *in Stratigraphy and Paleoenvironments of the Cretaceous Western Interior Seaway, USA: SEPM concepts in Sedimentology and Paleontology*, 6, 201–225.

Palmer, A.R., 1965, Biomere: A new kind of biostratigraphic unit: *Journal of Paleontology*, 39, 149–153.

Palmer, A.R., 1984, The biomere problem: evolution of an idea: *Journal of Paleontology*, 58, 599–611.

Pol, D., and M. A. Norell. 2006, Uncertainty in the age of fossils and the stratigraphic fit to phylogenies: *Syst. Biol*. 55, 512–521.

Ponder, W.F. and Lindberg, D.R., 1997, Towards a phylogeny of gastropod molluscs: an analysis using morphological characters: *Zoological Journal of the Linnean society*, 119, 83–265.

Shumard, B F, 1860, Descriptions of new Cretaceous fossils from Texas: *Academy Science St Louis Transactions*, 1, 590–510

Seilacher A, 1988, Why are nautiloid and ammonite sutures so different?: *Neues Jahrb Geol Paläontol Abh*, 177, 41–69

Sereno, P.C., 2007, Logical basis for morphological characters in phylogenetics: *Cladistics*, 23, 565–587.

Sessa, J.A., Larina, E., Knoll, K., Garb, M., Cochran, J.K., Huber, B.T., MacLeod, K.G. and Landman, N.H., 2015, Ammonite habitat revealed via isotopic composition and comparisons with co-occurring benthic and planktonic organisms: *Proceedings of the National Academy of Sciences*, 112, 15562–15567.

Slattery, J.S., 2011, Late Cretaceous faunal dynamics in the Western Interior Seaway: The record from the Red Bird Section, eastern Wyoming: University of South Florida Unpublished MS thesis, 119 pp.

Slattery, J.S., Cobban, W.A., McKinney, K.C., Harries, P.J., Sandness, A.L., 2015, Early Cretaceous to Paleocene Paleogeography of the Western Interior Seaway of North America and its relation to tectonics and eustasy: *in* Bingle-Davis, M. Ed., *WGA Field Guide, Cretaceous Conference. Evolution and Revolution,* 22–60.

Slattery, J.S., Harries, P.J. and Sandness, A.L., 2018, Do marine faunas track lithofacies? Faunal dynamics in the Upper Cretaceous Pierre Shale, Western Interior, USA. *Palaeogeography, Palaeoclimatology, Palaeoecology*, 496, 205–224.

Slingerland, R., Kump, L.R., Arthur, M.A., Fawcett, P.J., Sageman, B.B., and Barron, E.J., 1996, Esturine Circulation in the Turonian Western Interior Seaway of North America: *Geological Society of America Bulletin*, 108, 941–952.

Stanley, S.M., 2010, Thermal barriers and the fate of perched faunas: *Geology*, 38, 31–34.

Stephenson, L.W., 1941, The larger invertebrates of the Navarro Group of Texas (exclusive of corals and crustaceans and exclusive of the fauna of the Escondido Formation): *University of Texas Bulletin*, 4101, 641 pp.

Stöger, I., Sigwart, J.D., Kano, Y., Knebelsberger, T., Marshall, B.A., Schwabe, E. and Schrödl, M., 2013, The Continuing Debate on Deep Molluscan Phylogeny: Evidence for Serialia (Mollusca, Monoplacophora: *BioMed Research International*, 2013.

Tourtelot, H.A., and Rye, R.O., 1969, Distribution of oxygen and carbon isotopes in the fossils of Late Cretaceous age, Western Interior region of North America: *Geological Society of America Bulletin*, 80, 1903–1922.

Tsujita, C.J., Westermann, G.E.G., 1998, Ammonoid habitats and habits in the Western Interior Seaway: a case study from the Upper Cretaceous Bearpaw Formation of southern Alberta, Canada: *Palaeogeography, Palaeoclimatology, Palaeoecology*, 144, 135–160.

Waage, K.M., 1968, The type Fox Hills Formation, Cretaceous (Maestrichtian), South Dakota: Part I, stratigraphy and paleoenv ironments: *Peabody Museum of Natural History, Bulletin*, 27, 157 pp.

Ward, P.D., 1978, Baculitids from the Santonian-Maestrichtian Nanaimo Group, British Columbia, Canada and Washington State, USA: *Journal of Paleontology*, 52, 1143–1154.

Ward, P.D., Kennedy, W.J., MacLeod, K.G. and Mount, J.F., 1991, Ammonite and inoceramid bivalve extinction patterns in Cretaceous/Tertiary boundary sections of the Biscay region (southwestern France, northern Spain): *Geology*, 19, 1181–1184.

Ward, P.D., Haggart, J.W., Mitchell, R., Kirschvink, J.L. and Tobin, T., 2012, Integration of macrofossil biostratigraphy and magnetostratigraphy for the Pacific Coast Upper Cretaceous (Campanian–Maastrichtian) of North America and implications for correlation with the Western Interior and Tethys: *Geological Society of America Bulletin*, 124, 957–974.

Ward, P.D., Haggart, J.W., Mitchell, R. and Catlin, E., 2015, Quantitative morphological description of the Late Cretaceous ammonite Baculites inornatus Meek from western North America: implications for species concepts in the biostratigraphically important Baculitidae: *Journal of Paleontology*, 89, 594–610

Westermann, G.E.G, 1996, Ammonoid Life and Habitat, *in* Landman, N.H., Tanabe, K., and Davis, A.G., eds., *Ammonoid Paleobiology: Topics in Paleobiology*, 13, 608–704.

Westermann, G.E.G., 2013, Hydrostatics, propulsion and life-habits of the Cretaceous ammonoid Baculites: *Revue de Paléobiologie*, 32, 249–265.

Wills, M. A. 1998, Crustacean disparity through the Phanerozoic: Comparing morphological and stratigraphic data: *Biolological. Journal of the Linnean Society*, 65, 455–500.

Wills, M. A. 2002, The tree of life and the rock of ages: Are we getting better at estimating phylogeny?: *Bioessays*, 24, 203–207.

Wills, M. A. 2007, Fossil ghost ranges are most common in some of the oldest and some of the youngest strata: *Proceedings of the Royal Societies Lond. B Biol.*, 274, 2421–2427

Wills, M.A., Barrett, P.M. and Heathcote, J.F., 2008, The modified gap excess ratio (GER*) and the stratigraphic congruence of dinosaur phylogenies: *Systematic Biology*, 57, 891–904.

Wingard, G.L., 1993, A detailed taxonomy of Upper Cretaceous and lower Tertiary Crassatellidae in the Eastern United States; an example of the nature of extinction at the boundary (No. 1535).

Williams, M. Y. 1930, New species of marine invertebrate fossils from the Bearpaw Formation of Southern Alberta: *Bulletin National Museum of Canada*, 63, 71 pp.

Wright, E.K., 1987, Stratification and paleocirculation of the late Cretaceous western interior seaway of North America: *Geological Society of America Bulletin*, 99, 480–490.

Yacobucci, M.M., 2012, Meta-analysis of character utility and phylogenetic information content in cladistic studies of ammonoids: *Geobios*,45, 139–143.

Yacobucci, M.M., 2016, Towards a model for speciation in ammoniods, *Species and speciation in the fossil record*: 238–27

APPENDIX A:

LETTER OF PERMISSION FROM PUBLISHER TO REPRINT TEXT

IN CHAPTER TWO

WYOMING GEOLOGICAL ASSOCIATION
PO Box 545, Casper, WY 82602 602 S David St, Casper, WY 82601
www.wyogeo.org wygeology@gmail.com 307-237-0027

April 1, 2019

Joshua Slattery
14604 Grenadine Dr. Apt 1
Tampa, FL 33613

Dear Joshua:

The Board of Directors of Wyoming Geological Association gives you, Joshua Slattery, permission to reprint the following excerpt in your PhD dissertation:

Slattery, J.S., Cobban, W.A., McKinney, K.C., Harries, P.J. and Sandness, A.L., 2015. Early Cretaceous to Paleocene paleogeography of the Western Interior Seaway: the interaction of eustasy and tectonism. *Wyoming Geological Association Guidebook, 2015*, pp.22-60.

Sincerely,

Melanie D Peterson

Melanie Peterson, President
And the Board of Directors of Wyoming Geological Association

APPENDIX B:

NUCULA DATA

Table B1. Data for *Nucula* specimens used for size and shape analysis. Data includes taxon name, valve side (i.e., right (R) or left (L)), museum catalog number, locality, formation/Age, and size data. All fossil specimens are reposited in the Florida Museum of Natural History (FLMNH) Invertebrate Paleontology Collection, Mississippi Museum of Nature and Science (MMNS) Paleontolgy Collection, Yale Peabody Museum of Natural History (YPM) collection of invertebrate fossils, Monmouth Amateur Paleontologist's Society (MAPS) collection, and the authors (JS) personel research collection.

Taxon Name	Valve	Museum	Locality	Formation	Width (mm)	Height (mm)
Nucula proxima	L	FLMNH 1923	St. Lucie, County FL	Pamlico	8.528	7.352
Nucula proxima	L	FLMNH 1923	St. Lucie, County FL	Pamlico	6.837	5.735
Nucula proxima	L	FLMNH 1923	St. Lucie, County FL	Pamlico	8.749	7.45
Nucula proxima	L	FLMNH 1923	St. Lucie, County FL	Pamlico	8.945	8.112
Nucula proxima	L	FLMNH 1923	St. Lucie, County FL	Pamlico	5.759	4.436
Nucula proxima	L	FLMNH 1923	St. Lucie, County FL	Pamlico	6.347	5.759
Nucula proxima	L	FLMNH 1923	St. Lucie, County FL	Pamlico	5.024	4.338
Nucula proxima	L	FLMNH 1923	St. Lucie, County FL	Pamlico	5.514	5.122
Nucula proxima	L	FLMNH 1923	St. Lucie, County FL	Pamlico	5.539	4.999
Nucula proxima	L	FLMNH 1923	St. Lucie, County FL	Pamlico	4.387	3.946

Taxon Name	Valve	Museum	Locality	Formation	Width (mm)	Height (mm)
Nucula proxima	L	FLMNH 1923	St. Lucie, County FL	Pamlico	8.676	9.386
Nucula proxima	L	FLMNH 1923	St. Lucie, County FL	Pamlico	6.543	7.009
Nucula proxima	L	FLMNH 1923	St. Lucie, County FL	Pamlico	7.009	6.176
Nucula proxima	L	FLMNH 1923	St. Lucie, County FL	Pamlico	9.043	8.063
Nucula proxima	L	FLMNH 1923	St. Lucie, County FL	Pamlico	7.622	7.083
Nucula proxima	L	FLMNH 1923	St. Lucie, County FL	Pamlico	6.102	4.901
Nucula proxima	L	FLMNH 1923	St. Lucie, County FL	Pamlico	7.622	7.107
Nucula proxima	L	FLMNH 1923	St. Lucie, County FL	Pamlico	5.71	5.563
Nucula proxima	L	FLMNH 1923	St. Lucie, County FL	Pamlico	4.73	4.46
Nucula proxima	L	FLMNH 1923	St. Lucie, County FL	Pamlico	4.999	4.142
Nucula proxima	L	FLMNH 1923	St. Lucie, County FL	Pamlico	4.166	3.578
Nucula proxima	L	FLMNH 1923	St. Lucie, County FL	Pamlico	6.298	6.225
Nucula proxima	L	FLMNH 1923	St. Lucie, County FL	Pamlico	4.558	4.411
Nucula proxima	L	FLMNH 1923	St. Lucie, County FL	Pamlico	7.965	7.181
Nucula proxima	L	FLMNH 1923	St. Lucie, County FL	Pamlico	8.774	7.205
Nucula proxima	L	FLMNH 121705	Flagler County, FL	Pamlico	6.372	5.294
Nucula proxima	L	FLMNH 121705	Flagler County, FL	Pamlico	4.877	3.946

Taxon Name	Valve	Museum	Locality	Formation	Width (mm)	Height (mm)
Nucula proxima	L	FLMNH 121705	Flagler County, FL	Pamlico	6.617	6.372
Nucula proxima	L	FLMNH 121705	Flagler County, FL	Pamlico	5.171	4.73
Nucula proxima	L	FLMNH 121705	Flagler County, FL	Pamlico	4.509	4.485
Nucula proxima	L	FLMNH 121705	Flagler County, FL	Pamlico	5.686	4.779
Nucula proxima	L	FLMNH 121705	Flagler County, FL	Pamlico	5.343	4.24
Nucula proxima	L	FLMNH 121705	Flagler County, FL	Pamlico	6.421	6.837
Nucula proxima	L	FLMNH 121705	Flagler County, FL	Pamlico	6.494	6.764
Nucula proxima	L	FLMNH 121705	Flagler County, FL	Pamlico	6.764	6.396
Nucula proxima	L	FLMNH 121705	Flagler County, FL	Pamlico	5.147	4.436
Nucula proxima	L	FLMNH 121705	Flagler County, FL	Pamlico	5.122	4.191
Nucula proxima	L	FLMNH 121705	Flagler County, FL	Pamlico	7.034	6.568
Nucula proxima	L	FLMNH 121705	Flagler County, FL	Pamlico	-	-
Nucula proxima	L	FLMNH 121705	Flagler County, FL	Pamlico	3.823	3.357
Nucula proxima	L	FLMNH 121705	Flagler County, FL	Pamlico	5.906	5.514
Nucula proxima	R	FLMNH 1923	St. Lucie, County FL	Pamlico	6.592	5.514
Nucula proxima	R	FLMNH 1923	St. Lucie, County FL	Pamlico	9.092	7.426
Nucula proxima	R	FLMNH 1923	St. Lucie, County FL	Pamlico	5.539	4.95

Taxon Name	Valve	Museum	Locality	Formation	Width (mm)	Height (mm)
Nucula proxima	R	FLMNH 1923	St. Lucie, County FL	Pamlico	8.676	8.063
Nucula proxima	R	FLMNH 1923	St. Lucie, County FL	Pamlico	5.686	4.705
Nucula proxima	R	FLMNH 1923	St. Lucie, County FL	Pamlico	7.205	6.298
Nucula proxima	R	FLMNH 1923	St. Lucie, County FL	Pamlico	6.862	5.808
Nucula proxima	R	FLMNH 1923	St. Lucie, County FL	Pamlico	3.848	3.259
Nucula proxima	R	FLMNH 1923	St. Lucie, County FL	Pamlico	4.387	3.701
Nucula proxima	R	FLMNH 1923	St. Lucie, County FL	Pamlico	4.313	3.357
Nucula proxima	R	FLMNH 1923	St. Lucie, County FL	Pamlico	3.357	3.701
Nucula proxima	R	FLMNH 1923	St. Lucie, County FL	Pamlico	9.852	8.676
Nucula proxima	R	FLMNH 1923	St. Lucie, County FL	Pamlico	7.744	6.568
Nucula proxima	R	FLMNH 1923	St. Lucie, County FL	Pamlico	8.528	7.793
Nucula proxima	R	FLMNH 1923	St. Lucie, County FL	Pamlico	7.205	6.298
Nucula proxima	R	FLMNH 1923	St. Lucie, County FL	Pamlico	6.617	5.759
Nucula proxima	R	FLMNH 1923	St. Lucie, County FL	Pamlico	7.107	6.69
Nucula proxima	R	FLMNH 1923	St. Lucie, County FL	Pamlico	9.95	8.332
Nucula proxima	R	FLMNH 1923	St. Lucie, County FL	Pamlico	7.181	6.151
Nucula proxima	R	FLMNH 1923	St. Lucie, County FL	Pamlico	5.294	4.289

Taxon Name	Valve	Museum	Locality	Formation	Width (mm)	Height (mm)
Nucula proxima	R	FLMNH 1923	St. Lucie, County FL	Pamlico	4.926	4.117
Nucula proxima	R	FLMNH 1923	St. Lucie, County FL	Pamlico	4.705	3.921
Nucula proxima	R	FLMNH 1923	St. Lucie, County FL	Pamlico	6.127	5.539
Nucula proxima	R	FLMNH 1923	St. Lucie, County FL	Pamlico	7.646	6.519
Nucula proxima	R	FLMNH 1923	St. Lucie, County FL	Pamlico	5.71	4.999
Nucula proxima	R	FLMNH 1923	St. Lucie, County FL	Pamlico	3.995	3.161
Nucula proxima	R	FLMNH 121705	Flagler County, FL	Pamlico	5.71	5.441
Nucula proxima	R	FLMNH 121705	Flagler County, FL	Pamlico	4.95	4.607
Nucula proxima	R	FLMNH 121705	Flagler County, FL	Pamlico	4.754	4.24
Nucula proxima	R	FLMNH 121705	Flagler County, FL	Pamlico	6.47	5.294
Nucula proxima	R	FLMNH 121705	Flagler County, FL	Pamlico	5.539	4.73
Nucula proxima	R	FLMNH 121705	Flagler County, FL	Pamlico	5.98	5.367
Nucula proxima	R	FLMNH 121705	Flagler County, FL	Pamlico	5.22	4.901
Nucula proxima	R	FLMNH 121705	Flagler County, FL	Pamlico	7.254	6.347
Nucula proxima	R	FLMNH 121705	Flagler County, FL	Pamlico	5.857	5.784
Nucula proxima	R	FLMNH 121705	Flagler County, FL	Pamlico	5.588	4.656
Nucula proxima	R	FLMNH 121705	Flagler County, FL	Pamlico	4.999	3.774

Taxon Name	Valve	Museum	Locality	Formation	Width (mm)	Height (mm)
Nucula proxima	R	FLMNH 121705	Flagler County, FL	Pamlico	5.073	3.872
Nucula proxima	L	FLMNH 175733	Hendry County, FL	Ft. Thompson	4.975	4.46
Nucula proxima	L	FLMNH 175733	Hendry County, FL	Ft. Thompson	3.823	4.019
Nucula proxima	L	FLMNH 175733	Hendry County, FL	Ft. Thompson	3.578	3.406
Nucula proxima	L	FLMNH 175733	Hendry County, FL	Ft. Thompson	4.289	4.019
Nucula proxima	L	FLMNH 175733	Hendry County, FL	Ft. Thompson	3.995	3.578
Nucula proxima	L	FLMNH 175733	Hendry County, FL	Ft. Thompson	4.681	4.289
Nucula proxima	L	FLMNH 175733	Hendry County, FL	Ft. Thompson	4.338	3.603
Nucula proxima	L	FLMNH 175733	Hendry County, FL	Ft. Thompson	3.774	3.161
Nucula proxima	L	FLMNH 175733	Hendry County, FL	Ft. Thompson	4.191	3.652
Nucula proxima	L	FLMNH 175733	Hendry County, FL	Ft. Thompson	4.558	4.068
Nucula proxima	L	FLMNH 175733	Hendry County, FL	Ft. Thompson	5.49	5.048
Nucula proxima	L	FLMNH 175733	Hendry County, FL	Ft. Thompson	4.387	4.24
Nucula proxima	L	FLMNH 175733	Hendry County, FL	Ft. Thompson	4.044	4.019
Nucula proxima	L	FLMNH 175733	Hendry County, FL	Ft. Thompson	4.681	4.558
Nucula proxima	L	FLMNH 175733	Hendry County, FL	Ft. Thompson	4.852	4.142
Nucula proxima	L	FLMNH 175733	Hendry County, FL	Ft. Thompson	4.754	4.191

Taxon Name	Valve	Museum	Locality	Formation	Width (mm)	Height (mm)
Nucula proxima	L	FLMNH 175733	Hendry County, FL	Ft. Thompson	3.823	3.823
Nucula proxima	L	FLMNH 175733	Hendry County, FL	Ft. Thompson	5.441	4.828
Nucula proxima	L	FLMNH 175733	Hendry County, FL	Ft. Thompson	5.318	4.754
Nucula proxima	L	FLMNH 175733	Hendry County, FL	Ft. Thompson	4.583	3.848
Nucula proxima	L	FLMNH 175733	Hendry County, FL	Ft. Thompson	5.147	5.073
Nucula proxima	L	FLMNH 175733	Hendry County, FL	Ft. Thompson	4.534	4.142
Nucula proxima	L	FLMNH 175733	Hendry County, FL	Ft. Thompson	4.24	3.823
Nucula proxima	L	FLMNH 175733	Hendry County, FL	Ft. Thompson	6.102	5.808
Nucula proxima	L	FLMNH 175733	Hendry County, FL	Ft. Thompson	6.053	5.196
Nucula proxima	L	FLMNH 175733	Hendry County, FL	Ft. Thompson	4.362	3.97
Nucula proxima	L	FLMNH 175733	Hendry County, FL	Ft. Thompson	5.196	4.632
Nucula proxima	L	FLMNH 175733	Hendry County, FL	Ft. Thompson	-	-
Nucula proxima	L	FLMNH 175733	Hendry County, FL	Ft. Thompson	7.132	5.857
Nucula proxima	L	FLMNH 175733	Hendry County, FL	Ft. Thompson	6.936	6.813
Nucula proxima	L	FLMNH 175733	Hendry County, FL	Ft. Thompson	4.632	3.774
Nucula proxima	L	FLMNH 175733	Hendry County, FL	Ft. Thompson	4.607	4.264
Nucula proxima	L	FLMNH 175733	Hendry County, FL	Ft. Thompson	-	-

Taxon Name	Valve	Museum	Locality	Formation	Width (mm)	Height (mm)
Nucula proxima	L	FLMNH 175733	Hendry County, FL	Ft. Thompson	5.588	5.612
Nucula proxima	L	FLMNH 175733	Hendry County, FL	Ft. Thompson	5.882	5.097
Nucula proxima	L	FLMNH 175733	Hendry County, FL	Ft. Thompson	6.004	4.926
Nucula proxima	L	FLMNH 175733	Hendry County, FL	Ft. Thompson	5.196	5.196
Nucula proxima	L	FLMNH 175733	Hendry County, FL	Ft. Thompson	5.441	5.097
Nucula proxima	L	FLMNH 175733	Hendry County, FL	Ft. Thompson	5.539	5.269
Nucula proxima	L	FLMNH 175733	Hendry County, FL	Ft. Thompson	5.49	5.563
Nucula proxima	L	FLMNH 175733	Hendry County, FL	Ft. Thompson	5.661	5.024
Nucula proxima	L	FLMNH 175733	Hendry County, FL	Ft. Thompson	4.338	4.142
Nucula proxima	L	FLMNH 175733	Hendry County, FL	Ft. Thompson	5.441	5.367
Nucula proxima	L	FLMNH 175733	Hendry County, FL	Ft. Thompson	4.779	4.705
Nucula proxima	L	FLMNH 175733	Hendry County, FL	Ft. Thompson	4.95	5.122
Nucula proxima	L	FLMNH 175733	Hendry County, FL	Ft. Thompson	4.828	4.485
Nucula proxima	L	FLMNH 175733	Hendry County, FL	Ft. Thompson	4.705	4.534
Nucula proxima	L	FLMNH 175733	Hendry County, FL	Ft. Thompson	4.901	3.946
Nucula proxima	L	FLMNH 175733	Hendry County, FL	Ft. Thompson	5.392	5.392
Nucula proxima	L	FLMNH 175733	Hendry County, FL	Ft. Thompson	4.289	4.387

Taxon Name	Valve	Museum	Locality	Formation	Width (mm)	Height (mm)
Nucula proxima	L	FLMNH 175733	Hendry County, FL	Ft. Thompson	4.95	4.264
Nucula proxima	L	FLMNH 175733	Hendry County, FL	Ft. Thompson	5.073	4.485
Nucula proxima	L	FLMNH 175733	Hendry County, FL	Ft. Thompson	4.215	3.799
Nucula proxima	L	FLMNH 175733	Hendry County, FL	Ft. Thompson	6.69	5.71
Nucula proxima	L	FLMNH 175733	Hendry County, FL	Ft. Thompson	4.387	4.191
Nucula proxima	L	FLMNH 175733	Hendry County, FL	Ft. Thompson	4.583	4.093
Nucula proxima	L	FLMNH 175733	Hendry County, FL	Ft. Thompson	5.686	5.857
Nucula proxima	L	FLMNH 175733	Hendry County, FL	Ft. Thompson	6.666	5.735
Nucula proxima	L	FLMNH 175733	Hendry County, FL	Ft. Thompson	6.151	5.735
Nucula proxima	L	FLMNH 175733	Hendry County, FL	Ft. Thompson	6.078	5.343
Nucula proxima	L	FLMNH 175733	Hendry County, FL	Ft. Thompson	5.416	5.024
Nucula proxima	L	FLMNH 175733	Hendry County, FL	Ft. Thompson	5.759	5.22
Nucula proxima	L	FLMNH 175733	Hendry County, FL	Ft. Thompson	4.068	4.093
Nucula proxima	L	FLMNH 175733	Hendry County, FL	Ft. Thompson	6.274	5.416
Nucula proxima	L	FLMNH 175733	Hendry County, FL	Ft. Thompson	4.926	4.73
Nucula proxima	L	FLMNH 175733	Hendry County, FL	Ft. Thompson	4.73	4.828
Nucula proxima	L	FLMNH 175733	Hendry County, FL	Ft. Thompson	4.583	4.142

Taxon Name	Valve	Museum	Locality	Formation	Width (mm)	Height (mm)
Nucula proxima	L	FLMNH 175733	Hendry County, FL	Ft. Thompson	4.656	4.46
Nucula proxima	L	FLMNH 175733	Hendry County, FL	Ft. Thompson	5.343	4.975
Nucula proxima	L	FLMNH 175733	Hendry County, FL	Ft. Thompson	6.102	5.294
Nucula proxima	L	FLMNH 175733	Hendry County, FL	Ft. Thompson	6.519	5.955
Nucula proxima	L	FLMNH 175733	Hendry County, FL	Ft. Thompson	6.445	5.98
Nucula proxima	L	FLMNH 175733	Hendry County, FL	Ft. Thompson	5.294	5.294
Nucula proxima	L	FLMNH 175733	Hendry County, FL	Ft. Thompson	4.607	4.73
Nucula proxima	L	FLMNH 175733	Hendry County, FL	Ft. Thompson	6.323	5.784
Nucula proxima	L	FLMNH 175733	Hendry County, FL	Ft. Thompson	5.49	5.147
Nucula proxima	L	FLMNH 175733	Hendry County, FL	Ft. Thompson	6.298	5.539
Nucula proxima	L	FLMNH 175733	Hendry County, FL	Ft. Thompson	6.274	5.539
Nucula proxima	L	FLMNH 175733	Hendry County, FL	Ft. Thompson	4.632	4.068
Nucula proxima	L	FLMNH 175733	Hendry County, FL	Ft. Thompson	5.686	5.392
Nucula proxima	L	FLMNH 175733	Hendry County, FL	Ft. Thompson	5.196	4.779
Nucula proxima	L	FLMNH 175733	Hendry County, FL	Ft. Thompson	6.494	6.494
Nucula proxima	L	FLMNH 175733	Hendry County, FL	Ft. Thompson	6.078	5.416
Nucula proxima	L	FLMNH 175733	Hendry County, FL	Ft. Thompson	7.499	7.352

Taxon Name	Valve	Museum	Locality	Formation	Width (mm)	Height (mm)
Nucula proxima	L	FLMNH 175733	Hendry County, FL	Ft. Thompson	6.053	4.999
Nucula proxima	L	FLMNH 175733	Hendry County, FL	Ft. Thompson	5.171	5.073
Nucula proxima	L	FLMNH 175733	Hendry County, FL	Ft. Thompson	6.029	5.294
Nucula proxima	L	FLMNH 175733	Hendry County, FL	Ft. Thompson	5.514	5.073
Nucula proxima	L	FLMNH 175733	Hendry County, FL	Ft. Thompson	5.171	4.411
Nucula proxima	L	FLMNH 175733	Hendry County, FL	Ft. Thompson	5.784	5.735
Nucula proxima	L	FLMNH 175733	Hendry County, FL	Ft. Thompson	4.926	4.387
Nucula proxima	L	FLMNH 175733	Hendry County, FL	Ft. Thompson	6.47	6.396
Nucula proxima	L	FLMNH 175733	Hendry County, FL	Ft. Thompson	6.396	6.445
Nucula proxima	L	FLMNH 175733	Hendry County, FL	Ft. Thompson	6.445	6.445
Nucula proxima	L	FLMNH 175733	Hendry County, FL	Ft. Thompson	6.274	6.592
Nucula proxima	L	FLMNH 175733	Hendry County, FL	Ft. Thompson	6.445	6.445
Nucula proxima	L	FLMNH 175733	Hendry County, FL	Ft. Thompson	6.274	6.592
Nucula proxima	L	FLMNH 175733	Hendry County, FL	Ft. Thompson	6.225	6.47
Nucula proxima	L	FLMNH 175733	Hendry County, FL	Ft. Thompson	5.808	5.98
Nucula proxima	L	FLMNH 175733	Hendry County, FL	Ft. Thompson	5.931	5.857
Nucula proxima	L	FLMNH 175733	Hendry County, FL	Ft. Thompson	5.122	5.048

Taxon Name	Valve	Museum	Locality	Formation	Width (mm)	Height (mm)
Nucula proxima	R	FLMNH 175733	Hendry County, FL	Ft. Thompson	4.264	3.995
Nucula proxima	R	FLMNH 175733	Hendry County, FL	Ft. Thompson	4.534	3.652
Nucula proxima	R	FLMNH 175733	Hendry County, FL	Ft. Thompson	5.343	4.901
Nucula proxima	R	FLMNH 175733	Hendry County, FL	Ft. Thompson	4.436	3.97
Nucula proxima	R	FLMNH 175733	Hendry County, FL	Ft. Thompson	5.097	4.436
Nucula proxima	R	FLMNH 175733	Hendry County, FL	Ft. Thompson	4.068	3.456
Nucula proxima	R	FLMNH 175733	Hendry County, FL	Ft. Thompson	5.147	4.289
Nucula proxima	R	FLMNH 175733	Hendry County, FL	Ft. Thompson	5.465	4.558
Nucula proxima	R	FLMNH 175733	Hendry County, FL	Ft. Thompson	5.392	4.656
Nucula proxima	R	FLMNH 175733	Hendry County, FL	Ft. Thompson	5.097	4.975
Nucula proxima	R	FLMNH 175733	Hendry County, FL	Ft. Thompson	4.436	3.774
Nucula proxima	R	FLMNH 175733	Hendry County, FL	Ft. Thompson	4.485	4.093
Nucula proxima	R	FLMNH 175733	Hendry County, FL	Ft. Thompson	4.975	4.607
Nucula proxima	R	FLMNH 175733	Hendry County, FL	Ft. Thompson	5.514	4.975
Nucula proxima	R	FLMNH 175733	Hendry County, FL	Ft. Thompson	4.852	3.995
Nucula proxima	R	FLMNH 175733	Hendry County, FL	Ft. Thompson	4.828	3.946
Nucula proxima	R	FLMNH 175733	Hendry County, FL	Ft. Thompson	5.612	4.852

Taxon Name	Valve	Museum	Locality	Formation	Width (mm)	Height (mm)
Nucula proxima	R	FLMNH 175733	Hendry County, FL	Ft. Thompson	4.632	4.117
Nucula proxima	R	FLMNH 175733	Hendry County, FL	Ft. Thompson	7.23	6.617
Nucula proxima	R	FLMNH 175733	Hendry County, FL	Ft. Thompson	4.558	3.725
Nucula proxima	R	FLMNH 175733	Hendry County, FL	Ft. Thompson	4.019	3.529
Nucula proxima	R	FLMNH 175733	Hendry County, FL	Ft. Thompson	4.926	4.411
Nucula proxima	R	FLMNH 175733	Hendry County, FL	Ft. Thompson	3.97	3.774
Nucula proxima	R	FLMNH 175733	Hendry County, FL	Ft. Thompson	4.558	4.264
Nucula proxima	R	FLMNH 175733	Hendry County, FL	Ft. Thompson	4.926	4.313
Nucula proxima	R	FLMNH 175733	Hendry County, FL	Ft. Thompson	5.686	4.901
Nucula proxima	R	FLMNH 175733	Hendry County, FL	Ft. Thompson	4.803	4.754
Nucula proxima	R	FLMNH 175733	Hendry County, FL	Ft. Thompson	4.166	3.725
Nucula proxima	R	FLMNH 175733	Hendry County, FL	Ft. Thompson	4.338	3.848
Nucula proxima	R	FLMNH 175733	Hendry County, FL	Ft. Thompson	5.465	4.705
Nucula proxima	R	FLMNH 175733	Hendry County, FL	Ft. Thompson	4.485	4.558
Nucula proxima	R	FLMNH 175733	Hendry County, FL	Ft. Thompson	4.607	3.774
Nucula proxima	R	FLMNH 175733	Hendry County, FL	Ft. Thompson	4.093	3.921
Nucula proxima	R	FLMNH 175733	Hendry County, FL	Ft. Thompson	4.754	4.436

Taxon Name	Valve	Museum	Locality	Formation	Width (mm)	Height (mm)
Nucula proxima	R	FLMNH 175733	Hendry County, FL	Ft. Thompson	4.019	3.48
Nucula proxima	R	FLMNH 175733	Hendry County, FL	Ft. Thompson	5.931	5.563
Nucula proxima	R	FLMNH 175733	Hendry County, FL	Ft. Thompson	5.588	4.852
Nucula proxima	R	FLMNH 175733	Hendry County, FL	Ft. Thompson	6.102	5.147
Nucula proxima	R	FLMNH 175733	Hendry County, FL	Ft. Thompson	5.612	4.656
Nucula proxima	R	FLMNH 175733	Hendry County, FL	Ft. Thompson	5.955	5.441
Nucula proxima	R	FLMNH 175733	Hendry County, FL	Ft. Thompson	3.823	3.259
Nucula proxima	R	FLMNH 175733	Hendry County, FL	Ft. Thompson	4.166	3.603
Nucula proxima	R	FLMNH 175733	Hendry County, FL	Ft. Thompson	5.22	4.705
Nucula proxima	R	FLMNH 175733	Hendry County, FL	Ft. Thompson	4.387	3.823
Nucula proxima	R	FLMNH 175733	Hendry County, FL	Ft. Thompson	4.681	4.264
Nucula proxima	R	FLMNH 175733	Hendry County, FL	Ft. Thompson	4.558	3.799
Nucula proxima	R	FLMNH 175733	Hendry County, FL	Ft. Thompson	4.485	4.142
Nucula proxima	R	FLMNH 175733	Hendry County, FL	Ft. Thompson	4.999	4.558
Nucula proxima	R	FLMNH 175733	Hendry County, FL	Ft. Thompson	4.779	3.897
Nucula proxima	R	FLMNH 175733	Hendry County, FL	Ft. Thompson	4.779	4.877
Nucula proxima	R	FLMNH 175733	Hendry County, FL	Ft. Thompson	6.421	5.416

Taxon Name	Valve	Museum	Locality	Formation	Width (mm)	Height (mm)
Nucula proxima	R	FLMNH 175733	Hendry County, FL	Ft. Thompson	4.901	4.46
Nucula proxima	R	FLMNH 175733	Hendry County, FL	Ft. Thompson	5.196	4.607
Nucula proxima	R	FLMNH 175733	Hendry County, FL	Ft. Thompson	4.852	4.215
Nucula proxima	R	FLMNH 175733	Hendry County, FL	Ft. Thompson	4.607	4.142
Nucula proxima	R	FLMNH 175733	Hendry County, FL	Ft. Thompson	5.024	4.95
Nucula proxima	R	FLMNH 175733	Hendry County, FL	Ft. Thompson	5.392	4.632
Nucula proxima	R	FLMNH 175733	Hendry County, FL	Ft. Thompson	5.073	4.387
Nucula proxima	R	FLMNH 175733	Hendry County, FL	Ft. Thompson	5.441	4.901
Nucula proxima	R	FLMNH 175733	Hendry County, FL	Ft. Thompson	6.225	5.097
Nucula proxima	R	FLMNH 175733	Hendry County, FL	Ft. Thompson	6.519	5.686
Nucula proxima	R	FLMNH 175733	Hendry County, FL	Ft. Thompson	4.656	4.289
Nucula proxima	R	FLMNH 175733	Hendry County, FL	Ft. Thompson	5.392	4.656
Nucula proxima	R	FLMNH 175733	Hendry County, FL	Ft. Thompson	4.534	3.75
Nucula proxima	R	FLMNH 175733	Hendry County, FL	Ft. Thompson	4.558	3.799
Nucula proxima	R	FLMNH 175733	Hendry County, FL	Ft. Thompson	5.147	4.485
Nucula proxima	R	FLMNH 175733	Hendry County, FL	Ft. Thompson	5.465	4.681
Nucula proxima	R	FLMNH 175733	Hendry County, FL	Ft. Thompson	5.416	5.097

Taxon Name	Valve	Museum	Locality	Formation	Width (mm)	Height (mm)
Nucula proxima	R	FLMNH 175733	Hendry County, FL	Ft. Thompson	5.906	5.71
Nucula proxima	R	FLMNH 175733	Hendry County, FL	Ft. Thompson	5.245	4.46
Nucula proxima	R	FLMNH 175733	Hendry County, FL	Ft. Thompson	5.686	4.754
Nucula proxima	R	FLMNH 175733	Hendry County, FL	Ft. Thompson	4.607	4.044
Nucula proxima	R	FLMNH 175733	Hendry County, FL	Ft. Thompson	4.558	3.946
Nucula proxima	R	FLMNH 175733	Hendry County, FL	Ft. Thompson	7.989	7.181
Nucula proxima	R	FLMNH 175733	Hendry County, FL	Ft. Thompson	6.249	5.392
Nucula proxima	R	FLMNH 175733	Hendry County, FL	Ft. Thompson	6.69	5.98
Nucula proxima	R	FLMNH 175733	Hendry County, FL	Ft. Thompson	6.053	5.588
Nucula proxima	R	FLMNH 175733	Hendry County, FL	Ft. Thompson	6.274	5.343
Nucula proxima	R	FLMNH 175733	Hendry County, FL	Ft. Thompson	5.759	4.73
Nucula proxima	R	FLMNH 175733	Hendry County, FL	Ft. Thompson	4.852	4.24
Nucula proxima	R	FLMNH 175733	Hendry County, FL	Ft. Thompson	6.592	6.298
Nucula proxima	R	FLMNH 175733	Hendry County, FL	Ft. Thompson	5.245	4.362
Nucula proxima	R	FLMNH 175733	Hendry County, FL	Ft. Thompson	4.583	3.946
Nucula proxima	R	FLMNH 175733	Hendry County, FL	Ft. Thompson	5.808	5.392
Nucula proxima	R	FLMNH 175733	Hendry County, FL	Ft. Thompson	6.078	5.318

Taxon Name	Valve	Museum	Locality	Formation	Width (mm)	Height (mm)
Nucula proxima	R	FLMNH 175733	Hendry County, FL	Ft. Thompson	6.788	5.759
Nucula proxima	R	FLMNH 175733	Hendry County, FL	Ft. Thompson	6.47	5.441
Nucula proxima	R	FLMNH 175733	Hendry County, FL	Ft. Thompson	5.955	5.367
Nucula proxima	R	FLMNH 175733	Hendry County, FL	Ft. Thompson	4.46	4.093
Nucula proxima	R	FLMNH 175733	Hendry County, FL	Ft. Thompson	5.759	4.705
Nucula proxima	R	FLMNH 175733	Hendry County, FL	Ft. Thompson	5.073	4.215
Nucula proxima	R	FLMNH 175733	Hendry County, FL	Ft. Thompson	5.097	4.313
Nucula proxima	R	FLMNH 175733	Hendry County, FL	Ft. Thompson	6.176	5.441
Nucula proxima	R	FLMNH 175733	Hendry County, FL	Ft. Thompson	6.347	5.416
Nucula proxima	R	FLMNH 175733	Hendry County, FL	Ft. Thompson	3.897	3.382
Nucula proxima	L	FLMNH 242766	Glades County, FL	Caloosahatchee/ Bermont	0.72	0.939
Nucula proxima	L	FLMNH 242766	Glades County, FL	Caloosahatchee/ Bermont	0.75	0.971
Nucula proxima	L	FLMNH 242766	Glades County, FL	Caloosahatchee/ Bermont	0.748	0.972
Nucula proxima	L	FLMNH 242766	Glades County, FL	Caloosahatchee/ Bermont	0.754	0.95
Nucula proxima	L	FLMNH 242766	Glades County, FL	Caloosahatchee/ Bermont	0.754	0.97
Nucula proxima	L	FLMNH 242766	Glades County, FL	Caloosahatchee/ Bermont	0.747	0.95
Nucula proxima	L	FLMNH 242766	Glades County, FL	Caloosahatchee/ Bermont	0.764	0.953

Taxon Name	Valve	Museum	Locality	Formation	Width (mm)	Height (mm)
Nucula proxima	L	FLMNH 242766	Glades County, FL	Caloosahatchee/ Bermont	0.732	0.973
Nucula proxima	L	FLMNH 242766	Glades County, FL	Caloosahatchee/ Bermont	0.745	0.948
Nucula proxima	L	FLMNH 242766	Glades County, FL	Caloosahatchee/ Bermont	0.76	0.956
Nucula proxima	L	FLMNH 242766	Glades County, FL	Caloosahatchee/ Bermont	0.77	0.949
Nucula proxima	L	FLMNH 242766	Glades County, FL	Caloosahatchee/ Bermont	0.759	0.967
Nucula proxima	L	FLMNH 242766	Glades County, FL	Caloosahatchee/ Bermont	0.776	0.975
Nucula proxima	L	FLMNH 242766	Glades County, FL	Caloosahatchee/ Bermont	0.739	0.949
Nucula proxima	L	FLMNH 242766	Glades County, FL	Caloosahatchee/ Bermont	0.732	0.944
Nucula proxima	L	FLMNH 242766	Glades County, FL	Caloosahatchee/ Bermont	0.733	0.956
Nucula proxima	L	FLMNH 242766	Glades County, FL	Caloosahatchee/ Bermont	0.773	0.977
Nucula proxima	L	FLMNH 242766	Glades County, FL	Caloosahatchee/ Bermont	0.796	0.948
Nucula proxima	L	FLMNH 242766	Glades County, FL	Caloosahatchee/ Bermont	0.754	0.948
Nucula proxima	L	FLMNH 242766	Glades County, FL	Caloosahatchee/ Bermont	0.747	0.939
Nucula proxima	L	FLMNH 242766	Glades County, FL	Caloosahatchee/ Bermont	0.773	0.95
Nucula proxima	L	FLMNH 242766	Glades County, FL	Caloosahatchee/ Bermont	0.773	0.973
Nucula proxima	L	FLMNH 242766	Glades County, FL	Caloosahatchee/ Bermont	0.801	0.974
Nucula proxima	L	FLMNH 242766	Glades County, FL	Caloosahatchee/ Bermont	0.77	0.972

Taxon Name	Valve	Museum	Locality	Formation	Width (mm)	Height (mm)
Nucula proxima	L	FLMNH 242766	Glades County, FL	Caloosahatchee/ Bermont	0.769	0.941
Nucula proxima	L	FLMNH 242766	Glades County, FL	Caloosahatchee/ Bermont	0.763	0.973
Nucula proxima	L	FLMNH 242766	Glades County, FL	Caloosahatchee/ Bermont	0.77	0.974
Nucula proxima	L	FLMNH 242766	Glades County, FL	Caloosahatchee/ Bermont	0.782	0.975
Nucula proxima	L	FLMNH 242766	Glades County, FL	Caloosahatchee/ Bermont	0.752	0.923
Nucula proxima	L	FLMNH 242766	Glades County, FL	Caloosahatchee/ Bermont	0.762	0.935
Nucula proxima	L	FLMNH 242766	Glades County, FL	Caloosahatchee/ Bermont	0.731	0.97
Nucula proxima	L	FLMNH 242766	Glades County, FL	Caloosahatchee/ Bermont	0.754	0.946
Nucula proxima	L	FLMNH 242766	Glades County, FL	Caloosahatchee/ Bermont	0.755	0.971
Nucula proxima	L	FLMNH 242766	Glades County, FL	Caloosahatchee/ Bermont	0.756	0.973
Nucula proxima	L	FLMNH 242766	Glades County, FL	Caloosahatchee/ Bermont	0.741	0.967
Nucula proxima	L	FLMNH 242766	Glades County, FL	Caloosahatchee/ Bermont	0.746	0.945
Nucula proxima	L	FLMNH 242766	Glades County, FL	Caloosahatchee/ Bermont	0.767	0.95
Nucula proxima	L	FLMNH 242766	Glades County, FL	Caloosahatchee/ Bermont	0.759	0.972
Nucula proxima	L	FLMNH 242766	Glades County, FL	Caloosahatchee/ Bermont	0.739	0.941
Nucula proxima	L	FLMNH 242766	Glades County, FL	Caloosahatchee/ Bermont	0.71	0.957
Nucula proxima	L	FLMNH 242766	Glades County, FL	Caloosahatchee/ Bermont	0.735	0.973

Taxon Name	Valve	Museum	Locality	Formation	Width (mm)	Height (mm)
Nucula proxima	L	FLMNH 242766	Glades County, FL	Caloosahatchee/ Bermont	0.763	0.97
Nucula proxima	L	FLMNH 242766	Glades County, FL	Caloosahatchee/ Bermont	0.755	0.949
Nucula proxima	L	FLMNH 242766	Glades County, FL	Caloosahatchee/ Bermont	0.738	0.975
Nucula proxima	L	FLMNH 242766	Glades County, FL	Caloosahatchee/ Bermont	0.752	0.937
Nucula proxima	L	FLMNH 242766	Glades County, FL	Caloosahatchee/ Bermont	0.735	0.922
Nucula proxima	L	FLMNH 242766	Glades County, FL	Caloosahatchee/ Bermont	0.75	0.937
Nucula proxima	L	FLMNH 242766	Glades County, FL	Caloosahatchee/ Bermont	0.75	0.942
Nucula proxima	L	FLMNH 242766	Glades County, FL	Caloosahatchee/ Bermont	0.75	0.937
Nucula proxima	L	FLMNH 242766	Glades County, FL	Caloosahatchee/ Bermont	0.749	0.969
Nucula proxima	L	FLMNH 242766	Glades County, FL	Caloosahatchee/ Bermont	0.769	0.97
Nucula proxima	L	FLMNH 242766	Glades County, FL	Caloosahatchee/ Bermont	0.751	0.931
Nucula proxima	L	FLMNH 242766	Glades County, FL	Caloosahatchee/ Bermont	0.736	0.93
Nucula proxima	L	FLMNH 242766	Glades County, FL	Caloosahatchee/ Bermont	0.741	0.973
Nucula proxima	L	FLMNH 242766	Glades County, FL	Caloosahatchee/ Bermont	0.76	0.975
Nucula proxima	L	FLMNH 242766	Glades County, FL	Caloosahatchee/ Bermont	0.746	0.976
Nucula proxima	L	FLMNH 242766	Glades County, FL	Caloosahatchee/ Bermont	0.771	0.937
Nucula proxima	L	FLMNH 242766	Glades County, FL	Caloosahatchee/ Bermont	0.731	0.924

Taxon Name	Valve	Museum	Locality	Formation	Width (mm)	Height (mm)
Nucula proxima	L	FLMNH 242766	Glades County, FL	Caloosahatchee/ Bermont	0.767	0.94
Nucula proxima	L	FLMNH 242766	Glades County, FL	Caloosahatchee/ Bermont	0.755	0.969
Nucula proxima	L	FLMNH 242766	Glades County, FL	Caloosahatchee/ Bermont	0.749	0.94
Nucula proxima	L	FLMNH 242766	Glades County, FL	Caloosahatchee/ Bermont	0.747	0.937
Nucula proxima	L	FLMNH 242766	Glades County, FL	Caloosahatchee/ Bermont	0.762	0.938
Nucula proxima	L	FLMNH 242766	Glades County, FL	Caloosahatchee/ Bermont	0.754	0.933
Nucula proxima	L	FLMNH 242766	Glades County, FL	Caloosahatchee/ Bermont	0.76	0.939
Nucula proxima	L	FLMNH 242766	Glades County, FL	Caloosahatchee/ Bermont	0.763	0.935
Nucula proxima	L	FLMNH 242766	Glades County, FL	Caloosahatchee/ Bermont	0.769	0.973
Nucula proxima	L	FLMNH 242766	Glades County, FL	Caloosahatchee/ Bermont	0.747	0.946
Nucula proxima	L	FLMNH 242766	Glades County, FL	Caloosahatchee/ Bermont	0.758	0.978
Nucula proxima	L	FLMNH 242766	Glades County, FL	Caloosahatchee/ Bermont	0.739	0.981
Nucula proxima	L	FLMNH 242766	Glades County, FL	Caloosahatchee/ Bermont	0.762	0.952
Nucula proxima	L	FLMNH 242766	Glades County, FL	Caloosahatchee/ Bermont	0.768	0.943
Nucula proxima	L	FLMNH 242766	Glades County, FL	Caloosahatchee/ Bermont	0.753	0.96
Nucula proxima	L	FLMNH 242766	Glades County, FL	Caloosahatchee/ Bermont	0.744	0.977
Nucula proxima	L	FLMNH 242766	Glades County, FL	Caloosahatchee/ Bermont	0.761	0.941

Taxon Name	Valve	Museum	Locality	Formation	Width (mm)	Height (mm)
Nucula proxima	L	FLMNH 242766	Glades County, FL	Caloosahatchee/ Bermont	0.731	0.959
Nucula proxima	L	FLMNH 242766	Glades County, FL	Caloosahatchee/ Bermont	0.721	0.974
Nucula proxima	L	FLMNH 242766	Glades County, FL	Caloosahatchee/ Bermont	0.713	0.981
Nucula proxima	L	FLMNH 242766	Glades County, FL	Caloosahatchee/ Bermont	0.751	0.976
Nucula proxima	L	FLMNH 242766	Glades County, FL	Caloosahatchee/ Bermont	0.814	0.978
Nucula proxima	L	FLMNH 242766	Glades County, FL	Caloosahatchee/ Bermont	0.741	0.976
Nucula proxima	L	FLMNH 242766	Glades County, FL	Caloosahatchee/ Bermont	0.731	0.977
Nucula proxima	L	FLMNH 242766	Glades County, FL	Caloosahatchee/ Bermont	0.727	0.951
Nucula proxima	L	FLMNH 242766	Glades County, FL	Caloosahatchee/ Bermont	0.751	0.94
Nucula proxima	L	FLMNH 242766	Glades County, FL	Caloosahatchee/ Bermont	0.73	0.946
Nucula proxima	L	FLMNH 242766	Glades County, FL	Caloosahatchee/ Bermont	0.743	0.938
Nucula proxima	L	FLMNH 242766	Glades County, FL	Caloosahatchee/ Bermont	0.775	0.974
Nucula proxima	L	FLMNH 242766	Glades County, FL	Caloosahatchee/ Bermont	0.751	0.979
Nucula proxima	L	FLMNH 242766	Glades County, FL	Caloosahatchee/ Bermont	0.737	0.925
Nucula proxima	L	FLMNH 242766	Glades County, FL	Caloosahatchee/ Bermont	0.747	0.938
Nucula proxima	L	FLMNH 242766	Glades County, FL	Caloosahatchee/ Bermont	0.765	0.961
Nucula proxima	L	FLMNH 242766	Glades County, FL	Caloosahatchee/ Bermont	0.746	0.948

Taxon Name	Valve	Museum	Locality	Formation	Width (mm)	Height (mm)
Nucula proxima	L	FLMNH 242766	Glades County, FL	Caloosahatchee/ Bermont	0.747	0.971
Nucula proxima	L	FLMNH 242766	Glades County, FL	Caloosahatchee/ Bermont	0.764	0.975
Nucula proxima	L	FLMNH 242766	Glades County, FL	Caloosahatchee/ Bermont	0.754	0.945
Nucula proxima	L	FLMNH 242766	Glades County, FL	Caloosahatchee/ Bermont	0.721	0.955
Nucula proxima	L	FLMNH 242766	Glades County, FL	Caloosahatchee/ Bermont	0.743	0.933
Nucula proxima	L	FLMNH 242766	Glades County, FL	Caloosahatchee/ Bermont	0.743	0.976
Nucula proxima	L	FLMNH 242766	Glades County, FL	Caloosahatchee/ Bermont	0.766	0.957
Nucula proxima	L	FLMNH 242766	Glades County, FL	Caloosahatchee/ Bermont	0.746	0.96
Nucula proxima	L	FLMNH 242766	Glades County, FL	Caloosahatchee/ Bermont	0.75	0.949
Nucula proxima	L	FLMNH 242766	Glades County, FL	Caloosahatchee/ Bermont	0.745	0.941
Nucula proxima	L	FLMNH 242766	Glades County, FL	Caloosahatchee/ Bermont	0.747	0.974
Nucula proxima	L	FLMNH 242766	Glades County, FL	Caloosahatchee/ Bermont	0.757	0.973
Nucula proxima	L	FLMNH 242766	Glades County, FL	Caloosahatchee/ Bermont	0.749	0.978
Nucula proxima	L	FLMNH 242766	Glades County, FL	Caloosahatchee/ Bermont	0.759	0.952
Nucula proxima	L	FLMNH 242766	Glades County, FL	Caloosahatchee/ Bermont	0.759	0.945
Nucula proxima	R	FLMNH 242766	Glades County, FL	Caloosahatchee/ Bermont	0.738	0.943
Nucula proxima	R	FLMNH 242766	Glades County, FL	Caloosahatchee/ Bermont	0.761	0.937

Taxon Name	Valve	Museum	Locality	Formation	Width (mm)	Height (mm)
Nucula proxima	R	FLMNH 242766	Glades County, FL	Caloosahatchee/ Bermont	0.789	0.936
Nucula proxima	R	FLMNH 242766	Glades County, FL	Caloosahatchee/ Bermont	0.749	0.942
Nucula proxima	R	FLMNH 242766	Glades County, FL	Caloosahatchee/ Bermont	0.714	0.971
Nucula proxima	R	FLMNH 242766	Glades County, FL	Caloosahatchee/ Bermont	0.765	0.92
Nucula proxima	R	FLMNH 242766	Glades County, FL	Caloosahatchee/ Bermont	0.769	0.97
Nucula proxima	R	FLMNH 242766	Glades County, FL	Caloosahatchee/ Bermont	0.77	0.966
Nucula proxima	R	FLMNH 242766	Glades County, FL	Caloosahatchee/ Bermont	0.756	0.941
Nucula proxima	R	FLMNH 242766	Glades County, FL	Caloosahatchee/ Bermont	0.77	0.933
Nucula proxima	R	FLMNH 242766	Glades County, FL	Caloosahatchee/ Bermont	0.758	0.929
Nucula proxima	R	FLMNH 242766	Glades County, FL	Caloosahatchee/ Bermont	0.772	0.926
Nucula proxima	R	FLMNH 242766	Glades County, FL	Caloosahatchee/ Bermont	0.783	0.944
Nucula proxima	R	FLMNH 242766	Glades County, FL	Caloosahatchee/ Bermont	0.781	0.974
Nucula proxima	R	FLMNH 242766	Glades County, FL	Caloosahatchee/ Bermont	0.764	0.939
Nucula proxima	R	FLMNH 242766	Glades County, FL	Caloosahatchee/ Bermont	0.79	0.939
Nucula proxima	R	FLMNH 242766	Glades County, FL	Caloosahatchee/ Bermont	0.753	0.937
Nucula proxima	R	FLMNH 242766	Glades County, FL	Caloosahatchee/ Bermont	0.77	0.927
Nucula proxima	R	FLMNH 242766	Glades County, FL	Caloosahatchee/ Bermont	0.773	0.911

Taxon Name	Valve	Museum	Locality	Formation	Width (mm)	Height (mm)
Nucula proxima	R	FLMNH 242766	Glades County, FL	Caloosahatchee/ Bermont	0.774	0.974
Nucula proxima	R	FLMNH 242766	Glades County, FL	Caloosahatchee/ Bermont	0.742	0.94
Nucula proxima	R	FLMNH 242766	Glades County, FL	Caloosahatchee/ Bermont	0.765	0.974
Nucula proxima	R	FLMNH 242766	Glades County, FL	Caloosahatchee/ Bermont	0.712	0.947
Nucula proxima	R	FLMNH 242766	Glades County, FL	Caloosahatchee/ Bermont	0.769	0.982
Nucula proxima	R	FLMNH 242766	Glades County, FL	Caloosahatchee/ Bermont	0.769	0.975
Nucula proxima	R	FLMNH 242766	Glades County, FL	Caloosahatchee/ Bermont	0.75	0.979
Nucula proxima	R	FLMNH 242766	Glades County, FL	Caloosahatchee/ Bermont	0.801	0.974
Nucula proxima	R	FLMNH 242766	Glades County, FL	Caloosahatchee/ Bermont	0.746	0.97
Nucula proxima	R	FLMNH 242766	Glades County, FL	Caloosahatchee/ Bermont	0.753	0.959
Nucula proxima	R	FLMNH 242766	Glades County, FL	Caloosahatchee/ Bermont	0.765	0.941
Nucula proxima	R	FLMNH 242766	Glades County, FL	Caloosahatchee/ Bermont	0.764	0.942
Nucula proxima	R	FLMNH 242766	Glades County, FL	Caloosahatchee/ Bermont	0.736	0.938
Nucula proxima	R	FLMNH 242766	Glades County, FL	Caloosahatchee/ Bermont	0.761	0.95
Nucula proxima	R	FLMNH 242766	Glades County, FL	Caloosahatchee/ Bermont	0.771	0.946
Nucula proxima	R	FLMNH 242766	Glades County, FL	Caloosahatchee/ Bermont	0.711	0.952
Nucula proxima	R	FLMNH 242766	Glades County, FL	Caloosahatchee/ Bermont	0.754	0.98

Taxon Name	Valve	Museum	Locality	Formation	Width (mm)	Height (mm)
Nucula proxima	R	FLMNH 242766	Glades County, FL	Caloosahatchee/ Bermont	0.738	0.974
Nucula proxima	R	FLMNH 242766	Glades County, FL	Caloosahatchee/ Bermont	0.757	0.979
Nucula proxima	R	FLMNH 242766	Glades County, FL	Caloosahatchee/ Bermont	0.744	0.978
Nucula proxima	R	FLMNH 242766	Glades County, FL	Caloosahatchee/ Bermont	0.738	0.95
Nucula proxima	R	FLMNH 242766	Glades County, FL	Caloosahatchee/ Bermont	0.755	0.95
Nucula proxima	R	FLMNH 242766	Glades County, FL	Caloosahatchee/ Bermont	0.756	0.977
Nucula proxima	R	FLMNH 242766	Glades County, FL	Caloosahatchee/ Bermont	0.73	0.941
Nucula proxima	R	FLMNH 242766	Glades County, FL	Caloosahatchee/ Bermont	0.707	0.977
Nucula proxima	R	FLMNH 242766	Glades County, FL	Caloosahatchee/ Bermont	0.722	0.939
Nucula proxima	R	FLMNH 242766	Glades County, FL	Caloosahatchee/ Bermont	0.768	0.946
Nucula proxima	R	FLMNH 242766	Glades County, FL	Caloosahatchee/ Bermont	0.702	0.96
Nucula proxima	R	FLMNH 242766	Glades County, FL	Caloosahatchee/ Bermont	0.779	0.947
Nucula proxima	R	FLMNH 242766	Glades County, FL	Caloosahatchee/ Bermont	0.73	0.978
Nucula proxima	R	FLMNH 242766	Glades County, FL	Caloosahatchee/ Bermont	0.758	0.946
Nucula proxima	R	FLMNH 242766	Glades County, FL	Caloosahatchee/ Bermont	0.76	0.958
Nucula proxima	R	FLMNH 242766	Glades County, FL	Caloosahatchee/ Bermont	0.772	0.953
Nucula proxima	R	FLMNH 242766	Glades County, FL	Caloosahatchee/ Bermont	0.781	0.977

Taxon Name	Valve	Museum	Locality	Formation	Width (mm)	Height (mm)
Nucula proxima	R	FLMNH 242766	Glades County, FL	Caloosahatchee/ Bermont	0.754	0.957
Nucula proxima	R	FLMNH 242766	Glades County, FL	Caloosahatchee/ Bermont	0.71	0.956
Nucula proxima	R	FLMNH 242766	Glades County, FL	Caloosahatchee/ Bermont	0.754	0.976
Nucula proxima	R	FLMNH 242766	Glades County, FL	Caloosahatchee/ Bermont	0.772	0.975
Nucula proxima	R	FLMNH 242766	Glades County, FL	Caloosahatchee/ Bermont	0.751	0.943
Nucula proxima	R	FLMNH 242766	Glades County, FL	Caloosahatchee/ Bermont	0.776	0.97
Nucula proxima	R	FLMNH 242766	Glades County, FL	Caloosahatchee/ Bermont	0.757	0.973
Nucula proxima	R	FLMNH 242766	Glades County, FL	Caloosahatchee/ Bermont	0.762	0.958
Nucula proxima	R	FLMNH 242766	Glades County, FL	Caloosahatchee/ Bermont	0.779	0.954
Nucula proxima	R	FLMNH 242766	Glades County, FL	Caloosahatchee/ Bermont	0.784	0.95
Nucula proxima	R	FLMNH 242766	Glades County, FL	Caloosahatchee/ Bermont	0.76	0.948
Nucula proxima	R	FLMNH 242766	Glades County, FL	Caloosahatchee/ Bermont	0.754	0.945
Nucula proxima	L	FLMNH 99967	Hendry County, FL	Caloosahatchee	5.844	5.091
Nucula proxima	L	FLMNH 99967	Hendry County, FL	Caloosahatchee	6.255	5.479
Nucula proxima	L	FLMNH 99967	Hendry County, FL	Caloosahatchee	5.639	5.091
Nucula proxima	L	FLMNH 99967	Hendry County, FL	Caloosahatchee	3.493	3.31
Nucula proxima	L	FLMNH 242766	Glades County, FL	Caloosahatchee/ Bermont	5.707	4.84

Taxon Name	Valve	Museum	Locality	Formation	Width (mm)	Height (mm)
Nucula proxima	L	FLMNH 242766	Glades County, FL	Caloosahatchee/ Bermont	5.73	4.748
Nucula proxima	L	FLMNH 242766	Glades County, FL	Caloosahatchee/ Bermont	5.593	4.771
Nucula proxima	L	FLMNH 242766	Glades County, FL	Caloosahatchee/ Bermont	5.114	4.269
Nucula proxima	L	FLMNH 242766	Glades County, FL	Caloosahatchee/ Bermont	6.575	5.433
Nucula proxima	L	FLMNH 242766	Glades County, FL	Caloosahatchee/ Bermont	4.474	4.292
Nucula proxima	L	FLMNH 242766	Glades County, FL	Caloosahatchee/ Bermont	6.209	4.977
Nucula proxima	L	FLMNH 242766	Glades County, FL	Caloosahatchee/ Bermont	5.091	4.201
Nucula proxima	L	FLMNH 242766	Glades County, FL	Caloosahatchee/ Bermont	8.401	6.917
Nucula proxima	L	FLMNH 242766	Glades County, FL	Caloosahatchee/ Bermont	5.159	4.452
Nucula proxima	L	FLMNH 242766	Glades County, FL	Caloosahatchee/ Bermont	5.844	5.433
Nucula proxima	L	FLMNH 242766	Glades County, FL	Caloosahatchee/ Bermont	5.753	5
Nucula proxima	L	FLMNH 242766	Glades County, FL	Caloosahatchee/ Bermont	5.936	4.794
Nucula proxima	L	FLMNH 242766	Glades County, FL	Caloosahatchee/ Bermont	4.84	4.315
Nucula proxima	L	FLMNH 242766	Glades County, FL	Caloosahatchee/ Bermont	4.178	3.493
Nucula proxima	L	FLMNH 242766	Glades County, FL	Caloosahatchee/ Bermont	5.273	4.178
Nucula proxima	L	FLMNH 242766	Glades County, FL	Caloosahatchee/ Bermont	4.68	4.109
Nucula proxima	L	FLMNH 242766	Glades County, FL	Caloosahatchee/ Bermont	5.57	5.022

Taxon Name	Valve	Museum	Locality	Formation	Width (mm)	Height (mm)
Nucula proxima	L	FLMNH 242766	Glades County, FL	Caloosahatchee/ Bermont	5.958	4.748
Nucula proxima	L	FLMNH 242766	Glades County, FL	Caloosahatchee/ Bermont	4.246	3.721
Nucula proxima	L	FLMNH 242766	Glades County, FL	Caloosahatchee/ Bermont	5.73	5.205
Nucula proxima	L	FLMNH 242766	Glades County, FL	Caloosahatchee/ Bermont	5.662	4.657
Nucula proxima	L	FLMNH 242766	Glades County, FL	Caloosahatchee/ Bermont	4.817	3.767
Nucula proxima	L	FLMNH 242766	Glades County, FL	Caloosahatchee/ Bermont	4.726	4.109
Nucula proxima	L	FLMNH 242766	Glades County, FL	Caloosahatchee/ Bermont	5.205	4.337
Nucula proxima	L	FLMNH 242766	Glades County, FL	Caloosahatchee/ Bermont	5.981	4.634
Nucula proxima	L	FLMNH 242766	Glades County, FL	Caloosahatchee/ Bermont	5.844	5.228
Nucula proxima	L	FLMNH 242766	Glades County, FL	Caloosahatchee/ Bermont	6.826	5.502
Nucula proxima	L	FLMNH 242766	Glades County, FL	Caloosahatchee/ Bermont	5.296	4.223
Nucula proxima	L	FLMNH 242766	Glades County, FL	Caloosahatchee/ Bermont	4.771	4.018
Nucula proxima	L	FLMNH 242766	Glades County, FL	Caloosahatchee/ Bermont	5.342	4.474
Nucula proxima	L	FLMNH 242766	Glades County, FL	Caloosahatchee/ Bermont	5.273	4.337
Nucula proxima	L	FLMNH 242766	Glades County, FL	Caloosahatchee/ Bermont	5.137	4.109
Nucula proxima	L	FLMNH 242766	Glades County, FL	Caloosahatchee/ Bermont	5.479	4.52
Nucula proxima	L	FLMNH 242766	Glades County, FL	Caloosahatchee/ Bermont	4.84	4.543

Taxon Name	Valve	Museum	Locality	Formation	Width (mm)	Height (mm)
Nucula proxima	L	FLMNH 242766	Glades County, FL	Caloosahatchee/ Bermont	4.246	3.835
Nucula proxima	L	FLMNH 242766	Glades County, FL	Caloosahatchee/ Bermont	4.611	3.904
Nucula proxima	L	FLMNH 242766	Glades County, FL	Caloosahatchee/ Bermont	5.205	4.543
Nucula proxima	L	FLMNH 242766	Glades County, FL	Caloosahatchee/ Bermont	4.611	4.246
Nucula proxima	L	FLMNH 242766	Glades County, FL	Caloosahatchee/ Bermont	5.365	4.703
Nucula proxima	L	FLMNH 242766	Glades County, FL	Caloosahatchee/ Bermont	5.022	4.109
Nucula proxima	L	FLMNH 242766	Glades County, FL	Caloosahatchee/ Bermont	3.721	2.785
Nucula proxima	L	FLMNH 242766	Glades County, FL	Caloosahatchee/ Bermont	4.817	4.041
Nucula proxima	L	FLMNH 242766	Glades County, FL	Caloosahatchee/ Bermont	5.684	4.726
Nucula proxima	L	FLMNH 242766	Glades County, FL	Caloosahatchee/ Bermont	4.726	4.429
Nucula proxima	L	FLMNH 242766	Glades County, FL	Caloosahatchee/ Bermont	5.936	5.844
Nucula proxima	L	FLMNH 242766	Glades County, FL	Caloosahatchee/ Bermont	5.41	4.452
Nucula proxima	L	FLMNH 242766	Glades County, FL	Caloosahatchee/ Bermont	7.031	5.41
Nucula proxima	L	FLMNH 242766	Glades County, FL	Caloosahatchee/ Bermont	4.703	4.748
Nucula proxima	L	FLMNH 242766	Glades County, FL	Caloosahatchee/ Bermont	4.452	4.406
Nucula proxima	L	FLMNH 242766	Glades County, FL	Caloosahatchee/ Bermont	5.205	4.406
Nucula proxima	L	FLMNH 242766	Glades County, FL	Caloosahatchee/ Bermont	4.634	3.744

Taxon Name	Valve	Museum	Locality	Formation	Width (mm)	Height (mm)
Nucula proxima	L	FLMNH 242766	Glades County, FL	Caloosahatchee/ Bermont	5.593	5.228
Nucula proxima	L	FLMNH 242766	Glades County, FL	Caloosahatchee/ Bermont	5.57	5.205
Nucula proxima	L	FLMNH 242766	Glades County, FL	Caloosahatchee/ Bermont	4.908	4.178
Nucula proxima	L	FLMNH 242766	Glades County, FL	Caloosahatchee/ Bermont	5.433	4.429
Nucula proxima	L	FLMNH 242766	Glades County, FL	Caloosahatchee/ Bermont	5.068	4.611
Nucula proxima	L	FLMNH 99967	Hendry County, FL	Caloosahatchee	5.65	4.453
Nucula proxima	L	FLMNH 99967	Hendry County, FL	Caloosahatchee	5.739	5.345
Nucula proxima	L	FLMNH 99967	Hendry County, FL	Caloosahatchee	3.356	3.059
Nucula proxima	L	FLMNH 99967	Hendry County, FL	Caloosahatchee	3.881	3.219
Nucula proxima	L	FLMNH 99967	Hendry County, FL	Caloosahatchee	5.205	4.931
Nucula proxima	L	FLMNH 99967	Hendry County, FL	Caloosahatchee	5.296	4.589
Nucula proxima	L	FLMNH 242766	Glades County, FL	Caloosahatchee/ Bermont	5.137	4.452
Nucula proxima	L	FLMNH 242766	Glades County, FL	Caloosahatchee/ Bermont	5	4.406
Nucula proxima	L	FLMNH 242766	Glades County, FL	Caloosahatchee/ Bermont	4.566	4.406
Nucula proxima	L	FLMNH 242766	Glades County, FL	Caloosahatchee/ Bermont	4.337	4.018
Nucula proxima	L	FLMNH 242766	Glades County, FL	Caloosahatchee/ Bermont	4.201	3.675
Nucula proxima	L	FLMNH 242766	Glades County, FL	Caloosahatchee/ Bermont	4.863	4.885

Taxon Name	Valve	Museum	Locality	Formation	Width (mm)	Height (mm)
Nucula proxima	L	FLMNH 242766	Glades County, FL	Caloosahatchee/ Bermont	4.771	4.36
Nucula proxima	L	FLMNH 242766	Glades County, FL	Caloosahatchee/ Bermont	4.954	4.383
Nucula proxima	L	FLMNH 242766	Glades County, FL	Caloosahatchee/ Bermont	4.954	4.064
Nucula proxima	L	FLMNH 242766	Glades County, FL	Caloosahatchee/ Bermont	3.79	3.013
Nucula proxima	L	FLMNH 242766	Glades County, FL	Caloosahatchee/ Bermont	4.383	3.653
Nucula proxima	L	FLMNH 242766	Glades County, FL	Caloosahatchee/ Bermont	4.84	3.721
Nucula proxima	L	FLMNH 242766	Glades County, FL	Caloosahatchee/ Bermont	4.794	4.863
Nucula proxima	L	FLMNH 242766	Glades County, FL	Caloosahatchee/ Bermont	4.452	4.337
Nucula proxima	L	FLMNH 242766	Glades County, FL	Caloosahatchee/ Bermont	4.452	4.064
Nucula proxima	L	FLMNH 242766	Glades County, FL	Caloosahatchee/ Bermont	3.949	2.991
Nucula proxima	L	FLMNH 242766	Glades County, FL	Caloosahatchee/ Bermont	4.977	4.36
Nucula proxima	L	FLMNH 242766	Glades County, FL	Caloosahatchee/ Bermont	5.319	4.543
Nucula proxima	L	FLMNH 242766	Glades County, FL	Caloosahatchee/ Bermont	4.269	4.155
Nucula proxima	L	FLMNH 242766	Glades County, FL	Caloosahatchee/ Bermont	4.611	4.018
Nucula proxima	L	FLMNH 242766	Glades County, FL	Caloosahatchee/ Bermont	5.045	4.452
Nucula proxima	L	FLMNH 242766	Glades County, FL	Caloosahatchee/ Bermont	7.762	5.684
Nucula proxima	L	FLMNH 242766	Glades County, FL	Caloosahatchee/ Bermont	6.209	4.726

Taxon Name	Valve	Museum	Locality	Formation	Width (mm)	Height (mm)
Nucula proxima	L	FLMNH 242766	Glades County, FL	Caloosahatchee/ Bermont	4.36	3.721
Nucula proxima	L	FLMNH 242766	Glades County, FL	Caloosahatchee/ Bermont	5.936	5.045
Nucula proxima	L	FLMNH 242766	Glades County, FL	Caloosahatchee/ Bermont	5.365	4.337
Nucula proxima	L	FLMNH 242766	Glades County, FL	Caloosahatchee/ Bermont	3.858	3.972
Nucula proxima	L	FLMNH 242766	Glades County, FL	Caloosahatchee/ Bermont	4.634	4.132
Nucula proxima	L	FLMNH 242766	Glades County, FL	Caloosahatchee/ Bermont	4.041	3.402
Nucula proxima	L	FLMNH 242766	Glades County, FL	Caloosahatchee/ Bermont	4.589	4.086
Nucula proxima	L	FLMNH 242766	Glades County, FL	Caloosahatchee/ Bermont	5.114	4.178
Nucula proxima	L	FLMNH 242766	Glades County, FL	Caloosahatchee/ Bermont	4.657	4.041
Nucula proxima	L	FLMNH 242766	Glades County, FL	Caloosahatchee/ Bermont	4.246	3.675
Nucula proxima	L	FLMNH 242766	Glades County, FL	Caloosahatchee/ Bermont	4.292	3.47
Nucula proxima	L	FLMNH 242766	Glades County, FL	Caloosahatchee/ Bermont	3.79	3.812
Nucula proxima	L	FLMNH 242766	Glades County, FL	Caloosahatchee/ Bermont	4.292	3.653
Nucula proxima	L	FLMNH 242766	Glades County, FL	Caloosahatchee/ Bermont	5.045	4.429
Nucula proxima	L	FLMNH 242766	Glades County, FL	Caloosahatchee/ Bermont	5.776	4.954
Nucula proxima	L	FLMNH 242766	Glades County, FL	Caloosahatchee/ Bermont	5.296	4.726
Nucula proxima	L	FLMNH 242766	Glades County, FL	Caloosahatchee/ Bermont	4.429	3.995

Taxon Name	Valve	Museum	Locality	Formation	Width (mm)	Height (mm)
Nucula proxima	L	FLMNH 242766	Glades County, FL	Caloosahatchee/ Bermont	4.452	3.721
Nucula proxima	L	FLMNH 242766	Glades County, FL	Caloosahatchee/ Bermont	5.045	4.452
Nucula proxima	L	FLMNH 242766	Glades County, FL	Caloosahatchee/ Bermont	4.794	4.109
Nucula proxima	L	FLMNH 242766	Glades County, FL	Caloosahatchee/ Bermont	4.589	3.995
Nucula proxima	L	FLMNH 242766	Glades County, FL	Caloosahatchee/ Bermont	4.589	4.018
Nucula proxima	L	FLMNH 242766	Glades County, FL	Caloosahatchee/ Bermont	4.634	4.064
Nucula proxima	L	FLMNH 242766	Glades County, FL	Caloosahatchee/ Bermont	4.155	3.927
Nucula proxima	L	FLMNH 242766	Glades County, FL	Caloosahatchee/ Bermont	5.137	4.086
Nucula proxima	L	FLMNH 242766	Glades County, FL	Caloosahatchee/ Bermont	3.653	3.242
Nucula proxima	L	FLMNH 204489	Hendry County, FL	Caloosahatchee	3.698	3.287
Nucula proxima	L	FLMNH 204489	Hendry County, FL	Caloosahatchee	3.47	3.105
Nucula proxima	R	FLMNH 222156	Charolette County, FL	Caloosahatchee	4.726	4.041
Nucula proxima	R	FLMNH 222156	Charolette County, FL	Caloosahatchee	3.744	3.31
Nucula proxima	R	FLMNH 222156	Charolette County, FL	Caloosahatchee	3.904	3.196
Nucula proxima	R	FLMNH 222156	Charolette County, FL	Caloosahatchee	5.159	4.817
Nucula proxima	R	FLMNH 222158	Charolette County, FL	Caloosahatchee	4.315	3.584
Nucula proxima	R	FLMNH 99967	Hendry County, FL	Caloosahatchee	4.611	3.79

Taxon Name	Valve	Museum	Locality	Formation	Width (mm)	Height (mm)
Nucula proxima	R	FLMNH 99967	Hendry County, FL	Caloosahatchee	5.388	4.611
Nucula proxima	R	FLMNH 99967	Hendry County, FL	Caloosahatchee	4.703	3.812
Nucula proxima	R	FLMNH 242766	Glades County, FL	Caloosahatchee/ Bermont	4.109	3.402
Nucula proxima	R	FLMNH 242766	Glades County, FL	Caloosahatchee/ Bermont	6.05	5.273
Nucula proxima	R	FLMNH 242766	Glades County, FL	Caloosahatchee/ Bermont	5.639	4.84
Nucula proxima	R	FLMNH 242766	Glades County, FL	Caloosahatchee/ Bermont	6.095	5.022
Nucula proxima	R	FLMNH 242766	Glades County, FL	Caloosahatchee/ Bermont	4.794	3.995
Nucula proxima	R	FLMNH 242766	Glades County, FL	Caloosahatchee/ Bermont	5.114	4.155
Nucula proxima	R	FLMNH 242766	Glades County, FL	Caloosahatchee/ Bermont	5.776	4.794
Nucula proxima	R	FLMNH 242766	Glades County, FL	Caloosahatchee/ Bermont	5.045	5.022
Nucula proxima	R	FLMNH 242766	Glades County, FL	Caloosahatchee/ Bermont	4.566	3.927
Nucula proxima	R	FLMNH 242766	Glades County, FL	Caloosahatchee/ Bermont	5.388	4.337
Nucula proxima	R	FLMNH 242766	Glades County, FL	Caloosahatchee/ Bermont	5.799	4.406
Nucula proxima	R	FLMNH 242766	Glades County, FL	Caloosahatchee/ Bermont	6.529	5.433
Nucula proxima	R	FLMNH 242766	Glades County, FL	Caloosahatchee/ Bermont	6.209	5.502
Nucula proxima	R	FLMNH 242766	Glades County, FL	Caloosahatchee/ Bermont	5.388	4.337
Nucula proxima	R	FLMNH 242766	Glades County, FL	Caloosahatchee/ Bermont	5.388	5

Taxon Name	Valve	Museum	Locality	Formation	Width (mm)	Height (mm)
Nucula proxima	R	FLMNH 242766	Glades County, FL	Caloosahatchee/ Bermont	4.863	4.223
Nucula proxima	R	FLMNH 242766	Glades County, FL	Caloosahatchee/ Bermont	5.159	4.748
Nucula proxima	R	FLMNH 242766	Glades County, FL	Caloosahatchee/ Bermont	5.913	5.022
Nucula proxima	R	FLMNH 242766	Glades County, FL	Caloosahatchee/ Bermont	4.817	3.812
Nucula proxima	R	FLMNH 242766	Glades County, FL	Caloosahatchee/ Bermont	5.525	4.178
Nucula proxima	R	FLMNH 242766	Glades County, FL	Caloosahatchee/ Bermont	5.091	4.452
Nucula proxima	R	FLMNH 242766	Glades County, FL	Caloosahatchee/ Bermont	7.123	5.342
Nucula proxima	R	FLMNH 242766	Glades County, FL	Caloosahatchee/ Bermont	5.137	5.114
Nucula proxima	R	FLMNH 242766	Glades County, FL	Caloosahatchee/ Bermont	5.821	4.657
Nucula proxima	R	FLMNH 242766	Glades County, FL	Caloosahatchee/ Bermont	4.589	3.79
Nucula proxima	R	FLMNH 242766	Glades County, FL	Caloosahatchee/ Bermont	6.187	5.296
Nucula proxima	R	FLMNH 242766	Glades County, FL	Caloosahatchee/ Bermont	5.388	5.045
Nucula proxima	R	FLMNH 242766	Glades County, FL	Caloosahatchee/ Bermont	5.41	5.137
Nucula proxima	R	FLMNH 242766	Glades County, FL	Caloosahatchee/ Bermont	5.936	4.589
Nucula proxima	R	FLMNH 242766	Glades County, FL	Caloosahatchee/ Bermont	5.502	3.972
Nucula proxima	R	FLMNH 242766	Glades County, FL	Caloosahatchee/ Bermont	6.118	5.388
Nucula proxima	R	FLMNH 242766	Glades County, FL	Caloosahatchee/ Bermont	4.977	4.269

Taxon Name	Valve	Museum	Locality	Formation	Width (mm)	Height (mm)
Nucula proxima	R	FLMNH 242766	Glades County, FL	Caloosahatchee/ Bermont	5	4.155
Nucula proxima	R	FLMNH 242766	Glades County, FL	Caloosahatchee/ Bermont	5.114	4.201
Nucula proxima	R	FLMNH 242766	Glades County, FL	Caloosahatchee/ Bermont	6.369	5.182
Nucula proxima	R	FLMNH 99967	Hendry County, FL	Caloosahatchee	4.292	3.561
Nucula proxima	R	FLMNH 99967	Hendry County, FL	Caloosahatchee	4.178	3.333
Nucula proxima	R	FLMNH 242766	Glades County, FL	Caloosahatchee/ Bermont	4.863	4.36
Nucula proxima	R	FLMNH 242766	Glades County, FL	Caloosahatchee/ Bermont	6.369	4.771
Nucula proxima	R	FLMNH 242766	Glades County, FL	Caloosahatchee/ Bermont	5.319	4.497
Nucula proxima	R	FLMNH 242766	Glades County, FL	Caloosahatchee/ Bermont	4.977	3.835
Nucula proxima	R	FLMNH 242766	Glades County, FL	Caloosahatchee/ Bermont	5.342	4.36
Nucula proxima	R	FLMNH 242766	Glades County, FL	Caloosahatchee/ Bermont	5.707	4.52
Nucula proxima	R	FLMNH 242766	Glades County, FL	Caloosahatchee/ Bermont	5.616	4.52
Nucula proxima	R	FLMNH 242766	Glades County, FL	Caloosahatchee/ Bermont	5.114	4.064
Nucula proxima	R	FLMNH 242766	Glades County, FL	Caloosahatchee/ Bermont	4.771	3.881
Nucula proxima	R	FLMNH 242766	Glades County, FL	Caloosahatchee/ Bermont	4.497	3.972
Nucula proxima	R	FLMNH 242766	Glades County, FL	Caloosahatchee/ Bermont	5.022	3.995
Nucula proxima	R	FLMNH 242766	Glades County, FL	Caloosahatchee/ Bermont	3.698	3.607

Taxon Name	Valve	Museum	Locality	Formation	Width (mm)	Height (mm)
Nucula proxima	R	FLMNH 242766	Glades County, FL	Caloosahatchee/ Bermont	4.155	3.584
Nucula proxima	R	FLMNH 242766	Glades County, FL	Caloosahatchee/ Bermont	4.086	3.356
Nucula proxima	R	FLMNH 242766	Glades County, FL	Caloosahatchee/ Bermont	4.543	4.337
Nucula proxima	R	FLMNH 242766	Glades County, FL	Caloosahatchee/ Bermont	4.771	4.064
Nucula proxima	R	FLMNH 242766	Glades County, FL	Caloosahatchee/ Bermont	4.566	3.812
Nucula proxima	R	FLMNH 242766	Glades County, FL	Caloosahatchee/ Bermont	4.817	4.383
Nucula proxima	R	FLMNH 242766	Glades County, FL	Caloosahatchee/ Bermont	5.273	4.908
Nucula proxima	R	FLMNH 242766	Glades County, FL	Caloosahatchee/ Bermont	4.52	3.584
Nucula proxima	R	FLMNH 242766	Glades County, FL	Caloosahatchee/ Bermont	5	4.589
Nucula proxima	R	FLMNH 242766	Glades County, FL	Caloosahatchee/ Bermont	5.251	4.383
Nucula proxima	R	FLMNH 242766	Glades County, FL	Caloosahatchee/ Bermont	4.657	3.858
Nucula proxima	R	FLMNH 242766	Glades County, FL	Caloosahatchee/ Bermont	5.456	4.52
Nucula proxima	R	FLMNH 242766	Glades County, FL	Caloosahatchee/ Bermont	5.57	4.703
Nucula proxima	R	FLMNH 242766	Glades County, FL	Caloosahatchee/ Bermont	5.844	4.657
Nucula proxima	R	FLMNH 204489	Hendry County, FL	Caloosahatchee	4.566	3.561
Nucula proxima	R	FLMNH 204489	Hendry County, FL	Caloosahatchee	4.931	3.904
Nucula Proxima	L	FLMNH 186696	Craven County, NC	James City	9.117	8.479

Taxon Name	Valve	Museum	Locality	Formation	Width (mm)	Height (mm)
Nucula Proxima	L	FLMNH 186696	Craven County, NC	James City	8.725	8.945
Nucula Proxima	L	FLMNH 186696	Craven County, NC	James City	9.386	8.774
Nucula Proxima	L	FLMNH 186696	Craven County, NC	James City	8.798	8.406
Nucula Proxima	L	FLMNH 186696	Craven County, NC	James City	6.176	6.053
Nucula Proxima	R	FLMNH 186696	Craven County, NC	James City	10.048	8.896
Nucula Proxima	R	FLMNH 186696	Craven County, NC	James City	9.95	8.7
Nucula Proxima	R	FLMNH 186696	Craven County, NC	James City	9.166	7.842
Nucula proxima	L	FLMNH 161833	Glynn County, GA	Duplin/Raysor	9.73	8.309
Nucula proxima	L	FLMNH 161833	Glynn County, GA	Duplin/Raysor	9.24	8.064
Nucula proxima	L	FLMNH 161833	Glynn County, GA	Duplin/Raysor	9.73	8.162
Nucula proxima	L	FLMNH 161833	Glynn County, GA	Duplin/Raysor	9.412	8.358
Nucula proxima	L	FLMNH 161833	Glynn County, GA	Duplin/Raysor	10.27	8.407
Nucula proxima	L	FLMNH 161833	Glynn County, GA	Duplin/Raysor	6.814	6.348
Nucula proxima	L	FLMNH 161833	Glynn County, GA	Duplin/Raysor	9.069	8.456
Nucula proxima	L	FLMNH 161833	Glynn County, GA	Duplin/Raysor	5.882	5.172
Nucula proxima	L	FLMNH 161833	Glynn County, GA	Duplin/Raysor	10.196	8.676
Nucula proxima	L	FLMNH 161833	Glynn County, GA	Duplin/Raysor	7.77	6.74

Taxon Name	Valve	Museum	Locality	Formation	Width (mm)	Height (mm)
Nucula proxima	L	FLMNH 161833	Glynn County, GA	Duplin/Raysor	9.142	9.118
Nucula proxima	L	FLMNH 169464	Darling County, SC	Raysor	5.76	5.588
Nucula proxima	L	FLMNH 169464	Darling County, SC	Raysor	7.892	7.549
Nucula proxima	L	FLMNH 169464	Darling County, SC	Raysor	7.549	7.525
Nucula proxima	L	FLMNH 169464	Darling County, SC	Raysor	6.593	6.74
Nucula proxima	L	FLMNH 169464	Darling County, SC	Raysor	5	4.044
Nucula proxima	L	FLMNH 169464	Darling County, SC	Raysor	6.961	7.059
Nucula proxima	L	FLMNH 169464	Darling County, SC	Raysor	6.912	6.887
Nucula proxima	L	FLMNH 169464	Darling County, SC	Raysor	4.853	4.118
Nucula proxima	L	FLMNH 169464	Darling County, SC	Raysor	8.113	7.941
Nucula proxima	L	FLMNH 169464	Darling County, SC	Raysor	6.887	7.525
Nucula proxima	L	FLMNH 169464	Darling County, SC	Raysor	6.054	6.078
Nucula proxima	L	FLMNH 169464	Darling County, SC	Raysor	6.789	5.858
Nucula proxima	L	FLMNH 169464	Darling County, SC	Raysor	6.078	6.029
Nucula proxima	L	FLMNH 169464	Darling County, SC	Raysor	8.627	7.5
Nucula proxima	L	FLMNH 169464	Darling County, SC	Raysor	6.838	5.686
Nucula proxima	L	FLMNH 169464	Darling County, SC	Raysor	6.569	6.74

Taxon Name	Valve	Museum	Locality	Formation	Width (mm)	Height (mm)
Nucula proxima	L	FLMNH 169464	Darling County, SC	Raysor	6.299	5.637
Nucula proxima	L	FLMNH 185920	Darling County, SC	Raysor	6.201	6.078
Nucula proxima	L	FLMNH 185920	Darling County, SC	Raysor	-	-
Nucula proxima	L	FLMNH 185920	Darling County, SC	Raysor	-	-
Nucula proxima	L	FLMNH 185920	Darling County, SC	Raysor	-	-
Nucula proxima	L	FLMNH 185920	Darling County, SC	Raysor	5.735	5.27
Nucula proxima	L	FLMNH 185920	Darling County, SC	Raysor	6.691	6.152
Nucula proxima	L	FLMNH 185920	Darling County, SC	Raysor	7.451	6.887
Nucula proxima	L	FLMNH 185920	Darling County, SC	Raysor	6.054	5.319
Nucula proxima	L	FLMNH 185920	Darling County, SC	Raysor	5.49	5.49
Nucula proxima	L	FLMNH 185920	Darling County, SC	Raysor	6.005	5.784
Nucula proxima	L	FLMNH 185920	Darling County, SC	Raysor	6.642	5.637
Nucula proxima	L	FLMNH 185920	Darling County, SC	Raysor	5.123	5.196
Nucula proxima	L	FLMNH 185920	Darling County, SC	Raysor	5.147	4.632
Nucula proxima	L	FLMNH 185920	Darling County, SC	Raysor	6.127	6.348
Nucula proxima	L	FLMNH 185920	Darling County, SC	Raysor	5.441	5.074
Nucula proxima	L	FLMNH 185920	Darling County, SC	Raysor	6.127	6.348

Taxon Name	Valve	Museum	Locality	Formation	Width (mm)	Height (mm)
Nucula proxima	L	FLMNH 185920	Darling County, SC	Raysor	5.956	4.706
Nucula proxima	L	FLMNH 185920	Darling County, SC	Raysor	5.882	4.583
Nucula proxima	L	FLMNH 185920	Darling County, SC	Raysor	8.162	8.015
Nucula proxima	L	FLMNH 185920	Darling County, SC	Raysor	5.637	5.907
Nucula proxima	L	FLMNH 185920	Darling County, SC	Raysor	6.422	6.716
Nucula proxima	L	FLMNH 185920	Darling County, SC	Raysor	7.426	6.985
Nucula proxima	L	FLMNH 185920	Darling County, SC	Raysor	5.49	4.73
Nucula proxima	L	FLMNH 185920	Darling County, SC	Raysor	6.029	6.299
Nucula proxima	L	FLMNH 185920	Darling County, SC	Raysor	6.618	6.716
Nucula proxima	L	FLMNH 185920	Darling County, SC	Raysor	7.279	6.544
Nucula proxima	L	FLMNH 185920	Darling County, SC	Raysor	6.52	5.956
Nucula proxima	L	FLMNH 185920	Darling County, SC	Raysor	6.422	5.564
Nucula proxima	L	FLMNH 185920	Darling County, SC	Raysor	6.618	5.907
Nucula proxima	L	FLMNH 185920	Darling County, SC	Raysor	6.667	5.882
Nucula proxima	L	FLMNH 185920	Darling County, SC	Raysor	5.637	5.417
Nucula proxima	L	FLMNH 185920	Darling County, SC	Raysor	5.613	5.27
Nucula proxima	L	FLMNH 185920	Darling County, SC	Raysor	5.662	4.534

Taxon Name	Valve	Museum	Locality	Formation	Width (mm)	Height (mm)
Nucula proxima	R	FLMNH 161833	Glynn County, GA	Duplin/Raysor	9.457	8.403
Nucula proxima	R	FLMNH 161833	Glynn County, GA	Duplin/Raysor	6.348	6.275
Nucula proxima	R	FLMNH 161833	Glynn County, GA	Duplin/Raysor	-	-
Nucula proxima	R	FLMNH 161833	Glynn County, GA	Duplin/Raysor	7.917	8.186
Nucula proxima	R	FLMNH 161833	Glynn County, GA	Duplin/Raysor	7.5	7.034
Nucula proxima	R	FLMNH 161833	Glynn County, GA	Duplin/Raysor	5.417	5.343
Nucula proxima	R	FLMNH 169464	Darling County, SC	Raysor	8.922	8.529
Nucula proxima	R	FLMNH 169464	Darling County, SC	Raysor	8.113	7.941
Nucula proxima	R	FLMNH 169464	Darling County, SC	Raysor	8.873	7.279
Nucula proxima	R	FLMNH 169464	Darling County, SC	Raysor	7.745	6.422
Nucula proxima	R	FLMNH 169464	Darling County, SC	Raysor	9.167	8.676
Nucula proxima	R	FLMNH 169464	Darling County, SC	Raysor	6.985	6.324
Nucula proxima	R	FLMNH 169464	Darling County, SC	Raysor	6.961	6.275
Nucula proxima	R	FLMNH 169464	Darling County, SC	Raysor	7.99	6.716
Nucula proxima	R	FLMNH 169464	Darling County, SC	Raysor	7.181	5.686
Nucula proxima	R	FLMNH 169464	Darling County, SC	Raysor	8.775	7.402
Nucula proxima	R	FLMNH 169464	Darling County, SC	Raysor	6.373	5.319

Taxon Name	Valve	Museum	Locality	Formation	Width (mm)	Height (mm)
Nucula proxima	R	FLMNH 169464	Darling County, SC	Raysor	6.348	5.27
Nucula proxima	R	FLMNH 169464	Darling County, SC	Raysor	6.912	6.127
Nucula proxima	R	FLMNH 169464	Darling County, SC	Raysor	8.113	7.034
Nucula proxima	R	FLMNH 169464	Darling County, SC	Raysor	5.833	4.73
Nucula proxima	R	FLMNH 169464	Darling County, SC	Raysor	7.402	6.52
Nucula proxima	R	FLMNH 169464	Darling County, SC	Raysor	7.23	6.275
Nucula proxima	R	FLMNH 169464	Darling County, SC	Raysor	8.113	7.77
Nucula proxima	R	FLMNH 169464	Darling County, SC	Raysor	5.025	4.191
Nucula proxima	R	FLMNH 169464	Darling County, SC	Raysor	8.235	7.353
Nucula proxima	R	FLMNH 169464	Darling County, SC	Raysor	6.495	5.441
Nucula proxima	R	FLMNH 185920	Darling County, SC	Raysor	5.662	5.515
Nucula proxima	R	FLMNH 185920	Darling County, SC	Raysor	7.304	6.25
Nucula proxima	R	FLMNH 185920	Darling County, SC	Raysor	7.819	7.304
Nucula proxima	R	FLMNH 185920	Darling County, SC	Raysor	7.279	6.005
Nucula proxima	R	FLMNH 185920	Darling County, SC	Raysor	6.985	5.686
Nucula proxima	R	FLMNH 185920	Darling County, SC	Raysor	6.961	6.544
Nucula proxima	R	FLMNH 185920	Darling County, SC	Raysor	7.696	7.108

Taxon Name	Valve	Museum	Locality	Formation	Width (mm)	Height (mm)
Nucula proxima	R	FLMNH 185920	Darling County, SC	Raysor	7.745	7.206
Nucula proxima	R	FLMNH 185920	Darling County, SC	Raysor	5.098	4.853
Nucula proxima	R	FLMNH 185920	Darling County, SC	Raysor	5.49	5.294
Nucula proxima	R	FLMNH 185920	Darling County, SC	Raysor	6.299	5
Nucula proxima	R	FLMNH 185920	Darling County, SC	Raysor	5.515	4.853
Nucula proxima	R	FLMNH 185920	Darling County, SC	Raysor	6.225	5.735
Nucula proxima	R	FLMNH 185920	Darling County, SC	Raysor	6.25	5.27
Nucula proxima	R	FLMNH 185920	Darling County, SC	Raysor	7.304	6.471
Nucula proxima	R	FLMNH 185920	Darling County, SC	Raysor	7.132	6.691
Nucula proxima	R	FLMNH 185920	Darling County, SC	Raysor	6.029	4.853
Nucula proxima	R	FLMNH 185920	Darling County, SC	Raysor	5.172	4.804
Nucula proxima	R	FLMNH 185920	Darling County, SC	Raysor	6.642	6.716
Nucula proxima	R	FLMNH 185920	Darling County, SC	Raysor	7.279	5.809
Nucula proxima	R	FLMNH 185920	Darling County, SC	Raysor	7.721	6.765
Nucula proxima	R	FLMNH 185920	Darling County, SC	Raysor	4.951	4.436
Nucula proxima	L	FLMNH 120105	Leon County, FL	Jackson Bluff	6.664	5.746
Nucula proxima	L	FLMNH 120105	Leon County, FL	Jackson Bluff	4.539	3.96

Taxon Name	Valve	Museum	Locality	Formation	Width (mm)	Height (mm)
Nucula proxima	L	FLMNH 120105	Leon County, FL	Jackson Bluff	4.563	3.911
Nucula proxima	L	FLMNH 120105	Leon County, FL	Jackson Bluff	4.974	5.022
Nucula proxima	L	FLMNH 120105	Leon County, FL	Jackson Bluff	4.684	4.056
Nucula proxima	L	FLMNH 120105	Leon County, FL	Jackson Bluff	4.805	4.225
Nucula proxima	L	FLMNH 120105	Leon County, FL	Jackson Bluff	5.529	5.215
Nucula proxima	L	FLMNH 120105	Leon County, FL	Jackson Bluff	4.587	3.911
Nucula proxima	L	FLMNH 120105	Leon County, FL	Jackson Bluff	4.443	3.911
Nucula proxima	L	FLMNH 120105	Leon County, FL	Jackson Bluff	3.501	3.018
Nucula proxima	L	FLMNH 120105	Leon County, FL	Jackson Bluff	3.308	2.752
Nucula proxima	L	FLMNH 120108	Leon County, FL	Jackson Bluff	6.078	5.539
Nucula proxima	L	FLMNH 120108	Leon County, FL	Jackson Bluff	7.107	6.102
Nucula proxima	L	FLMNH 120108	Leon County, FL	Jackson Bluff	3.995	3.676
Nucula proxima	L	FLMNH 120108	Leon County, FL	Jackson Bluff	5.71	5.367
Nucula proxima	L	FLMNH 120108	Leon County, FL	Jackson Bluff	5.343	4.632
Nucula proxima	L	FLMNH 120108	Leon County, FL	Jackson Bluff	3.848	3.259
Nucula proxima	L	FLMNH 120108	Leon County, FL	Jackson Bluff	5.416	4.436
Nucula proxima	L	FLMNH 120108	Leon County, FL	Jackson Bluff	4.509	3.701

Taxon Name	Valve	Museum	Locality	Formation	Width (mm)	Height (mm)
Nucula proxima	L	FLMNH 120108	Leon County, FL	Jackson Bluff	4.436	3.75
Nucula proxima	L	FLMNH 120108	Leon County, FL	Jackson Bluff	5.465	4.338
Nucula proxima	L	FLMNH 120108	Leon County, FL	Jackson Bluff	4.117	3.652
Nucula proxima	L	FLMNH 120108	Leon County, FL	Jackson Bluff	3.406	2.622
Nucula proxima	L	FLMNH 120108	Leon County, FL	Jackson Bluff	3.456	2.818
Nucula proxima	L	FLMNH 120108	Leon County, FL	Jackson Bluff	4.068	3.603
Nucula proxima	L	FLMNH 120108	Leon County, FL	Jackson Bluff	4.166	3.652
Nucula proxima	L	FLMNH 120108	Leon County, FL	Jackson Bluff	3.676	3.137
Nucula proxima	L	FLMNH 120108	Leon County, FL	Jackson Bluff	3.039	2.72
Nucula proxima	L	FLMNH 140035	Leon County, FL	Jackson Bluff	8.823	8.504
Nucula proxima	L	FLMNH 140035	Leon County, FL	Jackson Bluff	5.906	5.122
Nucula proxima	L	FLMNH 140035	Leon County, FL	Jackson Bluff	7.205	6.47
Nucula proxima	L	FLMNH 140035	Leon County, FL	Jackson Bluff	7.107	5.808
Nucula proxima	L	FLMNH 140035	Leon County, FL	Jackson Bluff	6.078	5.514
Nucula proxima	L	FLMNH 120067	Leon County, FL	Jackson Bluff	4.926	3.995
Nucula proxima	L	FLMNH 120067	Leon County, FL	Jackson Bluff	4.73	4.289
Nucula proxima	L	FLMNH 120067	Leon County, FL	Jackson Bluff	6.813	6.225

Taxon Name	Valve	Museum	Locality	Formation	Width (mm)	Height (mm)
Nucula proxima	L	FLMNH 120067	Leon County, FL	Jackson Bluff	4.926	4.117
Nucula proxima	L	FLMNH 120067	Leon County, FL	Jackson Bluff	103.494	78.815
Nucula proxima	L	FLMNH 120067	Leon County, FL	Jackson Bluff	6.396	6.176
Nucula proxima	L	FLMNH 120067	Leon County, FL	Jackson Bluff	5.245	4.583
Nucula proxima	L	FLMNH 120067	Leon County, FL	Jackson Bluff	6.347	6.102
Nucula proxima	L	FLMNH 120067	Leon County, FL	Jackson Bluff		
Nucula proxima	L	FLMNH 120108	Leon County, FL	Jackson Bluff	7.769	6.862
Nucula proxima	L	FLMNH 120108	Leon County, FL	Jackson Bluff	8.063	6.764
Nucula proxima	L	FLMNH 120108	Leon County, FL	Jackson Bluff	6.641	6.421
Nucula proxima	L	FLMNH 120108	Leon County, FL	Jackson Bluff	4.583	3.995
Nucula proxima	L	FLMNH 120108	Leon County, FL	Jackson Bluff	6.127	6.127
Nucula proxima	L	FLMNH 120108	Leon County, FL	Jackson Bluff	4.583	3.921
Nucula proxima	L	FLMNH 120108	Leon County, FL	Jackson Bluff	3.259	3.039
Nucula proxima	L	FLMNH 120108	Leon County, FL	Jackson Bluff	5.759	5.294
Nucula proxima	L	FLMNH 120108	Leon County, FL	Jackson Bluff	3.97	3.357
Nucula proxima	L	FLMNH 120108	Leon County, FL	Jackson Bluff	5.882	5.245
Nucula proxima	L	FLMNH 120108	Leon County, FL	Jackson Bluff	5.833	5.318

Taxon Name	Valve	Museum	Locality	Formation	Width (mm)	Height (mm)
Nucula proxima	L	FLMNH 120108	Leon County, FL	Jackson Bluff	4.975	4.093
Nucula proxima	L	FLMNH 120108	Leon County, FL	Jackson Bluff	4.779	3.97
Nucula proxima	L	FLMNH 120108	Leon County, FL	Jackson Bluff	4.73	3.872
Nucula proxima	L	FLMNH 120108	Leon County, FL	Jackson Bluff	3.97	3.946
Nucula proxima	L	FLMNH 120108	Leon County, FL	Jackson Bluff	3.676	3.382
Nucula proxima	L	FLMNH 120108	Leon County, FL	Jackson Bluff	4.142	4.387
Nucula proxima	L	FLMNH 120108	Leon County, FL	Jackson Bluff	4.068	3.872
Nucula proxima	L	FLMNH 120108	Leon County, FL	Jackson Bluff	2.549	2.157
Nucula proxima	L	FLMNH 120108	Leon County, FL	Jackson Bluff	5.637	4.852
Nucula proxima	L	FLMNH 120108	Leon County, FL	Jackson Bluff	4.779	4.656
Nucula proxima	L	FLMNH 120108	Leon County, FL	Jackson Bluff	3.799	3.039
Nucula proxima	L	FLMNH 120108	Leon County, FL	Jackson Bluff	4.387	4.24
Nucula proxima	L	FLMNH 120108	Leon County, FL	Jackson Bluff	5.588	4.485
Nucula proxima	L	FLMNH 120108	Leon County, FL	Jackson Bluff	6.813	5.955
Nucula proxima	L	FLMNH 120108	Leon County, FL	Jackson Bluff	8.676	7.94
Nucula proxima	L	FLMNH 120105	Leon County, FL	Jackson Bluff	5.98	4.926
Nucula proxima	L	FLMNH 120105	Leon County, FL	Jackson Bluff	5.22	4.632

Taxon Name	Valve	Museum	Locality	Formation	Width (mm)	Height (mm)
Nucula proxima	L	FLMNH 120105	Leon County, FL	Jackson Bluff	6.323	5.294
Nucula proxima	L	FLMNH 120105	Leon County, FL	Jackson Bluff	4.754	3.946
Nucula proxima	L	FLMNH 120105	Leon County, FL	Jackson Bluff	5.048	4.509
Nucula proxima	L	FLMNH 120105	Leon County, FL	Jackson Bluff	4.705	4.387
Nucula proxima	L	FLMNH 120105	Leon County, FL	Jackson Bluff	3.774	2.72
Nucula proxima	L	FLMNH 120105	Leon County, FL	Jackson Bluff	4.926	4.436
Nucula proxima	L	FLMNH 120105	Leon County, FL	Jackson Bluff	6.47	5.637
Nucula proxima	L	FLMNH 120105	Leon County, FL	Jackson Bluff	6.641	5.784
Nucula proxima	L	FLMNH 120105	Leon County, FL	Jackson Bluff	5.22	4.313
Nucula proxima	L	FLMNH 120105	Leon County, FL	Jackson Bluff	5.416	5.367
Nucula proxima	L	FLMNH 120105	Leon County, FL	Jackson Bluff	4.926	4.583
Nucula proxima	L	FLMNH 120105	Leon County, FL	Jackson Bluff	9.729	9.705
Nucula proxima	L	FLMNH 120105	Leon County, FL	Jackson Bluff	7.769	7.279
Nucula proxima	L	FLMNH 120105	Leon County, FL	Jackson Bluff	5.539	5.22
Nucula proxima	L	FLMNH 120105	Leon County, FL	Jackson Bluff	8.161	7.352
Nucula proxima	L	FLMNH 120105	Leon County, FL	Jackson Bluff	6.47	5.416
Nucula proxima	L	FLMNH 120105	Leon County, FL	Jackson Bluff	6.764	6.053

Taxon Name	Valve	Museum	Locality	Formation	Width (mm)	Height (mm)
Nucula proxima	L	FLMNH 120105	Leon County, FL	Jackson Bluff	7.769	7.842
Nucula proxima	L	FLMNH 120105	Leon County, FL	Jackson Bluff	6.347	5.441
Nucula proxima	R	FLMNH 120105	Leon County, FL	Jackson Bluff	6.347	5.441
Nucula proxima	R	FLMNH 120105	Leon County, FL	Jackson Bluff	7.769	6.862
Nucula proxima	R	FLMNH 120105	Leon County, FL	Jackson Bluff	5.906	5.759
Nucula proxima	R	FLMNH 120105	Leon County, FL	Jackson Bluff	4.093	3.799
Nucula proxima	R	FLMNH 120105	Leon County, FL	Jackson Bluff	4.534	3.995
Nucula proxima	R	FLMNH 120105	Leon County, FL	Jackson Bluff	4.607	3.725
Nucula proxima	R	FLMNH 120105	Leon County, FL	Jackson Bluff		
Nucula proxima	R	FLMNH 120108	Leon County, FL	Jackson Bluff	6.69	5.882
Nucula proxima	R	FLMNH 120108	Leon County, FL	Jackson Bluff	4.509	4.215
Nucula proxima	R	FLMNH 120108	Leon County, FL	Jackson Bluff	4.142	3.406
Nucula proxima	R	FLMNH 120108	Leon County, FL	Jackson Bluff	4.73	4.289
Nucula proxima	R	FLMNH 120108	Leon County, FL	Jackson Bluff	4.852	4.24
Nucula proxima	R	FLMNH 120108	Leon County, FL	Jackson Bluff	5.294	4.607
Nucula proxima	R	FLMNH 120108	Leon County, FL	Jackson Bluff	2.99	2.353
Nucula proxima	R	FLMNH 120108	Leon County, FL	Jackson Bluff	2.598	2.157

Taxon Name	Valve	Museum	Locality	Formation	Width (mm)	Height (mm)
Nucula proxima	R	FLMNH 140035	Leon County, FL	Jackson Bluff	6.029	5.171
Nucula proxima	R	FLMNH 140035	Leon County, FL	Jackson Bluff	5.539	4.362
Nucula proxima	R	FLMNH 120067	Leon County, FL	Jackson Bluff	5.22	4.338
Nucula proxima	R	FLMNH 120067	Leon County, FL	Jackson Bluff	5.563	4.583
Nucula proxima	R	FLMNH 120067	Leon County, FL	Jackson Bluff	5.686	4.607
Nucula proxima	R	FLMNH 120067	Leon County, FL	Jackson Bluff	5.49	5.294
Nucula proxima	R	FLMNH 120067	Leon County, FL	Jackson Bluff	8.087	7.426
Nucula proxima	R	FLMNH 120067	Leon County, FL	Jackson Bluff	5.637	4.852
Nucula proxima	R	FLMNH 120067	Leon County, FL	Jackson Bluff	5.71	4.803
Nucula proxima	R	FLMNH 120067	Leon County, FL	Jackson Bluff	6.053	5.539
Nucula proxima	R	FLMNH 120067	Leon County, FL	Jackson Bluff	6.862	6.151
Nucula proxima	R	FLMNH 120067	Leon County, FL	Jackson Bluff	4.754	3.75
Nucula proxima	R	FLMNH 120067	Leon County, FL	Jackson Bluff	5.441	4.877
Nucula proxima	R	FLMNH 120108	Leon County, FL	Jackson Bluff	7.622	6.372
Nucula proxima	R	FLMNH 120108	Leon County, FL	Jackson Bluff	5.294	4.436
Nucula proxima	R	FLMNH 120108	Leon County, FL	Jackson Bluff	6.911	5.882
Nucula proxima	R	FLMNH 120108	Leon County, FL	Jackson Bluff	5.637	4.828

Taxon Name	Valve	Museum	Locality	Formation	Width (mm)	Height (mm)
Nucula proxima	R	FLMNH 120108	Leon County, FL	Jackson Bluff	5.931	5.024
Nucula proxima	R	FLMNH 120108	Leon County, FL	Jackson Bluff	5.269	4.828
Nucula proxima	R	FLMNH 120108	Leon County, FL	Jackson Bluff	5.294	4.509
Nucula proxima	R	FLMNH 120108	Leon County, FL	Jackson Bluff	5.147	4.24
Nucula proxima	R	FLMNH 120108	Leon County, FL	Jackson Bluff	4.46	3.725
Nucula proxima	R	FLMNH 120108	Leon County, FL	Jackson Bluff	3.995	3.406
Nucula proxima	R	FLMNH 120108	Leon County, FL	Jackson Bluff	3.701	2.72
Nucula proxima	R	FLMNH 120108	Leon County, FL	Jackson Bluff	3.603	2.867
Nucula proxima	R	FLMNH 120105	Leon County, FL	Jackson Bluff	7.23	5.857
Nucula proxima	R	FLMNH 120105	Leon County, FL	Jackson Bluff	6.862	5.931
Nucula proxima	R	FLMNH 120105	Leon County, FL	Jackson Bluff	5.048	3.921
Nucula proxima	R	FLMNH 120105	Leon County, FL	Jackson Bluff	5.097	4.215
Nucula proxima	R	FLMNH 120105	Leon County, FL	Jackson Bluff	4.975	4.191
Nucula proxima	R	FLMNH 120105	Leon County, FL	Jackson Bluff	7.671	6.666
Nucula proxima	R	FLMNH 120105	Leon County, FL	Jackson Bluff	5.661	4.656
Nucula proxima	R	FLMNH 120105	Leon County, FL	Jackson Bluff	4.852	3.774
Nucula proxima	R	FLMNH 120105	Leon County, FL	Jackson Bluff	5.955	5.269

Taxon Name	Valve	Museum	Locality	Formation	Width (mm)	Height (mm)
Nucula proxima	R	FLMNH 140035	Leon County, FL	Jackson Bluff	6.985	6.445
Nucula proxima	R	FLMNH 140035	Leon County, FL	Jackson Bluff	6.151	4.901
Nucula proxima	R	FLMNH 140035	Leon County, FL	Jackson Bluff	6.764	5.612
Nucula proxima	R	FLMNH 140035	Leon County, FL	Jackson Bluff	4.877	3.897
Nucula proxima	L	FLMNH 173222	Broward County, FL	Tamiami	5.539	5.073
Nucula proxima	L	FLMNH 173222	Broward County, FL	Tamiami	5.171	4.583
Nucula proxima	L	FLMNH 173222	Broward County, FL	Tamiami	4.803	4.828
Nucula proxima	L	FLMNH 173222	Broward County, FL	Tamiami	4.779	4.313
Nucula proxima	L	FLMNH 200813	Sarasota County, FL	Tamiami	7.132	7.524
Nucula proxima	L	FLMNH 173222	Broward County, FL	Tamiami	6.347	5.465
Nucula proxima	L	FLMNH 173222	Broward County, FL	Tamiami	5.686	5.171
Nucula proxima	L	FLMNH 173222	Broward County, FL	Tamiami	6.102	4.828
Nucula proxima	L	FLMNH 173222	Broward County, FL	Tamiami	5.465	4.583
Nucula proxima	R	FLMNH 173222	Broward County, FL	Tamiami	4.387	3.725
Nucula proxima	R	FLMNH 200813	Sarasota County, FL	Tamiami	7.769	6.788
Nucula proxima	R	FLMNH 173222	Broward County, FL	Tamiami	4.95	4.215
Nucula proxima	L	FLMNH 177563	Hampton County, VA	Yorktown	6.157	5.94

Taxon Name	Valve	Museum	Locality	Formation	Width (mm)	Height (mm)
Nucula proxima	L	FLMNH 177563	Hampton County, VA	Yorktown	7.219	6.181
Nucula proxima	L	FLMNH 210427	Norfolk Naval Res. VA	Yorktown	8.113	7.267
Nucula proxima	R	FLMNH 177563	Hampton County, VA	Yorktown	8.014	6.323
Nucula proxima	R	FLMNH 177563	Hampton County, VA	Yorktown	7.744	6.225
Nucula proxima	R	FLMNH 177563	Hampton County, VA	Yorktown	10.661	9.411
Nucula proxima	R	FLMNH 177563	Hampton County, VA	Yorktown	7.058	6.764
Nucula proxima	R	FLMNH 177563	Hampton County, VA	Yorktown	7.573	5.735
Nucula chipolana	L	FLMNH 104159	Calhoun County, FL	Chipola	1.887	1.421
Nucula chipolana	L	FLMNH 104159	Calhoun County, FL	Chipola	2.034	1.544
Nucula chipolana	L	FLMNH 104159	Calhoun County, FL	Chipola	3.48	2.647
Nucula chipolana	L	FLMNH 104159	Calhoun County, FL	Chipola	2.941	2.304
Nucula chipolana	L	FLMNH 104159	Calhoun County, FL	Chipola	2.5	1.863
Nucula chipolana	L	FLMNH 104159	Calhoun County, FL	Chipola	2.941	2.304
Nucula chipolana	L	FLMNH 104159	Calhoun County, FL	Chipola	2.353	1.74
Nucula chipolana	L	FLMNH 104159	Calhoun County, FL	Chipola	2.451	1.961
Nucula chipolana	L	FLMNH 104159	Calhoun County, FL	Chipola	2.549	2.132
Nucula chipolana	L	FLMNH 104159	Calhoun County, FL	Chipola	2.524	2.132

Taxon Name	Valve	Museum	Locality	Formation	Width (mm)	Height (mm)
Nucula chipolana	L	FLMNH 104159	Calhoun County, FL	Chipola	2.573	2.132
Nucula chipolana	L	FLMNH 104159	Calhoun County, FL	Chipola	2.72	2.255
Nucula chipolana	L	FLMNH 104159	Calhoun County, FL	Chipola	2.475	2.083
Nucula chipolana	L	FLMNH 93860	Calhoun County, FL	Chipola	4.779	4.068
Nucula chipolana	L	FLMNH 93860	Calhoun County, FL	Chipola	4.362	4.289
Nucula chipolana	L	FLMNH 93860	Calhoun County, FL	Chipola	4.142	3.505
Nucula chipolana	L	FLMNH 93860	Calhoun County, FL	Chipola	4.95	4.411
Nucula chipolana	L	FLMNH 93860	Calhoun County, FL	Chipola	4.632	3.823
Nucula chipolana	L	FLMNH 93860	Calhoun County, FL	Chipola	4.558	3.676
Nucula chipolana	L	FLMNH 93860	Calhoun County, FL	Chipola	3.725	3.039
Nucula chipolana	L	FLMNH 93860	Calhoun County, FL	Chipola	5.097	4.95
Nucula chipolana	L	FLMNH 93860	Calhoun County, FL	Chipola	4.705	4.24
Nucula chipolana	L	FLMNH 93860	Calhoun County, FL	Chipola	4.387	3.603
Nucula chipolana	L	FLMNH 93860	Calhoun County, FL	Chipola	3.725	2.769
Nucula chipolana	L	FLMNH 93860	Calhoun County, FL	Chipola	3.725	2.769
Nucula chipolana	L	FLMNH 93860	Calhoun County, FL	Chipola	4.681	3.578
Nucula chipolana	L	FLMNH 93860	Calhoun County, FL	Chipola	4.215	3.505

Taxon Name	Valve	Museum	Locality	Formation	Width (mm)	Height (mm)
Nucula chipolana	L	FLMNH 93860	Calhoun County, FL	Chipola	4.656	4.019
Nucula chipolana	L	FLMNH 93860	Calhoun County, FL	Chipola	3.284	3.431
Nucula chipolana	L	FLMNH 93860	Calhoun County, FL	Chipola	3.97	3.774
Nucula chipolana	L	FLMNH 93860	Calhoun County, FL	Chipola	3.627	3.21
Nucula chipolana	L	FLMNH 93860	Calhoun County, FL	Chipola	4.093	3.701
Nucula chipolana	L	FLMNH 93860	Calhoun County, FL	Chipola	3.97	3.627
Nucula chipolana	L	FLMNH 93860	Calhoun County, FL	Chipola	4.068	3.872
Nucula chipolana	R	FLMNH 104159	Calhoun County, FL	Chipola	2.206	1.863
Nucula chipolana	R	FLMNH 104159	Calhoun County, FL	Chipola	2.132	1.765
Nucula chipolana	R	FLMNH 104159	Calhoun County, FL	Chipola	2.108	1.74
Nucula chipolana	R	FLMNH 104159	Calhoun County, FL	Chipola	2.108	1.716
Nucula chipolana	R	FLMNH 104159	Calhoun County, FL	Chipola	2.108	1.716
Nucula chipolana	R	FLMNH 93860	Calhoun County, FL	Chipola	4.485	3.652
Nucula chipolana	R	FLMNH 93860	Calhoun County, FL	Chipola	4.411	3.848
Nucula chipolana	R	FLMNH 93860	Calhoun County, FL	Chipola	3.48	2.696
Nucula chipolana	R	FLMNH 93860	Calhoun County, FL	Chipola	3.431	3.063
Nucula chipolana	R	FLMNH 93860	Calhoun County, FL	Chipola	5.269	4.264

Taxon Name	Valve	Museum	Locality	Formation	Width (mm)	Height (mm)
Nucula chipolana	R	FLMNH 93860	Calhoun County, FL	Chipola	4.362	3.872
Nucula chipolana	R	FLMNH 93860	Calhoun County, FL	Chipola	3.627	2.892
Nucula chipolana	R	FLMNH 93860	Calhoun County, FL	Chipola	4.852	4.093
Nucula chipolana	R	FLMNH 93860	Calhoun County, FL	Chipola	3.995	3.308
Nucula chipolana	R	FLMNH 93860	Calhoun County, FL	Chipola	3.382	2.867
Nucula chipolana	R	FLMNH 93860	Calhoun County, FL	Chipola	4.362	4.068
Nucula chipolana	R	FLMNH 93860	Calhoun County, FL	Chipola	3.897	3.235
Nucula chipolana	R	FLMNH 93860	Calhoun County, FL	Chipola	3.848	3.578
Nucula chipolana	R	FLMNH 93860	Calhoun County, FL	Chipola	4.509	3.774
Nucula chipolana	R	FLMNH 93860	Calhoun County, FL	Chipola	4.215	3.921
Nucula chipolana	R	FLMNH 93860	Calhoun County, FL	Chipola	3.897	4.068
Nucula chipolana	R	FLMNH 93860	Calhoun County, FL	Chipola	4.411	4.313
Nucula chipolana	R	FLMNH 93860	Calhoun County, FL	Chipola	4.166	3.308
Nucula chipolana	R	FLMNH 93860	Calhoun County, FL	Chipola	4.362	3.382
Nucula chipolana	R	FLMNH 93860	Calhoun County, FL	Chipola	3.554	3.235
Nucula chipolana	R	FLMNH 93860	Calhoun County, FL	Chipola	4.191	3.529
Nucula chipolana	R	FLMNH 93860	Calhoun County, FL	Chipola	4.093	3.456

Taxon Name	Valve	Museum	Locality	Formation	Width (mm)	Height (mm)
Nucula percrassa	L	MMNS 3277	Tippah, MS	Owl Creek	19.336	13.058
Nucula percrassa	L	MMNS 3277	Tippah, MS	Owl Creek	29.541	18.286
Nucula percrassa	L	MMNS 4004	Tippah, MS	Owl Creek	30.773	17.852
Nucula percrassa	L	MMNS 4004	Tippah, MS	Owl Creek	25.751	15.866
Nucula percrassa	L	MMNS 4004	Tippah, MS	Owl Creek	24.815	15.341
Nucula percrassa	L	MMNS 4004	Tippah, MS	Owl Creek	24.861	16.619
Nucula percrassa	L	MMNS 4004	Tippah, MS	Owl Creek	26.002	17.236
Nucula percrassa	L	MMNS 4004	Tippah, MS	Owl Creek	25.546	16.094
Nucula percrassa	L	MMNS 4004	Tippah, MS	Owl Creek	27.851	16.323
Nucula percrassa	L	MMNS 3065	Tippah, MS	Owl Creek	26.55	16.939
Nucula percrassa	L	MMNS 3065	Tippah, MS	Owl Creek	26.208	15.752
Nucula percrassa	L	MMNS 5627	Tippah, MS	Owl Creek	25.911	16.482
Nucula percrassa	L	MMNS 5627	Tippah, MS	Owl Creek	27.623	17.281
Nucula percrassa	L	MMNS 3287	Tippah, MS	Owl Creek	25.546	15.843
Nucula percrassa	L		Tippah, MS	Owl Creek	28.194	17.259
Nucula percrassa	L		Tippah, MS	Owl Creek	26.778	16.3
Nucula percrassa	L		Tippah, MS	Owl Creek	21.482	14.154

Taxon Name	Valve	Museum	Locality	Formation	Width (mm)	Height (mm)
Nucula percrassa	L		Tippah, MS	Owl Creek	26.664	16.46
Nucula percrassa	R	MMNS 5627	Tippah, MS	Owl Creek	24.29	15.25
Nucula percrassa	R	MMNS 5627	Tippah, MS	Owl Creek	28.856	17.122
Nucula percrassa	R	MMNS 5627	Tippah, MS	Owl Creek	26.23	16.323
Nucula percrassa	R	MMNS 3287	Tippah, MS	Owl Creek	26.185	16.254
Nucula percrassa	R	MMNS 3287	Tippah, MS	Owl Creek		
Nucula percrassa	R	JS15OC	Tippah, MS	Owl Creek	24.906	15.067
Nucula percrassa	R	JS15OC	Tippah, MS	Owl Creek	18.24	12.122
Nucula percrassa	R	JS15OC	Tippah, MS	Owl Creek	31.801	19.427
Nucula percrassa	R	JS15OC	Tippah, MS	Owl Creek	26.208	16.026
Nucula percrassa	R	JS15OC	Tippah, MS	Owl Creek	29.632	18.971
Nucula percrassa	R	MMNS 3065	Tippah, MS	Owl Creek	28.445	16.962
Nucula percrassa	R	JS15OC	Tippah, MS	Owl Creek	31.207	19.975
Nucula percrassa	R	JS15OC	Tippah, MS	Owl Creek	24.564	16.186
Nucula percrassa	R	MMNS 3277	Tippah, MS	Owl Creek	19.496	13.332
Nucula percrassa	R	MMNS 3277	Tippah, MS	Owl Creek	29.221	17.715
Nucula percrassa	R	MMNS 3277	Tippah, MS	Owl Creek		

Taxon Name	Valve	Museum	Locality	Formation	Width (mm)	Height (mm)
Nucula percrassa	R	MMNS 4004	Tippah, MS	Owl Creek	27.486	16.209
Nucula percrassa	R	MMNS 4004	Tippah, MS	Owl Creek	31.002	17.692
Nucula percrassa	R	MMNS 4004	Tippah, MS	Owl Creek	26.048	16.505
Nucula percrassa	R	MMNS 4004	Tippah, MS	Owl Creek	25.683	16.14
Nucula percrassa	R	MMNS 4004	Tippah, MS	Owl Creek	16.574	11.209
Nucula percrassa	R	MMNS 3065	Tippah, MS	Owl Creek	29.426	18.491
Nucula percrassa	R	MMNS 3065	Tippah, MS	Owl Creek	24.884	15.866
Nucula percrassa	R	MMNS 3065	Tippah, MS	Owl Creek	18.788	12.328
Nucula percrassa	R	MMNS 3065	Tippah, MS	Owl Creek	26.002	15.432
Nucula percrassa	R	MMNS 3065	Tippah, MS	Owl Creek	30.591	17.989
Nucula percrassa	R	MMNS 5627	Tippah, MS	Owl Creek	24.564	15.295
Nucula percrassa	R	MMNS 5627	Tippah, MS	Owl Creek	24.906	15.843
Nucula percrassa	R	MMNS 5627	Tippah, MS	Owl Creek	24.336	15.569
Nucula percrassa	L	JS15OC	Tippah, MS	Owl Creek		
Nucula percrassa	L	JS15OC	Tippah, MS	Owl Creek		
Nucula percrassa	L	JS15OC	Tippah, MS	Owl Creek		
Nucula percrassa	R	JS15OC	Tippah, MS	Owl Creek		

Taxon Name	Valve	Museum	Locality	Formation	Width (mm)	Height (mm)
Nucula percrassa	R	JS15OC	Tippah, MS	Owl Creek	-	-
Nucula slackiana	L	MAPS Collection	Brightseat County, MD	Severn	24.704	18.116
Nucula slackiana	L	MAPS Collection	Brightseat County, MD	Severn	27.998	19.058
Nucula slackiana	R	MAPS Collection	Brightseat County, MD	Severn	35.363	24.51
Nucula slackiana	R	MAPS Collection	Brightseat County, MD	Severn	29.763	21.998
Nucula slackiana	R	MAPS Collection	Brightseat County, MD	Severn	34.351	23.645
Nucula slackiana	R	MAPS Collection	Brightseat County, MD	Severn	32.468	25.057
Nucula slackiana	R	MAPS Collection	Brightseat County, MD	Severn	30.704	22.234
Nucula percrassa	L	MMNS 1782	Union County, MS	Ripley	33.695	23.034
Nucula percrassa	L	MMNS 6820	Union County, MS	Ripley	29.678	20.592
Nucula percrassa	L	MMNS 6820	Union County, MS	Ripley	19.427	12.83
Nucula percrassa	L	MMNS 6820	Union County, MS	Ripley	25.797	17.213
Nucula percrassa	L	MMNS 6820	Union County, MS	Ripley	27.6	18.423
Nucula percrassa	R	MMNS 1782	Union County, MS	Ripley	34.403	22.669
Nucula percrassa	R	MMNS 1782	Union County, MS	Ripley	30.066	23.034
Nucula percrassa	R	MMNS 1782	Union County, MS	Ripley	27.212	18.902
Nucula percrassa	R	MMNS 1782	Union County, MS	Ripley	31.298	20.774

Taxon Name	Valve	Museum	Locality	Formation	Width (mm)	Height (mm)
Nucula percrassa	R	MMNS 6820	Union County, MS	Ripley	26.733	17.327
Nucula percrassa	L	JS15BS	Union County, MS	Ripley	26.812	17.681
Nucula percrassa	L	JS15BS	Union County, MS	Ripley	21.787	15.024
Nucula percrassa	L	JS15BS	Union County, MS	Ripley	19.758	12.077
Nucula percrassa	L	JS15BS	Union County, MS	Ripley	32.85	21.594
Nucula percrassa	L	JS15BS	Union County, MS	Ripley	21.159	14.251
Nucula percrassa	L	JS15BS	Union County, MS	Ripley	27.295	17.536
Nucula percrassa	L	JS15BS	Union County, MS	Ripley	39.42	27.053
Nucula percrassa	R	JS15BS	Union County, MS	Ripley	33.865	21.932
Nucula percrassa	R	JS15BS	Union County, MS	Ripley	31.401	20.773
Nucula percrassa	R	JS15BS	Union County, MS	Ripley	26.908	17.391
Nucula percrassa	R	JS15BS	Union County, MS	Ripley	25.749	17.585
Nucula percrassa	R	JS15BS	Union County, MS	Ripley	25.894	17.246
Nucula percrassa	R	JS15BS	Union County, MS	Ripley	28.357	18.599
Nucula percrassa	R	JS15BS	Union County, MS	Ripley	29.565	19.517
Nucula percrassa	R	JS15BS	Union County, MS	Ripley	24.686	16.522
Nucula percrassa	R	JS15BS	Union County, MS	Ripley	30.821	20.725

Taxon Name	Valve	Museum	Locality	Formation	Width (mm)	Height (mm)
Nucula percrassa	L	MMNS 6820	Union County, MS	Ripley	31.253	21.208
Nucula percrassa	L	MMNS 6820	Union County, MS	Ripley	20.683	13.926
Nucula percrassa	L	MMNS 2809	Union County, MS	Ripley	30.979	19.93
Nucula percrassa	L	MMNS 2809	Union County, MS	Ripley	31.572	20.135
Nucula percrassa	L	MMNS 2809	Union County, MS	Ripley	29.426	20.957
Nucula percrassa	L	MMNS 2809	Union County, MS	Ripley	22.441	14.953
Nucula percrassa	L	MMNS 2809	Union County, MS	Ripley	27.189	17.944
Nucula percrassa	L	MMNS 2809	Union County, MS	Ripley	24.495	15.912
Nucula percrassa	L	MMNS 2809	Union County, MS	Ripley	21.756	14.222
Nucula percrassa	L	MMNS 2809	Union County, MS	Ripley	30.773	21.299
Nucula percrassa	L	MMNS 2809	Union County, MS	Ripley	30.773	21.322
Nucula percrassa	L	MMNS 1483	Union County, MS	Ripley	35.02	23.628
Nucula percrassa	L	MMNS 1483	Union County, MS	Ripley	35.02	23.605
Nucula percrassa	L	MMNS 2486	Union County, MS	Ripley	25.043	16.619
Nucula percrassa	L	MMNS 2486	Union County, MS	Ripley	28.354	18.811
Nucula percrassa	L	MMNS 2486	Union County, MS	Ripley	27.372	18.925
Nucula percrassa	L	MMNS 1632	Union County, MS	Ripley	24.427	15.204

Taxon Name	Valve	Museum	Locality	Formation	Width (mm)	Height (mm)
Nucula percrassa	L	MMNS 3177	Union County, MS	Ripley	24.473	15.295
Nucula percrassa	L	MMNS 2388	Union County, MS	Ripley	29.906	19.45
Nucula percrassa	L	MMNS 2388	Union County, MS	Ripley	22.715	14.884
Nucula percrassa	L	MMNS 2388	Union County, MS	Ripley	23.719	16.368
Nucula percrassa	L	MMNS 2388	Union County, MS	Ripley	22.258	15.41
Nucula percrassa	R	MMNS 6820	Union County, MS	Ripley	27.212	18.286
Nucula percrassa	R	MMNS 6820	Union County, MS	Ripley	19.77	13.355
Nucula percrassa	R	MMNS 6820	Union County, MS	Ripley	26.208	17.67
Nucula percrassa	R	MMNS 6820	Union County, MS	Ripley	18.948	12.807
Nucula percrassa	R	MMNS 2809	Union County, MS	Ripley	30.751	20.021
Nucula percrassa	R	MMNS 2809	Union County, MS	Ripley	21.802	14.245
Nucula percrassa	R	MMNS 2809	Union County, MS	Ripley	30.157	19.77
Nucula percrassa	R	MMNS 2809	Union County, MS	Ripley	25.043	16.756
Nucula percrassa	R	MMNS 2809	Union County, MS	Ripley	18.354	11.255
Nucula percrassa	R	MMNS 2809	Union County, MS	Ripley	30.636	20.5
Nucula percrassa	R	MMNS 1483	Union County, MS	Ripley	18.354	11.277
Nucula percrassa	R	MMNS 1483	Union County, MS	Ripley	30.636	20.5

Taxon Name	Valve	Museum	Locality	Formation	Width (mm)	Height (mm)
Nucula percrassa	R	MMNS 1483	Union County, MS	Ripley	29.655	20.112
Nucula percrassa	R	MMNS 2486	Union County, MS	Ripley	33.65	22.555
Nucula percrassa	R	MMNS 2486	Union County, MS	Ripley	28.171	19.359
Nucula percrassa	R	MMNS 2486	Union County, MS	Ripley	30.066	20.66
Nucula percrassa	R	MMNS 2388	Union County, MS	Ripley	27.486	18.88
Nucula percrassa	R	MMNS 2388	Union County, MS	Ripley	30.636	19.633
Nucula percrassa	R	MMNS 1632	Union County, MS	Ripley	22.852	15.592
Nucula percrassa	R	MMNS 1632	Union County, MS	Ripley	22.03	15.866
Nucula percrassa	R	MMNS 1633	Union County, MS	Ripley	25.911	17.67
Nucula percrassa	R	MMNS 1634	Union County, MS	Ripley	26.39	16.893
Nucula percrassa	L	FLMNH 213777	McNairy County, TN	Coon Creek	34.586	24.039
Nucula percrassa	L	FLMNH 213777	McnNairy County, TN	Coon Creek	42.028	24.929
Nucula percrassa	L	FLMNH 213777	McNairy County, TN	Coon Creek	34.517	21.505
Nucula percrassa	L	FLMNH 213777	McNairy County, TN	Coon Creek	31.276	20.866
Nucula percrassa	L	FLMNH 213777	McNairy County, TN	Coon Creek	36.298	22.715
Nucula percrassa	L	FLMNH 213777	McNairy County, TN	Coon Creek	34.883	21.802
Nucula percrassa	L	FLMNH 213777	McNairy County, TN	Coon Creek	29.86	18.72

Taxon Name	Valve	Museum	Locality	Formation	Width (mm)	Height (mm)
Nucula percrassa	L	FLMNH 213777	McNairy County, TN	Coon Creek	23.833	15.775
Nucula percrassa	L	YPM 507066	McNairy County, TN	Coon Creek	43.717	25.865
Nucula percrassa	L	YPM 534808	McNairy County, TN	Coon Creek	36.184	22.144
Nucula percrassa	L	YPM 534809	McNairy County, TN	Coon Creek	33.399	20.98
Nucula percrassa	L	YPM 534815	McNairy County, TN	Coon Creek	30.614	19.016
Nucula percrassa	L	YPM 534822	McNairy County, TN	Coon Creek	33.079	21.984
Nucula percrassa	L	YPM 534834	McNairy County, TN	Coon Creek	33.262	20.569
Nucula percrassa	L	YPM 534836	McNairy County, TN	Coon Creek	36.595	21.939
Nucula percrassa	L	YPM 534837	McNairy County, TN	Coon Creek	34.494	22.19
Nucula percrassa	R	FLMNH 213777	McNairy County, TN	Coon Creek	34.654	21.025
Nucula percrassa	R	FLMNH 213777	McNairy County, TN	Coon Creek	37.508	22.235
Nucula percrassa	R	FLMNH 213777	McNairy County, TN	Coon Creek	29.974	19.039
Nucula percrassa	R	YPM 534807	McNairy County, TN	Coon Creek	33.17	20.226
Nucula percrassa	R	YPM 534810	McNairy County, TN	Coon Creek	31.321	19.93
Nucula percrassa	R	YPM 534815	Mcnairy County, TN	Coon Creek	30.728	18.56
Nucula percrassa	R	YPM 534817	McNairy County, TN	Coon Creek	30.248	18.583
Nucula percrassa	R	YPM 534818	McNairy County, TN	Coon Creek	31.23	19.61

Taxon Name	Valve	Museum	Locality	Formation	Width (mm)	Height (mm)
Nucula percrassa	R	YPM 534819	McNairy County, TN	Coon Creek	28.742	18.286
Nucula percrassa	R	YPM 534848	McNairy County, TN	Coon Creek	28.217	18.126
Nucula percrassa	R	YPM 534850	McNairy County, TN	Coon Creek	32.257	20.66
Nucula percrassa	R	YPM 534876	McNairy County, TN	Coon Creek	35.408	20.888
Nucula percrassa	R	JS15CCTN	McNairy County, TN	Coon Creek		
Nucula percrassa	R	JS15CCTN	McNairy County, TN	Coon Creek		
Nucula percrassa	L	JS15CCTN	McNairy County, TN	Coon Creek		
Nucula percrassa	L	JS15CCTN	McNairy County, TN	Coon Creek		
Nucula percrassa	R	JS15CCTN	McNairy County, TN	Coon Creek		

APPENDIX C:

LUCINA AND *ANODONTIA* DATA

Table C1. Data for *Lucina* specimens used for size and shape analysis. Data includes taxon name, valve side (i.e., right (R) or left (L)), museum catalog number, locality, formation/Age, and size data. All fossil specimens are reposited in the Florida Museum of Natural History (FLMNH) Invertebrate Paleontology Collection.

Taxon Name	Valve	Museum	Locality	Formation	Width (mm)	Height (mm)
Lucina roquesana	R	-	San Salvador, Bahamas	Holocene	15.959	15.009
Lucina roquesana	R	-	San Salvador, Bahamas	Holocene	3.42	3.333
Lucina roquesana	R	-	San Salvador, Bahamas	Holocene	6.647	6.56
Lucina roquesana	R	-	San Salvador, Bahamas	Holocene	7.258	6.792
Lucina roquesana	R	-	San Salvador, Bahamas	Holocene	8.372	8.188
Lucina roquesana	R	-	San Salvador, Bahamas	Holocene	4.767	4.515
Lucina roquesana	R	-	San Salvador, Bahamas	Holocene	4.67	4.331
Lucina roquesana	R	-	San Salvador, Bahamas	Holocene	7.674	7.383
Lucina roquesana	R	-	San Salvador, Bahamas	Holocene	15.6	15.319
Lucina roquesana	R	-	San Salvador, Bahamas	Holocene	9.631	8.953
Lucina roquesana	R	-	San Salvador, Bahamas	Holocene	8.818	8.372

Taxon Name	Valve	Museum	Locality	Formation	Width (mm)	Height (mm)
Lucina roquesana	R	-	San Salvador, Bahamas	Holocene	8.285	7.742
Lucina roquesana	R	-	San Salvador, Bahamas	Holocene	5.659	5.513
Lucina roquesana	R	-	San Salvador, Bahamas	Holocene	5.238	4.945
Lucina roquesana	R	-	San Salvador, Bahamas	Holocene	8.791	8.498
Lucina roquesana	R	-	San Salvador, Bahamas	Holocene	8.773	8.104
Lucina roquesana	R	-	San Salvador, Bahamas	Holocene	7.711	7.289
Lucina roquesana	R	-	San Salvador, Bahamas	Holocene	5.861	5.861
Lucina roquesana	R	-	San Salvador, Bahamas	Holocene	3.727	3.599
Lucina roquesana	R	-	San Salvador, Bahamas	Holocene	4.954	4.533
Lucina roquesana	R	-	San Salvador, Bahamas	Holocene	8.113	7.756
Lucina roquesana	R	-	San Salvador, Bahamas	Holocene	4.313	4.112
Lucina roquesana	R	-	San Salvador, Bahamas	Holocene	8.498	8.681
Lucina roquesana	R	-	San Salvador, Bahamas	Holocene	5.183	4.982
Lucina roquesana	R	-	San Salvador, Bahamas	Holocene	4.423	4.313
Lucina roquesana	R	-	San Salvador, Bahamas	Holocene	7.665	7.399
Lucina roquesana	R	-	San Salvador, Bahamas	Holocene	5.604	5.54
Lucina roquesana	R	-	San Salvador, Bahamas	Holocene	9.222	8.709

Taxon Name	Valve	Museum	Locality	Formation	Width (mm)	Height (mm)
Lucina roquesana	R	-	San Salvador, Bahamas	Holocene	8.874	8.233
Lucina roquesana	L	-	San Salvador, Bahamas	Holocene	15.736	15.106
Lucina roquesana	L	-	San Salvador, Bahamas	Holocene	3.488	3.382
Lucina roquesana	L	-	San Salvador, Bahamas	Holocene	6.618	6.473
Lucina roquesana	L	-	San Salvador, Bahamas	Holocene	7.238	6.812
Lucina roquesana	L	-	San Salvador, Bahamas	Holocene	8.449	8.12
Lucina roquesana	L	-	San Salvador, Bahamas	Holocene	4.709	4.525
Lucina roquesana	L	-	San Salvador, Bahamas	Holocene	4.661	4.312
Lucina roquesana	L	-	San Salvador, Bahamas	Holocene	7.645	7.422
Lucina roquesana	L	-	San Salvador, Bahamas	Holocene	15.562	15.445
Lucina roquesana	L	-	San Salvador, Bahamas	Holocene	9.573	8.827
Lucina roquesana	L	-	San Salvador, Bahamas	Holocene	8.692	8.333
Lucina roquesana	L	-	San Salvador, Bahamas	Holocene	8.343	7.732
Lucina roquesana	L	-	San Salvador, Bahamas	Holocene	5.707	5.475
Lucina roquesana	L	-	San Salvador, Bahamas	Holocene	8.672	8.226
Lucina roquesana	L	-	San Salvador, Bahamas	Holocene	8.827	8.982
Lucina roquesana	L	-	San Salvador, Bahamas	Holocene	4.331	4.263

Taxon Name	Valve	Museum	Locality	Formation	Width (mm)	Height (mm)
Lucina roquesana	L	-	San Salvador, Bahamas	Holocene	4.409	4.448
Lucina roquesana	L	-	San Salvador, Bahamas	Holocene	5.261	4.99
Lucina roquesana	L	-	San Salvador, Bahamas	Holocene	8.159	7.606
Lucina roquesana	L	-	San Salvador, Bahamas	Holocene	6.075	6.124
Lucina roquesana	L	-	San Salvador, Bahamas	Holocene	3.992	3.731
Lucina roquesana	L	-	San Salvador, Bahamas	Holocene	5.271	4.903
Lucina roquesana	L	-	San Salvador, Bahamas	Holocene	3.982	3.963
Lucina roquesana	L	-	San Salvador, Bahamas	Holocene	9.447	8.779
Lucina roquesana	L	-	San Salvador, Bahamas	Holocene	8.585	8.197
Lucina roquesana	L	-	San Salvador, Bahamas	Holocene	13.275	13.003
Lucina roquesana	L	-	San Salvador, Bahamas	Holocene	12.461	11.967
Lucina roquesana	L	-	San Salvador, Bahamas	Holocene	6.899	6.928
Lucina roquesana	L	-	San Salvador, Bahamas	Holocene	10.135	9.864
Lucina roquesana	L	-	San Salvador, Bahamas	Holocene	9.67	9.321
Lucina roquesana	L	-	San Salvador, Bahamas	Holocene	9.544	9.661
Lucina roquesana	L	-	San Salvador, Bahamas	Holocene	9.254	8.43
Lucina roquesana	L	-	San Salvador, Bahamas	Holocene	8.44	8.12

Taxon Name	Valve	Museum	Locality	Formation	Width (mm)	Height (mm)
Lucina roquesana	L	-	San Salvador, Bahamas	Holocene	8.178	7.994
Lucina roquesana	L	-	San Salvador, Bahamas	Holocene	3.653	3.537
Lucina pensylvinica	L	-	Honey Moon Island, Dunedin, FL	Holocene	39.844	40.104
Lucina pensylvinica	L	-	Honey Moon Island, Dunedin, FL	Holocene	40.833	41.406
Lucina pensylvinica	L	-	Honey Moon Island, Dunedin, FL	Holocene	39.062	37.865
Lucina pensylvinica	L	-	Honey Moon Island, Dunedin, FL	Holocene	40.156	40.104
Lucina pensylvinica	L	-	Honey Moon Island, Dunedin, FL	Holocene	37.396	36.458
Lucina pensylvinica	L	-	Honey Moon Island, Dunedin, FL	Holocene	37.917	35.573
Lucina pensylvinica	L	-	Honey Moon Island, Dunedin, FL	Holocene	41.25	37.76
Lucina pensylvinica	L	-	Honey Moon Island, Dunedin, FL	Holocene	36.458	35.469
Lucina pensylvinica	L	-	Honey Moon Island, Dunedin, FL	Holocene	38.021	37.448
Lucina pensylvinica	L	-	Honey Moon Island, Dunedin, FL	Holocene	38.073	37.656
Lucina pensylvinica	L	-	Honey Moon Island, Dunedin, FL	Holocene	35.677	37.656
Lucina pensylvinica	L	-	Honey Moon Island, Dunedin, FL	Holocene	29.271	27.917
Lucina pensylvinica	L	-	Honey Moon Island, Dunedin FL	Holocene	35.104	33.385
Lucina pensylvinica	L	-	Honey Moon Island, Dunedin, FL	Holocene	35.104	33.594
Lucina pensylvinica	R	-	Honey Moon Island, Dunedin, FL	Holocene	38.385	36.823

Taxon Name	Valve	Museum	Locality	Formation	Width (mm)	Height (mm)
Lucina pensylvinica	R	-	Honey Moon Island, Dunedin, FL	Holocene	40.573	42.083
Lucina pensylvinica	R	-	Honey Moon Island, Dunedin, FL	Holocene	47.656	47.76
Lucina pensylvinica	R	-	Honey Moon Island, Dunedin, FL	Holocene	35.208	38.542
Lucina pensylvinica	R	-	Honey Moon Island, Dunedin, FL	Holocene	39.583	36.615
Lucina pensylvinica	R	-	Honey Moon Island, Dunedin, FL	Holocene	38.802	40.885
Lucina pensylvinica	R	-	Honey Moon Island, Dunedin, FL	Holocene	33.333	31.927
Lucina pensylvinica	R	-	Honey Moon Island, Dunedin, FL	Holocene	35.885	35.573
Lucina pensylvinica	R	-	Honey Moon Island, Dunedin, FL	Holocene	42.292	42.604
Lucina pensylvinica	R	-	Honey Moon Island, Dunedin, FL	Holocene	35.729	35.885
Lucina pensylvinica	R	-	Honey Moon Island, Dunedin, FL	Holocene	36.458	38.385
Lucina pensylvinica	R	-	Honey Moon Island, Dunedin, FL	Holocene	32.24	32.917
Lucina pensylvinica	R	-	Honey Moon Island, Dunedin, FL	Holocene	32.292	32.448
Lucina pensylvinica	R	-	Honey Moon Island, Dunedin, FL	Holocene	31.771	31.51
Lucina pensylvinica	R	-	Honey Moon Island, Dunedin, FL	Holocene	32.188	32.76
Lucina pensylvinica	R	-	Honey Moon Island, Dunedin, FL	Holocene	34.583	34.167
Lucina pensylvinica	R	-	Honey Moon Island, Dunedin, FL	Holocene	34.323	34.688
Lucina pensylvinica	R	-	Honey Moon Island, Dunedin, FL	Holocene	31.51	30.573

Taxon Name	Valve	Museum	Locality	Formation	Width (mm)	Height (mm)
Lucina pensylvinica	L	-	Honey Moon Island, Dunedin, FL	Holocene	38.802	39.688
Lucina pensylvinica	L	-	Honey Moon Island, Dunedin, FL	Holocene	34.375	31.562
Lucina pensylvinica	L	-	Honey Moon Island, Dunedin, FL	Holocene	31.406	30.625
Lucina pensylvinica	L	-	Honey Moon Island, Dunedin, FL	Holocene	39.688	41.042
Lucina pensylvinica	L	-	Honey Moon Island, Dunedin, FL	Holocene	33.333	33.229
Lucina pensylvinica	L	-	Honey Moon Island, Dunedin, FL	Holocene	24.479	25.417
Lucina pensylvinica	L	-	Honey Moon Island, Dunedin, FL	Holocene	35.833	35.208
Lucina pensylvinica	L	-	Honey Moon Island, Dunedin, FL	Holocene	32.656	31.25
Lucina pensylvinica	L	-	Honey Moon Island, Dunedin, FL	Holocene	32.552	33.542
Lucina pensylvinica	L	-	Honey Moon Island, Dunedin, FL	Holocene	30	28.698
Lucina pensylvinica	L	-	Honey Moon Island, Dunedin, FL	Holocene	30.26	27.865
Lucina pensylvinica	L	-	Honey Moon Island, Dunedin, FL	Holocene	36.927	35.208
Lucina pensylvinica	L	-	Honey Moon Island, Dunedin, FL	Holocene	36.615	35.312
Lucina pensylvinica	L	-	Honey Moon Island, Dunedin, FL	Holocene	35.781	35.365
Lucina pensylvinica	L	-	Honey Moon Island, Dunedin, FL	Holocene	34.792	35.365
Lucina pensylvinica	R	-	Honey Moon Island, Dunedin, FL	Holocene	41.927	39.219
Lucina pensylvinica	R	-	Honey Moon Island, Dunedin, FL	Holocene	29.427	29.531

Taxon Name	Valve	Museum	Locality	Formation	Width (mm)	Height (mm)
Lucina pensylvinica	R	-	Honey Moon Island, Dunedin, FL	Holocene	37.865	37.5
Lucina pensylvinica	R	-	Honey Moon Island, Dunedin, FL	Holocene	34.688	33.906
Lucina pensylvinica	R	-	Honey Moon Island, Dunedin, FL	Holocene	39.062	36.302
Lucina pensylvinica	R	-	Honey Moon Island, Dunedin, FL	Holocene	40.729	40
Lucina pensylvinica	R	-	Honey Moon Island, Dunedin, FL	Holocene	31.146	33.333
Lucina pensylvinica	R	-	Honey Moon Island, Dunedin, FL	Holocene	30.938	32.552
Lucina pensylvinica	R	-	Honey Moon Island, Dunedin, FL	Holocene	34.062	35
Lucina pensylvinica	R	-	Honey Moon Island, Dunedin, FL	Holocene	31.146	32.604
Lucina pensylvinica	R	-	Honey Moon Island, Dunedin, FL	Holocene	35	36.042
Lucina pensylvinica	R	-	Honey Moon Island, Dunedin, FL	Holocene	37.24	37.917
Lucina pensylvinica	R	-	Honey Moon Island, Dunedin, FL	Holocene	34.271	33.854
Lucina pensylvinica	L	-	Honey Moon Island, Dunedin, FL	Holocene	34.896	35.312
Lucina pensylvinica	L	-	Honey Moon Island, Dunedin, FL	Holocene	34.583	32.5
Lucina pensylvinica	L	-	Honey Moon Island, Dunedin, FL	Holocene	33.542	34.427
Lucina pensylvinica	L	-	Honey Moon Island, Dunedin, FL	Holocene	30.938	30.365
Lucina pensylvinica	L	-	Honey Moon Island, Dunedin, FL	Holocene	40.469	38.177
Lucina pensylvinica	L	-	Honey Moon Island, Dunedin, FL	Holocene	32.969	32.448

Taxon Name	Valve	Museum	Locality	Formation	Width (mm)	Height (mm)
Lucina pensylvinica	L	-	Honey Moon Island, Dunedin, FL	Holocene	39.167	38.698
Lucina pensylvinica	L	-	Honey Moon Island, Dunedin, FL	Holocene	34.635	34.427
Lucina pensylvinica	L	-	Honey Moon Island, Dunedin, FL	Holocene	37.188	37.76
Lucina pensylvinica	R	-	Honey Moon Island, Dunedin, FL	Holocene	35.573	35.104
Lucina pensylvinica	R	-	Honey Moon Island, Dunedin, FL	Holocene	30.26	29.583
Lucina pensylvinica	R	-	Honey Moon Island, Dunedin FL	Holocene	29.375	30.052
Lucina pensylvinica	R	-	Honey Moon Island, Dunedin, FL	Holocene	35.521	33.906
Lucina pensylvinica	R	-	Honey Moon Island, Dunedin, FL	Holocene	36.094	35.885
Lucina pensylvinica	R	-	Honey Moon Island, Dunedin, FL	Holocene	34.271	33.333
Lucina pensylvinica	R	-	Honey Moon Island, Dunedin, FL	Holocene	39.583	39.167
Lucina pensylvanica	L	FLMNH 172943	Sarasota County, FL	Fort Thompson	32.491	32.753
Lucina pensylvanica	L	FLMNH 172943	Sarasota County, FL	Fort Thompson	38.435	39.284
Lucina pensylvanica	L	FLMNH 135172	St. Lucie County, FL	Fort Thompson	36.639	35.855
Lucina pensylvanica	L	FLMNH 135172	St. Lucie County, FL	Fort Thompson	36.116	32.818
Lucina pensylvanica	L	FLMNH 135172	St. Lucie County, FL	Fort Thompson	24.262	25.503
Lucina pensylvanica	L	FLMNH 135172	St. Lucie County, FL	Fort Thompson	33.308	34.222
Lucina pensylvanica	R	FLMNH 172943	Sarasota, County FL	Fort Thompson	38.075	39.284

Taxon Name	Valve	Museum	Locality	Formation	Width (mm)	Height (mm)
Lucina pensylvanica	R	FLMNH 172943	Sarasota, County FL	Fort Thompson	39.937	40.492
Lucina pensylvanica	R	FLMNH 135172	St. Lucie County, FL	Fort Thompson	24.132	24.426
Lucina pensylvanica	R	FLMNH 135172	St. Lucie County, FL	Fort Thompson	25.275	25.601
Lucina pensylvanica	R	FLMNH 135172	St. Lucie County, FL	Fort Thompson	19.527	19.038
Lucina pensylvanica	L	FLMNH 123384	Palm Beach County, FL	Bermont	40.349	42.077
Lucina pensylvanica	L	FLMNH 123384	Palm Beach County, FL	Bermont	43.145	42.643
Lucina pensylvanica	L	FLMNH 123384	Palm Beach County, FL	Bermont	45.251	45.659
Lucina pensylvanica	L	FLMNH 123384	Palm Beach County, FL	Bermont	40.789	42.988
Lucina pensylvanica	L	FLMNH 123384	Palm Beach County, FL	Bermont	41.637	41.134
Lucina pensylvanica	L	FLMNH 123384	Palm Beach County, FL	Bermont	43.208	40.757
Lucina pensylvanica	L	FLMNH 123384	Palm Beach County, FL	Bermont	42.391	40.6
Lucina pensylvanica	L	FLMNH 123384	Palm Beach County, FL	Bermont	42.423	41.574
Lucina pensylvanica	L	FLMNH 123384	Palm Beach County, FL	Bermont	44.402	41.448
Lucina pensylvanica	L	FLMNH 123384	Palm Beach County, FL	Bermont	36.892	36.201
Lucina pensylvanica	L	FLMNH 123384	Palm Beach County, FL	Bermont	40.286	39.06
Lucina pensylvanica	L	FLMNH 123384	Palm Beach County, FL	Bermont	39.752	38.809
Lucina pensylvanica	L	FLMNH 123384	Palm Beach County, FL	Bermont	32.493	31.487

Taxon Name	Valve	Museum	Locality	Formation	Width (mm)	Height (mm)
Lucina pensylvanica	L	FLMNH 123384	Palm Beach County, FL	Bermont	33.372	33.812
Lucina pensylvanica	L	FLMNH 134748	Guantanamo Province, Cuba	Bermont	29.539	29.884
Lucina pensylvanica	L	FLMNH 125575	Palm Beach County, FL	Bermont	32.775	33.624
Lucina pensylvanica	L	FLMNH 214410	Miami-Dade County, FL	Bermont	39.312	38.903
Lucina pensylvanica	L	FLMNH 214410	Miami-Dade County, FL	Bermont	33.153	33.687
Lucina pensylvanica	L	FLMNH 214410	Miami-Dade County, FL	Bermont	43.522	44.088
Lucina pensylvanica	L	FLMNH 214410	Miami-Dade County, FL	Bermont	44.874	44.245
Lucina pensylvanica	L	FLMNH 214410	Miami-Dade County, FL	Bermont	45.408	45.879
Lucina pensylvanica	L	FLMNH 52971	Miami-Dade County, FL	Bermont	46.068	45.942
Lucina pensylvanica	L	FLMNH 52971	Miami-Dade County, FL	Bermont	42.485	43.208
Lucina pensylvanica	L	FLMNH 125613	Palm Beach County, FL	Bermont	48.236	47.388
Lucina pensylvanica	L	FLMNH 125613	Palm Beach County, FL	Bermont	52.164	50.153
Lucina pensylvanica	L	FLMNH 125613	Palm Beach County, FL	Bermont	47.796	48.456
Lucina pensylvanica	L	FLMNH 125613	Palm Beach County, FL	Bermont	42.611	42.14
Lucina pensylvanica	L	FLMNH 125613	Palm Beach County, FL	Bermont	32.335	29.067
Lucina pensylvanica	L	FLMNH 125613	Palm Beach County, FL	Bermont	47.262	43.522
Lucina pensylvanica	L	FLMNH 125613	Palm Beach County, FL	Bermont	33.718	33.498

Taxon Name	Valve	Museum	Locality	Formation	Width (mm)	Height (mm)
Lucina pensylvanica	L	FLMNH 56929	Miami-Dade County, FL	Bermont	32.995	33.184
Lucina pensylvanica	L	FLMNH 56929	Miami-Dade County, FL	Bermont	35.384	35.792
Lucina pensylvanica	L	FLMNH 56929	Miami-Dade County, FL	Bermont	33.624	33.844
Lucina pensylvanica	L	FLMNH 56929	Miami-Dade County, FL	Bermont	33.53	32.995
Lucina pensylvanica	L	FLMNH 56929	Miami-Dade County, FL	Bermont	33.498	34.221
Lucina pensylvanica	L	FLMNH 56929	Miami-Dade County, FL	Bermont	32.744	33.75
Lucina pensylvanica	L	FLMNH 125614	Palm Beach County, FL	Bermont	45.722	46.979
Lucina pensylvanica	L	FLMNH 125614	Palm Beach County, FL	Bermont	46.288	44.057
Lucina pensylvanica	L	FLMNH 125614	Palm Beach County, FL	Bermont	47.67	49.022
Lucina pensylvanica	L	FLMNH 125614	Palm Beach County, FL	Bermont	47.073	49.147
Lucina pensylvanica	L	FLMNH 125614	Palm Beach County, FL	Bermont	49.462	48.865
Lucina pensylvanica	L	FLMNH 125614	Palm Beach County, FL	Bermont	35.227	35.541
Lucina pensylvanica	L	FLMNH 27697	Hillsborough County, FL	Bermont	33.372	34.252
Lucina pensylvanica	R	FLMNH 123384	Palm Beach County, FL	Bermont	42.894	41.888
Lucina pensylvanica	R	FLMNH 123384	Palm Beach County, FL	Bermont	40.16	39.972
Lucina pensylvanica	R	FLMNH 123384	Palm Beach County, FL	Bermont	41.48	40.663
Lucina pensylvanica	R	FLMNH 123384	Palm Beach County, FL	Bermont	38.903	37.835

Taxon Name	Valve	Museum	Locality	Formation	Width (mm)	Height (mm)
Lucina pensylvanica	R	FLMNH 123384	Palm Beach County, FL	Bermont	45.345	43.742
Lucina pensylvanica	R	FLMNH 123384	Palm Beach County, FL	Bermont	41.009	39.783
Lucina pensylvanica	R	FLMNH 123384	Palm Beach County, FL	Bermont	35.289	35.824
Lucina pensylvanica	R	FLMNH 123384	Palm Beach County, FL	Bermont	42.674	38.086
Lucina pensylvanica	R	FLMNH 134748	Guantanamo Province, Cuba	Bermont	32.65	31.55
Lucina pensylvanica	R	FLMNH 125732	St. Lucie County, FL	Bermont	29.633	29.727
Lucina pensylvanica	R	FLMNH 125576	Palm Beach County, FL	Bermont	38.4	40.537
Lucina pensylvanica	R	FLMNH 214410	Miami-Dade County, FL	Bermont	42.203	42.108
Lucina pensylvanica	R	FLMNH 214410	Miami-Dade County, FL	Bermont	44.402	44.214
Lucina pensylvanica	R	FLMNH 214410	Miami-Dade County, FL	Bermont	44.151	43.868
Lucina pensylvanica	R	FLMNH 214410	Miami-Dade County, FL	Bermont	39.123	39.374
Lucina pensylvanica	R	FLMNH 214410	Miami-Dade County, FL	Bermont	42.485	41.229
Lucina pensylvanica	R	FLMNH 214410	Miami-Dade County, FL	Bermont	33.027	33.812
Lucina pensylvanica	R	FLMNH 214410	Miami-Dade County, FL	Bermont	28.376	30.639
Lucina pensylvanica	R	FLMNH 52971	Miami-Dade County, FL	Bermont	45.062	46.476
Lucina pensylvanica	R	FLMNH 52971	Miami-Dade County, FL	Bermont	48.582	50.31
Lucina pensylvanica	R	FLMNH 52971	Miami-Dade County, FL	Bermont	48.362	48.362

Taxon Name	Valve	Museum	Locality	Formation	Width (mm)	Height (mm)
Lucina pensylvanica	R	FLMNH 125613	Palm Beach County, FL	Bermont	34.692	33.561
Lucina pensylvanica	R	FLMNH 125613	Palm Beach County, FL	Bermont	49.65	50.876
Lucina pensylvanica	R	FLMNH 125613	Palm Beach County, FL	Bermont	47.451	48.456
Lucina pensylvanica	R	FLMNH 125613	Palm Beach County, FL	Bermont	44.591	44.34
Lucina pensylvanica	R	FLMNH 125613	Palm Beach County, FL	Bermont	38.18	39.626
Lucina pensylvanica	R	FLMNH 125613	Palm Beach County, FL	Bermont	46.633	49.179
Lucina pensylvanica	R	FLMNH 125613	Palm Beach County, FL	Bermont	46.539	44.277
Lucina pensylvanica	R	FLMNH 125613	Palm Beach County, FL	Bermont	42.454	42.485
Lucina pensylvanica	R	FLMNH 125613	Palm Beach County, FL	Bermont	41.637	42.643
Lucina pensylvanica	R	FLMNH 56929	Miami-Dade County, FL	Bermont	23.788	22.091
Lucina pensylvanica	R	FLMNH 56929	Miami-Dade County, FL	Bermont	34.032	34.975
Lucina pensylvanica	R	FLMNH 56929	Miami-Dade County, FL	Bermont	37.081	36.326
Lucina pensylvanica	R	FLMNH 56929	Miami-Dade County, FL	Bermont	33.467	32.901
Lucina pensylvanica	R	FLMNH 56929	Miami-Dade County, FL	Bermont	33.09	34.472
Lucina pensylvanica	R	FLMNH 56929	Miami-Dade County, FL	Bermont	30.67	31.33
Lucina pensylvanica	R	FLMNH 56929	Miami-Dade County, FL	Bermont	30.419	30.607
Lucina pensylvanica	R	FLMNH 125614	Palm Beach County, FL	Bermont	30.167	32.524

Taxon Name	Valve	Museum	Locality	Formation	Width (mm)	Height (mm)
Lucina pensylvanica	R	FLMNH 125614	Palm Beach County, FL	Bermont	42.894	43.585
Lucina pensylvanica	R	FLMNH 125614	Palm Beach County, FL	Bermont	47.67	48.645
Lucina pensylvanica	R	FLMNH 125614	Palm Beach County, FL	Bermont	43.648	41.668
Lucina pensylvanica	R	FLMNH 125614	Palm Beach County, FL	Bermont	41.574	44.214
Lucina pensylvanica	R	FLMNH 125614	Palm Beach County, FL	Bermont	48.833	48.707
Lucina pensylvanica	R	FLMNH 125614	Palm Beach County, FL	Bermont	38.746	41.826
Lucina pensylvanica	R	FLMNH 125614	Palm Beach County, FL	Bermont	48.362	49.022
Lucina pensylvanica	R	FLMNH 27697	Hillsborough County, FL	Bermont	41.983	42.234
Lucina pensylvanica	R	FLMNH 14087	Palm Beach County, FL	Bermont	33.718	34.315
Lucina pensylvanica	R	FLMNH 14087	Palm Beach County, FL	Bermont	42.611	42.266
Lucina pensylvanica	R	FLMNH 136148	Glades County,FL	Bermont	37.803	38.935
Lucina pensylvanica	R	FLMNH 136148	Glades County,FL	Bermont	29.476	30.23
Lucina pensylvanica	R	FLMNH 136148	Glades County,FL	Bermont	32.933	34.472
Lucina pensylvanica	L	FLMNH 125340	Hendry County, FL	Caloosahatchee	41.093	40.901
Lucina pensylvanica	L	FLMNH 248667	Lee County, FL	Caloosahatchee	28.746	30.086
Lucina pensylvanica	L	FLMNH 248667	Lee County, FL	Caloosahatchee	27.374	29.065
Lucina pensylvanica	L	FLMNH 248667	Lee County, FL	Caloosahatchee	31.553	32.861

Taxon Name	Valve	Museum	Locality	Formation	Width (mm)	Height (mm)
Lucina pensylvanica	L	FLMNH 248667	Lee County, FL	Caloosahatchee	35.828	36.147
Lucina pensylvanica	L	FLMNH 24047	Hendry County, FL	Caloosahatchee	45.814	48.75
Lucina pensylvanica	L	FLMNH 24047	Hendry County, FL	Caloosahatchee	44.57	45.495
Lucina pensylvanica	L	FLMNH 24047	Hendry County, FL	Caloosahatchee	35.86	35.637
Lucina pensylvanica	L	FLMNH 24047	Hendry County, FL	Caloosahatchee	37.136	38.923
Lucina pensylvanica	L	FLMNH 24047	Hendry County, FL	Caloosahatchee	40.965	42.847
Lucina pensylvanica	L	FLMNH 24047	Hendry County, FL	Caloosahatchee	37.36	35.669
Lucina pensylvanica	L	FLMNH 24047	Hendry County, FL	Caloosahatchee	36.562	38.094
Lucina pensylvanica	L	FLMNH 24047	Hendry County, FL	Caloosahatchee	39.529	40.742
Lucina pensylvanica	L	FLMNH 24047	Hendry County, FL	Caloosahatchee	42.082	42.847
Lucina pensylvanica	L	FLMNH 24047	Hendry County, FL	Caloosahatchee	43.772	41.635
Lucina pensylvanica	L	FLMNH 24047	Hendry County, FL	Caloosahatchee	36.785	37.551
Lucina pensylvanica	L	FLMNH 24047	Hendry County, FL	Caloosahatchee	35.828	35.956
Lucina pensylvanica	L	FLMNH 24047	Hendry County, FL	Caloosahatchee	35.956	35.924
Lucina pensylvanica	L	FLMNH 123829	Glades County, Florida	Caloosahatchee	39.402	38.668
Lucina pensylvanica	L	FLMNH 123829	Glades County, Florida	Caloosahatchee	33.946	34.488
Lucina pensylvanica	L	FLMNH 123829	Glades County, Florida	Caloosahatchee	38.285	37.2

Taxon Name	Valve	Museum	Locality	Formation	Width (mm)	Height (mm)
Lucina pensylvanica	L	FLMNH 123829	Glades County, Florida	Caloosahatchee	36.913	38.349
Lucina pensylvanica	L	FLMNH 123829	Glades County, Florida	Caloosahatchee	33.85	35.828
Lucina pensylvanica	L	FLMNH 123829	Glades County, Florida	Caloosahatchee	31.968	33.212
Lucina pensylvanica	L	FLMNH 123829	Glades County, Florida	Caloosahatchee	33.34	33.755
Lucina pensylvanica	L	FLMNH 123829	Glades County, Florida	Caloosahatchee	33.436	34.329
Lucina pensylvanica	L	FLMNH 125424	Hendry County, FL	Caloosahatchee	45.687	46.133
Lucina pensylvanica	L	FLMNH 125424	Hendry County, FL	Caloosahatchee	45.623	46.229
Lucina pensylvanica	L	FLMNH 125600	Hendry County, FL	Caloosahatchee	38.732	38.955
Lucina pensylvanica	L	FLMNH 24118	Hendry County, FL	Caloosahatchee	46.867	48.016
Lucina pensylvanica	L	FLMNH 24118	Hendry County, FL	Caloosahatchee	43.932	44.762
Lucina pensylvanica	L	FLMNH 24118	Hendry County, FL	Caloosahatchee	41.316	40.805
Lucina pensylvanica	L	FLMNH 24118	Hendry County, FL	Caloosahatchee	46.229	49.005
Lucina pensylvanica	L	FLMNH 24118	Hendry County, FL	Caloosahatchee	48.271	49.228
Lucina pensylvanica	L	FLMNH 4178	Hendry County, FL	Caloosahatchee	39.114	40.518
Lucina pensylvanica	L	FLMNH 4178	Hendry County, FL	Caloosahatchee	39.051	40.486
Lucina pensylvanica	L	FLMNH 4178	Hendry County, FL	Caloosahatchee	42.72	40.965
Lucina pensylvanica	L	FLMNH 4178	Hendry County, FL	Caloosahatchee	43.836	48.526

Taxon Name	Valve	Museum	Locality	Formation	Width (mm)	Height (mm)
Lucina pensylvanica	L	FLMNH 4178	Hendry County, FL	Caloosahatchee	35.445	35.063
Lucina pensylvanica	L	FLMNH 133377	Palm Beach County, FL	Caloosahatchee	37.296	36.594
Lucina pensylvanica	L	FLMNH 133377	Palm Beach County, FL	Caloosahatchee	48.941	51.908
Lucina pensylvanica	L	FLMNH 133377	Palm Beach County, FL	Caloosahatchee	36.785	38.859
Lucina pensylvanica	L	FLMNH 133377	Palm Beach County, FL	Caloosahatchee	36.466	38.189
Lucina pensylvanica	L	FLMNH 133377	Palm Beach County, FL	Caloosahatchee	38.221	40.423
Lucina pensylvanica	L	FLMNH 133377	Palm Beach County, FL	Caloosahatchee	35.509	36.53
Lucina pensylvanica	L	FLMNH 133377	Palm Beach County, FL	Caloosahatchee	35.605	35.382
Lucina pensylvanica	L	FLMNH 133377	Palm Beach County, FL	Caloosahatchee	37.934	39.051
Lucina pensylvanica	L	FLMNH 133377	Palm Beach County, FL	Caloosahatchee	39.721	40.742
Lucina pensylvanica	L	FLMNH 133377	Palm Beach County, FL	Caloosahatchee	33.276	34.648
Lucina pensylvanica	L	FLMNH 136696	Palm Beach County, FL	Caloosahatchee	29.192	29.001
Lucina pensylvanica	L	FLMNH 52530	Hendry County, FL	Caloosahatchee	37.296	37.041
Lucina pensylvanica	L	FLMNH 52530	Hendry County, FL	Caloosahatchee	41.858	41.029
Lucina pensylvanica	L	FLMNH 52530	Hendry County, FL	Caloosahatchee	38.253	39.561
Lucina pensylvanica	L	FLMNH 52530	Hendry County, FL	Caloosahatchee	41.731	40.901
Lucina pensylvanica	L	FLMNH 52530	Hendry County, FL	Caloosahatchee	37.2	37.136

Taxon Name	Valve	Museum	Locality	Formation	Width (mm)	Height (mm)
Lucina pensylvanica	R	FLMNH 125306	Hendry County, FL	Caloosahatchee	42.783	42.433
Lucina pensylvanica	R	FLMNH 125340	Hendry County, FL	Caloosahatchee	36.243	36.881
Lucina pensylvanica	R	FLMNH 125340	Hendry County, FL	Caloosahatchee	34.074	34.839
Lucina pensylvanica	R	FLMNH 125340	Hendry County, FL	Caloosahatchee	21.408	21.503
Lucina pensylvanica	R	FLMNH 125340	Hendry County, FL	Caloosahatchee	31.298	32.127
Lucina pensylvanica	R	FLMNH 248667	Lee County, FL	Caloosahatchee	31.553	33.34
Lucina pensylvanica	R	FLMNH 248667	Lee County, FL	Caloosahatchee	28.586	30.405
Lucina pensylvanica	R	FLMNH 248667	Lee County, FL	Caloosahatchee	27.055	28.363
Lucina pensylvanica	R	FLMNH 248667	Lee County, FL	Caloosahatchee	14.58	14.708
Lucina pensylvanica	R	FLMNH 24047	Hendry County, FL	Caloosahatchee	36.849	36.02
Lucina pensylvanica	R	FLMNH 24047	Hendry County, FL	Caloosahatchee	38.349	41.093
Lucina pensylvanica	R	FLMNH 24047	Hendry County, FL	Caloosahatchee	35.796	35.605
Lucina pensylvanica	R	FLMNH 24047	Hendry County, FL	Caloosahatchee	42.082	42.815
Lucina pensylvanica	R	FLMNH 24047	Hendry County, FL	Caloosahatchee	36.722	37.296
Lucina pensylvanica	R	FLMNH 24047	Hendry County, FL	Caloosahatchee	44.347	45.208
Lucina pensylvanica	R	FLMNH 24047	Hendry County, FL	Caloosahatchee	37.838	39.657
Lucina pensylvanica	R	FLMNH 24047	Hendry County, FL	Caloosahatchee	36.817	37.647

Taxon Name	Valve	Museum	Locality	Formation	Width (mm)	Height (mm)
Lucina pensylvanica	R	FLMNH 24047	Hendry County, FL	Caloosahatchee	45.655	48.59
Lucina pensylvanica	R	FLMNH 24047	Hendry County, FL	Caloosahatchee	30.724	32.032
Lucina pensylvanica	R	FLMNH 24047	Hendry County, FL	Caloosahatchee	35.477	34.488
Lucina pensylvanica	R	FLMNH 24047	Hendry County, FL	Caloosahatchee	37.328	36.275
Lucina pensylvanica	R	FLMNH 24047	Hendry County, FL	Caloosahatchee	30.756	31.202
Lucina pensylvanica	R	FLMNH 24047	Hendry County, FL	Caloosahatchee	39.274	40.678
Lucina pensylvanica	R	FLMNH 24047	Hendry County, FL	Caloosahatchee	43.485	41.763
Lucina pensylvanica	R	FLMNH 24047	Hendry County, FL	Caloosahatchee	35.86	36.275
Lucina pensylvanica	R	FLMNH 24047	Hendry County, FL	Caloosahatchee	40.55	42.528
Lucina pensylvanica	R	FLMNH 24047	Hendry County, FL	Caloosahatchee	36.243	37.998
Lucina pensylvanica	R	FLMNH 123829	Glades County, Florida	Caloosahatchee	36.052	35.796
Lucina pensylvanica	R	FLMNH 123829	Glades County, Florida	Caloosahatchee	41.507	41.699
Lucina pensylvanica	R	FLMNH 123829	Glades County, Florida	Caloosahatchee	34.169	34.712
Lucina pensylvanica	R	FLMNH 123829	Glades County, Florida	Caloosahatchee	33.244	33.627
Lucina pensylvanica	R	FLMNH 123829	Glades County, Florida	Caloosahatchee	38.381	37.424
Lucina pensylvanica	R	FLMNH 123829	Glades County, Florida	Caloosahatchee	38.381	37.392
Lucina pensylvanica	R	FLMNH 123829	Glades County, Florida	Caloosahatchee	30.883	31.553

Taxon Name	Valve	Museum	Locality	Formation	Width (mm)	Height (mm)
Lucina pensylvanica	R	FLMNH 123829	Glades County, Florida	Caloosahatchee	31.84	33.978
Lucina pensylvanica	R	FLMNH 123829	Glades County, Florida	Caloosahatchee	34.393	35.956
Lucina pensylvanica	R	FLMNH 123829	Glades County, Florida	Caloosahatchee	34.648	35.605
Lucina pensylvanica	R	FLMNH 123829	Glades County, Florida	Caloosahatchee	36.179	37.2
Lucina pensylvanica	R	FLMNH 125600	Hendry County, FL	Caloosahatchee	42.656	43.326
Lucina pensylvanica	R	FLMNH 125600	Hendry County, FL	Caloosahatchee	45.687	47.824
Lucina pensylvanica	R	FLMNH 125600	Hendry County, FL	Caloosahatchee	20.674	20.419
Lucina pensylvanica	R	FLMNH 24118	Hendry County, FL	Caloosahatchee	43.772	45.017
Lucina pensylvanica	R	FLMNH 24118	Hendry County, FL	Caloosahatchee	41.252	40.869
Lucina pensylvanica	R	FLMNH 24118	Hendry County, FL	Caloosahatchee	46.708	48.367
Lucina pensylvanica	R	FLMNH 24118	Hendry County, FL	Caloosahatchee	47.984	49.132
Lucina pensylvanica	R	FLMNH 24118	Hendry County, FL	Caloosahatchee	35.477	35.286
Lucina pensylvanica	R	FLMNH 4178	Hendry County, FL	Caloosahatchee	43.517	48.654
Lucina pensylvanica	R	FLMNH 4178	Hendry County, FL	Caloosahatchee	39.178	40.327
Lucina pensylvanica	R	FLMNH 4178	Hendry County, FL	Caloosahatchee	40.742	42.401
Lucina pensylvanica	R	FLMNH 4178	Hendry County, FL	Caloosahatchee	36.084	37.743
Lucina pensylvanica	R	FLMNH 133377	Palm Beach County, FL	Caloosahatchee	36.722	38.413

Taxon Name	Valve	Museum	Locality	Formation	Width (mm)	Height (mm)
Lucina pensylvanica	R	FLMNH 133377	Palm Beach County, FL	Caloosahatchee	32.797	34.169
Lucina pensylvanica	R	FLMNH 133377	Palm Beach County, FL	Caloosahatchee	36.849	38.891
Lucina pensylvanica	R	FLMNH 133377	Palm Beach County, FL	Caloosahatchee	34.712	34.169
Lucina pensylvanica	R	FLMNH 133377	Palm Beach County, FL	Caloosahatchee	38.317	41.986
Lucina pensylvanica	R	FLMNH 133377	Palm Beach County, FL	Caloosahatchee	41.603	40.742
Lucina pensylvanica	R	FLMNH 133377	Palm Beach County, FL	Caloosahatchee	33.308	34.52
Lucina pensylvanica	R	FLMNH 136696	Palm Beach County, FL	Caloosahatchee	40.263	41.252
Lucina pensylvanica	R	FLMNH 136696	Palm Beach County, FL	Caloosahatchee	35.669	37.679
Lucina pensylvanica	R	FLMNH 136696	Palm Beach County, FL	Caloosahatchee	41.348	41.252
Lucina pensylvanica	R	FLMNH 52530	Hendry County, FL	Caloosahatchee	37.168	37.264
Lucina pensylvanica	R	FLMNH 52530	Hendry County, FL	Caloosahatchee	44.953	45.527
Lucina pensylvanica	R	FLMNH 52530	Hendry County, FL	Caloosahatchee	40.391	41.252
Lucina pensylvanica	R	FLMNH 52530	Hendry County, FL	Caloosahatchee	37.232	37.519
Lucina pensylvanica	L	FLMNH 59344	Okeechobee County, FL	Tamiami	41.7	42.699
Lucina pensylvanica	L	FLMNH 59344	Okeechobee County, FL	Tamiami	42.85	42.517
Lucina pensylvanica	L	FLMNH 59344	Okeechobee County, FL	Tamiami	35.885	36.976
Lucina pensylvanica	L	FLMNH 59344	Okeechobee County, FL	Tamiami	48.725	47.393

Taxon Name	Valve	Museum	Locality	Formation	Width (mm)	Height (mm)
Lucina pensylvanica	L	FLMNH 59344	Okeechobee County, FL	Tamiami	42.638	43.426
Lucina pensylvanica	L	FLMNH 59344	Okeechobee County, FL	Tamiami	38.005	38.247
Lucina pensylvanica	L	FLMNH 59344	Okeechobee County, FL	Tamiami	37.763	39.792
Lucina pensylvanica	L	FLMNH 59344	Okeechobee County, FL	Tamiami	35.28	35.492
Lucina pensylvanica	L	FLMNH 59344	Okeechobee County, FL	Tamiami	42.548	41.094
Lucina pensylvanica	L	FLMNH 59344	Okeechobee County, FL	Tamiami	34.068	35.128
Lucina pensylvanica	L	FLMNH 59344	Okeechobee County, FL	Tamiami	34.129	35.007
Lucina pensylvanica	L	FLMNH 93027	Charlotte County, FL	Tamiami	23.5	23.378
Lucina pensylvanica	L	FLMNH 93027	Charlotte County, FL	Tamiami	34.644	36.249
Lucina pensylvanica	L	FLMNH 93027	Charlotte County, FL	Tamiami	32.13	33.432
Lucina pensylvanica	L	FLMNH 93027	Charlotte County, FL	Tamiami	38.459	37.854
Lucina pensylvanica	L	FLMNH 93027	Charlotte County, FL	Tamiami	33.766	33.13
Lucina pensylvanica	L	FLMNH 93027	Charlotte County, FL	Tamiami	35.855	36.37
Lucina pensylvanica	L	FLMNH 93027	Charlotte County, FL	Tamiami	33.826	34.735
Lucina pensylvanica	L	FLMNH 93027	Charlotte County, FL	Tamiami	36.915	37.127
Lucina pensylvanica	L	FLMNH 93027	Charlotte County, FL	Tamiami	33.13	33.493
Lucina pensylvanica	L	FLMNH 93027	Charlotte County, FL	Tamiami	35.159	36.37

Taxon Name	Valve	Museum	Locality	Formation	Width (mm)	Height (mm)
Lucina pensylvanica	L	FLMNH 145904	Collier County, FL	Tamiami	31.827	30.646
Lucina pensylvanica	L	FLMNH 125345	Collier County, FL	Tamiami	15.656	15.444
Lucina pensylvanica	L	FLMNH 125345	Collier County, FL	Tamiami	30.192	31.373
Lucina pensylvanica	L	FLMNH 125345	Collier County, FL	Tamiami	33.675	33.705
Lucina pensylvanica	L	FLMNH 125345	Collier County, FL	Tamiami	29.889	31.525
Lucina pensylvanica	L	FLMNH 125345	Collier County, FL	Tamiami	32.009	31.949
Lucina pensylvanica	L	FLMNH 35635	Miami-Dade County, FL	Pincrest Beds	24.953	26.467
Lucina pensylvanica	L	FLMNH 35635	Miami-Dade County, FL	Pincrest Beds	35.613	34.947
Lucina pensylvanica	L	FLMNH 35635	Miami-Dade County, FL	Pincrest Beds	33.523	34.099
Lucina pensylvanica	L	FLMNH 35635	Miami-Dade County, FL	Pincrest Beds	29.435	30.283
Lucina pensylvanica	L	FLMNH 35635	Miami-Dade County, FL	Pincrest Beds	35.795	35.643
Lucina pensylvanica	L	FLMNH 35635	Miami-Dade County, FL	Pincrest Beds	27.77	27.618
Lucina pensylvanica	L	FLMNH 35635	Miami-Dade County, FL	Pincrest Beds	35.734	36.037
Lucina pensylvanica	L	FLMNH 35635	Miami-Dade County, FL	Pincrest Beds	33.463	35.189
Lucina pensylvanica	L	FLMNH 35635	Miami-Dade County, FL	Pincrest Beds	36.128	35.734
Lucina pensylvanica	L	FLMNH 35635	Miami-Dade County, FL	Pincrest Beds	36.764	35.189
Lucina pensylvanica	L	FLMNH 35635	Miami-Dade County, FL	Pincrest Beds	33.796	35.28

Taxon Name	Valve	Museum	Locality	Formation	Width (mm)	Height (mm)
Lucina pensylvanica	L	FLMNH 35635	Miami-Dade County, FL	Pincrest Beds	25.317	27.315
Lucina pensylvanica	L	FLMNH 35635	Miami-Dade County, FL	Pincrest Beds	30.253	30.646
Lucina pensylvanica	L	FLMNH 35635	Miami-Dade County, FL	Pincrest Beds	36.279	36.218
Lucina pensylvanica	L	FLMNH 35635	Miami-Dade County, FL	Pincrest Beds	34.28	34.28
Lucina pensylvanica	L	FLMNH 35635	Miami-Dade County, FL	Pincrest Beds	31.646	31.888
Lucina pensylvanica	L	FLMNH 35635	Miami-Dade County, FL	Pincrest Beds	35.431	35.401
Lucina pensylvanica	L	FLMNH 35635	Miami-Dade County, FL	Pincrest Beds	33.584	33.008
Lucina pensylvanica	L	FLMNH 35635	Miami-Dade County, FL	Pincrest Beds	31.494	32.978
Lucina pensylvanica	L	FLMNH 35635	Miami-Dade County, FL	Pincrest Beds	33.039	33.372
Lucina pensylvanica	L	FLMNH 35635	Miami-Dade County, FL	Pincrest Beds	34.159	34.099
Lucina pensylvanica	L	FLMNH 35635	Miami-Dade County, FL	Pincrest Beds	33.402	32.554
Lucina pensylvanica	L	FLMNH 35635	Miami-Dade County, FL	Pincrest Beds	28.86	30.222
Lucina pensylvanica	L	FLMNH 35635	Miami-Dade County, FL	Pincrest Beds	32.736	34.735
Lucina pensylvanica	L	FLMNH 35635	Miami-Dade County, FL	Pincrest Beds	30.283	30.556
Lucina pensylvanica	L	FLMNH 35635	Miami-Dade County, FL	Pincrest Beds	28.345	29.496
Lucina pensylvanica	L	FLMNH 35635	Miami-Dade County, FL	Pincrest Beds	26.165	26.134
Lucina pensylvanica	L	FLMNH 35635	Miami-Dade County, FL	Pincrest Beds	28.345	26.619

Taxon Name	Valve	Museum	Locality	Formation	Width (mm)	Height (mm)
Lucina pensylvanica	L	FLMNH 35635	Miami-Dade County, FL	Pincrest Beds	35.037	35.128
Lucina pensylvanica	L	FLMNH 35635	Miami-Dade County, FL	Pincrest Beds	29.859	30.041
Lucina pensylvanica	L	FLMNH 35635	Miami-Dade County, FL	Pincrest Beds	33.796	33.584
Lucina pensylvanica	L	FLMNH 35635	Miami-Dade County, FL	Pincrest Beds	29.556	29.253
Lucina pensylvanica	L	FLMNH 35635	Miami-Dade County, FL	Pincrest Beds	33.16	32.585
Lucina pensylvanica	L	FLMNH 35635	Miami-Dade County, FL	Pincrest Beds	30.132	29.102
Lucina pensylvanica	L	FLMNH 35635	Miami-Dade County, FL	Pincrest Beds	34.916	34.856
Lucina pensylvanica	L	FLMNH 35635	Miami-Dade County, FL	Pincrest Beds	31.918	32.918
Lucina pensylvanica	L	FLMNH 35635	Miami-Dade County, FL	Pincrest Beds	33.402	35.976
Lucina pensylvanica	L	FLMNH 35635	Miami-Dade County, FL	Pincrest Beds	35.613	36.067
Lucina pensylvanica	L	FLMNH 35635	Miami-Dade County, FL	Pincrest Beds	28.92	30.101
Lucina pensylvanica	L	FLMNH 35635	Miami-Dade County, FL	Pincrest Beds	30.98	30.101
Lucina pensylvanica	L	FLMNH 35635	Miami-Dade County, FL	Pincrest Beds	30.374	29.193
Lucina pensylvanica	L	FLMNH 35635	Miami-Dade County, FL	Pincrest Beds	20.835	20.441
Lucina pensylvanica	L	FLMNH 125713	Collier County, FL	Tamiami	16.535	15.626
Lucina pensylvanica	L	FLMNH 125713	Collier County, FL	Tamiami	19.533	18.2
Lucina pensylvanica	L	FLMNH 125713	Collier County, FL	Tamiami	37.612	39.186

Taxon Name	Valve	Museum	Locality	Formation	Width (mm)	Height (mm)
Lucina pensylvanica	L	FLMNH 125713	Collier County, FL	Tamiami	34.099	34.613
Lucina pensylvanica	L	FLMNH 125713	Collier County, FL	Tamiami	42.911	43.638
Lucina pensylvanica	L	FLMNH 125713	Collier County, FL	Tamiami	33.13	33.16
Lucina pensylvanica	L	FLMNH 125713	Collier County, FL	Tamiami	30.525	30.465
Lucina pensylvanica	L	FLMNH 125713	Collier County, FL	Tamiami	34.523	34.402
Lucina pensylvanica	L	FLMNH 125713	Collier County, FL	Tamiami	32.403	32.797
Lucina pensylvanica	L	FLMNH 125713	Collier County, FL	Tamiami	27.043	29.102
Lucina pensylvanica	L	FLMNH 59344	Okeechobee County, FL	Tamiami	29.102	29.344
Lucina pensylvanica	L	FLMNH 35635	Miami-Dade County, FL	Pincrest Beds	22.288	23.167
Lucina pensylvanica	R	FLMNH 59344	Okeechobee County, FL	Tamiami	48.453	47.242
Lucina pensylvanica	R	FLMNH 59344	Okeechobee County, FL	Tamiami	42.548	40.852
Lucina pensylvanica	R	FLMNH 59344	Okeechobee County, FL	Tamiami	42.517	42.487
Lucina pensylvanica	R	FLMNH 59344	Okeechobee County, FL	Tamiami	37.49	38.52
Lucina pensylvanica	R	FLMNH 59344	Okeechobee County, FL	Tamiami	42.699	42.972
Lucina pensylvanica	R	FLMNH 59344	Okeechobee County, FL	Tamiami	37.914	40.004
Lucina pensylvanica	R	FLMNH 59344	Okeechobee County, FL	Tamiami	34.038	35.31
Lucina pensylvanica	R	FLMNH 59344	Okeechobee County, FL	Tamiami	34.068	34.947

Taxon Name	Valve	Museum	Locality	Formation	Width (mm)	Height (mm)
Lucina pensylvanica	R	FLMNH 59344	Okeechobee County, FL	Tamiami	41.185	42.881
Lucina pensylvanica	R	FLMNH 59344	Okeechobee County, FL	Tamiami	23.56	23.5
Lucina pensylvanica	R	FLMNH 59344	Okeechobee County, FL	Tamiami	35.583	35.461
Lucina pensylvanica	R	FLMNH 93027	Charlotte County, FL	Tamiami	37.066	38.671
Lucina pensylvanica	R	FLMNH 93027	Charlotte County, FL	Tamiami	40.004	43.486
Lucina pensylvanica	R	FLMNH 93027	Charlotte County, FL	Tamiami	38.399	38.55
Lucina pensylvanica	R	FLMNH 93027	Charlotte County, FL	Tamiami	33.281	33.069
Lucina pensylvanica	R	FLMNH 93027	Charlotte County, FL	Tamiami	35.401	37.097
Lucina pensylvanica	R	FLMNH 93027	Charlotte County, FL	Tamiami	30.616	31.525
Lucina pensylvanica	R	FLMNH 93027	Charlotte County, FL	Tamiami	35.431	35.795
Lucina pensylvanica	R	FLMNH 93027	Charlotte County, FL	Tamiami	28.769	28.163
Lucina pensylvanica	R	FLMNH 93027	Charlotte County, FL	Tamiami	30.132	32.373
Lucina pensylvanica	R	FLMNH 93027	Charlotte County, FL	Tamiami	38.944	40.125
Lucina pensylvanica	R	FLMNH 93027	Charlotte County, FL	Tamiami	35.492	35.431
Lucina pensylvanica	R	FLMNH 93027	Charlotte County, FL	Tamiami	39.913	40.579
Lucina pensylvanica	R	FLMNH 93027	Charlotte County, FL	Tamiami	31.585	31.858
Lucina pensylvanica	R	FLMNH 93027	Charlotte County, FL	Tamiami	29.708	30.495

Taxon Name	Valve	Museum	Locality	Formation	Width (mm)	Height (mm)
Lucina pensylvanica	R	FLMNH 125345	Collier County, FL	Tamiami	22.47	23.651
Lucina pensylvanica	R	FLMNH 125345	Collier County, FL	Tamiami	45.515	45.909
Lucina pensylvanica	R	FLMNH 125345	Collier County, FL	Tamiami	45.485	45.909
Lucina pensylvanica	R	FLMNH 125345	Collier County, FL	Tamiami	24.832	25.407
Lucina pensylvanica	R	FLMNH 125345	Collier County, FL	Tamiami	28.981	27.043
Lucina pensylvanica	R	FLMNH 35635	Miami-Dade County, FL	Pincrest Beds	28.769	30.101
Lucina pensylvanica	R	FLMNH 35635	Miami-Dade County, FL	Pincrest Beds	35.885	37.733
Lucina pensylvanica	R	FLMNH 35635	Miami-Dade County, FL	Pincrest Beds	33.766	34.492
Lucina pensylvanica	R	FLMNH 35635	Miami-Dade County, FL	Pincrest Beds	36.007	35.795
Lucina pensylvanica	R	FLMNH 35635	Miami-Dade County, FL	Pincrest Beds	35.522	36.007
Lucina pensylvanica	R	FLMNH 35635	Miami-Dade County, FL	Pincrest Beds	34.977	35.825
Lucina pensylvanica	R	FLMNH 35635	Miami-Dade County, FL	Pincrest Beds	35.795	35.946
Lucina pensylvanica	R	FLMNH 35635	Miami-Dade County, FL	Pincrest Beds	30.374	30.858
Lucina pensylvanica	R	FLMNH 35635	Miami-Dade County, FL	Pincrest Beds	35.946	34.704
Lucina pensylvanica	R	FLMNH 35635	Miami-Dade County, FL	Pincrest Beds	34.129	34.644
Lucina pensylvanica	R	FLMNH 35635	Miami-Dade County, FL	Pincrest Beds	33.493	34.28
Lucina pensylvanica	R	FLMNH 35635	Miami-Dade County, FL	Pincrest Beds	31.343	32.13

Taxon Name	Valve	Museum	Locality	Formation	Width (mm)	Height (mm)
Lucina pensylvanica	R	FLMNH 35635	Miami-Dade County, FL	Pincrest Beds	28.072	29.647
Lucina pensylvanica	R	FLMNH 35635	Miami-Dade County, FL	Pincrest Beds	33.493	32.706
Lucina pensylvanica	R	FLMNH 35635	Miami-Dade County, FL	Pincrest Beds	36.976	35.492
Lucina pensylvanica	R	FLMNH 35635	Miami-Dade County, FL	Pincrest Beds	31.646	32.857
Lucina pensylvanica	R	FLMNH 35635	Miami-Dade County, FL	Pincrest Beds	33.22	35.159
Lucina pensylvanica	R	FLMNH 35635	Miami-Dade County, FL	Pincrest Beds	33.887	33.311
Lucina pensylvanica	R	FLMNH 35635	Miami-Dade County, FL	Pincrest Beds	30.707	30.495
Lucina pensylvanica	R	FLMNH 35635	Miami-Dade County, FL	Pincrest Beds	25.256	27.315
Lucina pensylvanica	R	FLMNH 35635	Miami-Dade County, FL	Pincrest Beds	31.767	33.22
Lucina pensylvanica	R	FLMNH 35635	Miami-Dade County, FL	Pincrest Beds	34.341	35.643
Lucina pensylvanica	R	FLMNH 35635	Miami-Dade County, FL	Pincrest Beds	34.492	35.249
Lucina pensylvanica	R	FLMNH 35635	Miami-Dade County, FL	Pincrest Beds	34.825	35.583
Lucina pensylvanica	R	FLMNH 35635	Miami-Dade County, FL	Pincrest Beds	32.918	33.432
Lucina pensylvanica	R	FLMNH 35635	Miami-Dade County, FL	Pincrest Beds	32.887	33.796
Lucina pensylvanica	R	FLMNH 35635	Miami-Dade County, FL	Pincrest Beds	33.13	34.19
Lucina pensylvanica	R	FLMNH 35635	Miami-Dade County, FL	Pincrest Beds	29.223	30.253
Lucina pensylvanica	R	FLMNH 35635	Miami-Dade County, FL	Pincrest Beds	30.374	31.979

Taxon Name	Valve	Museum	Locality	Formation	Width (mm)	Height (mm)
Lucina pensylvanica	R	FLMNH 35635	Miami-Dade County, FL	Pincrest Beds	29.587	29.738
Lucina pensylvanica	R	FLMNH 125713	Collier County, FL	Tamiami	32.251	33.766
Lucina pensylvanica	R	FLMNH 125713	Collier County, FL	Tamiami	32.282	33.796
Lucina pensylvanica	R	FLMNH 125713	Collier County, FL	Tamiami	29.98	30.919
Lucina pensylvanica	R	FLMNH 125713	Collier County, FL	Tamiami	34.886	35.401
Lucina pensylvanica	R	FLMNH 125713	Collier County, FL	Tamiami	37.642	38.066
Lucina pensylvanica	R	FLMNH 125713	Collier County, FL	Tamiami	32.857	32.948
Lucina pensylvanica	R	FLMNH 125713	Collier County, FL	Tamiami	36.097	36.37
Lucina pensylvanica	R	FLMNH 125713	Collier County, FL	Tamiami	31.827	32.282
Lucina pensylvanica	R	FLMNH 125713	Collier County, FL	Tamiami	35.249	36.491
Lucina glenni	L	FLMNH 36271	Liberty County, FL	Chipola	21.915	21.915
Lucina glenni	L	FLMNH 36271	Liberty County, FL	Chipola	24.803	24.552
Lucina glenni	L	FLMNH 36271	Liberty County, FL	Chipola	25.557	26.812
Lucina glenni	L	FLMNH 36271	Liberty County, FL	Chipola	24.834	23.108
Lucina glenni	L	FLMNH 36271	Liberty County, FL	Chipola	25.557	26.75
Lucina glenni	L	FLMNH 36271	Liberty County, FL	Chipola	25.651	26.373
Lucina glenni	L	FLMNH 36271	Liberty County, FL	Chipola	26.687	27.158

Taxon Name	Valve	Museum	Locality	Formation	Width (mm)	Height (mm)
Lucina glenni	L	FLMNH 36271	Liberty County, FL	Chipola	25.211	25.619
Lucina glenni	L	FLMNH 36271	Liberty County, FL	Chipola	25.651	26.373
Lucina glenni	L	FLMNH 36271	Liberty County, FL	Chipola	26.844	27.252
Lucina glenni	L	FLMNH 36271	Liberty County, FL	Chipola	27.786	27.88
Lucina glenni	L	FLMNH 36271	Liberty County, FL	Chipola	29.23	28.759
Lucina glenni	L	FLMNH 36271	Liberty County, FL	Chipola	23.265	22.762
Lucina glenni	L	FLMNH 36271	Liberty County, FL	Chipola	23.61	23.453
Lucina glenni	L	FLMNH 36271	Liberty County, FL	Chipola	24.207	24.646
Lucina glenni	L	FLMNH 36271	Liberty County, FL	Chipola	26.624	27.346
Lucina glenni	L	FLMNH 36271	Liberty County, FL	Chipola	24.834	25.18
Lucina glenni	L	FLMNH 36271	Liberty County, FL	Chipola	24.897	25.368
Lucina glenni	L	FLMNH 36271	Liberty County, FL	Chipola	23.17	23.547
Lucina glenni	L	FLMNH 36271	Liberty County, FL	Chipola	22.072	22.229
Lucina glenni	L	FLMNH 36271	Liberty County, FL	Chipola	23.39	24.364
Lucina glenni	L	FLMNH 36271	Liberty County, FL	Chipola	25.619	26.341
Lucina glenni	L	FLMNH 36271	Liberty County, FL	Chipola	25.588	26.247
Lucina glenni	L	FLMNH 36271	Liberty County, FL	Chipola	24.489	24.081

Taxon Name	Valve	Museum	Locality	Formation	Width (mm)	Height (mm)
Lucina glenni	L	FLMNH 36271	Liberty County, FL	Chipola	23.484	23.233
Lucina glenni	L	FLMNH 36271	Liberty County, FL	Chipola	27.943	29.104
Lucina glenni	L	FLMNH 36271	Liberty County, FL	Chipola	24.175	23.39
Lucina glenni	L	FLMNH 36271	Liberty County, FL	Chipola	26.718	26.09
Lucina glenni	L	FLMNH 36271	Liberty County, FL	Chipola	18.43	19.215
Lucina glenni	L	FLMNH 36271	Liberty County, FL	Chipola	24.677	24.05
Lucina glenni	L	FLMNH 36271	Liberty County, FL	Chipola	27.346	27.566
Lucina glenni	L	FLMNH 36271	Liberty County, FL	Chipola	22.448	21.726
Lucina glenni	L	FLMNH 36271	Liberty County, FL	Chipola	23.767	24.269
Lucina glenni	L	FLMNH 36271	Liberty County, FL	Chipola	19.466	19.591
Lucina glenni	L	FLMNH 36271	Liberty County, FL	Chipola	23.641	24.175
Lucina glenni	L	FLMNH 36271	Liberty County, FL	Chipola	23.955	23.484
Lucina glenni	L	FLMNH 74601	Cahloun County, FL	Chipola	32.495	34.693
Lucina glenni	L	FLMNH 74601	Cahloun County, FL	Chipola	25.808	26.373
Lucina glenni	L	FLMNH 74601	Cahloun County, FL	Chipola	29.293	29.23
Lucina glenni	L	FLMNH 74601	Cahloun County, FL	Chipola	28.759	28.696
Lucina glenni	L	FLMNH 74601	Cahloun County, FL	Chipola	24.301	23.861

Taxon Name	Valve	Museum	Locality	Formation	Width (mm)	Height (mm)
Lucina glenni	L	FLMNH 74601	Cahloun County, FL	Chipola	22.511	22.229
Lucina glenni	L	FLMNH 74601	Cahloun County, FL	Chipola	27.629	27.786
Lucina glenni	L	FLMNH 74601	Cahloun County, FL	Chipola	31.02	31.145
Lucina glenni	L	FLMNH 74601	Cahloun County, FL	Chipola	26.247	26.09
Lucina glenni	L	FLMNH 74601	Cahloun County, FL	Chipola	29.45	30.894
Lucina glenni	L	FLMNH 74601	Cahloun County, FL	Chipola	32.213	33.374
Lucina glenni	L	FLMNH 74601	Cahloun County, FL	Chipola	18.461	18.335
Lucina glenni	L	FLMNH 74601	Cahloun County, FL	Chipola	30.894	30.392
Lucina glenni	L	FLMNH 74601	Cahloun County, FL	Chipola	29.104	29.042
Lucina glenni	L	FLMNH 74601	Cahloun County, FL	Chipola	22.26	22.072
Lucina glenni	L	FLMNH 74601	Cahloun County, FL	Chipola	22.605	21.758
Lucina glenni	L	FLMNH 74601	Cahloun County, FL	Chipola	25.965	27.346
Lucina glenni	L	FLMNH 74601	Cahloun County, FL	Chipola	22.982	24.74
Lucina glenni	L	FLMNH 74601	Cahloun County, FL	Chipola	25.996	27.66
Lucina glenni	L	FLMNH 74601	Cahloun County, FL	Chipola	27.283	27.723
Lucina glenni	L	FLMNH 74601	Cahloun County, FL	Chipola	16.985	16.075
Lucina glenni	L	FLMNH 74601	Cahloun County, FL	Chipola	17.833	17.362

Taxon Name	Valve	Museum	Locality	Formation	Width (mm)	Height (mm)
Lucina glenni	L	FLMNH 96425	Cahloun County, FL	Chipola	30.015	31.239
Lucina glenni	L	FLMNH 96425	Cahloun County, FL	Chipola	28.665	30.831
Lucina glenni	L	FLMNH 96425	Cahloun County, FL	Chipola	24.364	24.364
Lucina glenni	L	FLMNH 96425	Cahloun County, FL	Chipola	27.001	28.257
Lucina glenni	L	FLMNH 96425	Cahloun County, FL	Chipola	28.005	27.629
Lucina glenni	L	FLMNH 96425	Cahloun County, FL	Chipola	28.696	29.544
Lucina glenni	L	FLMNH 96425	Cahloun County, FL	Chipola	22.951	22.605
Lucina glenni	L	FLMNH 96425	Cahloun County, FL	Chipola	16.577	16.483
Lucina glenni	L	FLMNH 96425	Cahloun County, FL	Chipola	31.208	31.773
Lucina glenni	L	FLMNH 96425	Cahloun County, FL	Chipola	22.762	22.637
Lucina glenni	L	FLMNH 96425	Cahloun County, FL	Chipola	24.395	23.924
Lucina glenni	R	FLMNH 36271	Liberty County, FL	Chipola	24.897	25.619
Lucina glenni	R	FLMNH 36271	Liberty County, FL	Chipola	26.75	26.687
Lucina glenni	R	FLMNH 36271	Liberty County, FL	Chipola	20.031	19.811
Lucina glenni	R	FLMNH 36271	Liberty County, FL	Chipola	25.18	26.844
Lucina glenni	R	FLMNH 36271	Liberty County, FL	Chipola	25.557	24.929
Lucina glenni	R	FLMNH 36271	Liberty County, FL	Chipola	25.619	26.404

Taxon Name	Valve	Museum	Locality	Formation	Width (mm)	Height (mm)
Lucina glenni	R	FLMNH 36271	Liberty County, FL	Chipola	25.871	25.462
Lucina glenni	R	FLMNH 36271	Liberty County, FL	Chipola	24.426	24.803
Lucina glenni	R	FLMNH 36271	Liberty County, FL	Chipola	25.274	27.221
Lucina glenni	R	FLMNH 36271	Liberty County, FL	Chipola	19.434	19.685
Lucina glenni	R	FLMNH 36271	Liberty County, FL	Chipola	29.481	28.759
Lucina glenni	R	FLMNH 36271	Liberty County, FL	Chipola	25.431	26.122
Lucina glenni	R	FLMNH 36271	Liberty County, FL	Chipola	23.987	23.955
Lucina glenni	R	FLMNH 36271	Liberty County, FL	Chipola	26.436	25.462
Lucina glenni	R	FLMNH 36271	Liberty County, FL	Chipola	25.996	26.122
Lucina glenni	R	FLMNH 36271	Liberty County, FL	Chipola	21.883	21.852
Lucina glenni	R	FLMNH 36271	Liberty County, FL	Chipola	23.202	24.646
Lucina glenni	R	FLMNH 36271	Liberty County, FL	Chipola	22.794	24.175
Lucina glenni	R	FLMNH 36271	Liberty County, FL	Chipola	21.318	21.946
Lucina glenni	R	FLMNH 36271	Liberty County, FL	Chipola	20.502	20.879
Lucina glenni	R	FLMNH 36271	Liberty County, FL	Chipola	22.543	24.018
Lucina glenni	R	FLMNH 36271	Liberty County, FL	Chipola	25.431	25.996
Lucina glenni	R	FLMNH 36271	Liberty County, FL	Chipola	23.265	23.673

Taxon Name	Valve	Museum	Locality	Formation	Width (mm)	Height (mm)
Lucina glenni	R	FLMNH 36271	Liberty County, FL	Chipola	22.103	23.17
Lucina glenni	R	FLMNH 36271	Liberty County, FL	Chipola	23.798	23.987
Lucina glenni	R	FLMNH 36271	Liberty County, FL	Chipola	24.96	25.274
Lucina glenni	R	FLMNH 36271	Liberty County, FL	Chipola	24.05	24.803
Lucina glenni	R	FLMNH 36271	Liberty County, FL	Chipola	24.615	25.18
Lucina glenni	R	FLMNH 36271	Liberty County, FL	Chipola	25.086	26.247
Lucina glenni	R	FLMNH 36271	Liberty County, FL	Chipola	25.117	26.247
Lucina glenni	R	FLMNH 36271	Liberty County, FL	Chipola	26.687	27.001
Lucina glenni	R	FLMNH 36271	Liberty County, FL	Chipola	27.786	28.005
Lucina glenni	R	FLMNH 36271	Liberty County, FL	Chipola	20.439	20.722
Lucina glenni	R	FLMNH 36271	Liberty County, FL	Chipola	20.125	19.058
Lucina glenni	R	FLMNH 36271	Liberty County, FL	Chipola	23.422	25.305
Lucina glenni	R	FLMNH 36271	Liberty County, FL	Chipola	21.349	21.381
Lucina glenni	R	FLMNH 36271	Liberty County, FL	Chipola	26.122	26.279
Lucina glenni	R	FLMNH 36271	Liberty County, FL	Chipola	25.745	26.185
Lucina glenni	R	FLMNH 36271	Liberty County, FL	Chipola	28.068	29.01
Lucina glenni	R	FLMNH 36271	Liberty County, FL	Chipola	25.808	27.409

Taxon Name	Valve	Museum	Locality	Formation	Width (mm)	Height (mm)
Lucina glenni	R	FLMNH 36271	Liberty County, FL	Chipola	19.56	19.528
Lucina glenni	R	FLMNH 36271	Cahloun County, FL	Chipola	23.076	22.04
Lucina glenni	R	FLMNH 74601	Cahloun County, FL	Chipola	30.078	31.553
Lucina glenni	R	FLMNH 74601	Cahloun County, FL	Chipola	30.392	30.957
Lucina glenni	R	FLMNH 74601	Cahloun County, FL	Chipola	31.02	31.051
Lucina glenni	R	FLMNH 74601	Cahloun County, FL	Chipola	32.275	34.034
Lucina glenni	R	FLMNH 74601	Cahloun County, FL	Chipola	29.104	28.79
Lucina glenni	R	FLMNH 74601	Cahloun County, FL	Chipola	20.47	20.627
Lucina glenni	R	FLMNH 74601	Cahloun County, FL	Chipola	29.167	30.078
Lucina glenni	R	FLMNH 74601	Cahloun County, FL	Chipola	23.893	24.615
Lucina glenni	R	FLMNH 74601	Cahloun County, FL	Chipola	30.674	30.8
Lucina glenni	R	FLMNH 74601	Cahloun County, FL	Chipola	34.661	34.913
Lucina glenni	R	FLMNH 74601	Cahloun County, FL	Chipola	23.547	27.692
Lucina glenni	R	FLMNH 74601	Cahloun County, FL	Chipola	27.597	28.382
Lucina glenni	R	FLMNH 74601	Cahloun County, FL	Chipola	26.812	28.602
Lucina glenni	R	FLMNH 74601	Cahloun County, FL	Chipola	22.605	21.789
Lucina glenni	R	FLMNH 96425	Cahloun County, FL	Chipola	24.175	25.839

Taxon Name	Valve	Museum	Locality	Formation	Width (mm)	Height (mm)
Lucina glenni	R	FLMNH 96425	Cahloun County, FL	Chipola	26.75	27.126
Lucina glenni	R	FLMNH 96425	Cahloun County, FL	Chipola	29.921	30.266
Lucina glenni	R	FLMNH 96425	Cahloun County, FL	Chipola	26.75	27.346
Lucina glenni	R	FLMNH 96425	Cahloun County, FL	Chipola	28.633	29.858
Lucina glenni	R	FLMNH 96425	Cahloun County, FL	Chipola	23.798	23.453
Lucina glenni	R	FLMNH 96425	Cahloun County, FL	Chipola	21.381	20.722
Lucina glenni	R	FLMNH 96425	Cahloun County, FL	Chipola	24.897	24.426
Lucina glenni	R	FLMNH 96425	Cahloun County, FL	Chipola	27.566	27.472
Lucina glenni	R	FLMNH 96425	Cahloun County, FL	Chipola	23.076	22.668
Lucina glenni	R	FLMNH 96425	Cahloun County, FL	Chipola	19.089	19.842
Lucina glenni	R	FLMNH 96425	Cahloun County, FL	Chipola	19.277	18.775
Lucina glenni	R	FLMNH 96425	Cahloun County, FL	Chipola	20.313	19.152
Lucina glenni	R	FLMNH 96425	Cahloun County, FL	Chipola	27.315	28.696
Lucina glenni	R	FLMNH 96425	Cahloun County, FL	Chipola	18.744	17.896

Table B2. Data for *Anodontia* specimens used for size and shape analysis. Data includes taxon name, valve side (i.e., right (R) or left (L)), museum catalog number, locality, formation/Age, and size data. All fossil specimens are reposited in the Florida Museum of Natural History (FLMNH) Invertebrate Paleontology Collection.

Taxon Name	Valve	Museum #	Locality	Formation or Age	Width (mm)	Height (mm)
Anodontia alba	R	-	Honeymoon Island	Holocene	50.665	47.186
Anodontia alba	R	-	Honeymoon Island	Holocene	48.194	42.649
Anodontia alba	R	-	Honeymoon Island	Holocene	47.035	42.699
Anodontia alba	R	-	Honeymoon Island	Holocene	42.145	39.07
Anodontia alba	R	-	Honeymoon Island	Holocene	45.472	41.54
Anodontia alba	R	-	Honeymoon Island	Holocene	36.146	33.726
Anodontia alba	R	-	Honeymoon Island	Holocene	43.204	38.918
Anodontia alba	R	-	Honeymoon Island	Holocene	42.447	39.423
Anodontia alba	R	-	Honeymoon Island	Holocene	52.933	49.707
Anodontia alba	R	-	Honeymoon Island	Holocene	49.253	42.901
Anodontia alba	R	-	Honeymoon Island	Holocene	51.622	47.489
Anodontia alba	R	-	Honeymoon Island, FL	Holocene	40.633	35.289
Anodontia alba	R	-	Honeymoon Island, FL	Holocene	49.102	44.766
Anodontia alba	R	-	Honeymoon Island, FL	Holocene	46.127	42.397

Taxon Name	Valve	Museum #	Locality	Formation or Age	Width (mm)	Height (mm)
Anodontia alba	R	-	Honeymoon Island, FL	Holocene	56.966	52.732
Anodontia alba	R	-	Honeymoon Island, FL	Holocene	44.817	41.187
Anodontia alba	R	-	Honeymoon Island, FL	Holocene	47.136	42.246
Anodontia alba	R	-	Honeymoon Island, FL	Holocene	49.253	44.918
Anodontia alba	R	-	Honeymoon Island, FL	Holocene	50.413	47.489
Anodontia alba	R	-	Honeymoon Island, FL	Holocene	50.009	48.396
Anodontia alba	R	-	Honeymoon Island, FL	Holocene	57.672	51.875
Anodontia alba	R	-	Honeymoon Island, FL	Holocene	44.161	41.137
Anodontia alba	R	-	Honeymoon Island, FL	Holocene	43.607	40.733
Anodontia alba	R	-	Honeymoon Island, FL	Holocene	44.766	41.691
Anodontia alba	R	-	Honeymoon Island, FL	Holocene	48.799	44.968
Anodontia alba	R	-	Honeymoon Island, FL	Holocene	44.867	41.288
Anodontia alba	R	-	Honeymoon Island, FL	Holocene	50.211	46.783
Anodontia alba	R	-	Honeymoon Island, FL	Holocene	41.237	38.364
Anodontia alba	R	-	Honeymoon Island, FL	Holocene	33.625	30.046
Anodontia alba	R	-	Honeymoon Island, FL	Holocene	34.23	30.348
Anodontia alba	R	-	Honeymoon Island, FL	Holocene	39.574	36.448

Taxon Name	Valve	Museum #	Locality	Formation or Age	Width (mm)	Height (mm)
Anodontia alba	R	-	Honeymoon Island, FL	Holocene	39.423	35.289
Anodontia alba	R	-	Honeymoon Island, FL	Holocene	37.507	34.381
Anodontia alba	R	-	Honeymoon Island, FL	Holocene	40.028	34.936
Anodontia alba	R	-	Honeymoon Island, FL	Holocene	45.825	42.548
Anodontia alba	R	-	Honeymoon Island, FL	Holocene	48.749	43.355
Anodontia alba	R	-	Honeymoon Island, FL	Holocene	49.051	45.875
Anodontia alba	R	-	Honeymoon Island, FL	Holocene	48.85	43.506
Anodontia alba	R	-	Honeymoon Island, FL	Holocene	48.295	42.599
Anodontia alba	R	-	Honeymoon Island, FL	Holocene	51.37	46.178
Anodontia alba	R	-	Honeymoon Island, FL	Holocene	39.826	35.642
Anodontia alba	R	-	Honeymoon Island, FL	Holocene	41.237	33.978
Anodontia alba	R	-	Honeymoon Island, FL	Holocene	42.246	36.65
Anodontia alba	R	-	Honeymoon Island, FL	Holocene	46.682	43.607
Anodontia alba	R	-	Honeymoon Island, FL	Holocene	41.641	38.717
Anodontia alba	R	-	Honeymoon Island, FL	Holocene	45.775	40.028
Anodontia alba	R	-	Honeymoon Island, FL	Holocene	45.069	42.347
Anodontia alba	R	-	Honeymoon Island, FL	Holocene	42.75	39.776

Taxon Name	Valve	Museum #	Locality	Formation or Age	Width (mm)	Height (mm)
Anodontia alba	R	-	Honeymoon Island, FL	Holocene	38.213	34.835
Anodontia alba	R	-	Honeymoon Island, FL	Holocene	42.699	37.91
Anodontia alba	R	-	Honeymoon Island, FL	Holocene	40.229	36.6
Anodontia alba	R	-	Honeymoon Island, FL	Holocene	40.532	35.289
Anodontia alba	R	-	Honeymoon Island, FL	Holocene	41.641	38.061
Anodontia alba	R	-	Honeymoon Island, FL	Holocene	38.818	33.877
Anodontia alba	R	-	Honeymoon Island, FL	Holocene	36.448	33.222
Anodontia alba	R	-	Honeymoon Island, FL	Holocene	41.137	36.095
Anodontia alba	R	-	Honeymoon Island, FL	Holocene	49.757	46.228
Anodontia alba	R	-	Honeymoon Island, FL	Holocene	53.689	47.589
Anodontia alba	R	-	Honeymoon Island, FL	Holocene	36.448	33.222
Anodontia alba	R	-	Honeymoon Island, FL	Holocene	41.137	36.095
Anodontia alba	R	-	Honeymoon Island, FL	Holocene	49.757	46.228
Anodontia alba	R	-	Honeymoon Island, FL	Holocene	53.689	47.589
Anodontia alba	R	-	Honeymoon Island, FL	Holocene	51.925	46.279
Anodontia alba	R	-	Honeymoon Island, FL	Holocene	46.178	41.641
Anodontia alba	R	-	Honeymoon Island, FL	Holocene	45.119	39.725

Taxon Name	Valve	Museum #	Locality	Formation or Age	Width (mm)	Height (mm)
Anodontia alba	R	-	Honeymoon Island, FL	Holocene	41.187	37.154
Anodontia alba	R	-	Honeymoon Island, FL	Holocene	47.942	44.666
Anodontia alba	R	-	Honeymoon Island, FL	Holocene	48.295	44.464
Anodontia alba	R	-	Honeymoon Island, FL	Holocene	42.851	38.112
Anodontia alba	R	-	Honeymoon Island, FL	Holocene	43.052	38.666
Anodontia alba	R	-	Honeymoon Island, FL	Holocene	35.642	30.953
Anodontia alba	L	-	Honeymoon Island, FL	Holocene	52.933	47.993
Anodontia alba	L	-	Honeymoon Island, FL	Holocene	52.379	46.884
Anodontia alba	L	-	Honeymoon Island, FL	Holocene	55.706	49.656
Anodontia alba	L	-	Honeymoon Island, FL	Holocene	51.471	45.825
Anodontia alba	L	-	Honeymoon Island, FL	Holocene	47.136	42.044
Anodontia alba	L	-	Honeymoon Island, FL	Holocene	50.614	45.775
Anodontia alba	L	-	Honeymoon Island, FL	Holocene	46.884	42.548
Anodontia alba	L	-	Honeymoon Island, FL	Holocene	42.246	38.465
Anodontia alba	L	-	Honeymoon Island, FL	Holocene	46.43	42.8
Anodontia alba	L	-	Honeymoon Island, FL	Holocene	45.018	41.237
Anodontia alba	L	-	Honeymoon Island, FL	Holocene	45.119	41.288

Taxon Name	Valve	Museum #	Locality	Formation or Age	Width (mm)	Height (mm)
Anodontia alba	L	-	Honeymoon Island, FL	Holocene	46.934	40.38
Anodontia alba	L	-	Honeymoon Island, FL	Holocene	41.59	38.112
Anodontia alba	L	-	Honeymoon Island, FL	Holocene	45.17	40.38
Anodontia alba	L	-	Honeymoon Island, FL	Holocene	52.681	46.329
Anodontia alba	L	-	Honeymoon Island, FL	Holocene	45.674	41.338
Anodontia alba	L	-	Honeymoon Island, FL	Holocene	43.758	38.717
Anodontia alba	L	-	Honeymoon Island, FL	Holocene	46.43	40.28
Anodontia alba	L	-	Honeymoon Island, FL	Holocene	42.699	37.809
Anodontia alba	L	-	Honeymoon Island, FL	Holocene	38.515	34.785
Anodontia alba	L	-	Honeymoon Island, FL	Holocene	49.606	44.968
Anodontia alba	L	-	Honeymoon Island, FL	Holocene	43.809	40.733
Anodontia alba	L	-	Honeymoon Island, FL	Holocene	45.573	41.389
Anodontia alba	L	-	Honeymoon Island, FL	Holocene	45.27	39.423
Anodontia alba	L	-	Honeymoon Island, FL	Holocene	39.624	34.986
Anodontia alba	L	-	Honeymoon Island, FL	Holocene	40.28	36.549
Anodontia alba	L	-	Honeymoon Island, FL	Holocene	46.984	42.447
Anodontia alba	L	-	Honeymoon Island, FL	Holocene	48.245	43.556

Taxon Name	Valve	Museum #	Locality	Formation or Age	Width (mm)	Height (mm)
Anodontia alba	L	-	Honeymoon Island, FL	Holocene	38.112	32.214
Anodontia alba	L	-	Honeymoon Island, FL	Holocene	51.068	45.976
Anodontia alba	L	-	Honeymoon Island, FL	Holocene	49.051	42.044
Anodontia alba	L	-	Honeymoon Island, FL	Holocene	41.792	37.91
Anodontia alba	L	-	Honeymoon Island, FL	Holocene	42.498	37.961
Anodontia alba	L	-	Honeymoon Island, FL	Holocene	45.875	42.901
Anodontia alba	L	-	Honeymoon Island, FL	Holocene	50.16	45.321
Anodontia alba	L	-	Honeymoon Island, FL	Holocene	50.009	45.119
Anodontia alba	L	-	Honeymoon Island, FL	Holocene	46.228	41.943
Anodontia alba	L	-	Honeymoon Island, FL	Holocene	43.153	38.515
Anodontia alba	L	-	Honeymoon Island, FL	Holocene	42.951	37.457
Anodontia alba	L	-	Honeymoon Island, FL	Holocene	47.136	41.137
Anodontia alba	L	-	Honeymoon Island, FL	Holocene	42.246	38.314
Anodontia alba	L	-	Honeymoon Island, FL	Holocene	45.724	40.885
Anodontia alba	L	-	Honeymoon Island, FL	Holocene	45.17	39.574
Anodontia alba	L	-	Honeymoon Island, FL	Holocene	40.633	38.566
Anodontia alba	L	-	Honeymoon Island, FL	Holocene	41.893	37.457

Taxon Name	Valve	Museum #	Locality	Formation or Age	Width (mm)	Height (mm)
Anodontia alba	L	-	Honeymoon Island, FL	Holocene	56.512	48.699
Anodontia alba	L	-	Honeymoon Island, FL	Holocene	44.716	39.675
Anodontia alba	L	-	Honeymoon Island, FL	Holocene	50.665	46.43
Anodontia alba	L	-	Honeymoon Island, FL	Holocene	49.959	43.052
Anodontia alba	L	-	Honeymoon Island, FL	Holocene	42.044	36.196
Anodontia alba	L	-	Honeymoon Island, FL	Holocene	37.759	33.978
Anodontia alba	L	-	Honeymoon Island, FL	Holocene	50.211	44.666
Anodontia alba	L	-	Honeymoon Island, FL	Holocene	42.649	36.852
Anodontia alba	L	-	Honeymoon Island, FL	Holocene	41.086	36.146
Anodontia alba	L	-	Honeymoon Island, FL	Holocene	39.826	34.482
Anodontia alba	L	-	Honeymoon Island, FL	Holocene	37.658	33.524
Anodontia alba	L	-	Honeymoon Island, FL	Holocene	35.138	32.567
Anodontia alba	L	-	Honeymoon Island, FL	Holocene	44.111	38.414
Anodontia alba	L	-	Honeymoon Island, FL	Holocene	36.902	32.718
Anodontia alba	L	-	Honeymoon Island, FL	Holocene	33.071	27.777
Anodontia alba	L	-	Honeymoon Island, FL	Holocene	49.303	44.565
Anodontia alba	L	-	Honeymoon Island, FL	Holocene	46.48	41.943

Taxon Name	Valve	Museum #	Locality	Formation or Age	Width (mm)	Height (mm)
Anodontia alba	L	-	Honeymoon Island, FL	Holocene	38.414	35.39
Anodontia alba	L	-	Honeymoon Island, FL	Holocene	43.153	40.028
Anodontia alba	L	-	Honeymoon Island, FL	Holocene	49.404	44.817
Anodontia alba	L	-	Honeymoon Island, FL	Holocene	50.513	46.43
Anodontia alba	L	-	Honeymoon Island, FL	Holocene	44.615	39.826
Anodontia alba	L	-	Honeymoon Island, FL	Holocene	44.01	39.473
Anodontia alba	L	-	Honeymoon Island, FL	Holocene	41.943	38.616
Anodontia alba	L	FLMNH 37357	Hillsborough, County, FL	Fort Thompson	51.216	47.851
Anodontia alba	L	FLMNH 37357	Hillsborough, County, FL	Fort Thompson	52.065	48.089
Anodontia alba	L	FLMNH 38085	Hillsborough, County, FL	Fort Thompson	36.568	31.946
Anodontia alba	L	FLMNH 38085	Hillsborough, County, FL	Fort Thompson	24.401	21.105
Anodontia alba	L	FLMNH 10431	Hillsborough, County, FL	Fort Thompson	58.387	54.241
Anodontia alba	L	FLMNH 10431	Hillsborough, County, FL	Fort Thompson	21.513	17.706
Anodontia alba	L	FLMNH 37472	Hillsborough, County, FL	Fort Thompson	60.052	54.071
Anodontia alba	L	FLMNH 37472	Hillsborough County, FL	Fort Thompson	58.421	54.275
Anodontia alba	L	FLMNH 37472	Hillsborough County, FL	Fort Thompson	56.076	51.046
Anodontia alba	L	FLMNH 37472	Hillsborough County, FL	Fort Thompson	51.454	46.866

Taxon Name	Valve	Museum #	Locality	Formation or Age	Width (mm)	Height (mm)
Anodontia alba	L	FLMNH 37472	Hillsborough County, FL	Fort Thompson	59.576	57.333
Anodontia alba	L	FLMNH 37472	Hillsborough County, FL	Fort Thompson	49.347	44.011
Anodontia alba	L	FLMNH 37472	Hillsborough County, FL	Fort Thompson	59.984	54.037
Anodontia alba	L	FLMNH 37472	Hillsborough County, FL	Fort Thompson	58.489	54.376
Anodontia alba	L	FLMNH 37472	Hillsborough County, FL	Fort Thompson	56.484	51.012
Anodontia alba	L	FLMNH 37472	Hillsborough County, FL	Fort Thompson	51.352	46.934
Anodontia alba	L	FLMNH 37472	Hillsborough County, FL	Fort Thompson	49.551	44.385
Anodontia schrammi	L	FLMNH 15056	Hendry County, FL	Fort Thompson	58.319	54.376
Anodontia schrammi	L	FLMNH 15056	Hendry County, FL	Fort Thompson	54.071	49.381
Anodontia schrammi	L	FLMNH 15056	Hendry County, FL	Fort Thompson	60.494	56.314
Anodontia schrammi	L	FLMNH 15056	Hendry County, FL	Fort Thompson	61.717	57.877
Anodontia schrammi	L	FLMNH 15056	Hendry County, FL	Fort Thompson	59.712	56.246
Anodontia schrammi	L	FLMNH 15056	Hendry County, FL	Fort Thompson	56.789	53.391
Anodontia schrammi	L	FLMNH 15056	Hendry County, FL	Fort Thompson	57.367	52.133
Anodontia alba	R	FLMNH 37357	Hillsborough County, FL	Fort Thompson	52.439	48.531
Anodontia alba	R	FLMNH 38085	Hillsborough County, FL	Fort Thompson	36.5	31.742
Anodontia alba	R	FLMNH 38085	Hillsborough County, FL	Fort Thompson	24.673	21.037

Taxon Name	Valve	Museum #	Locality	Formation or Age	Width (mm)	Height (mm)
Anodontia alba	R	FLMNH 37472	Hillsborough County, FL	Fort Thompson	58.217	54.139
Anodontia alba	R	FLMNH 37472	Hillsborough County, FL	Fort Thompson	56.042	51.046
Anodontia alba	R	FLMNH 37472	Hillsborough County, FL	Fort Thompson	60.018	54.037
Anodontia alba	R	FLMNH 37472	Hillsborough County, FL	Fort Thompson	59.984	54.784
Anodontia alba	R	FLMNH 37472	Hillsborough County, FL	Fort Thompson	56.008	51.25
Anodontia alba	R	FLMNH 37472	Hillsborough County, FL	Fort Thompson	49.856	44.759
Anodontia alba	R	FLMNH 37472	Hillsborough County, FL	Fort Thompson	57.945	54.139
Anodontia alba	R	FLMNH 37472	Hillsborough County, FL	Fort Thompson	55.94	51.114
Anodontia alba	R	FLMNH 37472	Hillsborough County, FL	Fort Thompson	59.984	54.207
Anodontia alba	R	FLMNH 37472	Hillsborough County, FL	Fort Thompson	60.018	54.852
Anodontia alba	R	FLMNH 37472	Hillsborough County, FL	Fort Thompson	56.042	51.352
Anodontia alba	R	FLMNH 37472	Hillsborough County, FL	Fort Thompson	49.788	44.793
Anodontia schrammi	R	FLMNH 15056	Hendry County, FL	Fort Thompson	61.174	56.959
Anodontia schrammi	R	FLMNH 15056	Hendry County, FL	Fort Thompson	60.256	56.042
Anodontia schrammi	R	FLMNH 15056	Hendry County, FL	Fort Thompson	56.484	52.541
Anodontia schrammi	R	FLMNH 15056	Hendry County, FL	Fort Thompson	53.901	49.653
Anodontia schrammi	R	FLMNH 15056	Hendry County, FL	Fort Thompson	56.552	53.323

Taxon Name	Valve	Museum #	Locality	Formation or Age	Width (mm)	Height (mm)
Anodontia schrammi	R	FLMNH 15056	Hendry County, FL	Fort Thompson	60.154	56.586
Anodontia schrammi	R	FLMNH 15056	Hendry County, FL	Fort Thompson	58.523	54.512
Anodontia alba	L	FLMNH 138312	St. Lucie County, FL	Bermont	55.871	49.74
Anodontia alba	L	FLMNH 138312	St. Lucie County, FL	Bermont	42.099	37.981
Anodontia alba	L	FLMNH 138312	St. Lucie County, FL	Bermont	45.526	41.911
Anodontia alba	L	FLMNH 138312	St. Lucie County, FL	Bermont	52.035	46.03
Anodontia alba	L	FLMNH 138312	St. Lucie County, FL	Bermont	40.056	36.314
Anodontia alba	L	FLMNH 138312	St. Lucie County, FL	Bermont	41.628	38.892
Anodontia alba	L	FLMNH 137872	Palm Beach County, FL	Bermont	44.52	40.842
Anodontia alba	L	FLMNH 137872	Palm Beach County, FL	Bermont	43.86	40.15
Anodontia alba	L	FLMNH 137872	Palm Beach County, FL	Bermont	42.885	38.421
Anodontia alba	L	FLMNH 137872	Palm Beach County, FL	Bermont	45.212	41.156
Anodontia alba	L	FLMNH 137872	Palm Beach County, FL	Bermont	40.527	36.377
Anodontia alba	L	FLMNH 144441	Glades County, FL	Bermont	55.965	50.211
Anodontia alba	L	FLMNH 122295	Palm Beach County, FL	Bermont	41.282	37.855
Anodontia alba	L	FLMNH 122295	Palm Beach County, FL	Bermont	41.439	37.949
Anodontia alba	L	FLMNH 122295	Palm Beach County, FL	Bermont	40.527	36.975

Taxon Name	Valve	Museum #	Locality	Formation or Age	Width (mm)	Height (mm)
Anodontia alba	L	FLMNH 122295	Palm Beach County, FL	Bermont	42.791	39.458
Anodontia alba	L	FLMNH 122295	Palm Beach County, FL	Bermont	39.113	34.962
Anodontia alba	L	FLMNH 122295	Palm Beach County, FL	Bermont	28.108	25.121
Anodontia alba	L	FLMNH 122295	Palm Beach County, FL	Bermont	52.003	46.753
Anodontia alba	L	FLMNH 122295	Palm Beach County, FL	Bermont	17.324	14.809
Anodontia alba	L	FLMNH 122291	Palm Beach County, FL	Bermont	41.911	37.069
Anodontia alba	L	FLMNH 122291	Palm Beach County, FL	Bermont	26.033	23.392
Anodontia alba	L	FLMNH 122291	Palm Beach County, FL	Bermont	42.728	39.49
Anodontia alba	L	FLMNH 122291	Palm Beach County, FL	Bermont	31.347	27.479
Anodontia alba	L	FLMNH 122291	Palm Beach County, FL	Bermont	33.044	29.051
Anodontia alba	L	FLMNH 122291	Palm Beach County, FL	Bermont	41.659	36.88
Anodontia alba	L	FLMNH 122291	Palm Beach County, FL	Bermont	48.419	43.42
Anodontia alba	L	FLMNH 122291	Palm Beach County, FL	Bermont	27.134	23.266
Anodontia alba	L	FLMNH 122291	Palm Beach County, FL	Bermont	36.692	32.007
Anodontia alba	L	FLMNH 136161	Charolette County, FL	Bermont	53.795	48.671
Anodontia alba	L	FLMNH 136161	Charolette County, FL	Bermont	47.57	43.357
Anodontia alba	L	FLMNH 136161	Charolette County, FL	Bermont	52.192	46.973

Taxon Name	Valve	Museum #	Locality	Formation or Age	Width (mm)	Height (mm)
Anodontia alba	L	FLMNH 136161	Charolette County, FL	Bermont	48.293	43.294
Anodontia alba	L	FLMNH 136161	Charolette County, FL	Bermont	43.514	39.584
Anodontia alba	L	FLMNH 136161	Charolette County, FL	Bermont	44.52	40.37
Anodontia alba	L	FLMNH 136161	Charolette County, FL	Bermont	43.546	40.37
Anodontia alba	L	FLMNH 136161	Charolette County, FL	Bermont	45.904	41.596
Anodontia alba	L	FLMNH 136161	Charolette County, FL	Bermont	46.375	42.037
Anodontia alba	L	FLMNH 136161	Charolette County, FL	Bermont	45.621	41.03
Anodontia alba	L	FLMNH 136161	Charolette County, FL	Bermont	44.961	39.49
Anodontia alba	L	FLMNH 136161	Charolette County, FL	Bermont	45.118	41.785
Anodontia alba	L	FLMNH 136161	Charolette County, FL	Bermont	42.98	38.735
Anodontia alba	L	FLMNH 136161	Charolette County, FL	Bermont	39.616	36.063
Anodontia alba	L	FLMNH 136161	Charolette County, FL	Bermont	39.018	34.994
Anodontia alba	L	FLMNH 136161	Charolette County, FL	Bermont	21.977	20.751
Anodontia alba	L	FLMNH 13710	Hillsborough County, FL	Bermont	53.292	48.639
Anodontia alba	L	FLMNH 13710	Hillsborough County, FL	Bermont	48.639	43.671
Anodontia alba	L	FLMNH 13710	Hillsborough County, FL	Bermont	50.18	47.193
Anodontia alba	L	FLMNH 13710	Hillsborough County, FL	Bermont	49.394	46.124

Taxon Name	Valve	Museum #	Locality	Formation or Age	Width (mm)	Height (mm)
Anodontia alba	R	FLMNH 138312	St. Lucie County, FL	Bermont	56.499	52.129
Anodontia alba	R	FLMNH 138312	St. Lucie County, FL	Bermont	51.123	47.067
Anodontia alba	R	FLMNH 138312	St. Lucie County, FL	Bermont	39.741	36.377
Anodontia alba	R	FLMNH 138312	St. Lucie County, FL	Bermont	45.212	41.219
Anodontia alba	R	FLMNH 137872	Palm Beach County, FL	Bermont	46.595	40.873
Anodontia alba	R	FLMNH 137872	Palm Beach County, FL	Bermont	43.766	40.339
Anodontia alba	R	FLMNH 137872	Palm Beach County, FL	Bermont	39.427	36.88
Anodontia alba	R	FLMNH 137872	Palm Beach County, FL	Bermont	42.602	38.83
Anodontia alba	R	FLMNH 144441	Glades County, FL	Bermont	47.664	43.734
Anodontia alba	R	FLMNH 144441	Glades County, FL	Bermont	42.917	42.382
Anodontia alba	R	FLMNH 144441	Glades County, FL	Bermont	51.186	48.105
Anodontia alba	R	FLMNH 144441	Glades County, FL	Bermont	48.828	44.52
Anodontia alba	R	FLMNH 144441	Glades County, FL	Bermont	42.257	38.169
Anodontia alba	R	FLMNH 144441	Glades County, FL	Bermont	24.461	21.254
Anodontia alba	R	FLMNH 122295	Palm Beach County, FL	Bermont	37.792	33.61
Anodontia alba	R	FLMNH 122291	Palm Beach County, FL	Bermont	37.069	33.422
Anodontia alba	R	FLMNH 122291	Palm Beach County, FL	Bermont	33.076	29.932

Taxon Name	Valve	Museum #	Locality	Formation or Age	Width (mm)	Height (mm)
Anodontia alba	R	FLMNH 122291	Palm Beach County, FL	Bermont	32.95	29.083
Anodontia alba	R	FLMNH 122291	Palm Beach County, FL	Bermont	23.109	19.965
Anodontia alba	R	FLMNH 122291	Palm Beach County, FL	Bermont	37.792	32.164
Anodontia alba	R	FLMNH 122291	Palm Beach County, FL	Bermont	39.238	35.025
Anodontia alba	R	FLMNH 122291	Palm Beach County, FL	Bermont	34.491	31.378
Anodontia alba	R	FLMNH 122291	Palm Beach County, FL	Bermont	36.44	33.202
Anodontia alba	R	FLMNH 122291	Palm Beach County, FL	Bermont	50.809	47.13
Anodontia alba	R	FLMNH 136161	Charolette County, FL	Bermont	51.406	46.124
Anodontia alba	R	FLMNH 136161	Charolette County, FL	Bermont	48.042	43.42
Anodontia alba	R	FLMNH 136161	Charolette County, FL	Bermont	45.935	41.848
Anodontia alba	R	FLMNH 136161	Charolette County, FL	Bermont	45.841	41.785
Anodontia alba	R	FLMNH 136161	Charolette County, FL	Bermont	40.433	37.037
Anodontia alba	R	FLMNH 136161	Charolette County, FL	Bermont	47.633	43.451
Anodontia alba	R	FLMNH 136161	Charolette County, FL	Bermont	49.331	45.181
Anodontia alba	R	FLMNH 136161	Charolette County, FL	Bermont	47.696	43.483
Anodontia alba	R	FLMNH 136161	Charolette County, FL	Bermont	43.829	40.81
Anodontia alba	R	FLMNH 136161	Charolette County, FL	Bermont	50.368	46.878

Taxon Name	Valve	Museum #	Locality	Formation or Age	Width (mm)	Height (mm)
Anodontia alba	R	FLMNH 136161	Charolette County, FL	Bermont	43.923	39.678
Anodontia alba	R	FLMNH 136161	Charolette County, FL	Bermont	41.879	38.389
Anodontia alba	R	FLMNH 136161	Charolette County, FL	Bermont	45.432	41.691
Anodontia alba	R	FLMNH 136161	Charolette County, FL	Bermont	45.275	41.156
Anodontia alba	R	FLMNH 136161	Charolette County, FL	Bermont	38.295	32.887
Anodontia alba	R	FLMNH 136161	Charolette County, FL	Bermont	36	31.975
Anodontia alba	R	FLMNH 13710	Hillsborough County, FL	Bermont	49.205	45.872
Anodontia alba	R	FLMNH 13710	Hillsborough County, FL	Bermont	53.292	48.356
Anodontia alba	R	FLMNH 13710	Hillsborough County, FL	Bermont	49.457	45.904
Anodontia alba	R	FLMNH 13710	Hillsborough County, FL	Bermont	50.526	47.036
Anodontia alba	R	FLMNH 13710	Hillsborough County, FL	Bermont	50.84	47.853
Anodontia alba	L	FLMNH 136397	Glades County, Florida	Caloosahatchee	30.073	27.119
Anodontia alba	L	FLMNH 144406	Charolette County, FL	Caloosahatchee	34.598	30.481
Anodontia alba	L	FLMNH 144406	Charolette County, FL	Caloosahatchee	40.977	37.678
Anodontia alba	L	FLMNH 199850	Hendry County, FL	Caloosahatchee	42.517	37.049
Anodontia alba	L	FLMNH 144250	Hendry County, FL	Caloosahatchee	38.589	33.687
Anodontia alba	L	FLMNH 144250	Hendry County, FL	Caloosahatchee	49.493	43.9

Taxon Name	Valve	Museum #	Locality	Formation or Age	Width (mm)	Height (mm)
Anodontia alba	L	FLMNH 144250	Hendry County, FL	Caloosahatchee	46.539	43.522
Anodontia alba	L	FLMNH 144250	Hendry County, FL	Caloosahatchee	49.65	45.377
Anodontia alba	L	FLMNH 144250	Hendry County, FL	Caloosahatchee	37.426	33.592
Anodontia alba	L	FLMNH 144406	Charolette County, FL	Caloosahatchee	40.883	37.646
Anodontia alba	L	FLMNH 144406	Charolette County, FL	Caloosahatchee	34.849	30.419
Anodontia alba	L	FLMNH 2717	Charolette County, FL	Caloosahatchee	52.447	47.67
Anodontia alba	L	FLMNH 2717	Charolette County, FL	Caloosahatchee	45.345	39.909
Anodontia alba	L	FLMNH 2717	Charolette County, FL	Caloosahatchee	43.334	38.997
Anodontia alba	L	FLMNH 2717	Charolette County, FL	Caloosahatchee	36.798	32.367
Anodontia alba	L	FLMNH 2717	Charolette County, FL	Caloosahatchee	37.992	34.127
Anodontia alba	L	FLMNH 2717	Charolette County, FL	Caloosahatchee	45.062	40.317
Anodontia alba	L	FLMNH 2717	Charolette County, FL	Caloosahatchee	45.502	40.883
Anodontia alba	L	FLMNH 2717	Charolette County, FL	Caloosahatchee	36.641	33.215
Anodontia alba	L	FLMNH 2717	Charolette County, FL	Caloosahatchee	44.811	40.569
Anodontia alba	L	FLMNH 2717	Charolette County, FL	Caloosahatchee	50.247	44.779
Anodontia alba	L	FLMNH 2717	Charolette County, FL	Caloosahatchee	40.097	35.478
Anodontia alba	L	FLMNH 2717	Charolette County, FL	Caloosahatchee	43.868	38.935

Taxon Name	Valve	Museum #	Locality	Formation or Age	Width (mm)	Height (mm)
Anodontia alba	L	FLMNH 2717	Charolette County, FL	Caloosahatchee	41.229	36.515
Anodontia alba	L	FLMNH 2717	Charolette County, FL	Caloosahatchee	37.206	32.838
Anodontia alba	L	FLMNH 2717	Charolette County, FL	Caloosahatchee	34.472	30.073
Anodontia alba	L	FLMNH 2717	Charolette County, FL	Caloosahatchee	31.204	26.931
Anodontia alba	L	FLMNH 2717	Charolette County, FL	Caloosahatchee	36.986	33.372
Anodontia alba	L	FLMNH 2717	Charolette County, FL	Caloosahatchee	48.079	43.774
Anodontia alba	L	FLMNH 2717	Charolette County, FL	Caloosahatchee	47.105	41.637
Anodontia alba	L	FLMNH 2717	Charolette County, FL	Caloosahatchee	31.644	28.03
Anodontia alba	L	FLMNH 2717	Charolette County, FL	Caloosahatchee	45.408	41.983
Anodontia alba	L	FLMNH 2717	Charolette County, FL	Caloosahatchee	48.425	44.371
Anodontia alba	L	FLMNH 2717	Charolette County, FL	Caloosahatchee	37.709	33.184
Anodontia alba	L	FLMNH 2717	Charolette County, FL	Caloosahatchee	36.483	32.335
Anodontia alba	L	FLMNH 2717	Charolette County, FL	Caloosahatchee	36.389	31.676
Anodontia alba	L	FLMNH 2717	Charolette County, FL	Caloosahatchee	31.267	27.088
Anodontia alba	L	FLMNH 2717	Charolette County, FL	Caloosahatchee	32.021	27.81
Anodontia alba	L	FLMNH 2717	Charolette County, FL	Caloosahatchee	40.38	36.389
Anodontia alba	L	FLMNH 2717	Charolette County, FL	Caloosahatchee	37.929	33.215

Taxon Name	Valve	Museum #	Locality	Formation or Age	Width (mm)	Height (mm)
Anodontia alba	L	FLMNH 2717	Charolette County, FL	Caloosahatchee	37.772	33.31
Anodontia alba	L	FLMNH 2717	Charolette County, FL	Caloosahatchee	48.739	44.245
Anodontia alba	L	FLMNH 2717	Charolette County, FL	Caloosahatchee	31.33	27.873
Anodontia alba	L	FLMNH 2717	Charolette County, FL	Caloosahatchee	41.606	38.243
Anodontia alba	L	FLMNH 2717	Charolette County, FL	Caloosahatchee	40.977	37.709
Anodontia alba	L	FLMNH 2717	Charolette County, FL	Caloosahatchee	36.012	32.335
Anodontia alba	L	FLMNH 2717	Charolette County, FL	Caloosahatchee	39.657	34.567
Anodontia alba	L	FLMNH 2717	Charolette County, FL	Caloosahatchee	39.752	34.912
Anodontia alba	L	FLMNH 2717	Charolette County, FL	Caloosahatchee	24.762	21.62
Anodontia alba	L	FLMNH 2717	Charolette County, FL	Caloosahatchee	35.384	31.833
Anodontia alba	L	FLMNH 2717	Charolette County, FL	Caloosahatchee	43.334	38.966
Anodontia alba	L	FLMNH 2717	Charolette County, FL	Caloosahatchee	38.337	34.19
Anodontia alba	L	FLMNH 2717	Charolette County, FL	Caloosahatchee	39.72	36.515
Anodontia alba	L	FLMNH 2717	Charolette County, FL	Caloosahatchee	27.936	25.108
Anodontia alba	L	FLMNH 2717	Charolette County, FL	Caloosahatchee	36.892	32.335
Anodontia alba	L	FLMNH 2717	Charolette County, FL	Caloosahatchee	31.518	27.685
Anodontia alba	L	FLMNH 2717	Charolette County, FL	Caloosahatchee	27.999	24.479

Taxon Name	Valve	Museum #	Locality	Formation or Age	Width (mm)	Height (mm)
Anodontia alba	L	FLMNH 147372	Sarasota County,FL	Caloosahatchee	48.645	43.617
Anodontia alba	L	FLMNH 147372	Sarasota County,FL	Caloosahatchee	50.656	45.848
Anodontia alba	L	FLMNH 147372	Sarasota County,FL	Caloosahatchee	55.527	49.524
Anodontia alba	L	FLMNH 147372	Sarasota County,FL	Caloosahatchee	45.251	41.637
Anodontia alba	L	FLMNH 147372	Sarasota County,FL	Caloosahatchee	55.024	48.236
Anodontia alba	L	FLMNH 147372	Sarasota County,FL	Caloosahatchee	42.517	36.546
Anodontia alba	L	FLMNH 147372	Sarasota County,FL	Caloosahatchee	50.97	46.319
Anodontia alba	L	FLMNH 147372	Sarasota County,FL	Caloosahatchee	49.587	46.256
Anodontia alba	L	FLMNH 147372	Sarasota County,FL	Caloosahatchee	36.515	33.718
Anodontia alba	L	FLMNH 23968	Hendry County, FL	Caloosahatchee	46.979	42.8
Anodontia alba	L	FLMNH 23968	Hendry County, FL	Caloosahatchee	46.288	43.02
Anodontia alba	L	FLMNH 23968	Hendry County, FL	Caloosahatchee	42.014	38.463
Anodontia alba	L	FLMNH 23968	Hendry County, FL	Caloosahatchee	33.75	29.193
Anodontia alba	L	FLMNH 23968	Hendry County, FL	Caloosahatchee	37.206	33.687
Anodontia alba	L	FLMNH 23968	Hendry County, FL	Caloosahatchee	54.112	47.702
Anodontia alba	L	FLMNH 23968	Hendry County, FL	Caloosahatchee	35.761	31.33
Anodontia alba	L	FLMNH 23968	Hendry County, FL	Caloosahatchee	42.674	39.814

Taxon Name	Valve	Museum #	Locality	Formation or Age	Width (mm)	Height (mm)
Anodontia alba	L	FLMNH 23968	Hendry County, FL	Caloosahatchee	33.687	30.764
Anodontia alba	L	FLMNH 23968	Hendry County, FL	Caloosahatchee	34.032	29.947
Anodontia alba	L	FLMNH 23968	Hendry County, FL	Caloosahatchee	35.289	30.827
Anodontia alba	L	FLMNH 23968	Hendry County, FL	Caloosahatchee	27.308	23.82
Anodontia alba	L	FLMNH 23968	Hendry County, FL	Caloosahatchee	36.766	32.65
Anodontia alba	L	FLMNH 23968	Hendry County, FL	Caloosahatchee	58.166	51.598
Anodontia alba	L	FLMNH 23968	Hendry County, FL	Caloosahatchee	54.427	50.247
Anodontia alba	L	FLMNH 23968	Hendry County, FL	Caloosahatchee	53.075	47.545
Anodontia alba	L	FLMNH 23968	Hendry County, FL	Caloosahatchee	38.777	35.069
Anodontia alba	L	FLMNH 23968	Hendry County, FL	Caloosahatchee	41.857	37.646
Anodontia alba	L	FLMNH 23968	Hendry County, FL	Caloosahatchee	46.665	41.983
Anodontia alba	L	FLMNH 23968	Hendry County, FL	Caloosahatchee	42.643	38.557
Anodontia alba	L	FLMNH 23968	Hendry County, FL	Caloosahatchee	34.158	30.733
Anodontia alba	L	FLMNH 23968	Hendry County, FL	Caloosahatchee	38.432	34.19
Anodontia alba	L	FLMNH 23968	Hendry County, FL	Caloosahatchee	40.569	36.923
Anodontia alba	L	FLMNH 23968	Hendry County, FL	Caloosahatchee	26.333	23.82
Anodontia alba	L	FLMNH 23968	Hendry County, FL	Caloosahatchee	49.399	46.036

Taxon Name	Valve	Museum #	Locality	Formation or Age	Width (mm)	Height (mm)
Anodontia alba	L	FLMNH 23968	Hendry County, FL	Caloosahatchee	46.539	41.48
Anodontia alba	L	FLMNH 23968	Hendry County, FL	Caloosahatchee	45.816	42.517
Anodontia alba	L	FLMNH 23968	Hendry County, FL	Caloosahatchee	35.227	31.676
Anodontia alba	L	FLMNH 23968	Hendry County, FL	Caloosahatchee	56.312	51.473
Anodontia alba	L	FLMNH 23968	Hendry County, FL	Caloosahatchee	39.312	35.478
Anodontia alba	L	FLMNH 23968	Hendry County, FL	Caloosahatchee	41.197	36.641
Anodontia alba	L	FLMNH 23968	Hendry County, FL	Caloosahatchee	21.274	18.855
Anodontia alba	L	FLMNH 23968	Hendry County, FL	Caloosahatchee	49.65	46.099
Anodontia alba	L	FLMNH 23968	Hendry County, FL	Caloosahatchee	47.388	43.554
Anodontia alba	L	FLMNH 23968	Hendry County, FL	Caloosahatchee	48.519	44.685
Anodontia alba	L	FLMNH 23968	Hendry County, FL	Caloosahatchee	36.829	32.021
Anodontia alba	L	FLMNH 23968	Hendry County, FL	Caloosahatchee	35.478	32.147
Anodontia alba	L	FLMNH 23968	Hendry County, FL	Caloosahatchee	43.9	40.569
Anodontia alba	L	FLMNH 23968	Hendry County, FL	Caloosahatchee	23.222	20.677
Anodontia alba	L	FLMNH 23968	Hendry County, FL	Caloosahatchee	29.633	25.705
Anodontia alba	L	FLMNH 23968	Hendry County, FL	Caloosahatchee	22.374	18.98
Anodontia alba	R	FLMNH 2717	Hendry County, FL	Caloosahatchee	48.048	44.905

Taxon Name	Valve	Museum #	Locality	Formation or Age	Width (mm)	Height (mm)
Anodontia alba	R	FLMNH 23968	Hendry County, FL	Caloosahatchee	28.187	25.799
Anodontia alba	R	FLMNH 23968	Hendry County, FL	Caloosahatchee	42.171	37.426
Anodontia alba	R	FLMNH 136397	Glades County, Florida	Caloosahatchee	47.482	43.428
Anodontia alba	R	FLMNH 136397	Glades County, Florida	Caloosahatchee	47.608	43.397
Anodontia alba	R	FLMNH 199850	Hendry County, FL	Caloosahatchee	47.293	43.68
Anodontia alba	R	FLMNH 144250	Hendry County, FL	Caloosahatchee	46.633	42.328
Anodontia alba	R	FLMNH 144250	Hendry County, FL	Caloosahatchee	38.275	33.781
Anodontia alba	R	FLMNH 144250	Hendry County, FL	Caloosahatchee	41.668	37.143
Anodontia alba	R	FLMNH 144250	Hendry County, FL	Caloosahatchee	22.5	19.734
Anodontia alba	R	FLMNH 144250	Hendry County, FL	Caloosahatchee	36.829	32.933
Anodontia alba	R	FLMNH 144250	Hendry County, FL	Caloosahatchee	48.896	43.585
Anodontia alba	R	FLMNH 144250	Hendry County, FL	Caloosahatchee	49.619	45.251
Anodontia alba	R	FLMNH 144250	Hendry County, FL	Caloosahatchee	47.922	43.68
Anodontia alba	R	FLMNH 144250	Hendry County, FL	Caloosahatchee	37.238	33.592
Anodontia alba	R	FLMNH 144250	Hendry County, FL	Caloosahatchee	44.685	40.6
Anodontia alba	R	FLMNH 2717	Hendry County, FL	Caloosahatchee	48.11	43.9
Anodontia alba	R	FLMNH 2717	Hendry County, FL	Caloosahatchee	31.99	28.282

Taxon Name	Valve	Museum #	Locality	Formation or Age	Width (mm)	Height (mm)
Anodontia alba	R	FLMNH 2717	Hendry County, FL	Caloosahatchee	41.323	36.483
Anodontia alba	R	FLMNH 2717	Hendry County, FL	Caloosahatchee	41.291	36.452
Anodontia alba	R	FLMNH 2717	Hendry County, FL	Caloosahatchee	41.103	36.515
Anodontia alba	R	FLMNH 2717	Hendry County, FL	Caloosahatchee	48.613	44.277
Anodontia alba	R	FLMNH 2717	Hendry County, FL	Caloosahatchee	37.583	31.801
Anodontia alba	R	FLMNH 2717	Hendry County, FL	Caloosahatchee	50.279	46.916
Anodontia alba	R	FLMNH 2717	Hendry County, FL	Caloosahatchee	50.153	45.031
Anodontia alba	R	FLMNH 2717	Hendry County, FL	Caloosahatchee	45.534	41.448
Anodontia alba	R	FLMNH 2717	Hendry County, FL	Caloosahatchee	45.125	40.003
Anodontia alba	R	FLMNH 2717	Hendry County, FL	Caloosahatchee	36.515	32.775
Anodontia alba	R	FLMNH 2717	Hendry County, FL	Caloosahatchee	28.187	25.076
Anodontia alba	R	FLMNH 2717	Hendry County, FL	Caloosahatchee	37.678	34.127
Anodontia alba	R	FLMNH 2717	Hendry County, FL	Caloosahatchee	37.709	32.87
Anodontia alba	R	FLMNH 2717	Hendry County, FL	Caloosahatchee	46.979	41.857
Anodontia alba	R	FLMNH 2717	Hendry County, FL	Caloosahatchee	36.735	31.958
Anodontia alba	R	FLMNH 2717	Hendry County, FL	Caloosahatchee	28.942	27.905
Anodontia alba	R	FLMNH 2717	Hendry County, FL	Caloosahatchee	39.657	35.384

Taxon Name	Valve	Museum #	Locality	Formation or Age	Width (mm)	Height (mm)
Anodontia alba	R	FLMNH 2717	Hendry County, FL	Caloosahatchee	48.55	44.559
Anodontia alba	R	FLMNH 2717	Hendry County, FL	Caloosahatchee	41.103	36.044
Anodontia alba	R	FLMNH 2717	Hendry County, FL	Caloosahatchee	38.18	35.415
Anodontia alba	R	FLMNH 2717	Hendry County, FL	Caloosahatchee	37.709	32.995
Anodontia alba	R	FLMNH 2717	Hendry County, FL	Caloosahatchee	35.384	29.57
Anodontia alba	R	FLMNH 2717	Hendry County, FL	Caloosahatchee	39.783	36.138
Anodontia alba	R	FLMNH 2717	Hendry County, FL	Caloosahatchee	28.91	25.705
Anodontia alba	R	FLMNH 2717	Hendry County, FL	Caloosahatchee	38.997	34.535
Anodontia alba	R	FLMNH 2717	Hendry County, FL	Caloosahatchee	36.672	33.027
Anodontia alba	R	FLMNH 2717	Hendry County, FL	Caloosahatchee	48.362	42.957
Anodontia alba	R	FLMNH 2717	Hendry County, FL	Caloosahatchee	27.779	24.731
Anodontia alba	R	FLMNH 2717	Hendry County, FL	Caloosahatchee	45.691	40.003
Anodontia alba	R	FLMNH 2717	Hendry County, FL	Caloosahatchee	28.847	25.202
Anodontia alba	R	FLMNH 2717	Hendry County, FL	Caloosahatchee	54.364	48.645
Anodontia alba	R	FLMNH 2717	Hendry County, FL	Caloosahatchee	47.293	44.34
Anodontia alba	R	FLMNH 147372	Sarasota County,FL	Caloosahatchee	51.001	46.099
Anodontia alba	R	FLMNH 147372	Sarasota County,FL	Caloosahatchee	49.242	45.471

Taxon Name	Valve	Museum #	Locality	Formation or Age	Width (mm)	Height (mm)
Anodontia alba	R	FLMNH 147372	Sarasota County,FL	Caloosahatchee	42.297	36.798
Anodontia alba	R	FLMNH 147372	Sarasota County,FL	Caloosahatchee	54.961	50.216
Anodontia alba	R	FLMNH 147372	Sarasota County,FL	Caloosahatchee	34.221	31.361
Anodontia alba	R	FLMNH 147372	Sarasota County,FL	Caloosahatchee	50.907	45.282
Anodontia alba	R	FLMNH 147372	Sarasota County,FL	Caloosahatchee	34.598	30.701
Anodontia alba	R	FLMNH 147372	Sarasota County,FL	Caloosahatchee	45.785	41.417
Anodontia alba	R	FLMNH 147372	Sarasota County,FL	Caloosahatchee	37.175	33.215
Anodontia alba	R	FLMNH 147372	Sarasota County,FL	Caloosahatchee	42.014	37.458
Anodontia alba	R	FLMNH 23968	Hendry County, FL	Caloosahatchee	42.014	37.615
Anodontia alba	R	FLMNH 23968	Hendry County, FL	Caloosahatchee	47.733	43.68
Anodontia alba	R	FLMNH 23968	Hendry County, FL	Caloosahatchee	44.999	42.266
Anodontia alba	R	FLMNH 23968	Hendry County, FL	Caloosahatchee	47.042	42.674
Anodontia alba	R	FLMNH 23968	Hendry County, FL	Caloosahatchee	47.513	43.585
Anodontia alba	R	FLMNH 23968	Hendry County, FL	Caloosahatchee	33.592	30.136
Anodontia alba	R	FLMNH 23968	Hendry County, FL	Caloosahatchee	34.755	31.393
Anodontia alba	R	FLMNH 23968	Hendry County, FL	Caloosahatchee	34.629	30.701
Anodontia alba	R	FLMNH 23968	Hendry County, FL	Caloosahatchee	38.84	35.195

Taxon Name	Valve	Museum #	Locality	Formation or Age	Width (mm)	Height (mm)
Anodontia alba	R	FLMNH 23968	Hendry County, FL	Caloosahatchee	56.469	51.253
Anodontia alba	R	FLMNH 23968	Hendry County, FL	Caloosahatchee	57.82	51.787
Anodontia alba	R	FLMNH 23968	Hendry County, FL	Caloosahatchee	52.635	48.11
Anodontia alba	R	FLMNH 23968	Hendry County, FL	Caloosahatchee	48.488	44.874
Anodontia alba	R	FLMNH 23968	Hendry County, FL	Caloosahatchee	54.395	50.31
Anodontia alba	R	FLMNH 23968	Hendry County, FL	Caloosahatchee	34.818	30.859
Anodontia alba	R	FLMNH 23968	Hendry County, FL	Caloosahatchee	36.798	33.278
Anodontia alba	R	FLMNH 23968	Hendry County, FL	Caloosahatchee	46.319	42.768
Anodontia alba	R	FLMNH 23968	Hendry County, FL	Caloosahatchee	35.132	31.613
Anodontia alba	R	FLMNH 23968	Hendry County, FL	Caloosahatchee	35.258	31.644
Anodontia alba	R	FLMNH 23968	Hendry County, FL	Caloosahatchee	53.358	48.236
Anodontia alba	R	FLMNH 23968	Hendry County, FL	Caloosahatchee	51.976	45.848
Anodontia alba	R	FLMNH 23968	Hendry County, FL	Caloosahatchee	49.87	46.005
Anodontia alba	R	FLMNH 23968	Hendry County, FL	Caloosahatchee	28.407	26.931
Anodontia alba	R	FLMNH 23968	Hendry County, FL	Caloosahatchee	41.794	38.369
Anodontia alba	R	FLMNH 23968	Hendry County, FL	Caloosahatchee	45.785	42.548
Anodontia alba	R	FLMNH 23968	Hendry County, FL	Caloosahatchee	49.147	45.879

Taxon Name	Valve	Museum #	Locality	Formation or Age	Width (mm)	Height (mm)
Anodontia alba	R	FLMNH 23968	Hendry County, FL	Caloosahatchee	40.38	36.452
Anodontia alba	R	FLMNH 23968	Hendry County, FL	Caloosahatchee	34.724	30.953
Anodontia alba	R	FLMNH 23968	Hendry County, FL	Caloosahatchee	43.428	38.557
Anodontia alba	R	FLMNH 23968	Hendry County, FL	Caloosahatchee	42.108	38.306
Anodontia alba	R	FLMNH 23968	Hendry County, FL	Caloosahatchee	37.332	32.618
Anodontia alba	R	FLMNH 23968	Hendry County, FL	Caloosahatchee	39.217	35.415
Anodontia alba	R	FLMNH 23968	Hendry County, FL	Caloosahatchee	35.446	32.43
Anodontia alba	R	FLMNH 23968	Hendry County, FL	Caloosahatchee	36.735	32.807
Anodontia alba	R	FLMNH 23968	Hendry County, FL	Caloosahatchee	43.46	38.212
Anodontia alba	R	FLMNH 23968	Hendry County, FL	Caloosahatchee	52.038	46.822
Anodontia alba	R	FLMNH 23968	Hendry County, FL	Caloosahatchee	29.822	25.862
Anodontia alba	R	FLMNH 23968	Hendry County, FL	Caloosahatchee	34.409	30.953
Anodontia alba	R	FLMNH 23968	Hendry County, FL	Caloosahatchee	33.31	29.507
Anodontia alba	R	FLMNH 23968	Hendry County, FL	Caloosahatchee	21.368	18.855
Anodontia schrammi	L	FLMNH 58593	Hendry County, FL	Caloosahatchee	87.226	77.974
Anodontia schrammi	L	FLMNH 58593	Hendry County, FL	Caloosahatchee	87.066	91.501
Anodontia schrammi	L	FLMNH 58593	Hendry County, FL	Caloosahatchee	81.898	73.252

Taxon Name	Valve	Museum #	Locality	Formation or Age	Width (mm)	Height (mm)
Anodontia schrammi	L	FLMNH 58593	Hendry County, FL	Caloosahatchee	74.081	70.093
Anodontia schrammi	R	FLMNH 85520	Charolette County, FL	Caloosahatchee	41.252	37.296
Anodontia schrammi	R	FLMNH 85520	Charolette County, FL	Caloosahatchee	46.867	42.209
Anodontia schrammi	R	FLMNH 58593	Hendry County, FL	Caloosahatchee	74.305	70.03
Anodontia schrammi	R	FLMNH 58593	Hendry County, FL	Caloosahatchee	87.162	78.357
Anodontia schrammi	R	FLMNH 58593	Hendry County, FL	Caloosahatchee	81.515	73.316
Anodontia alba	L	FLMNH 122528	LeonCounty, FL	Jackson Bluff	42.809	38.526
Anodontia alba	L	FLMNH 122528	LeonCounty, FL	Jackson Bluff	43.761	40.8
Anodontia alba	L	FLMNH 122528	LeonCounty, FL	Jackson Bluff	45.348	40.218
Anodontia alba	L	FLMNH 122526	LeonCounty, FL	Jackson Bluff	41.831	37.653
Anodontia alba	L	FLMNH 122526	LeonCounty, FL	Jackson Bluff	40.826	37.997
Anodontia alba	L	FLMNH 122526	LeonCounty, FL	Jackson Bluff	40.376	37.865
Anodontia alba	L	FLMNH 122526	LeonCounty, FL	Jackson Bluff	43.444	39.398
Anodontia alba	L	FLMNH 122526	LeonCounty, FL	Jackson Bluff	44.819	39.292
Anodontia alba	L	FLMNH 122526	LeonCounty, FL	Jackson Bluff	36.437	32.206
Anodontia alba	L	FLMNH 122527	LeonCounty, FL	Jackson Bluff	42.968	39.61
Anodontia alba	L	FLMNH 122527	LeonCounty, FL	Jackson Bluff	41.461	38.684

Taxon Name	Valve	Museum #	Locality	Formation or Age	Width (mm)	Height (mm)
Anodontia alba	L	FLMNH 122527	LeonCounty, FL	Jackson Bluff	43.312	40.112
Anodontia alba	L	FLMNH 122527	LeonCounty, FL	Jackson Bluff	45.612	41.011
Anodontia alba	L	FLMNH 122527	LeonCounty, FL	Jackson Bluff	41.646	37.071
Anodontia alba	L	FLMNH 122527	LeonCounty, FL	Jackson Bluff	42.307	38.578
Anodontia alba	R	FLMNH 122528	LeonCounty, FL	Jackson Bluff	45.215	41.619
Anodontia alba	R	FLMNH 122528	LeonCounty, FL	Jackson Bluff	42.624	38.367
Anodontia alba	R	FLMNH 122528	LeonCounty, FL	Jackson Bluff	43.444	39.663
Anodontia alba	R	FLMNH 122528	LeonCounty, FL	Jackson Bluff	42.386	38.605
Anodontia alba	R	FLMNH 122528	LeonCounty, FL	Jackson Bluff	38.922	35.22
Anodontia alba	R	FLMNH 122528	LeonCounty, FL	Jackson Bluff	42.016	37.203
Anodontia alba	R	FLMNH 122528	LeonCounty, FL	Jackson Bluff	43.206	39.689
Anodontia alba	R	FLMNH 122528	LeonCounty, FL	Jackson Bluff	38.843	34.744
Anodontia alba	R	FLMNH 122528	LeonCounty, FL	Jackson Bluff	35.749	31.254
Anodontia alba	R	FLMNH 122526	LeonCounty, FL	Jackson Bluff	47.41	45.215
Anodontia alba	R	FLMNH 122526	LeonCounty, FL	Jackson Bluff	48.097	43.206
Anodontia alba	R	FLMNH 122526	LeonCounty, FL	Jackson Bluff	39.266	35.617
Anodontia alba	R	FLMNH 122526	LeonCounty, FL	Jackson Bluff	42.915	38.658

Taxon Name	Valve	Museum #	Locality	Formation or Age	Width (mm)	Height (mm)
Anodontia alba	R	FLMNH 122526	LeonCounty, FL	Jackson Bluff	40.112	35.723
Anodontia alba	R	FLMNH 122526	LeonCounty, FL	Jackson Bluff	42.624	38.499
Anodontia alba	R	FLMNH 122526	LeonCounty, FL	Jackson Bluff	34.004	31.069
Anodontia alba	R	FLMNH 122527	LeonCounty, FL	Jackson Bluff	43.126	38.129
Anodontia alba	R	FLMNH 122527	LeonCounty, FL	Jackson Bluff	43.682	40.826
Anodontia alba	R	FLMNH 122527	LeonCounty, FL	Jackson Bluff	42.994	38.843
Anodontia alba	R	FLMNH 122527	LeonCounty, FL	Jackson Bluff	42.016	38.578
Anodontia alba	R	FLMNH 122527	LeonCounty, FL	Jackson Bluff	42.148	37.917
Anodontia alba	R	FLMNH 122527	LeonCounty, FL	Jackson Bluff	41.593	37.256
Anodontia alba	R	FLMNH 122527	LeonCounty, FL	Jackson Bluff	36.913	33.555
Anodontia schrammi	L	FLMNH 79903	LeonCounty, FL	Jackson Bluff	60.444	55.48
Anodontia schrammi	L	FLMNH 79903	LeonCounty, FL	Jackson Bluff	60.542	55.578
Anodontia schrammi	L	FLMNH 79903	LeonCounty, FL	Jackson Bluff	54.762	51.202
Anodontia schrammi	L	FLMNH 79903	LeonCounty, FL	Jackson Bluff	51.072	46.5
Anodontia schrammi	L	FLMNH 79903	LeonCounty, FL	Jackson Bluff	51.66	45.259
Anodontia schrammi	L	FLMNH 79903	LeonCounty, FL	Jackson Bluff	53.39	49.178
Anodontia schrammi	L	FLMNH 79903	LeonCounty, FL	Jackson Bluff	49.504	44.476

Taxon Name	Valve	Museum #	Locality	Formation or Age	Width (mm)	Height (mm)
Anodontia schrammi	L	FLMNH 79903	LeonCounty, FL	Jackson Bluff	45.586	40.328
Anodontia schrammi	L	FLMNH 79903	LeonCounty, FL	Jackson Bluff	44.541	40.688
Anodontia schrammi	L	FLMNH 79903	LeonCounty, FL	Jackson Bluff	51.692	46.631
Anodontia schrammi	L	FLMNH 79903	LeonCounty, FL	Jackson Bluff	58.321	54.631
Anodontia schrammi	L	FLMNH 79903	LeonCounty, FL	Jackson Bluff	49.57	45.096
Anodontia schrammi	L	FLMNH 79903	LeonCounty, FL	Jackson Bluff	60.085	54.37
Anodontia schrammi	L	FLMNH 79903	LeonCounty, FL	Jackson Bluff	52.084	47.055
Anodontia schrammi	L	FLMNH 79903	LeonCounty, FL	Jackson Bluff	56.395	50.125
Anodontia schrammi	L	FLMNH 79903	LeonCounty, FL	Jackson Bluff	53.586	50.06
Anodontia schrammi	R	FLMNH 79903	LeonCounty, FL	Jackson Bluff	51.986	49.276
Anodontia schrammi	R	FLMNH 79903	LeonCounty, FL	Jackson Bluff	47.643	43.986
Anodontia schrammi	R	FLMNH 79903	LeonCounty, FL	Jackson Bluff	44.41	40.786
Anodontia schrammi	R	FLMNH 79903	LeonCounty, FL	Jackson Bluff	46.827	43.757
Anodontia schrammi	R	FLMNH 79903	LeonCounty, FL	Jackson Bluff	51.692	46.304
Anodontia schrammi	R	FLMNH 79903	LeonCounty, FL	Jackson Bluff	47.055	42.418
Anodontia schrammi	R	FLMNH 79903	LeonCounty, FL	Jackson Bluff	49.276	45.357
Anodontia schrammi	R	FLMNH 79903	LeonCounty, FL	Jackson Bluff	53.325	49.08

Taxon Name	Valve	Museum #	Locality	Formation or Age	Width (mm)	Height (mm)
Anodontia schrammi	R	FLMNH 79903	LeonCounty, FL	Jackson Bluff	47.839	41.961
Anodontia schrammi	R	FLMNH 79903	LeonCounty, FL	Jackson Bluff	46.598	43.431
Anodontia schrammi	R	FLMNH 79903	LeonCounty, FL	Jackson Bluff	53.978	49.341
Anodontia schrammi	R	FLMNH 79903	LeonCounty, FL	Jackson Bluff	48.557	43.594
Anodontia schrammi	R	FLMNH 79903	LeonCounty, FL	Jackson Bluff	48.525	44.116
Anodontia schrammi	R	FLMNH 79903	LeonCounty, FL	Jackson Bluff	47.545	43.725
Anodontia schrammi	R	FLMNH 79903	LeonCounty, FL	Jackson Bluff	47.708	43.953
Anodontia schrammi	R	FLMNH 79903	LeonCounty, FL	Jackson Bluff	49.341	44.28
Anodontia schrammi	R	FLMNH 79903	LeonCounty, FL	Jackson Bluff	46.239	43.006
Anodontia schrammi	R	FLMNH 79903	LeonCounty, FL	Jackson Bluff	48.133	43.92
Anodontia schrammi	R	FLMNH 79903	LeonCounty, FL	Jackson Bluff	45.684	42.32
Anodontia schrammi	R	FLMNH 79903	LeonCounty, FL	Jackson Bluff	41.471	36.377
Anodontia alba	L	FLMNH 144279	Sarasota County, FL	Tamiami	39.663	34.665
Anodontia alba	L	FLMNH 135372	Highlands County, FL	Tamiami	40.165	38.367
Anodontia alba	L	FLMNH 135372	Highlands County, FL	Tamiami	43.47	41.038
Anodontia alba	L	FLMNH 135373	Highlands County, FL	Tamiami	44.819	41.566
Anodontia alba	L	FLMNH 135373	Highlands County, FL	Tamiami	40.694	38.235

Taxon Name	Valve	Museum #	Locality	Formation or Age	Width (mm)	Height (mm)
Anodontia alba	L	FLMNH 135373	Highlands County, FL	Tamiami	51.588	47.859
Anodontia alba	L	FLMNH 135373	Highlands County, FL	Tamiami	47.754	43.179
Anodontia alba	L	FLMNH 135373	Highlands County, FL	Tamiami	45.665	41.963
Anodontia alba	L	FLMNH 135373	Highlands County, FL	Tamiami	45.665	41.91
Anodontia alba	L	FLMNH 135373	Highlands County, FL	Tamiami	49.314	45.083
Anodontia alba	R	FLMNH 144279	Sarasota County, FL	Tamiami	35.3	33.026
Anodontia alba	R	FLMNH 144279	Sarasota County, FL	Tamiami	29.535	25.966
Anodontia alba	R	FLMNH 227196	Sarasota County, FL	Tamiami	33.713	30.699
Anodontia alba	R	FLMNH 227196	Sarasota County, FL	Tamiami	28.24	25.331
Anodontia alba	R	FLMNH 227196	Sarasota County, FL	Tamiami	33.475	30.805
Anodontia alba	R	FLMNH 227196	Sarasota County, FL	Tamiami	28.16	25.41
Anodontia alba	R	FLMNH 135372	Highlands County, FL	Tamiami	43.602	41.461
Anodontia alba	R	FLMNH 135373	Highlands County, FL	Tamiami	51.429	47.939
Anodontia alba	R	FLMNH 135373	Highlands County, FL	Tamiami	39.901	37.997
Anodontia alba	R	FLMNH 135373	Highlands County, FL	Tamiami	44.184	41.381
Anodontia alba	R	FLMNH 135373	Highlands County, FL	Tamiami	43.444	40.614
Anodontia alba	R	FLMNH 135373	Highlands County, FL	Tamiami	44.792	41.778

Taxon Name	Valve	Museum #	Locality	Formation or Age	Width (mm)	Height (mm)
Anodontia alba	R	FLMNH 135373	Highlands County, FL	Tamiami	44.819	41.725
Anodontia alba	R	FLMNH 135373	Highlands County, FL	Tamiami	47.569	43.417
Anodontia alba	R	FLMNH 135373	Highlands County, FL	Tamiami	45.797	41.778
Anodontia alba	R	FLMNH 135373	Highlands County, FL	Tamiami	54.364	48.917
Anodontia alba	R	FLMNH 135373	Highlands County, FL	Tamiami	46.299	42.518
Anodontia alba	R	FLMNH 135373	Highlands County, FL	Tamiami	50.133	44.607
Anodontia santarosana	L	FLMNH 89641	Walton County, FL	Shoal River	33.74	28.874
Anodontia santarosana	L	FLMNH 89641	Walton County, FL	Shoal River	35.009	30.091
Anodontia santarosana	L	FLMNH 89641	Walton County, FL	Shoal River	23.903	20.968
Anodontia santarosana	L	FLMNH 89641	Walton County, FL	Shoal River	21.867	18.721
Anodontia santarosana	L	FLMNH 89641	Walton County, FL	Shoal River	20.915	18.086
Anodontia santarosana	L	FLMNH 89641	Walton County, FL	Shoal River	14.596	12.718
Anodontia santarosana	L	FLMNH 89641	Walton County, FL	Shoal River	30.619	27.526
Anodontia santarosana	L	FLMNH 89641	Walton County, FL	Shoal River	31.228	28.002
Anodontia santarosana	L	FLMNH 89641	Walton County, FL	Shoal River	31.043	27.341
Anodontia santarosana	L	FLMNH 89641	Walton County, FL	Shoal River	28.848	24.379
Anodontia santarosana	L	FLMNH 89641	Walton County, FL	Shoal River	21.841	18.694

Taxon Name	Valve	Museum #	Locality	Formation or Age	Width (mm)	Height (mm)
Anodontia santarosana	L	FLMNH 89641	Walton County, FL	Shoal River	15.045	13.432
Anodontia santarosana	L	FLMNH 89641	Walton County, FL	Shoal River	12.771	10.973
Anodontia santarosana	L	FLMNH 89641	Walton County, FL	Shoal River	11.449	10.339
Anodontia santarosana	L	FLMNH 89641	Walton County, FL	Shoal River	11.449	9.916
Anodontia santarosana	L	FLMNH 76040	Walton County, FL	Shoal River	26.68	24.062
Anodontia santarosana	L	FLMNH 76040	Walton County, FL	Shoal River	26.627	23.903
Anodontia santarosana	L	FLMNH 76040	Walton County, FL	Shoal River	25.834	23.057
Anodontia santarosana	L	FLMNH 76040	Walton County, FL	Shoal River	25.886	23.11
Anodontia santarosana	L	FLMNH 76040	Walton County, FL	Shoal River	32.999	28.795
Anodontia santarosana	L	FLMNH 76040	Walton County, FL	Shoal River	32.18	29.588
Anodontia santarosana	L	FLMNH 76040	Walton County, FL	Shoal River	31.069	27.87
Anodontia santarosana	L	FLMNH 76040	Walton County, FL	Shoal River	20.334	17.901
Anodontia santarosana	L	FLMNH 76040	Walton County, FL	Shoal River	20.677	18.007
Anodontia santarosana	L	FLMNH 76040	Walton County, FL	Shoal River	18.853	16.367
Anodontia santarosana	L	FLMNH 76040	Walton County, FL	Shoal River	23.586	21.18
Anodontia santarosana	L	FLMNH 76040	Walton County, FL	Shoal River	20.625	17.557
Anodontia santarosana	L	FLMNH 76040	Walton County, FL	Shoal River	15.151	13.538

Taxon Name	Valve	Museum #	Locality	Formation or Age	Width (mm)	Height (mm)
Anodontia santarosana	L	FLMNH 45771	Walton County, FL	Shoal River	25.49	22.766
Anodontia santarosana	L	FLMNH 45771	Walton County, FL	Shoal River	25.331	22.555
Anodontia santarosana	L	FLMNH 45645	Walton County, FL	Shoal River	23.454	19.593
Anodontia santarosana	L	FLMNH 45645	Walton County, FL	Shoal River	29.906	25.966
Anodontia santarosana	L	FLMNH 45645	Walton County, FL	Shoal River	25.41	21.656
Anodontia santarosana	L	FLMNH 45645	Walton County, FL	Shoal River	24.617	22.423
Anodontia santarosana	L	FLMNH 45645	Walton County, FL	Shoal River	20.651	17.531
Anodontia santarosana	L	FLMNH 45645	Walton County, FL	Shoal River	16.526	14.358
Anodontia santarosana	L	FLMNH 45645	Walton County, FL	Shoal River	17.372	14.754
Anodontia santarosana	L	FLMNH 45648	Walton County, FL	Shoal River	29.8	26.072
Anodontia santarosana	L	FLMNH 45648	Walton County, FL	Shoal River	19.382	16.843
Anodontia santarosana	L	FLMNH 45648	Walton County, FL	Shoal River	17.848	15.627
Anodontia santarosana	L	FLMNH 45648	Walton County, FL	Shoal River	22.026	19.54
Anodontia santarosana	L	FLMNH 45648	Walton County, FL	Shoal River	24.723	21.471
Anodontia santarosana	L	FLMNH 45648	Walton County, FL	Shoal River	16.738	14.464
Anodontia santarosana	L	FLMNH 45648	Walton County, FL	Shoal River	11.661	9.995
Anodontia santarosana	L	FLMNH 45648	Walton County, FL	Shoal River	12.057	10.497

Taxon Name	Valve	Museum #	Locality	Formation or Age	Width (mm)	Height (mm)
Anodontia santarosana	L	FLMNH 46049	Walton County, FL	Shoal River	14.146	12.11
Anodontia santarosana	L	FLMNH 67172	Walton County, FL	Shoal River	11.396	9.731
Anodontia santarosana	L	FLMNH 46038	Walton County, FL	Shoal River	35.009	31.201
Anodontia santarosana	L	FLMNH 46038	Walton County, FL	Shoal River	35.035	31.148
Anodontia santarosana	L	FLMNH 45630	Walton County, FL	Shoal River	21.206	19.012
Anodontia santarosana	R	FLMNH 89641	Walton County, FL	Shoal River	34.982	32.1
Anodontia santarosana	R	FLMNH 89641	Walton County, FL	Shoal River	31.809	29.615
Anodontia santarosana	R	FLMNH 89641	Walton County, FL	Shoal River	25.278	22.211
Anodontia santarosana	R	FLMNH 89641	Walton County, FL	Shoal River	21.894	18.536
Anodontia santarosana	R	FLMNH 89641	Walton County, FL	Shoal River	20.757	18.139
Anodontia santarosana	R	FLMNH 89641	Walton County, FL	Shoal River	17.875	15.706
Anodontia santarosana	R	FLMNH 89641	Walton County, FL	Shoal River	18.007	15.733
Anodontia santarosana	R	FLMNH 89641	Walton County, FL	Shoal River	18.747	16.473
Anodontia santarosana	R	FLMNH 89641	Walton County, FL	Shoal River	15.759	13.565
Anodontia santarosana	R	FLMNH 89641	Walton County, FL	Shoal River	25.278	22.211
Anodontia santarosana	R	FLMNH 76040	Walton County, FL	Shoal River	20.387	18.086
Anodontia santarosana	R	FLMNH 76040	Walton County, FL	Shoal River	20.545	17.69

Taxon Name	Valve	Museum #	Locality	Formation or Age	Width (mm)	Height (mm)
Anodontia santarosana	R	FLMNH 76040	Walton County, FL	Shoal River	22.079	19.567
Anodontia santarosana	R	FLMNH 76040	Walton County, FL	Shoal River	28.689	26.468
Anodontia santarosana	R	FLMNH 76040	Walton County, FL	Shoal River	22.581	20.281
Anodontia santarosana	R	FLMNH 76040	Walton County, FL	Shoal River	28.901	25.252
Anodontia santarosana	R	FLMNH 76040	Walton County, FL	Shoal River	20.545	16.288
Anodontia santarosana	R	FLMNH 76040	Walton County, FL	Shoal River	23.454	20.889
Anodontia santarosana	R	FLMNH 76040	Walton County, FL	Shoal River	32.761	28.874
Anodontia santarosana	R	FLMNH 76040	Walton County, FL	Shoal River	29.879	25.886
Anodontia santarosana	R	FLMNH 76040	Walton County, FL	Shoal River	21.92	19.382
Anodontia santarosana	R	FLMNH 76040	Walton County, FL	Shoal River	12.401	10.868
Anodontia santarosana	R	FLMNH 76040	Walton County, FL	Shoal River	14.331	12.533
Anodontia santarosana	R	FLMNH 45771	Walton County, FL	Shoal River	22.661	19.937
Anodontia santarosana	R	FLMNH 45645	Walton County, FL	Shoal River	23.454	19.831
Anodontia santarosana	R	FLMNH 45645	Walton County, FL	Shoal River	24.697	21.524
Anodontia santarosana	R	FLMNH 45645	Walton County, FL	Shoal River	17.134	14.728
Anodontia santarosana	R	FLMNH 45645	Walton County, FL	Shoal River	21.497	18.509
Anodontia santarosana	R	FLMNH 45648	Walton County, FL	Shoal River	25.701	23.031

Taxon Name	Valve	Museum #	Locality	Formation or Age	Width (mm)	Height (mm)
Anodontia santarosana	R	FLMNH 45648	Walton County, FL	Shoal River	16.817	14.464
Anodontia santarosana	R	FLMNH 45648	Walton County, FL	Shoal River	19.144	17.478
Anodontia santarosana	R	FLMNH 45648	Walton County, FL	Shoal River	24.644	21.444
Anodontia santarosana	R	FLMNH 45648	Walton County, FL	Shoal River	17.584	15.548
Anodontia santarosana	R	FLMNH 46049	Walton County, FL	Shoal River	30.593	27.05
Anodontia santarosana	R	FLMNH 46049	Walton County, FL	Shoal River	14.12	12.137
Anodontia santarosana	R	FLMNH 67172	Walton County, FL	Shoal River	12.031	10.312
Anodontia santarosana	R	FLMNH 67172	Walton County, FL	Shoal River	11.476	9.81
Anodontia santarosana	R	FLMNH 45630	Walton County, FL	Shoal River	34.454	30.434
Anodontia santarosana	R	FLMNH 45630	Walton County, FL	Shoal River	31.756	27.235
Anodontia santarosana	R	FLMNH 45630	Walton County, FL	Shoal River	32.576	27.42
Anodontia santarosana	R	FLMNH 45745	Walton County, FL	Shoal River	22.74	20.043
Anodontia santarosana	L	FLMNH 73294	Okaloosa County,FL	Oak Grove	39.717	35.106
Anodontia santarosana	L	FLMNH 73294	Okaloosa County,FL	Oak Grove	38.689	34.412
Anodontia santarosana	L	FLMNH 73294	Okaloosa County,FL	Oak Grove	27.524	24.33
Anodontia santarosana	L	FLMNH 73294	Okaloosa County,FL	Oak Grove	28.496	25.135
Anodontia santarosana	L	FLMNH 73294	Okaloosa County,FL	Oak Grove	19.914	17.164

Taxon Name	Valve	Museum #	Locality	Formation or Age	Width (mm)	Height (mm)
Anodontia santarosana	L	FLMNH 73294	Okaloosa County,FL	Oak Grove	23.025	20.636
Anodontia santarosana	L	FLMNH 73294	Okaloosa County,FL	Oak Grove	32.051	29.468
Anodontia santarosana	L	FLMNH 73294	Okaloosa County,FL	Oak Grove	25.858	22.913
Anodontia santarosana	L	FLMNH 73294	Okaloosa County,FL	Oak Grove	22.136	19.497
Anodontia santarosana	L	FLMNH 73294	Okaloosa County,FL	Oak Grove	16.581	14.331
Anodontia santarosana	L	FLMNH 73294	Okaloosa County,FL	Oak Grove	12.165	10.276
Anodontia santarosana	L	FLMNH 73294	Okaloosa County,FL	Oak Grove	12.109	10.332
Anodontia santarosana	R	FLMNH 73294	Okaloosa County,FL	Oak Grove	35.828	33.079
Anodontia santarosana	R	FLMNH 73294	Okaloosa County,FL	Oak Grove	39.467	35.301
Anodontia santarosana	R	FLMNH 73294	Okaloosa County,FL	Oak Grove	29.19	25.691
Anodontia santarosana	R	FLMNH 73294	Okaloosa County,FL	Oak Grove	28.94	25.135
Anodontia santarosana	R	FLMNH 73294	Okaloosa County,FL	Oak Grove	17.137	14.192
Anodontia janus	L	FNHM 89514	Cahloun County, FL	Chipola	35.995	31.356
Anodontia janus	L	FNHM 89514	Cahloun County, FL	Chipola	37.25	33.457
Anodontia janus	L	FNHM 89514	Cahloun County, FL	Chipola	30.946	26.389
Anodontia janus	L	FNHM 89514	Cahloun County, FL	Chipola	30.264	26.225
Anodontia janus	L	FNHM 89514	Cahloun County, FL	Chipola	29.118	26.171

Taxon Name	Valve	Museum #	Locality	Formation or Age	Width (mm)	Height (mm)
Anodontia janus	L	FNHM 89514	Cahloun County, FL	Chipola	22.459	20.303
Anodontia janus	L	FNHM 89514	Cahloun County, FL	Chipola	22.705	20.412
Anodontia janus	L	FNHM 89514	Cahloun County, FL	Chipola	28.19	25.734
Anodontia janus	L	FNHM 89514	Cahloun County, FL	Chipola	22.787	19.949
Anodontia janus	L	FNHM 89514	Cahloun County, FL	Chipola	29.582	26.662
Anodontia janus	L	FNHM 89514	Cahloun County, FL	Chipola	25.325	22.65
Anodontia janus	L	FNHM 89514	Cahloun County, FL	Chipola	24.779	21.995
Anodontia janus	L	FNHM 89514	Cahloun County, FL	Chipola	29.691	26.744
Anodontia janus	L	FNHM 89514	Cahloun County, FL	Chipola	29.827	26.634
Anodontia janus	L	FNHM 89514	Cahloun County, FL	Chipola	31.001	27.781
Anodontia janus	L	FNHM 89514	Cahloun County, FL	Chipola	27.071	24.042
Anodontia janus	L	FNHM 89514	Cahloun County, FL	Chipola	13.89	12.389
Anodontia janus	L	FNHM 89514	Cahloun County, FL	Chipola	26.716	23.387
Anodontia janus	L	FNHM 89514	Cahloun County, FL	Chipola	26.771	23.523
Anodontia janus	L	FNHM 89514	Cahloun County, FL	Chipola	27.371	25.052
Anodontia janus	L	FNHM 89514	Cahloun County, FL	Chipola	15.064	12.881
Anodontia janus	L	FNHM 89514	Cahloun County, FL	Chipola	16.183	14.955

Taxon Name	Valve	Museum #	Locality	Formation or Age	Width (mm)	Height (mm)
Anodontia janus	L	FNHM 89514	Cahloun County, FL	Chipola	15.118	12.799
Anodontia janus	L	FNHM 89514	Cahloun County, FL	Chipola	25.079	21.013
Anodontia janus	L	FNHM 89514	Cahloun County, FL	Chipola	16.674	14.218
Anodontia janus	L	FNHM 89514	Cahloun County, FL	Chipola	12.417	10.588
Anodontia janus	L	FNHM 89514	Cahloun County, FL	Chipola	13.481	11.844
Anodontia janus	L	FNHM 89514	Cahloun County, FL	Chipola	14.845	13.044
Anodontia janus	L	FNHM 89514	Cahloun County, FL	Chipola	15.992	13.89
Anodontia janus	L	FNHM 89514	Cahloun County, FL	Chipola	13.235	11.434
Anodontia janus	L	FNHM 89514	Cahloun County, FL	Chipola	12.962	11.161
Anodontia janus	L	FNHM 89514	Cahloun County, FL	Chipola	10.888	9.142
Anodontia janus	L	FNHM 89514	Cahloun County, FL	Chipola	29.527	26.525
Anodontia janus	R	FNHM 89514	Cahloun County, FL	Chipola	29.391	26.471
Anodontia janus	R	FNHM 89514	Cahloun County, FL	Chipola	30.482	26.334
Anodontia janus	R	FNHM 89514	Cahloun County, FL	Chipola	33.102	29.773
Anodontia janus	R	FNHM 89514	Cahloun County, FL	Chipola	29.991	26.498
Anodontia janus	R	FNHM 89514	Cahloun County, FL	Chipola	24.861	21.095
Anodontia janus	R	FNHM 89514	Cahloun County, FL	Chipola	29.745	26.798

Taxon Name	Valve	Museum #	Locality	Formation or Age	Width (mm)	Height (mm)
Anodontia janus	R	FNHM 89514	Cahloun County, FL	Chipola	29.418	26.498
Anodontia janus	R	FNHM 89514	Cahloun County, FL	Chipola	22.759	19.485
Anodontia janus	R	FNHM 89514	Cahloun County, FL	Chipola	29.554	26.143
Anodontia janus	R	FNHM 89514	Cahloun County, FL	Chipola	27.944	24.315
Anodontia janus	R	FNHM 89514	Cahloun County, FL	Chipola	28.245	25.57
Anodontia janus	R	FNHM 89514	Cahloun County, FL	Chipola	25.652	22.596
Anodontia janus	R	FNHM 89514	Cahloun County, FL	Chipola	21.368	18.557
Anodontia janus	R	FNHM 89514	Cahloun County, FL	Chipola	13.481	11.789
Anodontia janus	R	FNHM 89514	Cahloun County, FL	Chipola	13.044	11.325
Anodontia janus	R	FNHM 89514	Cahloun County, FL	Chipola	9.278	7.75
Anodontia janus	R	FNHM 89514	Cahloun County, FL	Chipola	11.653	10.152
Anodontia janus	R	FNHM 89514	Cahloun County, FL	Chipola	9.797	8.487
Anodontia janus	R	FNHM 89514	Cahloun County, FL	Chipola	9.879	8.542
Anodontia santarosana	L	FNHM 43938	Cahloun County, FL	Chipola	29.282	26.471
Anodontia santarosana	L	FNHM 41513	Cahloun County, FL	Chipola	25.215	21.968
Anodontia santarosana	L	FNHM 42687	Cahloun County, FL	Chipola	28.954	25.707
Anodontia santarosana	L	FNHM 67452	Cahloun County, FL	Chipola	29.745	25.707

Taxon Name	Valve	Museum #	Locality	Formation or Age	Width (mm)	Height (mm)
Anodontia santarosana	L	FNHM 67406	Cahloun County, FL	Chipola	23.633	20.74
Anodontia santarosana	L	FNHM 67406	Cahloun County, FL	Chipola	15.091	13.699
Anodontia santarosana	L	FNHM 38104	Cahloun County, FL	Chipola	17.984	14.982
Anodontia santarosana	L	FNHM 69689	Cahloun County, FL	Chipola	19.676	17.056
Anodontia santarosana	L	FNHM 69689	Cahloun County, FL	Chipola	15.064	12.826
Anodontia santarosana	L	FNHM 69689	Cahloun County, FL	Chipola	10.834	9.251
Anodontia santarosana	L	FNHM 43519	Cahloun County, FL	Chipola	33.702	30.128
Anodontia santarosana	L	FNHM 43519	Cahloun County, FL	Chipola	33.975	30.619
Anodontia santarosana	L	FNHM 202510	Cahloun County, FL	Chipola	28.736	24.97
Anodontia santarosana	L	FNHM 73204	Cahloun County, FL	Chipola	14.764	13.454
Anodontia santarosana	L	FNHM 35748	Cahloun County, FL	Chipola	21.368	18.557
Anodontia santarosana	L	FNHM 3082	Cahloun County, FL	Chipola	14.709	12.853
Anodontia santarosana	L	FNHM 3082	Cahloun County, FL	Chipola	15.664	13.536
Anodontia santarosana	R	FNHM 42687	Cahloun County, FL	Chipola	28.927	25.707
Anodontia santarosana	R	FNHM 67452	Cahloun County, FL	Chipola	29.473	25.843
Anodontia santarosana	R	FNHM 48831	Cahloun County, FL	Chipola	26.907	24.015
Anodontia santarosana	R	FNHM 4167	Cahloun County, FL	Chipola	15.446	13.563

Taxon Name	Valve	Museum #	Locality	Formation or Age	Width (mm)	Height (mm)
Anodontia santarosana	R	FNHM 4167	Cahloun County, FL	Chipola	18.393	16.565
Anodontia santarosana	R	FNHM 4167	Cahloun County, FL	Chipola	21.067	18.502
Anodontia santarosana	R	FNHM 4167	Cahloun County, FL	Chipola	11.216	9.633
Anodontia santarosana	R	FNHM 38104	Cahloun County, FL	Chipola	8.896	7.641
Anodontia santarosana	R	FNHM 69689	Cahloun County, FL	Chipola	17.82	15.337
Anodontia santarosana	R	FNHM 69689	Cahloun County, FL	Chipola	19.594	17.383
Anodontia santarosana	R	FNHM 69689	Cahloun County, FL	Chipola	17.11	14.6
Anodontia santarosana	R	FNHM 69689	Cahloun County, FL	Chipola	10.861	9.469
Anodontia santarosana	R	FNHM 45095	Cahloun County, FL	Chipola	14.654	12.28
Anodontia santarosana	R	FNHM 45095	Cahloun County, FL	Chipola	14.627	11.734
Anodontia santarosana	R	FNHM 43519	Cahloun County, FL	Chipola	17.574	14.709
Anodontia santarosana	R	FNHM 43519	Cahloun County, FL	Chipola	29.8	26.716
Anodontia santarosana	R	FNHM 43519	Cahloun County, FL	Chipola	29.909	26.58
Anodontia santarosana	R	FNHM 73204	Cahloun County, FL	Chipola	14.873	12.717
Anodontia santarosana	R	FNHM 35783	Cahloun County, FL	Chipola	22.405	19.457
Anodontia santarosana	R	FNHM 35748	Cahloun County, FL	Chipola	21.067	18.338
Anodontia santarosana	R	FNHM 67727	Cahloun County, FL	Chipola	36.295	32.42

Taxon Name	Valve	Museum #	Locality	Formation or Age	Width (mm)	Height (mm)
Anodontia janus	L	FNHM 97409	Cahloun County, FL	Chipola	26.826	24.479
Anodontia janus	L	FNHM 97409	Cahloun County, FL	Chipola	26.061	23.442
Anodontia janus	L	FNHM 97409	Cahloun County, FL	Chipola	26.826	24.451
Anodontia janus	L	FNHM 97409	Cahloun County, FL	Chipola	25.516	23.196
Anodontia janus	L	FNHM 97409	Cahloun County, FL	Chipola	29.5	27.017
Anodontia janus	L	FNHM 97409	Cahloun County, FL	Chipola	28.49	25.27
Anodontia janus	L	FNHM 97409	Cahloun County, FL	Chipola	26.307	23.633
Anodontia janus	L	FNHM 97409	Cahloun County, FL	Chipola	20.522	18.502
Anodontia janus	L	FNHM 97409	Cahloun County, FL	Chipola	21.067	18.475
Anodontia janus	L	FNHM 97409	Cahloun County, FL	Chipola	26.907	24.097
Anodontia janus	L	FNHM 97409	Cahloun County, FL	Chipola	24.124	21.722
Anodontia janus	L	FNHM 97409	Cahloun County, FL	Chipola	29.936	26.88
Anodontia janus	L	FNHM 97409	Cahloun County, FL	Chipola	29.282	26.143
Anodontia janus	L	FNHM 97409	Cahloun County, FL	Chipola	28.736	25.243
Anodontia janus	L	FNHM 97409	Cahloun County, FL	Chipola	26.089	23.578
Anodontia janus	L	FNHM 97409	Cahloun County, FL	Chipola	26.935	24.697
Anodontia janus	L	FNHM 97409	Cahloun County, FL	Chipola	22.432	19.894

Taxon Name	Valve	Museum #	Locality	Formation or Age	Width (mm)	Height (mm)
Anodontia janus	L	FNHM 97409	Cahloun County, FL	Chipola	23.906	21.886
Anodontia janus	L	FNHM 97409	Cahloun County, FL	Chipola	18.366	15.828
Anodontia janus	L	FNHM 97409	Cahloun County, FL	Chipola	17.411	15.773
Anodontia janus	L	FNHM 97409	Cahloun County, FL	Chipola	13.727	12.062
Anodontia janus	L	FNHM 97409	Cahloun County, FL	Chipola	13.399	11.543
Anodontia janus	L	FNHM 97409	Cahloun County, FL	Chipola	23.032	21.149
Anodontia janus	L	FNHM 97409	Cahloun County, FL	Chipola	21.886	19.703
Anodontia janus	L	FNHM 97409	Cahloun County, FL	Chipola	21.04	18.311
Anodontia janus	L	FNHM 97409	Cahloun County, FL	Chipola	25.816	23.087
Anodontia janus	L	FNHM 97409	Cahloun County, FL	Chipola	15.419	13.29
Anodontia janus	L	FNHM 97409	Cahloun County, FL	Chipola	18.775	16.701
Anodontia janus	L	FNHM 97409	Cahloun County, FL	Chipola	14.736	12.826
Anodontia janus	L	FNHM 97409	Cahloun County, FL	Chipola	13.781	11.871
Anodontia janus	L	FNHM 97409	Cahloun County, FL	Chipola	9.497	8.214
Anodontia janus	L	FNHM 97409	Cahloun County, FL	Chipola	8.896	7.75
Anodontia janus	L	FNHM 97409	Cahloun County, FL	Chipola	10.425	8.869
Anodontia janus	L	FNHM 104135	Cahloun County, FL	Chipola	24.806	21.559

Taxon Name	Valve	Museum #	Locality	Formation or Age	Width (mm)	Height (mm)
Anodontia janus	L	FNHM 104135	Cahloun County, FL	Chipola	19.294	17.11
Anodontia janus	L	FNHM 97588	Cahloun County, FL	Chipola	13.836	12.117
Anodontia janus	L	FLMNH 97505	Cahloun County, FL	Chipola	25.597	22.459
Anodontia janus	L	FLMNH 114127	Cahloun County, FL	Chipola	19.676	17.165
Anodontia janus	L	FLMNH 72985	Cahloun County, FL	Chipola	15.691	14.109
Anodontia janus	L	FLMNH 69683	Cahloun County, FL	Chipola	20.249	17.956
Anodontia janus	R	FNHM 97409	Cahloun County, FL	Chipola	32.584	30.264
Anodontia janus	R	FNHM 97409	Cahloun County, FL	Chipola	29.445	26.061
Anodontia janus	R	FNHM 97409	Cahloun County, FL	Chipola	29.5	26.116
Anodontia janus	R	FNHM 97409	Cahloun County, FL	Chipola	26.962	23.824
Anodontia janus	R	FNHM 97409	Cahloun County, FL	Chipola	21.995	19.785
Anodontia janus	R	FNHM 97409	Cahloun County, FL	Chipola	22.568	19.567
Anodontia janus	R	FNHM 97409	Cahloun County, FL	Chipola	20.986	18.12
Anodontia janus	R	FNHM 97409	Cahloun County, FL	Chipola	21.067	18.42
Anodontia janus	R	FNHM 97409	Cahloun County, FL	Chipola	13.918	11.953
Anodontia janus	R	FNHM 97409	Cahloun County, FL	Chipola	19.184	16.947
Anodontia janus	R	FNHM 97409	Cahloun County, FL	Chipola	29.664	26.198

Taxon Name	Valve	Museum #	Locality	Formation or Age	Width (mm)	Height (mm)
Anodontia janus	R	FNHM 97409	Cahloun County, FL	Chipola	26.662	23.605
Anodontia janus	R	FNHM 97409	Cahloun County, FL	Chipola	19.048	16.128
Anodontia janus	R	FNHM 97409	Cahloun County, FL	Chipola	15.337	13.399
Anodontia janus	R	FNHM 97409	Cahloun County, FL	Chipola	17.875	15.828
Anodontia janus	R	FNHM 97409	Cahloun County, FL	Chipola	13.563	11.462
Anodontia janus	R	FNHM 97409	Cahloun County, FL	Chipola	13.208	11.571
Anodontia janus	R	FNHM 97409	Cahloun County, FL	Chipola	17.274	14.927
Anodontia janus	R	FNHM 97409	Cahloun County, FL	Chipola	22.787	20.276
Anodontia janus	R	FNHM 97409	Cahloun County, FL	Chipola	26.607	23.223
Anodontia janus	R	FNHM 97409	Cahloun County, FL	Chipola	26.007	23.196
Anodontia janus	R	FNHM 97409	Cahloun County, FL	Chipola	14.9	13.126
Anodontia janus	R	FNHM 97409	Cahloun County, FL	Chipola	23.332	21.204
Anodontia janus	R	FNHM 97409	Cahloun County, FL	Chipola	20.194	17.574
Anodontia janus	R	FNHM 97409	Cahloun County, FL	Chipola	20.167	17.574
Anodontia janus	R	FNHM 97409	Cahloun County, FL	Chipola	19.839	17.411
Anodontia janus	R	FNHM 97409	Cahloun County, FL	Chipola	15.555	14.054
Anodontia janus	R	FNHM 97409	Cahloun County, FL	Chipola	13.072	10.861

Taxon Name	Valve	Museum #	Locality	Formation or Age	Width (mm)	Height (mm)
Anodontia janus	R	FNHM 97409	Cahloun County, FL	Chipola	9.524	8.241
Anodontia janus	R	FNHM 97409	Cahloun County, FL	Chipola	12.553	10.752
Anodontia janus	R	FNHM 97829	Cahloun County, FL	Chipola	28.49	25.57
Anodontia janus	R	FNHM 104135	Cahloun County, FL	Chipola	28.654	25.106
Anodontia janus	R	FNHM 104135	Cahloun County, FL	Chipola	24.479	21.395
Anodontia janus	R	FNHM 104135	Cahloun County, FL	Chipola	19.457	17.465
Anodontia janus	R	FNHM 97588	Cahloun County, FL	Chipola	24.233	21.258
Anodontia janus	R	FLMNH 119995	Cahloun County, FL	Chipola	15.664	13.508
Anodontia janus	R	FLMNH 72985	Cahloun County, FL	Chipola	19.785	17.247
Anodontia janus	R	FLMNH 72985	Cahloun County, FL	Chipola	14.955	13.126
Anodontia janus	R	FLMNH 69683	Cahloun County, FL	Chipola	20.249	18.202

APPENDIX D:

TAXON-CHARACTER MATRIX TNT EXECUTABLE FILE FORMAT FOR WESTERN INTERIOR *BACULITES*

nstates cont;
xread
'Character matrix for TNT analysis of Western Interior Baculites. The following text should be copied and pasted into a text editor without line breaks within the character arrays. Then save the text file to your home directory with a new file name such as "Baculites.txt". Open TNT and type "procedure Baculites.txt" to execute the phylogenetic analysis.'
55 25
&[continuous]
Sciponoceras_gracile 0.419 0.921 0.254 ? 0.547 0.731 0.749 0.370 0.403 0.616 0.411 0.913 0.690 0.605 4.500 4.500 4.500 ? ? ? 0.893 0.051 2.899 0.055 3.173 0.996 0.982 4.300 ? 1.167 ?
Baculites_obtusus 0.411 0.273 0.324 0.173 0.335 0.396 0.953 0.254 0.300 0.428 0.749 ? 0.424 0.197 2.500 1.800 4.000 0.830 0.336 0.735 0.709 0.020 1.160 0.102 5.822 1.022 1.011 5.000 ? ? ?
Baculites_mclearni 0.647 0.572 0.497 0.224 0.535 0.430 ? 0.328 0.352 0.435 0.699 ? 0.504 0.459 2.000 1.300 4.000 1.355 ? 0.747 0.713 0.027 1.560 0.035 2.013 0.988 ? 5.500 0.373 0.828 ?
Baculites_asperiformis 0.373 0.517 0.369 0.287 0.349 0.271 0.754 0.351 0.509 0.378 0.564 0.615 0.653 0.404 1.000 1.200 5.000 1.765 ? 0.691 0.712 0.034 1.924 0.052 2.991 1.036 1.023 5.500 0.171 1.419 ?
Baculites_sp_smooth 0.371 0.768 0.490 0.235 0.380 0.271 0.701 0.354 0.357 0.219 0.510 0.760 0.417 0.400 ? ? ? ? ? ? 0.639 0.033 1.878 ? 2.300 0.985 ? 6.500 ? ? ?
Baculites_perplexus 0.268 0.541 0.235 0.216 0.271 0.301 0.647 0.237 0.394 0.288 0.387 0.797 0.447 0.376 2.000 1.700 4.000 0.265 0.390 0.754 0.555 0.029 1.634 0.064 3.664 1.004 1.066 5.600 ? ? ?
Baculites_gilberti 0.304 0.449 0.390 0.293 0.443 0.438 0.714 0.438 0.538 0.395 ? ? ? 0.300 2.000 1.600 6.000 0.705 0.420 0.610 0.600 0.057 2.800 0.097 3.500 1.007 0.977 5.600 ? ? ?
Baculites_gregoryensis 0.329 0.548 0.289 0.279 0.243 0.333 0.847 0.441 0.479 0.382 0.379 0.821 0.487 0.394 2.000 ? 5.500 ? 0.706 0.500 0.590 0.068 3.889 0.140 7.997 0.996 0.990 6.000 ? ? ?
Baculites_reduncus 0.202 0.624 0.291 0.244 0.226 0.327 0.832 0.342 0.438 0.270 0.434 0.789 0.482 0.514 2.000 1.600 9.000 0.208 ? 0.446 0.646 0.110 6.254 0.075 6.100 1.015 0.987 6.000 ? ? ?
Baculites_scotti 0.161 0.617 0.118 0.383 0.225 0.165 0.491 0.431 0.516 0.202 0.226 0.404 0.318 0.132 ? ? 10.000 ? ? ? 0.638 0.025 1.442 0.127 3.500 1.018 1.015 6.000 0.184 1.340 ?
Baculites_texanus 0.391 0.453 0.219 0.195 0.380 0.321 0.983 0.426 0.472 0.301 0.605 1.263 0.320 0.507 1.000 2.000 ? 0.265 0.550 0.803 0.647 0.057 3.290 0.123 7.023 1.003 0.990 6.000 0.180 0.784 ?
Baculites_pseudovatus 0.200 0.802 0.209 0.341 0.207 0.228 0.391 0.379 0.539 0.182 0.374 0.697 0.488 0.137 ? ? ? ? ? ? 0.625 0.060 3.440 0.090 5.162 0.987 0.124 7.500 0.248 1.091 ?
Baculites_crickmayi 0.200 0.794 0.260 0.218 0.261 0.250 0.433 0.338 0.365 0.205 0.225 0.720 0.301 0.273 1.000 ? ? 1.585 ? 0.662 0.653 0.114 6.485 0.100 5.716 1.037 0.998 7.500 ? ? ?
Baculites_rugosus 0.135 0.713 0.207 0.301 0.208 0.182 0.234 0.395 0.344 0.159 0.225 0.171 0.349 0.274 2.000 ? 4.000 1.405 1.230 0.451 0.484 0.008 0.463 0.101 5.741 0.946 1.002 11.000 0.340 2.890 2.912

Baculites_corrugatus 0.226 0.915 0.201 0.259 0.194 0.137 0.193 0.296 0.507 0.254 0.239 0.663 0.479 0.180 ? ? 6.000 0.088 0.128 0.564 0.578 0.065 3.697 0.068 3.913 1.027 1.000 9.000 0.243 0.701 2.424
Baculites_undatus 0.596 0.387 0.373 0.286 0.476 0.404 0.587 0.410 0.395 0.332 0.622 0.546 0.510 0.388 1.000 1.500 3.000 0.096 ? 0.516 0.773 0.112 6.404 0.104 5.965 1.015 0.997 4.200 0.156 0.660 ?
Baculites_compressus 0.282 0.471 0.192 0.312 0.327 0.276 0.255 0.352 0.485 0.257 0.504 0.956 0.407 0.267 1.000 ? 8.000 0.218 ? ? 0.429 0.034 1.965 0.112 6.373 0.974 1.006 8.500 0.323 1.195 ?
Baculites_cuneatus 0.230 0.527 0.224 0.324 0.320 0.265 0.172 0.370 0.488 0.319 0.389 0.445 0.233 0.208 3.000 ? 8.000 0.533 0.332 0.323 0.521 0.052 2.993 0.063 3.600 1.033 1.031 9.000 0.316 1.087 3.688
Baculites_reesidei 0.251 0.493 0.290 0.314 0.193 0.146 0.095 0.392 0.458 0.227 0.470 0.598 0.494 0.412 1.000 ? 8.000 ? ? 0.581 0.588 0.049 2.792 0.052 2.980 1.021 1.008 8.500 ? ? ?
Baculites_jenseni 0.256 0.548 0.182 0.254 0.245 0.153 0.172 0.245 0.602 0.200 0.433 0.690 0.225 0.268 ? ? 9.000 ? ? 0.496 0.571 0.028 1.616 0.026 1.494 0. 968 0.997 7.000 ? ? ?
Baculites_eliasi 0.241 0.591 0.266 0.365 0.215 0.198 0.257 0.476 0.510 0.327 0.249 0.562 0.277 0.252 ? ? ? ? ? ? 0.614 0.047 2.706 0.092 5.251 1.019 1.004 7.000 ? ? ?
Baculites_baculus 0.331 0.525 0.380 0.344 0.421 0.405 0.826 0.480 0.663 0.324 0.804 1.517 0.672 0.326 2.000 ? 1.000 0.540 ? 0.627 0.854 0.099 5.646 0.084 4.785 1.015 1.023 10.500 0.225 0.892 3.112
Baculites_grandis 0.260 0.571 0.211 0.356 0.393 0.321 0.511 0.496 0.406 0.338 0.633 0.756 0.551 0.314 2.000 ? ? 0.174 1.420 0.697 0.728 0.105 5.991 0.090 5.138 1.003 1.014 11.000 0.266 0.849 5.625
Baculites_clinolobatus 0.298 0.434 0.191 0.290 0.244 0.287 0.770 0.415 0.459 0.312 0.475 0.747 0.307 0.465 1.000 ? ? 0.496 ? 0.632 0.705 0.033 1.899 0.029 1.660 1.024 0.979 10.000 ? ? ?
B_larsoni 0.841 0.288 0.388 ? 0.527 ? 0.906 0.210 0.336 0.894 0.741 1.031 0.806 0.780 2.000 ? ? ? ? 0.547 0.846 0.075 4.286 0.066 3.780 ? 1.010 1.010 ? ? ?

&[numeric]
Sciponoceras_gracile 0 0 0 0 0 0 0 0 0 0 0 0 0 0 0 0 0 0 0 0 0 0 0 0 0 0 0
Baculites_obtusus 1 0 0 0 0 0 1 1 1 0 0 0 0 1 1 0 0 0 0 0 1 1 0 1
Baculites_mclearni 1 0 0 0 0 0 1 1 1 0 0 0 0 1 1 0 0 0 0 0 0 ? 0 1
Baculites_asperiformis 1 0 0 1 0 0 1 1 1 0 0 0 0 2 1 0 0 0 0 0 1 1 0 1
Baculites_sp_smooth 1 0 0 1 0 0 ? ? ? 1 1 1 1 2 1 1 1 0 0 0 0 ? ? ?
Baculites_perplexus 1 0 1 1 0 0 2 2 2 0 0 0 0 2 1 1 1 0 0 0 1 1 0 1
Baculites_gilberti 1 0 1 1 0 0 2 2 2 0 0 0 0 2 1 0 1 0 1 0 1 0 ? ?
Baculites_gregoryensis 1 1 1 1 0 1 2 ? 1 0 1 0 1 3 2 0 1 0 1 0 0 0 ? ?
Baculites_reduncus 1 1 1 [12] 0 1 2 2 1 0 0 0 0 3 2 0 1 0 1 0 1 0 ? ?
Baculites_scotti 1 1 1 2 0 1 ? ? 1 0 1 0 1 3 2 0 0 0 1 [01] 1 1 1 0
Baculites_texanus 1 [02] 0 1 0 0 1 2 3 0 0 1 0 1 2 0 1 0 1 0 1 0 0 0
Baculites_pseudovatus 1 1 2 2 1 1 ? ? 1 1 1 [01] 1 1 2 1 0 0 0 0 0 0 1 0
Baculites_crickmayi 1 1 2 2 1 1 2 ? 1 0 1 [01] 1 1 2 0 1 0 1 0 1 0 1 0
Baculites_rugosus 1 1 2 2 1 1 2 ? 2 0 1 0 0 4 2 1 1 1 1 0 0 1 1 0
Baculites_corrugatus 1 1 2 2 1 1 2 ? 2 1 1 0 0 4 3 0 1 1 1 0 1 0 1 0
Baculites_undatus 1 2 0 2 0 0 1 2 3 0 0 0 0 0 4 0 1 0 0 0 1 0 1 0
Baculites_compressus 1 1 0 1 1 1 2 ? 1 0 1 [01] 1 3 3 0 1 0 1 0 0 1 1 0
Baculites_cuneatus 1 1 0 2 1 1 2 ? 1 0 1 0 1 5 3 0 1 0 1 0 1 1 1 0
Baculites_reesidei 1 1 0 2 1 1 2 ? 1 0 1 0 0 5 3 0 0 0 1 1 1 1 ? ?
Baculites_jenseni 1 1 0 2 1 1 ? ? 1 1 1 0 0 1 [13] 0 0 0 1 1 0 0 ? ?
Baculites_eliasi 1 1 0 2 1 1 ? ? ? 1 1 1 0 [16] 4 0 0 0 [01] 0 1 1 1 0
Baculites_baculus 1 2 0 1 0 0 1 ? 3 0 1 1 0 0 4 0 1 0 0 0 1 1 1 0
Baculites_grandis 1 2 0 1 0 0 1 ? ? 0 1 1 1 5 4 0 1 0 1 0 1 1 1 0
Baculites_clinolobatus 1 2 0 1 0 1 1 ? ? 0 1 1 1 5 4 0 1 0 1 0 1 0 ? ?
Baculites_larsoni 0 0 2 0 0 0 2 ? ? 0 1 1 1 2 2 0 1 0 0 0 ? 1 ? ?
;

```
nstates stand;
hold 50000;
collapse auto;
mult= replic 2000 keepall;
best;
procedure/;
```